DEVELOPMENT OF CHIRAL METAL-CATALYSTS FOR THE SELECTIVE FORMATION OF C-H, C-C AND C-X BONDS. FROM DESIGN TO APPLICATION

Pol De La Cruz Sanchez Badia

UNIVERSITAT
ROVIRA i VIRGILI

Development of chiral metal-catalysts for the selective formation of C-H, C-C and C-X bonds. From design to application.

Pol De La Cruz – Sánchez Badia

DOCTORAL THESIS
2023

UNIVERSITAT ROVIRA I VIRGILI
DEVELOPMENT OF CHIRAL METAL-CATALYSTS FOR THE SELECTIVE FORMATION OF C-H, C-C AND C-X BONDS. FROM DESIGN TO APPLICATION
Pol De La Cruz Sanchez Badia

UNIVERSITAT ROVIRA I VIRGILI
DEVELOPMENT OF CHIRAL METAL-CATALYSTS FOR THE SELECTIVE FORMATION OF C-H, C-C AND C-X BONDS. FROM DESIGN TO APPLICATION
Pol De La Cruz Sanchez Badia

UNIVERSITAT ROVIRA I VIRGILI
DEVELOPMENT OF CHIRAL METAL-CATALYSTS FOR THE SELECTIVE FORMATION OF C-H, C-C AND C-X BONDS. FROM DESIGN TO APPLICATION
Pol De La Cruz Sanchez Badia

Pol De La Cruz-Sánchez Badia

Development of chiral metal-catalysts for the selective formation of C-H, C-C and C-X bonds. From design to application.

Doctoral Thesis
Supervised by Prof. Montserrat Diéguez and Prof. Oscar Pàmies

Departament de Química Física i Inorgànica
Inncat Group

UNIVERSITAT ROVIRA I VIRGILI
TARRAGONA
2023

UNIVERSITAT ROVIRA I VIRGILI
DEVELOPMENT OF CHIRAL METAL-CATALYSTS FOR THE SELECTIVE FORMATION OF C-H, C-C AND C-X BONDS. FROM DESIGN TO APPLICATION
Pol De La Cruz Sanchez Badia

UNIVERSITAT ROVIRA i VIRGILI

Profs. Montserrat Diéguez Fernández and Oscar Pàmies Ollé, full professors of the Department de Química Física i Inorgànica at Universitat Rovira i Virgili

WE STATE that the present study, entitled "Development of chiral metal-catalysts for the selective formation of C-H, C-C and C-X bonds. From design to application", presented by Pol De La Cruz – Sánchez Badia for the award of the degree of Doctor, has been carried out under our supervision at the Department of Química Física i Inorgànica of this university and meets the requirements to qualify for the European mention.

Tarragona, September 2023

Doctoral Thesis Supervisors

Prof. Montserrat Diéguez Fernández Prof. Oscar Pàmies Ollé

UNIVERSITAT ROVIRA I VIRGILI
DEVELOPMENT OF CHIRAL METAL-CATALYSTS FOR THE SELECTIVE FORMATION OF C-H, C-C AND C-X BONDS. FROM DESIGN TO APPLICATION
Pol De La Cruz Sanchez Badia

The present Doctoral Thesis has been developed with a "Programa Martí I Franquès" scholarship (2019PMF-PIPF-1).

It has been possible thanks to the financial support from the following research projects:

- Ministerio de Economía y Competitividad (MINECO), Ministerio de Ciencia e Innovación (MICINN) and Agencia Estatal de Investigación (AEI). CTQ2016-74878-P, CTQ2016-81293-REDC/AEI and PID2019104904GB–I00 funded by MCIN/AEI/10.13039/501100011033

- European Regional Development fund (AEI/FEDER, UE)

- Generalitat de Catalunya. 2014SGR670 and 2017SGR1472.

- ICREA Foundation (ICREA Academia award to M.D).

- URV, Programa Martí i Franquès. 2019PMF-PIPF-1.

UNIVERSITAT ROVIRA I VIRGILI
DEVELOPMENT OF CHIRAL METAL-CATALYSTS FOR THE SELECTIVE FORMATION OF C-H, C-C AND C-X BONDS. FROM DESIGN TO APPLICATION
Pol De La Cruz Sanchez Badia

Acknowledgements/Agraïments

Des que vaig començar el màster a la URV allà pel 2017 moltes coses han transcorregut en els passadissos dels laboratoris del Departament de Química Física i Inorgànica. Abans de començar a endinsar-nos en el tema científic crec important agrair a totes les persones amb les qui he compartit el dia a dia aquests últims sis anys.

En primer lloc, m'agradaria agrair als meus supervisors el **Prof. Oscar Pàmies** i la **Prof. Montserrat Diéguez**. Des que em vau adoptar al començament del màster fins avui heu aconseguit canvis en mi que fins i tot jo pensava impossibles. Heu instaurat en mi valors molt importants: dedicació, compromís i rigor científic. Sense el vostre suport, esforç i constància aquesta tesi no hauria sigut. La vostra passió per la química fa que el més petit resultat (per nosaltres els doctorands) sembli un gran pas en la direcció correcta. Aquesta tesi és tan vostra com ho és meva.

També vull aprofitar aquesta oportunitat per agrair al personal investigador, d'administració i de serveis del departament, la facultat i la universitat que han fet que el dia a dia dels doctorands sigui més fàcil. Especialment, m'agradaria agrair a la **Prof. Anna Maria Masdeu**, per acollir-me durant el treball de fi de grau i fer-me enamorar de la catàlisi. A **l'Elisenda** per sempre solucionar tots els embolics de l'impressora i trobar solució a totes les "mac issues". Al **Josep** per estar sempre passes el que passes. Del servei de recursos científics i tècnics, a la **Sonia** per ajudar-me amb els embolics de les masses i els HPLC i sobretot al **Ramon** per sempre estar disposat a ajudar-nos incondicionalment, encara que arribéssim tard al matí per ficar el ASAP. Finalment vull agrair a la **Raquel** tot el que fa per nosaltres i pel departament. El primer dia que vaig arribar al laboratori em vas rebre amb un somriure, em vas dir que també eres de Lleida i vaig saber que tot aniria bé. La teva dedicació pels altres és l'engranatge que fa que tot el grup funcioni a la perfecció.

No vull oblidar tampoc de tots aquells amb qui hem col·laborat científicament en el transcorregut de la meva tesi. Especialment, vull agrair al **Prof. Miquel A. Pericàs** per la seva predisposició i tots els inavaluables consells científics.

To **Dr. Eric Manoury** and **Prof. Rinaldo Poli**, thanks for letting me conduct part of my thesis work in LCC/CNRS center in Toulouse in the middle of a pandemic in 2020. Even during the hardships of confinement, I had the time of my life discovering new ferrocene complexes as well as the beautiful city of Toulouse. I do not forget the kindness of everybody in Équipe G that, since day one, made me feel like one more in the group. Thanks to: **Agnes**, **Sandrine**, **Christophe**, **Uchchal**, **Hui**, **Ilia**, **Maxime** and **Meenu**.

Vull fer menció també de tota la gent que amb el qual he compartit espais de la facultat. Com per exemple els meus companys d'orgànica **Miguel**, **Isabel** i **Albert**, amb

els quals compartim moments des del màster i amb alguns des de la carrera. Que tan sols creuant unes paraules pel passadís/ascensor/RMN ja sabíem de quin "mood" estàvem aquella setmana. També menció als companys de polímers, sobretot a **Javi** l'organometàl·lic "traïdor" i **Jordi G.** el destí va ajuntar a dos descarrilats en el labo de termodinàmica de segon de carrera.

I ara si que si, és el torn dels anteriorment coneguts com a TECAT-OMICHIS, ara coneguts com a Inncat, CatBorChem i Greencat. Els companys del dia a dia, els que veus més que a la teva familia.

Del Lab 218, tenim a **Nassima**. Cuantas veces me quede hablando contigo media hora cuando solo iba a buscar hexano para la columna. Recuerdo mucho nuestro viaje a Toulouse cuando estuvimos de congreso, y aunque nos separaba una puerta metálica para mi, eras una más.

Del Lab 216, del qual sol una porta assassina ens separa. Primer començarem pels fanàtics del *syn-gas* i el CO_2, els doctorands de Cyril. **Toni**, vas ser de les primeres persones que vaig conèixer a l'entrar al grup i el que més em va sorprendre és que entenguessis el meu humor bastat 100% en referències del Simpson. A **Joris**, el francès majo, en singular porque solo he conocido uno. Muchas gracias por tu eterna positividad. **Lola**, no tengo paginas para describir los momentos que recuerdo contigo, mi compañera/enemiga de escritorio. Solo diré que si algun dia necesitas alguien con quien hacer un telemaraton de música cristiana llámame. Finalment a **Jèssica**, no sabia on ficar-te, així que em guiaré per la distribució actual. Però tenir-te al costat durant una temporada va ser, com a mínim, educatiu. A part de enseñarme els basics de com ser un real fooder també m'has ensenyat a ser una miiiiiiqueta millor persona, gràcies. Per una altra banda, al 216, tenim el subgrup dels famosament coneguts com borillos. Els primers que vaig conèixer en aquests grup van ser **Núria** i **Jordi R.** gràcies per ensenyar-me els primers passos per sobreviure en el departament. Després òbviament tenim a la **Jana**, companya de màster que em va abandonar (no la culpo), però els moments junts i els nostres esmorzars improvisats de quan baixaves de Bilbo sense avisar-me els guardo per a mi. A **Ricardo M.** aún recuerdo ese hola de cuando estaba en el lab 218 haciendo el TFG. Es muy topico andaluz decir esto, però gracias por enseñarme que esto tambien puede ser divertido. Després tenim a **Uri**, sempre estaré orgullós d'haver enganxat algú als crucigrames. Bromes a part, gràcies per la servitud amb els altres i les teves ganes de sempre donar un cop de mà quan se't necessita. A **Paula**, la meva geme de Vans (jo no faig skate es postureo), gràcies per sempre estar amb un somriu-re a la cara i per pressionar amb mi per anar a dinar a l'hora que toca. **Mireia**, la meva companya de cops de cap quan movem un mil·limetre la cadira, continua sent com ets d'autèntica i d'ebrenca et portarà a molts llocs. Això si, practica com dissimular el *side-eye*, t'evitarà problemes. A **Sara**, creo que nuestra amistad se basa en ocultar los sentimientos moñas hasta que llega un momento supercringe como

este. Solo diré que creo que el universo junta gente afin (o al menos con las misma carències mentales) para que se hagan companyia un rato. Eso o necesitaba a alguien que se riera de mis paridas mentales.

Davant del seminari solia haver-hi un laboratori del qual no en sabíem res. Però de sobte dues pobladores estranyes ens van ocupar dues taules. A **Anna**, companya de concerts Kpop, gràcies per obrir-me portes a altres cultures i demostrar-me fins a quin punt es pot ser resilient envers l'adversitat. A **Angie**, mi carachimba fav, que bonito tenir tiempo de conocerte y de que me traigas más desayunos. Algo me dice que nos quedan mas aventuras juntos.

Finalment, el Lab 217, amb els qui he compartit mes temps de treball (i xarrameca). **Daniel**, al principio tenia mis dudas de que te pudiera ensenyar algo de utilidad en el lab. Despues me di cuenta que al menos algun refran si que he conseguido que se te quede. Sigue aprendiendo, sigue preguntando y te deseo todo lo mejor para tu tesis. A **Joan**, opino que la vida moltes vegades et posa proves, tu has sigut una de paciència i comprensió. **Jordi F.** realment no sé què posar aquí, ja són molt anys junts, la primera vegada que ens vam conèixer se suposava que havia d'ensenyar-te jo a tu, però jo opino que ha sigut més un aprenentatge en paral·lel, i com hem crescut des d'aquells dies que compartíem vitrina. Una part teva se me'n va amb mi del lab 217. A **Maria**, qualsevol mena d'agraïment es queda curt amb el que m'has aportat tant científicament com personalment. Des del dia que ens vam conèixer es va fer obvi que estem en dues ondes diferents, però això mai et va impedir ensenyar-me amb amabilitat i perseverança, i sobretot en dir-me les coses com són i no d'una altra manera, que a vegades, ho necessito. Aquesta tesi també es graciés a tu. Finalment, a **Carlota**, la primera persona que vaig interactuar mai del laboratori. Encara sort que la teva paciència era infinita perquè si no m'hagués aviat la primera setmana. La teva professionalitat i la teva confiança en mi va ser el catalitzador que va fer que volgués continuar en aquest món. Sempre seràs un exemple per a mi.

També m'agradaria agrair a tota la gent que, fora del laboratori, ha aportat el seu granet de sorra en què aquests anys es fessin menys durs.

A las maris, **Dani**, **Luis** y **Alba**. Lo que unieron las cervecitas que no lo separe el hombre, muchas gracias por ser autenticos al 100% y siempre estar dispuestos ha hacer meetings llueva, truene o haya un terremoto. Especialmente a mi **Alba**, quiero agradecerte el incondicional apoyo durante estos años. Para lo bueno, para lo malo y para compartir un plato de sushi como dices tu, estaré ahi cuando me necesites.

A mis compañeros de pandèmia en Toulouse. **Lorena**, **Sara** y **Hugo** nos conocimos pocos meses pero me adentrasteis en vuestro grupo como si fuera uno mas y hicisteis Toulouse (Arenes) mi casa lejos de casa.

A mis queridisimos amigos del grupo mixto Barcelona/Ibiza. **Joan**, **Javi**, **Mar**, **Fati** i **Toni**. Muchas gracias por acojerme en vuestros sofàs siempre que lo he necesitado y siempre estar dispuestos a una buena rumbatronica cada vez que se propone. A **Sergio**, gracias por regalarme la portada de esta tesis, y tu que decias que Bellas Artes no te llevaria a ningun lado. A **Carlos**, te queria dedicar unes palabritas extra solo porque nos conocimos de hace ya muchos años y no dudaste en introducirme en tu mundo des de el minuto uno. Sin ti yo no estaria escribiendo estas palabras, te lo aseguro. Muchas gracias por todo.

A **Laila**, nunca pensé que una desconocida con al que compartes piso pudiera caerme tan y tan bien. Me has acompañado durante la mayoria de mis años haciendo el doctorado y has convertido el numero 7 de la baixada de misericòrdia un hogar con todas las letras. No dejes de luchar nunca por ti y tu felicidad, te la mereces. Estare aquí siempre. Un saludito a mis/tus niños **Jagger** y **Annakin** (aunque él no quiera).

Finalment, toca agrair als originadors, a la meva família. Sempre al meu costat, aguantant els meus canvis d'humor constants. **Padre**, gràcies per ensenyar-me que no totes les lliçons importants són les que s'aprenen assegut en una classe, les teves "armes" estan en la meva ment. **Madre**, gràcies per ensenyar-me paciència i perseverança, ah, i ha que m'agradessin les mates, sense tu no seria científic. **Neus**, pesi a qui li pesi ets la única persona que conec des que tinc memòria, gràcies per seguir-me sempre el rollo, sense fer moltes preguntes, em tindràs sempre. **Ascen**, ho sento, però ets la "tieta" enrollada, gràcies per infectar-me del teu sentit de l'humor. Abuela (**Carmen**), gracias por cuidar-me y preocuparte por mi desde bien pequeñito, espero algun dia poder pagar-te todo lo que has hecho por mi. Als meus altres avis, **Salvador**, **Juanita** i **Paco**, que ja no estan en el món terrenal; us porto presents cada dia que passa i les lliçons que em vau aplicar en vida es queden amb mi per sempre.

Sé ben segur que aquí no està reflectida en la seva totalitat les persones que he conegut i interactuat durant 5 o 6 anys. Però l'important no és que jo hagi escrit el teu nom en un tros de paper, sinó que és el que ha quedat imprès en la nostra consciència; l'un de l'altre.

Moltes gràcies a tots.

"I imagined in the beginning, that a few experiments would determine the problem, but experience soon convinced me that a very great number indeed were necessary, before such an art could be brought to any tolerable degree of perfection."

Elizabeth Fulhame, 1794.

Inventor of the concept of catalysis and discoverer of photoreduction

UNIVERSITAT ROVIRA I VIRGILI
DEVELOPMENT OF CHIRAL METAL-CATALYSTS FOR THE SELECTIVE FORMATION OF C-H, C-C AND C-X BONDS. FROM DESIGN TO APPLICATION
Pol De La Cruz Sanchez Badia

Table of Contents

UNIVERSITAT ROVIRA I VIRGILI
DEVELOPMENT OF CHIRAL METAL-CATALYSTS FOR THE SELECTIVE FORMATION OF C-H, C-C AND C-X BONDS. FROM DESIGN TO APPLICATION
Pol De La Cruz Sanchez Badia

Structure of the thesis

Some of the results of the thesis have already been published in international journals. These papers have been reedited and changed to tell a history of the work performed and to provide a uniform format throughout the thesis. It is to note that the numeration in Chapter 1 is independent of the rest of the chapters. Starting from Chapter 2 until the end of this thesis, the numeration is consecutive, including substrates and final products.

The thesis is divided into 6 Chapters.

Chapter 1. *General introduction*. This chapter first presents the importance of metal asymmetric catalysis in the synthesis of enantiomerically pure compounds and the relevance of the design of tailored chiral ligand libraries in its success. This chapter then focuses on the antecedents, performance and main achievements for each of the enantioselective catalytic transformations studied in this thesis, with emphasis on the most successful ligand libraries developed. The state of the art and current needs in the field justify the objectives of the thesis.

Chapter 2. *Objectives*. Based on the aspects discussed in Chapter 1, this Chapter presents the objectives of the thesis. These include the development of tailor-made ligand libraries and their subsequent utilization in the Rh- and Ir-catalyzed asymmetric hydrogenation, as well as in the Pd-catalyzed asymmetric allylic substitution. These processes have been chosen for their green chemistry properties and their industrial interest, since they give rise to chiral products with a high added value. Although they have a long history behind, our goal is to reach challenging and more complex substrates/nucleophiles. To achieve this objective several tailor-made ligand libraries have been synthetized. In their design we have taken into account their industrial applicability (synthetized in few steps and from inexpensive starting materials, and simple manipulation). Finally, the objectives also include to develop a novel Pd-catalyzed [3+2] cycloaddition of vinyl heterocycles to double-stabilized Michael acceptors.

Chapter 3. *Rh and Ir-catalyzed asymmetric hydrogenation*. This Chapter contains six sections on the development and application of tailor-made ligand libraries, specially designed with the needs of the substrates under study. The first section, *P-stereogenic N-phosphine-phosphite ligands for the Rh-Catalyzed asymmetric hydrogenation of chelating olefins,* identified a successful family of easy-to-synthesize P-stereogenic *N*-phosphine-phosphite ligands for the Rh-catalyzed asymmetric hydrogenation of chelating olefins. The corresponding catalysts show excellent enantiocontrol for α-dehydroamino acid derivatives and α-enamides (ee's up to >99%) and promising results for the more challenging β-analogues (ee's up to 80%). The usefulness of these catalytic

systems was further demonstrated with the synthesis of several valuable precursors of pharmacologically active compounds, with ee's at least as high (up to >99%) as the best ones reported. The results included in this section have been published in *J. Org. Chem*. **2020**, *7*, 4730-4739. I have participated in the synthesis of substrates and ligands and in part of the catalysts screening. The second section, *Privileged P-stereogenic Ir-MaxPHOX catalysts for the highly enantioselective hydrogenation of a diverse scope of non-chelating olefins,* which has been done in a collaboration framework with the groups of T. Riera (IRB, Barcelona) and F. Maseras (ICIQ, Tarragona), demonstrated that Ir-MaxPHOX-type catalysts, containing P-stereogenic aminophosphine-oxazoline ligands, provide high catalytic performance in the hydrogenation of a wide range of non-chelating olefins with different geometries, substitution patterns and degree of functionalization. These air-stable and readily available catalysts have been successfully applied in the asymmetric hydrogenation of di-, tri- and tetrasubstituted olefins (ee's up to 99%). The combination of theoretical calculations and deuterium labeling experiments led to the uncover of the factors responsible for the enantioselectivity observed in the reaction, allowing the rationalization of the most suitable substrates for these Ir-catalysts. The results included in this Chapter have been published in two papers: *Org. Lett.* **2019**, *21*, 807–811 and *ACS Catal.* **2023**, *13*, 3020–3035. I have participated in the synthesis of new substrates, most of the catalysts screening and in the deuterium experiments. The third section, *Phosphine-triazole based ligands for the Ir-catalyzed asymmetric hydrogenation of challenging exocyclic benzofused-based alkenes*, which has been done in a collaboration framework with the group of M. A. Pericàs (ICIQ, Tarragona), describes novel chiral phosphine-triazole ligands for the Ir-catalyzed asymmetric hydrogenation of exocyclic benzofused alkenes. Overcoming previous limitations, the catalytic system is able to successfully hydrogenate exocyclic olefins bearing a benzofused five- and six-membered ring motif (ee's up to 99%). The catalyst tolerates well the presence of several substituents and substitution patterns at both aromatic rings. The absence of a competing isomerization process together with the perfect fit of the olefins in the catalyst chiral pocket are key to surpass the previous limitations in the hydrogenation of both 5- and 6-membered ring benzofused exocyclic olefins. The results included in this section have been published in *Adv. Synth. Catal.* **2022**, *365*, 167–177. I have participated in the synthesis of new substrates, the ligands and in most of the catalysts screening. The fourth section, *Indene-based phosphorus-thioether ligands for the Ir-catalyzed asymmetric hydrogenation of olefins with diverse functional groups and substitution patterns*, which has been done in a collaboration framework with the group of M. A. Pericàs (ICIQ, Tarragona), shows the utility of an indene-based phosphite/phosphinite-thioether ligand library for the Ir-catalyzed asymmetric hydrogenation. These ligands were synthetized in only 3 steps from inexpensive indene. The high modularity of these ligands helped identify highly enantioselective catalysts

for asymmetric hydrogenation of substrates covering different substitution patterns with different functional groups and coordination abilities, ranging from non-chelating olefins, through olefins with poorly coordinative groups, to olefins with coordinative functional groups (ee's up to 99%). The results included in this section have been published in *Adv. Synth. Catal.* **2021***, 363,* 4561–4574. I have participated in most of the catalysts screening. In the next two sections two carbene-thioether ligand families have been developed with the aim to combine the advantages of thioether and *N*-heterocyclic carbene functionalities. In this respect, the fifth section, *Ir/thioether–carbene, –phosphinite and –phosphite complexes for asymmetric hydrogenation. A case for comparison*, compiles for the first time the application of novel and simple Ir/thioether-NHC complexes in the asymmetric hydrogenation of non-chelating olefins and cyclic β-enamides. For comparison, thioether–phosphinite/phosphite analogues complexes were prepared and applied in the reduction of the same olefins. Catalytic performance of Ir/thioether-carbene catalyst precursors was lower than their related Ir/thioether-P complexes in the hydrogenation of non-chelating olefins but they presented similar good performance for the reduction of chelating olefins. Reactivity studies with H_2 revealed that the low activities of the new NHC-based complexes in the hydrogenation of non-chelating tri- and bulky disubstituted olefins is due the formation of inactive trinuclear species. The results included in this section have been published in *Organometallics* **2019**, *38*, 4193−4205. I have worked in the synthesis of the ligands, done the catalysts screening and the reactivity studies with H_2. The sixth section, *Chiral ferrocene-based thioether-carbene ligands for the Ir-catalyzed hydrogenation of non-chelating olefins*, which has been done in a collaboration framework, during my PhD research stay, with the groups of E. Manoury and R. Poli (CNRS, Toulouse), describes the potential of novel ferrocene-based Ir/thioether-NHC complexes in the asymmetric hydrogenation of non-chelating olefins and olefins with polar neighboring groups. The introduction of an extended chelate ring overcame the previously observed activity issues. Catalytic performance of these complexes was still not satisfactory in most of the cases, except for lactones and acyclic esters (up to 99% ee). The reactivity with hydrogen of selected Ir-catalyst precursors was studied. In contrast to the results from previous section, the presence of catalytically inactive trinuclear hydride was not observed. I have done the synthesis of the ligands, the catalysts screening and the reactivity studies with H_2.

Chapter 4. *Pd-catalyzed asymmetric allylic substitution.* This chapter contains one section, *Pd-catalyzed asymmetric allylic substitution using a methylene linked phosphite-oxazoline PHOX-based ligands*, describing a small library of phosphite-oxazoline ligands for Pd-catalyzed allylic substitution of a wide range of substrates and nucleophiles with high enantioselectivities (up to 99%). By replacing the phosphine moiety in the PHOX ligands by biaryl phosphites and by introducing a methylene spacer between the oxazoline and the phenyl ring allowed to increase the substrate and

nucleophile scope of the previous phosphine-based ligands. Good performance for a range of hindered and cyclic substrates, with several nucleophiles was observed. Mechanistic studies based on DFT calculations and NMR spectroscopy of the key Pd-intermediates allowed us to better understand the origin of the enantioselectivities. The wide substrate scope found is due to the ability of the ligand to adapt their ligand parameters to the reacting substrate. The results included in this section have been published in a special issue dedicated to Prof. R. Poli in occasion of his 65th birthday, *Eur. J. Inorg. Chem.* **2022**, *10*, e202100988. I have done the catalysts screening and leading the *in situ*-NMR mechanistic studies.

Chapter 5. *Pd-catalyzed [3+2] cycloaddition reaction.* This chapter contains one section, *Synthesis of tetrahydrofuran-fused spirocyclic Meldrum's acid derivatives via asymmetric Pd-catalyzed [3+2] cycloaddition*, on the developed of an efficient method for the synthesis of spirocyclic tetrahydrofurans via the Pd-catalyzed [3+2] cycloaddition reaction of vinyl epoxides with 5-alkylidene Meldrum's acid derivatives. The cycloaddition reaction provided the corresponding Meldrum's acid spiro-fused tetrahydrofurans in high yields and high enantio- and diastereoselectivities (dr's up to 15:1 and ee's up to >99%). Several aryl, alkyl and heterocyclic groups were successfully introduced in different positions of the tetrahydrofuran without compromising the high enantioselectivities obtained. I have done all the work.

Chapter 6. *General conclusions*. This Chapter presents de conclusions of the work included in this thesis.

CHAPTER 1

General introduction

UNIVERSITAT ROVIRA I VIRGILI
DEVELOPMENT OF CHIRAL METAL-CATALYSTS FOR THE SELECTIVE FORMATION OF C-H, C-C AND C-X BONDS. FROM DESIGN TO APPLICATION
Pol De La Cruz Sanchez Badia

1. General introduction

A large list of pharmaceutical formulations, agrochemicals and fine chemicals are manufactured using enantiopure chemicals. The main technology for obtaining chiral chemicals is the resolution of racemates. However, asymmetric catalysis is gaining preference, especially in the pharmaceutical industry, where the discovery of safer drugs with better therapeutic value requires versatile, high yield, low-cost processes to synthesize enantiomers.[1] Actually, catalysis is a key player in sustainable production processes and one of the principles that support green chemistry as well as a facilitator of other green chemistry principles such as atom economy and energy efficiency.[2] Compared to non-catalyzed processes, catalytic processes can provide higher production in fewer reaction steps, under more favorable energy conditions and generate fewer by-products. Undoubtedly, the path to sustainable growth goes through the improvement of catalytic synthetic processes, either by increasing the stability and selectivity of catalysts for existing processes, the development of catalysts for processes for which they are not widely available or improving the manufacturing process itself.[1]

To attain elevated levels of reactivity and selectivity in catalytic enantioselective reactions, various reaction parameters must be considered and optimized. Among these parameters, the design and selection of the chiral ligand is considered to be one of the most relevant. Hence, the synthesis of novel chiral ligands is crucial for advancing the development of catalytic systems that yield successful outcomes in asymmetric catalysis.[1,3] In this context, the utilization of highly modular ligand scaffolds confers significant advantages as it enables the synthesis and screening of a series of new more specific *tailored* ligand libraries, which take into account the needs of the reaction under study. This approach aims to attain the optimal activities and selectivities for each specific asymmetric catalytic reaction.[1,3]

This thesis specifically, addresses the development of tailor-made ligand libraries and their subsequent utilization in several metal-catalyzed asymmetric processes. These ligand libraries were not only designed with the objective of performance but also having in mind their industrial applicability (few synthetic steps, inexpensive starting materials, stability in the air and simple manipulation). In this thesis, we investigate the synthesis and application of various heterodonor bidentate ligand libraries, P-P', P-N, P-S, and C-S ligands, for the Rh- and Ir-catalyzed asymmetric hydrogenation, as well as for the Pd-catalyzed asymmetric allylic substitution. These processes have been chosen for their green chemistry properties and their industrial interest, since they give rise to chiral products with a high added value. Although they have a long history behind, our goal is to reach challenging and more complex substrates. Additionally, we also studied novel [3+2] Pd-catalyzed cycloaddition of vinyl heterocycles to double-stabilized Michael acceptors. In the subsequent sections, we provide a detailed background of each of the asymmetric catalytic reactions examined in this thesis.

1.1. Metal-catalyzed asymmetric hydrogenation of olefins

This 100% atom economy process has a large record of successful examples in the production of single enantiomer intermediates, especially in the pharmaceutical industry, using substrates ranging from olefins with coordinating functional groups to their non-coordinating counterparts, passing through olefins with intermediate coordinating properties.[1,3-4] It is estimated that around 10% of all chemical steps in the synthesis of enantiomerically pure compounds are hydrogenations. In this strategy the addition of hydrogen, catalyzed by a chiral metal complex, to a prochiral substrate containing a double bond gives rise to new carbon chiral centers (Scheme 1.1). This reaction has been the subject of extensive research and development by both academic and industrial research groups for several decades.

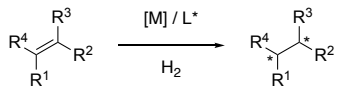

Scheme 1.1. Metal-catalyzed asymmetric hydrogenation of olefins.

As the number of substrates continues to increase to reach more complex molecules, finding a catalyst that performs well with many of them regardless of geometry, substitution pattern and functionalization remains a challenge. While the reduction of non-chelating olefins has a long story and the already known catalysts (mainly Rh- and Ru-catalysts with diphosphine ligands)[3] can efficiently reduce olefins with very diverse structures, the reduction of non-chelating olefins is less mature and has fewer synthetic applications, being the Ir-P,X compounds (X=N, S and O; mainly with phosphine/phosphinite/phosphite-oxazoline ligands)[4] the catalysts of choice The introduction by Pfaltz in 1998 of Ir-catalysts modified with chiral heterodonor ligands of P,N-type opened the race for enantiocontrol in the hydrogenation of non-chelating olefins, and many efforts have been devoted over the last two decades to the development of new Ir-catalysts that can expand the substrate scope to include even the most reluctant examples (see section 1.1.2.2 below for details).[4] Our research group has been an important player in this area with the development of highly versatile Ir-catalysts able to hydrogenate olefins with different substitution patterns and functionalization. The key to such versatility was the concept of "tailor-made" ligand libraries, a systematic series of ligands formulated from a variety of readily available, enantiopure starting backbones and the variation of the modularly introduced substituents. This proved to be an efficient approach to generate a diversity of ligands with very varied electronic and steric characteristics, able to adapt to the requirements of each substrate class (see section 1.1.2.2 below).

1.1.1. Metal-catalyzed asymmetric hydrogenation of chelating olefins

1.1.1.1. Mechanism

Scheme 1.2 illustrates the mechanism for the asymmetric hydrogenation of dehydroamino acids (e.g. methyl α-acetamidoacrylate) and their esters using cationic Rh-precursors incorporating diphosphine ligands.[5] This mechanism has also been found applicable to other phosphorus-based ligands, such as diphosphinites and diphosphites.[6] The catalytic cycle consists in two coupled diastereomeric manifolds. The cycle begins with the reaction of the substrate with the intermediate **A**, a square planar Rh(I) complex containing the chelating diphosphine and two molecules of solvent. In this first step, the substrate displaces the solvent molecules to give rise the square planar diastereomeric adducts $\mathbf{B}^{maj}$ and $\mathbf{B}^{min}$, where the substrate acts as a bidentate ligand bonded via the olefinic double bond and the oxygen atom of the acetyl group. The next step is the irreversible oxidative addition of hydrogen, which converts the square planar diastereoisomers **B** into the octahedral *cis*-dihydridorhodium complex **C**. Following this, the coordinated olefin is inserted into one of the Rh-H bonds, generating the two diastereomeric alkyl complexes **D**. Through reductive elimination, these complexes yield the enantiomeric forms of the hydrogenated product and regenerate the catalytically active square planar species **A**.[5]

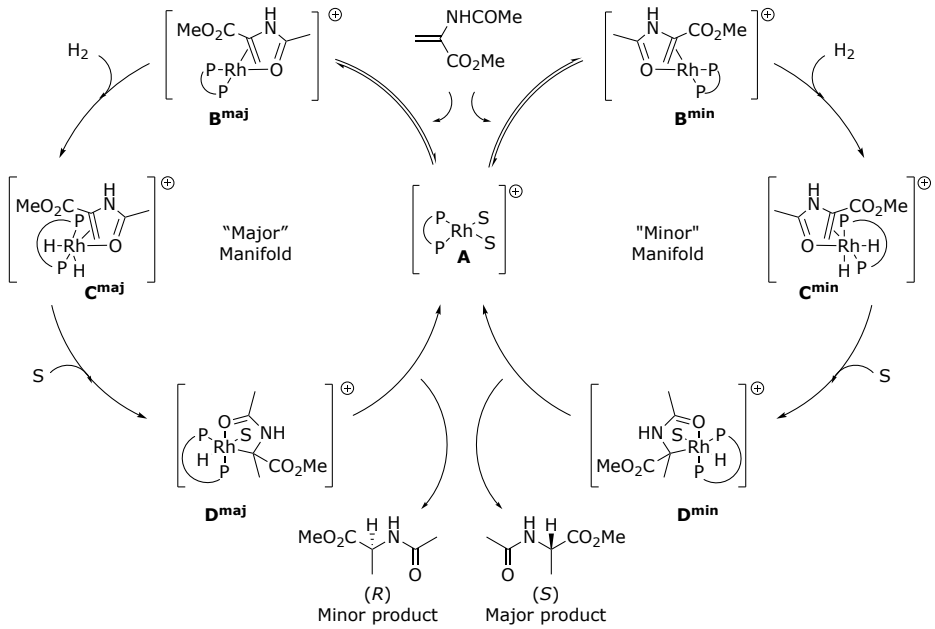

Scheme 1.2. Catalytic cycle for the Rh-catalyzed asymmetric hydrogenation of methyl α-acetamidoacrylate (S= solvent molecule, P-P= chiral diphosphine ligand).

The rate- and enantioselectivity-determining step in this process is widely accepted to be the oxidative addition of hydrogen. In this catalytic cycle, the reactivity of the minor diastereoisomer **B^{min}** is much higher than that of the major diastereoisomer **B^{maj}**. Consequently, the formation of the minor diastereoisomer governs the overall product outcome. In order to explain this phenomenon, Brown, Landis, *et al*. have conducted mechanistic studies which revealed that the oxidative addition of both major and minor adducts requires the rotation of substrates in the opposite direction to the rhodium phosphine axis. In the minor adduct, which is less stable, there is a more hindered configuration that can rotate more easily. Therefore, the minor species displays heightened reactivity towards dihydrogen compared to the major species.[6-7]

1.1.1.2. Ligands

The initial progress in asymmetric hydrogenation of olefins emerged during the 1960s, following the breakthrough discovery of Wilkinson's hydrogenation catalyst,[8] when Knowles[9] and Horner[10] simultaneously developed the earliest examples of enantioselective hydrogenation, albeit with poor enantioselectivities. They substituted the triphenylphosphine in Wilkinson's catalyst with resolved chiral monophosphines (**L1**, Figure 1.1). Following that, two significant advancements were achieved in the field of asymmetric hydrogenation. Kagan *et al*. documented the first C_2-symmetric diphosphine ligand (DIOP, Figure 1.1) which was non-P-stereogenic but has chirality in the carbon backbone. This ligand was tested in the Rh-catalyzed asymmetric hydrogenation of several α-dehydroamino acids, with ee's up to 80%.[11] These results proved that chirality at the P atom vas not essential to induce high enantioselectivity and the good results could be due to the conformational rigidity conferred by the diphosphine chelation to Rh. Following this concept, Knowles *et al*. made a notable breakthrough by discovering the C_2-symmetric chelating diphosphine ligand DIPAMP (Figure 1.1), with P-stereogenic phosphine groups, that provided higher enantioselectivities (up to 96%) than the DIOP.[12] The remarkable catalytic efficiency of DIPAMP led to its utilization in the industrial synthesis of L-DOPA, a medication employed for the treatment of Parkinson's disease.[13] In recognition of his groundbreaking contributions, Knowles was honored with the Nobel Prize in 2001.[14]

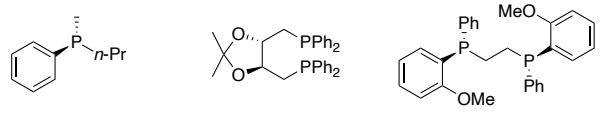

L1
Knowles, Horner *et al.*

DIOP
Kagan *et al.*

DIPAMP
Knowles *et al.*

Figure 1.1. Pioneering ligands in the asymmetric hydrogenation of chelating olefins.

Despite the success of DIPAMP, the methods to prepare P-stereogenic ligands at that time were scarce and challenging. Thus, most of the research groups opted for the

development of non-P-stereogenic chiral ligands, such as BPPFA, Prophos, Chiraphos and BINAP among others (Figure 1.2). The latter two ligands proved that ligand with backbone chirality could surpass the DIPAMP in the Rh-catalyzed hydrogenation of some types of dehydroamino acids. In addition, the discovery of Ru-BINAP catalysts by Noyori *et al*. expanded the substrate scope to other olefin types and ketones. With this groundbreaking discovery, Noyori was awarded the Nobel Prize in 2001 alongside Knowles. [15] Afterwards, several non-P-stereogenic diphosphine ligands such as DuPhos,[16] BICP,[17] *o*-HexaMeO-BIPHEP,[18] BPMPI,[19] among others,[20] have proven to be successful for the hydrogenation of *E*-β-dehydroamino acids (Figure 1.2). However, only the chiral diphosphine ligands BDPMI,[19] (Figure 1.2) provided high enantioselectivities in the reduction of *Z*-β-dehydroamino acids. The introduction of highly effective chiral diphosphorus ligands, such as BPE ligands developed by Burk *et al.*, greatly broadened the application range of asymmetric hydrogenation of various chelating olefins, including cyclic α-enamides (Figure 1.2).[21] Also concerning the reduction of these substrates, Zhang *et al*. developed conformationally rigid chiral bisphosphine PennPhos (Figure 1.2) which was successfully applied in the Rh-catalyzed asymmetric hydrogenation of 5- and 6- membered cyclic α-enamides.[22]

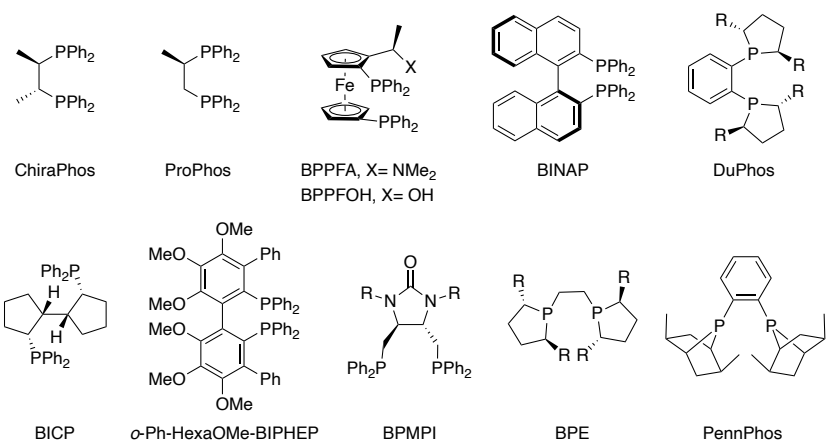

Figure 1.2. Representative non-P-stereogenic diphosphine ligands used in the metal-catalyzed asymmetric hydrogenation of chelating olefins.

The successful results with non-P-stereogenic ligands, along with the difficulty of preparing enantioenriched P-stereogenic compounds in their early days, diminished interest in these for many years. However, during that time the methods for the P-stereogenic ligands kept improving slowly.[23] So, in 1998, Imamoto *et al.* reported the BisP* ligands,[24] setting a milestone on the synthesis of the second generation of stereogenic phosphine ligands (Figure 1.3). The chirality is generated by the desymmetrization of *tert*-butyl(dimethyl)phosphine-boranes through an enantioselective deprotonation with a stoichiometric amount of (-)-sparteine and *sec*-

butyllithium, already developed by Jugé and Evans.[25] BisP* proved to be highly effective in the Rh-catalyzed asymmetric hydrogenation of di-, tri- and tetra-substituted chelating olefins.[24, 26] Following this work several other P-stereogenic ligand libraries were developed using this stereoselective deprotonation approach. Some successful examples of this second generation, include TangPhos[27] and QuinoxP*[28] ligands, which were synthesized using the (-)-sparteine method (Figure 1.3) and provided excellent results in the Rh-catalyzed asymmetric hydrogenation of α-dehydroamino acid derivatives, γ,δ-unsaturated amidoesters, acetoxy β-enamidoesters, among other olefins.[29] This second generation of diphosphine ligands are bulky, containing in general the *tert*-butyl, methyl pair attached to the P that provides a large steric bias that is extremely beneficial in terms of selectivity. On the other hand, they are electron-rich alkyl phosphines which make the catalysts very active in hydrogenation, but that also has drawbacks, making these ligands very prone to oxidation. In fact, the introduction of an aromatic flat backbone in the QuinoxP* ligand provide stability towards oxidation of the free ligand and a more rigid metal-chelate complex, which were responsible of the improved selectivity.

As previously said, the same features that are beneficial for catalysis become a drawback when attempting to synthesize these P-stereogenic electron-rich bulky phosphine ligands. For instance, the reactions on the P center are hampered by the steric hindrance of the bulky *tert*-butyl group. In addition, this type of phosphines is highly prone to oxidation in air, thus making the protection of phosphorus as an oxide or borane complex mandatory during the synthesis. However, due to the σ-donor properties of these phosphines, harsh deprotection conditions are usually needed, which compromises the chemical and stereochemical integrity of the ligand. Thus, the synthesis of bulky P-stereogenic ligands is highly challenging. Established methods that work well in the synthesis of aryl-containing P-stereogenic compounds fail when a *tert*-butyl group is attached to phosphorus. In this context, dedicated methods have been developed for the preparation of such classes of compounds.

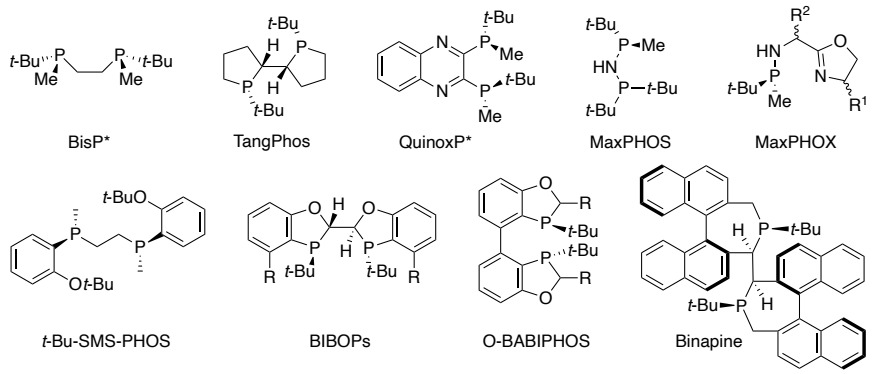

Figure 1.3. Representative of second generation of P-stereogenic containing ligands in asymmetric hydrogenation of chelating olefins.

So, one of the preferred strategies to achieve for crafting P-stereogenic ligands is the use of chiral auxiliaries. These auxiliaries react with phosphorus precursors, forming enriched intermediates where they're bound together. The auxiliary's chiral details influence diastereomer preference. This is a more direct strategy since it provides high yields of the desired phosphine diastereomer. Common auxiliaries are accessible alcohols, amines, or amino alcohols.[23] For instance, one of the most successful examples of utilization of the chiral auxiliary methodology are the MaxPHOS ligands (Figure 1.3).[30] Developed by Riera, Verdaguer *et al*. using a chiral aminophosphine the Rh-MaxPHOS complex showed excellent results in the asymmetric hydrogenation of a wide range of *E*- and *Z*- α-dehydroamino acid derivatives, β-ketoenamides, dimethyl itaconates and vinyl acetamides.[30, 31] Shortly after, the same group, developed the C_1-symmetric MAXPHOX ligands (Figure 1.3), that replaced one of the phosphine moieties by a oxazoline group.[32] The stereoselective synthesis of this family was aided by the use of *cis*-1-amino-2-indanol as chiral auxiliary. Furthermore, since the catalyst has three stereocenters originate from three separate chiral building blocks, it was easy to create a variety of ligands. Their Ir complexes were able to hydrogenate a broad range of challenging cyclic-β-enamides[33] and 2-aryl allyl phthalimides[34] obtaining outstanding enantioselectivities, outperforming the most successful Rh and Ru catalysts.

This methodology has also been extended to the synthesis of a diverse range of ligand families. For example, Stephan, Mohar *et al.* reported an analog of DIPAMP, named *t*-Bu-SMS-PHOS, which bear bulkier substituents in the alkoxy group of the functionalized aryl ring, using (-)-menthol as chiral auxiliary (Figure 1.3).[35] The rhodium complexes of several of these ligands have demonstrated marked ability to hydrogenate a wide range of di- and tri-substituted olefins and certain tetrasubstituted ones.[35] BIBOP[36] and BABIPHOS[37] ligands are also synthesized using a common intermediate achieved by the use of a chiral tosyl phenol (Figure 1.3). These P-stereogenic diphosphines showed very high enantioselectivity in the Rh-catalyzed asymmetric hydrogenation of α- and β-(acylamino)acrylic acids, as well for enamides.[36-37]

In recent years there have been several other ways to obtain enantiomerically pure phosphine ligands for subsequent use in asymmetric hydrogenation of chelating olefins, such as the resolution of racemic mixtures by chiral HPLC or via crystallization with a resolving agent and carbon or carbon-metal chiral templates.[23] One example of the utilization of the later technique is the Binapine ligands (Figure 1.3).[38] Zhang *et al.* prepared this ligand by taking advantage of the axially chiral (*S*)-2,2′-dimethylbinaphthyl template, which has shown success in the Rh-catalyzed asymmetric hydrogenation of typical *E*- and *Z*- β-dehydroamino acid derivatives as well as for more challenging tetrasubstituted cyclic enamides.[39]

From all these approaches, in Section 3.1 we prepared P-stereogenic *N*-phosphine-phosphite ligands by using the chiral auxiliar strategy since the obtained chiral P-

stereogenic phosphine containing ligands are usually less prone to oxidation than the ones from the stereoselective deprotonation. The novelty of the ligand design presented in Section 3.1 is that we use the chiral auxiliary both for preparing the P-stereogenic moiety and as a ligand backbone. The latter allows to reduce the number of synthetic steps. In addition, it facilitates the introduction of a biaryl phosphite moiety in the ligand which further increases the ligand stability as well as the electronic differentiation between both P-donor groups of the ligands.

1.1.2. Metal-catalyzed asymmetric hydrogenation of non-chelating olefins

1.1.2.1. Mechanism

The mechanism for the asymmetric hydrogenation of non-chelating olefins with Ir-catalysts has been investigated computationally and experimentally and several pathways have been proposed. The most accepted catalytic cycle proceeds via Ir(III)/Ir(V) intermediates as theoretically identified independently by Andersson and co-workers[40] and Burgess and co-workers[41] and later supported by NMR studies under hydrogenation conditions by Pfaltz's group (Scheme 1.3). [42] Andersson's DFT calculations agree with a migratory-insertion/reductive elimination cycle (3/5-MI) while Burgess studies involve a sigma-metathesis/reductive elimination pathway (3/5-Meta).

In the Pfaltz's study they were able to synthetize and characterize the elusive catalytically competent intermediates Ir-dihydride alkene complexes ($[Ir(H)_2(alkene)(L)]^+$).[42] Upon investigating the reactivity of these complexes, it was observed that an additional molecule of H_2 was required to facilitate the conversion of the catalyst bond-alkene into the hydrogenated product but no signals corresponding to a dihydride complex with an extra coordinated H_2 molecule were detected, thus indicating that these Ir-dihydride alkene complexes represent the resting state of the catalyst. This observation further supports the Ir(III)/Ir(V) mechanism via an $[Ir(H)_2(alkene)(H_2)(L)]^+$ intermediate. Additionally, they discovered that there are two dihydride-alkene intermediates in equilibrium through a dissociation/association process, resulting from an enantioface exchange of the coordinated olefin within the complexes. The configuration of the hydrogenated product aligns with the one that would typically correspond to the formation of the minor isomer. That suggests that the minor intermediate, which is less stable, is converted to the major product enantiomer, similar to the mechanism of the Rh-catalyzed asymmetric hydrogenation.[5]

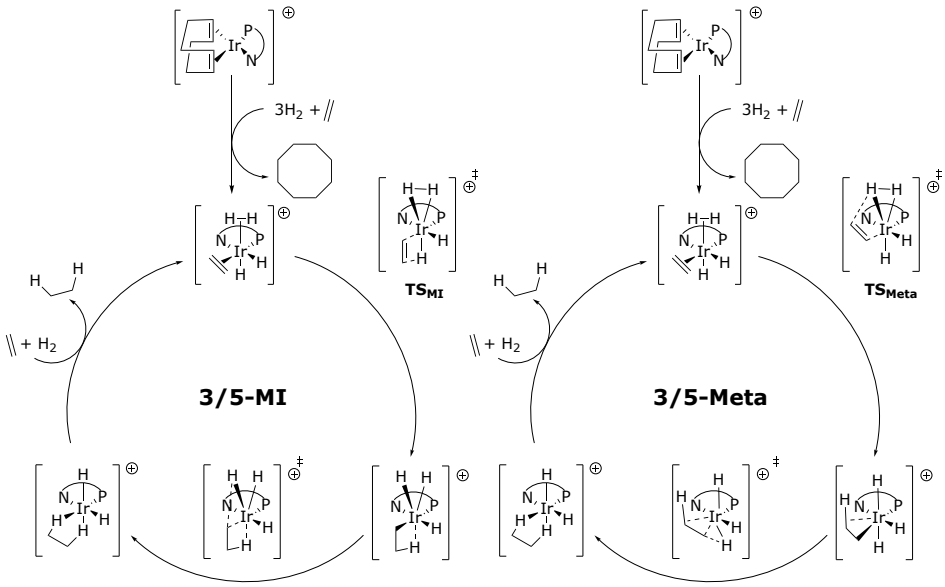

Scheme 1.3. Proposed catalytic cycles 3/5-MI and 3/5-Meta for asymmetric hydrogenation of non-chelating olefins.

1.1.2.2. Ligands.

In the 1970s, Crabtree *et al*. studied the catalytic performance in the alkene hydrogenation of metal complexes of the type $[M(cod)L_2]X$ (M=Rh or Ir; cod= 1,5-cyclooctadiene; L= phosphine ligand; X= Cl, BF_4 or PF_6). After careful ligand-screening experiments, they found that substituting one of the phosphine ligands in the Ir-catalyst with a pyridine ligand resulted in a substantial improvement in its catalytic performance. Thus, $[Ir(cod)(Py)(PCy_3)]PF_6$ catalytic precursor (Figure 1.4), so-called Crabtree's catalysts, demonstrates superior reactivity compared to the corresponding diphosphine catalyst. It exhibits enhanced performance in the efficient reduction of tri- and tetrasubstituted non-chelating olefins.[43]

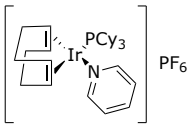

Figure 1.4. Crabtree's catalyst.

In 1997, Pfaltz *et al*. made a significant breakthrough in the field of hydrogenation of non-chelating olefins when they used phosphine-oxazoline ligands PHOX (Figure 1.5) to design $[Ir(cod)(PHOX)]PF_6$,[44] a chiral analogue of the Crabtree's catalyst. Despite its capability to achieve highly enantioselective hydrogenation of prochiral olefins, this catalyst exhibited instability under the given reaction conditions. Pfaltz *et al*. successfully resolved the problem by substituting the catalyst anion

hexafluorophosphate with a less coordinative anion, tetrakis[3,5-bis(trifluoromethyl)phenyl]borate ([3,5-$(F_3C)_2$-$(C_6H_3)_4B]^-$; BAr_F^-). The outcome of this modification was the [Ir(cod)(PHOX)]BAr_F an active, enantioselective and stable catalyst for hydrogenation of some non-chelating olefins. Despite this success, the applicability of this catalyst was mainly limited to *E*-trisubstituted olefins.[44,45]

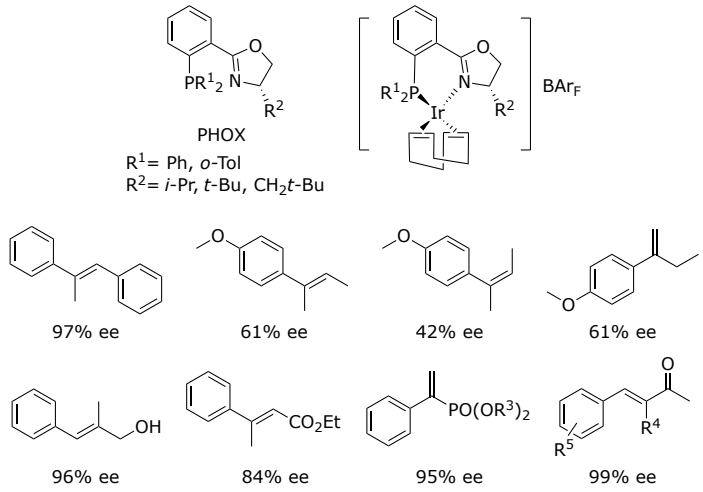

Figure 1.5. Selected Ir-hydrogenation results using PHOX ligands.

Since then, the research in this field has predominantly concentrated on the design and synthesis of new chiral P,N-ligands.[4] The composition of these P,N-ligands has been expanded by modifying the ligand backbone (replacing the phenyl backbone by an alkyl backbone chain or a bicycle, etc.) and also by substituting the phosphine moiety with a phosphinite, *N*-phosphine or carbene group (Figure 1.6). Furthermore, the oxazoline moiety has been replaced with other N-donor groups, such as pyridine, imidazole, thiazole, thiazoline and oxazole, or by O-donor group (Figure 1.6).[4,46] However, success in achieving high enantioselectivities in the reduction of non-chelating olefins was limited to trisubstituted olefins with *E*-geometry while their *Z*-isomers, as well as di- and tetra-substituted olefins, were hydrogenated with low enantioselectivities. The exception was the family of ligands **L2** (Figure 1.6), that have provided high enantioselectivities for some cyclic tetrasubstituted[47] and a broad range of acyclic olefins [48] mainly trimethyl styrene derivatives. However, **L2** provided low enantioselectivities for tri- and di-substituted olefins as well as tetrasubstituted olefins with poorly coordinative groups that are useful for further synthesis. Also to highlight is the family of ligands **L6** (Figure 1.6), that successfully reduced *E*-trisubstituted and some specific groups of acyclic tetrasubstituted olefins with poorly coordinative groups.[49] Finally, there is the family of phosphinite-pyridine ligands **L11**–**L12** (Figure 1.6), which successfully hydrogenated *E*- and *Z*-trisubstituted olefins but were not able to efficiently reduce di- and tetrasubstituted olefins.[50]

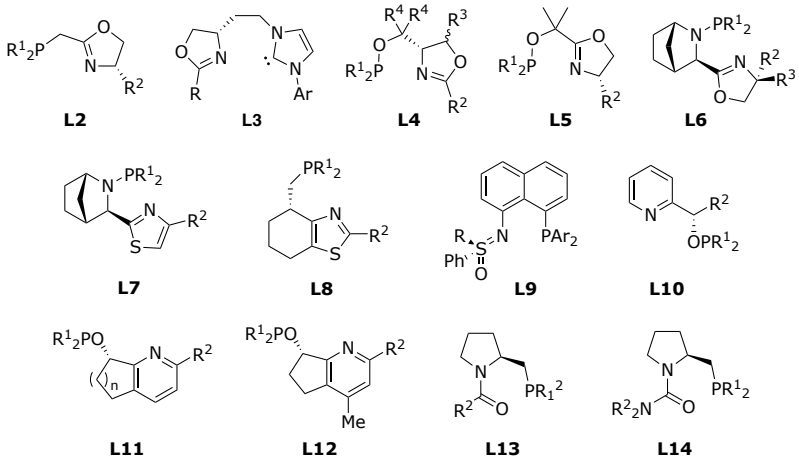

Figure 1.6. Representative ligands for the Ir-catalyzed hydrogenation of non-chelating olefins.

In 2005, our group started a research line to address this underdeveloped topic. We found that the introduction of a conformationally adaptable biaryl phosphite group in the catalyst enlarged the substrate scope (Figure 1.7). Surpassing previous results in the literature, Ir/phosphite-oxazoline catalysts were able to hydrogenate *E* and *Z*-trisubstituted and, for the first time, a wide range of unsolved 1,1'-disubstituted olefins.[4e, 51] Our mechanistic studies based on HP-NMR, deuterogenation and DFT calculations showed that the presence of the bulky and flexible biaryl phosphite group was responsible for this success. More recently, we also found that the oxazoline moiety can be replaced by more robust N-containing groups such as triazole and pyridine,[52] and also by non N-donor groups such as thioethers (Figure 1.7).[4e,53] The thioether moiety imparts higher stability with respect to commonly used oxazolines and involves the introduction of an additional chiral center close to the metal with a different steric environment around the metal center than that exerted by the oxazoline group. These findings allowed us to further expand the hydrogenation to di- and tri-substituted olefins with relevant poorly coordinative groups (e.g. vinyl boronates, α,β-unsaturated ketones, …). The relevance of the asymmetric hydrogenation of these substrates lies in the fact that high-value compounds can be produced more efficiently than with traditional non-asymmetric hydrogenation methods. In these recent developments, DFT calculations were crucial in identifying the key ligand parameters that maximized enantioselectivity. In addition, these studies revealed that the bulkiness of the phosphite moiety made our phosphite-based catalysts inefficient for the AH of tetrasubstituted olefins. This knowledge allowed us to work out new catalyst designs with the recent finding of an Ir-phosphinite,N family that is able to reduce non-chelating tetrasubstituted olefins (ligands **L18**,[54] Figure 1.7), however it provided low enantioselectivities for di- and trisubstituted olefins.

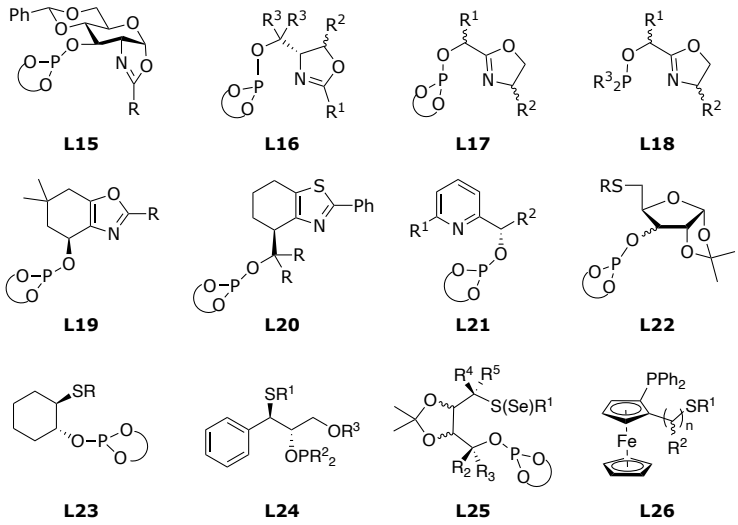

Figure 1.7. Selected ligands developed in our group for the asymmetric hydrogenation of non-chelating olefins.

Despite all the advances in the field, even for the most studied trisubstituted olefins there is still room for improvement. For example, the reduction of the so called purely alkyl-trisubstituted olefins, those without functional groups or aryl substituents, has been achieved in very few cases[50c,55] and the effectiveness for exocyclic substrates needs to be improved, since the hydrogenation of such substrates is highly influenced by the size of the substrate ring.[54,56] As we've seen, for tetrasubstituted olefins only a few specific Ir-catalysts have provided high performance for certain substrates, with variable enantioselectivity and low functional group tolerance. Most of the alkenes studied were restricted to cyclic olefins and only a few were acyclic, mainly trimethylstyrene derivatives,[47] until recently when Gosselin's group in collaboration with Bigler, Pfaltz and Denmark[48] presented the reduction of a wide range of acyclic olefins with two or more aryl substituents. In addition, there are fewer reports of tetrasubstituted olefins with poorly coordinative groups that are useful for further synthesis and, in most cases, the same catalyst was unsuccessful for tetrasubstituted olefins without a poorly coordinative group.[49h-i] Thus, the finding of a catalyst that could work on all of them is highly desirable to limit time-consuming catalyst design and avoid a variety of preparation methods. With this idea in mind, we focus this thesis on developing air stable, easy-to-synthetize and modular ligand libraries with the needs of the substrates under study. In this respect, we have synthesized a family of phosphine-triazole ligands, specially designed to solve the asymmetric hydrogenation of exocyclic benzofused based non-chelating alkenes (see Section 3.3). They are based on the phosphine-oxazolines PHOX in which a chiral carbon spacer has been added between the oxazoline and the phenyl ring to increase its flexibility. The oxazoline moiety has

also been replaced by a triazole with the aim to facilitate the stabilization of the substrate in the catalyst chiral pocket via N---H interactions. The ligand design has been completed by attaching a silyl group on the carbon spacer, according to the Pfaltz's first generation of phosphine-pyridine design, that showed a positive effect on catalytic performance of this silyl group due its interaction with the active site of the catalysts.[57] We also take advantage of the thioether moiety with a phosphite/phosphinite-thioether ligand library, synthetized in three steps from inexpensive indene, that was able to overcome the substrate specificity in the asymmetric hydrogenation with the successful reduction of a broad scope of olefins with a variety of coordination abilities, ranging from non-chelating olefins, through olefins with poorly coordinative groups to olefins with a coordinative functional group (see Section 3.4). Two carbene-thioether ligand families, designed with the aim to combine the advantages of thioether and N-heterocyclic carbene functionalities were also prepared (see Section 3.5 and 3.6). Finally, we find the first family of ligands, P-stereogenic aminophosphine-oxazolines, that is able to successfully reduce a broad range of di, tri- and tetrasubstituted olefins (see Section 3.2).

1.2. Pd-catalyzed asymmetric allylic substitution

Pd-catalyzed asymmetric allylic substitution has emerged as a highly effective synthetic strategy for the formation of stereoselective C-C, C-N, and C-O bonds in organic synthesis. In this process, a nucleophile (Nu; typically, a carbon or a nitrogen nucleophile) reacts, catalyzed by a chiral metal complex, with an allylic racemic substrate that contains a leaving group (LG; normally a malonate or acetate), that gives rise to new chiral C-C, C-N or C-O bonds (Scheme 1.4). This method offers several advantages, including mild reaction conditions, compatibility with diverse functional groups, and the resulting products can be further transformed by taking advantage of the alkene functionality. As a result, it has become a valuable approach for the synthesis of optically active compounds.[58]

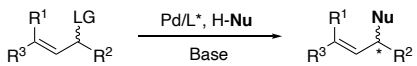

Scheme 1.4. Pd-catalyzed asymmetric allylic substitution reaction.

Over the last ten years, significant achievements have been realized in advancing highly efficient catalytic systems through the exploration of new iterations of ligands, catalysts, and reaction conditions.[59] As in the case of asymmetric hydrogenation, the design of catalysts heavily relies on structural insights, and the utilization of computational studies has grown significantly due to advancements in computational power and methodologies. This shift is moving away from the resource-intensive approach of trial-and-error-based discovery. Significant efforts have been dedicated to

expanding the range of substrates and nucleophiles, thus augmenting the potential applications for synthesizing increasingly complex organic molecules.

1.2.1. Substrate and nucleophile types

The catalyst performance depends fundamentally on the nature of the substrate.[58] Most of developed Pd-catalysts which are well suited for unhindered disubstituted substrates (both linear and cyclic) prove to be unsuitable for the alkylation of hindered disubstituted substrates or vice versa. In this context, extensive research into Pd-catalyzed allylic substitution has predominantly focused on diminishing the catalyst's reliance on specific substrates. Substantial research has also been made to enlarge the scope of substrates and nucleophiles, thereby increasing the possibilities for applications to the synthesis of more complex organic molecules.

The majority of the substrates fall into the category of activated allylic substrates, characterized by having easily reactive leaving groups, with acetates and carbonates being prevalent examples. The first type of activated substrates comprises 1,3-disubstituted allyl esters featuring identical substituents. These substrates yield symmetrical allyl intermediates, which are highly prevalent in Pd-catalyzed allylic substitution reactions. Notably, linear 1,3-diarylallyl esters are employed in this type of reactions, with rac-1,3-diphenylallyl acetate frequently being employed as a representative model substrate (Figure 1.8). This class of substrates holds the advantage that, unlike substrates with non-identical substituents, there are no concerns regarding regioselectivity (Figure 1.8).

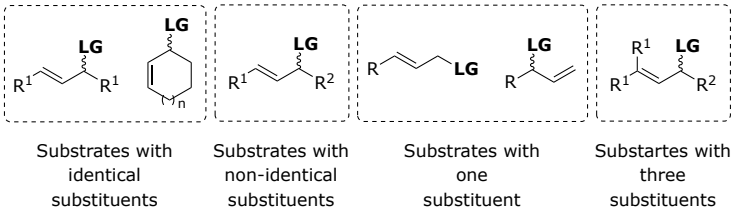

Figure 1.8. The most common substrates used in the enantioselective allylic substitution.

The second class of substrates is racemic 1,3-disubstituted substrates with different substituents on the allylic termini (Figure 1.8), which is a challenging class of substrates due to the added complexities of regiocontrol. Furthermore, the formation of two isomeric allyl intermediates, which cannot be converted through π−σ−π isomerization, adds to the challenge. Nevertheless, in certain instances, it has been observed that one of the potential products can be achieved with both regio- and enantioselectivity through either kinetic or dynamic kinetic resolution methods. Moreover, the inclusion of challenging monosubstituted substrates (Figure 1.8) introduces an additional hurdle: the potential formation of two regioisomers, the α- and γ-products, necessitating careful control of regioselectivity. Most Pd-catalysts exhibit a preference for generating linear

isomers, which can yield unintended achiral products unless a prochiral nucleophile is employed. While specific ligands have been documented to encourage the formation of branched products, their applicability remains somewhat restricted in comparison to catalysts built upon Ir and Mo (for stabilized carbon nucleophiles) as well as Cu (for non-stabilized carbon nucleophiles).[60] Lastly, trisubstituted substrates form another complex category (Figure 1.8). To summarize, a significant portion of these substrates bear two identical geminal substituents, allowing regioselectivity to be governed by steric hindrances that promote nucleophilic attack on the less substituted allylic carbon terminus.

Regarding the nucleophiles, dimethyl malonate has emerged as the conventional nucleophile for evaluating these processes. Nonetheless, various other carbon-stabilized nucleophiles containing functional groups such as carbonyl, sulfone, nitrile, or nitro groups have also been employed in a less extend.[58] Enantioselective reactions involving non-stabilized carbon-nucleophiles, such as diorganozinc or Grignard reagents, are relatively scarce and limited in number.[61] Amination and etherification reactions have also been the subject of extensive study. Various amines, including primary and secondary alkyl amines, aryl amines, and nitrogen heterocycles, have been commonly used as nucleophiles in these reactions. Benzylamine is often employed as a model N-nucleophile in these studies.[58d,58j] Efficient Pd-catalyzed allylic etherification has been achieved primarily in the presence of benzylic alcohols. However, aliphatic alcohols have been found to be ineffective nucleophiles in this reaction, limiting the scope of Pd-catalyzed asymmetric etherification. Consequently, the development of effective and selective Pd-catalyzed asymmetric etherification remains a significant challenge.[58l]

1.2.2. The mechanism

The established catalytic cycle involved for Pd-catalyzed asymmetric allylic substitution reactions with stabilized carbon nucleophiles and heteronucleophiles involves four main steps (Scheme 1.5). The initial step involves the coordination of the allylic substrate **E** *trans* to its leaving group, leading to olefin complex **G**. Subsequently, the cycle proceeds with the oxidative addition of complex **G** with dissociation of the leaving group, resulting in the formation of two equilibrating key Pd η^3-allyl intermediates **H** (identical for C_2-symmetric ligands) and, normally minor, *syn,anti* and *anti,anti* isomers, followed by nucleophilic attack to give unstable olefin complex **I**. The final step is the release of the substituted product **J** by dissociation and regeneration of the Pd catalyst.

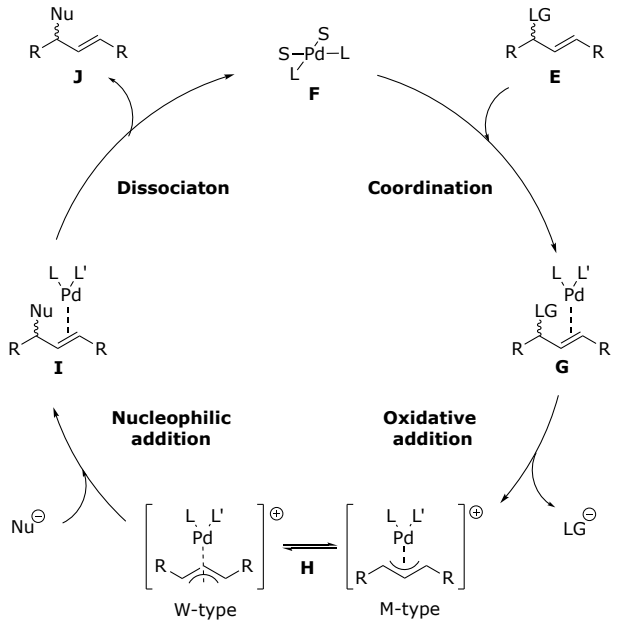

Scheme 1.5. Accepted mechanism for Pd-catalyzed asymmetric allylic substitutions.

For this process, the enantiodetermining step can be either the oxidative addition or the nucleophilic attack. For substrates with enantiotopic leaving groups (in geminal or 1,3-positions), the enantiodiscriminating step is the oxidative addition, whereas for substrates with identical substituents at the 1-and 3-positions, enantiodiscrimination occurs during nucleophilic attack at one of the diastereotopic sites (enantiotopic in the presence of achiral ligands). For other substrates, the relative rates of the different steps, including interconversion of isomeric allyl complexes, govern in which step the enantioselectivity is determined. Use of prochiral nucleophiles, finally, may also lead to enantiodiscrimination.[58]

The key Pd η^3-allyl intermediates can undergo isomerizations under the conditions of the catalytic reactions. One type of isomerization is apparent allyl rotation, that is, interconversion of M- and W-type isomers (Scheme 1.5). This process can proceed via a dissociative mechanism, or via intermediate η^1-complexes and rotation around the C−Pd bond.[1c] Another possible mechanism involves coordination of an external ligand to form a five-coordinated Pd complex, which undergoes pseudorotation.[62] Furthermore, for noncyclic substrates, *syn,syn*, *syn,anti* and *anti,anti* η^3-allyl complexes equilibrate via η^1-complexes, a process that changes the configuration at a terminal allyl carbon atom, but which does not change the relative positions of the allyl carbons and the ligands (Figure 1.9).

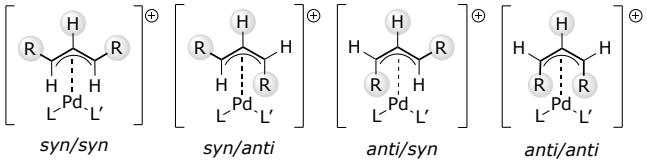

Figure 1.9. Possible isomers adopted by key Pd η³-allyl intermediates **H**.

Assuming similar reaction rates for all possible isomers, the formation of a single isomer is crucial to achieve high enantioselectivities in the reaction. Both the oxidative addition and nucleophilic attack steps occur with stereoselectivity, with an inversion of configuration. If the intermediate **H** remains unchanged in terms of its configuration without undergoing any isomerization, the overall process proceeds with retention of configuration; *i.e* the nucleophile is introduced on the same side of the allyl plane that was occupied by the leaving group.

1.2.3. Ligands

Initially, Pd-catalyzed allylic substitution reactions employed the chiral bidentate diphosphines ligands already developed for asymmetric hydrogenation. However, in contrast to their remarkable efficacy in asymmetric hydrogenation, only a limited number of these diphosphines yielded good enantioselectivities (e.g. 50% ee using BINAP). The low efficiency of these ligands was attributed to the fact that the enantiodiscriminating nucleophilic attack on the Pd-η^3-allyl intermediate occurs outside the coordination sphere. This external interaction made it challenging for the ligand to govern the stereochemical trajectory of the process.[58] New successful ligands appeared later and can be grouped into four main categories based on the underlying design principles.

The first strategy involves the use of secondary interactions of the nucleophile with the chiral ligand. This makes the latter capable to direct the nucleophilic attack towards one of the allylic terminal carbon atoms. For example, Hayashi and coworkers, designed ligand **L27**, which incorporates a side chain capable of directing the nucleophile towards one of the allylic terminal carbon atoms, thereby achieving significant levels of enantioinduction (81% ee, Figure 1.10).[63]

In the past decade, further examples of secondary interactions other than hydrogen bonding have been developed like electrostatic, coordinating and orbital interactions, that not only help the enantioselectivity but also the regioselectivity outcome.[64]

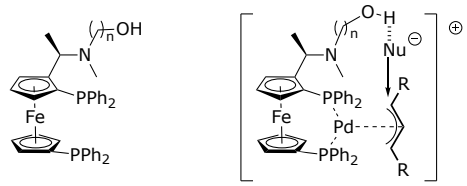

L27

Figure 1.10. Ferrocene-based phosphine ligand **L27**.

The second strategy involves the idea of increasing the ligand's bite angle by enlarging the chelate ring, thus creating a more confined chiral cavity, which interacts more strongly with the substituents of the allyl system and the nucleophile. This design concept was pioneered by Trost through the design of diphosphine ligands, like (*R,R*)-Ph-DACH (**L28**, Figure 1.11).[65] Ligands of this type represent one of the most effective ligand families for asymmetric allylic substitution, which has found widespread use in natural product synthesis. The fundamental concept aimed at enlarging the ligand's bite angle by expanding the chelate ring, thereby creating a more confined chiral pocket. The mechanistic model originally proposed to explain the enantioselectivity results from steric interactions with the four P-phenyl groups, constituting the chiral cavity, which block one of the allylic termini against nucleophilic attack (Figure 1.11). The model aligned with the observed absolute configuration of the products and also explain why substrates with small substituents exhibited high enantioselectivities and yields, while hindered substrates, which do not fit into the chiral cavity, such as 1,3-diphenylallyl acetate, reacted with low enantioselectivity.[65]

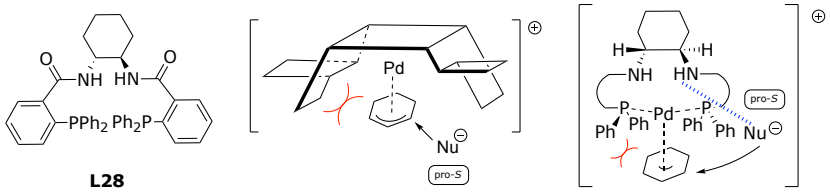

L28

Figure 1.11. Chiral pocket and secondary interactions of Trost ligand **L28**.

However, it was not clear why the sodium salt of diethyl malonate gave much lower ee than analogous tetraalkylammonium salts. A refined model, which rationalized the observed counterion effect and also provided a deeper insight into the relevant enantioselectivity-determining interactions, was reported in 2009 by Lloyd-Jones, Norrby, and co-workers. They conducted a combination of NMR spectroscopic studies, isotopic labeling and a DFT analysis that revealed the presence of a secondary interaction that directs the nucleophilic attack, similar to ligand **L27** (Figure 1.10).[66] This interaction is facilitated by a hydrogen bonding interaction between the enolate oxygen of the dimethyl malonate and the amide group of the ligand backbone. It guides the enolate carbon towards the proximal (pro-(*S*)) terminus of the η^3-carbon of the allyl

group with perfect selectivity. Therefore, the enantiocontrol achieved with Trost's ligand (**L28**) is not solely attributed to the chiral cavity provided by the ligand scaffold, but also to the interaction between the nucleophile and the ligand itself.

There is a third strategy of ligand-design, which neither form a chiral cavity around the metal center nor possess a functionalized side chain that can interact with the nucleophile, but still induce high enantioselectivity in allylic substitutions with symmetrically substituted allyl substrates. The regioselectivity of nucleophilic attack in this case results from interactions of the ligand with the allyl system, which influence the reactivity at the terminal carbon atoms. This phenomenon was observed with C_2-symmetric bisoxazolines, where comprehensive analyses including X-ray crystallography and NMR spectroscopy of their respective Pd-allyl complexes unveiled how repulsive steric interactions can distinctly heighten reactivity at one of the allylic termini by elongating one of the Pd−C bonds.[67] From the absolute configuration of the allylation product, which is formed with high ee, it can be inferred that the nucleophile preferentially attacks the longer, more strained Pd−C bond. The reactivity at the allylic termini can also be modulated by electronic interactions with the ligand, which are transmitted by the *trans* influence of the donor atoms coordinated to the metal center.[68] If the Pd atom is coordinated by two electronically different donor atoms, the allylic termini become electronically nonequivalent and, thus, are expected to exhibit different reactivity. On the basis of this concept, the phosphine-oxazoline PHOX ligands (Scheme 1.6), with a nitrogen and a phosphorus donor atom were developed in parallel by the groups of Helmchen, Pfaltz, and Williams.[58a] Analysis of X-ray data for allyl Pd-PHOX complexes unveiled a notable distinction: the Pd−C bond positioned opposite the P atom is visibly longer than the bond positioned opposite the N atom, implying heightened reactivity. Under usual reaction conditions, Pd allyl intermediates swiftly equilibrate between their *exo* and *endo* conformations (M- and W-type, Scheme 1.5). Through comprehensive NMR spectroscopic investigations, it was established that nucleophilic attack predominantly occurs on the more stable *exo* isomer, characterized by the elongated Pd−C bond *trans* to the P atom (Scheme 1.6).[58a]

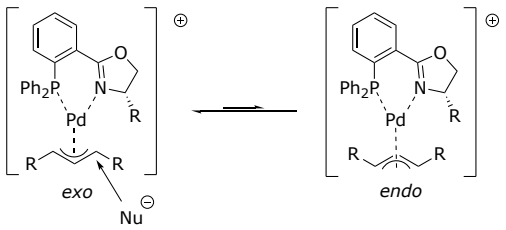

Scheme 1.6. Exemplification of the nucleophilic attack *trans* to the donor atom in Pd-allyl complexes with PHOX ligands.

Subsequently, many other heterodonor ligands, mainly P,N ligands (P = phosphine or phosphinite, N = oxazoline, pyridine, imidazole, etc.) have been developed.[58]

Although these ligands yield significant ee values in allylic substitutions involving highly sterically hindered substrates, the majority of them exhibit only moderate to low enantioselectivities when applied to substrates featuring small substituents on the allyl system. In this respect, the P,N ligands and the Trost diphosphine ligands have complementary scope.

A fourth strategy emerged from the search for ligands displaying wider substrate scope, focuses on conformational flexibility. Traditionally, chiral ligands were devised using conformationally rigid structural components, enabling easy prediction of steric interactions with substrates. Nonetheless, recent evidence has accumulated, suggesting that a certain level of flexibility can be advantageous in promoting enantioselectivity.[69]

The work of Moberg and coworkers with flexible phosphepine and azepine ligands **L29** and **L30** is an example (Figure 1.12).[70] By conducting a comprehensive investigation by NMR spectroscopy and DFT studies, they demonstrated that these ligands adapt their conformation to the structure of the substrate.[71] However, this self-adaptation mode proved to be less effective than desired because the conformational changes were slow in comparison with nucleophilic attack. Therefore, the flexible ligands behaved essentially as a mixture of the analogous rigid ligands.[72]

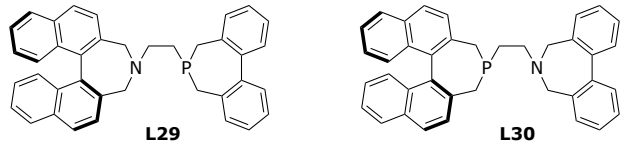

L29 **L30**

Figure 1.12. Flexible phosphepine and azepine ligands **L29** and **L30**.

An alternative method to create self-adaptable Pd-catalysts, which addresses the restricted substrate range of Pd-catalyzed allylic substitutions, involved integrating a flexible biaryl phosphite moiety into heterodonor P,N ligands.[58,73] The first examples of this approach were developed in our group, with ligands **L31** (Figure 1.13), in which the phosphine group of the PHOX ligands had been replaced by biaryl phosphite moieties. Pd complexes of these ligands proved to be very effective catalysts for reactions of both hindered and unhindered linear and cyclic substrates, outperforming Pd-PHOX catalysts, which give outstanding enantioselectivities with rac-(*E*)-1,3-diarylallyl substrates, moderate to good enantioselectivities with 1,3-dialkylallyl substrates but provide essentially racemic products with cyclic substrates.[74] Their wide substrate scope was rationalized by NMR spectroscopic and DFT studies of its Pd-η^2-olefin and Pd-η^3-allyl complexes, which results from their capacity to adjust the size of the binding pocket to the substrate type thanks to the flexibility of the biaryl phosphite moieties.[74]

Subsequently, a large variety of heterodonor biaryl phosphite-containing ligands, mainly belonging to the P,N (N= oxazoline, pyridine, oxazole, thiazole etc., Figure

1.13)[75] and more recently in our group we observed that the introduction of the thioether[76] moiety yields results comparable to the best reported in the literature (Figure 1.13). Pd complexes of these ligands proved to be very effective catalysts for reactions of both hindered, unhindered linear, monosubstituted and cyclic substrates, outperforming Pd-PHOX catalysts, yielding outstanding enantioselectivities overall.

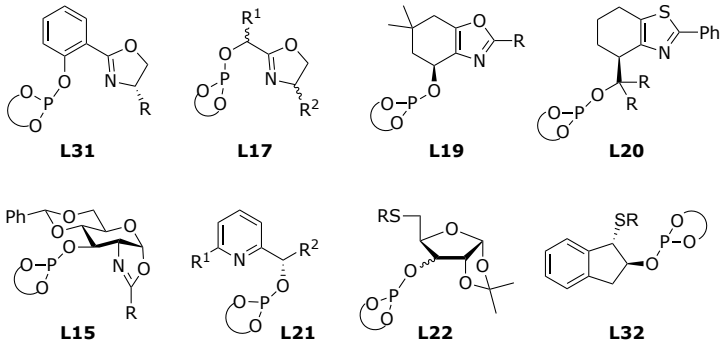

Figure 1.13. Representative phosphite-heterodonor ligands for the Pd-catalyzed allylic substitution reaction.

Following our interest in the use of air stable and easy-to-phosphite analogues of PHOX-type ligands for Pd-catalyzed allylic substitutions, in this thesis we present the application of solid and air stable phosphite-oxazoline family of ligands with a methylene spacer between the oxazoline ring and the phenyl ring of PHOX ligand which was synthetized in only 2 steps from readily available starting materials (see Section 4.1).

1.3. Pd-catalyzed allylic cycloaddition reaction

Chiral heterocyclic compounds are abundant in nature and have demonstrated considerable potential in various fields, including medicinal and crop protecting chemistry, materials science among many others.[77] Hence, significant research efforts to achieve the efficient construction of structurally diverse chiral heterocycles.[78] Metal-catalyzed dipolar cycloaddition reactions play a crucial role in organic synthesis, offering an efficient and convergent route to cyclic motifs, which are core motifs in numerous bioactive natural products and drugs.[79] In addition metal-catalyzed cycloadditions represents a highly attractive alternative to classical cycloaddition reactions, including the Diels-Alder reaction. Classical cycloaddition reactions are predominantly governed by orbital symmetry considerations, which can restrict the range of cyclic synthons accessible through those reactions. In recent decades, significant advancements have been made in the field by using a wide range of transition metal-stabilized heteroatom dipoles. These dipoles have been effectively employed in catalytic asymmetric cyclization reactions, enabling the construction of diverse chiral carbo- and heterocyclic scaffolds (Figure 1.14).[78]

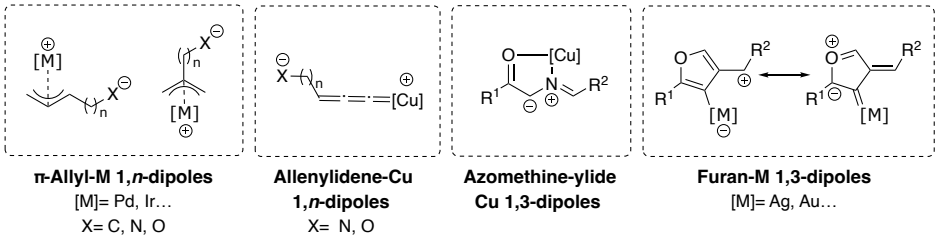

Figure 1.14. Examples of common transition metal stabilized heteroatom dipoles.

In this context, the Pd-catalyzed cycloaddition reactions via interceptive allylic substitution has become an extremely powerful and popular tool to achieve cyclic synthons.[80] Interestingly, the Pd-zwitterionic species can react through the terminal carbon (γ position) or the substituted carbon (α position), giving rise to different sized cycloadducts, which opens the opportunity to create (hetero)carbocycles with different ring sizes from the same reactants by proper tuning of the ligand and reaction conditions (Scheme 1.7).[80]

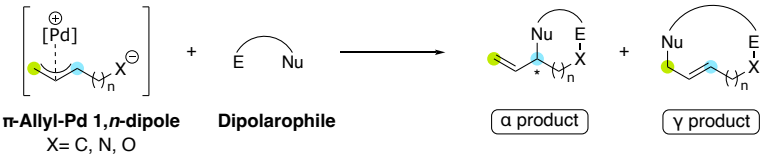

Scheme 1.7. Asymmetric Pd-catalyzed cycloaddition reactions via interceptive allylic substitution.

1.3.1. The mechanism

Although extensive research has been conducted in expanding the Pd-catalyzed cycloaddition reaction to novel combinations of dipoles and dipolarophiles, the efforts to stablish a concise mechanism have been rather scarce[81], being in most cases devoted to unravel the origin of regio- and stereoselectivity.[82] The general mechanism for the Pd-catalyzed cycloaddition reaction is shown in Scheme 1.8.[83] The initial step is the coordination of the 1,*n*-dipole precursor to the catalytic active species, which enters the cycle in the Pd(0) oxidation state. Subsequently, the cycle proceeds with the oxidative addition of the formed complex resulting in a π-allyl intermediate (via ring opening or leaving group elimination). Afterwards, in most reported cases, the reaction proceeds through a sequence where the metal-zwitterionic species initiates the process with a nucleophilic attack on the dipolarophile, followed by a subsequent nucleophilic attack of the dipolarophile on the metal-allyl fragment prompting the cyclization step (path A; Scheme 1.8). However, in recent years, there have been several successful examples where the dipolarophile behaves as a nucleophile in its initial interaction with the metal-zwitterionic species and then a subsequent nucleophilic attack of the metal-allyl fragment on the dipolarophile (path B; Scheme 1.8). As we've seen in previous sections,

after the nucleophilic attack and ring closing, an unstable Pd(0) olefin complex is generated, which rapidly undergoes dissociation, leading to the release of the cyclic adduct.

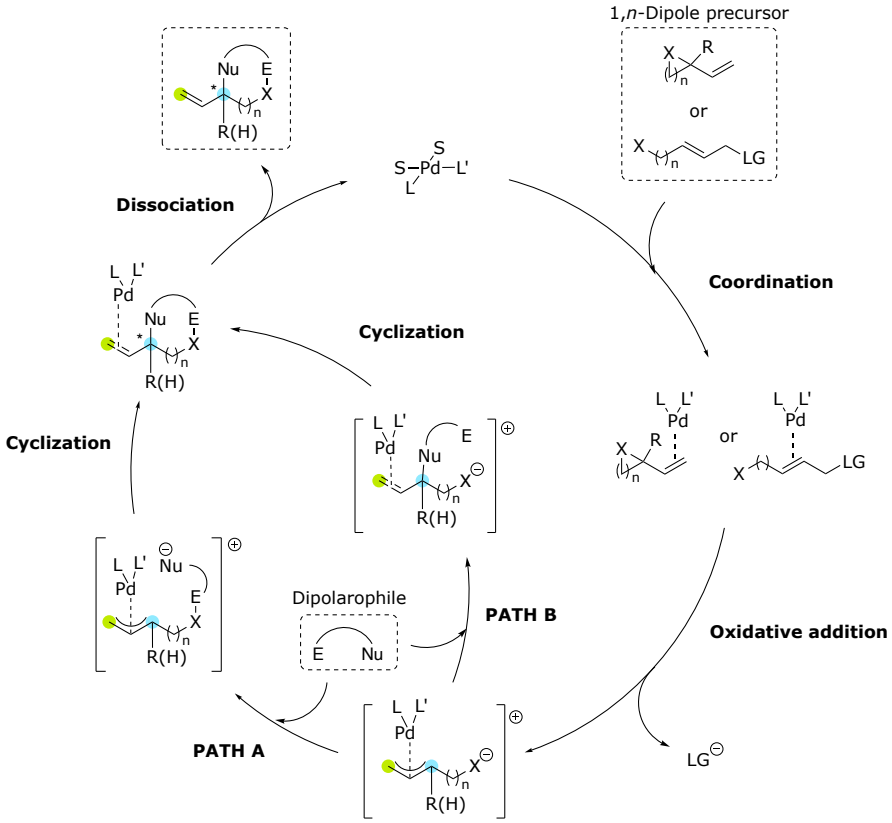

Scheme 1.8 Proposed mechanism pathways for the asymmetric metal-catalyzed cycloaddition reactions via interceptive allylic substitution.

Several experimentally and DFT guided mechanistic studies suggest that the rate-determining step can vary between the oxidative addition, the first nucleophilic addition or the ring closing step, depending on the dipole/dipolarophile used and reaction conditions (solvent, temperature, ligand…). Regarding the stereochemical aspects of the reaction, the ones that determine the enantio- and diastereoselectivity are the initial nucleophilic attack and the subsequent cyclization. However, in most cases, the initial nucleophilic attack is reversible, making the cyclization step the one that controls the stereochemistry of the reaction.[80,81b-c,84]

1.3.2. Previous work

The pioneering work in Pd-catalyzed cyclization reactions of metal-zwitterionic species came in the 1980s when Trost's research group developed Pd-trimethylenemethane (Pd-TMM), which is an all-carbon 1,3-dipole.[85] This category of dipolar reactions is characterized by the formation of exocyclic unsaturated bonds. As research in this field progressed rapidly more intricate dipole structures incorporating heteroatoms, extending carbon chains, or devising dipoles containing delocalized anions emerged, finding extensive utility (Figure 1.15).[80c,h]

Around the same time an alternate cycloaddition strategy emerged, pioneered by Tsuji and colleagues.[86] This approach involved the generation of a zwitterion *in situ* through the reaction of Pd with activated vinyl cyclopropanes (Figure 1.15). These reactions rely on the *in situ* formation of Pd-π-allyl 1,3- or 1,5-zwitterions through the reaction of Pd(0) species with vinyl three-membered rings and their analogs.[80,81] Subsequently, these zwitterions gained widespread utilization, marking a significant advancement in this since they have proven to be highly effective and atom-efficient methods for constructing diverse carbon- and heterocycles.

The discovery of new Pd-π-allyl zwitterions has enabled the construction of the diverse set of carbon- and heterocyclic compounds and improves the high potential of such transformation for the synthesis of highly complex organic molecules. The range of dipolarophiles has also grown over time therefore the scope includes activated alkenes as well as a wide range of unsaturated compounds (e.g. ketones, imines, aldehydes …). In addition, recent works have shown that dipolarophiles can be also generated by organo- and photocatalysis. [80,81c-d,87]

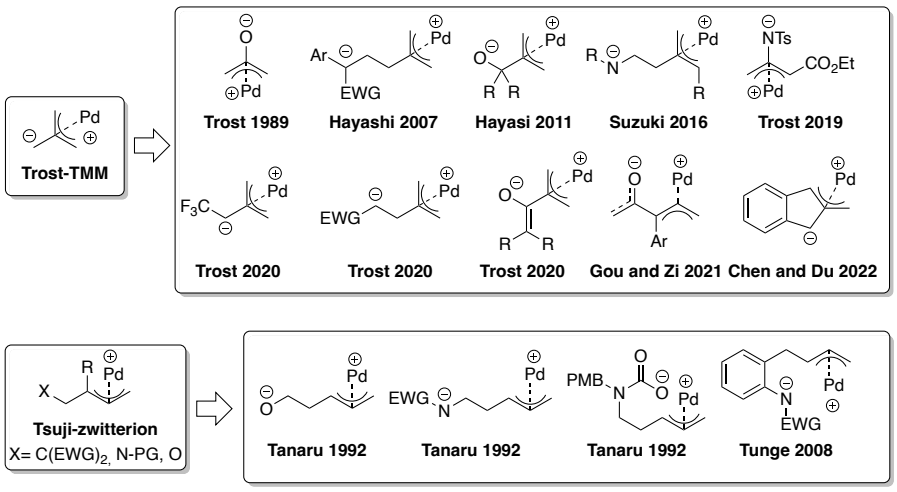

Figure 1.15. Representative Pd-π-allyl zwitterion developed over the years.

Following the main topic of Section 5.1 in this thesis, the following section compiles several recent and relevant [3+2] Pd-catalyzed cyclization reactions of metal-zwitterionic species to synthesize chiral tetrahydrofurans. Special attention will be paid to examples in which a chiral tetrahydrofuran-fused spirocyclic scaffolds are synthesized.

1.3.2.1. Synthesis of tetrahydrofurans via [3+2] Pd-catalyzed cyclization

One of the simplest ways to construct a furan ring via metal-catalyzed [3+2] cycloaddition is the reaction of either vinyl epoxides or vinylethylene carbonates, with electron-deficient olefins.[88] Thus, for instance, Ding, Peng, Hou and coworkers disclosed the Pd-catalyzed [3+2] cycloaddition of a range of vinyl epoxides with several linear α,β-unsaturated enones (Scheme 1.9a).[89] The use of Pd/(*R*)-BINAP catalyst gave the cycloaddition products in high yields, diastereo- and enantioselectivities (up to 99:1 dr and up to 99% ee; Scheme 1.9). Nevertheless, long reaction times (typically 5 days) are required to full conversions due to less activated nature of the enones. More recently and following a similar methodology the enones have been replaced by more reactive β-disubstituted keto enol esters to yield tetrahydrofuran acetals.[90]

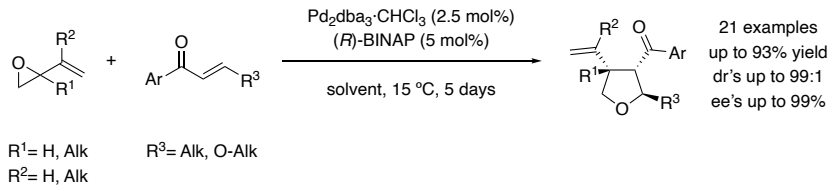

Scheme 1.9. Pd catalyzed [3+2] cycloaddition of vinyl epoxides with linear α,β-disubstituted enones.

Another Michael acceptor that has been widely used is nitroalkenes. Thus, for instance, Zhang and coworkers reported the decarboxylative [3+2] cycloaddition of vinylethylene carbonates to monoactivated β-nitroolefins.[91] The presence of the chiral squaramide **OC1** activates the nitroolefins by means of hydrogen bonding and, at the same time, has a synergistic effect with the chiral Pd-catalyst on the stereochemical outcome of the reaction (Scheme 1.10). Interestingly, Hou and coworkers reported a similar synthesis of nitrotetrahydrofurans in high diastereo- and enantioselectivities, without the use of an external organocatalyst.[92]

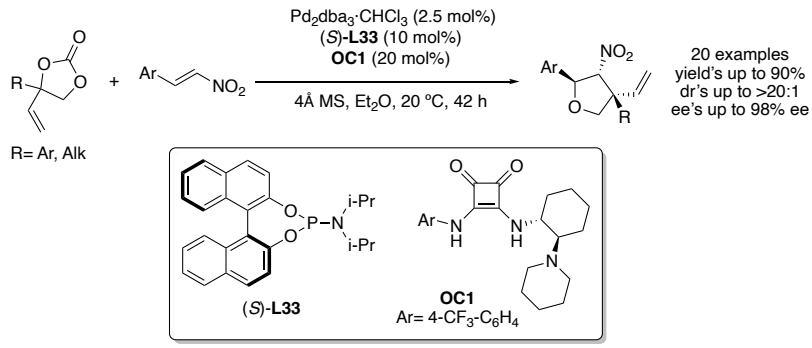

Scheme 1.10. Dual organocatalysis and Pd-catalyzed [3+2] cycloaddition of vinylethylene carbonates with linear β-nitroolefins.

The use of doubly activated Michael acceptors has also been widely explored. Thus, for instance, You and coworkers reported the Pd-catalyzed dearomative [3+2] cycloaddition of several vinyl epoxides with a range of nitro-benzofurans (Scheme 1.11).[88b] More recently, this methodology has been used in the cyclization of nitrobenzothiophenes,[88b] nitroindoles,[93] 3-cyanochromanones,[94] 2-nitroacrylates,[95] α-*N*-heterocyclic acrylates[96] among others.

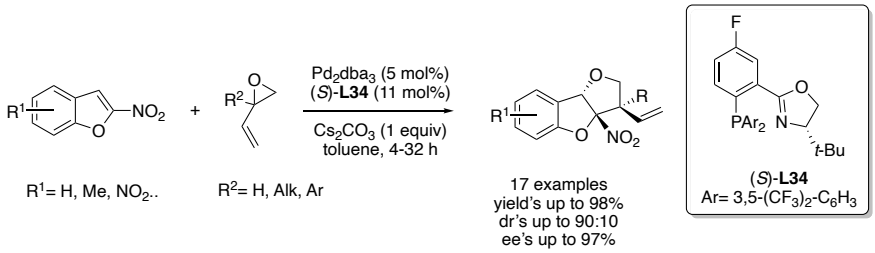

Scheme 1.11. Synthesis of tetrahydrofurobenzofurans via Pd-catalyzed dearomative [3+2] cycloaddition.

Less typical Michael acceptors that have been recently used include α-allenamides[97] and *gem*-difluoroalkenes[98]. Whereas the former gave rise to alkylidene derived tetrahydrofurans, the later produced 2,2-difluorotetrahydrofurans in high diastereo- and enantioselectivities for both set of compounds.

Another important class of compounds that has been synthesized via Pd-catalyzed [3+2] cycloaddition reaction is tetrahydrofuran-fused spirocyclic compounds. Nevertheless, despite the growing interest of chiral spirocyclic compounds in medicinal chemistry,[99] there are very few reports on the synthesis of such compounds over the last years.

Zhao and coworkers in 2016 studied the formal [3+2] cycloaddition of *para*-quinone methides with vinyl epoxides or cyclopropanes using PHOX-based ligand (S,S_P)-**L35**

(Scheme 1.12). The sequential 1,6-addition and cyclization gave rise to a diverse array of spiro[4.5]decanes in high diastereo- and enantioselectivities (up to >20:1 dr and up to >99% ee's).[100]

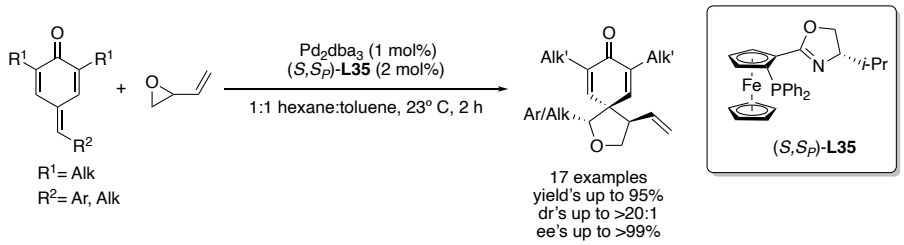

Scheme 1.12. Pd-catalyzed [3+2] cycloaddition of vinyl oxirane with *para*-quinone methides.

Yang and coworkers approached the synthesis of spirofused-tetrahydrofurans differently, using activated vinyl cyclopropanes as dipole precursor with a carbonyl moiety as dipolarophile (Scheme 1.13). Thus, one example of bispirooxindole cycloadduct was prepared via [3+2] cycloaddition of spirovinyl-cyclopropyl oxindole with 1-benzylindoline-2,3-dione using Pd/(*S,S,S*)-**L51** catalytic system. However, low yield and good diastereo- and enantioselectivity were obtained (up to 5:1 dr and up to 71% ee's).[101]

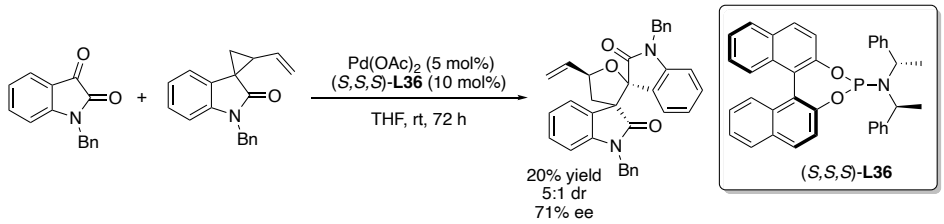

Scheme 1.13. Pd-catalyzed [3+2] cycloaddition of spirovinylcyclopropyl oxindole with 1-benzylindoline-2,3-dione.

In 2020, Hu and coworkers developed the synthesis of spirooxindoles through a decarboxylative [3+2] cycloaddition of vinylethylene carbonates with methylene indolinenones (Scheme 1.14).[102] After reaction optimization, high diastereo- and enantioselectivities were achieved (up to >20:1 dr and up to 99% ee) using DuPhos as the optimal ligand.

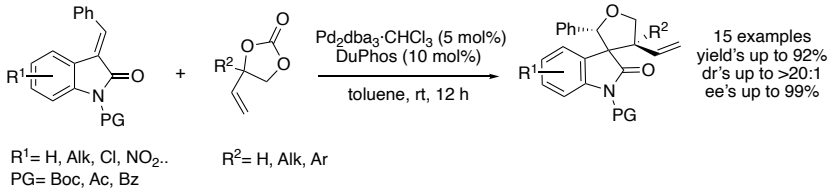

Scheme 1.14. Pd-catalyzed [3+2] cycloaddition of vinylethylene carbonates with methylene indolinenones.

Shortly after, Guo and coworkers presented in a similar manner an efficient synthesis of spirofused tetrahydrofurans with 1,3-indandiones (Scheme 1.15).[103] Thus, the decarboxylative cycloaddition of vinylethylene carbonate derivatives with several benzylidene 1,3-indandiones employing phosphoromidite ligand (*R,S,S)*-**L37** led to high diastereo- and enantioselectivities (up to 4:1 dr and up to 99% ee).

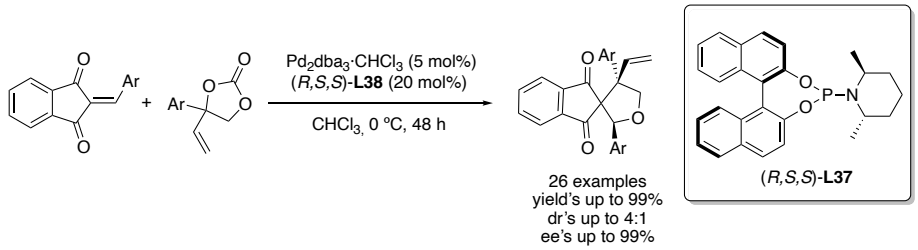

Scheme 1.15. Pd-catalyzed [3+2] decarboxylative cycloaddition of vinylethylene carbonate with benzylidene 1,3-indandiones.

More recently in 2022, Lee and coworkers reported the stereodivergent synthesis of spiro-furanoindolines via the Pd-catalyzed cycloaddition of vinylethylene carbonate with indolinone-based azadienes (Scheme 1.16).[104] More interestingly, by careful selection of the ligand, access to all four stereoisomers of the cyclic product was possible. For example, by using PHOX-based ligand (*S*)-**L38** the reaction yielded "*cis*" diastereomer in good diastereoselectivity and high enantioselectivity (up to 6:1 dr and up to 99% ee, Scheme 1.16a). On the other hand, when using diphosphine ligand (*R*)-**L39** the reaction yielded the opposite diastereomer in high diastereo- and enantioselectivity (up to 15:1 dr and up to 99% ee, Scheme 1.16b). Furthermore, when using the inverse configuration on both ligands the reaction provided the opposite enantiomers of each diastereoisomer in both cases.

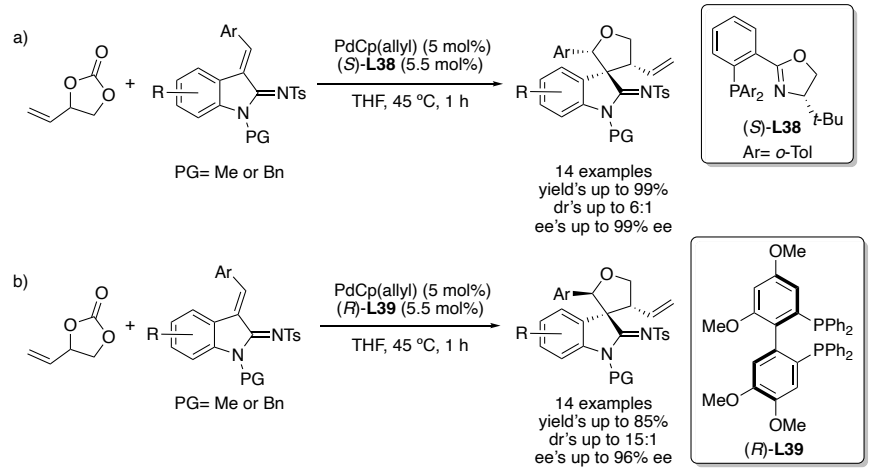

Scheme 1.16. Pd-catalyzed [3+2] decarboxylative cycloaddition of vinylethylene carbonate with indole-based azadienes.

As stated earlier, despite all the advancements made in this field, the synthesis of tetrahydrofuran-fused spirocyclic scaffolds via asymmetric Pd-catalyzed [3+2] cyclization is still underdeveloped. Encourage by the fact that this transformation offers an efficient pathway to annulated complexes in a single step with the possibility to simultaneously construct multiple stereogenic centers, in this thesis we investigate the cycloaddition of 2-substituted vinyl epoxides and 5-substituted Meldrum's acid derivatives as novel reaction partners combination for the synthesis of spirocyclic tetrahydrofurans (see Section 5.1).

1.4. References

[1] (a) Blaser, H. U.; Federsel, H.–J., Eds. *Asymmetric Catalysis on Industrial Scale: Challenges, Approaches and Solutions*, 2nd ed.; Wiley–VCH: Weinheim, **2010**. (b) Ojima, I., Ed. *Catalytic Asymmetric Synthesis*; 3rd ed.; John Wiley & Sons, Inc.: Hoboken, **2010**. (c) Jacobsen, E. N.; Pfaltz, A.; Yamamoto, H., Eds. *Comprehensive Asymmetric Catalysis*; Springer–Verlag: Berlin, **1999**. (d) Noyori, R., Ed. *Asymmetric Catalysis in Organic Synthesis*; Wiley: New York, **1994**. (e) Cornils, B.; Hermann, W. A., Eds. *Applied Homogeneous Catalysis with Organometallic Compounds*, 2nd ed.; Wiley–VCH: Wienhein, **2002**. (f) de Vries, J. G.; Elsevier, C. J., Eds. *Handbook of Homogeneous Hydrogenation*; Wiley–VCH: Weinheim, **2007**. (g) Akiyama, T.; Ojima, I., Eds. *Catalytic Asymmetric Synthesis*, 4th Ed; John Wiley & Sons, Inc.: Hoboken, **2022**. (h) Busacca, C. A.; Fandrick, D. R.; Song, J. J.; Senanayake, C. H. The Growing Impact of Catalysis in the Pharmaceutical Industry. *Adv. Synth. Catal.* **2011**, *353*, 1825–1864. (i) Ager, D. J.; de Vries, A. H. M.; de Vries, J. G. Asymmetric Homogeneous Hydrogenations at Scale. *Chem. Soc. Rev*. **2012**, *41*, 3340–3380. (j) Diéguez, M.; Pizzano, A., Eds. *Metal–Catalyzed Asymmetric Hydrogenation. Evolution and Prospect* in Advances in Catalysis; Elsevier: Oxford, Vol. 68, **2021**. (k) Biosca, M.; Diéguez, M.; Zanotti–Gerosa, A. Asymmetric Hydrogenation in Industry. *Adv. Catal.* **2021**, *68*, 341–384. (l) Catalysis from A to Z: A Concise Encyclopedia, 5th ed; Cornils, B.,Herrmann, W. A., Xu, J.-H., Zanthoff, H.-W., Eds.; Wiley-VCH:Weinheim, **2019**.

[2] American Chemical Society. 12 Principles of Green Chemistry. https://www.acs.org/greenchemistry/principles/12-principles-of-green-chemistry.html accessed 2023-08-28.

[3] See for example: (a) Genet, J. P. *In Modern Reduction Methods*; Andersson, P. G., Munslow, I. J., Eds; Wiley-VCH, Weinheim, **2008**, pp 3–38. (b) Tang, W.; Zhang, X. New Chiral Phosphorus Ligands for Enantioselective Hydrogenation. *Chem. Rev.* **2003**, *103*, 3029–3069. (c) Chi, Y.; Tang, W.; Zhang, X. In *Modern Rhodium-Catalyzed Organic Reactions*; Evans, P. A., Ed; Wiley-VCH: Weinheim, **2005**, pp 1–31. (d) Kitamura, M., Noyori, R. in *Ruthenium in Organic Synthesis*; Murahashi, S.-I., Ed.; Wiley-VCH: Weinheim, **2004**, pp 3–52. (e) Weiner, B.; Szymanski, W.; Janssen, D. B.; Minnaard, A. J.; Feringa, B. L. Recent Advances in the Catalytic Asymmetric Synthesis of Beta-amino Acids. *Chem. Soc. Rev.* **2010**, *39*, 1656–1691. (f) Xie, J.-H.; Zhu, S.-F.; Zhou, Q.-L. Transition Metal-Catalyzed Enantioselective Hydrogenation of Enamines and Imines. *Chem. Rev.* **2011**, *111*, 1713–1760. (g) Etayo, P.; Vidal-Ferran, A. Rhodium-Catalyzed Asymmetric Hydrogenation as a Valuable Synthetic Tool for the Preparation of Chiral Drugs. *Chem. Soc. Rev.* **2013**, *42*, 728–754. (h) Pizzano, A. Asymmetric Hydrogenation of Functionalized Olefins. *Adv. Catal.* **2021**, *68*, 1–134. (i) Kim, A. N.; Stoltz, B. M. Recent Advances in Homogeneous Catalysts for the Asymmetric Hydrogenation of Heteroarenes. *ACS Catal.* **2020**, *10*, 13834–13851. (j) Cabré, A.; Verdaguer, X.;

Riera, A. Recent Advances in the Enantioselective Synthesis of Chiral Amines via Transition Metal-Catalyzed Asymmetric Hydrogenation. *Chem. Rev.* **2022**, *122*, 269–339. (k) Zhang, Z.; Butt, N. A.; Zhang, W. Asymmetric Hydrogenation of Nonaromatic Cyclic Substrates. *Chem. Rev.* **2016**, *16*, 14769–14827. (l) Pfaltz, A.; Drury III, W.J. Design of Chiral Ligands for Asymmetric Catalysis: From C_2-symmetric P,P- and N,N-Ligands to Sterically and Electronically Nonsymmetrical P,N-Ligands. *PNAS* **2004**, *101*, 5723-5726. (m).Yoon, T.P.; Jacobsen, E.N. Privileged Chiral Catalysts. *Science* **2003**, *299*, 1691-1693. (n) Sommer, W.; Weibel, D. Asymmetric Catalysis, Privileged Ligands and Complexes. *Sigma Aldrich's Chemfiles* **2008**, 1-91. (o) Zhou, Q.-L. *Privileged Chiral Ligands and Catalysts*; Wiley-VCH, Weinheim, **2011**. (p) Chiral Ligands. Evolution of Ligand Libraries for Asymmetric Catalysis; Dieguez, M., Ed.; CRC Press, **2021**. (q) Margalef, J.; Biosca, M.; De La Cruz-Sánchez, P.; Faiges, J.; Pàmies, O.; Diéguez, M. Evolution in Heterodonor P-N, P-S and P-O Chiral Ligands for Preparing Efficient Catalysts for Asymmetric Catalysis. From Design to Applications and references therein. *Coord. Chem. Rev*. **2021**, *446*, 214120-214205.

[4] (a) Cui, X.; Burgess, K. Catalytic Homogeneous Asymmetric Hydrogenations of Largely Unfunctionalized Alkenes. *Chem. Rev.* **2005**, *105*, 3272–3296. (b) Roseblade, S. J.; Pfaltz, A. Iridium-Catalyzed Asymmetric Hydrogenation of Olefins. *Acc. Chem. Res.* **2007**, *40*, 1402–1411. (c) Woodmansee, D. H.; Pfaltz, A. Asymmetric Hydrogenation of Alkenes Lacking Coordinating Groups. *Chem. Commun.* **2011**, *47*, 7912–7916. (d) Zhu, Y.; Burgess, K. Filling Gaps in Asymmetric Hydrogenation Methods for Acyclic Stereocontrol: Application to Chirons for Polyketide-Derived Natural Products. *Acc. Chem. Res.* **2012**, *45*, 1623–1636. (e) Verendel, J. J.; Pàmies, O.; Diéguez, M.; Andersson, P. G. Asymmetric Hydrogenation of Olefins Using Chiral Crabtree-type Catalysts: Scope and Limitations. *Chem. Rev.* **2014**, *114*, 2130–2169. (f) Margarita, C.; Andersson, P. G. Evolution and Prospects of the Asymmetric Hydrogenation of Unfunctionalized Olefins. *J. Am. Chem. Soc.* **2017**, *139*, 1346–1356. (g) Pàmies, O.; Zheng, J.; Faiges, J.; Andersson, P. G. Asymmetric Hydrogenation of Unfunctionalized Olefins or with Poorly Coordinative groups. *Adv. Catal.* **2021**, *68*, 135–203. For specific examples of application of P,O and P,S-ligands in the Ir-catalyzed asymmetric hydrogenation see: (h) Margalef, J.; Pàmies,O. ; Pericas, M. A.; Diéguez, M. Evolution of Phosphorus-Thioether Ligands for Asymmetric Catalysis, *Chem. Comm*. **2020**, *56*, 10795–10808, (i) Rageot, D.; Woodmansee, D. H.; Pugin, B.; Pfaltz, A. Proline-Based P,O Ligand/Iridium Complexes as Highly Selective Catalysts: Asymmetric Hydrogenation of Trisubstituted Alkenes. *Angew. Chem*. Int. Ed. **2011**, *50*, 9598–9601.

[5] (a) Halpern, J.; Riley, D. P.; Chan, A. S. C.; Pluth, J. J. Novel Coordination Chemistry and Catalytic Properties of Cationic 1,2-Bis(diphenylphosphino)ethanerhodium(I) Complexes. *J. Am. Chem. Soc.* **1977**, *99*, 8055-8057. (b) Chan, A. S. C.; Pluth, J. J.; Halpern, J. Identification of the Enantioselective Step in the Asymmetric Catalytic Hydrogenation of a Prochiral Olefin. *J. Am. Chem. Soc.* **1980**, *102*, 5952-5954. (c) Wilczynski, R.; Fordyce, W. A.; Halpern, J. Coordination Chemistry and Catalytic Properties of Hydrido(phosphine)ruthenate Complexes. *J. Am. Chem. Soc.* **1983**, *105*, 2066-2068. (d) Brown, J. M. Tilden Lecture. Selectivity and Mechanism in Catalytic Asymmetric Synthesis. *Chem. Soc. Rev.* **1993**, *22*, 25-41. (e) Giovannetti, J. S.; Kelly, C. M.; Landis, C. R. Molecular Mechanics and NOE Investigations of the Solution Structures of Intermediates in the [Rhodium(chiral bisphosphine)]+-Catalyzed Hydrogenation of Prochiral Enamides. *J. Am. Chem. Soc.* **1993**, *115*, 4040-4057. (f) Kimmich, B. F. M.; Somsook, E.; Landis, C. R. Oxidative Addition of Dihydrogen to [Ir(bisphosphine)(1,5-cyclooctadiene)]BF_4 Complexes: Kinetic and Thermodynamic Selectivity. *J. Am. Chem. Soc.* **1998**, *120*, 10115-10125. (g) Landis, C. R.; Brauch, T. W. Probing the Nature of H_2 Activation in Catalytic Asymmetric Hydrogenation. *Inorg. Chim. Acta* **1998**, *270*, 285-297. (h) Landis, C. R.; Hilfenhaus, P.; Feldgus, S. Structures and Reaction Pathways

in Rhodium(I)-Catalyzed Hydrogenation of Enamides: A Model DFT Study. *J. Am. Chem. Soc.* **1999**, *121*, 8741-8754. (i) Feldgus, S.; Landis, C. R. Large-Scale Computational Modeling of $[Rh(DuPHOS)]^+$-Catalyzed Hydrogenation of Prochiral Enamides: Reaction Pathways and the Origin of Enantioselection. *J. Am. Chem. Soc.* **2000**, *122*, 12714-12727. (j) Landis, C. R.; Feldgus, S. A Simple Model for the Origin of Enantioselection and the Anti "Lock-and-Key" Motif in Asymmetric Hydrogenation of Enamides as Catalyzed by Chiral Diphosphine Complexes of Rh(I). *Angew. Chem. Int. Ed.* **2000**, *39*, 2863-2866. (k) Feldgus, S.; Landis, C. R. Origin of Enantioreversal in the Rhodium-Catalyzed Asymmetric Hydrogenation of Prochiral Enamides and the Effect of the α-Substituent. *Organometallics* **2001**, *20*, 2374-2386.

[6] (a) Fernández-Pérez, H.; Donald, S. M. A.; Munslow, I. J.; Benet-Buchholz, J.; Maseras, F.; Vidal-Ferran, A. Highly Modular P-OP Ligands for Asymmetric Hydrogenation: Synthesis, Catalytic Activity, and Mechanism. *Chem. Eur. J.* **2010**, *16*, 6495-6508. (b) Deerenberg, S.; Kamer, P. C. J.; van Leeuwen, P. W. N. M. New Chiral Phosphine−Phosphite Ligands in the Enantioselective Rhodium-Catalyzed Hydroformylation of Styrene. *Organometallics* **2000**, *19*, 2065-2072. (c) Pàmies, O.; Diéguez, M.; Net, G.; Ruiz, A.; Claver, C. Synthesis and Coordination Chemistry of Novel Chiral P,S-Ligands with a Xylofuranose Backbone: Use in Asymmetric Hydroformylation and Hydrogenation. *Organometallics* **2000**, *19*, 1488-1496.

[7] However, more recent mechanistic studies made with electron-rich diphosphines showed that the major/minor concept is unlikely to be universal acceptable. See: Gridnev, I. D.; Imamoto, T. Challenging the Major/Minor Concept in Rh-Catalyzed Asymmetric Hydrogenation. *ACS Catal.* **2015**, *5*, 2911-2915.

[8] Osborn, J. A.; Jardine, F. H.; Young, J. F.; Wilkinson, G. The Preparation and Properties of Tris(triphenylphosphine)halogenorhodium(I) and Some Reactions Thereof Including Catalytic Homogeneous Hydrogenation of Olefins and Acetylenes and their Derivatives *J. Chem. Soc. A* **1966**, 1711-1732.

[9] Knowles, W. S.; Sabacky, M. J. Catalytic Asymmetric Hydrogenation Employing a Soluble, Optically Active, Rhodium Complex**.** *Chem. Commun.* **1968**, 1445-1446.

[10] Horner, L.; Siegel, H.; Büthe, H. Asymmetric Catalytic Hydrogenation with an Optically Active Phosphinerhodium Complex in Homogeneous Solution**.** *Angew. Chem. Int. Ed.* **1968**, *7*, 942-942.

[11] Kagan, H. B.; Dang Tuan, P. Asymmetric Catalytic Reduction with Transition Metal Complexes. I. Catalytic System of Rhodium(I) with (-)-2,3-0-Isopropylidene-2,3-dihydroxy-1,4-bis(diphenylphosphino)butane, a New Chiral Diphosphine**.** *J. Am. Chem. Soc.* **1972**, *94*, 6429-6433.

[12] Knowles, W. S.; Sabacky, M. J.; Vineyard, B. D. Catalytic asymmetric hydrogenation. *J. Chem. Soc., Chem. Commun.* **1972**, 10-11.

[13] Knowles, W. S. Application of Organometallic Catalysis to the Commercial Production of L-DOPA. *J. Chem. Educ.* **1986**, *63*, 222-222.

[14] Knowles, W. S. Asymmetric Hydrogenations (Nobel Lecture). *Angew. Chem. Int. Ed.* **2002**, *41*, 1998-2007.

[15] Noyori, R. Asymmetric Catalysis: Science and Opportunities (Nobel Lecture). *Angew. Chem. Int. Ed.* **2002**, *48*, 2008-2022.

[16] Heller, D.; Holz, J.; Drexler, H.-J.; Lang, J.; Drauz, K.; Krimmer, H.-P.; Börner, A. Pressure Dependent Highly Enantioselective Hydrogenation of Unsaturated β-Amino Acid Precursors. *J. Org. Chem.* **2001**, *66*, 6816-6817.

[17] Zhu, G.; Chen, Z.; Zhang, X. Highly Efficient Asymmetric Synthesis of β-Amino Acid Derivatives via Rhodium-Catalyzed Hydrogenation of β-(Acylamino)acrylates. *J. Org. Chem.* **1999**, *64*, 6907-6910.

[18] Tang, W.; Chi, Y.; Zhang, X. An *ortho*-Substituted BIPHEP Ligand and Its Applications in Rh-Catalyzed Hydrogenation of Cyclic Enamides. *Org. Lett.* **2002**, *4*, 1695-1698.

[19] Lee, S.-G.; Zhang, Y. J. Rh(I)-Catalyzed Enantioselective Hydrogenation of (*E*)- and (*Z*)-β-(Acylamino)acrylates Using 1,4-Bisphosphine Ligands under Mild Conditions. *Org. Lett.* **2002**, *4*, 2429-2431.

[20] (a) Hansen, K. B.; Hsiao, Y.; Xu, F.; Rivera, N.; Clausen, A.; Kubryk, M.; Krska, S.; Rosner, T.; Simmons, B.; Balsells, J.; Ikemoto, N.; Sun, Y.; Spindler, F.; Malan, C.; Grabowski, E. J. J.; Armstrong, J. D. Highly Efficient Asymmetric Synthesis of Sitagliptn. *J. Am. Chem. Soc.* **2009**, *131*, 8798-8804. (b) Hu, X.-P.; Zheng, Z. Practical Rh(I)-Catalyzed Asymmetric Hydrogenation of β-(Acylamino)acrylates Using a New Unsymmetrical Hybrid Ferrocenylphosphine−Phosphoramidite Ligand: Crucial Influence of an N−H Proton in the Ligand. *Org. Lett.* **2005**, *7*, 419-422. (c) You, J.; Drexler, H.-J. Zhang, S.; Fischer, C.; Heller.D. Preparation and Asymmetric Hydrogenation of β-Aryl-Substituted β-Acylaminoacrylates. *Angew. Chem. Int. Ed.* **2003**, *42*, 913-916.

[21] (a) Nugent, W. A.; RajanBabu, T. V.; Burk, M. J. Beyond Nature's Chiral Pool: Enantioselective Catalysis in Industry. *Science* **1993**, *259*, 479-483. (b) Burk, M. J. Modular Phospholane Ligands in Asymmetric Catalysis. *Acc. Chem. Res.* **2000**, *33*, 363-372. (c) Burk, M. J.; Casy, G.; Johnson, N. B. A Three-Step Procedure for Asymmetric Catalytic Reductive Amidation of Ketones. *J. Org. Chem.* **1998**, *63*, 6084-6085.

[22] Zhang, Z.; Zhu, G.; Jiang, Q.; Xiao, D.; Zhang, X. Highly Enantioselective Hydrogenation of Cyclic Enamides Catalyzed by a Rh-PennPhos Catalyst. *J. Org. Chem.* **1999**, *64*, 1774-1775.

[23] Rojo. P.; Riera, A.; Verdaguer, X. Bulky P-tereogenic Ligands. A Success Story in Asymmetric Catalysis. *Coord. Chem. Rev*. **2023**, *489*, 215192-215226.

[24] Imamoto, T.; Watanabe, J.; Wada, Y.; Masuda, H.; Yamada, H.; Tsuruta, H.; Matsukawa, S.; Yamaguchi, K. P-Chiral Bis(trialkylphosphine) Ligands and Their Use in Highly Enantioselective Hydrogenation Reactions. *J. Am. Chem. Soc.* **1998**, *120*, 1635–1636.

[25] (a) Jugé, S.; Stephan, M.; Laffite, J.A.; Genet, J.P. Efficient Asymmetric Synthesis of Optically Pure Tertiary Mono and Diphosphine Ligands. *Tetrahedron Lett*. **1990**, *31*, 6357–6360. (b) Muci, A.R.; Campos, K.R.; Evans, D.A. Enantioselective Deprotonation as a Vehicle for the Asymmetric Synthesis of C_2-Symmetric P-Chiral Diphosphines. *J. Am. Chem. Soc.* **1995**, *117*, 9075–9076.

[26] (a) Gridnev, I.D.; Yamanoi, Y.; Higashi, N.; Tsuruta, H.; Yasutake, M.; Imamoto, T. Asymmetric Hydrogenation Catalyzed by (*S,S*)-R-BisPast;-Rh and (*R,R*)-R-MiniPHOS Complexes: Scope, Limitations, and Mechanism. *Adv. Synth. Catal*. **2001**, *343*, 118–136. (b) Yasutake, M.; Gridnev, I.D.; Higashi, N.; Imamoto, T. Highly Enantioselective Hydrogenation of (*E*)-β-(Acylamino)acrylates Catalyzed by Rh(I)-Complexes of Electron-Rich P-Chirogenic Diphosphines. *Org. Lett.* **2001**, *3*, 1701–1704. (c) Gridnev, I.D.; Yasutake, M.; Higashi, N.; Imamoto, T. Asymmetric Hydrogenation of Enamides with Rh-BisP* and Rh-MiniPHOS Catalysts. Scope, Limitations, and Mechanism. *J. Am. Chem. Soc.* **2001**, *123*, 5268–5276.

[27] Tang, W.; Zhang, X. A Chiral 1,2-Bisphospholane Ligand with a Novel Structural Motif: Applications in Highly Enantioselective Rh-Catalyzed Hydrogenations. *Angew. Chem. Int. Ed.* **2002**, *41*, 1612–1614.

[28] Imamoto, T.; Sugita, K.; Yoshida, K. An Air-Stable P-Chiral Phosphine Ligand for Highly Enantioselective Transition-Metal-Catalyzed Reactions. *J. Am. Chem. Soc.* **2005**, *127*, 11934–11935.

[29] (a) O'Shea, P.D.; Gauvreau, D.; Gosselin, F.; Hughes, G.; Nadeau, C.; Roy, A.; Shultz, C. S. Practical Synthesis of a Potent Bradykinin B_1 Antagonist via Enantioselective Hydrogenation of a Pyridyl *N*-Acyl Enamide. *J. Org. Chem.* **2009**, *74*, 4547–4553. (b) Gao, M.; Meng, J.-J.; Lv, H.;

Zhang, X. Highly Regio- and Enantioselective Synthesis of γ,δ-Unsaturated Amido Esters by Catalytic Hydrogenation of Conjugated Enamides. *Angew. Chem. Int. Ed*. **2015**, *54* 1885–1887. (c) Jiang, J.; Wang, Y.; Zhang, X. Rhodium-Catalyzed Enantioselective Hydrogenation of Tetrasubstituted α-Acetoxy β-Enamido Esters: A New Approach to Chiral α-Hydroxyl-β-amino Acid Derivatives. *ACS Catal*. **2014**, *4*, 1570–1573. (d) Lei, A.; Chen, M.; He, M.; Zhang, X. Asymmetric Hydrogenation of Pyridines: Enantioselective Synthesis of Nipecotic Acid Derivatives. *Eur. J. Org. Chem.* **2006**, *19* 4343–4347. (e) Imamoto, T.; Tamura, K.; Zhang, Z.; Horiuchi, Y.; Sugiya, M.; Yoshida, K.; Yanagisawa, A.; Gridnev, I.D. Rigid P-Chiral Phosphine Ligands with *tert*-Butylmethylphosphino Groups for Rhodium-Catalyzed Asymmetric Hydrogenation of Functionalized Alkenes. *J. Am. Chem. Soc.* **2012**, *134*, 1754–1769.

[30] Revés, M.; Ferrer, C.; León, T.; Doran, S.; Etayo, P.; Vidal-Ferran, A.; Riera, A.; Verdaguer, X. Primary and Secondary Aminophosphines as Novel P-Stereogenic Building Blocks for Ligand Synthesis. *Angew. Chem. Int. Ed.* **2010**, *49*, 9452–9455.

[31] Cristóbal-Lecina, E.; Etayo, P.; Doran, S.; Revés, M.; Martín-Gago, P.; Grabulosa, A.; Costantino, A.R.; Vidal-Ferran, A.; Riera, A.; Verdaguer, X. MaxPHOS Ligand: PH/NH Tautomerism and Rhodium-Catalyzed Asymmetric Hydrogenations. *Adv. Synth. Catal.* **2014**, *356*, 795–804

[32] Orgué, S.; Flores-Gaspar, A.; Biosca, M.; Pàmies, O.; Diéguez, M.; Riera, A.; Verdaguer, X. Stereospecific SN_2@P Reactions: Novel Access to Bulky P-stereogenic Ligands. *Chem. Commun.*, **2015**, *51*, 17548-17551.

[33] Salomó, E.; Orgué, S.; Riera, A.; Verdaguer, X. Highly Enantioselective Iridium-Catalyzed Hydrogenation of Cyclic Enamides. *Angew. Chem. Int. Ed*. **2016**, *28*, 7988-7992.

[34] Cabré, A., Rimangoli, E.; Martínez-Balart, P.; Verdaguer, X.; Riera, A. Highly Enantioselective Iridium-Catalyzed Hydrogenation of 2-Aryl Allyl Phthalimides. *Org. Lett.* **2019**, *23*, 9709-9713

[35] (a) Zupančič, B.; Mohar, B.; Stephan, M. Heavyweight "R-SMS-Phos" Ligands in the Olefins' Hydrogenation Arena. *Org. Lett*. **2010**, *12*, 1296–1299. (b) Zupančič, B.; Mohar, B.; Stephan , M. Impact on Hydrogenation Catalytic Cycle of the R Groups' Cyclic Feature in "R-SMS-Phos". *Org. Lett*. **2010**, *12*, 3022–3025. (c) Stephan, M.; Šterk, D.; Zupančič, B.; Mohar, B. Profiling the Tuneable R-SMS-Phos Structure in the Rhodium(i)-Catalyzed Hydrogenation of Olefins: the Last Stand? *Org. Biomol. Chem.* **2011**, *9*, 5266–5271.

[36] (a) Reeves, J.T.; Tan, Z.; Reeves, D.C.; Song, J.J.; Han, S.Z.; Xu, Y.; Tang, W.; Yang, B.-S.; Razavi, H.; Harcken, C.; Kuzmich, D.; Mahaney, P.E.; Lee, H.; Busacca, C.A.; Senanayake, C.H. Development of an Enantioselective Hydrogenation Route to (*S*)-1-(2-(Methylsulfonyl)pyridin-4-yl)propan-1-amine. *Org. Process Res. Dev*. **2014**, *18*, 904–911. (b) Zhang, Z.; Wang, J.; Li, J.; Yang, F.; Liu, G.; Tang, W.; He, W.; Fu, J.J.; Shen, Y.H.; Li, A.; Zhang, W.D. Total Synthesis and Stereochemical Assignment of Delavatine A: Rh-Catalyzed Asymmetric Hydrogenation of Indene-Type Tetrasubstituted Olefins and Kinetic Resolution through Pd-Catalyzed Triflamide-Directed C–H Olefination. *J. Am. Chem. Soc.* **2017**, *139*, 5558–5567.

[37] Li, G.; Zatolochnaya, O.V.; Wang, X.J.; Rodríguez, S.; Qu, B.; Desrosiers, J.N.; Mangunuru, H.P.R.; Biswas, S.; Rivalti, D.; Karyakarte, S.D.; Sieber, J.D.; Grinberg, N.; Wu, L.; Lee, H.; Haddad, N.; Fandrick, D.R.; Yee, N.K.; Song, J.J.; Senanayake, C.H. BABIPhos Family of Biaryl Dihydrobenzooxaphosphole Ligands for Asymmetric Hydrogenation. *Org. Lett.* **2018**, *20*, 1725–1729.

[38] Tang, W.; Wang, W.; Chi, Y.; Zhang, X. A Bisphosphepine Ligand with Stereogenic Phosphorus Centers for the Practical Synthesis of β-Aryl-β-Amino Acids by Asymmetric Hydrogenation. *Angew. Chem. Int. Ed.* **2003**, *42*, 3509–3511.

[39] Li, X.; You, C.; Yang, H.; Che, J.; Chen, P.; Yang, Y.; Lv, H.; Zhang, X. Rhodium-Catalyzed Asymmetric Hydrogenation of Tetrasubstituted Cyclic Enamides: Efficient Access to Chiral Cycloalkylamine Derivatives. *Adv. Synth. Catal*. **2017**, *359*, 597–602.

[40] (a) Brandt, P.; Hedberg, C.; Andersson, P. G. New Mechanistic Insights into the Iridium–Phosphanooxazoline-Catalyzed Hydrogenation of Unfunctionalized Olefins: A DFT and Kinetic Study. *Chem. Eur. J.* **2003**, *9*, 339-347; (b) Church, T. L.; Rasmussen, T.; Andersson, P. G. Enantioselectivity in the Iridium-Catalyzed Hydrogenation of Unfunctionalized Olefins. *Organometallics* **2010**, *29*, 6769-6781.

[41] (a) Fan, Y.; Cui, X.; Burgess, K.; Hall, M. B. Electronic Effects Steer the Mechanism of Asymmetric Hydrogenations of Unfunctionalized Aryl-Substituted Alkenes. *J. Am. Chem. Soc.* **2004**, *126*, 16688-16689. (b) Cui, X.; Fan, Y.; Hall, M. B.; Burgess, K. Mechanistic Insights into Iridium-Catalyzed Asymmetric Hydrogenation of Dienes. *Chem. Eur. J.* **2005**, *11*, 6859-6868.

[42] Gruber, S.; Pfaltz, A. Asymmetric Hydrogenation with Iridium C,N and N,P Ligand Complexes: Characterization of Dihydride Intermediates with a Coordinated Alkene. *Angew. Chem. Int. Ed.* **2014**, *53*, 1896-1900.

[43] (a) Crabtree, R. H.; Gautier, A.; Giordano, G.; Khan, T. The Preparation and Some Catalytic Properties of a Number of Rhodium(I) Diolefin Complexes. *J. Organomet. Chem.* **1977**, *141*, 113-121. (b) Crabtree, R. H.; Felkin, H.; Morris, G. E. Cationic Iridium Diolefin Complexes as Alkene Hydrogenation Catalysts and the Isolation of Some Related Hydrido Complexes. *J. Organomet. Chem.* **1977**, *141*, 205-215.

[44] Lightfoot, A.; Schnider, P.; Pfaltz, A. Enantioselective Hydrogenation of Olefins with Iridium–Phosphanodihydrooxazole Catalysts. *Angew. Chem. Int. Ed.* **1998**, *37*, 2897-2899.

[45] (a) Tang, W.; Wang, W.; Zhang, X. Phospholane–Oxazoline Ligands for Ir-Catalyzed Asymmetric Hydrogenation. *Angew. Chem. Int. Ed.* **2003**, *42*, 943-946. (b) Hou, D. R.; Reibenspies, J.; Colacot, T. J.; Burgess, K. Enantioselective Hydrogenations of Arylalkenes Mediated by $[Ir(cod)(JM\text{-}Phos)]^+$ Complexes. *Chem. Eur. J.* **2001**, *7*, 5391-5400. (c) Menges, F.; Neuburger, M.; Pfaltz, A. Synthesis and Application of Chiral Phosphino-Imidazoline Ligands: Ir-Catalyzed Enantioselective Hydrogenation. *Org. Lett.* **2002**, *4*, 4713-4716. (d) Goulioukina, N. S.; Dolgina, T. Y. M.; Bondarenko, G. N.; Beletskaya, I. P.; Ilyin, M. M.; Davankov, V. A.; Pfaltz, A. Highly Enantioselective Hydrogenation of α,β-Unsaturated Phosphonates with Iridium–Phosphinooxazoline Complex: Synthesis of a Phosphorus Analogue of Naproxen. *Tetrahedron: Asymmetry* **2003**, *14*, 1397-1401. (e) Cozzi, P. G.; Menges, F.; Kaiser, S. Iridium-HetPHOX Complexes for the Catalytic Asymmetric Hydrogenation of Olefins and Imines. *Synlett* **2003**, 0833-0836. (f) Liu, D.; Tang, W.; Zhang, X. Synthesis of a New Class of Conformationally Rigid Phosphino-oxazolines: Highly Enantioselective Ligands for Ir-Catalyzed Asymmetric Hydrogenation. *Org. Lett.* **2004**, *6*, 513-516. (g) Schrems, M. G.; Pfaltz, A. *Neo*PHOX—an Easily Accessible P,N-Ligand for Iridium-Catalyzed Asymmetric Hydrogenation: Preparation, Scope and Application in the Synthesis of Demethyl Methoxycalamenene. *Chem. Commun.* **2009**, 6210-6212. (h) Lu, S. M.; Bolm, Highly Chemo- and Enantioselective Hydrogenation of Linear α,β-Unsaturated Ketones. C. *Chem. Eur. J.* **2008**, *14*, 7513-7516. (i) Lu, S. M.; Bolm, C. Highly Enantioselective Synthesis of Optically Active Ketones by Iridium-Catalyzed Asymmetric Hydrogenation. *Angew. Chem. Int. Ed.* **2008**, *47*, 8920-8923.

[46] (a) Rageot, D.; Pfaltz, A. Chiral Proline-Based P,O and P,N Ligands for Iridium-Catalyzed Asymmetric Hydrogenation. *Helv. Chim. Acta* **2012**, *95*, 2176-2193. (b) Elías-Rodríguez, P.; Borràs, C.; Carmona, A.T.; Faiges, J.; Robina, I.; Pàmies, O.; Diéguez, M. Pyrrolidine-Based P,O Ligands from Carbohydrates: Easily Accessible and Modular Ligands for the Ir-Catalyzed Asymmetric Hydrogenation of Minimally Functionalized Olefins. *ChemCatChem* **2018**, *10*, 5414-5424.

[47] Schrems, M. G.; Neumann, E.; Pfaltz, A. Iridium-catalyzed Asymmetric Hydrogenation of Unfunctionalized Tetrasubstituted Olefins. *Angew. Chem. Int. Ed.* **2007**, *46*, 8274-8276.

[48] Bigler, R.; Mack, K.A.; Shen, J.; Tosatti, P.; Han, C.; Bachmann, S.; Zhang, H.; Scalone, M.; Pfaltz, A.; Denmark, S.E.; Hildbrand, S.; Gosselin, F Asymmetric Hydrogenation of Unfunctionalized Tetrasubstituted Acyclic Olefins. *Angew. Chem. Int. Ed*. **2020**, *59*, 2844-2849.

[49] (a) Trifonova, A.; Diesen, J. S.; Andersson, P. G. Asymmetric Hydrogenation of Imines and Olefins Using Phosphine-Oxazoline Iridium Complexes as Catalysts. *Chem. Eur. J.* **2006**, *12*, 2318-2328. (b) Cheruku, P.; Diesen, J.; Andersson, P. G. Asymmetric Hydrogenation of Di and Trisubstituted Enol Phosphinates with N,P-Ligated Iridium Complexes. *J. Am. Chem. Soc.* **2008**, *130*, 5595-5599. (c) Cheruku, P.; Gohil, S.; Andersson, P. G. Asymmetric Hydrogenation of Enol Phosphinates by Iridium Catalysts Having N,P Ligands. *Org. Lett.* **2007**, *9*, 1659-1661. (d) Källström, K.; Munslow, I. J.; Hedberg, C.; Andersson, P. G. Iridium-Catalysed Asymmetric Hydrogenation of Vinylsilanes as a Route to Optically Active Silanes. *Adv. Synth. Catal.* **2006**, *348*, 2575-2578. (e) Engman, M.; Diesen, J. S.; Paptchikhine, A.; Andersson, P. G. Iridium-Catalyzed Asymmetric Hydrogenation of Fluorinated Olefins Using N,P-Ligands: A Struggle with Hydrogenolysis and Selectivity. *J. Am. Chem. Soc.* **2007**, *129*, 4536-4537. (f) Paptchikhine, A.; Cheruku, P.; Engman, M.; Andersson, P. G. Iridium-Catalyzed Enantioselective Hydrogenation of Vinyl Boronates.*Chem. Commun.* **2009**, 5996-5998. (g) Verendel, J. J.; Li, J. Q.; Quan, X.; Peters, B.; Zhou, T.; Gautun, O. R.; Govender, T.; Andersson, P. G. Chiral Hetero- and Carbocyclic Compounds from the Asymmetric Hydrogenation of Cyclic Alkenes. *Chem. Eur. J.* **2012**, *18*, 6507-6513. (h) Kerdphon, S.; Ponra, S.; Yang, J.; Wu, H.; Eriksson, L.; Andersson, P. G. Diastereo–and Enantioselective Synthesis of Structurally Diverse Succinate, Butyrolactone, and Trifluoromethyl Derivatives by Iridium-Catalyzed Hydrogenation of Tetrasubstituted Olefins. *ACS Catal.* **2019**, *9*, 6169–6176. (i) Ponra, S.; Rabten, W.; Yang, J.; Wu, H.; Kerdphon, S.; Andersson, P. G. Diastereo- and Enantioselective Synthesis of Fluorine Motifs with Two Contiguous Stereogenic centers. *J. Am. Chem. Soc.* **2018**, *140*, 13878–13883.

[50] (a) Kaiser, S.; Smidt, S. P.; Pfaltz, A. Iridium Catalysts with Bicyclic Pyridine–Phosphinite Ligands: Asymmetric Hydrogenation of Olefins and Furan Derivatives. *Angew. Chem. Int. Ed.* **2006**, *45*, 5194-5197. (b) Woodmansee, D. H.; Muller, M.-A.; Neuburger, M.; Pfaltz, A. Chiral Pyridyl Phosphinites with Large Aryl Substituents as Efficient Ligands for the Asymmetric Iridium-Catalyzed Hydrogenation of Difficult Substrates. *Chem. Sci.* **2010**, *1*, 72-78. (c) Wang, A.; Fraga, R. P. A.; Hörmann, E.; Pfaltz, A. Iridium-Catalyzed Asymmetric Hydrogenation of Unfunctionalized, Trialkyl-Substituted Olefins. *Chem. Asian J.* **2011**, *6*, 599-606. (d) Liu, Q.-B.; Yu, C.-B.; Zhou, Y.-G. Synthesis of Tunable Phosphinite–Pyridine Ligands and their Applications in Asymmetric Hydrogenation. *Tetrahedron Lett.* **2006**, *47*, 4733-4736. (e) Baeza, A.; Pfaltz, A. Iridium-Catalyzed Asymmetric Hydrogenation of N-Protected Indoles. *Chem. Eur. J.* **2010**, *16*, 2036-2039. (f) Woodmansee, D. H.; Müller, M. A.; Tröndlin, L.; Hörmann, E.; Pfaltz, A. Asymmetric Hydrogenation of α,β-Unsaturated Carboxylic Esters with Chiral Iridium N,P Ligand Complexes. *Chem. Eur. J.* **2012**, *18*, 13780-13786. (g) Pauli, L.; Tannert, R.; Scheil, R.; Pfaltz, A. Asymmetric Hydrogenation of Furans and Benzofurans with Iridium–Pyridine–Phosphinite Catalysts. *Chem. Eur. J.* **2015**, *21*, 1482-1487. (h) Jones, M.; Harris, D.; Struble, J.; Hayes, M.; Koeller, K.; Özgün, K.C.; Schirmer, H.; Heinrich, J.; Baechle, F.; Goudedranche, S.; Schotes C. Development of a Practical Process for the Large-Scale Preparation of the Chiral Pyridyl-Backbone for the Crabtree/Pfaltz-Type Iridium Complex Used in the Industrial Production of the Novel Fungicide Inpyrfluxam. *Org. Process Res. Dev.* **2022**, *26*, 2407-2414. (i) Schotes, C.; Müller, S. On the Importance of Collaboration in the Development of Sustainable Catalytic Processes: The Case of Inpyrfluxam. *ACS Sustainable Chem. Eng.* **2022**, *10*, 13244-13253.

[51] For early representative publications, see: (a) Diéguez, M.; Mazuela, J.; Pàmies, O.; Verendel, J. J.; Andersson, P. G. Chiral Pyranoside Phosphite−Oxazolines: A New Class of Ligand for Asymmetric Catalytic Hydrogenation of Alkenes. *J. Am. Chem. Soc.* **2008**, *130*, 7208-7209. (b) Mazuela, J.; Verendel, J. J.; Coll, M.; Schäffner, B.; Börner, A.; Andersson, P. G.; Pàmies, O.; Diéguez, M. Iridium Phosphite−Oxazoline Catalysts for the Highly Enantioselective Hydrogenation of Terminal Alkenes. *J. Am. Chem. Soc.* **2009**, *131*, 12344-12353. (c) Mazuela, J.; Norrby, P.-O.; Andersson, P. G.; Pàmies, O.; Diéguez, M. Pyranoside Phosphite–Oxazoline Ligands for the Highly Versatile and Enantioselective Ir-Catalyzed Hydrogenation of Minimally Functionalized Olefins. A Combined Theoretical and Experimental Study. *J. Am. Chem. Soc.* **2011**, *133*, 13634-13645.

[52] (a) Mazuela, J.; Pàmies, O.; Diéguez, M. A Phosphite-Pyridine/Iridium Complex Library as Highly Selective Catalysts for the Hydrogenation of Minimally Functionalized Olefins. *Adv. Synth. Catal*. **2013**, *355*, 2569-2583. (b) Biosca, M.; de la Cruz–Sánchez, P.; Tarr, D.; Llanes, P.; Karlsson, E. A.; Margalef, J.; Pàmies, O.; Pericàs, M. A.; Diéguez, M. Filling the Gaps in the Challenging Asymmetric Hydrogenation of Exocyclic Benzofused–Based Alkenes with Ir–P,N Catalysts. *Adv. Synth. Catal.* **2022**, *365*, 167–177.

[53] (a) Coll, M.; Pàmies, O.; Diéguez, M. Thioether–phosphite: New Ligands for the Highly Enantioselective Ir–Catalyzed Hydrogenation of Minimally Functionalized Olefins. *Chem. Commun.* **2011**, *47*, 9215–9217. (b) Coll, M.; Pàmies, O.; Diéguez, M. A Modular Furanoside Thioether–Phosphite/Phosphinite/ Phosphine Ligand Library for Asymmetric Iridium–Catalyzed Hydrogenation of Minimally Functionalized Olefins: Scope and Limitations. *Adv. Synth. Catal.* **2013**, *355*, 143–160. (c) Margalef, J.; Caldentey, X.; Karlsson, E. A.; Coll, M.; Mazuela, J.; Pàmies, O.; Diéguez, M.; Pericàs, M. A. A Theoretically–Guided Optimization of a New Family of Modular P,S–Ligands for Iridium–Catalyzed Hydrogenation of Minimally Functionalized Olefins. *Chem. Eur. J.* **2014**, *20*, 12201–12214. (d) Borràs, C.; Biosca, M.; Pàmies, O.; Diéguez, M. Iridium–Catalyzed Asymmetric Hydrogenation with Simple Cyclohexane–Based P/S Ligands: *In Situ* HP–NMR and DFT Calculations for the Characterization of Reaction Intermediates. *Organometallics* **2015**, *34*, 5321–5334. (e) Biosca, M.; Coll, M.; Lagarde, F.; Brémond, E.; Routaboul, L.; Manoury, E.; Pàmies, O.; Poli, R.; Diéguez, M. Chiral Ferrocene–Based P,S Ligands for Ir–Catalyzed Hydrogenation of Minimally Functionalized Olefins. Scope and limitations. *Tetrahedron* **2016**, *72*, 2623–2631. (f) Faiges, J.; Borràs, C.; Pastor, I. M.; Pàmies, O.; Besora, M.; Diéguez, M. Density Functional Theory–Inspired Design of Ir/P,S–Catalysts for Asymmetric Hydrogenation of Olefins. *Organometallics* **2021,** *40*, 20, 3424–3435.

[54] Biosca, M.; Magre, M.; Pàmies, O.; Diéguez, M. Asymmetric Hydrogenation of Disubstituted, Trisubstituted, and Tetrasubstituted Minimally Functionalized Olefins and Cyclic β-Enamides with Easily Accessible Ir–P,Oxazoline Catalysts. *ACS Catal.* **2018**, *8*, 10316–10320.

[55] Bell, S.; Wüstenberg, B.; Kaiser, S.; Menges, F.; Netscher, T.; Pfaltz, A. Asymmetric Hydrogenation of Unfunctionalized, Purely Alkyl-Substituted Olefins. *Science* **2006**, *311*, 642–644.

[56] (a) Xia, J.; Yang, G.; Zhuge, R.; Liu, Y.; Zhang, W. Iridium–Catalyzed Asymmetric Hydrogenation of Unfunctionalized Exocyclic C=C Bonds. *Chem. Eur. J.* **2016**, *22*, 18354–18357. (b) Biosca, M.; Magre, M.; Coll, M.; Pàmies, O.; Diéguez, M. Alternatives to Phosphinooxazoline (*t*–BuPHOX) Ligands in the Metal–Catalyzed Hydrogenation of Minimally Functionalized Olefins and Cyclic β–Enamides. *Adv. Synth. Catal.* **2017**, *359*, 2801–2814.

[57] Drury III, W. J.; Zimmermann, N.; Keenan, M.; Hayashi, M.; Kaiser, S.; Goddard, R.; Pfaltz, A. Synthesis of Versatile Chiral N,P Ligands Derived from Pyridine and Quinoline. *Angew. Chem. Int. Ed*. **2004**, *43*, 70–74. Angew. Chem. **2004**, *116*, 72–76.

[58] (a) Helmchen, G.; Pfaltz, A. Phosphinooxazolines A New Class of Versatile, Modular P,N-Ligands for Asymmetric Catalysis, *Acc. Chem. Res.* **2000**, *33*, 336-345. (b) *Palladium Reagents and Catalysis, Innovations in Organic Synthesis*; (Ed. Tsuji, J.), Wiley, New York, **1995**. (c) Trost, B. M.; Van Vranken, D. L. Asymmetric Transition Metal-Catalyzed Allylic Alkylations. *Chem. Rev.* **1996**, *96*, 395-422. (d) Johannsen, M.; Jørgensen, K. A. Allylic Amination**.** *Chem. Rev.* **1998**, *98*, 1689-1708. (e) Trost, B. M.; Crawley, M. L. Asymmetric Transition-Metal-Catalyzed Allylic Alkylations: Applications in Total Synthesis. *Chem. Rev.* **2003**, *103*, 2921-2944. (f) Lu, Z.; Ma, S. Metal-Catalyzed Enantioselective Allylation in Asymmetric Synthesis. *Angew. Chem. Int. Ed.* **2008**, *47*, 258-297. (g) Trost, B. M.; Zhang, T.; Sieber, J. D. Catalytic Asymmetric Allylic Alkylation Employing Heteroatom Nucleophiles: a Powerful Method for C–X Bond Formation. *Chem. Sci.* **2010**, *1*, 427-440. (h) Trost, B. M. Pd- and Mo-Catalyzed Asymmetric Allylic Alkylation. *Org. Process Res. Dev.* **2012**, *16*, 185-194. (i) Butt, N. A.; Zhang, W. Transition Metal-Catalyzed Allylic Substitution Reactions with Unactivated Allylic Substrates . *Chem. Soc. Rev.* **2015**, *44*, 7929-7967. (j) Grange, R. L.; Clizbe, E. A.; Evans, P. A. Recent Developments in Asymmetric Allylic Amination Reactions. *Synthesis* **2016**, *48*, 2911-2968. (k) Butt, N.; Yang, G.; Zhang, W. Allylic Alkylations with Enamine Nucleophiles. *Chem. Rec.* **2016**, *16*, 2687-2696. (l) *Transition Metal Catalyzed Enantioselective Allylic Substitution in Organic Synthesis*; (Ed. Kazmaier, U.), Springer-Verlag, Heidelberg, Berlin, **2012**. (m) Pàmies, O.; Margalef, J.; Cañellas, S.; James, J.; Judge, e.; Guiry, P.J.; Moberg, C.; Bäckvall, J.-E.; Pfaltz, A.; Pericàs, M.A.; Diéguez, M. Recent Advances in Enantioselective Pd-Catalyzed Allylic Substitution: From Design to Applications. *Chem. Rev.* **2021,** *121*, 8, 4373–4505**.**

[59] (a) Zhong, C.; Shi, X. When Organocatalysis Meets Transition-Metal Catalysis. *Eur. J. Org. Chem*. **2010**, *2010*, 2999−3025. (b) Afewerki, S.; Córdova, A. Combinations of Aminocatalysts and Metal Catalysts: A Powerful Cooperative Approach in Selective Organic Synthesis. *Chem. Rev.* **2016**, *116*, 13512−13570. (c) Fu, J.; Huo, X.; Li, B.; Zhang, W. Cooperative Bimetallic Catalysis in Asymmetric Allylic Substitution. *Org. Biomol. Chem*. **2017**, *15*, 9747−9759. (d) Wu, Y.; Huo, X.; Zhang, W. Synergistic Pd/Cu Catalysis in Organic Synthesis. *Chem.-Eur. J*. **2020**, *26*, 4895−4916.

[60] For a recent review, see: Cheng, Q.; Tu, H.-F.; Zheng, C.; Qu, J.-P.; Helmchen, G.; You, S.-L. Iridium-Catalyzed Asymmetric Allylic Substitution Reactions. *Chem. Rev*. **2019**, *119*, 1855−1969.

[61] (a) Hornillos, V.; Gualtierotti, J.-B.; Feringa, B. L. In *Progress in Enantioselective Cu(I)-catalyzed Formation of Stereogenic Centers*; Harutyunyan, S. R., Ed.; Springer International Publishing: Cham, **2016**. (b) Yorimitsu, H.; Oshima, K. Recent Progress in Asymmetric Allylic Substitutions Catalyzed by Chiral Copper Complexes. *Angew. Chem. Int. Ed.* **2005**, *44*, 4435-4439. (c) Harutyunyan, S. R.; den Hartog, T.; Geurts, K.; Minnaard, A. J.; Feringa, B. L. Catalytic Asymmetric Conjugate Addition and Allylic Alkylation with Grignard Reagents. *Chem. Rev.* **2008**, *108*, 2824-2852. (d) Cherney, A. H.; Kadunce, N. T.; Reisman, S. E. Enantioselective and Enantiospecific Transition-Metal-Catalyzed Cross-Coupling Reactions of Organometallic Reagents To Construct C–C Bonds. *Chem. Rev.* **2015**, *115*, 9587-9652. (e) Falciola, C. A.; Alexakis, A. Copper-Catalyzed Asymmetric Allylic Alkylation. *Eur. J. Org. Chem.* **2008**, 3755-8780.

[62] Gogoll, A.; Oernebro, J.; Grennberg, H.; Bäckvall, J.-E. Mechanism of Apparent π-Allyl Rotation in (π-Allyl)Palladium Complexes with Bidentate Nitrogen Ligands. *J. Am. Chem. Soc*. **1994**, *116*, 3631−3632.

[63] (a) Hayashi, T.; Yamamoto, A.; Ito, Y.; Nishioka, E.; Miura, H.; Yanagi, K. Asymmetric Synthesis Catalyzed by Chiral Ferrocenylphosphine-Transition-Metal Complexes. 8. Palladium-Catalyzed Asymmetric Allylic Amination. *J. Am. Chem. Soc.* **1989**, *111*, 6301-6311. (b) Hayashi, T.; Yamamoto, A.; Hagihara, T.; Ito, Y. Modification of Optically Active Ferrocenylphosphine Ligands for Palladium-Catalyzed Asymmetric Allylic Alkylation. *Tetrahedron Lett.* **1986**, *27*, 191-194.

[64] (a) Wang, Y.-N.; Lu, L.-Q.; Xiao, W.-J. Non-Bonding Interactions Enable the Selective Formation of Branched Products in Palladium-Catalyzed Allylic Substitution Reactions*. Chem. Asian J*. **2018**, *13*, 2174–2183. (b) Zhuo, C.-X.; Zhou, Y.; You, S.-L. Highly Regio- and Enantioselective Synthesis of Polysubstituted 2H-Pyrroles via Pd-Catalyzed Intermolecular Asymmetric Allylic Dearomatization of Pyrroles. *J. Am. Chem. Soc.* **2014**, *136*, 6590−6593.

[65] (a) Trost, B. M.; van Vranken, D. L.; Bingel, C. A Modular Approach for Ligand Design for Asymmetric Allylic Alkylations via Enantioselective Palladium-Catalyzed Ionizations. *J. Am. Chem. Soc.* **1992**, *114*, 9327-9343. (b) Trost, B. M. Designing a Receptor for Molecular Recognition in a Catalytic Synthetic Reaction: Allylic Alkylation. *Acc. Chem. Res.* **1996**, *29*, 355-364. (c) Trost, B. M.; Krueger, A. C.; Bunt, R. C.; Zambrano, J. On the Question of Asymmetric Induction with Acyclic Allylic Substrates. An Asymmetric Synthesis of (+)-Polyoxamic Acid. *J. Am. Chem. Soc.* **1996**, *118*, 6520-6521. (d) Trost, B. M.; Bunt, R. C. Asymmetric Induction in Allylic Alkylations of 3-(Acyloxy)Cycloalkenes. *J. Am. Chem. Soc.* **1994**, *116*, 4089-4090.

[66] Butts, C.P.; Filali, E.; Lloyd-Jones, G.C.; Norrby, P.-O.; Sale, D.A.; Schramm, Y. Structure-Based Rationale for Selectivity in the Asymmetric Allylic Alkylation of Cycloalkenyl Esters Employing the Trost 'Standard Ligand' (TSL): Isolation, Analysis and Alkylation of the Monomeric form of the Cationic η^3-Cyclohexenyl Complex $[(\eta^3\text{-}c\text{-}C_6H_9)Pd(TSL)]^+$ *J. Am. Chem. Soc.* **2009**, *131*, 9945-9957.

[67] Pfaltz, A. Chiral Semicorrins and Related Nitrogen Heterocycles as Ligands in Asymmetric Catalysis. *Acc. Chem. Res*. **1993**, *26*, 339−345.

[68](a) Prétôt, R.; Pfaltz, A. New Ligands for Regio- and Enantiocontrol in Pd-Catalyzed Allylic Alkylations. *Angew. Chem. Int. Ed.* **1998**, *37*, 323-325. (b) Prétôt, R.; Loyd-Jones, G. C.; Pfaltz, A. Enantio- and Regiocontrol in Palladium- and Tungsten-Catalyzed Allylic Substitutions. *Pure Appl. Chem.* **1998**, *70*, 1035-1040.

[69] Crawford, J. M.; Sigman, M. S. Conformational Dynamics in Asymmetric Catalysis: is Catalyst Flexibility a Design Element? *Synthesis* **2019**, *51*, 1021−1036.

[70] (a) Stranne, R.; Vasse, J.-L.; Moberg, C. Synthesis and Application of Chiral P,N-Ligands with Pseudo-Meso and Pseudo-C_2 symmetry. *Org. Lett*. **2001**, *3*, 2525−2528. (b) Vasse, J.-L.; Stranne, R.; Zalubovskis, R.; Gayet, C.; Moberg, C. Influence of Steric Symmetry and Electronic Dissymmetry on the Enantioselectivity in Palladium-Catalyzed Allylic Substitutions. *J. Org. Chem*. **2003**, *68*, 3258−3270.

[71] Zalubovskis, R.; Bouet, A.; Fjellander, E.; Constant, S.; Linder, D.; Fischer, A.; Lacour, J.; Privalov, T.; Moberg, C. Self-Adaptable Catalysts: Substrate-Dependent Ligand Configuration. *J. Am. Chem. Soc*. **2008**, 130, 1845−1855.

[72] Théveau, L.; Bellini, R.; Dydio, P.; Szabo, Z.; van der Werf, A.; Afshin Sander, R.; Reek, J. N. H.; Moberg, C. Cofactor-Controlled Chirality of Tropoisomeric Ligand. *Organometallics* **2016**, *35*, 1956−1963.

[73] (a) Diéguez, M.; Pàmies, O. Biaryl Phosphites: New Efficient Adaptative Ligands for Pd-catalyzed Asymmetric Allylic Substitution Reactions. *Acc. Chem. Res*. **2010**, *43*, 312−322. (b) van Leeuwen, P. W. N. M.; Kamer, P. C. J.; Claver, C.; Pàmies, O.; Diéguez, M. Phosphite-Containing Ligands for Asymmetric Catalysis. *Chem. Rev*. **2011**, *111*, 2077−2118. (c) Biosca, M.; Tarr, D.; Pàmies, O.; Diéguez, M. The Evolution of Phosphite-Oxazoline Ligandsf or the Pd-Allylic Substitution and Their Application in Building Chiral Molecules. *Eur. J. Org. Chem*.**2023**, e202300429.

[74] (a) Pàmies, O.; Diéguez, M.; Claver, C. New Phosphite−Oxazoline Ligands for Efficient Pd-Catalyzed Substitution Reactions. *J. Am. Chem. Soc.* **2005**, *127*, 3646-3647. (b) Bellini, R.; Magre, M.; Biosca, M.; Norrby, P.-O.; Pàmies, O.; Diéguez, M.; Moberg, C. Conformational Preferences of a

Tropos Biphenyl Phosphinooxazoline - a Ligand with Wide Substrate Scope. *ACS Catal*. **2016**, *6*, 1701−1712.

[75] See some examples: (a) Raluy, E.; Pàmies, O.; Diéguez, M. Modular Furanoside Phosphite-Phosphoroamidites, a Readily Available Ligand Library for Asymmetric Palladium-Catalyzed Allylic Substitution Reactions. Origin of Enantioselectivity. *Adv. Synth. Catal*. **2009**, *351*, 1648−1670. (b) Diéguez, M.; Pàmies, O. Modular Phosphite-Oxazoline/Oxazine Ligand Library for Asymmetric Pd-Catalyzed Allylic Substitution Reactions: Scope and Limitations-Origin of Enantioselectivity. *Chem. - Eur. J*. **2008**, *14*, 3653−3669. (c) Mata, Y.; Pàmies, O.; Diéguez, M. Pyranoside Phosphiteoxazoline Ligand Library: Highly Efficient Modular P,N Ligands for Palladium-Catalyzed Allylic Substitution Reactions. A Study of the Key Palladium Allyl Intermediates. *Adv. Synth. Catal*. **2009**, *351*, 3217−3234. (d) Mazuela, J.; Pàmies, O.; Diéguez, M. Phosphite-Thiazoline versus Phosphite-Oxazoline for Pd-Catalyzed Allylic Substitution Reactions: a Case for Comparison. *ChemCatChem* **2013**, *5*, 1504−1516. (e) Biosca, M.; Saltó, J.; Magre, M.; Norrby, P.-O.; Pàmies, O.; Diéguez, M. An Improved Class of Phosphite-Oxazoline Ligands for Pd-Catalyzed Allylic Substitution Reactions. *ACS Catal*. **2019**, *9*, 6033−6048. (f) Mazuela, J.; Paptchikhine, A.; Tolstoy, P.; Pàmies, O.; Diéguez, M.; Andersson, P. G. A New Class of Modular P,N-Ligand Library for aAymmetric Pd-Catalyzed Allylic Substitution Reactions: a Study of the Key Pd-π-Allyl Intermediates. *Chem. - Eur. J.* **2010**, *16*, 620−638. (g) Magre, M.; Biosca, M.; Norrby, P.-O.; Pàmies, O.; Diéguez, M. Theoretical and Experimental Optimization of a New Amino Phosphite Ligand Library for Asymmetric Palladium-Catalyzed Allylic Substitution. *ChemCatChem* **2015**, *7*, 4091−4107. (h) Pàmies, O.; Diéguez, M. Screening of a Phosphite-Phosphoramidite Ligand Library for Palladium-Catalysed Asymmetric Allylic Substitution Reactions: the Origin of Enantioselectivity. *Chem. -Eur. J*. **2008**, 14, 944−960.

[76] (a) Coll, M.; Pàmies, O.; Diéguez, M. Highly Versatile Pd/Thioether-Phosphite Catalytic Systems for Asymmetric Allylic Alkylation, Amination, and Etherification Reactions. *Org. Lett*. **2014**, *16*, 1892−1895. (b) Margalef, J.; Coll, M.; Norrby, P.-O.; Pàmies, O.; Diéguez, M. Asymmetric Catalyzed Allylic Substitution Using a Pd/P-S Catalyst Library with Exceptional High Substrate and Nucleophile Versatility: DFT and Pd-π-Allyl Key Intermediates Studies. *Organometallics* **2016**, *35*, 3323−3335. (c) Biosca, M.; Margalef, J.; Caldentey, X.; Besora, M.; Rodríguez-Escrich, C.; Saltó, J.; Cambeiro, X. C.; Maseras, F.; Pàmies, O.; Diéguez, M.; Pericàs. M.A. Computationally Guided Design of a Readily Assembled Phosphite-Thioether Ligand for a Broad Range of Pd Catalyzed Asymmetric Allylic Substitutions. *ACS Catal*. **2018**, *8*, 3587− 3601. (d) Margalef, J.; Borràs, C.; Alegre, S.; Pàmies, O.; Diéguez, M. A Readily Accessible and Modular Carbohydrate-Derived Thioether/Selenoether-Phosphite Ligand Library for Pd-Catalyzed Asymmetric Allylic Substitutions. *Dalton Trans*. **2019**, *48*, 12632−12643.

[77] (a) Royer, J. *Asymmetric Synthesis of Nitrogen Heterocycles*, Wiley-VCH, Weinhei, **2009**. (b) Louis, D. Q.; John, A. T. *Fundamentals of Heterocyclic Chemistry*, Wiley-VCH, Weinheim, **2010**. (c) Pozharskii, A. F.; Soldatenkov, A. T.; Katritzky, A. R *Heterocycles in Life and Society*, Wiley-VCH, Weinheim, **2011**. (d) Vitaku, E.; Smith, D. T.; Njardarson, J. T. Analysis of the Structural Diversity, Substitution Patterns, and Frequency of Nitrogen Heterocycles among U.S. FDA Approved Pharmaceuticals. *J. Med. Chem.* **2014**, 57, 10257-10274. (e) Taylor, R.D.; MacCoss, M.; Lawson, A.D.G. Rings in Drugs. *J. Med. Chem.* **2014**, 57, 5845-5859.

[78] (a) Hassner, A. *Synthesis of Heterocycles via Cycloadditions I*, Springer, Berlin, **2008**. (b) Hassner, A*. Synthesis of Heterocycles via Cycloadditions II*, Springer, Berlin, **2008**. (c) Eicher, T.; Hauptmann, S.; Speicher, A. *The Chemistry of Heterocycles: Structures, Reactions, Synthesis, and Applications*, Wiley-VCH, Weinheim, **2012**. (d) Hashimoto, T.; Maruoka, K. Recent Advances of Catalytic Asymmetric 1,3-Dipolar Cycloadditions. *Chem. Rev*. **2015**, 115, 5366-5412.

[79] See for example: (a)Yu, Z.X.; Wang, Y.; Wang, Y. Transition-Metal-Catalyzed Cycloadditions for the Synthesis of Eight-Membered Carbocycles. *Chem. Asian J.* **2010**, *5*, 1072-1088. (b) Nemoto, T.; Harada, S.; Nakajima, M. Synthetic Methods for 3,4-Fused Tricyclic Indoles via Indole Ring Formation. *Asian J. Org. Chem*. **2018**, *7*, 1730-1742. (c) Reyes, R.L.; Iwai, T.; Sawamura, M. Construction of Medium-Sized Rings by Gold Catalysis*. Chem. Rev*. **2021**, *121*, 8926-8947. (d) Zhang, X.; Lin, L.; Li, J.; Duan, S.; Long, Y.; Li, J. Recent Progress in the Synthesis of Medium-Sized Ring and Macrocyclic Compounds. *Chin. J. Org. Chem*. **2021**, *41*, 1878-1887. (e) Huisgen, R. 1,3-Dipolar Cycloadditions. Past and Future. *Angew. Chem. Int. Ed.* **1963**, *2*, 565-598.

[80] For reviews, see: (a) He, J.; Ling, J.; Chiu, P. Vinyl Epoxides in Organic Synthesis. *Chem. Rev*. **2014**, *114*, 8037-8128. (b) Allen, D.W.B.; Lakeland, C.P.; Harrity, J.P.A. Utilizing Palladium-Stabilized Zwitterions for the Construction of *N*-Heterocycles. *Chem. Eur. J*. **2017**, *23*, 13830-13857. (c) De, N.; Yoo, E.J. Recent Advances in the Catalytic Cycloaddition of 1,*n*-Dipoles. *ACS Catal*. **2018**, *8*, 48-58. (d) Liu, Y.; Oble, J.; Pradal, A.; Poli, G. Catalyic Domino Annulations through η^3-Allylpalladium Chemistry: A Never-Ending Story. *Eur. J. Inorg. Chem*. **2020**, 942-961. (e) Trost, B.M.; Mata. G. Forging Odd-Membered Rings: Palladium-Catalyzed Asymmetric Cycloadditions of Trimethylenemethane. *Acc. Chem. Res*. **2020**, *53*, 1293-1305. (f) Wang, J. Blaszczyk, S.A.; Li, X.; Tang, W. Transition Metal-Catalyzed Selective Carbon−Carbon Bond Cleavage of Vinylcyclopropanes in Cycloaddition Reactions. *Chem. Rev*. **2021**, *121*, 110-139. (g) Du, J.; Li, Y.-F.; Ding, C.-H. Recent Advances of Pd-π-Allyl Zwitterions in Cycloaddition Reactions. *Chin. Chem. Lett*, **2023**, 108401 (i) Niu, B.; Shi, M. Recent Advances in Annulation Reactions Based on Zwitterionic π-Allyl Palladium and Propargyl Palladium Complexes. *Org. Chem. Front.* **2021**, *8*, 3475-3501. (j) De La Cruz-Sánchez, P.; Pàmies, O. Metal-π-Allyl Mediated Asymmetric Cycloaddition Reactions. In Advances in Catalysis; Elsevier: Amsterdam, The Netherlands, **2021**; Volume 69, pp. 103–180.

[81] For some examples of full mechanism investigations: (a) Gao, X.; Xia, M.; Yuan, C.; Zhou, L.; Sun, W.; Li, C.; Wu, B.; Zhu, D.; Zhang, C.; Zheng, B.; Wang, D.; Guo, H. Enantioselective Synthesis of Chiral Medium-Sized Cyclic Compounds via Tandem Cycloaddition/Cope Rearrangement Strategy. *ACS Catal*, **2019**, *9*, 1645-1654. (b) Qi, T.; Fu, S.; Zhang, X.; Liu, T,-H.; Li, Q.-Z.; Gou, C.; Li. J.-L. Theoretical Insight into the Origins of Chemo- and Diastereoselectivity in the Palladium-Catalysed (3+2) Cyclisation of 5-Alkenyl Thiazolones. *Org. Chem. Front.* **2021**, *8,* 6203–6214. (c) Yang, C.; Yang, Z.-X.; Ding, C.-H.; Xu, B.; Hou, X.-L. Development of Dipolarophiles for Catalytic Asymmetric Cycloadditions through Pd-π-Allyl Zwitterions. *Chem. Rec.* **2021**, *21*, 1442–1454. (d) Guo, C.; Janssen-Mu̇ller, D.; Fleige, M.; Lerchen, A.; Daniliuc, C. G.; Glorius, F. Mechanistic Studies on a Cooperative NHC Organocatalysis/Palladium Catalysis System: Uncovering Significant Lessons for Mixed Chiral Pd(NHC)(PR_3) Catalyst Design. *J. Am. Chem. Soc.* **2017**, *139*, 4443−4451.

[82] Examples metal-zwitterionic species studies: (a) Chai, W.; Zhou, Q.; Ai, W.; Zheng, Y.; Qin, T.; Xu, X.; Zi, W. Lewis-Acid-Promoted Ligand-Controlled Regiodivergent Cycloaddition of Pd-Oxyallyl with 1,3-Dienes: Reaction Development and Origins of Selectivities. *J. Am. Chem. Soc.* **2021**, *143*, 3595–3603. (b) Zheng, Y.; Quin, T.; Zi, W. Enantioselective Inverse Electron Demand (3+2) Cycloaddition of Palladium-Oxyallyl Enabled by a Hydrogenbond-Donating Ligand. *J. Am. Chem. Soc.* **2021**, *143*, 1038–1045. (c) Liu, T.; Fang, Y.; Zuo, L.; Yang, Y.; Liu, Y.; Chen, W.; Dang, L.; Guo, W. Pd/LA-Catalyzed Decarboxylation Enabled Exclusive [5+2] Annulation Toward N-Aryl Azepanes and DFT Insights. *Org. Chem. Front.* **2021**, *8*, 1902–1909. (d) Khan, A.; Zheng, R.; Kan, Y.; Ye, J.; Xing, J.; Zhang, Y. J. Palladium-Catalyzed Decarboxylative Cycloaddition of Vinylethylene Carbonates with Formaldehyde: Enantioselective Construction of Tertiary Vinylglycols. *Angew. Chem. Int. Ed.* **2014**, *53*, 6439–6442. (e) Khan, A.; Xing, J.; Zhao, J.; Kan, Y.; Zhang, W.; Zhang, Y. J. Palladium-Catalyzed Enantioselective Decarboxylative Cycloaddition of Vinylethylene

Carbonates with Isocyanates. *Chem. Eur. J.* **2015**, *21*, 120–124. (f) Guo, W.; Martinez-Rodriguez, L.; Kuniyil, R.; Martin, E.; Escudero-Adan, E. C; Maseras, F.; Kleij, A. W. Stereoselective and Versatile Preparation of Tri- and Tetra-Substituted Allylic Amine Scaffolds Under Mild Conditions. *J. Am. Chem. Soc.* **2016**, *138*, 11970–11978. (g) Guo, W.; Kuniyil, R.; Gómez, J. E.; Maseras F.; Kleij A. W. A Domino Process Toward Functionally Dense Quaternary Carbons Through Pd-Catalyzed Decarboxylative C(sp^3)-C(sp^3) Bond Formation. *J. Am. Chem. Soc.* **2018**, *140*, 3981–3987. (h) Hu. L.; Cai, A.; Wu, Z.; Kleij, A. W.; Huang, G. A Mechanistic Analysis of the Palladium-Catalyzed Formation of Branched Allylic Amines Reveals the Origin of The Regio- And Enantioselectivity Through A Unique Inner-Sphere Pathway. *Angew. Chem. Int. Ed.* **2019**, *58*, 14694–14702. (i) Song, B.; Xie, P.; Li, Y.; Hao, J.; Wang, L.; Chen, X.; Xu, Z.; Quan H.; Lou, L.; Xia, Y.; Houk, K. N.; Yang, W. Pd-Catalyzed Decarboxylative Olefination: Stereoselective Synthesis of Polysubstituted Butadienes and Macrocyclic P-Glyco-Protein Inhibitors. *J. Am. Chem. Soc.* **2020**, *142*, 9982–9992.

[83] It is assumed that the mechanism follows the same elemental steps whether the nucleophilic attack is in the α- or γ-carbon of the Pd-allyl complex.

[84] Trost, B.M.; Morris, P.J.; Sprague, S.J. Palladium-Catalyzed Diastereo- and Enantioselective Formal [3+2]-Cycloadditions of Substituted Vinylcyclopropanes. *J. Am. Chem. Soc.* **2012**, *134*, 17823−17831.

[85] Trost, B. M.; Chan, D. M. T. New Conjunctive Reagents. 2- Acetoxymethyl-3-Allyltrimethylsilane for Methylenecyclopentane Annulations Catalyzed by Palladium (0). *J. Am. Chem. Soc*. **1979**, *101*, 6429−6432.

[86] Shimizu, I.; Ohashi, Y.; Tsuji, J. Palladium-Catalyzed [3+2] Cycloaddition Reaction of Vinylcyclopropanes with A,B-Unsaturated Esters Or Ketones. *Tetrahedron Lett.* **1985**, *26*, 3825-3828.

[87] See for instance: (a) Guo, C.; Fleige, M.; Janssen-Müller, D.; Daniliuc, C. G.; Glorius, F. Cooperative N-Heterocyclic Carbene/Palladium-Catalyzed Enantioselective Umpolung Annulations. *J. Am. Chem. Soc.* **2016**, *138*, 7840−7843. (b) Li, M.-M.; Wei, Y.; Liu, J.; Chen, H.-W.; Lu, L.-Q.; Xiao, W.-J. Sequential Visible-Light Photoactivation and Palladium Catalysis Enabling Enantioselective [4+2] Cycloadditions. *J.Am. Chem. Soc*. **2017**, *139*, 14707−14713.

[88] See for example: (a) Khan, A.; Yang, L.; Xu, J.; Jin, L. Y.; Zhang, Y. J. Palladium-Catalyzed Asymmetric Decarboxylative Cycloaddition of Vinylethylene Carbonates with Michael Acceptors: Construction of Vicinal Quaternary Stereocenters. *Angew. Chem. Int. Ed.* **2014**, *53*, 11257-11260. (b) Cheng, Q.; Zhang, H.-J.; Yue, W.-J.; You S.-L. Palladium-Catalyzed Highly Stereoselective Dearomative [3+2] Cycloaddition of Nitrobenzofurans. *Chem*, **2017**, *3*, 428-436. (c) Wu, Q.-Q; Ding, C.-H.; Hou, X.-L. Pd-Catalyzed Diastereo- and Enantioselective [3+2]-Cycloaddition Reaction of Vinyl Epoxide with Nitroalkenes. *Synlett*, **2012**, *23*, 1035-1038. (d) Shim, J.-G.; Yamamoto, Y. Palladium-Catalyzed Regioselective [3 + 2] Cycloaddition of Vinylic Oxiranes with Activated Olefins. A Facile Synthesis of Tetrahydrofuran Derivatives. *J. Org. Chem.* **1998**, 63, 9, 3067–3071.

[89] Suo, J.-J.; Du, J.; Liu, Q.-R.; Chen, D.; Ding, C.-H.; Peng, Q.; Hou, X.-L. Highly Diastereo- and Enantioselective Palladium-Catalyzed [3 + 2] Cycloaddition of Vinyl Epoxides and α,β-Unsaturated Ketones. *Org. Lett.* **2017**, *19*, 6658–6661.

[90] Li. M.; Liu, Y.; Zhang, Y.J. Route to Chiral Tetrahydrofuran Acetals via Pd-Catalyzed Asymmetric Allylic Cycloaddition of Vinyl Epoxides with β-Keto Enol Ethers. *Org.Lett.* **2022**, *24*, 6716−6721

[91] Liu, K.; Khan, I.; Cheng, J.; Hsueh, Y.-J.; Zhang, Y.-J. Asymmetric Decarboxylative Cycloaddition of Vinylethylene Carbonates with β-Nitroolefins by Cooperative Catalysis of Palladium Complex and Squaramide. *ACS Catal.* **2018**, *8*, 11600-11604.

[92] Du, J.; Jiang, Y.-J.; Suo, J.-J.; Wu, W.-Q; Liu, X.-Y.; Chen, Di; Ding, C.-H.; Wei, Y.; Hou, X.-L. Trisubstituted Alkenes with a Single Activator as Dipolarophiles in a Highly Diastereo- and Enantioselective [3+2] Cycloaddition with Vinyl Epoxides Under Pd-Catalysis. *Chem Commun*. **2018**, *54*, 13143-13146.

[93] Cheng, Q.; Zhang, F.; Yue, C.; Guo, Y.L.; You, S.-L. Stereodivergent Synthesis of Tetrahydrofuroindoles through Pd-Catalyzed Asymmetric Dearomative Formal [3+2] Cycloaddition. *Angew. Chem. Int. Ed.* **2018**, *57*, 2134-2138.

[94] Khan, I.; Zhao, C.; Zhang, Y.-J. Pd-Catalyzed Asymmetric Decarboxylative Cycloaddition of Vinylethylene Carbonates with 3-Cyanochromanones. *Chem. Commun,* **2018**, 54, 4708-4711.

[95] Zhao, C.; Khan, I.; Zhang, Y. J. Enantioselective Total Synthesis of Furofuran Lignans via Pd-Catalyzed Asymmetric Allylic Cycloaddition Of Vinylethylene Carbonates with 2-Nitroacrylates. *Chem. Comm.* **2020**, *56*, 12431-12434.

[96] Huang, K.-X; Xie, M.-S; Wang, D.-C; Sang, J.-Wei; Qu, G.-R.; Guo, H.-M. Palladium-Catalyzed Asymmetric Formal [3+2] Cycloaddition of α-*N*-Heterocyclic Acrylates with Vinyl Epoxides for Construction of Isonucleoside Analogs. *Chem. Commun*, **2019**, *55*, 13550-13553.

[97] Wang, W.-Y; Wu, J.-Y.; Liu, Q.-R.; Liu, X.-Y.; Ding, C.-H; Hou, X.-L. Palladium/N-Heterocyclic Carbene (NHC)-Catalyzed Asymmetric [3+2] Cycloaddition Reaction of Vinyl Epoxides with Allenic Amides. *Org. Lett*. **2018**, *20*, 4773-4776.

[98] Liu, J.; Yu, L.; Zheng, C.; Zhao, G. Asymmetric Synthesis of 2,2-Difluorotetrahydrofurans through Palladium-Catalyzed Formal [3+2] Cycloaddition. *Angew. Chem. Int. Ed.* **2021**, *60*, 23641–23645

[99] For some reviews and examples, see: (a) Chupakhin, E.; Babich, O.; Prosekov, A.; Asyakina, L.; Krasavin, M. Spirocyclic Motifs in Natural Products. *Molecules* **2019**, *24*, 4165. (b) Yadav, P.; Pratap, R.; Ji Ram, V. Naturaland Synthetic Spirobutenolides and Spirobutyrolactones. *Asian J. Org.Chem*. **2020**, *9*, 1377−1409. (c) Xie, J.; Wang, J.; Dong, G. Synthetic Study of Phainanoids. Highly Diastereoselective Construction of the 4,5-Spirocycle via Palladium-Catalyzed Intra-molecular Alkenylation. *Org. Lett.* **2017**, *19*, 3017−3020. (d) Half-penny, P. R.; Horwell, D. C.; Hughes, J.; Hunter, J. C.; Rees, D. C. Highly Selective Kappa-Opioid Analgesics. 3. Synthesis and Structure-Activity Relationships of Novel N-[2-(1-Pyrrolidinyl)-4- Or −5-Substituted Cyclohexyl]Arylacetamide Derivatives. *J. Med. Chem*. **1990**, *33*, 286−291. (e) Katsoulis, I. A.; Kythreoti, G.;Papakyriakou, A.; Koltsida, K.; Anastasopoulou, P.; Stathakis, C. I.;Mavridis, I.; Cottin, T.; Saridakis, E.; Vourloumis, D. Synthesis of 5,6-Spiroethers and Evaluation of their Affinities for the Bacterial A Site. *ChemBioChem*. **2011**, *12*, 1188−1192. (f) Yang, L.; Morriello, G.;Prendergast, K.; Cheng, K.; Jacks, T.; Chan, W. W.-S.; Schleim, K. D.;Smith, R. G.; Patchett, A. A. Potent 3-Spiropiperidine Growth hormone Secretagogues. *Bioorg. Med. Chem. Lett*. **1998**, *8*, 107−112.

[100] Ma, C.; Huang, Y.; Xhao, Y. Stereoselective 1,6-Conjugate Addition/Annulation of *para*-Quinone Methides with Vinyl Epoxides/Cyclopropanes. *ACS. Catal.* **2016**, *6*, 6408−6412.

[101] Xiao, J.-A.; Li, Y.-C.; Luo, Z.-J.; Cheng, X.-L.; Deng, Z.-X; Chen, W.-Q.; Su, W.; Yang, H. Construction of Bispirooxindole Heterocycles via Palladium-Catalyzed Ring-Opening Formal [3+2]-Cycloaddition of Spirovinylcyclopropyl Oxindole and 3-Oxindole Derivatives. *J. Org. Chem*. **2019**, 84, 2297-2306.

[102] Wang, J.; Zhao, L.; Rong, Q.; Lv, C.; Lu. Y.; Pan, X; Zhao, L.; Hu, L. Asymmetric Synthesis of 3,3'-Tetrahydrofuryl Spirooxindoles via Palladium-Catalyzed [3+2] Cycloadditions of Methyleneindolinones with Vinylethylene Carbonates. *Org. Lett*, **2020**, 5833-5838.

[103] Zhang, H.; Gao, X.; Jiang, F.; Shi, W.; Wang, W.; Wu, Y.; Zhang, C.; Shi, X.; Guo, H. Palladium-Catalyzed Asymmetric [3+2] Cycloaddition of Vinylethylene Carbonates with 2-Arylidene-1,3-

Indanones: Synthesis of Tetrahydrofuran-Fused Spirocyclic 1,3-indandiones. *Eur. J. Org. Chem*. **2020**, *30*, 4301-4804.

[104] Jeon, H.J.; Park, S.M.; Lee, Y.M.; Lee, S.-G. Divergent Asymmetric Synthesis of Chiral Spiroheterocycles through Pd-Catalyzed Enantio-and Diastereoselective [3+2] Spiroannulation. *Org. Lett*. **2022**, *24*, 9189−9193.

UNIVERSITAT ROVIRA I VIRGILI
DEVELOPMENT OF CHIRAL METAL-CATALYSTS FOR THE SELECTIVE FORMATION OF C-H, C-C AND C-X BONDS. FROM DESIGN TO APPLICATION
Pol De La Cruz Sanchez Badia

CHAPTER 2

Objectives

UNIVERSITAT ROVIRA I VIRGILI
DEVELOPMENT OF CHIRAL METAL-CATALYSTS FOR THE SELECTIVE FORMATION OF C-H, C-C AND C-X BONDS. FROM DESIGN TO APPLICATION
Pol De La Cruz Sanchez Badia

2. Objectives

The general objective of this thesis is to improve the state of the art in the design, synthesis and screening of catalysts for the following transformations: (1) Rh- and Ir-catalyzed asymmetric hydrogenation of olefins, (2) Pd-catalyzed asymmetric allylic substitution and (3) Pd-catalyzed [3+2] cycloaddition of vinyl heterocycles to double stabilized Michael acceptors. These processes have been chosen for their green chemistry properties and their industrial interest, since they give rise to chiral products with a high added value. Although they have a long history behind, our goal is to reach challenging substrates and novel combination of substrate/nucleophile/dipolarophile. For transformations (1) and (2) tailor-made ligand libraries, specially designed with the needs of the substrates/nucleophiles under study, will be prepared. In their design we have taken into account their industrial applicability (synthetized in few steps and from inexpensive starting materials, and simple manipulation). For the [3+2] cycloaddition reactions previously known ligands would be tested. The specific objectives for each transformation are:

1. The specific aims for the Rh and Ir-catalyzed asymmetric hydrogenation are:

1.1. To synthesize a modular easy-to-synthetize P-stereogenic *N*-phosphine-phosphite ligand library (**L1**–**L3**, Figure 2.1) for the ***Rh-catalyzed asymmetric hydrogenation*** of relevant chelating olefins. Ligands **L1**–**L3** possess a chiral phosphine moiety, with different R substituents (Me, *o*-anisyl and *i*-Pr), and several biaryl phosphite moieties (**a**–**c**) and a simple readily available ligand backbone. For comparison, ligands **L4b**–**c** without chirality on the phosphorous atom were also synthesized and applied.

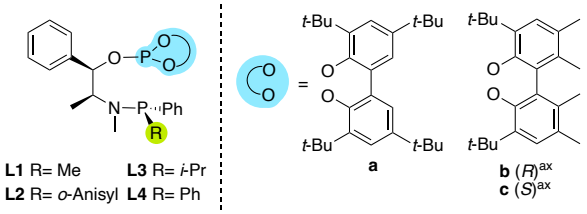

Figure 2.1. P-stereogenic *N*-phosphine–phosphite ligands **L1**–**L3a**–**c** and *N*-phosphine-phosphite ligands **L4b**–**c**.

1.2. To synthesize several tailor-made heterodonor ligand libraries (which consider the needs of the substrates under study) for the ***Ir-catalyzed asymmetric hydrogenation*** of olefins. Two of them are P-oxazoline/triazole ligand libraries (P= *N*-phosphine or phosphine moiety) and three of them are P-S/C ligand libraries (P= phosphite and phosphinite; S= thioether; C= carbene). The specific ligand libraries are collected below.

1.2.1. The P-stereogenic aminophosphine–oxazoline ligand library **L5**–**L8a**–**c** (Figure 2.2), specially synthetized to solve the substrate specificity of the Ir-catalyzed asymmetric hydrogenation of di-, tri- and tetrasubstituted non-chelating olefins. This family of ligands, prepared in only three steps from available starting materials, combine the advantages that a P-stereogenic moiety near the metal center can provide, together with an easy variation of the bulkiness of the oxazoline (R) and of its configuration and the configuration of the stereogenic center at the alkyl backbone chain. Mechanistic studies were also performed to uncover the factors responsible for enantioselectivities and to find the most suitable substrates.

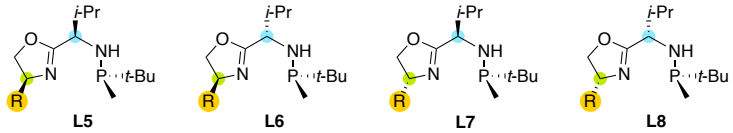

a R= Ph; **b** R= *i*-Pr; **c** R= *t*-Bu

Figure 2.2. P-stereogenic aminophosphine–oxazoline ligand library **L5**–**L8a**–**c**.

1.2.2. The phosphine-triazole ligands **L9**–**L10** (Figure 2.3) specially designed to solve the asymmetric hydrogenation of exocyclic benzofused based non-chelating alkenes. They are based on the phosphine-oxazolines PHOX in which a chiral carbon spacer has been added between the oxazoline and the phenyl ring to increase its flexibility. The oxazoline moiety has also been replaced by a triazole with the aim to facilitate the stabilization of the substrate in the catalyst chiral pocket via N---H interactions. The ligand design has been completed by attaching a silyl group on the carbon spacer, according to the Pfaltz's first generation of phosphine-pyridine design, that showed a positive effect on catalytic performance of this silyl group due its interaction with the active site of the catalysts. Mechanistic studies were performed to explain the origin of enantioselectivity.

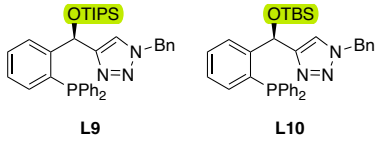

Figure 2.3. Phosphine-triazole ligands **L9**–**L10**.

1.2.3. The phosphite/phosphinite-thioether ligand library **L11**–**L18a**–**f** (Figure 2.4) for the Ir-catalyzed hydrogenation of a broad scope of olefins with a variety of coordination abilities, ranging from non-chelating olefins, through olefins with poorly coordinative groups to olefins with a coordinative functional group. The thioether moiety imparts higher stability with respect to commonly used oxazolines and involves the introduction of an additional chiral center close to the metal with a different steric environment around the metal center than that exerted by the

oxazoline group. This air stable ligand library was synthesized in only three steps from inexpensive indene and allowed easy variation of both, thioether (R) and P-donor moieties (**a**–**f**).

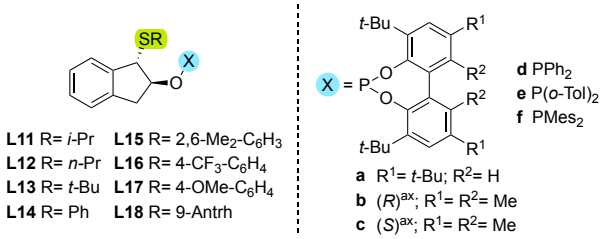

Figure 2.4. Phosphite/phosphinite-thioether ligands **L11**–**L18a**–**f**.

1.2.4. Two carbene-thioether ligand families, designed with the aim to combine the advantages of thioether and *N*-heterocyclic carbene functionalities. *N*-heterocyclic carbenes have emerged as powerful alternatives for phosphine-containing ligands thanks to their strong σ-donor ability, air stability and robustness. Concretely, we synthesized and applied:

1.2.4.1. The first example of mixed carbene-thioether compounds **L19**–**L20H·Br** (Figure 2.5) for the Ir-catalyzed asymmetric hydrogenation of alkenes, including cyclic β-enamides. For comparison, we also synthesized their related phosphite/phosphinite-thioether ligands **L21**–**L22a**–**e** (Figure 2.5).

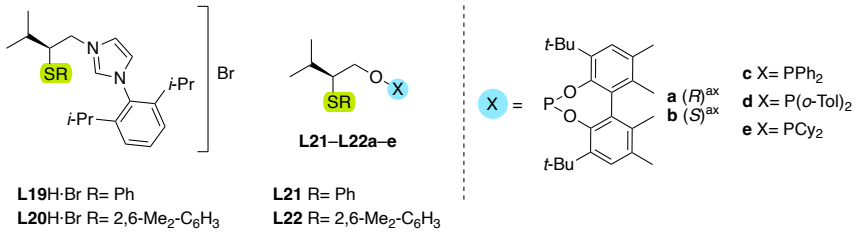

Figure 2.5. Carbene-thioether ligands **L19**–**L20**H·Br and their phosphite/phosphinite-thioether analogues **L21**–**L22a-e**.

1.2.4.2. The chiral ferrocene-based carbene-thioether compounds **L23**–**L30**H·Cl (Figure 2.6) for the Ir-catalyzed hydrogenation of alkenes. These carbene-thioether ligands incorporate the advantages in asymmetric catalysis of a ferrocene backbone and a bigger chelating ring size after coordination to Ir than previous carbene-thioether ligands **L19**–**L20**, to study their effect on the catalytic performance.

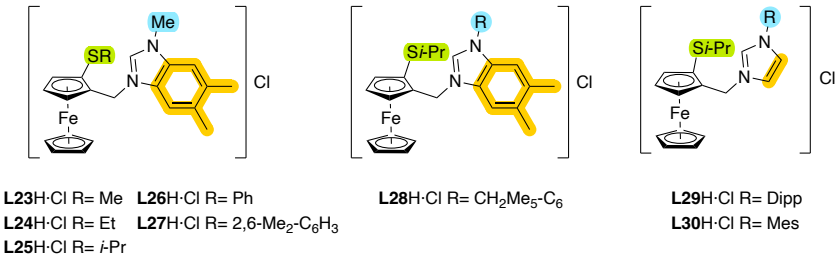

L23H·Cl R= Me **L26**H·Cl R= Ph
L24H·Cl R= Et **L27**H·Cl R= 2,6-Me_2-C_6H_3
L25H·Cl R= *i*-Pr

L28H·Cl R= CH_2Me_5-C_6

L29H·Cl R= Dipp
L30H·Cl R= Mes

Figure 2.6. Chiral ferrocene-based carbene-thioether compounds **L23**–**L30**H·Cl.

2. For the ***Pd-catalyzed asymmetric allylic substitution***, we tested a small library of easy to handle (solid and air stable) phosphite-oxazoline ligands **L31**–**L33a**–**c** (Figure 2.7). These ligands, which are readily available in only two synthetic steps, are derived from the PHOX ligand by replacing the phosphine moiety by biaryl phosphites and by introducing a methylene spacer between the oxazoline and the phenyl ring. These simple modifications allowed to increase the substrate and nucleophile scope of the PHOX ligands thanks to their ability to adapt the ligand parameters to the reacting substrate.

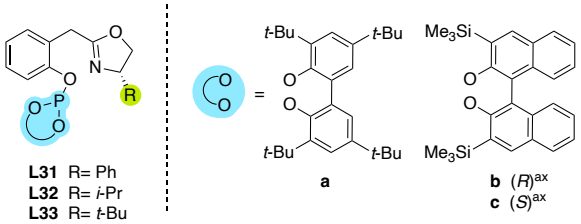

L31 R= Ph
L32 R= *i*-Pr
L33 R= *t*-Bu

a

b $(R)^{ax}$
c $(S)^{ax}$

Figure 2.7. Phosphite-oxazoline ligands **L31-L33a-c**.

3. With the aim to prepare structurally complex tetrahydrofuran-fused spirocyclic scaffolds we also studied novel ***Pd-catalyzed [3+2] cycloaddition reaction*** of vinyl epoxides with 5-alkylidene Meldrum's acid derivatives (Figure 2.8) using several previously known ligands.

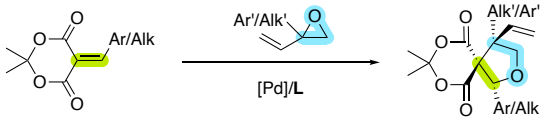

Figure 2.8. Pd-catalyzed [3+2] cycloaddition to construct structurally complex tetrahydrofuran-fused spirocyclic scaffolds.

CHAPTER 3

Rh- and Ir-catalyzed asymmetric hydrogenation

UNIVERSITAT ROVIRA I VIRGILI
DEVELOPMENT OF CHIRAL METAL-CATALYSTS FOR THE SELECTIVE FORMATION OF C-H, C-C AND C-X BONDS. FROM DESIGN TO APPLICATION
Pol De La Cruz Sanchez Badia

3.1. P-stereogenic *N*-phosphine-phosphite ligands for the Rh-catalyzed asymmetric hydrogenation of chelating olefins

3.1.1. Introduction

Catalytic asymmetric hydrogenation is one of the most reliable transformations for the preparation of enantiopure compounds. Its operational simplicity, high efficiency and perfect atom economy are key aspects that explain its predominant role in industry.[1] Over the years the scope of this transformation has been extended in terms of reactant structure and catalyst efficiency. Thus, while chiral analogues of the Ir-Crabtree catalyst dominate the reduction of non-chelating olefins,[2] the hydrogenation of chelating olefins is dominated by Rh- and Ru-catalysts containing chiral diphosphine, diphosphinite and diphosphite ligands.[3] Despite the early success of the P-stereogenic diphosphine ligand DIPAMP,[4] used in the industrial production of L-DOPA (a drug used to treat Parkinson's disease),[5] most of the diphosphine ligands have been designed by introducing the stereogenic center at the ligand backbone rather than in the P-atoms, thus losing the advantage that a stereogenic center near the metal center can provide.[3] The main reason for this placement is the difficulty in the preparation of phosphines bearing the chirality on the P atom. With the development of new, straightforward methodologies to obtain the chirality on the phosphine moiety, some P-stereogenic phosphine ligands have emerged and been successfully applied in this process (e.g. QuinoxP*, BenzP*, Binapine, Zhangphos, Duanphos, BIBOP, TCFP, MaxPHOS, etc.; Figure 3.1.1).[6]

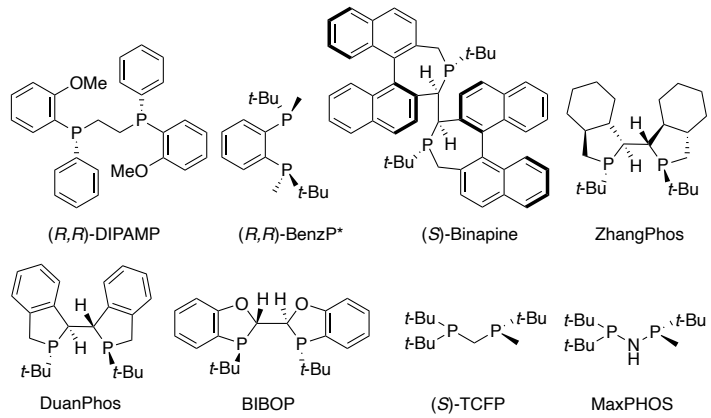

Figure 3.1.1. Example of some representative P-stereogenic diphosphine ligands.

Rh-catalyzed asymmetric hydrogenation has also benefited from the use of heterodonor ligands. The presence of the two functionalities not only enables electronic differentiation, but also facilitates catalyst optimization, since both functionalities can be independently boosted. Among the heterodonor ligands, mixed P,P'-ligands have been successfully applied in the Rh-catalyzed asymmetric hydrogenation of a broad

range of chelating substrates.[1i,7] Among them, ligands combining a phosphine group with a more π-acceptor phosphorus moiety (i.e., phosphite or phosphoromidite) have demonstrated a high potential in this process. In this context, some research groups made significant contributions in terms of substrate scope with the development of phosphine-phosphite/phosphoromidite ligands.[8,9] Nevertheless, for this latter class of ligands, the introduction of a P-stereogenic phosphine moiety on the ligand design has been overlooked.[8b,10] One of the simplest ways to introduce a P-stereogenic center is to use Jugé's approach using a chiral 1,2-aminoalcohol as the template.[11] Following this procedure, some P-stereogenic *N*-phosphine-phosphinite ligands were developed for this process.[12] To best of our knowledge, there is only one report by Kamer et al. more than 10 year ago on the use of heterodonor P-stereogenic *N*-phosphine-phosphite ligands.[13] They showed the application of a series of resin-bound P-stereogenic *N*-phosphine-phosphite ligands in the asymmetric hydrogenation of a limited range of α-dehydroamino acids, with only moderate to good enantioselectivities (ee's up to 89%). To further study the possibilities of this ligand design, we have expanded the range of ligands to include other substituents in the stereogenic *N*-phosphine group (ligands **L1**–**L3**; Figure 3.1.2) and other biaryl phosphite functionalities (**a**–**c**). In addition, for comparison, we also synthesized ligands **L4b**–**c** without chirality on the *N*-phosphine moiety.[14]

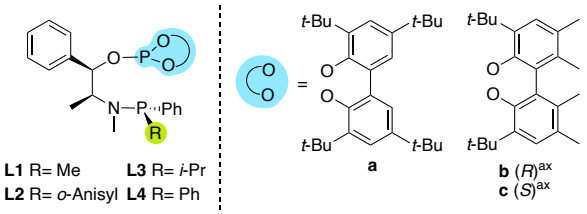

Figure 3.1.2. P-stereogenic *N*-phosphine-phosphite ligands **L1**–**L3a**–**c** and *N*-phosphine-phosphite ligands **L4b**–**c**.

3.1.2. Results and discussion

3.1.2.1. Synthesis of ligands

Ligands **L1**–**L4a**–**c** were easily accessible from readily available (1*R*,2*S*)-(−)-ephedrine **1** (Scheme 3.1.1). The synthesis of ligands **L1**–**L3a**–**c** started with the condensation of **1** with bis(diethylamino)phenyl phosphine followed by *in situ* protection of the P atom to obtain the key intermediate: borane-protected oxazaphospholidine **2** (Scheme 3.1.1, step (i)).[15] Then, the ring opening of **2** with the corresponding organolithium reagent resulted in exclusive cleavage of the P-O bond to give the desired hydroxyl compounds **3**–**5** (Scheme 3.1.1 , step (ii)).[15] The ring opening of compound **2** proceeded with retention of the configuration at the phosphorus atom, leading to the corresponding enantiopure compounds after recrystallization. The reaction of **3**–**5** with the desired phosphorochloridite ($ClP(OR)_2$; $(OR)_2$= **a**–**c**; Scheme 3.1.1, step (iii)) under

basic conditions followed by deprotection of the P-stereogenic *N*-phosphine moiety lead to ligands **L1**–**L3a**–**c**. Note that, for ligands **L2b** and **L2c**, the deprotection of phosphine takes place during the introduction of the phosphite moiety. Ligands **L4** were obtained in a two-step procedure by coupling **1** with the desired phosphorochloridite (Scheme 3.1.1, step (iii)) to form amino-phosphites **6**, followed by the subsequent reaction of these intermediates with chlorodiphenylphosphine (Scheme 3.1.1, step (v)).

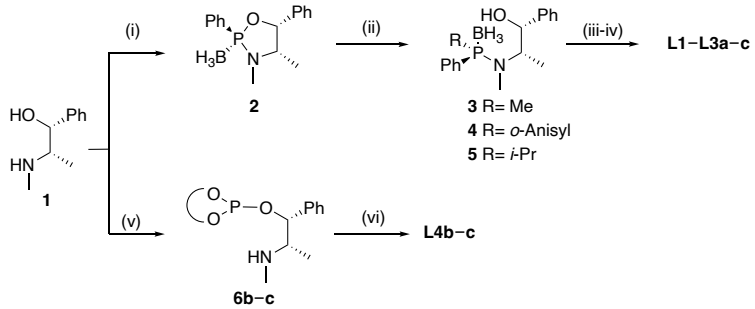

Scheme 3.1.1. Synthethic route for the preparation of *N*-phosphine-phosphite ligands **L1**–**L4a**–**c**: (i) $P(NEt_2)_2Ph$, toluene, reflux, 16 h then $BH_3{\cdot}(CH_3)_2S$, rt, 12 h; (ii) RLi, THF, -78 ºC, 30 min-16 h; (iii) $ClP(OR)_2$; $(OR)_2$=**a**–**c**, NEt_3, DMAP, toluene, 80 ºC, 16 h; (iv) $NHEt_2$, reflux, 16 h; (v) $ClP(OR)_2$; $(OR)_2$=**b**–**c**, NEt_3, DMAP, toluene, rt, 4 h; (vi) $ClPPh_2$, THF, NEt_3, 55 ºC, 16 h.

All ligands were obtained as white solids after purification on neutral silica or alumina and were stable to oxidation under air atmosphere if kept at low temperature. The ligands were therefore manipulated and stored in the air, and it was not necessary to use a dry box. All characterization data (NMR and HRMS-ESI) were as expected for these C_1-symmetric ligands. Thus, for example the ^{31}P NMR spectra showed the two typical signals for the phosphite (ca. 150 ppm), and for the *N*-phosphine (ca. 68 ppm) functionalities.

3.1.2.2. Asymmetric hydrogenation of chelating olefins

3.1.2.2.1. Rh-catalyzed hydrogenation of α-dehydroamino acid derivatives

In a first step of experiments, we evaluated *N*-phosphine-phosphite ligands **L1**–**L4a**–**c** in the Rh-catalyzed asymmetric hydrogenation of benchmark α-dehydroamino acid derivatives, methyl 2-acetamidoacrylate **S1** and methyl 2-acetamidocinnmate **S2** (Table 3.1.1). Full conversion was obtained in all cases after only two hours of reaction. Comparing the results obtained with ligands **L1a**–**c**, the fact that the highest enantioselectivity is obtained with ligand **L1c** indicates that the ephedrine ligand backbone is not able to control the tropoisomerism of the biaryl phosphite moiety **a** upon coordination to the rhodium (Table 3.1.1, entry 1 vs 2 and 3). It is also seen that there is a cooperative effect between the configuration of the biaryl phosphite group and that of the *N*-phosphine moiety that results in a matched combination for ligands

containing the enantiopure (*S*)-biaryl phosphite moiety **c** (e.g., Table 3.1.1, entry 3 vs 1 and 2). These results agree with the lower activities and enantioselectivities reported by Kamer et al. with related P-sterogenic *N*-phosphine-phosphite ligands with an achiral unsubstituted biaryl phosphite moiety.[16] We also found that the amino-phosphine substituent affect the catalytic performance (Table 3.1.1, entries 3, 5 and 7). Thus, the best enantioselectivity (>99%) was achieved with ligand **L2c**, with a bulky *o*-anisyl substituent at the P-stereogenic *N*-phosphine group. Finally, although enantioselectivities up to 96% ee (Table 3.1.1, entry 9) could be achieved with ligand **L4c**, with a diaryl *N*-phosphine group, the presence of a P-stereogenic unit is crucial to maximize enantioselectivities, up to ≥99% ee for both substrates (Table 3.1.1, entry 5). In summary, the best enantioselectivity was obtained with ligand **L2c** which contains the best combination of ligand parameters.

Interestingly, we also found that the replacement of THF for a more environmentally friendly solvent such as 1,2-propylene carbonate (PC)[17] did not deteriorate activity or enantioselectivity (Table 3.1.1, entry 10, 99% ee).

Table 3.1.1. Asymmetric hydrogenation of α-dehydroamino acid derivatives **S1** and **S2** using Rh/**L1**–**L4a**–**c** catalyst precursors.[a]

		 **S1**		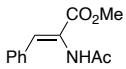 **S2**	
Entry	Ligand	% Conv[b]	% ee[c]	% Conv[b]	% ee[c]
1	**L1a**	100	61 (*R*)	100	61 (*R*)
2	**L1b**	100	66 (*R*)	100	64 (*R*)
3	**L1c**	100	85 (*R*)	100	80 (*R*)
4	**L2b**	100	40 (*R*)	100	37 (*R*)
5	**L2c**	100 (96)	99 (*R*)	100 (97)	>99 (*R*)
6	**L3b**	100	25 (*S*)	100	7 (*R*)
7	**L3c**	100	81 (*R*)	100	68 (*R*)
8	**L4b**	100	50 (*S*)	100	52 (*S*)
9	**L4c**	100	94 (*R*)	100	96 (*R*)
10[d]	**L2c**	99	99 (*R*)	95	99 (*R*)

[a] Reaction conditions: $[Rh(cod)_2]BF_4$ (1 mol%), ligand (1 mol%), substrate (0.25 mmol), THF (2 mL), H_2 (25 bar), 2 h at rt. [b] Conversions measured by GC. Isolated yields shown in parenthesis. [c] Enantiomeric excesses determined by GC. [d] Reaction carried out using PC as solvent. Conversion measured after 1 h.

3.1.2.2.2. Rh-catalyzed hydrogenation of β-dehydroamino acid derivatives and enamides

We then proceeded to study ligands **L1**–**L4a**–**c** in the hydrogenation of β-dehydroamino acid derivatives (Table 3.1.2). The hydrogenation of such type of substrates lead to important motifs present in many biologically active products (e.g., β-peptides and secondary amines, respectively). In most reported cases, the hydrogenation of β-dehydroamino acid derivatives is highly dependent upon the olefin geometry, since *Z*-isomers more difficult to be efficiently hydrogenated than the *E*-olefins.[18,19] We therefore chose *E*- and *Z*-methyl 3-acetamido-3-phenylacrylates (**S3** and **S4**) as model substrates. We obtained higher ee's in the hydrogenation of the *Z*-olefin than for the *E*-olefin. As expected, each isomer needs a different ligand to maximize the enantioselectivity. The ligands differ in the substituent of the P-stereogenic *N*-phosphine group and both have *S* configuration in the biaryl phosphite moiety. Thus, while for substrate **S3** (with *E*-geometry) the use of ligand **L2c**, with a bulky *o*-anisyl substituent at the P-stereogenic *N*-phosphine group, provided the best enantioselectivity (Table 3.1.2, entry 5, 60% ee), the ligand **L1c** afforded the best ee's for substrate **S4** (with *Z*-geometry; Table 3.1.2, entry 3, 80% ee). Results also showed that for this substrate the P-stereogenic *N*-phosphine moiety is crucial to achieve good enantioselectivities (the use of ligands **L4** led to poor ee's; Table 3.1.2, entries 8 and 9, up to 25% ee).

Table 3.1.2. Asymmetric hydrogenation of β-dehydroamino acid derivatives **S3** and **S4** Rh/**L1**–**L4a**–**c** catalyst precursors.[a]

		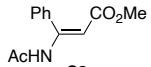 **S3**		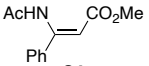 **S4**	
Entry	Ligand	% Conv[b]	% ee[c]	% Conv[b]	% ee[c]
1	**L1a**	100	14 (*R*)	100	31 (*R*)
2	**L1b**	100	3 (*S*)	100	21 (*S*)
3	**L1c**	100	22 (*R*)	100 (93)	80 (*R*)[d]
4	**L2b**	100	3 (*R*)	100	8 (*S*)
5	**L2c**	100 (94)	60 (*R*)[d]	100	20 (*S*)
6	**L3b**	100	15 (*S*)	100	76 (*S*)
7	**L3c**	100	2 (*S*)	100	15 (*R*)
8	**L4b**	100	25 (*R*)	100	15 (*S*)
9	**L4c**	100	16 (*R*)	100	1 (*S*)

[a] Reaction conditions: $[Rh(cod)_2]BF_4$ (1 mol%), ligand (1 mol%), substrate (0.25 mmol), THF (2 mL), H_2 (25 bar), 2 h at rt. [b] Conversions measured by GC. Isolated yields shown in parenthesis. [c] Enantiomeric excesses determined by GC or HPLC. [d] Full conversions and the same ee's were achieved using PC as solvent under typical reaction conditions.

Regarding the asymmetric hydrogenation of enamides, we selected *N*-(1-(4-methoxyphenyl)vinyl)acetamide **S5**, *N*-(3,4-dihydro-1-naphthalenyl)acetamide **S6**, *N*-(2H-chromen-4-yl)acetamide **S7** and *N*-(3,4-dihydro-2-naphthalenyl)acetamide **S8** as substrates (Table 3.1.3). High enantioselectivities have been obtained in α-enamide **S5** and the more challenging cyclic α-enamides **S6** and **S7**, for which only a few successful examples can be found in the literature.[20] Again, the results indicated that the ligand parameters have to be carefully selected for each substrate to maximize enantioselectivity. For instance, the highest enantioselectivities (ee's up to 96%) for the asymmetric hydrogenation of acyclic α-enamide **S5** were obtained using ligands **L1b** and **L1c**, with a methyl at the P-stereogenic *N*-phosphine group (Table 3.1.3, entries 2 and 3), while ligand **L2c** provided the highest ee's for cyclic α-enamides **S6** and **S7** (Table 3.1.3, entry 5, ee's up to 95%). In addition, for acyclic α-enamide **S5**, both enantiomers of the hydrogenated product were accessible by simply varying the configuration of the biaryl phosphite moiety (Table 3.1.3, entries 2 and 3). Although the hydrogenation of β-enamide **S8** proceeded with lower enantiocontrol (Table 3.1.3, entry 9, up to 80% ee) than for α-enamides, this was not unexpected, since the cyclic β-enamides are one of the most challenging substrates for this transformation.[20d,21]

Table 3.1.3. Asymmetric hydrogenation of enamides **S5**–**S8** using Rh/**L1**–**L4a**–**c** catalyst precursors.[a]

		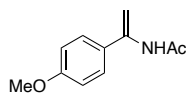	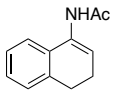	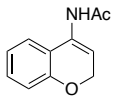	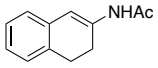
		S5	**S6**	**S7**	**S8**
Entry	Ligand	% ee[b]	% ee[b]	% ee[b]	% ee[b]
1	**L1a**	80 (*S*)	35 (*R*)	38 (*R*)	58 (*R*)
2	**L1b**	96 (*R*)[c,d]	53 (*S*)	51(*S*)	7 (*R*)
3	**L1c**	96 (*S*)[e]	74 (*R*)	73 (*R*)	55 (*R*)
4	**L2b**	64 (*S*)	5 (*S*)	2 (*S*)	17(*S*)
5	**L2c**	84 (*S*)	95 (*R*)[c,f]	94(*R*)[g]	44 (*R*)
6	**L3b**	76 (*S*)	61 (*R*)	63 (*R*)	5 (*S*)
7	**L3c**	2 (*R*)	24 (*S*)	22 (*S*)	4 (*R*)
8	**L4b**	7 (*R*)	2 (*R*)	1 (*R*)	9(*S*)
9	**L4c**	82 (*S*)	84 (*R*)	85 (*R*)	80 (*R*)[c,h]
10[d]	**L2c**	80 (*S*)	35 (*R*)	38 (*R*)	58 (*R*)

[a] Reaction conditions: $[Rh(cod)_2]BF_4$ (1 mol%), ligand (1 mol%), substrate (0.25 mmol), THF (2 mL), H_2 (25 bar), 2 h at rt. Full conversions were achieved in all cases. [b] Enantiomeric excesses determined by GC or HPLC. [c] Full conversions and the same ee's were achieved using PC as solvent under typical reaction conditions. [d] 92% yield. [e] 90% yield. [f] 93% yield. [g] 87% yield. [h] 91% yield.

We also performed the reactions in 1,2-propylene carbonate (Table 3.1.3). The enantioselectivities remained as high as those achieved with THF.

3.1.2.2.3. Rh-catalyzed hydrogenation of synthethically relevant chelating olefins

Encouraged by the previous results, we finally targeted substrates **S9**–**S13**, whose hydrogenation led to valuable chiral synthons for the synthesis of a range of drugs such as compound LY2497282,[22] receptor antagonist CCK1/CCK2,[23] analgesic SDZNKT343,[24] a renin inhibitor,[25] and AZ960 and JAK2 kinase inhibitors[26] (Figure 3.1.3). In all cases reactions proceeded smoothly with an excellent enantiocontrol (Scheme 3.1.2). Finally, it should be noted that ligands **L1**–**L4** are very robust to the different substrate decorations. Thus, the ee's (up to >99%) achieved in the hydrogenation of **S9**–**S13** are at least as high as the best achieved in the literature.[27] In addition, the hydrogenation can also be carried out at large scale (see the hydrogenation of **S9** and **S13** as examples) maintaining the high enantioselectivities.

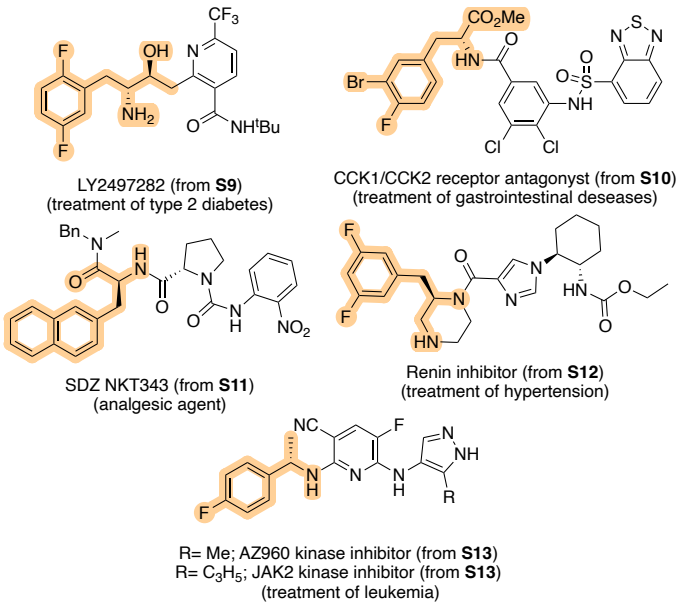

Figure 3.1.3. Examples of chiral drugs that can be synthesized by using asymmetric hydrogenation.

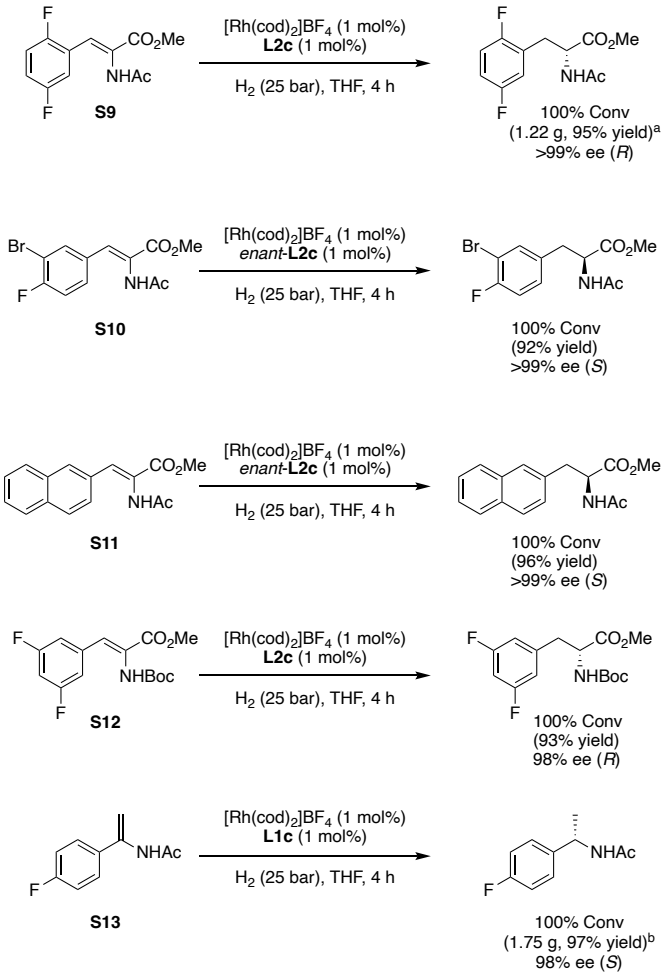

Scheme 3.1.2. Asymmetric hydrogenation of several valuable chiral synthons **S9**–**S13** with Rh/**L1**–**L4a**–**c** catalysts. [a] Rection carried out at 5 mmol scale. [b] Reaction carried out at 10 mmol scale.

3.1.3. Conclusions

In summary, we have identified a successful family of P-stereogenic *N*-phosphine-phosphite ligands with a simple backbone for the Rh-catalyzed asymmetric hydrogenation of chelating olefins (ee's up to >99%). All ligands can be modulated by a simple and efficient synthetic route from readily available sources. This modularity was key in finding the most efficient catalyst for the reduction of each type of olefin. A chiral biaryl phosphite moiety and a P-stereogenic *N*-phosphine group with the right choice of its substituent are needed to maximize the enantioselectivity. The exception is substrate **S8** that also has good enantioselectivity with an achiral *N*-phosphine group. Moreover, the reactions can be carried out in the environmentally friendly 1,2-propylene

carbonate solvent with no loss of enantioselectivity. Finally, in order to evaluate the potential impact of these Rh/P-sterogenic *N*-phosphine-phosphite catalysts in synthesis, we applied them to the synthesis of several chiral synthons for the preparation of pharmacological compounds, with ee's at least as high as the best ones reported (up to >99%). These results pave the way for the further development of new generation of modular P-stereogenic *N*-phosphine-phosphite ligands with a simple ligand backbone that are readily available and easy-to-synthesize, for the asymmetric hydrogenation of relevant olefins.

3.1.4. Experimental section

3.1.4.1. General considerations

All reactions were carried out using standard Schlenk techniques under an argon atmosphere. Solvents were purified and dried by standard procedures. Borane-protected oxazaphospholidine **2**,[15] borane-protected *N*-phosphine-hydroxyl compounds **3**–**5**[15] and phosphorochloridites[28] were prepared as previously reported. ^{1}H, ^{13}C{^{1}H}, and ^{31}P{^{1}H} NMR spectra were recorded using a 400 MHz spectrometer. Chemical shifts are relative to that of $SiMe_4$ (^{1}H and ^{13}C) as internal standard or H_3PO_4 (^{31}P) as external standard. ^{1}H, ^{13}C, and ^{31}P assignments were made on the basis of ^{1}H-^{1}H gCOSY, ^{1}H-^{13}C gHSQC and ^{1}H-^{31}P gHMBC experiments. Electrospray ionization (ESI) mass spectrometry analysis were run on a chromatographic system, an Agilent G3250AA liquid chromatography coupled to 6210 time of flight (TOF) mass spectrometer from Agilent Technologies with an ESI interface. Exact m/z values are reported in daltons. Substrates **S2**,[29] **S3**–**S4**,[30] **S5**,[31] **S6**–**S7**,[32] **S8**,[33] **S9**,[22] **S10**,[8f] **S11**,[27f] **S12**[8e] and **S13**[34] were prepared following the reported procedures, while substrate **S1** was commercially available and used as received. For characterization and ee determination details as well as copies of the NMR spectra and GC or HPLC traces see Supporting Information.

3.1.4.2. General procedure for the preparation of P-stereogenic *N*-phosphine-phosphite ligands L1–L3a–c

To a solution of *in situ* generated phosphorochloridite (1.1 mmol) in dry toluene (6 mL), was added triethylamine (0.27 mL, 2.0 mmol). Then, this solution was placed in a 0 ºC bath. After 2 min at that temperature, a solution of the corresponding borane-protected *N*-phosphine-hydroxyl compound (1.0 mmol) and triethylamine (0.27 mL, 2.0 mmol) in toluene (6 mL) was added dropwise at 0 °C. The mixture was left to warm to 80 ºC using an oil bath and stirred overnight at this temperature. The precipitate formed was filtered under argon and the solvent was evaporated under vacuum. The residue was purified by flash chromatography or by filtration over neutral silicato afford **L1**·BH_3**a**–**c**, **L2b**–**c** and **L3**·BH_3**b**–**c** as white solids.

L1a·BH_3: Yield: 367 mg (60%) (flash chromatography under argon, using neutral silica and dry toluene/hexane (1:1) as eluent system (1% NEt_3)). $^{31}P\{^1H\}$ NMR (161.9 MHz, C_6D_6): δ= 149.5 (bs, P-O), 68.6 (bs, P-N). ^1H NMR (400 MHz, C_6D_6): δ= 1.10 (pt, 6H, CH_3-CH, CH_3-P, *J*= 8.6 Hz), 1.18 (s, 9H, CH_3, *t*-Bu), 1.24 (s, 9H, CH_3, *t*-Bu), 1.49 (s, 18H, CH_3, *t*-Bu), 1.95 (d, 3H, CH_3-N, $^3J_{H-P}$= 8.2 Hz), 4.38-4.44 (m, 1H, CH-N), 5.51-5.54 (m, 1H, CH-O), 6.82-6.85 (m, 2H, CH=), 6.98-7.12 (m, 7H, CH=), 7.21 (s, 1H, CH=), 7.27 (s, 1H, CH=), 7.48-7.54 (m, 3H, CH=). $^{13}C\{^1H\}$ NMR (100.6 MHz, C_6D_6): δ= 10.8 (d, CH_3-P, J_{C-P}= 39.1 Hz), 13.4 (CH_3-CH), 28.4 (d, CH_3-N, J_{C-P}= 2.9 Hz), 31.0 (CH_3, *t*-Bu), 31.1 (CH_3, *t*-Bu), 31.2 (CH_3, *t*-Bu), 34.2 (d, C, *t*-Bu, J_{C-P}= 8.1 Hz), 35.2 (C, *t*-Bu), 57.8 (CH-N), 81.3 (CH-O), 124.0-146.4 (aromatic carbons). HRMS (ESI-TOF) m/z: $[M+H]^+$ Calcd for $C_{45}H_{65}BNO_3P_2$ 740.4527; Found 740.4528.

L1b·BH_3: Yield: 458 mg (68%) (filtration under argon over neutral silica using dry toluene/hexane (1:1) as eluent system (1% NEt_3)). $^{31}P\{^1H\}$ NMR (161.9 MHz, C_6D_6): δ= 143.1 (s, P-O), 68.3 (bs, P-N). ^1H NMR (400 MHz, C_6D_6): δ= 1.01 (d, 3H, CH_3-P, $^2J_{H-P}$= 6.8 Hz), 1.08 (d, 3H, CH_3-CH, $^3J_{H-H}$= 8.8 Hz), 1.45 (s, 9H, CH_3, *t*-Bu), 1.58 (s, 9H, CH_3, *t*-Bu), 1.64 (s, 3H, CH_3), 1.72 (s, 3H, CH_3), 1.84 (d, 3H, CH_3-N, $^3J_{H-P}$= 8.2 Hz), 2.00 (s, 3H, CH_3), 2.02 (s, 3H, CH_3), 4.34-4.44 (m, CH-N), 5.36 (dd, CH-O, $^3J_{H-P}$= 8.7 Hz, $^3J_{H-H}$= 6.6 Hz), 6.86-6.92 (m, 2H, CH=), 6.98-7.05 (m, 3H, CH=), 7.12-7.16 (m, 5H, CH=), 7.60-7.63 (m, 2H, CH=). $^{13}C\{^1H\}$ NMR (100.6 MHz, C_6D_6): δ= 11.0 (d, CH_3-P, $^1J_{C-P}$= 38.8 Hz), 13.4 (CH_3-CH), 16.1 (CH_3), 16.5 (CH_3), 19.9 (CH_3), 20.0 (CH_3), 28.1 (d, CH_3-N, $^2J_{C-P}$= 3.0 Hz), 31.3 (CH_3, *t*-Bu), 31.4 (CH_3, *t*-Bu), 31.5 (CH_3, *t*-Bu), 34.5 (C, *t*-Bu), 34.8 (C, *t*-Bu), 57.9 (d, CH-N, $^2J_{C-P}$= 10.1 Hz), 81.2 (CH-O), 127.4-145.4 (aromatic carbons). HRMS (ESI-TOF) m/z: $[M+H]^+$ Calcd for $C_{41}H_{57}BNO_3P_2$ 684.3901; Found 684.3905.

L1c·BH_3: Yield: 492 mg (72%) (filtration under argon over neutral silica using dry toluene/hexane (1:1) as eluent system (1% NEt_3)). $^{31}P\{^1H\}$ NMR (161.9 MHz, C_6D_6): δ= 140.9 (s, P-O), 68.4 (bs, P-N). ^1H NMR (400 MHz, C_6D_6): δ= 1.10 (d, 3H, CH_3-P, $^2J_{H-P}$= 8.7 Hz), 1.14 (d, 3H, CH_3-CH, $^3J_{H-H}$= 6.5 Hz), 1.40 (s, 9H, CH_3, *t*-Bu), 1.58 (s, 9H, CH_3, *t*-Bu), 1.59 (s, 3H, CH_3), 1.62 (s, 3H, CH_3), 1.98 (s, 3H, CH_3), 2.06 (s, 3H, CH_3), 2.13 (d, 3H, CH_3-N, $^3J_{H-P}$= 8.2 Hz), 4.31-4.37 (m, CH-N), 5.37 (dd, CH-O, $^3J_{H-P}$= 8.7 Hz, $^3J_{H-H}$= 6.6 Hz), 6.91-6.94 (m, 3H, CH=), 6.95-7.04 (m, 5H, CH=), 7.11 (s, 2H, CH=), 7.18-7.22 (m, 2H, CH=). $^{13}C\{^1H\}$ NMR (100.6 MHz, C_6D_6): δ= 10.7 (d, CH_3-P, $^1J_{C-P}$= 38.8 Hz), 13.9 (CH_3-CH), 16.2 (CH_3), 16.3 (CH_3), 20.0 (CH_3), 20.1 (CH_3), 28.8 (d, CH_3-N, $^2J_{C-P}$= 3.0 Hz), 31.0 (CH_3, *t*-Bu), 31.1 (CH_3, *t*-Bu), 31.4 (CH_3, *t*-Bu), 34.3 (C, *t*-Bu), 34.7 (C, *t*-Bu), 57.9 (d, CH-N, $^2J_{C-P}$= 10.1 Hz), 80.2 (CH-O), 125.7-145.5 (aromatic carbons). HRMS (ESI-TOF) m/z: $[M+H]^+$ Calcd for $C_{41}H_{57}BNO_3P_2$ 684.3901; Found 684.3903.

L2b: Yield: 259 mg (69%) (filtration under argon over neutral silica using dry toluene/hexane (1:1) as eluent system (1% NEt_3)). $^{31}P\{^1H\}$ NMR (161.9 MHz, C_6D_6):

δ= 143.4 (s, P-O), 55.9 (s, P-N). ^{1}H NMR (400 MHz, C_6D_6): δ= 1.34 (d, 3H, CH_3-N, $^{3}J_{H-H}$= 6.6 Hz), 1.52 (s, 18H, *t*-Bu), 1.66 (s, 3H, CH_3), 1.76 (s, 3H, CH_3), 2.02 (s, 3H, CH_3), 2.05 (s, 3H, CH_3), 2.07 (d, CH_3-N, $^{3}J_{H-P}$= 2.7 Hz), 3.09 (s, 3H, CH_3-O), 3.97-4.04 (m, 1H, CH-N), 5.35 (pt, 1H, CH-OP, *J*= 8.8 Hz), 6.44 (dd, 1H, CH=, $^{3}J_{H-H}$= 8.3 Hz, $^{4}J_{H-H}$= 4.1 Hz), 6.74 (t, 1H, CH=, $^{3}J_{H-H}$= 7.4 Hz), 6.85-6.86 (m, 2H, CH=), 6.93-7.05 (m, 4H, CH=), 7.06-7.20 (m, 6H, CH=), 7.47-7.50 (m, 2H, CH=). ^{13}C{^{1}H} NMR (100.6 MHz, C_6D_6): δ= 15.7 (d, CH_3-CH, $^{3}J_{C-P}$= 4.2 Hz), 16.2 (CH_3), 16.6 (CH_3), 20.0 (CH_3), 20.1 (CH_3), 31.3 (d, CH_3, *t*-Bu, J_{C-P}= 5.3 Hz), 31.5 (CH_3-N), 31.6 (CH_3, *t*-Bu), 34.6 (C, *t*-Bu), 34.8 (C, *t*-Bu), 54.4 (CH_3-O), 65.5 (d, CH-N, $^{2}J_{C-P}$= 41.8 Hz), 81.3 (dd, CH-O, $^{2}J_{C-P}$= 10.7 Hz, $^{3}J_{C-P}$= 6.6 Hz), 110.0-160.8 (aromatic carbons). HRMS (ESI-TOF) m/z: $[M+H]^+$ Calcd for $C_{47}H_{58}NO_4P_2$ 762.3836; Found 762.3841.

L2c: Yield: 224 mg (59%) (filtration under argon over neutral silica using dry toluene/hexane (1:1) as eluent system (1% NEt_3)). ^{31}P{^{1}H} NMR (161.9 MHz, C_6D_6): δ= 140.1 (s, P-O), 54.4 (s, P-N). ^{1}H NMR (400 MHz, C_6D_6): δ= 1.40 (s, 9H, CH_3, *t*-Bu), 1.53 (s, 12H, CH_3, *t*-Bu, CH_3-CH), 1.63 (s, 6H, CH_3), 2.00 (s, 3H, CH_3), 2.06 (s, 3H, CH_3), 2.26 (d, 3H, CH_3-N, $^{3}J_{H-P}$= 2.6 Hz), 3.11 (s, 3H, CH_3-O), 3.92-3.99 (m, 1H, CH-N), 5.49 (pt, 1H, CH-O, *J*= 7.7 Hz), 6.44-6.47 (m, 1H, CH=), 6.79 (t, 1H, CH=, $^{3}J_{H-H}$= 7.4 Hz), 6.77-6.81 (m, 1H, CH=), 6.90-7.01 (m, 8H, CH=), 7.08-7.13 (m, 5H, CH=). ^{13}C{^{1}H} NMR (100.6 MHz, C_6D_6): δ= 16.0 (d, CH_3-CH, $^{3}J_{C-P}$= 5.3 Hz), 16.1 (CH_3), 16.3 (CH_3), 20.0 (CH_3), 20.1 (CH_3), 31.1 (d, CH_3, *t*-Bu, J_{C-P}= 5.1 Hz), 31.4 (C, *t*-Bu), 32.7 (d, CH_3-N, $^{2}J_{C-P}$= 9.5 Hz), 34.4 (C, *t*-Bu), 34.6 (C, *t*-Bu), 54.4 (CH_3-O), 65.3 (dd, CH-N, $^{2}J_{C-P}$= 39.7 Hz, $^{3}J_{C-P}$= 5.0 Hz), 80.9 (dd, CH-O, $^{2}J_{C-P}$= 9.9 Hz, $^{3}J_{C-P}$= 5.3 Hz), 110.1-160.9 (aromatic carbons). HRMS (ESI-TOF) m/z: $[M+H]^+$ Calcd for $C_{47}H_{58}NO_4P_2$ 762.3836; Found 762.3840.

L3b·BH_3: Yield: 206 mg (58%) (filtration under argon over neutral silica using dry toluene/hexane (1:1) as eluent system (1% NEt_3)). ^{31}P{^{1}H} NMR (161.9 MHz, C_6D_6): δ= 144.2 (s, P-O), 77.2 (bs, P-N). ^{1}H NMR (400 MHz, C_6D_6): δ= 0.84-0.93 (m, 9H, CH_3, *i*-Pr, CH_3-CH), 1.43 (s, 9H, CH_3, *t*-Bu), 1.56 (s, 9H, CH_3, *t*-Bu), 1.62 (s, 3H, CH_3), 1.78 (s, 3H, CH_3), 1.92 (d, 3H, CH_3-N, $^{3}J_{H-P}$= 7.8 Hz), 1.98 (s, 3H, CH_3), 2.06 (s, 3H, CH_3), 2.09-2.14 (m, 1H, CH, *i*-Pr), 4.36-4.42 (m, 1H, CH-N), 5.50 (dd, 1H, CH-O, $^{3}J_{H-P}$= 8.8 Hz, $^{3}J_{H-H}$= 4.5 Hz), 6.97-7.01 (m, 4H, CH=), 7.07-7.16 (m, 4H, CH=), 7.50-7.54 (m, 2H, CH=), 7.62-7.64 (m, 2H, CH=). ^{13}C{^{1}H} NMR (100.6 MHz, C_6D_6): δ= 11.5 (CH_3-CH), 15.4 (CH_3), 16.1 (CH_3), 16.4 (CH_3), 16.5 (d, CH_3, *J*= 5.5 Hz), 20.0 (d, CH_3, *J*= 3.1 Hz), 21.4 (CH_3), 21.9 (CH_3), 28.0 (d, CH_3-N, $^{2}J_{C-P}$= 4.2 Hz), 29.4 (CH-*i*-Pr), 31.2 (d, CH_3, *t*-Bu, J_{C-P}= 5.4 Hz), 31.4 (CH_3, *t*-Bu), 34.5 (C, *t*-Bu), 34.8 (C, *t*-Bu), 58.3 (d, CH-N, $^{2}J_{C-P}$= 8.3 Hz), 82.3 (d, CH-O, $^{2}J_{C-P}$= 4.4 Hz), 125.3-145.5 (aromatic carbons). HRMS (ESI-TOF) m/z: $[M+H]^+$ Calcd for $C_{43}H_{61}BNO_3P_2$ 712.4214; Found 712.4218.

L3c·BH_3: Yield: 203 mg (57%) (filtration under argon over neutral silica using dry toluene/hexane (1:1) as eluent system (1% NEt_3)). ^{31}P{^{1}H} NMR (161.9 MHz, C_6D_6):

δ= 141.0 (s, P-O), 78.6 (bs, P-N). ^{1}H NMR (400 MHz, C_6D_6): δ= 0.94-0.96 (d, 3H, CH_3-CH, $^{4}J_{H-P}$= 6.9 Hz), 0.99-1.05 (dd, 3H, CH_3-*i*-Pr, *J*= 17.3 Hz, *J*= 7.0 Hz), 1.20-1.26 (dd, 3H, CH_3-*i*-Pr, *J*= 15.4 Hz, *J*= 7.0 Hz), 1.49 (s, 9H, CH_3, *t*-Bu), 1.63 (s, 3H, CH_3), 1.66 (s, 3H, CH_3), 1.70 (s, 9H, CH_3, *t*-Bu), 2.04 (s, 3H, CH_3), 2.18 (s, 3H, CH_3), 2.26-2.33 (m, 1H, CH-*i*-Pr), 2.47 (d, 3H, CH_3-N, $^{3}J_{H-P}$= 7.8 Hz), 4.54-4.61 (m, 1H, CH-N), 5.74 (dd, 1H, CH-O, $^{3}J_{H-P}$= 8.2 Hz, $^{3}J_{H-H}$= 3.8 Hz), 6.96-7.32 (m, 10H, CH=), 7.65-7.67 (m, 2H, CH=). ^{13}C{^{1}H} NMR (100.6 MHz, C_6D_6): δ= 11.3 (CH_3-CH), 15.9 (CH_3), 16.2 (CH_3), 16.4 (CH_3), 16.7 (CH_3), 20.0 (CH_3), 20.2 (CH_3), 29.1 (d, CH_3-N, $^{2}J_{C-P}$= 4.2 Hz), 29.5 (CH-*i*-Pr), 31.0 (d, CH_3, *t*-Bu, J_{C-P}= 5.4 Hz), 31.5 (CH_3, *t*-Bu), 34.4 (C, *t*-Bu), 34.8 (C, *t*-Bu), 58.2 (CH-N), 81.6 (CH-O), 121.0-150.6 (aromatic carbons). HRMS (ESI-TOF) m/z: $[M+H]^+$ Calcd for $C_{43}H_{61}BNO_3P_2$ 712.4214; Found 712.4219.

For deprotection, the borane-adduct (0.68 mmol) was dissolved in dry and deoxygenated diethylamine (20 mL) and heated to 55 ºC using an oil bath for 16 h. After this time, the mixture was evaporated to dryness and the residue was purified by flash chromatography to afford the corresponding ligands as white solids.

L1a: Yield: 221 mg (75%) (flash chromatography under argon using neutral alumina and dry and deoxygenated toluene/hexane (1:1) as eluent system (1% NEt_3). ^{31}P{^{1}H} NMR (161.9 MHz, C_6D_6): δ= 147.8 (bs, P-O), 49.5 (s, P-N). ^{1}H NMR (400 MHz, C_6D_6): δ= 1.10 (d, 3H, CH_3-P, $^{2}J_{H-P}$= 8.4 Hz), 1.24 (s, 9H, CH_3, *t*-Bu), 1.26 (s, 9H, CH_3, *t*-Bu), 1.31 (d, 3H, CH_3-CH, $^{3}J_{H-H}$= 6.6 Hz), 1.48 (s, 9H, CH_3, *t*-Bu), 1.53 (s, 9H, CH_3, *t*-Bu), 2.08 (d, 3H, CH_3-N, $^{3}J_{H-P}$= 8.0 Hz), 3.73-3.80 (m, 1H, CH-N), 5.38 (pt, 1H, CH-O, *J*= 8.4 Hz), 6.82-6.86 (m, 1H, CH=), 6.96-7.09 (m, 7H, CH=), 7.27 (s, 2H, CH=), 7.33-7.35 (m, 2H, CH=), 7.51-7.53 (m, 2H, CH=). ^{13}C{^{1}H} NMR (100.6 MHz, C_6D_6): δ= 12.2 (d, CH_3-P, $^{1}J_{C-P}$= 21.7 Hz), 16.3 (d, CH_3-CH, $^{3}J_{C-P}$= 6.5 Hz), 30.5 (d, CH_3-N, $^{2}J_{C-P}$= 8.2 Hz), 30.6 (CH_3, *t*-Bu), 31.1 (CH_3, *t*-Bu), 31.2 (d, CH_3, *t*-Bu, J_{C-P}= 5.4 Hz), 34.3 (C, *t*-Bu), 35.3 (C, *t*-Bu), 64.7 (d, CH-N, $^{3}J_{C-P}$= 38.1 Hz), 80.6 (CH-O), 123.9-146.4 (aromatic carbons). HRMS (ESI-TOF) m/z: $[M+H]^+$ Calcd for $C_{45}H_{62}NO_3P_2$ 726.4199; Found 726.4236.

L1b: Yield: 74 mg (60%) (flash chromatography under argon using neutral alumina and dry and deoxygenated toluene/hexane (1:1) as eluent system (1% NEt_3)). ^{31}P{^{1}H} NMR (161.9 MHz, C_6D_6): δ= 143.0 (s, P-O), 51.2 (s, P-N). ^{1}H NMR (400 MHz, C_6D_6): δ= 1.03 (d, 3H, CH_3-P, $^{1}J_{H-P}$= 6.3 Hz), 1.21 (d, CH_3-CH, $^{3}J_{H-H}$= 6.7 Hz), 1.53 (s, CH_3, 18H, *t*-Bu), 1.66 (s, CH_3), 1.74 (CH_3), 1.95 (d, CH_3-N, $^{2}J_{H-P}$= 3.5 Hz), 2.01 (s, 3H, CH_3), 2.07 (s, 3H, CH_3), 3.74-3.84 (m, 1H, CH-N), 5.23 (pt, CH-O, *J*= 8.9 Hz), 6.70-6.74 (m, 2H, CH=), 6.94-6.99 (m, 4H, CH=), 7.04-7.16 (m, 5H, CH=), 7.47-7.49 (m, 2H, CH=). ^{13}C{^{1}H} NMR (100.6 MHz, C_6D_6): δ= 12.2 (d, CH_3-P, $^{1}J_{C-P}$= 22.2 Hz), 16.2 (CH_3), 16.4 (d, CH_3-CH, $^{3}J_{C-P}$= 4.7 Hz), 16.5 (CH_3), 20.1 (CH_3), 29.7 (d, CH_3-N, $^{2}J_{C-P}$= 8.9 Hz), 31.2 (d, CH_3, *t*-Bu, J_{C-P}= 5.3 Hz), 31.6 (CH_3, *t*-Bu), 34.6 (C, *t*-Bu), 34.8 (C, *t*-Bu), 64.8 (CH-

N, $^{2}J_{C\text{-}P}$= 37.0 Hz), 80.7 (CH-O), 126.9-145.5 (aromatic carbons). HRMS (ESI-TOF) m/z: $[M+H]^+$ Calcd for $C_{41}H_{54}NO_3P_2$ 670.3573; Found 670.3576.

L1c: Yield: 60 mg (67%) (flash chromatography under argon using neutral alumina and dry and deoxygenated toluene/hexane (1:1) as eluent system (1% NEt_3)). $^{31}P\{^{1}H\}$ NMR (161.9 MHz, C_6D_6): δ= 140.6 (s, P-O), 49.0 (s, P-N). ^{1}H NMR (400 MHz, C_6D_6): δ= 1.11 (d, 3H, CH_3-P, $^{1}J_{H\text{-}P}$= 6.5 Hz), 1.40 (d, CH_3-CH, $^{3}J_{H\text{-}H}$= 6.7 Hz), 1.43 (s, CH_3, 9H, *t*-Bu), 1.57 (s, CH_3, 9H, *t*-Bu), 1.63 (s, CH_3), 1.99 (CH_3), 2.06 (s, 3H, CH_3), 2.09 (d, CH_3-N, $^{2}J_{H\text{-}P}$= 3.6 Hz), 3.72-3.78 (m, 1H, CH-N), 5.33 (pt, CH-O, J= 7.7 Hz), 6.80-6.84 (m, 2H, CH=), 6.95-7.16 (m, 10H, CH=). $^{13}C\{^{1}H\}$ NMR (100.6 MHz, C_6D_6): δ= 12.3 (d, CH_3-P, $^{1}J_{C\text{-}P}$= 21.4 Hz), 16.2 (CH_3), 16.3 (CH_3), 16.6 (d, CH_3-CH, $^{3}J_{C\text{-}P}$= 7.2 Hz), 20.0 (CH_3), 20.1 (CH_3), 30.8 (d, CH_3-N, $^{2}J_{C\text{-}P}$= 8.0 Hz), 31.0 (d, CH_3, *t*-Bu, $J_{C\text{-}P}$= 5.2 Hz), 31.5 (CH_3, *t*-Bu), 34.4 (C, *t*-Bu), 34.7 (C, *t*-Bu), 64.8 (CH-N), 80.2 (CH-O), 125.3-145.6 (aromatic carbons). HRMS (ESI-TOF) m/z: $[M+H]^+$ Calcd for $C_{41}H_{54}NO_3P_2$ 670.3573; Found 670.3578.

L3b: Yield: 92 mg (70%) (flash chromatography under argon using neutral alumina and dry and deoxygenated toluene/hexane (1:1) as eluent system (1% NEt_3)). $^{31}P\{^{1}H\}$ NMR (161.9 MHz, C_6D_6): δ= 143.6 (s, P-O), 70.4 (bs, P-N). ^{1}H NMR (400 MHz, C_6D_6): δ= 0.60-0.74 (m, 6H, CH_3, *i*-Pr), 1.05 (d, 3H, CH3-CH, $^{3}J_{H\text{-}H}$= 6.7 Hz), 1.49 (s, 9H, CH_3, *t*-Bu), 1.52 (s, 9H, CH_3, *t*-Bu), 1.63 (s, 3H, CH_3), 1.73 (s, 3H, CH_3), 1.97 (d, 3H, CH_3-N, $^{3}J_{H\text{-}P}$= 3.7 Hz), 1.99 (s, 3H, CH_3), 1.99-2.01 (m, 1H, CH, *i*-Pr), 2.06 (s, 3H, CH_3), 3.82-3.92 (m, 1H, CH-N), 5.13-5.17 (m, 1H, CH-O), 6.94-7.18 (m, 9H, CH=), 7.33-7.40 (m, 3H, CH=). $^{13}C\{^{1}H\}$ NMR (100.6 MHz, C_6D_6): δ= 14.7 (CH_3-CH), 16.1 (CH_3), 16.4 (CH_3), 17.5 (CH_3), 17.7 (CH_3), 17.9 (CH_3), 18.0 (CH_3), 19.9 (CH_3), 20.0 (CH_3), 22.7 (d, CH-*i*-Pr, $^{1}J_{C\text{-}P}$= 6.2 Hz), 29.6 (d, CH_3-N, $^{2}J_{C\text{-}P}$= 7.6 Hz), 31.2 (d, CH_3, *t*-Bu, $J_{C\text{-}P}$= 5.4 Hz), 31.6 (CH_3, *t*-Bu), 34.5 (C, *t*-Bu), 34.7 (C, *t*-Bu), 65.5 (d, CH-N, $^{2}J_{C\text{-}P}$= 36.7 Hz), 81.3 (CH-O), 125.3-145.5 (aromatic carbons). HRMS (ESI-TOF) m/z: $[M+H]^+$ Calcd for $C_{43}H_{58}NO_3P_2$ 698.3886; Found 698.3891.

L3c: Yield: 48 mg (68%) (flash chromatography under argon using neutral alumina and dry and deoxygenated toluene/hexane (1:1) as eluent system (1% NEt_3)). $^{31}P\{^{1}H\}$ NMR (161.9 MHz, C_6D_6): δ= 140.6 (s, P-O), 70.6 (bs, P-N). ^{1}H NMR (400 MHz, C_6D_6): δ= 0.79-0.87 (m, 6H, CH_3, *i*-Pr), 1.24 (d, 3H, CH3-CH, $^{3}J_{H\text{-}H}$= 6.8 Hz), 1.46 (s, 9H, CH_3, *t*-Bu), 1.60 (s, 9H, CH_3, *t*-Bu), 1.67 (s, 6H, CH_3), 2.02 (s, 3H, CH_3), 2.11 (s, 3H, CH_3), 2.13-2.15 (m, 1H, CH, *i*-Pr), 2.25 (d, 3H, CH_3-N, $^{3}J_{H\text{-}P}$= 3.7 Hz), 3.90-3.97 (m, 1H, CH-N), 5.34 (m, 1H, CH-O), 6.97-7.01 (m, 10H, CH=), 7.47 (m, 2H, CH=). $^{13}C\{^{1}H\}$ NMR (100.6 MHz, C_6D_6): δ= 14.5 (CH_3-CH), 15.6 (CH_3), 16.1 (CH_3), 16.3 (CH_3), 17.5 (CH_3), 17.8 (CH_3), 18.2 (CH_3), 19.9 (CH_3), 20.0 (CH_3), 22.6 (d, CH-*i*-Pr, $^{1}J_{C\text{-}P}$= 6.3 Hz), 29.4 (CH_3-N), 31.4 (d, CH_3, *t*-Bu, $J_{C\text{-}P}$= 5.1 Hz), 31.5 (CH_3, *t*-Bu), 34.3 (C, *t*-Bu), 34.7 (C, *t*-Bu), 65.7 (CH-N), 81.1 (CH-O), 120.9-150.5 (aromatic carbons). HRMS (ESI-TOF) m/z: $[M+H]^+$ Calcd for $C_{43}H_{58}NO_3P_2$ 698.3886; Found 698.3980.

3.1.4.3. Preparation of amino-phosphites 6b–c

To a solution of *in situ* generated phosphorochloridite (0.55 mmol) in dry toluene (3 mL), was added triethylamine (0.14 mL, 1.0 mmol). Then, this solution was placed in a 0 ºC bath. After 2 min at that temperature, a solution of ephedrine **1** (82.0 mg, 0.5 mmol), DMAP (6.7 mg, 0.055 mmol) and triethylamine (0.14 mL, 1.0 mmol) in toluene (3 mL) was added dropwise at 0 °C. The mixture was left to warm to rt and stirred for 4 h at this temperature. The precipitate formed was filtered under argon and the solvent was evaporated under vacuum. The residue was purified by flash chromatography to produce the corresponding to afford the corresponding amino-phosphite compound **6b** and **6c** as white solids.

6b: Yield: 197 mg (72%) (filtration under argon over neutral silica using toluene/NEt_3= 100/1 as eluent). $^{31}P\{^1H\}$ NMR (161.9 MHz, C_6D_6): δ= 142.7 (s). ^1H NMR (400 MHz, C_6D_6): δ= 0.71 (d, 3H, CH_3-CH, $^3J_{H-H}$= 6.5 Hz), 1.42 (s, 9H, CH_3, *t*-Bu), 1.54 (s, 9H, CH_3, *t*-Bu), 1.67 (s, 3H, CH_3), 1.73 (s, 3H, CH_3), 2.04 (s, 3H, CH_3), 2.09 (s, 3H, CH_3), 2.16 (s, 3H, CH_3-N), 2.56-2.59 (m, 1H, CH-N), 5.23 (dd, 1H, CH-O, $^3J_{H-P}$= 7.7 Hz, $^3J_{H-H}$= 3.1 Hz), 7.01-7.03 (m, 1H, CH=), 7.07-7.12 (m, 2H, CH=), 7.17-7.20 (m, 3H, CH=), 7.22 (s, 1H, CH=). $^{13}C\{^1H\}$ NMR (100.6 MHz, C_6D_6): δ= 14.2 (CH_3-CH), 16.2 (CH_3), 16.4 (CH_3), 20.0 (CH_3), 20.1 (CH_3), 30.8 (d, CH_3, *t*-Bu, J_{C-P}= 4.8 Hz), 31.3 (CH_3, *t*-Bu), 33.5 (CH_3-N), 34.5 (C, *t*-Bu), 34.7 (C, *t*-Bu), 61.1 (CH-N), 77.8 (d, CH-O, $^2J_{C-P}$= 8.7 Hz), 125.3-146.4 (aromatic carbons). HRMS (ESI-TOF) m/z: $[M+H]^+$ Calcd for $C_{34}H_{47}NO_3P$ 548.3288; Found 548.3291.

6c: Yield: 216 mg (79%) (filtration under argon over neutral silica using toluene/NEt_3= 100/1 as eluent). $^{31}P\{^1H\}$ NMR (161.9 MHz, C_6D_6): δ= 141.7 (s). ^1H NMR (400 MHz, C_6D_6): δ= 0.86 (d, CH_3-CH, $^3J_{H-H}$= 6.5 Hz), 1.34 (s, 9H, *t*-Bu), 1.56 (s, 9H, *t*-Bu), 1.65 (s, 6H, CH_3), 1.99 (s, 3H, CH_3), 2.06 (s, 3H, CH_3), 2.19 (s, 3H, CH_3-N), 2.89-2.95 (m, 1H, CH-N), 5.22 (dd, 1H, CH-O, $^3J_{C-P}$= 8.9 Hz, $^3J_{H-H}$= 3.9 Hz), 6.97-7.22 (m, 7H, CH=). $^{13}C\{^1H\}$ NMR (100.6 MHz, C_6D_6): δ= 15.1 (CH_3-CH), 16.2 (CH_3), 16.4 (CH_3), 20.0 (CH_3), 30.9 (d, CH_3, *t*-Bu, J_{C-P}= 5.2 Hz), 31.5 (CH_3, *t*-Bu), 33.8 (CH_3-N), 34.3 (C, *t*-Bu), 34.7 (C, *t*-Bu), 59.8 (d, CH-N, $^3J_{C-P}$= 6.0 Hz), 80.3 (d, CH-O, $^2J_{C-P}$= 11.2 Hz), 125.3-145.7 (aromatic carbons). HRMS (ESI-TOF) m/z: $[M+H]^+$ Calcd for $C_{34}H_{47}NO_3P$ 548.3288; Found 548.3289.

3.1.4.4. Preparation of *N*-phosphine–phosphite ligands L4b–c

The corresponding amino-phosphite compound **6b** and **6c** (136.9 mg, 0.25 mmol) was dissolved in THF (2 ml), and triethylamine was added (0.045 mL, 0.32 mmol) at rt, followed by the addition of chlorodiphenylphosphine (0.05 mL, 0.27 mmol) via syringe. The reaction was stirred for 16 h at 55 ºC using an oil bath. The solvent was removed *in vacuo*, and the product was purified by flash chromatography to produce the corresponding ligand as white solid.

L4b: Yield: 128 mg (70%) (flash chromatography under argon using neutral alumina and dry and deoxygenated toluene/NEt_3= 100/1). $^{31}P\{^1H\}$ NMR (161.9 MHz, C_6D_6): δ= 143.3 (s, P-O), 64.2 (s, P-N). ^1H NMR (400 MHz, C_6D_6): δ= 1.23 (d, 3H, CH_3-CH, $^3J_{H-H}$= 6.7 Hz), 1.53 (s, 9H, CH_3, *t*-Bu), 1.54 (s, 9H, CH_3, *t*-Bu), 1.66 (CH_3), 1.75 (CH_3), 2.01 (CH_3), 2.02 (d, 3H, CH_3-N, $^3J_{H-P}$= 2.9 Hz), 2.05 (s, 3H, CH_3), 3.92-4.03 (m, 1H, CH-N), 5.35 (pt, 1H, CH-O, *J*= 7.3 Hz), 6.85-6.89 (m, 1H, CH=), 6.91-7.12 (m, 9H, CH=), 7.17-7.22 (m, 4H, CH=), 7.45-7.49 (m, 2H, CH=). $^{13}C\{^1H\}$ NMR (100.6 MHz, C_6D_6): δ= 16.1 (d, CH_3-CH, $^3J_{C-P}$= 4.4 Hz), 16.2 (CH_3), 16.5 (CH_3), 20.0 (CH_3), 20.1 (CH_3), 31.3 (d, CH_3, *t*-Bu, J_{C-P}= 5.3 Hz), 31.5 (CH_3-N), 31.6 (CH_3, *t*-Bu), 34.6 (C, *t*-Bu), 34.8 (C, *t*-Bu), 65.6 (d, CH-N, $^2J_{C-P}$= 39.6 Hz), 81.1 (dd, CH-O, $^2J_{C-P}$= 11.0 Hz, $^3J_{C-P}$= 7.5 Hz), 125.3-145.4 (aromatic carbons). HRMS (ESI-TOF) m/z: $[M+H]^+$ Calcd for $C_{46}H_{56}NO_3P_2$ 732.3730; Found 732.3733.

L4c: Yield: 109 mg (60%) (flash chromatography under argon using neutral alumina and dry and deoxygenated toluene/NEt_3= 100/1). $^{31}P\{^1H\}$ NMR (161.9 MHz, C_6D_6): δ= 140.1 (s, P-O), 63.3 (s, P-N). ^1H NMR (400 MHz, C_6D_6): δ= 1.43 (d, 3H, CH_3-CH, $^3J_{H-H}$= 7.5 Hz), 1.45 (s, 9H, CH_3, *t*-Bu), 1.55 (s, 9H, CH_3, *t*-Bu), 1.64 (s, 3H, CH_3), 1.66 (s, 3H, CH_3), 2.01 (s, 3H, CH_3), 2.07 (s, 3H, CH_3), 2.18 (d, 3H, CH_3-N, $^3J_{H-P}$= 2.9 Hz), 3.92-3.96 (m, 1H, CH-N), 5.45 (pt, 1H, CH-O, *J*= 7.8 Hz), 6.93-7.02 (m, 10H, CH=), 7.05-7.14 (m, 5H, CH=), 7.21-7.26 (m, 2H, CH=). $^{13}C\{^1H\}$ NMR (100.6 MHz, C_6D_6): δ= 16.2 (CH_3), 16.3 (CH_3), 16.4 (d, CH_3-CH, $^3J_{C-P}$= 6.3 Hz), 20.0 (CH_3), 20.1 (CH_3), 31.0 (d, CH_3, *t*-Bu, J_{C-P}= 5.2 Hz), 31.4 (C, *t*-Bu), 32.1 (d, CH_3-N, $^2J_{C-P}$= 10.0 Hz), 34.4 (C, *t*-Bu), 34.7 (C, *t*-Bu), 65.4 (dd, CH-N, $^2J_{C-P}$= 37.8 Hz, $^3J_{C-P}$= 5.8 Hz), 80.7 (dd, CH-O, $^2J_{C-P}$= 10.6 Hz, $^3J_{C-P}$= 5.6 Hz), 125.3-145.7 (aromatic carbons). HRMS (ESI-TOF) m/z: $[M+H]^+$ Calcd for $C_{46}H_{56}NO_3P_2$ 732.3730; Found 732.3732.

3.1.4.5. General procedure for the asymmetric hydrogenation

$[Rh(cod)_2]BF_4$ (1 mg, 2.5 μmol), the corresponding ligand (2.5 μmol) and the desired substrate (0.25 mmol) were dissolved in THF (2 mL) and placed in a high-pressure autoclave. The autoclave was purged 4 times with hydrogen. Then, it was pressurized at the desired pressure. After the desired reaction time, the autoclave was depressurized, and the solvent evaporated off. The residue was dissolved in Et_2O (1.5 ml) and filtered through a short plug of Celite. Conversions were determined by ^1H NMR and enantiomeric excesses were determined by chiral HPLC or GCs.

3.1.5. References

[1] (a) Blaser, H. U.; Federsel, H.–J., Eds. *Asymmetric Catalysis on Industrial Scale: Challenges, Approaches and Solutions*, 2nd ed.; Wiley–VCH: Weinheim, **2010**. (b) Ojima, I., Ed. *Catalytic Asymmetric Synthesis*; 3rd ed.; John Wiley & Sons, Inc.: Hoboken, **2010**. (c) Jacobsen, E. N.; Pfaltz, A.; Yamamoto, H., Eds. *Comprehensive Asymmetric Catalysis*; Springer–Verlag: Berlin, **1999**. (d) Noyori, R., Ed. *Asymmetric Catalysis in Organic Synthesis*; Wiley: New York, **1994**. (e) Cornils, B.;

Hermann, W. A., Eds. *Applied Homogeneous Catalysis with Organometallic Compounds*, 2nd ed.; Wiley–VCH: Wienhein, **2002**. (f) de Vries, J. G.; Elsevier, C. J., Eds. *Handbook of Homogeneous Hydrogenation*; Wiley–VCH: Weinheim, **2007**. (g) Akiyama, T.; Ojima, I., Eds. *Catalytic Asymmetric Synthesis*, 4th Ed; John Wiley & Sons, Inc.: Hoboken, **2022**. (h) Busacca, C. A.; Fandrick, D. R.; Song, J. J.; Senanayake, C. H. The Growing Impact of Catalysis in the Pharmaceutical Industry. *Adv. Synth. Catal.* **2011**, *353*, 1825–1864. (i) Ager, D. J.; de Vries, A. H. M.; de Vries, J. G. Asymmetric homogeneous hydrogenations at scale. *Chem. Soc. Rev*. **2012**, *41*, 3340–3380. (j) Diéguez, M.; Pizzano, A., Eds. *Metal–catalyzed Asymmetric Hydrogenation. Evolution and Prospect* in Advances in Catalysis; Elsevier: Oxford, Vol. 68, **2021**. (k) Biosca, M.; Diéguez, M.; Zanotti–Gerosa, A. Asymmetric hydrogenation in Industry. *Adv. Catal.* **2021**, *68*, 341–384 and references therein.

[2] See for example: (a) Cui, X.; Burgess, K. Catalytic Homogeneous Asymmetric Hydrogenations of Largely Unfunctionalized Alkenes. *Chem. Rev.* **2005**, *105*, 3272−3296. (b) Roseblade, S. J.; Pfaltz, A. Iridium−Catalyzed Asymmetric Hydrogenation of Olefins. *Acc. Chem. Res.* **2007**, *40*, 1402−1411. (c) Woodmansee, D. H.; Pfaltz, A. Asymmetric Hydrogenation of Alkenes Lacking Coordinating Groups. *Chem. Commun.* **2011**, *47*, 7912−7916. (d) Zhu, Y.; Burgess, K. Filling Gaps in Asymmetric Hydrogenation Methods for Acyclic Stereocontrol: Application to Chirons for Polyketide–Derived Natural Products. *Acc. Chem. Res.* **2012**, *45*, 1623−1636. (e) Verendel, J. J.; Pàmies, O.; Diéguez, M.; Andersson, P. G. Asymmetric Hydrogenation of Olefins Using Chiral Crabtree–type Catalysts: Scope and Limitations. *Chem. Rev.* **2014**, *114*, 2130−2169. (f) Margarita, C.; Andersson, P. G. Evolution and Prospects of the Asymmetric Hydrogenation of Unfunctionalized Olefins. *J. Am. Chem. Soc.* **2017**, *139*, 1346−1356. (g) Pàmies, O.; Zheng, J.; Faiges, J.; Andersson, P. G. Asymmetric hydrogenation of unfunctionalized olefins or with poorly coordinative groups. *Adv. Catal.* **2021**, *68*, 135–203. For specific examples of application of P,O and P,S–ligands in the Ir–catalyzed asymmetric hydrogenation see: (h) Margalef, J.; Pàmies,O. ; Pericas, M. A.; Diéguez, M. Evolution of phosphorus–thioether ligands for asymmetric catalysis, *Chem. Comm*. **2020**, *56*, 10795–10808, (i) Margalef, J.; Pericàs, M. A. "Chiral bidentate heterodonor P–S/O ligands" in Chiral Ligands. Evolution of ligands for asymmetric catalysis; Diéguez, M., Ed.; CRC Press, **2021**, 81–108. (j) Rageot, D.; Woodmansee, D. H.; Pugin, B.; Pfaltz, A. Proline–Based P,O Ligand/Iridium Complexes as Highly Selective Catalysts: Asymmetric Hydrogenation of Trisubstituted Alkenes. *Angew. Chem*. Int. Ed. **2011**, *50*, 9598–9601.

[3] See for example: (a) Genet, J. P. In *Modern Reduction Methods*; Andersson, P. G.; Munslow, I. J., Eds.; Wiley–VCH: Weinheim, **2008**, pp 3–38. (b) Tang, W.; Zhang, X. New Chiral Phosphorus Ligands for Enantioselective Hydrogenation. *Chem. Rev.* **2003**, *103*, 3029–3069. (c) Kitamura, M.; Noyori, R. In *Ruthenium in Organic Synthesis*; Murahashi, S.–I., Ed.; Wiley–VCH, Weinheim, **2004**, pp 3–52. (d) Weiner, B.; Szymanski, W.; Janssen, D. B.; Minnaard, A. J.; Feringa, B. L. Recent Advances in the Catalytic Asymmetric Synthesis of β–Amino Acids. *Chem. Soc. Rev.* **2010**, *39*, 1656–1691.

[4] Knowles, W. S.; Sabacky, M. J.; Vineyard, B. D. Catalytic Asymmetric Hydrogenation. *J. Chem. Soc., Chem. Commun.* **1972**, 10–11.

[5] Knowles, W. S. Application of Organometallic Catalysis to the Commercial Production of L–DOPA. *J. Chem. Educ.* **1986**, *63*, 222–225.

[6] See for instance: (a) Imamoto, T.; Watanabe, J.; Wada, Y.; Masuda, H.; Yamada, H.; Tsuruta, H.; Matsukawa, S.; Yamaguchi, K. P–Chiral Bis(trialkylphosphine) Ligands and Their Use in Highly Enantioselective Hydrogenation Reactions. *J. Am. Chem. Soc.* **1998**, *120*, 1635–1636. (b) Hoge, G.; Wu, H.–P.; Kissel, W. S.; Pflum, D. A.; Greene, D. J.; Bao, J. Highly Selective Asymmetric Hydrogenation Using a Three Hindered Quadrant Bisphosphine Rhodium Catalyst. *J. Am. Chem. Soc.*

2004, *126*, 5966–5967. (c) Cristóbal–Lecina, E.; Etayo, P.; Doran, S.; Revés, M.; Martín–Gago, P.; Grabulosa, A.; Costantino, A. R.; Vidal–Ferran, A.; Riera, A.; Verdaguer, X. MaxPHOS Ligand: PH/NH Tautomerism and Rhodium-Catalyzed Asymmetric Hydrogenations. *Adv. Synth. Catal.* **2014**, *356*, 795–804. (d) Tang, W.; Wang, W.; Chi, Y.; Zhang, X. A bisphosphepin ligand with stereogenic phosphorus centers for the practical synthesis of β–aryl–β–amino acids by asymmetric hydrogenation. *Angew. Chem. Int. Ed.* **2003**, *42*, 3509–3511. (e) Zhang, X.; Huang, K.; Hou, G.; Cao, B.; Zhang, X. Electron–donating and rigid P–stereogenic bisphospholane ligands for highly enantioselective rhodium–catalyzed asymmetric hydrogenations. *Angew. Chem., Int. Ed.* **2010**, *49*, 6421–6424. (f) Liu, D.; Zhang, X. Practical P–chiral phosphane ligand for Rh–catalyzed asymmetric hydrogenation. *Eur. J. Org. Chem.* **2005**, 646–649. (g) Tang, W.; Qu, B.; Capacci, A. G; Rodriguez, S.; Wei, X.; Haddad, N.; Narayanan, B.; Ma, S.; Grinberg, N.; Yee, N. K.; Krishnamurthy, D.; Senanayake, C. H. Novel, Tunable, and Efficient Chiral Bisdihydrobenzooxaphosphole Ligands for Asymmetric Hydrogenation. *Org. Lett.* **2010**, *12*, 176–179.

[7] For representative reviews, see: (a) Agbossou–Niedercorn, F.; Suisse, I. Chiral Aminophosphine Phosphinite Ligands and Related Auxiliaries: Recent Advances in Their Design, Coordination Chemistry, and Use in Enantioselective Catalysis. *Coord. Chem. Rev.* **2003**, *242*, 145–158. (b) Agbossou, F.; Carpentier, J.–F.; Hapiot, F.; Suisse, I.; Mortreux, A. The Aminophosphine–Phosphinites and Related Ligands: Synthesis, Coordination Chemistry and Enantioselective Catalysis**.** *Coord. Chem. Rev.* **1998**, *178–180*, 1615–1645. (c) Fernández–Pérez, H.; Etayo, P.; Panossian, A.; Vidal–Ferran, A. Phosphine−Phosphinite and Phosphine−Phosphite Ligands: Preparation and Applications in Asymmetric Catalysis. *Chem. Rev.* **2011**, *111*, 2119–2176. (d) van Leeuwen, P. W. N. M.; Kamer, P. C. J.; Claver, C.; Pàmies, O.; Diéguez, M. Phosphite–Containing Ligands for Asymmetric Catalysis. *Chem. Rev.* **2011**, *111*, 2077–2118. (e) Wassenaar, J.; Reek, J. N. H. Hybrid Bidentate Phosphorus Ligands in Asymmetric Catalysis: Privileged Ligand Approach vs. Combinatorial Strategies. *Org. Biomol. Chem.* **2011**, *9*, 1704–1713. (f) Pizzano, A. Features and Application in Asymmetric Catalysis of Chiral Phosphine–Phosphite Ligands. *Chem. Rec.* **2016**, *16*, 2599–2622.

[8] For relevant examples, see: (a) Pàmies, O.; Diéguez, M.; Net, G.; Ruiz, A.; Claver, C. Phosphine–Phosphite, a New Class of Auxiliaries in Highly Active and Enantioselective Hydrogenation. *Chem. Commun.* **2000**, 2383–2384. (b) Suárez, A.; Méndez–Rojas, M. A.; Pizzano, A. Electronic Differences between Coordinating Functionalities of Chiral Phosphine−Phosphites and Effects in Catalytic Enantioselective Hydrogenation. *Organometallics* **2002**, *21*, 4611–4621. (c) Chávez M., Á.; Vargas, S.; Suárez, A.; Álvarez, E.; Pizzano, A. Highly Enantioselective Hydrogenation of β–Acyloxy and β–Acylamino α,β–Unsaturated Phosphonates Catalyzed by Rhodium Phosphane–Phosphite Complexes. *Adv. Synth. Catal.* **2011**, *353*, 2775–2794. (d) Kleman, P.; González–Liste, P. J.; García–Garrido, S. E.; Cadierno, V.; Pizzano, A. Asymmetric Hydrogenation of 1–Alkyl and 1–Aryl Vinyl Benzoates: A Broad Scope Procedure for the Highly Enantioselective Synthesis of 1–Substituted Ethyl Benzoates. *ACS Catal.* **2014**, *4*, 4398–4408. (e) Fernández-Pérez, H.; Donald, S. M. A.; Munslow, I. J.; Benet-Buchholz, J.; Maseras, F.; Vidal-Ferran, A. Highly Modular P–OP Ligands for Asymmetric Hydrogenation: Synthesis, Catalytic Activity, and Mechanism. *Chem. Eur. J.* **2010**, *16*, 6495–6508. (f) Etayo, P.; Núñez–Rico, J. L.; Fernández–Pérez, H.; Vidal–Ferran, A. Enantioselective Access to Chiral Drugs by using Asymmetric Hydrogenation Catalyzed by Rh(P–OP) Complexes. *Chem. Eur. J.* **2011**, *17*, 13978–13982. (g) Fernández–Pérez, H.; Benet–Buchholz, J.; Vidal–Ferran, A. Small Bite–Angle P–OP Ligands for Asymmetric Hydroformylation and Hydrogenation. *Org. Lett.* **2013**, *15*, 3634–3637. (h) Pullmann, T.; Engendahl, B.; Zhang, Z.; Hölscher, M.; Zanotti-Gerosa, A.; Dyke, A.; Franciò, G.; Leitner, W. Quinaphos and Dihydro–

Quinaphos Phosphine–Phosphoramidite Ligands for Asymmetric Hydrogenation. *Chem. Eur. J.* **2010**, *16*, 7517–7526. (i) Huang, J.–D.; Hu, X.–P.; Duan, Z.–C.; Zeng, Q.–H.; Yu, S.–B.; Deng, J.; Wang, D.–Y.; Zheng, Z. Readily Available Phosphine−Phosphoramidite Ligands for Highly Efficient Rh–Catalyzed Enantioselective Hydrogenations. *Org. Lett.* **2006**, *8*, 4367–4370. (j) Eggenstein, M.; Thomas, A.; Theuerkauf, J.; Franciò, G.; Leitner, W. Highly Efficient and Versatile Phosphine-Phosphoramidite Ligands for Asymmetric Hydrogenation. *Adv. Synth. Catal.* **2009**, *351*, 725–732.

[9] (a) Wang, D.–Y.; Hu, X.–P.; Huang, J.–D.; Deng, J.; Yu, S.–B.; Duan, Z.–C.; Xu, X.–F.; Zheng, Z. Highly Enantioselective Synthesis of a–Hydroxy Phosphonic Acid Derivatives by Rh–Catalyzed Asymmetric Hydrogenation with Phosphine–Phosphoramidite Ligands. *Angew. Chem. Int. Ed.* **2007**, *46*, 7810–7813. (b) Balogh, S.; Farkas, G.; Madarasz, J.; Szollosy, A.; Kovacs, J.; Darvas, F.; Urge, L.; Bakos, J. Asymmetric hydrogenation of C=C double bonds using Rh–complex under homogeneous, heterogeneous and continuous mode conditions. *Green Chemistry* **2012**, *14*, 1146–1151.

[10] (a) Deerenberg, S.; Pàmies, O.; Diéguez, M.; Claver, C.; Kamer, P. C. J.; van Leeuwen, P. W. N. M. Chiral Phosphine−Phosphite Ligands in the Highly Enantioselec–tive Rhodium–Catalyzed Asymmetric Hydrogenation. *J. Org. Chem.* **2001**, *66*, 7626–7631. (b) Vargas, S.; Rubio, M.; Suárez, A.; del Rio, D.; Álvarez, E.; Pizzano, A. Iridium Complexes with Phosphine−Phosphite Ligands. Structural Aspects and Application in the Catalytic Asymmetric Hydrogenation of N–Aryl Imines. *Organometallics* **2006**, *25*, 961–973. (c) León, F.; González–Liste, P. J.; García–Garrido, S. E.; Arribas, I.; Rubio, M.; Cadierno, V.; Pizzano, A. Broad Scope Synthesis of Ester Precursors of Nonfunctionalized Chiral Alcohols Based on the Asymmetric Hydrogenation of α,β–Dialkyl–, α,β–Diaryl–, and α–Alkyl–β–aryl–vinyl Esters. *J. Org. Chem*. **2017**, *82*, 5852–5867. (d) González–Liste, P. J.; León, F.;

, I.; Rubio, M.; García–Garrido, S. E.; Cadierno, V.; Pizzano, A. Highly Stereoselective Synthesis and Hydrogenation of (*Z*)–1–Alkyl–2–arylvinyl Acetates: a Wide Scope Procedure for the Preparation of Chiral Homobenzylic Esters. *ACS Catal.* **2016**, *6*, 3056–3060.

[11] Other methods to generate P–stereogenic ligands include: (a) Han, Z. S.; Zhang, L.; Xu, Y.; Sieber, J. D.; Marsini, M. A.; Li, Z.; Reeves, J. T.; Fandrick, K. R.; Patel, N. D.; Desrosiers, J.–N.; Qu, B.; Chen, A.; Rudzinski, D. M.; Samankumara, L. P.; Ma, S.; Grin–berg, N.; Roschangar, F.; Yee, N. K.; Wang, G.; Song, J. J.; Sena–nayake, C. H. Efficient Asymmetric Synthesis of Structurally Diverse P–Stereogenic Phosphinamides for Catalyst Design. *Angew. Chem. Int. Ed.* **2015**, *54*, 5474–5477 (for the synthesis of P–stereogenic phosphinamides). (b) Orgué, S.; Flores–Gaspar, A.; Biosca, M.; Pàmies, O.; Diéguez, M.; Riera, A.; Verdaguer, X. Stereospecific SN_2@P reactions: novel access to bulky P–stereogenic ligands. *Chem. Commun.* **2015**, *51*, 17548–17551 (for the synthesis of P–stereogenic *N*–phosphine–hydroxyl compounds).

[12] (a) Moulin, D.; Darcel, C.; Sugé, S. Versatile Synthesis of P–chiral (Ephedrine) AMPP Ligands via Their Borane Complexes. Structural Consequences in Rh–Catalyzed Hydrogenation of Methyl α–Acetamidocinnamate. *Tetrahedron: Asymmetry* **1999**, *10*, 4729–4743. (b) Darcel, C.; Moulin, D.; Henry, J.–C.; Lagrelette, M.; Richard, P.; Harvey, P. D.; Jugé, S. Modular P–Chirogenic Amino–phosphane–Phosphinite Ligands for Rh–Catalyzed Asymmetric Hydrogenation: A New Model for Prediction of Enantioselectivity. *Eur. J. Org. Chem.* **2007**, 2078–2090.

[13] den Heeten, R.; Swennenhuis, B. H. G.; van Leeuwen, P. W. N. M.; de Vries, J. G.; Kamer, P. C. J. Parallel Synthesis and Screening of Polymer–Supported Phosphorus–Stereogenic Aminophosphane–Phosphite and –Phosphinite Ligands. *Angew. Chem. Int. Ed.* **2008**, *47*, 6602–6605.

[14] Previous studies in the asymmetric hydrogenation of α–dehydroamino acids with related P–stereogenic *N*–phosphine–phosphinite ligands showed that the opposite configuration of carbons at the ephedrine moiety has a negative effect on enantioselectivity, see ref. 12.

[15] (a) Jugé, S.; Stephan, M.; Laffitte, J. A.; Genêt, J. P. Efficient Asymmetric Synthesis of Optically Pure Tertiary Mono and Diphosphine Ligands. *Tetrahedron Lett.* **1990**, *31*, 6357–6360. (b) Chaux, F.; Frynas, S.; Laureano, H.; Salomon, C.; Morata, G.; Auclair, M.–L.; Stephan, M.; Merdès, R.; Richard, P.; Ondel–Eymin, M.–J.; Henry, J.–C.; Bayardon, J.; Darcel, C.; Jugé, S. Enantiodivergent synthesis of P–chirogenic phosphines. *C. R. Chemie* **2010**, *13*, 1213–1126. (c) Zijlstra, H.; León, T.; de Cózar, A.; Fonseca Guerra, C.; Byrom, D.; Riera, A.; Verdaguer, X.; Bickelhaupt, F. M. Stereodivergent SN_2@P Reactions of Borane Oxazaphospholidines: Experimental and Theoretical Studies. *J. Am. Chem. Soc.* **2013**, *135*, 4483–4491.

[16] The hydrogenation of **S1** and **S2** proceeded with 89% ee and 52% conv and 73% ee and 13% conv, respectively.

[17] Schäffner, B.; Schäffner, F.; Verevkin, S. P.; Börner, A. Organic Carbonates as Solvents in Synthesis and Catalysis. *Chem. Rev.* **2010**, *110*, 4554–4581.

[18] (a) Bruneau, C.; Renaud, J.–L.; Jerphagnon, T. Synthesis of β–Aminoacid Derivatives via Enantioselective Hydrogenation of β–Substituted–β–(Acylamino)acrylates. *Coord. Chem. Rev.* **2008**, *252*, 532–544. (b) See ref 3d.

[19] For an example of the sucessful asymmetric hydrogenation of both isomers see ref. 6g.

[20] For the most successful examples, see: (a) Zhang. Z.; Zhu, G.; Jiang, Q.; Xiao, D.; Zhang, X. Highly Enantioselective Hydrogenation of Cyclic Enamides Catalyzed by a Rh–PennPhos Catalyst. *J. Org. Chem*. **1999**, *64*, 1774–1775 (ee's up to 98% for **S6** and 90% for **S7**). (b) Bernsmann, H.; van den Berg, M.; Hoen, R.; Minnaard, A. J.; Mehler, G.; Reetz, M. T.; de Vries, J. G.; Feringa, B. L. PipPhos and MorfPhos: Privileged Monodentate Phosphoramidite Ligands for Rhodium–Catalyzed Asymmetric Hydrogenation. *J. Org. Chem*. **2005**, *70*, 943–951 (ee's up to 98% for **S6** and 99% for **S7**). (c) Terrade, F. G.; Kluwer, A. M.; Detz, R. J.; Abiri, Z.; van der Burg, A. M.; Reek, J. N. H. Combinatorial Strategies to find New Catalysts for Asymmetric Hydrogenation Based on the Versatile Coordination Chemistry of METAMORPhos Ligands. *ChemCatChem* **2015**, *7*, 3368–3375 (ee's up to 88% for **S6**). (d) Salomó, E.; Orgué, S.; Riera, A.; Verdaguer, X. Highly Enantioselective Iridium-Catalyzed Hydrogenation of Cyclic Enamides. *Angew. Chem. Int. Ed.* **2016**, *55*, 7988–7992 (ee's up to 99% for **S6**).

[21] Magre, M.; Pàmies, O.; Diéguez, M. PHOX–Based Phosphite–Oxazoline Ligands for the Enantioselective Ir–Catalyzed Hydrogenation of Cyclic β–Enamides. *ACS Catal.* **2016**, *6*, 5186–5190.

[22] Yu, H.; Richey, R. N.; Stout, J. R.; LaPack, M. A.; Gu, R.; Khau, V. V.; Frank, S. A.; Ott, J. P.; Miller, R. D.; Carr, M. A.; Zhang, T. Y. Development of a Practical Synthesis of DPP IV Inhibitor LY2497282. *Org. Process Res. Dev.* **2008**, *12*, 218–225.

[23] Pippel, M.; Boyce, K.; Venkatesan, H.; Phuong, V. K.; Yan, W.; Barrett, T. D.; Lagaud, G.; Li, L.; Morton, M. F.; Prendergast, C.; Wu, X.; Shankley, N. P.; Rabinowitz, M. H. Anthranilic Sulfonamide CCK1/CCK2 Dual Receptor Antagonists II: Tuning of Receptor Selectivity and In Vivo Efficacy. *Bioorg. Med. Chem. Lett.* **2009**, *19*, 6376–6378.

[24] Walpole, C.; Ko, S. Y.; Brown, M.; Beattie, D.; Campbell, E.; Dickenson, F.; Ewan, S.; Hughes, G. A.; Lemaire, M.; Lerpiniere, J.; Patel, S.; Urban, L. 2–Nitrophenylcarbamoyl–(S)–prolyl–(S)–3–(2–naphthyl)alanyl–N–benzyl–N–methyl–amide (SDZ NKT 343), a Potent Human NK1 Tachykinin Receptor Antagonist with Good Oral Analgesic Activity in Chronic Pain Models. *J. Med. Chem.* **1998**, *41*, 3159–3173.

[25] P. V. Chaturvedula, L. Chen, R. Civiello, A. P. Degnan, G. M. Dubowchik, X. Han, X. J. J. Jiang, J. E. Macor, G. S. Poindexter, G. O. Tora, G. Luo, US 0149503, **2007**.

[26] (a) Gozgit, J. M.; Bebernitz, G.; Patil, P.; Ye, M.; Parmentier, J.; Wu, J.; Su, N.; Wang, T.; Ioannidis, S.; Davies, A.; Huszar, D.; Zinda, M. Effects of the JAK2 Inhibitor, AZ960, on Pim/BAD/BCL–xL Survival Signaling in the Human JAK2 V617F Cell Line SET–2. *J. Biol. Chem.* **2008**, *283*, 32334–32343. (b) Wang, T.; Ioannidis, S.; Almeida, L.; Block, M. H.; Davies, A. M.; Lamb, M. L.; Scott, D. A.; Su, M.; Zhang, H.–J.; Alimzhanov, M.; Bebernitz, G.; Bell, K.; Zinda, M. In Vitro and In Vivo Evaluation of 6–Aminopyrazolyl–pyridine–3–carbonitriles as JAK2 Kinase Inhibitors. *Bioorg. Med. Chem. Lett.* **2011**, *21*, 2958–2961.

[27] The highest enantioselectivities reported for **S9** (a) See ref 8f (99% ee). (b) See ref 21 (>99%ee). For **S10**: (c) See ref 8f (99% ee). (d) Liu, J.; Deng, X.; Fitzgerald, A. E.; Sales, Z. S.; Venkatesan, H.; Mani, N. S. Protecting–group–free Synthesis of a Dual CCK1/CCK2 Receptor Antagonist. *Org. Biomol. Chem.* **2011**, *9*, 2654–2660 (94% ee, industrial process). For **S11**: (e) Imamoto, T.; Tamura, K.; Zhang, Z.; Horiuchi, Y.; Sugiya, M.; Yoshida, K.; Yanagisawa, A.; Gridnev, I. D. Rigid P–Chiral Phosphine Ligands with tert–Butylmethylphosphino Groups for Rhodium–Catalyzed Asymmetric Hydrogenation of Functionalized Alkenes. *J. Am. Chem. Soc.* **2012**, *134*, 1754–1769 (>99% ee). (f) Boaz, N. W.; large, S. E.; Ponasik, J. A.; Moore, M. K.; Barnette, T.; Nottingham, W. D. The Preparation of Single Enantiomer 2–Naphthylalanine Derivatives Using Rhodium−Methyl BoPhoz–catalyzed Asymmetric Hydrogenation. *Org. Process Res. Dev.* **2005**, 9, 472–478 (98% ee, industrial process). For **S12**: (g) Etayo, P.; Núñez-Rico, J. L.; Vidal–Ferran, A. Chiral Rhodium Complexes Derived from Electron–Rich Phosphine–Phosphites as Asymmetric Hydrogenation Catalysts. *Organometallics* **2011**, *30*, 6718–6725 (93% ee). (h) Blake, J. F.; Kallan, N. C.; Xiao, D.; Xu, R.; Bencsik, J. R.; Skelton, N. J.; Spencer, K. L.; Mitchell. I. S.; Woessner, R. D.; Gloor, S. L.; Risom, T.; Gross, S. D.; Martison, M.; Morales, T. H.; Viger, G. P. A.; Brandhuber, B. J. Discovery of Pyrrolopyrimidine Inhibitors of Akt. *Bioorg. Med. Chem. Lett.* **2010**, *20*, 5607–5612 (>95% ee, industrial process). For **S13**: (i) Mohar, B.; Stephan, M. Practical Enantioselective Hydrogenation of α-Aryl- and α-Carboxyamido–ethylenes by Rhodium(I)-{1,2-Bis[(o-tert- butoxyphenyl)–(phenyl)phosphino]ethane}. *Adv. Synth. Catal.* **2013**, *355*, 594–600 (>99% ee).

[28] Buisman, G. J. H.; Kamer, P. C. J.; van Leeuwen, P. W. N. M. Rhodium Catalysed Asymmetric Hydroformylation with Chiral Diphosphite Ligands. *Tetrahedron: Asymmetry* **1993**, *4*, 1625–1634.

[29] Houston, T. A.; Wilkinson, B. L.; Blanchfield, J. T. Boric Acid Catalyzed Chemoselective Esterification of α–Hydroxy–carboxylic Acids. *Org. Lett.* **2004**, *6*, 679–681.

[30] Wu, Y.; Qi, S.–B.; Wu, F.–F.; Zhang, X.–C.; Li, M.; Wu, J.; Chan, A. S. C. Synthesis of β–Amino Acid Derivatives via Copper–Catalyzed Asymmetric 1,4–Reduction of β–(Acylamino)–acrylates. *Org. Lett.* **2011**, *13*, 1754–1757.

[31] Van den Berg, M.; Haak, R. M.; Minnaard, A. J.; de Vries, A. H. M.; de Vries, J. G.; Feringa, B. L. Rhodium/MonoPhos–Catalysed Asymmetric Hydrogenation of Enamides. *Adv. Synth. Catal.* **2002**, *344*, 1003–1007.

[32] Enthaler, S.; Hagemann, B.; Junge, K.; Erre, G.; Beller, M. Enantioselective Rhodium-Catalyzed Hydrogenation of Enamides in the Presence of Chiral Monodentate Phosphanes. *Eur. J. Org. Chem.* **2006**, *2006*, 2912–2917.

[33] Dupau, P.; Le Gendre, P.; Bruneau, C.; Dixneuf, P. H. Optically Active Amine Derivatives: Ruthenium–Catalyzed Enantioselective Hydrogenation of Enamides. *Synlett* **1999**, 1832–1834.

[34] Hu, N.; Zhao, G.; Zhang, Y.; Liu, X.; Li, G.; Tang, W. Synthesis of Chiral α–Amino Tertiary Boronic Esters by Enantio–selective Hydroboration of α–Arylenamides. *J. Am. Chem. Soc.* **2015**, *137*, 6746–6749.

3.2. Privileged P-stereogenic Ir-MaxPHOX catalysts for the highly enantioselective hydrogenation of a diverse scope of non-chelating olefins

3.2.1. Introduction

In the previous section we have highlighted that Rh- and Ru-catalysts, particularly those with diphosphine ligands, have been found to be effective for reducing olefins with coordinating functional groups.[1] In contrast, for the hydrogenation of non-chelating olefins Ir-P,X-catalysts (X=N, S and O; mainly with phosphine/phosphinite/phosphite-oxazoline ligands) have shown to yield the best results.[2] Particularly, the reduction of non-chelating olefins is the most difficult and less explored field since they do not have a coordinating group to help to transfer the chiral information to the product. Currently, Ir-catalysts only perform well for specific types of olefins. The most common substitution patterns are *E*-trisubstituted alkenes and, to a lesser extent, *Z*-trisubstituted and 1,1-disubstituted alkenes. The hydrogenation of tetrasubstituted olefins is the least developed category.[2] Even for the most studied trisubstituted olefins there is still room for improvement. For example, the reduction of the so called purely alkyl-trisubstituted olefins, those without functional groups or aryl substituents, has been achieved in very few cases[3] and the effectiveness for exocyclic substrates needs to be improved[4]. For tetrasubstituted olefins only a few specific Ir-catalysts have provided high performance for certain substrates, with variable enantioselectivity and low functional group tolerance. Most of the alkenes studied were restricted to cyclic olefins and only a few were acyclic, mainly trimethylstyrene derivatives,[4b,5] until recently when Gosselin's group in collaboration with Bigler, Pfaltz and Denmark[6] presented the reduction of a wide range of acyclic olefins with two or more aryl substituents. In addition, there are fewer reports of tetrasubstituted olefins with poorly coordinative groups that are useful for further synthesis and, in most cases, the same catalyst was unsuccessful for tetrasubstituted olefins without a poorly coordinative group.[7] The finding of a catalyst that could work on all of them is highly desirable to limit time-consuming catalyst design and avoid a variety of preparation methods.

The bottleneck in finding the best catalysts is the identification of the right ligands with a broad substrate scope.[8] To overcome the substrate scope limitation in the asymmetric hydrogenation of non-chelating olefins, we recently reported on the first P,N-ligand library that could reduce different types of non-chelating olefins.[4b] From a common backbone, the selection of the phosphite or phosphinite group lead to ligands that were suitable for 56 examples of di-, tri- and tetrasubstituted olefins. However, only 11 examples of tetrasubstituted olefins could be reduced, mainly indene derivatives and some acyclic olefins, to the detriment of tetrasubstituted acyclic alkenes with

relevant poorly coordinative groups. Even for trisubstituted olefins, only one example of *Z*-olefin was successfully reduced and none of purely alkyl-substituted were reported.

To advance the search for a ligand library capable of hydrogenating a large range of substituted non-chelating olefins, we decided to introduce in the P,N-ligand design the advantatges of having a bulky P-stereogenic center. However, this development was delayed by the difficulty of synthesizing bulky P-sterogenic phosphines in optically pure form. Fortunately, Riera and Verdaguer's group recently presented a novel, straightforward synthetic route that solved this problem and allowed the synthesis of a library of P-stereogenic aminophosphine-oxazoline (MaxPHOX, Figure 3.2.1) ligands in which both enantiomeric series are equally available.[9]

In this section, we highlight the effective use of Ir-MaxPHOX-type catalysts Ir/**L5**–**L8a**–**c** (Figure 3.2.1) in the hydrogenation of a wide range of di-, tri- and tetrasubstituted olefins, including those with poorly coordinative groups.[10] These catalyst precursors have the advantage that they are prepared in four steps from available starting materials[9b] and allow to easily study the effect of varying some ligand properties, such as the bulkiness of the oxazoline and its configuration and the configuration of the stereogenic center at the alkyl backbone chain. In addition, in a collaboration with Maseras and Besora's groups we performed DFT calculations that were able to explain the origin of enantioselectivity, identify the preferred pathway and predict enantioselectivities with good accuracy.

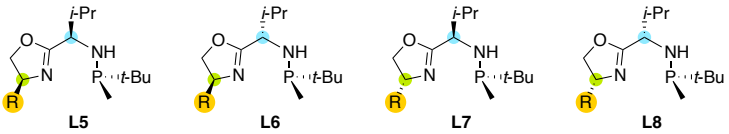

Figure 3.2.1. The family of P-stereogenic aminophosphine-oxazoline ligands **L5**–**L8a**–**c**.

3.2.2. Results and discussion

3.2.2.1. Initial catalytic screening

As mentioned in the introduction, the hydrogenation of non-chelating olefins depends largely on the substitution pattern of the substrate. The most successful examples have been reported for *E*-trisubstituted, while 1,1'-disubstituted olefins are usually hydrogenated less enantioselectively and tetrasubstituted olefins are still underdeveloped.[2] To explore the scope of the Ir-MaxPHOX catalysts (Ir/**L5**–**L8a**–**c**) we initially applied them in the asymmetric hydrogenation of the non-chelating disubstituted olefin **S14** and the widely used benchmark trisubstituted substrate **S15** and acyclic tetrasubstituted olefin **S16** (Table 3.2.1). The initial test conditions were the optimal conditions reported in previous studies with other P,N-ligands.[2] Therefore, the

reactions were carried out at room temperature using 1 mol% of the catalyst in dichloromethane under 1 bar of H_2 for the disubstituted substrate **S14**, 50 bar of H_2 for the trisubstituted olefin **S15** and 75 bar of H_2 for **S16**.

Table 3.2.1. Asymmetric hydrogenation of olefins **S14**, **S15** and **S16** with Ir/**L5**–**L8a**–**c**.[a]

		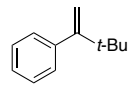 **S14**		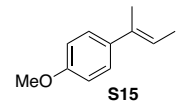 **S15**		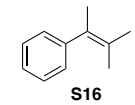 **S16**	
Entry	Ligand	% Conv[b]	% ee[c]	% Conv[b]	% ee[c]	% Conv[b]	% ee[c]
1	**L5a**	100	74 (*S*)	100	67 (*R*)	100	75 (*R*)
2	**L5b**	100	66 (*S*)	100	75 (*R*)	100	85 (*S*)[d]
3	**L5c**	100	81 (*S*)	100	77 (*R*)	85	44 (*R*)
4	**L6b**	100	15 (*S*)	100	15 (*S*)	85	33 (*S*)
5	**L7b**	100	80 (*R*)	100	23 (*S*)	100	44 (*R*)
6	**L8a**	100	83 (*R*)	100	82 (*S*)	100	28 (*R*)
7	**L8b**	100	88 (*R*)	100	85 (*S*)	100	25 (*R*)
8	**L8c**	100	91 (*S*)	100	88 (*S*)	100	31 (*R*)
9[e]	**L8c**	100	91 (*R*)	100	89 (*S*)	-	-
10[e]	**L5b**	-	-	-	-	100	98 (*S*)[f]

[a] Reaction conditions: Ir/**L5**–**L8a**–**c** (1 mol%), CH_2Cl_2, 1 bar of H_2 (**S14**) or 50 bar of H_2 (**S15**) or 75 bar of H_2 (**S16**), rt, 4 h (**S14** and **S15**) or 24 h (**S16**). [b] Conversions were measured by ^{1}H NMR spectroscopy after 4 h (**S14** and **S15**) or 24 h (**S16**). [c] Enantiomeric excess determined by GC. [d] Using 2 bar of H_2 - 98% (*S*) ee. [e] Reactions carried out in PC instead of CH_2Cl_2 after 6 h (**S14** and **S15**) and 30 h (**S16**). [f] Using 2 bar of H_2.

For substrates **S14** and **S15**, the best enantioselectivities were obtained with Ir/**L8c** (ee's up to 91%, entry 8) regardless of the substitution pattern of the substrate. The results showed that both the oxazoline substituent and the diastereoisomeric backbone of the ligand had a noticeable effect on the stereochemical outcome. This effect also occurred in the hydrogenation of the tetrasubstituted olefin **S16**. However, while for the di- and trisubstituted substrates (**S14** and **S15**) the best results were obtained with the bulkier *t*-Bu group in the oxazoline (e.g., entry 8 vs 6-7), the best results for the tetrasubstituted substrate **S16** were obtained with the less bulky *i*-Pr group, in accordance with the higher steric hindrance of **S16** (entry 2). Similarly, the effect of the diastereoisomeric backbone differed between the di/trisubstituted alkenes **S14** and **S15** and the tetrasubstituted olefin **S16**. While backbone **L8** (Figure 3.2.1) was best for **S14** and **S15** (ee's up to 91%), the best backbone for **S16** was **L5** (ee's up to 98% at 2 bars of H_2, entry 2)[11]. In summary, optimizing the ligand structure led us to identify Ir/**L5b**

and Ir/**L8c** as the best catalysts of the family for the hydrogenation of olefins with different substitution patterns.[12]

To make the process more sustainable, the reaction was carried out in 1,2-propylene carbonate (PC),[13] an eco-friendly alternative to standard organic solvents due to its high boiling point, low toxicity and green synthesis (Table 3.2.1, entries 9 and 10). Advantageously, enantioselectivities remained as high as those obtained with dichloromethane (ee's up to 98%). In addition, the catalyst could be recycled up to five times with a simple two-phase extraction with hexane with minimal decrease in enantioselectivity (see Supporting Information).

3.2.2.2. Mechanistic studies. The origin of the enantioselectivity

To understand why the best ligand for tetrasubstituted olefins is different from that of di- and trisubstituted analogues, we performed a density functional theory (DFT) study. The transition states (TSs) involved in the enantiodetermining step of the reaction for the tri- and tetrasubstituted olefins, **S15** with catalyst Ir/**L8c** and olefin **S16** with catalysts Ir/**L5b** and Ir/**L8c** were searched using the B3LYP[14] functional with the Grimme Dispersion correction, GD3[15]. As mentioned in the general introduction (Chapter 1), it is well known that Ir-catalyzed hydrogenation of non-chelating alkenes proceeds through an Ir(III)/Ir(V) mechanism[16] and enantioselectivity is determined in the first hydrogen transfer from the metal to the coordinated olefin. Our calculations also support this mechanism, the free energy reaction profile is presented in the Supporting Information. Consequently, enantioselectivity can be reliably estimated from the relative energies of the TSs of this step. Nevertheless, two different mechanisms can be considered for this process; therefore we computed the TSs for both migratory-insertion (**TS$_{MI}$**) and σ-bond metathesis (**TS$_{Meta}$**) pathways (see Supporting Information for the full set of calculated TSs). A data set collection of computational results is available in the ioChem-BD repository.[17]

The calculated relative energies for the most stable isomers of the TSs for both pathways (**TS$_{MI}$** and **TS$_{Meta}$**) are shown in Table 3.2.2. These key isomers are the result of the relative arrangement of the hydride (up or down), the coordination of the olefin through the *Re* or *Si* face and the attack of the hydride through the two olefinic carbons (C_1 or C_2). In addition, in these calculations we also considered the rotamers of the isopropyl group. As in other reported studies, the results show that in all cases the migratory insertion (**TS$_{MI}$**) is the preferred reaction pathway.

Positively, the calculations for the trisubstituted substrate **S15** with the Ir/**L8c** reproduce the experimental outcome. The favored pathway, TS$_{L}$ in Table 3.2.2, proceeds through the *Re*-face, which leads to the formation of the (*S*)-product and the energy difference between the two most stable TSs (TS$_{L}$ and TS$_{o}$, Table 3.2.2), which lead to opposite enantiomers, is 5.3 kJ/mol (ee_{calc}= 79% (*S*)) in agreement with the

experimental enantioselectivity (88% (*S*)). Single Point calculations on the most stable TSs with larger basis sets B97D3/cc-pVTZ & cc-pVTZ-PP improve the agreement ee_{calc}= 85% (*S*) (see Supporting Information for further details).

Table 3.2.2. Calculated relative energies (kJ/mol) for the transition states **TS_{MI}** and **TS_{Meta}** using Ir/**L8c** (for **S15**) and Ir/**L5b** and Ir/**L8c** (for **S16**).[a]

TS_{Meta}	L8c/S15	L8c/S16	L5b/S16	TS_{MI}	L8c/S15	L8c/S16	L5b/S16
 **A** attack through C_1 *Si*-face coordination	56.7	35.7	17.3	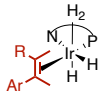 **I** attack through C_1 *Si*-face coordination	39.3	37.8	8.5
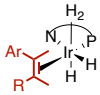 **B** attack through C_1 *Re*-face coordination	18.3	25.1	7.3	 **J** attack through C_1 *Re*-face coordination	60.3	49.7	21.3
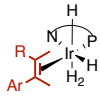 **C** attack through C_1 *Si*-face coordination	20.1	12.9	15.7	 **K** attack through C_1 *Si*-face coordination	26.3	7.3	27.0
 **D** attack through C_1 *Re*-face coordination	34.3	19.1	27.7	 **L** attack through C_1 *Re*-face coordination	**0.0**	10.7	24.9
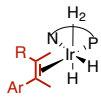 **E** attack through C_2 *Si*-face coordination	44.6	39.7	11.1	 **M** attack through C_2 *Si*-face coordination	61.7	37.2	**4.4**
 **F** attack through C_2 *Re*-face coordination	55.1	36.9	13.9	 **N** attack through C_2 *Re*-face coordination	19.1	28.3	**0.0**
 **G** attack through C_2 *Si*-face coordination	38.9	15.5	29.2	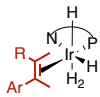 **O** attack through C_2 *Si*-face coordination	**5.3**	**0.0**	17.0
 **H** attack through C_2 *Re*-face coordination	5.6	9.9	24.8	 **P** attack through C_2 *Re*-face coordination	32.6	**6.4**	28.7

[a] Values in blue and bold indicate lowest *Re* and *Si* energy TSs for each combination of substrate and catalyst. [b] Relative Gibbs free energies (kJ/mol) in solution (B3LYP-D3/6-31G(d,p)&LANL2DZ) with respect to the corresponding lowest energy transition state; For **S15** Ar= 4-CH_3O-C_6H_4 and R= H and for **S16** Ar= C_6H_5 and R= CH_3; C_1 is the least electronegative olefinic carbon atom and C_2 is the most electronegative one. In all TSs the most stable rotamer was selected.

The factors responsible for enantioselectivity can be deduced by analyzing the structures of both TSs via quantitative quadrant-diagram representations using the MolQuO[18] software (Figure 3.2.2). Figure 3.2.2a shows the quadrant diagram obtained by analyzing the two most stable TSs for the hydrogenation of **S15** ($TS_{\mathbf{L}}$ and $TS_{\mathbf{o}}$, Table 3.2.2).[19] In this diagram, the oxazoline substituent (*t*-Bu) blocks the lower-left quadrant Q3 (quadrant occupancy= 3.8), while the methylenic carbon of the oxazoline partly occupies the upper-left quadrant Q1 (quadrant occupancy= 1.6) making it semi-hindered (Figure 3.2.2a). The other two quadrants Q2 and Q4, free from bulky groups, are empty (quadrant occupancy= 0). According to this model, the coordination of the trisubstituted olefin **S15** through the *Re*-face is favored because the smallest substituent, the olefinic hydrogen, is located in the most hindered quadrant Q3 and the aryl substituent (4-OMe-C_6H_5) is located in the semi-hindered quadrant Q1 (Figure 3.2.2b). In contrast, when the olefin coordinates through the *Si*-face, which leads to the opposite enantiomer ((*R*)-enantiomer, ($TS_{\mathbf{o}}$, Table 3.2.2), the aryl group is located at the most hindered quadrant resulting in a less favorable TS (Figure 3.2.2c). The occupancy value for this quadrant (3.1) is slightly lower than that obtained for the TS leading to the major product, indicating that the ligand adapts its chiral pocket to suit the olefin in this coordination manner. Noteworthy, all TSs with the methyl group located in Q3 are less stable, at least 26.3 kJ/mol higher in energy than the most stable one. Note that despite the small size of a methyl group, the flat 4-MeO-C_6H_5 group fits better into the cavity in Q3. In summary, the model indicates that the stereochemical outcome with trisubstituted olefin **S15** depends on steric factors. Following this observation, it can be hypothesized that the catalyst may also work for other aryl-containing trisubstituted olefins, including the less studied triaryltrisubstituted and *Z*-olefins (see below Scheme 3.2.2), where the TS with the olefinic hydrogen located in the most hindered quadrant Q3 will continue to be more stable than a TS with the aryl substituent (for triaryl olefins) or the methyl substituent (for *Z*-olefins) in Q3. In addition, this model suggests that if the olefinic aryl group is replaced by a bulkier substituent (e.g., purely alkyl-substituted olefins) then a higher destabilization of the $TS_{\mathbf{o}}$ could be expected, resulting in a higher energy gap between the TSs and high enantioselectivity (see results for **S33** and **S34**, Scheme 3.2.2).

In contrast, the most favorable TS with the same Ir-catalyst system Ir/**L8c** but with the tetrasubstituted olefin **S16** was $TS_{\mathbf{o}}$ (Table 3.2.2) where the olefin coordinates through the *Si*-face and the (*R*)-enantiomer would be obtained as observed experimentally.

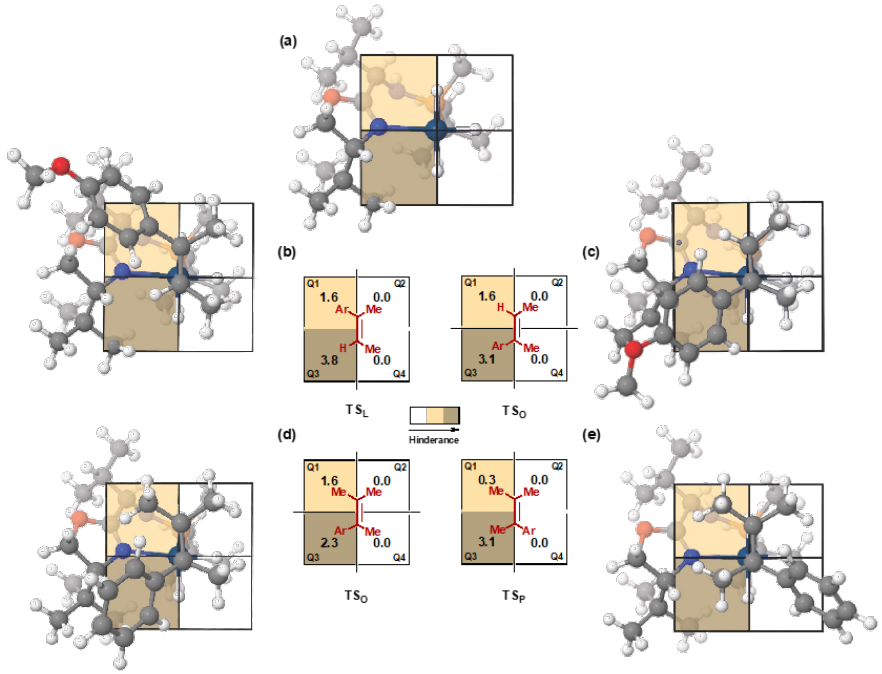

Figure 3.2.2. Models of the most favored TSs for the asymmetric hydrogenation of **S15** and **S16** with Ir/**L8c**; (a) Schematic quadrant model for Ir/**L8c** (the olefin coordinates above the plane of the paper), (b) The most favorable coordination of **S15** giving the major (*S*)-product, (c) The most favorable coordination of **S15** giving the minor (*R*)-product, (d) The most favorable coordination of **S16** giving the major (*R*)-product, (e) The most favorable coordination of **S16** giving the minor (*S*)-product.

The quadrant diagrams of the two most stable TSs ($TS_{\mathbf{O}}$ and $TS_{\mathbf{P}}$, Table 3.2.2) with the tetrasubstituted olefin **S16** and Ir/**L8c** were analyzed (Figure 3.2.2d and e). The diagrams show that the preferred coordination of **S16** is through the *Si*-face with the olefinic phenyl substituent occupying the most hindered quadrant (Q3, Figure 3.2.2d) which explains why the enantioselectivity is opposite to that of **S15**. Again, the planarity of the phenyl substituent makes the TS less crowded in Q3 than with a methyl group. This is reflected in the fact that the distance between the hydrogen of the C_4 of the oxazoline and the olefinic phenyl substituent ($TS_{\mathbf{O}}$) is greater than the distance between the hydrogen of the C_4 of the oxazoline and the methyl substituent in the $TS_{\mathbf{P}}$ (Figure 3.2.3).

When the Ir-catalyst Ir/**L5b** was used in the hydrogenation of the tetrasubstituted olefin **S16** the reverse enantioselectivity was obtained compared to Ir/**L8c**. This can be rationalized by analyzing the quadrant model of the most stable transition state, $TS_{\mathbf{N}}$ (Table 3.2.2), for the hydrogenation of **S16** with Ir/**L5b** (Figure 3.2.4). Ir/**L5b** has the opposite configuration in the oxazoline substituent compared to Ir/**L8c**, making the

upper-left quadrant Q1 the most hindered (Figure 3.2.4a). Therefore, the preferred coordination of **S16** is through the *Re*-face (the opposite of Ir/**L8c**) with the olefinic phenyl located in the most hindered quadrant (Q1) (Figure 3.2.4b).

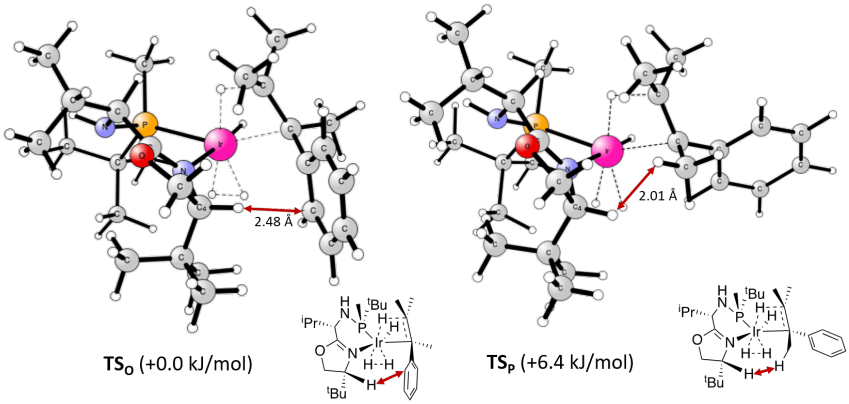

Figure 3.2.3. Representation of the two most stable TSs (TS**o** and TS**P**) for Ir/**L8c** and substrate **S16**. Relative Gibbs free energies in solution (kJ/mol) with respect to the corresponding lowest TS.

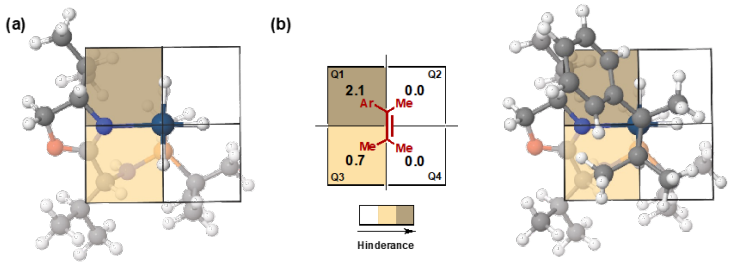

Figure 3.2.4. Model of the most favored TS for the asymmetric induction of **S16** with Ir/**L5b**; (a) Schematic quadrant model for Ir/**L5b** (the olefin coordinates above the plane of the paper), (b) The most favorable coordination of **S16** giving the major (*S*)-product.

Although the sense of enantioselectivity for **S16** was well predicted for both Ir-catalysts Ir/**L8c** and Ir/**L5b**, the enantioselectivity value was greatly overestimated with Ir/**L8c** (82% (*R*) B3LYP-D3/6-31G(d,p)&LANL2DZ and 85% B97D3/cc-pVTZ&cc-pVTZ-PP predicted ee vs 31% (*R*) observed ee). To explain this disagreement, we conducted deuterium labeling experiments with Ir/**L5b** and Ir/**L8c** (Scheme 3.2.1) in which the related tetrasubstituted olefin **S17** was reduced with deuterium. Note that in these deuterogenation experiments we used substrate **S17**, which differs from the tetrasubstituted olefin **S16** in a methoxy group in the aryl group, which was introduced to facilitate product analysis. Both substrates performed in the same way. As expected, no deuteration at the methyl groups was observed using Ir/**L5b**. However, in the case of Ir/**L8c** a substantial deuteration was found at the allylic position, indicating the

existence of a competing isomerization process. This isomerization would explain the lower enantioselectivity observed when using Ir/**L8c** in the hydrogenation of tetrasubstituted alkenes such as **S16** or **S17** (Table 3.2.1, entry 2 vs 7).

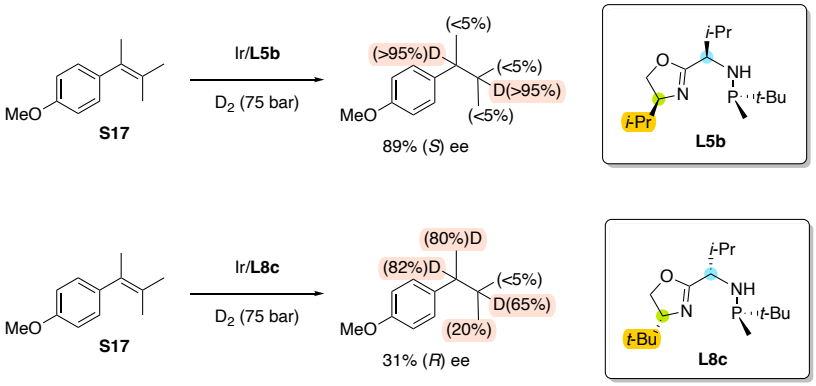

Scheme 3.2.1. Deuterium labeling experiments of tetrasubstituted substrate **S17**. The percentage of deuterium incorporation is shown in brackets.

3.2.2.3. Substrate scope. *1,1-Di- and trisubstituted olefins*

With the optimal Ir-complexes in hand and having elucidated the origin of the enantioselectivity the next step was to test de ligands with a variety of olefins. We first focused on the hydrogenation of non-chelating di- and trisubistututed olefins with aryl and/or alkyl substituents only (Scheme 3.2.2). According to the previous screening, Ir/**L8c** was selected for the hydrogenation of a wide range of 1,1'-disubstituted olefins. As expected, this catalyst provided high enantioselectivities (up to 94% ee) for other α-*tert*-butylstyrenes (substrates **S18**–**S24**) with a range of electronic and steric properties at the aryl group. These are significant results because disubstituted substrates suffer more face-selectivity indetermination than the trisubstituted equivalents and therefore there are fewer catalysts [20] that can provide those high ee's. Nevertheless, the hydrogenation of α-alkylstyrene **S25**, which has a less bulky ethyl group, proceeded with a lower enantioselectivity (ee' up to 80%) than α-*tert*-butylstyrenes. Although this is still a remarkable result for this challenging substrate, the lower ee was due to the isomerization of **S25** (as observed in deuteration experiments; see Supporting Information). Thus, like the most successful cases reported in the literature,[21] the competition between direct hydrogenation and isomerization is responsible for the observed decrease in enantioselectivity. Börner et al. found that the use of 1,2-propylene carbonate (PC) as a solvent reduces the isomerization rate.[13a] We therefore performed the reaction of **S25** in PC and we were glad to see that the enantioselectivity increased to 90% ee.

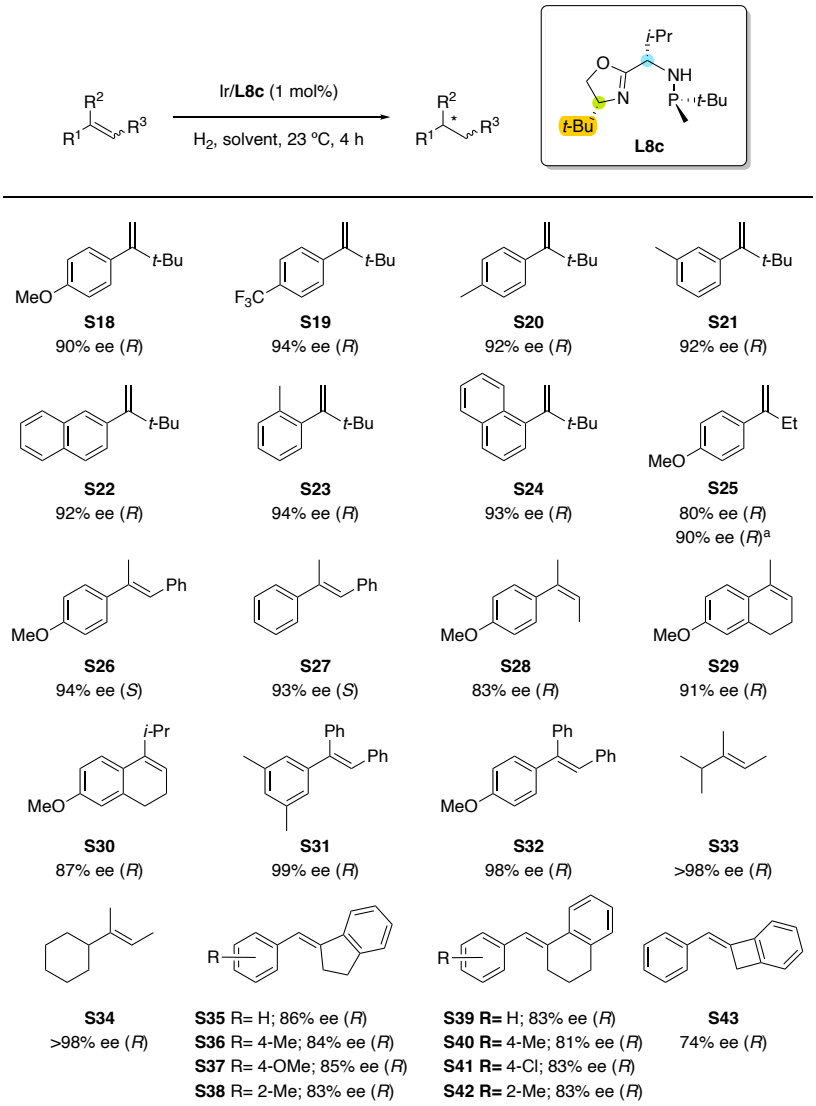

Scheme 3.2.2. Asymmetric hydrogenation of non-chelating disubstituted and trisubstituted olefins with only aryl and/or alkyl substituents **S18**–**S43**. Full conversions were achieved in all cases. Reaction conditions: Ir/**L8c** (1 mol%), CH_2Cl_2, 23 °C, 4 h, using 1 bar of H_2 for **S18**–**S25** or 50 bar of H_2 for **S26**–**S43**. [a] Reaction carried out using propylene carbonate (PC) as solvent for 6 h.

As far as the hydrogenation of aryl trisubstituted olefins is concerned (**S26**–**S32**; Scheme 3.2.2), the catalyst Ir/**L8c** also worked well for those with an *E*-geometry **S26** and **S27** (ee's up to 94%), which differ from **S15** in the substituent of the aryl ring and the substituent *trans* to the aryl group, as well as for the more challenging *Z*-geometry alkenes **S28**–**S30** (ee's up to 91%). In addition, the substrate scope was extended to the triaryltrisubstituted substrates **S31** and **S32** (ee's up to 99%), whose reduction has

been less studied despite the fact that they are an easy entry point to obtain diarylmethine chiral centers present in natural products and medicines.[22] These catalytic results are completely consistent with the calculated TSs (*vide supra*). The analysis of the TSs indicated that the stereochemical outcome for the *E*-olefins mainly depends on steric factors. This finding suggested that enantioselectivities could also be high for substrates such as **S15** with a bulkier group replacing the phenyl moiety. This hypothesis was confirmed with the high enantioselectivities (ee's >98%) found in the hydrogenation of substrates **S33** and **S34**, which contain a bulky isopropyl and cyclohexyl group, respectively (Scheme 3.2.2).[23] These are valuable results because the highly enantioselective hydrogenation of purely alkyl substrates is rare,[3] and indicate that the chiral pocket of the catalyst Ir/**L8c** is suitable for achieving the hydrogenation of these elusive substrates with excellent enantiocontrol.

The results up to this point led us to test the reduction of exocyclic trisubstituted olefins (**S35**–**S43**, Scheme 3.2.2). The hydrogenation of these substrates is of interest because the chiral benzofused ring motif is present in pharmaceuticals, natural products and intermediates of relevant bioactive drugs.[24] Despite the similarities with the acyclic olefins discussed above, the asymmetric hydrogenation of exocyclic olefins has hardly been explored and has yet to be resolved. The main challenge with exocyclic olefins is that the stereochemical outcome is highly influenced by ring size and, until recently, only a few examples had been able to provide high enantiocontrol, particularly for exocyclic olefins with a benzofused 5-membered ring[4a,4b,25] although enantioselectivity decreased when an *ortho*-substituent was present and required an additive to work.[26] Positively, the stereochemical outcome using Ir/**L8c** was barely affected by the size of the ring of the substrate, being able to hydrogenate five- and six-membered ring benzofused olefins with high enantioselectivities (up to 86% ee, Scheme 3.2.2) at room temperature without additives. In addition, Ir/**L8c** tolerates well the presence of several substituents that decorates the aryl group, even an *ortho* group. Note also that, surpassing the previously reported results, the more challenging benzofused olefin with a four-membered ring **S43** could also be hydrogenated with a significant enantioselectivity of 74% ee.

3.2.2.4. Substrate scope. *1,1-Di- and trisubstituted olefins with neighboring polar groups*

We then moved on to asymmetric hydrogenation of key acyclic olefins with neighboring polar groups. In this context, a set of α,β-unsaturated trisubstituted acyclic enones **S44**–**S49** (Scheme 3.2.3) could be hydrogenated with enantioselectivities comparable to the best ones reported but, in contrast to the asymmetric hydrogenation of di- and trisubstituted alkenes mentioned above, this was done with the catalytic system Ir/**L8a**.[2j,3d-f,27] The reduction of these olefins opens a direct, atom-efficient path to prepare optically pure ketones, the synthesis of which until now has been mainly

based on non-catalytic methods with a limited substrate scope. The attained enantioselectivities, between 95% and 98% ee, were quite independent of the nature of the substituents, which also allowed the successful hydrogenation of the highly appealing α-fluoride substituted enone **S49**.[28] It has been reported that the stereochemical outcome in the hydrogenation of acyclic enones is greatly influenced by the enone substitution pattern and, therefore, only a few catalysts have been able to hydrogenate both α,β- and β,β-unsaturated trisubstituted enones with high enantioselectivities.[27c,d] Gratifyingly, the catalytic system Ir/**L8a** also proved to be very efficient in the hydrogenation of β,β-unsaturated enones **S50** and **S51** (Scheme 3.2.3).

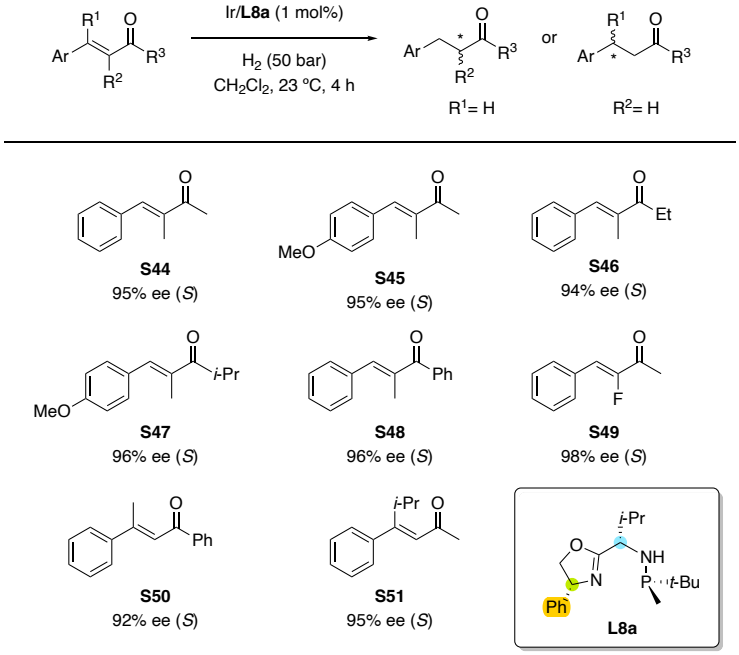

Scheme 3.2.3. Asymmetric hydrogenation of α,β- and β,β-unsaturated trisubstituted enones. Full conversions were achieved in all cases.

We then tested whether the high enantioselectivities were maintained for acyclic olefins containing other relevant neighboring polar groups (Scheme 3.2.4, substrates **S52**–**S61**). High enantioselectivities up to 98% in alkenylboronic esters and enol phosphinates were obtained. Among these results, one can highlight the effective hydrogenation of the pure alkyl trisubstituted enol phosphinates **S59** and **S60**, a good alternative to the hydrogenation of dialkyl ketones to alcohols whose hydrogenation is still elusive. While for the reduction of vinyl boronate the best enantioselectivity was achieved with Ir/**L8b** (95% ee), for enol phosphinates the highest enantioselectivities (up to 98% ee) were obtained with Ir/**L8a**. Both types of substrates are of interest because their reduction opens up straightforward routes for preparing enantiomerically pure organoboron and organophosphorous compounds, which can be easily transformed

into high-value compounds.[29] The excellent enantioselectivities obtained in the hydrogenation of the trisubstituted alkenylboronic ester and enol phosphinates were also reached in the even more challenging disubstituted analogues (**S53**–**S54** and **S60**–**S61**; up to 92% ee), including the hydrogenation of non-aromatic disubstituted olefins **S54** and **S60**.

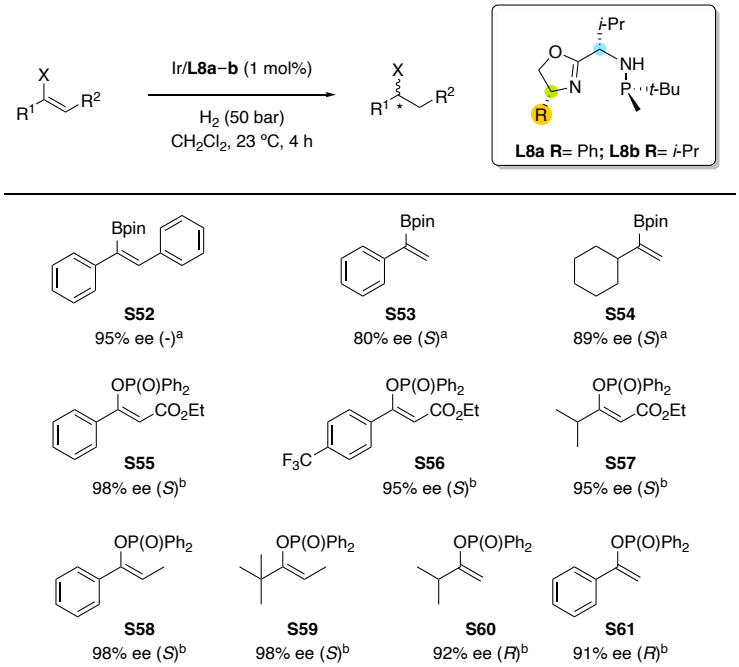

Scheme 3.2.4. Asymmetric hydrogenation of vinyl boronates **S52**–**S54** and enol phosphinates **S55**–**S61**. Full conversions were achieved in all cases. [a] Reactions carried out using Ir/**L8b**. [b] Reactions carried out with Ir/**L8a**.

Subsequently, we focused on the asymmetric hydrogenation of exocyclic olefins containing a neighboring polar group (Scheme 3.2.5, **S62**–**S81**). In particular, we considered the hydrogenation of α,α-unsaturated exocyclic enones and α,α-unsaturated lactones and lactams, since the reduced products of these olefins are encountered in natural products and drugs.[30] These substrates suffer from the same ring size limitation that was discussed for exocyclic olefins without a neighboring polar group.[3] In our case, however, the hydrogenation of the exocyclic enones **S62** and **S63** using Ir/**L8a** proceeded with high enantioselectivities (up to 97%), comparable to the best ones, regardless of the size of the ring. In addition, hydrogenation of α,α-unsaturated lactones **S64**–**S72** also proceeded with excellent levels of enantioselectivity (ee's up to 99%) regardless of the size of the lactone ring. In addition, ee's were found to be quite independent of the electronic and steric nature of the olefinic substituent. Chiral α-substituted-δ-valerolactones and γ-butyrolactones were therefore attained with ee's up to 99%. The hydrogenation of α,α-unsaturated lactams **S73**–**S81** followed the same

trend as related lactones, with ee's up to >99%. Note that the Ir-catalyst Ir/**L8a** also allows the presence of different protecting groups, such as Bn, Ac and Boc, albeit in the latter case the Boc group can also be partially cleaved under the reaction conditions.

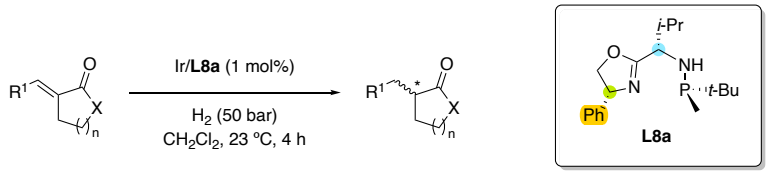

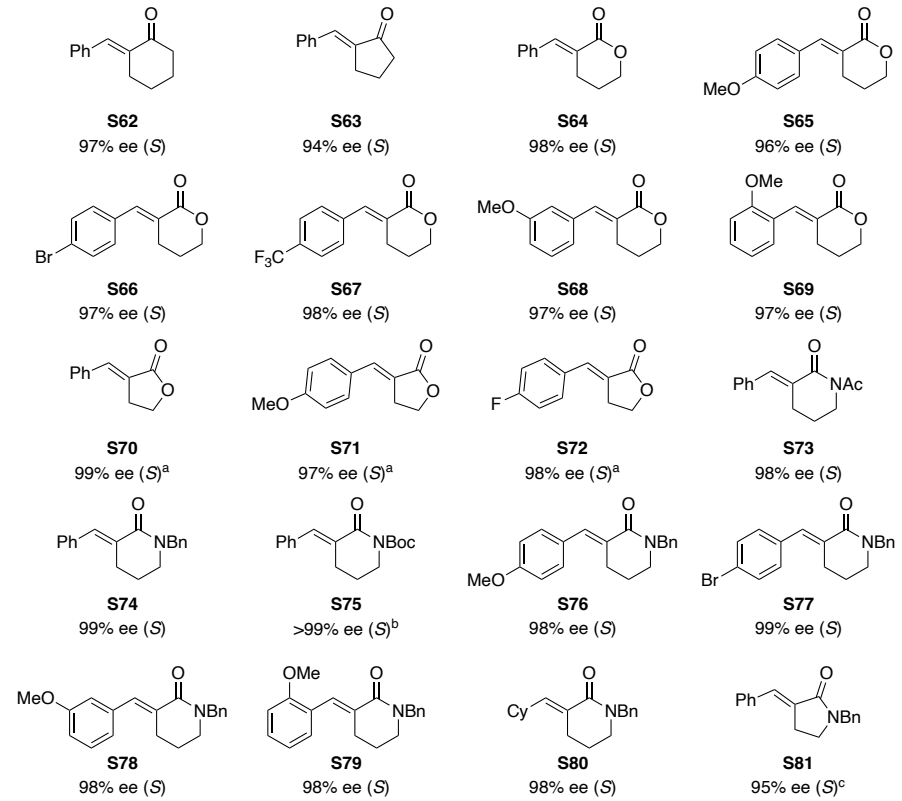

Scheme 3.2.5. Asymmetric hydrogenation of exocyclic α,α-unsaturated enones, lactones and lactams **S62**–**S81**. Full conversions were attained in all cases otherwise noted. [a] Reactions carried out using 2 mol% of catalysts. [b] 28% of deprotected lactam was also obtained. [c] 76% conversion was attained.

3.2.2.5. Substrate scope. *Tetrasubstituted olefins*

Tetrasubstituted acyclic olefins are considered to be some of the most challenging substrates to be hydrogenated due to the difficulty in differentiating the prochiral faces and due to the slow activities that result from their steric hindrance. The reduction of non-chelating tetrasubstituted acyclic olefins remains an open challenge. Furthermore,

there are only a few reports on the hydrogenation of tetrasubstituted olefins with poorly coordinative groups that can create intermediates useful for subsequent synthesis.[7]

So, following the excellent results obtained with acyclic olefin **S16** (Table 3.2.1), we wanted to further extend our work to the asymmetric hydrogenation of other non-chelating acylic tetrasubstituted olefins (**S82**–**S89**, Scheme 3.2.6). Advantageously, we found that with Ir/**L5b** catalyst enantioselectivity was neither affected by the electronic and steric decorations of the phenyl group of the substrate (**S16** and **S82**–**S85**), nor by the nature of the alkyl chain (**S83**, **S86** and **S87**), nor by the use of heteroaromatic olefins (**S88** and **S89**). Improving previously reported results,[4b,5a] a broad range of substituted acyclic tetrasubstituted olefins were therefore hydrogenated in excellent enantioselectivities (ee's ranging from 96% to 99%; Scheme 3.2.6).

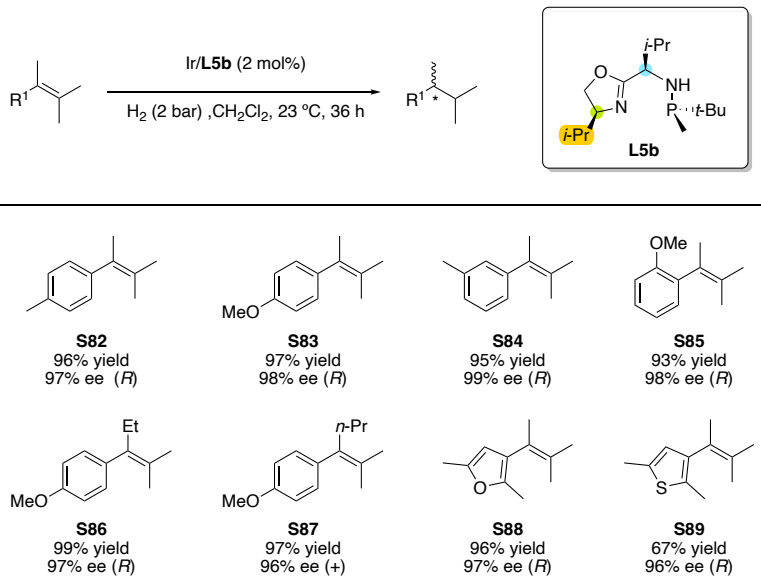

Scheme 3.2.6. Asymmetric hydrogenation of several acyclic tetrasubstituted olefins **S82**–**S89**.

We then moved to the asymmetric hydrogenation of acyclic tetrasubstituted olefins with relevant poorly coordinative groups. Due to the importance of chiral fluorine molecules, in particular those with two vicinal stereogenic centers,[31] we first focused on the asymmetric hydrogenation of acyclic vinyl fluorides containing an ester functionality such as substrates **S90**–**S94** (Scheme 3.2.7). The challenge of these substrates is that the catalysts must not only control enantioselectivity but also the diastereoselectivity (two vicinal stereogenic centers are created) and the defluorination side-reaction. Advantageously, the reaction proceeded smoothly without defluorination and in high diastereo- and enantioselectivities, regardless the nature of the olefin substituents (aryl or alkyl) and the olefin geometry under mild reaction conditions (**S90**–**S94**, Scheme

3.2.7).[32] Interestingly, the use of olefins with different geometries give access to both diastereoisomers of the hydrogenated products in high enantioselectivities. Thus, while substrate **S90**, with *E*-geometry, provides the *R,R*-diastereoisomer, the *Z*-analogue **S91** give access to the *R,S*-diastereoisomer. These results are comparable to the best ones reported in the literature.[7c] Moreover, the reduction of elusive vinyl fluorides **S95**–**S98** (Scheme 3.2.7) with an ester functionality and also a CF_3-functional group[33] instead of the methyl group improved previous results reported in the literature (67% ee).[7c] The reduction proceeded for the first time with high enantioselectivity (87% ee, Scheme 3.2.7), excellent diastereoselectivity without any defluorination with Ir/**L8c**. The result is in line with the quadrant model developed for Ir/**L8c** (vide supra, Figure 3.2.2a). The smallest substituent of the olefin (F) is placed in the most hindered quadrant (Q3) and the aryl substituent is in the semi-hindered quadrant Q1. According to this model, the predicted absolute configuration of the reduced product would be 2*S*,3*R*, in agreement with the experimental results. Positively, the high enantioselectivity was extended for the first time to substrates with different aryl substituents **S96**–**S98** (Scheme 3.2.7).

Encouraged by these results we then studied other functionalized tetrasubstituted olefins lacking a strong coordinative group. Due to the importance of succinic acid derivatives,[34] we focused on the asymmetric hydrogenation of tetrasubstituted maleates with two vicinal ester groups (substrates **S99**–**S104**; Scheme 3.2.7) as an atom-efficient method for their preparation. The reactions with Ir/**L8c** proceeded smoothly providing the hydrogenated products with excellent diastereoselectivity (>25/1 dr) and high enantioselectivities (up to 92%). Moreover, the enantioselectivity was almost unaffected by the electronic nature of the aromatic group (**S100**–**S102**) or the presence of heteroaromatic cyclic substituents (**S103**–**S104**). Next, we studied whether these results could be reproduced replacing one of the ester groups for other substituents (Scheme 3.2.7). While the exchange of any of the esters by a methyl group (**S105** and **S106**) led to a decrease in activity and enantioselectivity (ee's up to 73%), positively the reduction of **S107**, with a phosphate instead of one of the ester groups, proceeded with high enantioselectivity (>95% ee) and diastereoselectivity (>25/1 dr), being the first time that this substrate class was hydrogenated.

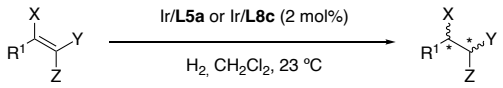

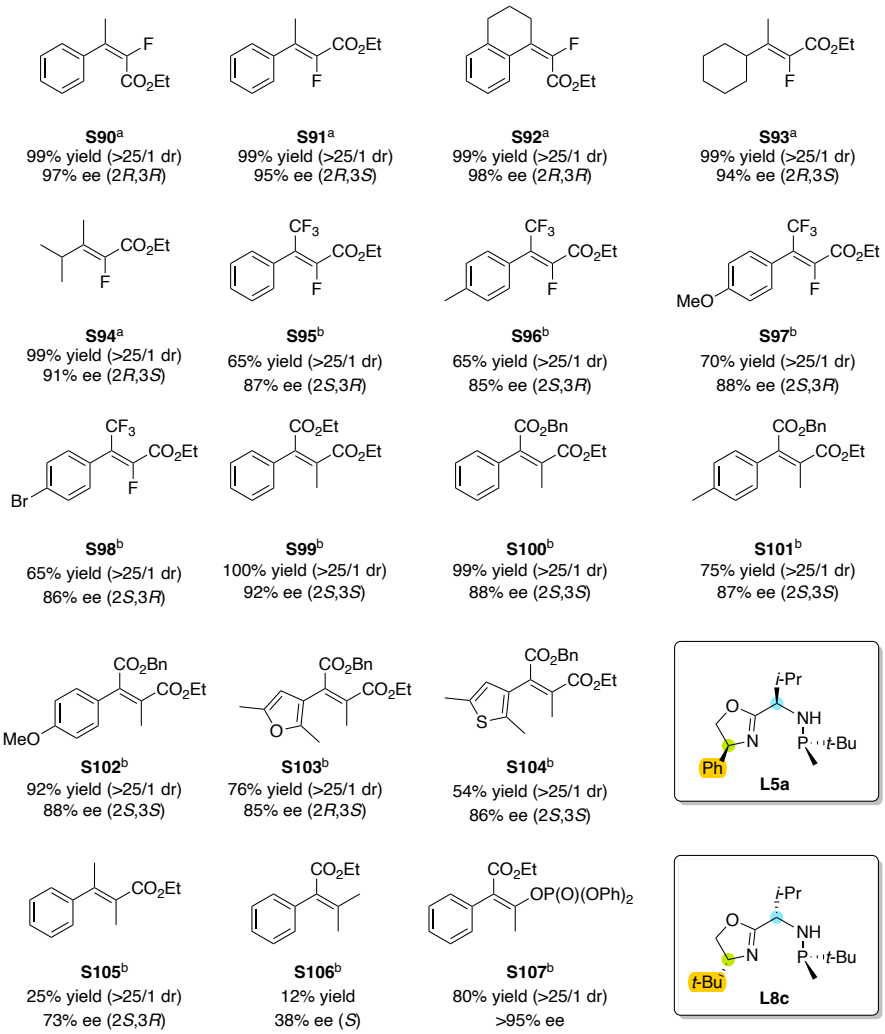

Scheme 3.2.7. Asymmetric hydrogenation of several acyclic tetrasubstituted olefins **S90**–**S107**. [a] Using Ir/**L5a** 2 bar of hydrogen using CH_2Cl_2 as solvent at 23 °C for 24 hours. [b] Using Ir/**L8c** 50 bar of hydrogen using CH_2Cl_2 as solvent at 23 °C for 4 h.

Based on the recent findings by Gosselin and collaborators of an Ir-P,N catalyst applicable to a wide range of non-chelating tetrasubstituted acyclic olefins containing two or three aryl substituents (Scheme 3.2.8 and Supporting Information for pressure and catalyst loading effects).[6] Initially,we studied the hydrogenation of substrate **S108**, having two phenyl groups in a *trans* disposition. In agreement with our quadrant model,

high diastereo- and enantioselectivities were attained (>25/1 dr and 99% ee). Calculations performed for substrate **S108** with the catalyst Ir/**L8c** reproduce the enantiomeric excess (computed 99% ee (*R,R*)) and support our quadrant model (see Supporting Information for further details). We then proceed to study several *E*-1,2-dialkyl-1,2-diaryl olefins (**S109**–**S111**). Overcoming the limitations of Gosselin's system[6] our catalyst was able to differentiate the *Re* and *Si* faces in substrates differentiated only in the length of an alkyl substituent **S109** and **S110** and in the electronic properties of the aromatic substituents **S111**. Thus, enantioselectivities >95% ee were achieved for these elusive substrate types.

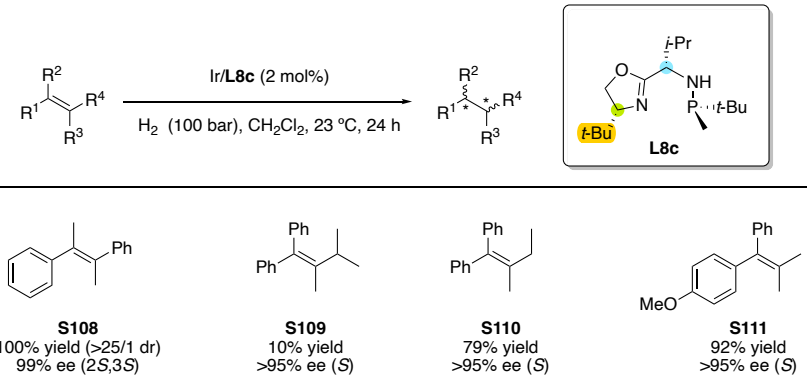

Scheme 3.2.8. Asymmetric hydrogenation of several acyclic tetrasubstituted olefins **S108**–**S111**.

Finally, we explored the asymmetric hydrogenation of cyclic tetrasubstituted olefins. For the initial reaction conditions we used the optimal mild reaction conditions from the previous studies with other Ir-catalysts (Table 3.2.3).[5a] The reactions were therefore carried out at room temperature using 1 mol% of the catalyst under 50 bar of H_2 in dichloromethane. The reactions proceeded smoothly to provide the *cis*-diasteroisomer only. It was observed that both the diastereomeric backbone of the ligand and the oxazoline substituent (entries 1–6) had a remarkable effect on the enantioselectivity. Catalyst precursor Ir/**L6b** provided the highest enantioselectivity of the series (entry 2, ee up to 93%). Interestingly, lowering the hydrogen pressure to 10 bar the enantioselectivity increased (entries 2, 7 and 8).[35] Enantioselectivities up to 95% ee were achieved at only 10 bars of H_2, while maintaining the full conversion (entry 8) under mild reaction conditions. This result is comparable to the best one reported in the literature.

We further studied the performance of Ir/**L6b** in the reduction of other indenes **S113**–**S119** and of the demanding 3,4-dimehtyl-1,2-dihydronapthalene **S120** (Scheme 3.2.9).

Table 3.2.3. Asymmetric hydrogenation of 2,3-dimethyl-1*H*-indene **S112** using Ir-catalyst precursors with Ir/**L5**–**L8a**–**c**

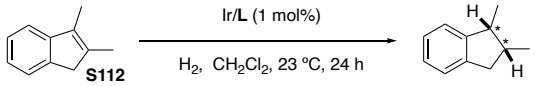

Entry	Ligand	H_2 (bar)	% Conv (% yield)[a]	% ee[b]
1	**L5b**	50	100 (95)	63 (*R,R*)
2	**L6b**	50	100 (96)	93 (*R,R*)
3	**L7b**	50	100 (96)	82 (*S,S*)
4	**L8b**	50	100 (95)	74 (*S,S*)
5	**L6a**	50	100 (-)[c]	83 (*R,R*)
6	**L6c**	50	100 (-)[c]	90 (*R,R*)
7	**L6b**	75	100 (-)[c]	92 (*R,R*)
8[d]	**L6b**	10	100 (96)	95 (*R,R*)

[a] Conversions were measured by ^{1}H NMR spectroscopy after 24 h. [b] Enantiomeric excesses determined by chiral GC. [c] Isolated yield not calculated. [d] Reaction performed using 2 mol% of catalysts.

Substrates **S113**–**S119** include several substituents at both benzylic (**S113**–**S115**) and vinylic position (**S118**–**S119**) and several substituents at the 6-position of the indene (**S116**–**S117**). We found that precatalyst Ir/**L6b** tolerated well variations of the alkyl substituent at both the benzylic and vinylic positions. The only exception was substrate **S115** with a phenyl substituent at the benzylic position that led to somewhat lower enantioselectivity. The results also indicated that conversion and yields were comparable for substrates **S116** and **S117** that contain a different substituent at the 6 position of the indene, although enantioselectivity was slightly better for the methoxy substituted indene **S117**. We should highlight the high enantioselectivity in the hydrogenation of 3,4-dimehtyl-1,2-dihydronapthalene **S120**, which is a more challenging substrate because the catalyst must avoid the dehydrogenation reaction towards the naphthalene derivative. This result improves the previous result by Pfaltz[5a] and is comparable to Busacca's result[5b] but with our catalyst we don't need to work at low temperature.

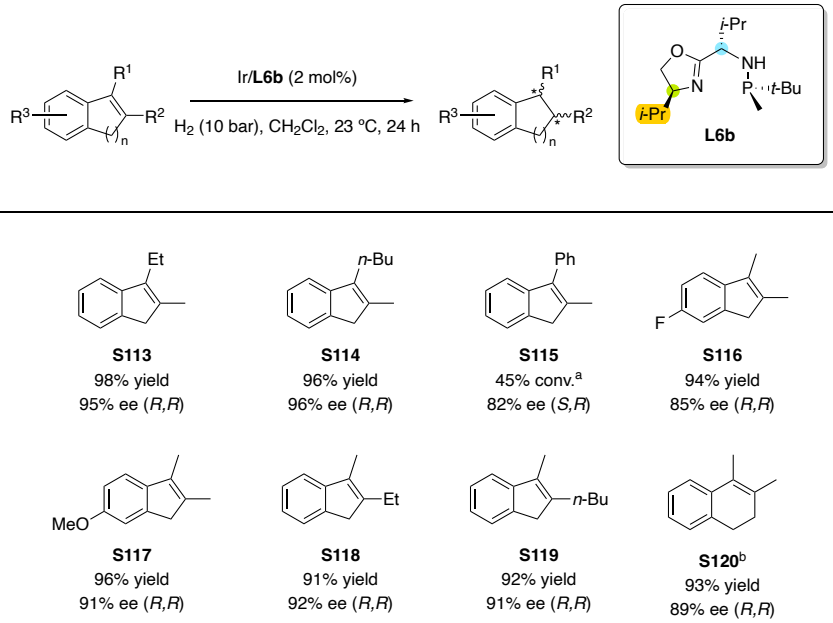

Scheme 3.2.9. Asymmetric hydrogenation of several indenes **S113**–**S119** and 1,2-dihydronapthalene **S120**. [a] Isolated yield not calculated. [b] Reaction performed using 75 bar of H_2.

3.2.3. Conclusions

In summary, we have shown that Ir-MaxPHOX catalysts (Ir/**L5**–**L8a**–**c**) are able to hydrogenate selectively up to 106 different olefins. The substrates included di- and trisubstituted olefins, some with key poorly coordinative groups (such as lactams, lactones, enol phosphinates, …) and a wide scope of the understudied tetrasubstituted alkenes. This family of Ir-MaxPHOX-type catalysts allowed the hydrogenation of exocyclic olefins, *Z*-olefins, pure alkyl substituted olefins and a broad range of tetrasubstituted olefins, thus improving over a previous family[4b], also based on P,N-ligands, that was so far the only one able to hydrogenate di-, tri- and tetrasubstituted olefins. DFT calculations and deuterium labeling experiments allowed the rationalization of the stereochemical outcomes of the reactions and helped in the selection of suitable substrates for these Ir-MaxPHOX-type catalysts. The analysis of the TSs indicated that the high catalytic performance of these catalysts is due to its ability to adapt to the demands of each substrate. This ability also explains the excellent performance of Ir-MaxPHOX catalysts in the hydrogenation of chelating olefins such as allyl amines and phthalimides,[36] and cyclic α- and β-enamides,[9] and imines.[37] These results open a new perspective for the growth of ligand libraries for the asymmetric hydrogenation of non-chelating olefins, where the Ir/P-stereogenic aminophosphine-oxazoline catalysts could be a good choice for further development.

3.2.4. Experimental section

3.2.4.1. General considerations

All reactions were carried out using standard Schlenk techniques under an atmosphere of argon. Solvents were purified and dried by standard procedures. All reagents were used as received. Ir-catalyst precursors Ir/**L5**–**L8a**–**c** were prepared as previously reported.[9] ^{1}H and ^{13}C{^{1}H}, were recorded using a 400 MHz spectrometer. Chemical shifts are relative to that of $SiMe_4$ (^{1}H and ^{13}C). ^{1}H and ^{13}C assignments were made based on ^{1}H-^{1}H gCOSY and ^{1}H-^{13}C gHSQC. Substrates **S14**,[21c] **S15**,[38] **S16**–**S17**,[10a] **S18**–**S24**,[21c] **S25**,[39] **S26**,[40] **S28**,[40] **S29**–**S30**,[41] **S31**,[42] **S32**,[43] **S35**–**S36**,[4a] **S39**,[4a] **S44**,[44] **S45**–**S48**,[27c] **S49**,[28] **S50**–**S51**,[45] **S54**,[29d] **S55**–**S61**,[29d] **S62**,[46] **S63**,[47] **S64**,[4d] **S65**,[48] **S66**,[49] **S67**–**S68**,[48] **S69**,[49] **S70**–**S74**,[4d] **S75**,[4e] **S80**–**S81**,[4d] **S82**,[50] **S83**,[51] **S85**,[52] **S90**–**S95**,[7c] **S99**–**S106**,[7a] **S107**,[53] **S108**–**S111**,[6] **S112**–**S113**,[54] **S114**,[5a] **S115**,[54] **S116**–**S117**,[55] **S118**[51] and **S119**–**S120**[54] were prepared following the reported procedures and **S27**, **S33**–**S34** and **S52**–**S53** were commercially available. For characterization and ee determination details, copies of the NMR spectra, copies of GC or HPLC traces as well as for DFT details and other mechanistic insights see Supporting Information.

3.2.4.2. Preparation of exocyclic olefins S37–S38 and S40–S41

According to the procedure reported by Zhang et al.,[4a] to a suspension of the substituted benzyltriphenylphosphonium chloride (15.14 mmol) in THF (40 ml), *n*-BuLi (6.06 mL, 2.5 M in hexanes, 15.14 mmol) was added dropwise. After stirring at room temperature for 2 h, a solution of the corresponding ketone (7.57 mmol) in THF (10 mL) was added. The reaction mixture was stirred at reflux for 18 h. After that, the solution was cooled to room temperature, quenched with water (20 mL) and extracted with EtOAc (3x30 mL). Then, the organic layers were combined, washed with brine (10 mL) and dried with anhydrous $MgSO_4$. The solution was filtered and concentrated *in vacuo*. The crude mixture containing a mixture of *Z*- and *E*-olefins was then purified with column chromatography (SiO_2, 100% petroleum ether or 95:5 petroleum ether-EtOAc) to yield the pure olefin.

(*E*)-1-(4-Methoxybenzylidene)-2,3-dihydro-1H-indene (S37). Prepared using 2,3-dihydro-1*H*-inden-1-one (1 g, 7.57 mmol). White solid (930 mg, 82% yield). ^{1}H NMR (400 MHz, $CDCl_3$), δ= 3.09 (s, 4H), 3.83 (s, 3H), 6.91–6.94 (m, 3H), 7.19–7.30 (m, 3H), 7.42 (d, $^{3}J_{H-H}$= 7.2 Hz, 2H), 7.59 (d, $^{3}J_{H-H}$= 9.1 Hz, 1H). ^{13}C NMR (100.6 MHz, $CDCl_3$), δ= 30.6, 30.9, 55.3, 2x113.9, 118.5, 119.9, 125.2, 126.6, 127.8, 2x129.7, 131.1, 141.9, 142.8, 145.5, 158.0.

(*E*)-1-(2-Methylbenzylidene)-2,3-dihydro-1H-indene (S38). Prepared using 2,3-dihydro-1*H*-inden-1-one (100 mg, 0.75 mmol). White solid (33 mg, 20% yield). ^{1}H

NMR (400 MHz, $CDCl_3$), δ= 2.40 (s, 3H), 3.03–3.05 (m, 4H), 7.06 (s, 1H), 7.17–7.32 (m, 6H), 7.49 (d, $^3J_{H-H}$= 7.3 Hz, 1H), 7.66 (d, $^3J_{H-H}$ = 7.3 Hz, 1H). ^{13}C NMR (100.6 MHz, $CDCl_3$), δ= 20.2, 30.4, 30.7, 117.1, 120.3, 125.3, 125.6, 126.5, 126.6, 127.8, 128.2, 130.1, 136.5, 137.0, 142.5, 144.2, 145.9.

(*E*)-1-(4-Methylbenzylidene)-1,2,3,4-tetrahydronaphthalene (S40). Prepared using 3,4-dihydronaphthalen-1(2*H*)-one (555 mg, 3.8 mmol). White solid (216 mg, 24% yield). ^{1}H NMR (400 MHz, $CDCl_3$), δ= 1.82–1.87 (quint, $^3J_{H-H}$= 6.4 Hz, 2H), 2.37 (s, 3H), 2.78–2.85 (m, 4H), 7.02 (s, 1H), 7.10–7.11 (m, 1H), 7.16–7.20 (m, 4H), 7.26-7.28 (m, 2H), 7.69–7.71 (m, 1H). ^{13}C NMR (100.6 MHz, $CDCl_3$), δ= 21.5, 23.9, 28.2, 30.5, 123.9, 124.5, 126.4, 127.4, 129.1, 3x129.2, 2x129.6, 135.6, 136.3, 136.8, 138.0.

(*E*)-1-(4-Chlorobenzylidene)-1,2,3,4-tetrahydronaphthalene (S41). Prepared using 3,4-dihydronaphthalen-1(2*H*)-one (536 mg, 3.6 mmol). White solid (140 mg, 15% yield). ^{1}H NMR (400 MHz, $CDCl_3$), δ= 1.85 (quint, $^3J_{H-H}$= 6.3 Hz, 2H), 2.74–2.78 (m, 2H), 2.84 (t, $^3J_{H-H}$= 6.3 Hz, 2H), 6.97 (s, 1H), 7.11–7.14 (m, 1H), 7.18–7.21 (m, 2H), 7.27–7.30 (m, 2H), 7.31–7.34 (m, 2H), 7.67–7.70 (m, 1H). ^{13}C NMR (100.6 MHz, $CDCl_3$), δ= 23.6, 27.9, 30.2, 122.4, 124.3, 126.2, 127.5, 2x128.3, 129.1, 2x130.6, 132.0, 136.0, 136.6, 2x138.0.

3.2.4.3. Preparation of exocyclic olefin S42

Based on a modified procedure by Chattopadhyay et al.,[56] to a suspension of 1-tetralone phosphonium salt[57] (1.7 g, 3.7 mmol) in THF (15 mL), *n*-BuLi (1.6 mL, 2.5M in hexanes, 4.1 mmol) was added gradually at 0ºC. The mixture was stirred at the same temperature for 1 h and then, a solution of *o*-tolualdehyde (0.4 mL, 3.1 mmol) in THF (5 mL) was added dropwise. The reaction mixture was warmed up to room temperature and stirred for 16 h. Then, the reaction was quenched with water (20 mL) and the aqueous phase extracted with Et_2O (3x10 mL). The combined organic extracts were washed with brine, dried with $MgSO_4$, filtered and concentrated *in vacuo*. The crude product was purified by column chromatography (SiO_2, 90:10 petroleum ether-EtOAc) and the E/Z isomers separated by means of semipreparative HPLC (Chiralcel OD-H column).

***(E)*-1-(2-Methylbenzylidene)-1,2,3,4-tetrahydronaphthalene (S42)**. White solid (65 mg, 10% yield). ^{1}H NMR (400 MHz, $CDCl_3$), δ= 1.83 (quint, $^3J_{H-H}$= 6.3 Hz, 2H), 2.30 (s, 3H), 2.59 (td, $^3J_{H-H}$= 6.3, 1.3 Hz, 2H), 2.87 (t, $^3J_{H-H}$= 6.3 Hz, 2H), 7.02 (s, 1H), 7.14–7.15 (m, 1H), 7.20–7.26 (m, 6H), 7.72–7.75 (m, 1H). ^{13}C NMR (100.6 MHz, $CDCl_3$), δ= 20.1, 23.8, 27.8, 30.3, 122.4, 124.3, 125.3, 126.0, 126.8, 127.3, 129.2, 129.4, 129.8, 136.2, 137.0, 137.3, 137.5, 137.6.

3.2.4.4. Preparation of exocyclic olefin S43

Based on a modified procedure by Matsuda et al.,[58] To a suspension of the benzyltriphenylphosphonium chloride (400 mg, 1.02 mmol) in THF (10 ml), *t*-BuOK (95 mg, 1.02 mmol) was added one portion. After stirring at room temperature for 30 min, a solution of benzocyclobutenone[59] (100 mg, 0.85 mmol) was added dropwise. The reaction mixture was stirred at room temperature for 18 h. After that, the solution was cooled to room temperature, quenched with water (10 mL) and extracted with Et_2O (3x10 mL). The organic layers were combined, washed with brine (15 mL), dried with anhydrous $MgSO_4$, filtered and concentrated *in vacuo*. The crude product was purified with silica gel column chromatography (SiO_2, 100% petroleum ether) to yield the pure *E*-olefin.

(*E*)-1-Benzylidenebenzocyclobutene (S43). Colorless oil, 20 mg (12% yield). ^{1}H NMR (400 MHz, $CDCl_3$), δ= 4.00 (s, 2H), 6.66 (s, 1H), 7.20–7.26 (m, 5H), 7.33–7.37 (m, 2H), 7.44-7.46 (m, 2H). ^{13}C NMR (100.6 MHz, $CDCl_3$), δ= 39.5, 117.8, 118.7, 122.6, 126.5, 126.8, 127.5, 127.6, 128.5, 128.6, 128.7, 137.4, 138.8, 145.6, 146.1.

3.2.4.5. Preparation of exocyclic lactams olefins S76–S79

Lactams **S76**–**S79** were prepared from 1-acetylpiperidin-2-one in two steps following an already reported procedure.[4d] A mixture of *N*-acetyl-2-pyrrolidinone (6 mmol, 847 mg) and THF (12 mL) was cooled to 0 °C. NaH (60% in mineral oil) (12 mmol, 480 mg) was then added, followed by addition of the corresponding aldehyde (3 mmol). The reaction was stirred at 0 °C for 1 h followed by warming to room temperature and stirring for 2 h. After quenching carefully with methanol at 0 °C, the solvent was removed under reduced pressure. The residue was diluted with water and extracted with ethyl acetate (3x10 mL). The organic extracts were washed with brine and dried over anhydrous Na_2SO_4. The solvent was removed under reduced pressure and the residue was dissolved in a small amount of ethyl acetate. Addition of petroleum ether resulted in precipitation of the unprotected lactam. The resulting solid was washed with petroleum ether and used without further purification.

(*E*)-3-(4-methoxybenzylidene)piperidin-2-one.[4e] White solid, 50% yield (328 mg). ^{1}H NMR (401 MHz, $CDCl_3$), δ= 1.76–1.86 (m, 2H), 2.71–2.82 (m, 2H), 3.26–3.42 (m, 2H), 3.76 (s, 3H), 5.97 (bs, 1H), 6.85 (d, *J* = 8.8 Hz, 2H), 7.35–7.27 (m, 2H), 7.70 (s, 1H).

(*E*)-3-(4-bromobenzylidene)piperidin-2-one.[4e] White solid, 24% yield (193 mg). ^{1}H NMR (401 MHz, $CDCl_3$), δ= 1.76–1.89 (m, 2H), 2.68–2.72 (m, 2H), 3.32–3.42 (m, 2H), 6.17 (bs, 1H), 7.14–7.21 (m, 2H), 7.40–7.48 (m, 2H), 7.66 (s, 1H).

(*E*)-3-(3-methoxybenzylidene)piperidin-2-one.[4e] White solid, 65% yield (390 mg). ^{1}H NMR (401 MHz, $CDCl_3$), δ= 1.78–1.83 (m, 2H), 2.73–2.77 (m, 2H), 3.34–3.38

(m, 2H), 3.75 (s, 3H), 5.88 (bs, 1H), 6.80 (dd, *J* = 8.3, 2.7, 1H), 6.85 (m, 1H), 6.91 (dd, *J* = 7.7, 1.4 Hz, 1H), 7.23 (t, *J* = 7.9 Hz, 1H), 7.71 (s, 1H),

(*E*)-3-(2-methoxybenzylidene)piperidin-2-one.[4e] White solid, 54% yield (343 mg). ^{1}H NMR (401 MHz, $CDCl_3$), δ= 1.74–1.88 (m, 2H), 2.63–2.77 (m, 2H), 3.22–3.48 (m, 2H), 3.82 (s, 3H), 6.21 (bs, 1H), 6.82–6.98 (m, 2H), 7.18–7.34 (m, 2H), 7.92 (s, 1H).

To a stirred solution of the corresponding (*E*)-3-aryl-pyrrolidin-2-one (1.0 mmol) in anhydrous THF (5 mL) over an ice bath, was added a suspension of sodium hydride (60% in mineral oil) (1.1 mmol, 43.9 mg). The mixture was stirred for 30 min at 0 °C and benzyl bromide (1.65 mmol, 133 µl) was then added dropwise. The reaction mixture was allowed to warm to room temperature and was stirred for a further 3 h. The solvent was evaporated in vacuo and the residue was extracted with ethyl acetate (3x10 mL). The organic phase was washed several times with brine, dried and evaporated. The residue was purified by column chromatography (silica gel, petroleum/ethyl acetate, 1:1) to afford the corresponding protected lactam.

(*E*)-1-benzyl-3-(4-methoxybenzylidene)piperidin-2-one (S76). Pale yellow solid, 88% yield (269.1 mg). ^{1}H NMR (401 MHz, $CDCl_3$), δ= 1.77–1.84 (m, 2H), 2.78–2.82 (m, 2H), 3.23–3.36 (m, 2H), 3.81 (s, 3H), 4.71 (s, 2H), 6.86–6.84 (m, 2H), 7.21–7.38 (m, 7H), 7.83 (s, 1H). ^{13}C NMR (401 MHz, $CDCl_3$), δ= 165.5, 159.4, 137.5, 135.4, 131.4, 128.8, 128.6, 128.1, 128.0, 127.3, 113.8, 55.3, 51.3, 47.2, 26.6, 23.0.

(*E*)-1-benzyl-3-(4-bromobenzylidene)piperidin-2-one (S77). White solid, 64% yield (272 mg). ^{1}H NMR (401 MHz, $CDCl_3$), δ= 1.70–1.80 (m, 2H), 2.64–2.72 (m, 2H), 3.23–3.31 (m, 2H), 4.65 (s, 2H), 7.14–7.28 (m, 7H), 7.39–7.46 (m, 2H), 7.74 (s, 1H). ^{13}C NMR (401 MHz, $CDCl_3$), δ= 22.9, 26.5, 47.2, 51.4, 122.1, 127.4, 128.1, 128.7, 130.7, 131.2, 131.5, 135.1, 137.2, 164.9.

(*E*)-1-benzyl-3-(3-methoxybenzylidene)piperidin-2-one (S78). White solid, 73% yield (224 mg). ^{1}H NMR (401 MHz, $CDCl_3$), δ= 1.70–1.80 (m, 2H), 2.70–2.78 (m, 2H), 3.24–3.31 (m, 2H), 3.75 (s, 3H), 4.66 (s, 2H), 6.78 (dd, *J* = 8.2, 2.6 Hz, 1H), 6.84 (t, *J* = 2.1 Hz, 1H), 6.89–6.91 (m, 1H), 7.22–7.29 (m, 6H), 7.79 (s, 1H). ^{13}C NMR (401 MHz, $CDCl_3$), δ= 23.0, 26.6, 47.2, 51.3, 55.3, 113.5, 115.3, 122.2, 127.4, 128.1, 128.6, 129.3, 130.3, 135.5, 137.4, 137.6, 159.4, 165.1.

(*E*)-1-benzyl-3-(2-methoxybenzylidene)piperidin-2-one (S79). White solid, 81% yield (248 mg). ^{1}H NMR (401 MHz, $CDCl_3$), δ= 1.68–1.75 (m, 2H), 2.61–2.64 (m, 2H), 3.24 (t, *J* = 5.9 Hz, 2H), 3.76 (s, 3H), 4.64 (s, 2H), 6.81–6.88 (m, 2H), 7.13–7.25 (m, 7H), 7.93 (s, 1H). ^{13}C NMR (401 MHz, $CDCl_3$), δ= 23.0, 26.6, 47.3, 51.2, 55.4, 110.6, 119.9, 125.3, 127.3, 128.2, 128.6, 129.4, 130.0, 130.1, 131.6, 137.5, 157.9, 165.2.

3.2.4.6. Preparation of tetrasubstituted olefins S84, S86–S89

A flame-dried Schkenk flask was charged with potassium *tert*-butoxide (4 mmol, 0.43 g) and stir bar. Dry DMSO (4 mL) was added, followed by isopropyltriphenyl phosphonium iodide (4 mmol, 0.43 g). This mixture was added dropwise with a syringe to a solution of the corresponding ketone (1 mmol) in toluene (3.5 mL). The reaction was heated to reflux overnight. It was allowed to cool to room temperature, and petroleum ether and water were added. The organic phase was separated and washed with water (2x25 mL) and brine (25 mL), dried over $MgSO_4$, filtered, and concentrated *in vacuo*. Compound **S84** was purified by flash column chromatography (petroleum ether), while compounds **S86**–**S89** were purified by distillation *in vacuo* at 130-170 °C.

1-Methyl-3-(3-methylbut-2-en-2-yl)benzene (S84). Colorless oil (222 mg, 84%). ^{1}H NMR (400 MHz, $CDCl_3$), δ= 1.61 (s, 3H, CH_3), 1.82 (s, 3H, CH_3), 1.96 (s, 3H, CH_3), 2.36 (s, 3H, CH_3, Me-Ar), 6.93-7.03 (m, 3H, CH=), 7.20 (td, 1H, CH=, Ar, *J*= 7.5 Hz, *J*=1.1 Hz). ^{13}C{^{1}H} NMR (100.6 MHz, $CDCl_3$), δ= 20.7 (CH_3), 21.0 (CH_3), 21.6 (CH_3), 22.2 (CH_3), 125.6 (CH=), 126.6 (CH=), 127.1 (C=), 127.9 (CH=), 129.2 (CH=), 130.2 (C=), 137.7 (C=), 145.4 (C=).

1-Methoxy-4-(2-methylpent-2-en-3-yl)benzene (S86). Colorless oil (57 mg, 30%). ^{1}H NMR (400 MHz, $CDCl_3$), δ= 0.9 (t, 3H, CH_3, Et, *J*= 7.5 Hz), 1.56 (s, 3H ,CH_3), 1.82 (s, 3H, CH_3), 2.34-2.39 (m, 1H, CH_2, Et), 3.84 (s, 3H, CH_3, OMe), 6.88 (d, 2H, CH=, *J*= 8.6 Hz), 7.04 (d, 2H, CH=, *J*= 8.6 Hz). ^{13}C{^{1}H} NMR (100.6 MHz, $CDCl_3$), δ= 12.9 (CH_3, Et), 19.9 (CH_3), 22.2 (CH_3), 27.6 (CH_2, Et), 55.2 (CH_3, MeO), 113.2 (CH=), 126.4 (C=), 129.9 (CH=), 136.3 (C=), 157.6 (C=).

1-Methoxy-4-(2-methylhex-2-en-3-yl)benzene (S87). Colorless oil (51 mg, 25%). ^{1}H NMR (400 MHz, $CDCl_3$), δ= 0.77 (t, 3H, CH_3, *n*-Pr, *J*= 7.3 Hz), 1.14-1.24 (m, 2H, CH_2, *n*-Pr), 1.47 (s, 3H, CH_3); 1.72 (s, 3H, CH_3), 2.20-2.24 (m, 2H, CH_2, *n*-Pr), 3.73 (s, 3H, CH_3, OMe), 6.77 (d, 2H, CH=, *J*= 8.6 Hz), 6.93 (d, 2H, CH=, *J*= 8.6 Hz). ^{13}C{^{1}H} NMR (100.6 MHz, $CDCl_3$), δ= 14.1 (CH_3, *n*-Pr), 20.2 (CH_3), 21.4 (CH_2, *n*-Pr), 22.2 (CH_3), 36.8 (CH_2, *n*-Pr), 55.2 (CH_3, OMe), 114.0 (CH=), 127.2 (C=), 129.9 (CH=), 134.8 (C=), 136.7 (C=), 157.2 (C=).

2,5-Dimethyl-3-(3-methylbut-2-en-2-yl)furan (S88). Colorless oil (59 mg, 36%). ^{1}H NMR (400 MHz, $CDCl_3$), δ= 1.57 (s, 3H, CH_3), 1.74 (s, 3H, CH_3), 1.80 (s, 3H, CH_3), 2.06 (s, 3H, CH_3), 2.22 (s, 3H, CH_3), 5.74 (s, 1H, CH=). ^{13}C{^{1}H} NMR (100.6 MHz, $CDCl_3$), δ= 12.5 (CH_3), 13.5 (CH_3), 19.8 (CH_3), 20.2 (CH_3), 22.0 (CH_3), 107.5 (CH=), 121.6 (C=), 123.5 (C=), 128.1 (C=), 144.7 (C=), 148.9 (C=).

2,5-Dimethyl-3-(3-methylbutan-2-yl)thiophene (S89). Colorless oil (72 mg, 40%). ^{1}H NMR (400 MHz, $CDCl_3$), δ= 1.54 (s, 3H, CH_3), 1.80 (s, 3H, CH_3), 1.84 (s, 3H, CH_3), 2.19 (s, 3H, CH_3), 2.41 (s, 3H, CH_3), 6.39 (s, 1H, CH=). ^{13}C{^{1}H} NMR (100.6 MHz,

$CDCl_3$), δ= 13.5 (CH_3), 15.2 (CH_3), 19.8 (CH_3), 20.0 (CH_3), 21.8 (CH_3), 124.7 (C=), 126.4 (CH=), 128.6 (C=), 130.3 (C=), 135.0 (C=), 141.4 (C=).

3.2.4.7. Preparation of tetrasubstituted olefins S96–S98

The tetrasubstituted vinyl-fluorides were synthetized according a literature procedure,[7c] to a stirred suspension of NaH (1 mmol, 1 equiv., 60 % mineral dispersion) in anhydrous THF (2mL) at 0°C corresponding substituted diethoxyphosphoryl-2-fluoroacetate (1.02 mmol, 1.02 equiv.) was added dropwise. The reaction mixture was then heated to 40 °C and stirred for 1 h. After cooling again to 0 °C, the corresponding ketone (1 mmol, 1 equiv.) was added dropwise and the resulting mixture was stirred at 40 °C for another 18 h. After this time, the reaction was quenched with water. The reaction mixture was extracted with diethyl ether (3x10 mL). The combined organic layers were dried over Na_2SO_4, filtered, and concentrated under reduced pressure. The crude product was purified by flash chromatography using petroleum ether, Et_2O mixture (95:5) to afford the desired tetrasubstituted vinyl fluorides

Ethyl (*E*)-2,4,4,4-tetrafluoro-3-(*p*-tolyl)but-2-enoate (S96). Colorless oil (87 mg, 35%). ^{1}H NMR (400 MHz, $CDCl_3$), δ= 1.32 (t, 3H, *J*= 7.2 Hz), 2.32 (s, 3H), 4.33 (q, 2H, *J*= 7.2 Hz), 6.98-7.33 (m, 4H). ^{19}F{^{1}H} NMR (564 MHz, $CDCl_3$), δ= -58.51 (d, *J*= 10.1 Hz), -107.39 (q, *J*= 9.9 Hz). ^{13}C{^{1}H} NMR (100.6 MHz, $CDCl_3$), δ= 13.7,21.3, 63.0, 118.9, 120.9 (d, *J*= 13.8 Hz), 123.7 (d, *J*= 14.0 Hz), 124.4, 129.0 (d, *J*= 2.6 Hz), 129.3, 139.7, 149.8 (d, *J*= 4.6 Hz), 152.5 (d, *J*= 4.5 Hz), 159.6 (d, *J*= 36.0 Hz)

Ethyl (*E*)-2,4,4,4-tetrafluoro-3-(4-methoxyphenyl)but-2-enoate (S97). Colorless oil (59 mg, 30%). ^{1}H NMR (400 MHz, $CDCl_3$), δ= 1.32 (t, 3H, J= 7.2 Hz), 3.77 (s, 3H), 4.33 (q, 2H, J= 7.2 Hz), 6.89 (d, 2H, J= 8.9 Hz), 7.20 (d, 2H, J= 9.0 Hz). ^{19}F{^{1}H} NMR (564 MHz, $CDCl_3$), δ= -58.58 (d, J= 9.8 Hz), -107.87 (q, J= 10.0 Hz). ^{13}C{^{1}H} NMR (100.6 MHz, $CDCl_3$), δ= 13.7, 55.3, 63.0, 114.1, 118.9-119.4 (m), 121.0 (d, J= 13.7 Hz), 123.2, 123.7 (d, J= 13.7 Hz), 129.5, 129.7, 130.6 (d, J=2.7 Hz), 149.7 (d, J= 4.3 Hz), 152.4 (d, J= 4.2 Hz), 159.6 (d, J= 36.3 Hz), 160.44.

Ethyl (E)-3-(4-bromophenyl)-2,4,4,4-tetrafluorobut-2-enoate (S98). Colorless oil (116 mg, 34%). ^{1}H NMR (400 MHz, $CDCl_3$), δ= 1.40 (t, 3H, *J*= 7.1 Hz), 4.41 (q, 2H, *J*= 7.1 Hz), 7.21 (dt, 2H, *J*= 8.9 Hz, *J*= 0.6 Hz), 7.49-7.69 (m, 2H).). ^{19}F{^{1}H} NMR (564 MHz, $CDCl_3$), δ= -58.44 (d, *J*= 9.8 Hz), -105.68 (q, *J*= 10.2 Hz). ^{13}C{^{1}H} NMR (100.6 MHz, $CDCl_3$), δ= 13.8, 63.4, 117.4-118.5 (m), 120.8 (d, *J*= 14.0 Hz), 123.5 (d, *J*= 14.0 Hz), 124.3, 126.4, 130.9 (d, *J*= 2.7 Hz), 132.1, 150.3 (d, *J*= 4.2 Hz), 153.0 (d, *J*= 4.3 Hz), 159.3 (d, *J*= 36.0 Hz).

3.2.4.8. Typical procedure for the hydrogenation of olefins

The alkene (0.5 mmol) and Ir complex (1 or 2 mol%) were dissolved in CH_2Cl_2 (2 mL) in a high-pressure autoclave, which was purged four times with hydrogen. The

apparatus was pressurized to the desired pressure and, after the required reaction time, the autoclave was depressurized and the solvent evaporated off. The residue was dissolved in Et_2O (1.5 mL) and filtered through a short Celite plug. Conversions were determined by ^1H NMR and enantiomeric excesses were determined by chiral HPLC or GCs.

3.2.4.9. Computational details

All species were optimized using B3LYP[14]-D3[15] functional as implemented in Gaussian 09.[60] The LANL2DZ[61] basis set together with the associated pseudopotential was used for iridium, and the 6-31G**[62] basis set was used for all other atoms. Implicit solvation using PCM[63] model with the parameters for dichloromethane was included in geometry optimizations. The reported energies are Gibbs free energies in solution within the quasi-harmonic approximation to the Rigid Rotor Harmonic Oscillator Model proposed by Cramer and Truhlar[64], corrections were done using the GoodVibes program.[65]

Quadrant analysis was done by means of MolQuO (Quantitative Quadrant-Diagram Representation of Molecular Systems)[18]. Note that this analysis was done taking the geometry of the whole TS, as shown in the figure, but removing the atoms of the olefin in the MolQuO calculation.

3.2.5. References

[1] See for example: (a) Genet, J. P. In Modern Reduction Methods; Andersson, P. G., Munslow, I. J., Eds; Wiley-VCH, Weinheim, **2008**, pp 3–38. (b) Tang, W.; Zhang, X. New Chiral Phosphorus Ligands for Enantioselective Hydrogenation. *Chem. Rev.* **2003**, *103*, 3029–3069. (c) Chi, Y.; Tang, W.; Zhang, X. In *Modern Rhodium-Catalyzed Organic Reactions*; Evans, P. A., Ed; Wiley-VCH: Weinheim, **2005**, pp 1–31. (d) Kitamura, M., Noyori, R. in *Ruthenium in Organic Synthesis*; Murahashi, S.-I., Ed.; Wiley-VCH: Weinheim, **2004**, pp 3–52. (e) Weiner, B.; Szymanski, W.; Janssen, D. B.; Minnaard, A. J.; Feringa, B. L. Recent Advances in the Catalytic Asymmetric Synthesis of Beta-amino Acids. *Chem. Soc. Rev.* **2010**, *39*, 1656–1691. (f) Xie, J.-H.; Zhu, S.-F.; Zhou, Q.-L. Transition Metal-Catalyzed Enantioselective Hydrogenation of Enamines and Imines. *Chem. Rev.* **2011**, *111*, 1713–1760. (g) Etayo, P.; Vidal-Ferran, A. Rhodium-catalysed asymmetric hydrogenation as a valuable synthetic tool for the preparation of chiral drugs. *Chem. Soc. Rev.* **2013**, *42*, 728–754. (h) Pizzano, A. Asymmetric hydrogenation of functionalized olefins. *Adv. Catal.* **2021**, *68*, 1–134. (i) Kim, A. N.; Stoltz, B. M. Recent advances in homogeneous catalysts for the asymmetric hydrogenation of heteroarenes. *ACS Catal.* **2020**, *10*, 13834–13851. (j) Cabré, A.; Verdaguer, X.; Riera, A. Recent advances in the enantioselective synthesis of chiral amines via transition metal-catalyzed asymmetric hydrogenation. *Chem. Rev.* **2022**, *122*, 269–339. (k) Zhang, Z.; Butt, N. A.; Zhang, W. Asymmetric Hydrogenation of Nonaromatic Cyclic Substrates. *Chem. Rev.* **2016**, *16*, 14769–14827.

[2] (a) Cui, X.; Burgess, K. Catalytic Homogeneous Asymmetric Hydrogenations of Largely Unfunctionalized Alkenes. *Chem. Rev.* **2005**, *105*, 3272–3296. (b) Roseblade, S. J.; Pfaltz, A. Iridium-Catalyzed Asymmetric Hydrogenation of Olefins. *Acc. Chem. Res.* **2007**, *40*, 1402–1411. (c) Woodmansee, D. H.; Pfaltz, A. Asymmetric Hydrogenation of Alkenes Lacking Coordinating Groups. *Chem. Commun.* **2011**, *47*, 7912–7916. (d) Zhu, Y.; Burgess, K. Filling Gaps in Asymmetric

Hydrogenation Methods for Acyclic Stereocontrol: Application to Chirons for Polyketide-Derived Natural Products. *Acc. Chem. Res.* **2012**, *45*, 1623–1636. (e) Verendel, J. J.; Pàmies, O.; Diéguez, M.; Andersson, P. G. Asymmetric Hydrogenation of Olefins Using Chiral Crabtree-type Catalysts: Scope and Limitations. *Chem. Rev.* **2014**, *114*, 2130–2169. (f) Margarita, C.; Andersson, P. G. Evolution and Prospects of the Asymmetric Hydrogenation of Unfunctionalized Olefins. *J. Am. Chem. Soc.* **2017**, *139*, 1346–1356. (g) Pàmies, O.; Zheng, J.; Faiges, J.; Andersson, P. G. Asymmetric hydrogenation of unfunctionalized olefins or with poorly coordinative groups. *Adv. Catal.* **2021**, *68*, 135–203. For specific examples of application of P,O and P,S-ligands in the Ir-catalyzed asymmetric hydrogenation see: (h) Margalef, J.; Pàmies,O. ; Pericas, M. A.; Diéguez, M. Evolution of phosphorus-thioether ligands for asymmetric catalysis, *Chem. Comm*. **2020**, *56*, 10795–10808, (i) Margalef, J.; Pericàs, M. A. Chiral Ligands. Evolution of ligands for asymmetric catalysis; Diéguez, M., Ed.; CRC Press, **2021**, pp 81–108. (j) Rageot, D.; Woodmansee, D. H.; Pugin, B.; Pfaltz, A. Proline-Based P,O Ligand/Iridium Complexes as Highly Selective Catalysts: Asymmetric Hydrogenation of Trisubstituted Alkenes. *Angew. Chem*. Int. Ed. **2011**, *50*, 9598–9601.

[3] (a) Bell, S.; Wüstenberg, B.; Kaiser, S.; Menges, F.; Netscher, T.; Pfaltz, A. Asymmetric Hydrogenation of Unfunctionalized, Purely Alkyl-Substituted Olefins. *Science* **2006**, *311*, 642–644. (b) Wang, A.; Fraga, R. P. A.; Hörmann, E.; Pfaltz, A. Iridium-Catalyzed Asymmetric Hydrogenation of Unfunctionalized, Trialkyl-Substituted Olefins. *Chem. Asian J.* **2011**, *6*, 599–606.

[4] The hydrogenation of such substrates is highly influenced by the size of substrate ring. So, for instance, a catalyst that provides high enantioselectivities in the hydrogenation of exocyclic olefins attached to a 5-membered ring motif is not suitable for the reduction of the 6-membered ring counterparts or vice versa. For non-functionalized olefins, see for instance: (a) Xia, J.; Yang, G.; Zhuge, R.; Liu, Y.; Zhang, W. Iridium-Catalyzed Asymmetric Hydrogenation of Unfunctionalized Exocyclic C=C Bonds. *Chem. Eur. J.* **2016**, *22*, 18354–18357 (up to 97% for benzofused 5-membered ring olefins and 75% ee for 6-membered ring counterparts). (b) Biosca, M.; Magre, M.; Pàmies, O.; Diéguez, M. Asymmetric Hydrogenation of Disubstituted, Trisubstituted, and Tetrasubstituted Minimally Functionalized Olefins and Cyclic β-Enamides with Easily Accessible Ir–P,Oxazoline Catalysts. *ACS Catal.* **2018**, *8*, 10316–10320 (up to 93% for benzofused 5-membered ring olefins and 30% ee for 6-membered ring counterparts). (c) Biosca, M.; de la Cruz-Sánchez, P.; Tarr, D.; Llanes, P.; Karlsson, E. A.; Margalef, J.; Pàmies, O.; Pericàs, M. A.; Diéguez, M. Filling the gaps in the challenging asymmetric hydrogenation of exocyclic benzofused-based alkenes with Ir-P,N catalysts. *Adv. Synth. Catal.* **2022**, *365*, 167-177 (up to 96% and 99% for benzofused 5–and 6-membered ring olefins, respectively, and 40% ee for the 4-memberd ring counterpart). For olefins with poorly coordinative groups, see for instance: (d) Tian, F.; Yao, D.; Liu, Y.; Xie, F.; Zhang, W. Iridium-Catalyzed Highly Enantioselective Hydrogenation of Exocyclic α,β-Unsaturated Carbonyl Compounds. *Adv. Synth. Catal.* **2010**, *352*, 1841–1845 (up to 99% ee for 5-membered ring cyclic enones, lactones and lactams and up to 75% ee for 6-membered ring counterparts). (e) Liu, X.; Han, Z.; Wang, Z.; Ding, K. SpinPhox/Iridium(I)-Catalyzed Asymmetric Hydrogenation of Cyclic α-Alkylidene Carbonyl Compounds. *Angew. Chem. Int. Ed.* **2014**, *53*, 1978–1982 (up to 98% ee for 6-membered ring cyclic enones, lactones and lactams and up to 83% ee for 5-membered ring counterparts). (f) Xia, J.; Nie, Y.; Yang, G.; Liu, Y.; Gridnev, I. D.; Zhang, W. Ir-Catalyzed Asymmetric Hydrogenation of α-Alkylidene β-Lactams and Cyclobutanones. *Chin. J. Chem.* **2018**, *36*, 612–618 (catalysts specially designed for 4-membered ring cyclic enones and lactams; ee's up to 98%). (g) Margalef, J.; Biosca, M.; de la Cruz-Sánchez, P.; Caldentey, X.; Rodríguez-Escrich, C.; Pàmies, O.; Pericàs, M. A.; Diéguez, M. Indene Derived Phosphorus-Thioether Ligands for the Ir-Catalyzed Asymmetric Hydrogenation of Olefins with Diverse Substitution Patterns and Different

Functional Groups. *Adv. Synth. Catal.* **2021**, *363*, 4561–4574 (catalysts designed for 6-membered ring cyclic enones, lactones and lactams; ee's up to 99%).

[5] (a) Schrems, M. G.; Neumann, E.; Pfaltz, A. Iridium-Catalyzed Asymmetric Hydrogenation of Unfunctionalized Tetrasubstituted Olefins. *Angew. Chem. Int. Ed.* **2007**, *46*, 8274–8276. (b) Busacca, C. A.; Qu, B.; Grett, N.; Fandrick, K. R.; Saha, A. K.; Marsini, M.; Reeves, D.; Haddad, N.; Eriksson, M.; Wu, J. P.; Grinberg, N.; Lee, H.; Li, Z.; Lu, B.; Chen, D.; Hong, Y.; Ma, S.; Senanayake, C. H. Tuning the Peri Effect for Enantioselectivity: Asymmetric Hydrogenation of Unfunctionalized Olefins with the BIPI Ligands. *Adv. Synth. Catal.* **2013**, *355*, 1455–1463.

[6] Bigler, R.; Mack, K. A.; Shen, J.; Tosatti, P.; Han, C.; Bachmann, S.; Zhang, H.; Scalone, M.; Pfaltz, A.; Denmark, S. E.; Hildbrand, S.; Gosselin, F. Asymmetric Hydrogenation of Unfunctionalized Tetrasubstituted Acyclic Olefins. *Angew. Chem. Int. Ed.* **2020**, *59*, 2844–2849.

[7] (a) Kerdphon, S.; Ponra, S.; Yang, J.; Wu, H.; Eriksson, L.; Andersson, P. G. Diastereo–and Enantioselective Synthesis of Structurally Diverse Succinate, Butyrolactone, and Trifluoromethyl Derivatives by Iridium-Catalyzed Hydrogenation of Tetrasubstituted Olefins. *ACS Catal.* **2019**, *9*, 6169–6176. (b) Zhao, Q.-K.; Wu, X.; Li, L.-P.; Yang, F.; Xie, J.-H.; Zhou, Q.-L. Asymmetric Hydrogenation of β-Aryl Alkylidene Malonate Esters: Installing an Ester Group Significantly Increases the Efficiency. *Org. Lett.* **2021**, *23*, 1675–1680. (c) Ponra, S.; Rabten, W.; Yang, J.; Wu, H.; Kerdphon, S.; Andersson, P. G. Diastereo-and enantioselective synthesis of fluorine motifs with two contiguous stereogenic centers. *J. Am. Chem. Soc.* **2018**, *140*, 13878–13883.

[8] (a) Pfaltz, A.; Drury III, W. J. Design of chiral ligands for asymmetric catalysis: From C2-symmetric P,P–and N,N-ligands to sterically and electronically nonsymmetrical P,N-ligands. *PNAS*, **2004**, *101*, 5723–5726. (b) Yoon, T. P.; Jacobsen, E. N. Privileged chiral catalysts. *Science* **2003**, *299*, 1691–1693. (c) Sommer, W.; Weibel, D. *Asymmetric Catalysis, Privileged Ligands and Complexes*, Sigma Aldrich's Chemfiles, **2008**, *2***,** 1–91. (d) Zhou, Q., Ed. *Privileged Chiral Ligands and Catalysts*, John Wiley& Sons Inc.: New York, **2011**. (e) Diéguez, M., Ed. *Chiral ligands. Evolution of ligand libraries for asymmetric Catalysis*, CRC Press: Boca Raton, **2021**.

[9] Salomó, E.; Orgué, S.; Riera, A.; Verdaguer, X. Highly Enantioselective Iridium-Catalyzed Hydrogenation of Cyclic Enamides. *Angew. Chem., Int. Ed.* **2016**, *55*, 7988–7992. The Ir-MaxPHOX library has also been applied in the asymmetric hydrogenation of functionalized olefins and imines as well as in the isomerization of alkenes, see: Cabré, A.; Riera, T.; Verdaguer, X. P-Stereogenic Amino-Phosphines as Chiral Ligands: From Privileged Intermediates to Asymmetric Catalysis. *Acc. Chem. Res.* **2020**, 53, 676–689.

[10] (a) Biosca, M.; Salomó, E.; de la Cruz-Sánchez, P.; Riera, A.; Verdaguer, X.; Pàmies, O.; Diéguez, M. Extending the Substrate Scope in the Hydrogenation of Unfunctionalized Tetrasubstituted Olefins with Ir-P Stereogenic Aminophosphine–Oxazoline Catalysts. *Org. Lett.* **2019**, *21*, 807–811. (b) Biosca, M.; de la Cruz-Sánchez, P.; Faiges, J.; Margalef, J.; Salomó, E.; Riera, A.; Verdaguer, X.; Ferré, J.; Maseras, F.; Besora, M.; Pàmies, O.; Diéguez, M. P-Stereogenic Ir-MaxPHOX: A Step toward Privileged Catalysts for Asymmetric Hydrogenation of Nonchelating Olefins. *ACS Catal.* **2023**, *13*, 5, 3020–3035.

[11] Enantioselectivities increased up to 98% ee when the reduction was done at only 2 bars of H_2. Similar hydrogen pressure effect on enantioselectivity has been reported in related tetrasubstituted susbtrates by Pfaltz and coworkers, see ref 5a.

[12] To the best of our knowledge so far only one family of Ir-catalysts has been successfully applied to di-, tri–and tetrasubstituted olefins, see ref 4b.

[13] (a) Bayardon, J.; Holz, J.; Schäffner, B.; Andrushko, V.; Verevkin, S. P.; Preetz, A.; Börner, A. Propylene Carbonate as a Solvent for Asymmetric Hydrogenations. *Angew. Chem., Int. Ed.* **2007**,

46, 5971–5974. (b) Schäffner, B.; Holz, J.; Verevkin, S. P.; Börner, A. Organic carbonates as alternative solvents for palladium-catalyzed substitution reactions. *ChemSusChem* **2008**, *1*, 249–253. (c) Schäffner, B.; Schäffner, F.; Verevkin, S. P.; Börner, A. Organic carbonates as solvents in synthesis and catalysis. *Chem. Rev.* **2010**, *110*, 4554–4581.

[14] (a) Becke, A. D. Density-functional thermochemistry. III. The role of exact Exchange. *J. Chem. Phys.* **1993**, *98*, 5648–5652. (b) Stephens, P. J.; Devlin, F. J.; Chabalowski, C. F.; Frisch, M. J. Ab Initio Calculation of Vibrational Absorption and Circular Dichroism Spectra Using Density Functional Force Fields. *J. Phys. Chem.* **1994**, *98*, 11623–11627.

[15] Grimme, S.; Antony, J.; Ehrlich, S.; Krieg, H. A consistent and accurate ab initio parametrization of density functional dispersion correction (DFT-D) for the 94 elements H-Pu. *J. Chem. Phys.* **2010**, *132*, 154104.

[16] (a) Brandt, P.; Hedberg, C.; Andersson, P. G. New Mechanistic Insights into the Iridium–Phosphanooxazoline-Catalyzed Hydrogenation of Unfunctionalized Olefins: A DFT and Kinetic Study. *Chem. Eur. J.* **2003**, *9*, 339–347. (b) Fan, Y.; Cui, X.; Burgess, K.; Hall, M. B. Electronic effects steer the mechanism of asymmetric hydrogenations of unfunctionalized aryl-substituted alkenes. *J. Am. Chem. Soc.* **2004**, *126*, 16688–16689. (c) Cui, X.; Fan, Y.; Hall, M. B.; Burgess, K. Mechanistic Insights into Iridium-Catalyzed Asymmetric Hydrogenation of Dienes. *Chem. Eur. J.* **2005**, *11*, 6859–6868. (d) Church, T. L.; Rasmussen, T.; Andersson, P. G. Enantioselectivity in the Iridium-Catalyzed Hydrogenation of Unfunctionalized Olefins. *Organometallics* **2010**, *29*, 6769–6781. (e) Hopmann, K. H.; Bayer, A. On the mechanism of iridium-catalyzed asymmetric hydrogenation of imines and alkenes: A theoretical study. *Organometallics* **2011**, *30*, 2483–2497. (f) Mazuela, J.; Norrby, P.-O.; Andersson, P. G.; Pam̀ies, O.; Diéguez, M. Pyranoside Phosphite–Oxazoline Ligands for the Highly Versatile and Enantioselective Ir-Catalyzed Hydrogenation of Minimally Functionalized Olefins. A Combined Theoretical and Experimental Study. *J. Am. Chem. Soc.* **2011**, *133*, 13634–13645. (g) Gruber, S.; Pfaltz, A. Asymmetric hydrogenation with iridium C, N and N, P ligand complexes: characterization of dihydride intermediates with a coordinated alkene. *Angew. Chem., Int. Ed.* **2014**, *53*, 1896–1900.

[17] Àlvarez-Moreno, M.; de Graaf, C.; Lopez, N.; Maseras, F.; Poblet, J.M.; Bo, C. Managing the Computational Chemistry Big Data Problem: The ioChem-BD Platform. *J. Chem. Inf. Model.* **2015**, *55*, 95–103.

[18] (a) Aguado-Ullate, S.; Saureu, S.; Guasch, L.; Carbó, J. J. Theoretical Studies of Asymmetric Hydroformylation Using the Rh–(*R*,*S*)-BINAPHOS Catalyst – Origin of Coordination Preferences and Stereoinduction. *Chem. Eur. J.* **2012**, *18*, 995–1005. (b) Aguado–Ullate, S.; Urbano-Cuadrado, M.; Villalba, I.; Pires, E.; García, J. I.; Bo, C.; Carbó, J. J. Predicting the Enantioselectivity of the Copper-Catalysed Cyclopropanation of Alkenes by Using Quantitative Quadrant-Diagram Representations of the Catalysts. *Chem. Eur. J.* **2012**, *18*, 14026–14036.

[19] Note, that this analysis was performed by taking the geometry of the whole TS, as shown in the figure, but removing the olefin atoms in the MolQuO calculation.

[20] (a) Mazuela, J.; Verendel, J. J.; Coll, M.; Schäffner, B.; Börner, A.; Andersson, P. G.; Pàmies, O.; Diéguez, M. Iridium Phosphite-Oxazoline Catalysts for the Highly Enantioselective Hydrogenation of Terminal Alkenes. *J. Am. Chem. Soc.* **2009**, *131*, 12344–12353. (b) Pàmies, O.; Andersson, P. G.; Diéguez, M. Asymmetric Hydrogenation of Minimally Functionalised Terminal Olefins: An Alternative Sustainable and Direct Strategy for Preparing Enantioenriched Hydrocarbons. *Chem. Eur. J.* **2010**, *16*, 14232–14240.

[21] (a) Blankenstein, J.; Pfaltz, A. A New Class of Modular Phosphinite–Oxazoline Ligands: Ir-Catalyzed Enantioselective Hydrogenation of Alkenes. *Angew. Chem., Int. Ed.* **2001**, *40*, 4445–

4447. (b) McIntyre, S.; Hörmann, E.; Menges, F.; Smidt, S. P.; Pfaltz, A. Iridium-Catalyzed Enantioselective Hydrogenation of Terminal Alkenes. *Adv. Synth. Catal.* **2005**, *347*, 282–288. (c) Biosca, M.; Paptchikhine, A.; Pàmies, O.; Andersson, P. G.; Diéguez, M. Extending the Substrate Scope of Bicyclic P-Oxazoline/Thiazole Ligands for Ir-Catalyzed Hydrogenation of Unfunctionalized Olefins by Introducing a Biaryl Phosphoroamidite Group. *Chem. Eur. J.* **2015**, *21*, 3455–3464. (d) Krajangsri, S.; Wu, H.; Liu, J.; Rabten, W.; Singhband, T.; Andersson, P. G. Tandem Peterson olefination and chemoselective asymmetric hydrogenation of β-hydroxy silanes. *Chem. Sci.* **2019**, *10*, 3649–3653.

[22] (a) Fessard, T. C.; Andrews, S. P.; Motoyohsi, H.; Carreira, E. Enantioselective Preparation of 1, 1-Diarylethanes: Aldehydes as Removable Steering Groups for Asymmetric Synthesis. *Angew. Chem., Int. Ed.* **2007**, *46*, 9331–9334. (b) Prat, L.; Dupas, G.; Duflos, J.; Quéguiner, G.; Bourguignon, J.; Levacher, V. Deracemization of alkyl diarylmethanes using (−)-sparteine or a chiral proton source. *Tetrahedron Lett.* **2001**, *42*, 4515–4518. (c) Wilkinson, J. A.; Rossington, S. B.; Ducki, S.; Leonard, J.; Hussain, N. Asymmetric alkylation of diarylmethane derivatives. *Tetrahedron* **2006**, *62*, 1833–1844.

[23] Pure alkyls are difficult to study because the enantiomers of pure hydrocarbons are difficult to separate. This was also the case of the substrate (*E*)-3,4,4-trimethylpent-2-ene (with a *t*-Bu group), whose measurement of ee failed despite we obtained 100% conversion.

[24] (a) Donde, Y.; Nguyen, J. H., WO Patent WO2015048553A1, **2015**. (b) Pohlski, F.; Lange, U.; Ochse, M.; Behi, B.; Hutchins, C. W., US Patent 2012040948A1, **2012**. (c) Lansbury, P. T.; Justman, C. J., WO Patent WO2009036275A1, **2009**. (d) Pontillo, J.; Gao, Y.; Wade, W. S.; Wu, D.; Eccles, W. K., U.S. Patent 2006276454A1, **2006**. (e) Kolanos, R.; Siripurapu, U.; Pullagurla, M.; Riaz, M.; Setola, V.; Roth, B. L.; Dukat, M.; Glennon, R. A. Binding of isotryptamines and indenes at h5-HT6 serotonin receptors. *Bioorg. Med. Chem. Lett.* **2005**, *15*, 1987–1991. (f) Horwell, D. C.; Howson, W.; Nolan, W. P.; Ratcliffe, G. S.; Rees, D. C.; Willems, H. M. G. The design of dipeptide helical mimetics, Part I: the synthesis of 1,6-disubstituted indanes. *Tetrahedron* **1995**, 51, 203-211. (g) Plummer, E. L.; Tonawanda, N., U.S. Patent 41362744A1, **1982**. (h) Ardalani, H.; Avan, A.; Ghayour-Mobarhan, M. Podophyllotoxin: a novel potential natural anticancer agent. *Avicenna J. Phytomed.* **2017**, 7, 285–294. (i) Cervo, L.; Samanin, R. Potential antidepressant properties of 8-hydroxy-2-(di-n-propylamino) tetralin, a selective serotonin IA receptor agonist. *Eur. J. Pharm*. **1987**, *144*, 223–229.

[25] Biosca, M.; Magre, M.; Coll, M.; Pàmies, O.; Diéguez, M. Alternatives to Phosphinooxazoline (*t*-BuPHOX) Ligands in the Metal-Catalyzed Hydrogenation of Minimally Functionalized Olefins and Cyclic β-Enamides. *Adv. Synth. Catal.* **2017**, *359*, 2801–2814.

[26] Much recently it has been disclosed that the high enantiocontrol for these substrates can be further expanded to both 5–and 6-membered ring counterparts by introducing a triazole in the ligand design, see ref 3c.

[27] (a) Xi, J. Q.; Quan, X.; Andersson, P. G. Highly Enantioselective Iridium-Catalyzed Hydrogenation of α,β–Unsaturated Esters. *Chem. Eur. J.* **2012**, *18*, 10609–10616. (b) Woodmansee, D. H.; Müller, M. A.; Tröndlin, L.; Hörmann, E.; Pfaltz, A. Asymmetric Hydrogenation of α,β-Unsaturated Carboxylic Esters with Chiral Iridium N, P Ligand Complexes. *Chem. Eur. J.* **2012**, *18*, 13780–13786. (c) Lu, S. M.; Bolm, C. Highly Enantioselective Synthesis of Optically Active Ketones by Iridium-Catalyzed Asymmetric Hydrogenation. *Angew. Chem., Int. Ed.* **2008**, *47*, 8920–8923. (d) Lu, W.-J.; Chen, Y.-W.; Hou, X.-L. Iridium–Catalyzed Highly Enantioselective Hydrogenation of the C–C Bond of α,β-Unsaturated Ketones. *Angew. Chem., Int. Ed.* **2008**, *47*, 10133–10136. (e) Shang, J.; Han, Z.; Li, Y.; Wang, Z.; Ding, K. Highly enantioselective asymmetric hydrogenation of (E)-β,β-disubstituted

α,β-unsaturated Weinreb amides catalyzed by Ir (I) complexes of SpinPhox ligands. *Chem. Commun.* **2012**, *48*, 5172–5174. (f) Biosca, M.; Pamìes, O.; Diéguez, M. Giving a Second Chance to Ir/ Sulfoximine-Based Catalysts for the Asymmetric Hydrogenation of Olefins Containing Poorly Coordinative Groups. *J. Org. Chem.* **2019**, *84*, 8259–8266.

[28] Chiral organofluorines are important in agrochemicals and drug synthesis among other applications due to its unique physical properties. For a recent hydrogenation of this substrate class, see: Ponra, S.; Yang, J.; Kerdphon, S.; Andersson, P. G. Asymmetric Synthesis of Alkyl Fluorides: Hydrogenation of Fluorinated Olefins. *Angew. Chem. Int. Ed.* **2019**, *58*, 9282–9287.

[29] (a) Cheruku, P.; Gohil, S.; Andersson, P. G. Asymmetric hydrogenation of enol phosphinates by iridium catalysts having N,P ligands. *Org. Lett.* **2007**, *9*, 1659– 1661. (b) Cheruku, P.; Diesen, J.; Andersson, P. G. Asymmetric Hydrogenation of Di and Trisubstituted Enol Phosphinates with N,P–Ligated Iridium Complexes. *J. Am. Chem. Soc.* **2008**, *130*, 5595–5599. (c) Paptchikhine, A.; Cheruku, P.; Engman, M.; Andersson, P. G. Iridium-catalyzed enantioselective hydrogenation of vinyl boronates. *Chem. Commun.* **2009**, 5996–5998. (d) Ganic, A.; Pfaltz, A. Iridium-Catalyzed Enantioselective Hydrogenation of Alkenylboronic Esters. *Chem. Eur. J.* **2012**, *18*, 6724–6728.

[30] See for instance: (a) Theodore, L. J.; Nelson, W. L. Stereospecific synthesis of the enantiomers of verapamil and gallopamil. *J. Org. Chem.* **1987**, *52*, 1309–1315. (b) Procopiou, P. A.; Biggadike, K.; English, A. F.; Farrell, R. M.; Hagger, G. N.; Hancock, A. P.; Haase, M. V.; Irving, W. R.; Snowden, M. A.; Solanke, Y. E.; Tralau-Stewart, C. J.; Walton, S. E.; Wood, J. A. Novel Glucocorticoid Antedrugs Possessing a 17β-(γ-Lactone) Ring. *J. Med. Chem.* **2001**, *44*, 602–612. (c) Adlington, R. M.; Baldwin, J. E.; Becker, G. W.; Chen, B.; Cheng, L.; Cooper, S. L.; Hermann, R. B.; Howe, T. J.; McCoull, W.; McNulty, A. M.; Neubauer, B. L.; Pritchard, G. J. Design, synthesis, and proposed active site binding analysis of monocyclic 2-azetidinone inhibitors of prostate specific antigen. *J. Med. Chem.* **2001**, *44*, 1491–1508. (d) Aoyama, Y.; Uenaka, M.; Kii, M.; Tanaka, M.; Konoike, T.; Hayasaki-Kajiwara, Y.; Naya, N.; Nakajima, M. Design, synthesis and pharmacological evaluation of 3-benzylazetidine-2-one-based human chymase inhibitors. *Bioorg. Med. Chem.* **2001**, *9*, 3065–3075. (e) Kottirsch, G.; Koch, G.; Feifel, R.; Neumann, U. β-Aryl-Succinic Acid Hydroxamates as Dual Inhibitors of Matrix Metalloproteinases and Tumor Necrosis Factor Alpha Converting Enzyme. *J. Med. Chem.* **2002**, *45*, 2289–2293. (f) Higashi, T.; Isobe, Y.; Ouchi, H.; Suzuki, H.; Okazaki, Y.; Asakawa, T.; Furuta, T.; Wakimoto, T.; Kan, T. Stereocontrolled Synthesis of (+)-Methoxyphenylkainic Acid and (+)-Phenylkainic Acid. *Org. Lett.* **2011**, *13*, 1089–1091. (g) Shan, W.; Balog, A.; Quesnelle, C.; Gill, P.; Han, W.-C.; Norris, D.; Mandal, S.; Thiruvenkadam, R.; Gona, K. B.; Thiyagarajan, K.; Kandeula, S.; McGlinchey, K.; Menard, K.; Wen, M.-L.; Rose, A.; White, R.; Guarino, V.; Shen, D. R.; Cvijic, M. E.; Ranasinghe, A.; Dai, J.; Zhang, Y.; Wu, D.-R.; Mathur, A.; Rampulla, R.; Trainor, G.; Hunt, J. T.; Vite, G. D.; Westhouse, R.; Lee, F. Y.; Gavai, A. V. BMS-871: A novel orally active pan-Notch inhibitor as an anticancer agent. *Bioorg. Med. Chem. Lett.* **2015**, *25*, 1905–1909. (h) Lin, X.; Yuen, P.-W.; Mendonca, R.; Parr, B.; Pastor, R.; Pei, Z.; Gaz-zard, L.; Jaipuri, F.; Kumar, S.; Li, X.; Pavana, R.; Potturi, H.; Velvadapu, V.; Waldo, J.; Zhang, Z.; Wu, G. WO 2017107979 A1, **2017**. (i) Kaieda, A.; Toyofuku, M.; Daini, M.; Nara, H.; Yoshikawa, M.; Ishii, N.; Hidaka, K. US 20170015655 A1, **2017**. (j) Huang, X.; Brubaker, J.; Peterson, S. L.; Butcher, J. W.; Close, J. T.; Martinez, M.; Maccoss, R. N.; Jung, J. O.; Siliphaivanh, P.; Zhang, H.; Aslanian, R. G.; Biju, P. J.; Dong, L.; Huang, Y.; Mccormick, K. D.; Palani, A.; Shao, N.; Zhou, W. WO 2012174176 A1, **2017**.

[31] During the last decade, the synthesis of chiral fluorinated molecules with two vicinal chiral centers has received a great deal of attention because of their presence in several drugs, such as dexamethasone and fluticasone propionate. Despite this, the number of successful methods for their

preparation is very limited and those methods also require high catalyst loading, drastic reaction conditions and multiple steps among other drawbacks. See for instance: Ma, J.-A.; Cahard, D. *Chem. Rev.* **2008**, *108*, PR1–PR43.

[32] For the full optimization of acyclic vinyl fluoride olefins, see Supporting Information.

[33] Chiral CF_3-containing molecules are of interest because the trifluoromethyl motif often occurs in pharmaceuticals and agrochemical products, see for instance: (a) Jeschke, P. The Unique Role of Fluorine in the Design of Active Ingredients for Modern Crop Protection. *ChemBioChem* **2004**, *5*, 570–589. (b) Zhou, Y.; Wang, J.; Gu, Z.; Wang, S.; Zhu, W.; Aceña, J. L.; Soloshonok, V. A.; Izawa, K.; Liu, H. Next Generation of Fluorine–Containing Pharmaceuticals, Compounds Currently in Phase II–III Clinical Trials of Major Pharmaceutical Companies: New Structural Trends and Therapeutic Areas. *Chem. Rev.* **2016**, *116*, 422–518. (c) Yang, J.; Ponra, S.; Li, X.; Peters, B. B. C.; Massaro, L.; Zhou, T.; Andersson, P. G. Catalytic enantioselective synthesis of fluoromethylated stereocenters by asymmetric hydrogenation. *Chem. Sci.* **2022**, 13, 8590–8596.

[34] See for example: (a) Kammermeier, B.; Beck, G.; Holla, W.; Jacobi, D.; Napierski, B.; Jendralla, H. Vanadium(II)–and Niobium(III)-Induced, Diastereoselective Pinacol Coupling of Peptide Aldehydes to Give a C_2-Symmetrical HIV Protease Inhibitor. *Chem. Eur. J.* **1996**, *2*, 307–315. (b) Fabre, B.; Ramos, A.; Pascual-Teresa, B. Targeting Matrix Metalloproteinases: Exploring the Dynamics of the S1′ Pocket in the Design of Selective, Small Molecule Inhibitors. *J. Med. Chem.* **2014**, *57*, 10205–10219. (c) Vandenbroucke, R. E.; Libert, C. Is there new hope for therapeutic matrix metalloproteinase inhibition? *Nat. Rev. Drug Discovery* **2014**, *13*, 904–927. (d) Stuart, A.; McCallum, M. M.; Fan, D.; LeCaptain, D. J.; Lee, C. Y.; Mohanty, D. K. Poly(vinyl chloride) plasticized with succinate esters: synthesis and characterization. *Polym. Bull.* **2010**, *65*, 589–598.

[35] Similar hydrogen pressure effect on enantioselectivity has been reported by Pfaltz and coworkers, see ref 5a

[36] (a) Cabré A.; Romagnoli, E.; Martínez-Balart, P.; Verdaguer, X.; Riera, A. Highly Enantioselective Iridium-Catalyzed Hydrogenation of 2-Aryl Allyl Phthalimides. *Org. Lett.* **2019**, 21, 9709–9713. (b) Rojo, P.; Molinari, M.; Cabré, A.; García-Mateos, C.; Riera, A.; Verdaguer, X. Iridium-Catalyzed Asymmetric Hydrogenation of 2,3-Diarylallyl Amines with a Threonine-Derived P-Stereogenic Ligand for the Synthesis of Tetrahydroquinolines and Tetrahydroisoquinolines. *Angew. Chem. Int. Ed.* **2022**, *61*, e202204300.

[37] Salomó, E.; Gallen, A.; Sciortino, G.; Ujaque, G.; Grabulosa, A.; Lledós, A.; Riera, A.; Verdaguer, X. Direct Asymmetric Hydrogenation of N-Methyl and N-Alkyl Imines with an Ir(III)H Catalyst. *J. Am. Chem. Soc.* **2018**, *140*, 16967–16970.

[38] Gupton, J. T.; Layman, W. J. Reaction of 2-aryl-3-(N,N-dimethylamino)-1-propenes and their corresponding quaternary ammonium salts with organometallic species and reducing agents. *J. Org. Chem*. **1987**, *52*, 3683–3686.

[39] Berthiol, F.; Doucet, H.; Santelli, M. Synthesis of Polysubstituted Alkenes by Heck Vinylation or Suzuki Cross-Coupling Reactions in the Presence of a Tetraphosphane–Palladium Catalyst. *Eur. J. Org. Chem*. **2003**, *2003*, 1091–1096

[40] Yanagisawa, A.; Nezu, T.; Mohri, S.-I. Brønsted Acid-Promoted Hydrocyanation of Arylalkenes. *Org. Lett*. **2009**, *11*, 5286–5289.

[41] Schrems, M. G.; Pfaltz, A. NeoPHOX—an easily accessible P,N-ligand for iridium-catalyzed asymmetric hydrogenation: preparation, scope and application in the synthesis of demethylmethoxycalamenene. *Chem. Commun*. **2009**, 6210–6212.

[42] Tolstoy, P.; Engman, M.; Paptchikhine, A.; Bergquist, J.; Church, T. L.; Leung, A. W. M.; Andersson, P. G. Iridium-Catalyzed Asymmetric Hydrogenation Yielding Chiral Diarylmethines with Weakly Coordinating or Noncoordinating Substituents. *J. Am. Chem. Soc*. **2009**, *131*, 8855–8860.

[43] Terao, Y.; Nomoto, M.; Satoh, T.; Miura, M.; Nomura, M. Palladium-Catalyzed Dehydroarylation of Triarylmethanols and Their Coupling with Unsaturated Compounds Accompanied by C–C Bond Cleavage. *J. Org. Chem*. **2004**, *69*, 6942–6944.

[44] Too, P. C.; Noji, T.; Lim, Y. J.; Li, X.; Chiba, S. Rhodium(III)-Catalyzed Synthesis of Pyridines from α,β-Unsaturated Ketoximes and Internal Alkynes. *Synlett* **2011**, *19*, 2789–2794.

[45] Lu, S.-M.; Bolm, C. Highly Chemo–and Enantioselective Hydrogenation of Linear α,β-Unsaturated Ketones. *Chem. Eur. J.* **2008**, *14*, 7513–7516.

[46] Galambos, J.; Wágner, G.; Nógrádi, K.; Bielik, A.; Molnár, L.; Bobok, A.; Horváth, A.; Kiss, B.; Kolok, S.; Nagy, J.; Kurkó, D.; Bakk, M. L.; Vastag, M.; Sághy, K.; Gyertyán, I.; Gál, K.; Greiner, I.; Szombathelyi, Z.; Keserű, G. M.; Domány, G. Carbamoyloximes as novel non-competitive mGlu5 receptor antagonists. *Bioorg. Med. Chem. Lett*. **2010**, *20*, 4371–4375.

[47] Peters, B. B. C.; Jongcharoenkamol, J.; Krajangsri, S.; Andersson, P. G. Highly Enantioselective Iridium-Catalyzed Hydrogenation of Conjugated Trisubstituted Enones. *Org. Lett.* **2021**, *23*, 242–246.

[48] Yang, J.; Li, X.; You, C.; Li, S.; Guan, Y.-Q.; Lv, H.; Zhang, X. Rhodium-catalyzed asymmetric hydrogenation of exocyclic α,β-unsaturated carbonyl compounds. *Org. Biomol. Chem.* **2020**, *18*, 856–859.

[49] Wu, Y.-L.; Gao, Y.-Q.; Wang, D.-L.; Zhong, C.-Q.; Feng, J.-T.; Zhang, X. Bioactivity-guided mixed synthesis and evaluation of α-alkenyl-γ and δ-lactone derivatives as potential fungicidal agents. *RSC Adv.* **2017**, *7*, 56496–56508.

[50] Richardson, W. H.; Stiggal-Estbergm D.L.; Chen, Z.; Baker, J. C. Burns, D.M.; Sherman, D.G. Substituent effects upon efficiency of excited-state acetophenones produced on thermolysis of 3,4-diaryl-3,4-dimethyl-1,2-dioxetanes. *J. Org. Chem*. **1987**, *52*, 3143–3150.

[51] Morrison, H.; Giacherio, D.; Palensky, F.J. Organic photochemistry. 50. Photoinduced skeletal rearrangement of alkylindenes *J. Org. Chem*. **1982**, *47*, 1051–1058.

[52] Vila, C.; Cembellín, S.; Hornillos, V.; Giannerini, M.; Fañanás-Mastral, M.; Feringa, B. L. *t*BuLi-Mediated One-Pot Direct Highly Selective Cross-Coupling of Two Distinct Aryl Bromides**.** *Chem. Eur. J.* **2015**, *21*, 15520–15524.

[53] Nakatsuji, H.; Ashida, Y.; Hori, H.; Sato, Y.; Honda, A.; Taira, M.; Tanabe, Y. (*E*)–and (*Z*)-stereodefined enol phosphonates derived from β-ketoesters: stereocomplementary synthesis of fully-substituted α,β-unsaturated esters. *Org. Biomol. Chem*. **2015**, *13*, 8205–8210.

[54] Troutman, M.V.; Appella, D.H.; Buchwald, S.L. Asymmetric Hydrogenation of Unfunctionalized Tetrasubstituted Olefins with a Cationic Zirconocene Catalyst *J. Am. Chem. Soc*. **1999**, *121*, 4916–4917.

[55] Zhang, Z.; Wang, J.; Li, J.; Yang, F.; Liu, G.; Tang, W.; He, W.; Fu, J.-J; Shen, Y.-H; Li, A.; Zhang, W.-D. Total Synthesis and Stereochemical Assignment of Delavatine A: Rh-Catalyzed Asymmetric Hydrogenation of Indene-Type Tetrasubstituted Olefins and Kinetic Resolution through Pd-Catalyzed Triflamide-Directed C–H Olefination. *J. Am. Chem. Soc*. **2017**, *139*, 5558–5567.

[56] Roy, S.; Das, S. K.; Khatua, H.; Das, S.; Singh, K. N.; Chattopadhyay, B. Iron-Catalyzed Radical Activation Mechanism for Denitrogenative Rearrangement Over C(sp^3)–H Amination. *Angew. Chem. Int. Ed.* **2021**, *60*, 8772-8780.

[57] Sun, K.; Liu, S.; Bec, P. M.; Driver, T. G. Rhodium-Catalyzed Synthesis of 2,3-Disubstituted Indoles from β,β-Disubstituted Stryryl Azides. *Angew. Chem. Int. Ed.* **2011**, *50*, 1702-1706.

[58] Matsuda, T.; Yuihara, I.; Kondo, K. Rhodium(I)-catalysed skeletal reorganisation of benzofused spiro[3.3]heptanes via consecutive carbon–carbon bond cleavage. *Org. Biomol. Chem.* **2016**, *14*, 7024-7027.

[59] Synthesis performed in two steps from chlorobenzene: a) Kraus, G. A.; Wu, T. A Three-component reaction between benzynes, the enolate of acetaldehyde, and unsaturated esters and dihydroisoquinolines. *Tetrahedron* **2010**, *66*, 569-572; b) Bubb, W.A.; Sternhell, S. Proton N.M.R. spectra of 1-substituted benzocyclobutenes (Bicyclo[4,2,0]octa-1,3,5-trienes). *Aust. J. Chem*. **1976**, *29*, 1685–1697.

[60] Frisch, M. J.; Trucks, G. W.; Schlegel, H. B.; Scuseria, G. E.; Robb, M. A.; Cheeseman, J. R.; Scalmani, G.; Barone, V.; Petersson, G. A.; Nakatsuji, H.; Li, X.; Caricato, M.; Marenich, A.; Bloino, J.; Janesko,B.G.;Gomperts,R.;Mennucci,B.;Hratchian,H.P.;Ortiz,J. V.; Izmaylov, A. F.; Sonnenberg, J. L.; Williams-Young, D.; Ding, F.; Lipparini, F.; Egidi, F.; Goings, J.; Peng, B.; Petrone, A.; Henderson, T.; Ranasinghe, D.; Zakrzewski, V. G.; Gao, J.; Rega, N.; Zheng, G.; Liang, W.; Hada, M.; Ehara, M.; Toyota, K.; Fukuda, R.; Hasegawa, J.; Ishida, M.; Nakajima, T.; Honda, Y.; Kitao, O.; Nakai, H.; Vreven, T.; Throssell, K.; Montgomery, J. A., Jr.; Peralta, J. E.; Ogliaro, F.; Bearpark, M.; Heyd, J. J.; Brothers, E.; Kudin, K. N.; Staroverov, V. N.; Keith, T.; Kobayashi, R.; Normand, J.; Raghavachari, K.; Rendell, A.; Burant, J. C.; Iyengar, S. S.; Tomasi, J.; Cossi, M.; Millam, J. M.; Klene, M.; Adamo, C.; Cammi, R.; Ochterski, J. W.; Martin, R. L.; Morokuma, K.; Farkas, O.; Foresman, J. B.; Fox, D. J. Gaussian 09, Revision A.02; Gaussian, Inc.: Wallingford CT, 2016.

[61] (a) Hay, P. J.; Wadt, W. R. Ab initio effective core potentials for molecular calculations. Potentials for the transition metal atoms Sc to Hg*. J. Chem. Phys.* **1985**, *82*, 270–283. (b) Hay, P. J.; Wadt, W. R. Ab initio effective core potentials for molecular calculations. Potentials for K to Au including the outermost core orbitals. *J. Chem. Phys.* **1985**, *82*, 299–310.

[62] Petersson, G. A.; Bennett, A.; Tensfeldt, T. G.; Al-Laham, M. A.; Shirley, W. A.; Mantzaris, J. "A complete basis set model chemistry. I. The total energies of closed-shell atoms and hydrides of the first-row atoms," *J. Chem. Phys.* **1988**, 89, 2193–2218.

[63] Tomasi, J.; Mennucci, B.; Cammi, R. Quantum Mechanical Continuum Solvation Models. *Chem. Rev.* **2005**, *105*, 2999–3094.

[64] Ribeiro, R. F.; Marenich, A. V.; Cramer, C. J.; Truhlar, D. G. Use of Solution-Phase Vibrational Frequencies in Continuum Models for the Free Energy of Solvation*. J. Phys. Chem. B*, **2011**, *115*, 14556–14562.

[65] Luchini, G.; Alegre-Requena, J. V.; Funes-Ardoiz, I.; Paton, R. S. GoodVibes: Automated Thermochemistry for Heterogeneous Computational Chemistry Data. *F1000Research*, **2020**, *9*, 291.

UNIVERSITAT ROVIRA I VIRGILI
DEVELOPMENT OF CHIRAL METAL-CATALYSTS FOR THE SELECTIVE FORMATION OF C-H, C-C AND C-X BONDS. FROM DESIGN TO APPLICATION
Pol De La Cruz Sanchez Badia

3.3. Phosphine-triazole based ligands for the Ir-catalyzed asymmetric hydrogenation of challenging exocyclic benzofused-based alkenes

3.3.1. Introduction

As previously discussed, the metal-catalyzed asymmetric hydrogenation of alkenes is still a growing field. It offers some of the most sustainable and straightforward processes for producing a broad range of pharmaceuticals and fine chemicals, which justify the interest of top pharmaceutical companies.[1] A thorough patent review by Glorius, Leker et al. recently highlighted the industrial relevance of asymmetric hydrogenation.[2] They concluded that catalytic hydrogenation is a mature technology that yet has to reach its maximum economic relevance and will continue to generate valuable patents and innovations. In this respect, to fully exploit the application of asymmetric hydrogenation there is still a constant need to expand the range of substrates undergoing the process with high enantioselectivity, thus making the synthesis of the most diverse chiral molecules possible.

Among the most challenging non-chelating substrates, the exocyclic olefins containing a benzofused five/six-membered ring motif, whose hydrogenation products are present in pharmaceutical natural products and key bioactive drug intermediates (Figure 3.3.1), represent an unmet goal.[3]

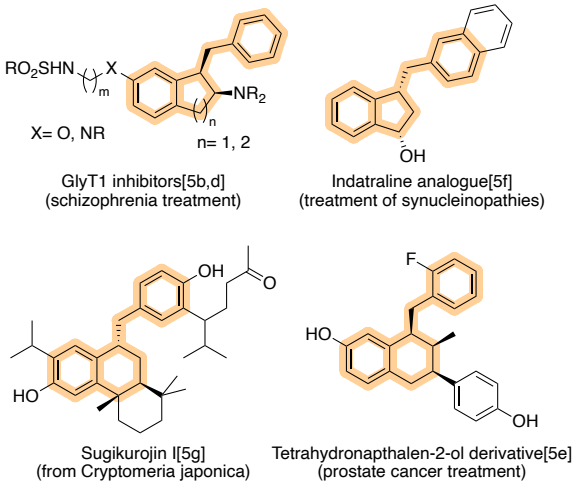

Figure 3.3.1. Representative examples of natural occurring compounds and drugs containing a chiral benzofused five/six-membered ring motif.

Compared to the considerable number of reports dealing with the reduction of non-chelating acyclic and endocyclic olefins, the reduction of non-chelating exocyclic olefins is clearly underdeveloped. Only a few publications have reported high catalytic

performance, albeit with a limited substrate scope (Figure 3.3.2).[4] One with comparatively broader scope is the Ir/In-BiphPHOX catalyst which is able to hydrogenate a range of olefins exocyclic to a five-membered benzofused ring with high enantioselectivities (Figure 3.3.2, 93-98% ee).[4a] However, the recorded enantioselectivities sharply decreased when an *ortho* substituent was present on the aromatic ring (Ar group in Figure 3.3.2, top) and was also lower in the reduction of the parent olefin exocyclic to a benzofused six-membered olefin (75% ee). Note that a similar ring size dependence has been observed in the hydrogenation of other olefins with an exocyclic double bond such as α,β-disubstituted unsaturated lactones and lactams.[5] Additionally, the reaction required an additive and a specific solvent (*o*-xylene), moving away from the commonly used solvents in Ir-catalyzed asymmetric hydrogenation. The difficulty in the reduction of this type of exocyclic olefins at benzofused five/six-membered rings is even more evident if we consider that PHOX, which are the most successful ligands for Ir-catalyzed hydrogenation, did not work in these cases.[4b-c] More recently, as dicussed in Section 3.2, Ir-MaxPHOX catalysts provided good levels of enantioselectivity for both 5- and 6-membered benzofused olefins (ee's up to 86%, Figure 3.3.2) without the use of any additive.[4d] However, we aimed for a wider substrate scope as well as maximizing the enantioselectivities for both ring sizes.

In this section, we report a new P,N-ligand design specially well suited for the Ir-catalyzed hydrogenation of exocyclic olefins at benzofused five-membered rings, the more challenging analogues involving six-membered rings, and with promising results for a seven-membered analogue (Figure 3.3.2, bottom).[6] The new phosphine-triazole ligands **L9** and **L10** are based on the phosphine-oxazolines PHOX in which a chiral carbon spacer has been added between the oxazoline and the phenyl ring to study how the size of the chelate ring influences the catalytic performance. The ligand design has been completed by attaching a silyl group on the carbon spacer. This latter design feature was inspired by Pfaltz's first generation of phosphine-pyridine design that showed that the silyl groups are interacting with the active site of the catalysts and therefore they have shown to be important in their success.[7] In addition, the oxazoline moiety in the PHOX ligand has also been replaced by a triazole with the aim to facilitate the stabilization of the substrate in the catalyst chiral pocket via N---H interactions.[8] We have also performed mechanistic studies (deuterogenation experiments and DFT calculations) to explain the origin of enantioselectivity in the reactions mediated by ligands **L9** and **L10**.

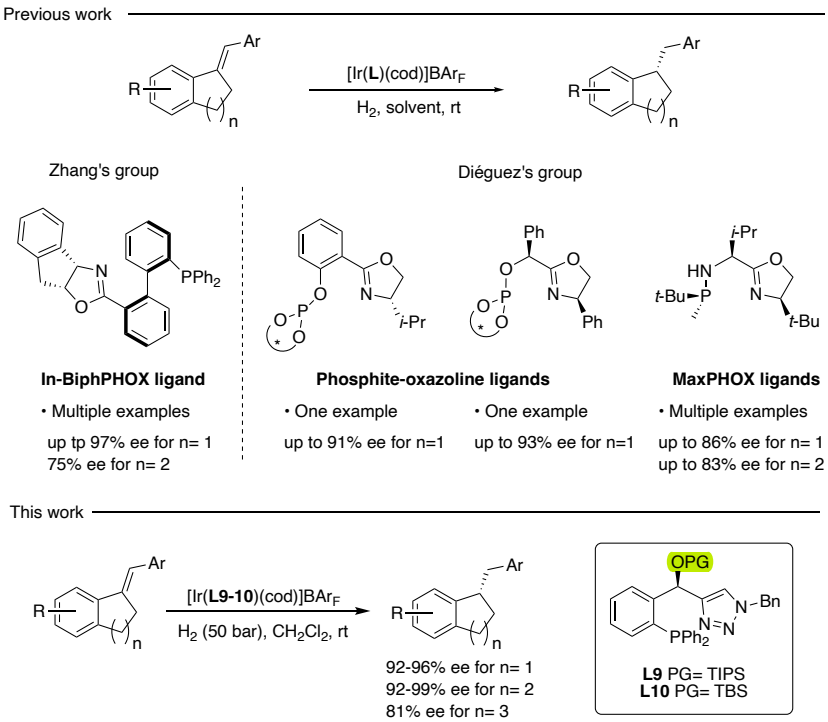

Figure 3.3.2. Precedents in the Ir-catalyzed asymmetric hydrogenation of non-chlating exocyclic olefins.

3.3.2. Results and discussion

3.3.2.1. Synthesis of Ir-catalyst precursors

The synthesis of the new phosphine-triazole ligands **L9**–**L10** is straightforward from (*R*)-(1-benzyl-1H-1,2,3-triazol-4-yl)(2-iodophenyl)methanol **7** (Scheme 3.3.1). Compound **7** was synthesized from the readily accessible 2-iodobenzaldehyde using a simple three step procedure developed by Pericàs and Nachtsheim groups.[9] Thus, the synthesis of enantiopure **7** (>99.9% ee) involves the non-enantioselective propargylation of 2-iodobenzaldehyde, the CALB-catalyzed enzymatic kinetic resolution of the intermediate propargyl alcohol, and a final Cu-catalyzed alkyne-azide Huisgen-type cycloaddition. Then, the Pd-catalyzed phosphination of **7** gave the corresponding phosphine-triazole compound **8** in 78% yield. Finally, the hydroxyl group in **8** was protected with two different bulky silyl ether groups (TIPS and TBS) to yield the desired enantiopure phosphine-triazole ligands **L9** and **L10** in 78% and 91% yield, respectively.

Coordination of ligands **L9**–**L10** to iridium using $[Ir(\mu\text{-Cl})(cod)]_2$ as precursor in dichloromethane at room temperature, followed by the replacement of the Cl anion by BAr_F^- using $NaBAr_F$ in an aqueous suspension led to desired Ir-catalyst precursors (Scheme 3.3.1). Advantageously, they were obtained as orange air stable solids. They

were therefore handled and stored in air. The formation of ligands and Ir-complexes was confirmed by ^{1}H, ^{13}C and ^{31}P NMR spectroscopy and HRMS-ESI spectrometry (see Experimental Section and Supporting Information for details). The HRMS-ESI spectra agree with the assigned structures displaying the heaviest ions at m/z values corresponding to the loss of BAr_F anion.

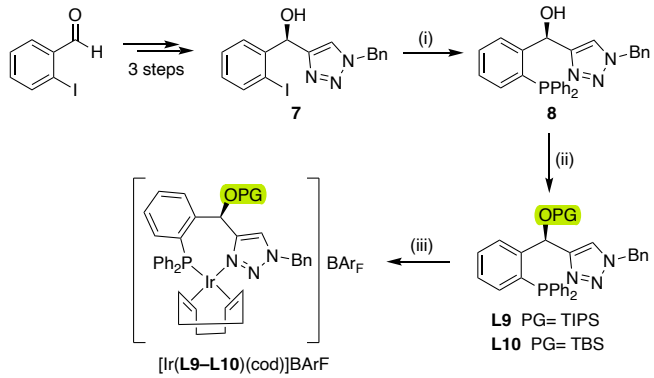

Scheme 3.3.1. Synthesis of ligands **L19** an **L10** and of [Ir(**L9**–**L10**)(cod)]BAr_F catalyst precursors: (i) $Pd_2(dba)_3$, dippf, $HPPh_2$, NEt_3, toluene, 110 °C, 2.5 h; (ii) TIPSOTf or TBSOTf, 2,6-lutidine, CH_2Cl_2, rt, 2 h; (iii) [Ir(μ-Cl)(cod)]$_2$, CH_2Cl_2, reflux, 1 h then $NaBAr_F$, H_2O, rt, 30 min.

3.3.2.2. Asymmetric hydrogenation of challenging exocyclic benzofused-based alkenes

3.3.2.2.1. Initial catalytic screening. Ir-catalyzed asymmetric hydrogenation of two model exocyclic olefins S35 and S39

The Ir-catalyst precursors containing phosphine-triazole ligands **L9**–**L10** were first tested in the hydrogenation of olefins **S35** (exocyclic to a benzofused five-membered ring) and the more challenging **S39** (exocyclic to a 1,2,3,4-tetrahydronaphthalene analogue). The results are summarized in Table 3.3.1, entries 1-4. We applied in these experiments the most commonly used reaction conditions in the Ir-catalyzed asymmetric hydrogenation of unfunctionalized olefins (50 bar of H_2 at room temperature using dichloromethane and 1 mol% of the catalysts precursor [Ir(cod)(**L9**–**L10**)]BAr_F).[4b] Positively, full conversion and high enantioselectivities (ee's up to 99%) in both substrate types were achieved by selecting the right silyl group, in only 4 hours and without any additive. We next studied the effect of the hydrogen pressure on the catalytic outcome (Table 3.3.1, entries 5-8). The results show a small decrease in conversion and enantioselectivity when the hydrogen pressure was lowered to 10 bars (Table 3.3.1, entries 5 and 6). Nevertheless, the catalytic performance is not affected by increasing the hydrogen pressure (Table 3.3.1, entries 7 and 8).

For comparison purposes, we also studied whether the high enantioselectivities achieved in the hydrogenation of **S35** using previously reported ligands **9**[4b] and **10**[4c] were maintained in the hydrogenation of 6-membered ring analogue **S39** (Table 3.3.1, entries 10 and 12). In line with previous results using Ir/In-BiphPHOX catalysts,[4a] the use of both Ir-phosphite-oxazoline based catalysts provided lower enantiocontrol in the hydrogenation of **S39** than for **S35** (Table 3.3.1, entries 9 and 11 vs 10 and 12 respectively).

Table 3.3.1. Asymmetric hydrogenation of olefins **S35** and **S39**.[a]

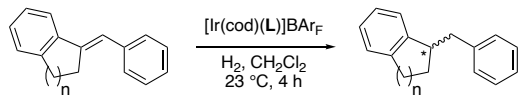

S35 n=1 ; **S39** n= 2

Entry	Substrate	H_2 (bar)	L	% Conv[b]	% ee[c]
1	**S35**	50	**L9**	100	85 (*S*)
2	**S35**	50	**L10**	100 (98)	95 (*S*)
3	**S39**	50	**L9**	100	87 (*S*)
4	**S39**	50	**L10**	100 (97)	99 (*S*)
5	**S35**	10	**L10**	99	92 (*S*)
6	**S39**	10	**L10**	88	95 (*S*)
7	**S35**	75	**L10**	100	95 (*S*)
8	**S39**	75	**L10**	100	99 (*S*)
9[d]	**S35**	50	**9**	100	91 (*R*)
10	**S39**	50	**9**	95	87 (*R*)
11[e]	**S35**	50	**10**	100	93 (*S*)
12	**S39**	50	**10**	79	30 (*S*)

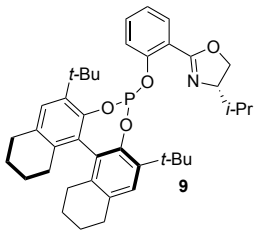

9

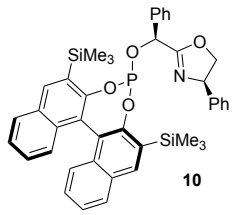

10

[a] Reaction conditions: 1 mol % [Ir(cod)(**L**)]BAr_F, CH_2Cl_2 as solvent at 23 °C for 4 h. [b] Conversions measured by ^1H NMR. Isolated yields in parenthesis. [c] Enantiomeric excesses determined by chiral HPLC. [d] Data from ref. 4b. [e] Data from ref. 4c

3.3.2.2.2. Scope and limitations. Ir-catalyzed asymmetric hydrogenation of a range of benzofused-based exocyclic olefins

We next studied the scope of the Ir/**L10** catalytic system by extending our work to the hydrogenation of other exocyclic olefins based on benzofused systems with different ring sizes and diverse substituents at both aromatic rings present in the structures of the substrates.

We initially considered the reduction of substrates **S36**–**S38** and **S121**–**S124** with double bonds exocyclic to a benzofused five-membered ring (Table 3.3.2, entries 1-7). As observed for the Ir/In-BiphPHOX system,[4a] Ir/**L10** tolerates very well the presence of several substituents and substitution patterns at both aromatic rings (**S36**–**S38** and **S121**–**S124**). In addition, note that improving the performance of the Ir/In-BiphPHOX, whose ability to hydrogenate substrates with *ortho* substituents on the aromatic ring (Ar group) is not optimal (ee's up to 78%), the Ir/**L10** was also able to provide high enantioselectivity in the reduction of substrate **S38**, bearing such an *ortho* substituent (Table 3.3.3, entry 5, 95% ee). Finally, the enantiomeric outcome was also maintained in the reduction of the dihydrobenzofuran analogue **S124** (Table 3.3.2, entry 7, 95% ee).

Table 3.3.2. Asymmetric hydrogenation of benzylidene-containing 2,3-dihydro-1*H*-indenes **S36**–**S38**, **S121**–**S123** and 2,3-dihydrobenzofuran **S124**.[a]

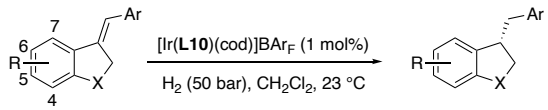

Entry	Substrate	Ar	R	X	% Yield	% ee[b]
1	**S36**	4-Me-C_6H_4	H	CH_2	98	93 (*S*)
2	**S37**	4-OMe-C_6H_4	H	CH_2	97	94 (*S*)
3	**S38**	2-Me-C_6H_4	H	CH_2	99	95 (*S*)
4	**S121**	4-Cl-C_6H_4	H	CH_2	99	94 (*S*)
5	**S122**	3-Me-C_6H_4	H	CH_2	97	96 (*S*)
6	**S123**	C_6H_5	5-Br	CH_2	98	92 (*S*)
7	**S124**	C_6H_5	H	O	95	95 (*S*)

[a] Full conversions were attained in all cases after 4 h. [b] Enantiomeric excesses determined by chiral HPLC.

We next applied Ir/**L10** in the hydrogenation of a series of olefins with the double bond exocyclic to a benzofused six-membered ring (Table 3.3.3). Positively, the catalytic performance was highly independent of the substitution pattern of the Ar group (**S40**–**S42** and **S125**, ee's up to 99%). Although the hydrogenation of the *ortho*-substituted derivative **S42** led to the lowest enantioselectivity (ee's up to 92%,) this is still remarkable for this challenging substrate. An electronegative, yet π-donating chloro substituent (Table 3.3.3, entry 2) was also well tolerated (99% ee). We were also pleased to find that Ir/**L10** tolerates well variations in the substitution pattern at the fused benzene ring (**S126**–**S130**, ≥ 98% ee).

Table 3.3.3. Asymmetric hydrogenation of benzylidene-1,2,3,4-tetrahydronaphtalenes **S40**–**S42** and **S125**–**S130**.[a]

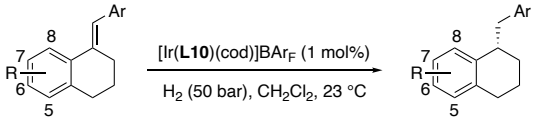

Entry	Substrate	Ar	R	% Yield	% ee[b]
1	**S40**	4-Me-C_6H_4	H	97	98 (*S*)
2	**S41**	4-Cl-C_6H_4	H	99	99 (*S*)
3	**S42**	2-Me-C_6H_4	H	97	92 (*S*)
4	**S125**	3-Me-C_6H_4	H	96	98 (*S*)
5	**S126**	C_6H_5	5-Br	97	98 (*S*)
6	**S127**	C_6H_5	5-OMe	98	99 (*S*)
7	**S128**	C_6H_5	6-Br	96	99 (*S*)
8	**S129**	C_6H_5	7-Br	99	98 (*S*)
9	**S130**	C_6H_5	7-OMe	98	98 (*S*)

[a] Full conversions were attained in all cases after 4 h. [b] Enantiomeric excesses determined by chiral HPLC.

To explore the possibilities beyond those already described for the Ir/**L10** catalytic system, we studied the hydrogenation of exocyclic olefins with an even larger benzofused seven-membered ring (**S131**) and, with a benzofused four-membered ring (**S43**, Scheme 3.3.2). The hydrogenation of **S43** provided the hydrogenated product with moderate enantioselectivity (40% ee), which did not improve the results obtained in Section 3.2. (74% ee).[4d] However, the hydrogenation of **S131** proceed with a remarkable enantioselectivity of 81% ee.

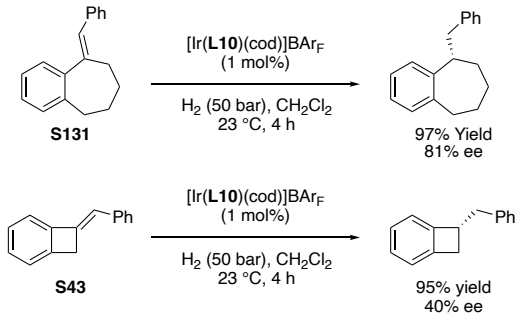

Scheme 3.3.2. Asymmetric hydrogenation of (*E*)-5-benzylidene-6,7,8,9-tetrahydro-5H-benzo[7]annulene **S131** and (*E*)-7-benzylidenebicyclo[4.2.0]octa-1,3,5-triene **S43**. Full conversions were attained in both cases.

Finally, having in mind that the enantiocontrol in the hydrogenation of non-chelating olefins is drastically affected by the olefin geometry,[10] we studied the asymmetric hydrogenation of the *Z*-olefins **S132**–**S134** (Scheme 3.3.3). In line with previous reports, the hydrogenation of these *Z*-analogues led to much lower enantioselectivities than the *E*-analogues.

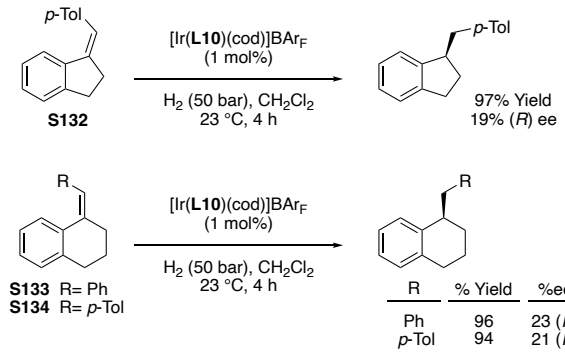

Scheme 3.3.3. Asymmetric hydrogenation of exocyclic olefins with *Z*-geometry. Full conversions were attained in all cases.

3.3.2.3. Mechanistic insights

The elusiveness of olefins exocyclic to benzofused rings as asymmetric hydrogenation substrates has been mainly attributed to the fact that they can easily isomerize into the corresponding endocyclic olefins under hydrogenation conditions. To study if the enantioselectivities attained in the hydrogenation of *E*-olefins with different ring size could be related to the isomerization extent, we studied the deuterogenation of olefins **S36**, **S40**, **S130** and **S43** (Scheme 3.3.4). The deuterium incorporation was only observed in the olefinic carbons, indicating that isomerization does not take place regardless of the size of the benzofused ring. This clearly indicates that the enantioselectivity is mainly governed by the constrains of the catalyst chiral pocket.

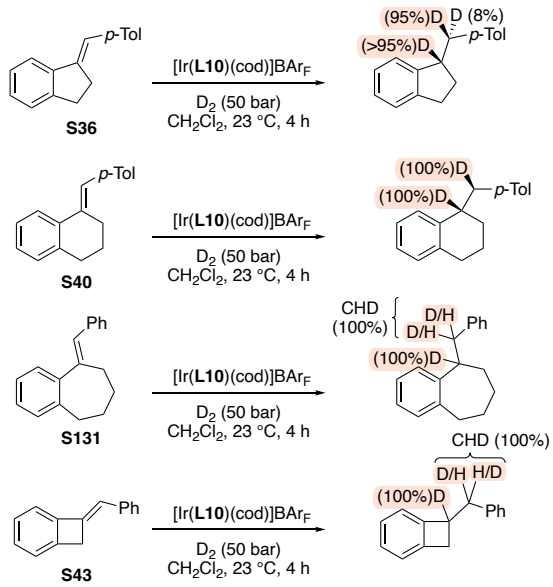

Scheme 3.3.4. Deuterogenation experiments.

To gain further insight about the effect of the ligand structure on this chiral pocket, we performed a DFT study of the species involved in the enantiodetermining step. Mechanistically, we reiterate that the Ir-catalyzed hydrogenation of non-chelating olefins proceeds via the Ir(III)/Ir(V) catalytic cycle, where the enantioselectivity is determined in the first hydrogen transfer from the metal to the coordinated olefin.[11, 12] This step, however, can be accomplished via migratory insertion (Figure 3.3.3, **TS_{MI}**) or via σ-bond metathesis (Figure 3.3.3, **TS_{Meta}**).[11,12] We therefore computed all the transition states (TSs) for both pathways with Ir/**L10** catalyst using substrate **S39**.

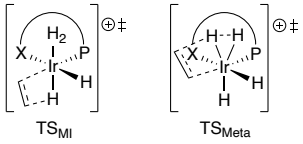

Figure 3.3.3. Schematic representation of the TSs for the migratory insertion (**TS_{MI}**) and σ-bond metathesis (**TS_{Meta}**) pathways.

The results show that the migratory insertion TSs are more favorable than the σ-bond metathesis TSs (see Supporting Information). The calculated energies of the most stable isomers of the **TS_{MI}** are shown in Table 3.3.4. These key TSs are the result of the coordination to the two enantiotopic faces (*Re* and *Si*) of the olefin, the attack of the hydride at the two olefinic carbons and the relative disposition of the hydride (up or down). For each of them, a conformational search was carried out to make sure that the conformation with the lowest energy was found.

Table 3.3.4. Calculated energies (kcal/mol) for transition states of the migratory insertion pathway with substrate **S39** using Ir/**L10**.[a]

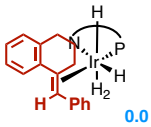 0.0	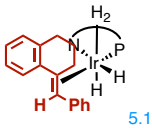 5.1	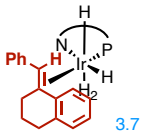 3.7	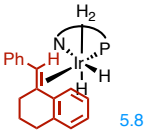 5.8
TS_A attack at C_1 *Re*-face coordination pro (*S*)	**TS_B** attack at C_2 *Re*-face coordination pro (*S*)	**TS_C** attack at C_2 *Re*-face coordination pro (*S*)	**TS_D** attack at C_1 *Re*-face coordination pro (*S*)
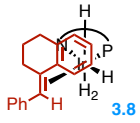 3.8	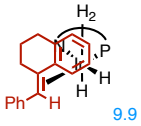 9.9	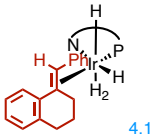 4.1	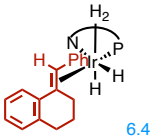 6.4
TS_E attack at C_1 *Si*-face coordination pro (*R*)	**TS_F** attack at C_2 *Si*-face coordination pro (*R*)	**TS_G** attack at C_2 *Si*-face coordination pro (*R*)	**TS_H** attack at C_1 *Si*-face coordination pro (*R*)

[a] C_1 is the olefinic carbon that is located in the ring structure and C_2 is the olefinic carbon that is located outside the ring structure. In all TSs the most stable conformer was selected.

Positively, the calculated energy difference of the two most stable TSs (**TS_A** and **TS_E**), that lead to opposite enantiomers, is in good agreement with the experimental enantioselectivity (Table 3.3.1, entry 4, ee of 99% (*S*)). The factors responsible for the enantioselectivity can therefore be deduced by examining the structures of **TS_A** and **TS_E**.

We first did a steric interaction assessment by analyzing the structures of the two most stable TSs, leading to opposite enantiomers, via a quantitative quadrant-diagram using the MolQuO software.[13] However, in contrast to previous studies in Section 3.2. the quadrant analysis did not provide a clear relationship between the olefin arrangement and the quadrant occupancy.

Both structures show attractive interactions between the substrate and the ligand that were analyzed with a non-covalent interaction (NCI)-plot (Figure 3.3.4). However, while the **TS_A** is stabilized by three CH---N, two CH-π and one T-shaped π-π interactions (Figure 3.3.4a), **TS_E** is only stabilized by two CH---N and one T-shaped π-π interactions (Figure 3.3.4b). Concretely, in **TS_A**, two of the CH---N interactions are located between the tetrahydronaphthalene phenyl ring of the substrate and two N of the triazole moiety of the ligand, and the third CH---N interaction is found between the H of the olefinic carbon and a N of the triazole unit (Figure 3.3.4a). These interactions show the importance of having a triazole instead of the most commonly oxazoline group into the ligand where some of these attractive CH---N interactions would not exist. Figure 3.3.4a also illustrates the T-shaped CH-π interaction of the benzyl substituent of the triazole group and two CH-π interactions of the tetrahydronaphthalene phenyl ring of the

substrate with the methyl substituents of the TBS group. The presence of a TBS group in the ligand is therefore crucial.

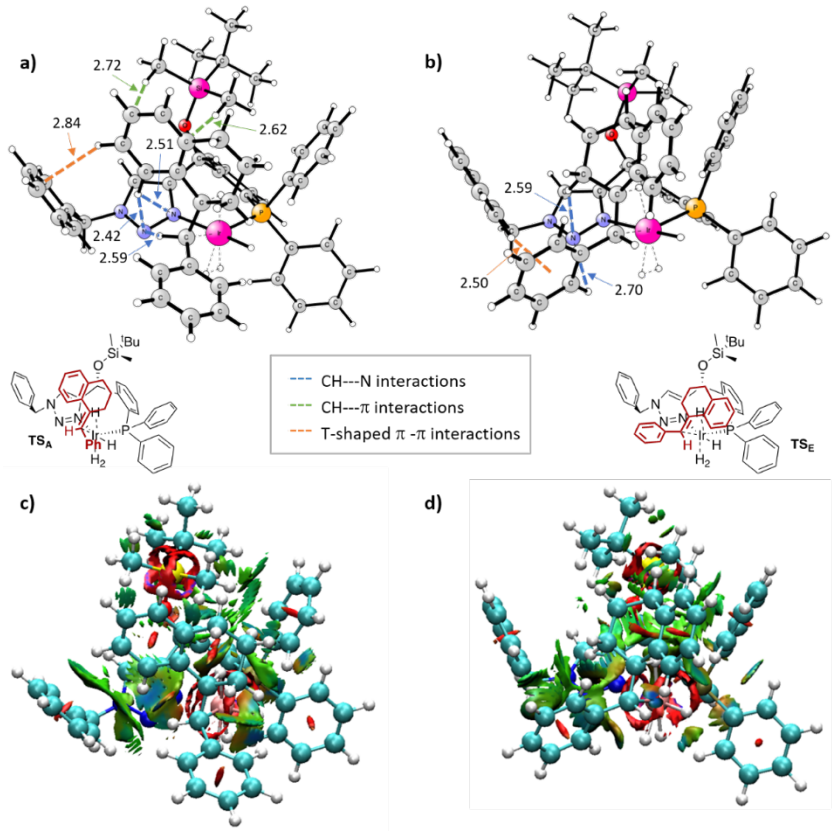

Figure 3.3.4. Optimized geometries of the most TSs resulting from the first hydrogen transfer from the metal to the coordinated olefin for the migratory insertion pathway for **S39** using Ir/**L10**: (a) **TS$_A$**: coordination from the *Re*-face, leading to the *S*-enantiomer; (b) **TS$_E$**: coordination from the *Si*-face, leading to the *R*-enantiomer; (c) NCI plot of **TS$_A$**; (d) NCI plot of **TS$_E$**. For the NCI plots; strong and attractive interactions are blue, weak interactions are green and strong and repulsive interactions are red.

In summary, the attractive interactions above described in **TS$_A$** make its chiral pocket better suited for the 6-membered exocyclic olefin **S39** than the cavity of **TS$_E$**, where only two CH---N interactions and a T-shaped π-π interaction are found[14] (Figure 3.3.4b), whereas the attractive interactions between the substrate and the protecting silyl group are not present.

In addition, the stereochemical model also showed that the relative position of the tetrahydronaphthalene phenyl ring is important to facilitate the necessary attractive interactions in **TS$_A$**. Ultimately, the position of this group is largely affected by the ring size of the benzofuzed moiety (Scheme 3.3.5a), and this can be related to the

differences in the enantiomeric excesses found when the size of the benzofuzed moiety varies. While the fit in the chiral pocket is adequate for the exocyclic olefins containing a benzofused five- or six-membered ring and to a less extend the seven-membered ring, the 4-membered exocyclic substrate **S43** shifts the position of the tetrahydronaphthalene phenyl ring in such a way that results in the loss of the aforementioned attractive interactions that make **TS_A** superior.

Finally, to identify whether the low ee's achieved in the hydrogenation of *Z*-olefins compared with those of the *E*-analogues can be caused by the constrains of the catalyst chiral pocket or by the existence of isomerization, we studied the deuterogenation of **S132** (Scheme 3.3.5b). In contrast to the *E*-analogue **S36**, we observed the incorporation of deuterium at the 2-position which clearly indicates that isomerization takes place. So, we can conclude that the isomerization rate of *Z*-olefins to *E*-olefins is in the same order as hydrogenation of both isomers, which leads to low enantioselectivities.

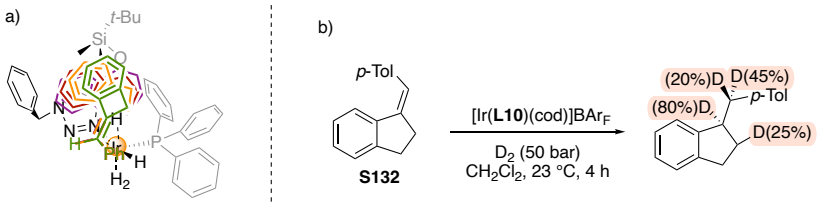

Scheme 3.3.5. (a) Representation of the effect of the substrate's size of the cycle in **TS_A**. Substrates **S42** (in green), **S35** (in orange), **S39** (in red) and **S130** (in violet) are superimposed; (b) Deuterogenation experiment of **S131**.

3.3.3. Conclusions

In summary, we have developed an Ir/phosphine-triazole catalysts for the asymmetric hydrogenation of olefins whose double bonds are exocyclic to benzofused rings of different sizes. We have identified a catalyst that is able to successfully hydrogenate exocyclic olefins containing a benzofused six-membered ring motif (with ee's typically of 99%). Significantly, the results also extended to olefins bearing a five-membered benzofused ring (ee's typically ca 95%) and for the first time a promising enantioselectivity of 81% was reached for a seven-membered benzofused analogue. Moreover, the catalyst tolerated well different substituents and substitution patterns at both aromatic rings present in the substrates, which opens up its potential use in the synthesis of high-value compounds such as drugs and natural products. The absence of a competing isomerization process together with the perfect fit of the *E*-olefins in the catalyst chiral pocket are the keys for the success of this catalyst. In this fit the presence of non-covalent attractive interactions between the substrate and the ligand components has been crucial as well as the presence in the ligand of a triazole instead

of the commonly oxazoline group and a silyl group. Finally, as observed for other non-chelating functionalized olefins, the enantiomeric excess was highly dependent on the olefin geometry. Thus, the high enantioselectivities were only attained in the hydrogenation of *E*-olefins. The decrease of enantioselectivity observed for *Z*-olefins was due to an isomerization process competing with the hydrogenation.

3.3.4. Experimental section

3.3.4.1. General considerations

All reactions were carried out using standard Schlenk techniques under an argon atmosphere unless otherwise noted. Solvents were purified and dried by standard procedures. Compound **7**[9] and substrates **S35**–**S36**,[4a] **S37–S38**,[15] **S39**,[4a] **S40–S41**,[15] **S43**[15] and **S121**–**S124**[4a] were prepared following the reported procedures. ^{1}H, ^{13}C and ^{31}P NMR spectra were recorded using a 400 MHz spectrometer. Chemical shifts are relative to that of NMR solvent for ^{1}H and $^{13}C\{^{1}H\}$ and of H_3PO_4 as internal standard for $^{31}P\{^{1}H\}$. For characterization and ee determination details, copies of the NMR spectra, copies of GC or HPLC traces as well as for DFT details and other mechanistic insights see Supporting Information.

3.3.4.2. Synthesis of (*R*)-(1-benzyl-1H-1,2,3-triazol-4-yl)(2-(diphenyl-phosphaneyl)phenyl) methanol 8

$Pd_2(dba)_3$ (4.58 mg, 5 µmol) and **7** (0.391 g, 1 mmol) were placed in a Schlenk tube. The tube was then entered into a N_2-filled glove box were 1,1'-bis(diisopropylphosphino)ferrocene (dippf; 4.18 mg, 10 µmol), and dry degassed toluene (2 mL) were added. After stirring for 20 min, degassed triethylamine (0.21 mL, 1.5 mmol), and diphenylphosphine (0.26 mL, 1 mmol) were added and the tube was sealed, taken out of the glove box, and heated in an oil bath at 110 ºC for 2.5 h. The reaction mixture was allowed to cool to room temperature and was then kept at -20 ºC overnight to induce crystallization. Filtration, followed by washing with toluene (5x0.5 mL), water (5x1 mL), and isopropanol (5x0.5 mL) resulted in an off-white powder that was recrystallized from hot deoxygenated isopropanol (9 mL) under Ar, filtered and washed with isopropanol (3x1 mL) to obtain compound **2** (0.336 g, 75 % yield) as a white powder. ^{31}P NMR (162 MHz, $CDCl_3$) δ: -18.0. ^{1}H NMR (400 MHz, $CDCl_3$) δ: 3.26 (br, 1H, O*H*), 5.20 (d, 1H, $^{2}J_{H-H}$= 14.9 Hz, C*H*$_2$Ph), 5.23 (d, 1H, $^{2}J_{H-H}$= 14.9 Hz, C*H*$_2$Ph), 6.69 (s, 1H, C*H*=N, trz), 6.76 (d, 1H, $^{3}J_{P-H}$= 7.2 Hz, C*H*OH), 6.95–6.98 (m, 1H, C*H*=, Ar), 7.12–7.16 (m, 4H, C*H*=, Ar), 7.19–7.24 (m, 5H, C*H*=, Ar), 7.24–7.29 (m, 1H, C*H*=, Ar), 7.29–7.34 (m, 6H, C*H*=, Ar), 7.40 (t, 1H, $^{3}J_{H-H}$= 7.6 Hz, C*H*=, Ar), 7.68–7.71 (m, 1H, C*H*=, Ar). ^{13}C NMR (100 MHz, $CDCl_3$) δ: 53.8 (*C*H$_2$Ph), 66.6 (d, $^{3}J_{C-P}$= 27.7 Hz, *C*HOH), 121.6 (*C*H=N, trz), 127.2–135.8 (aromatic carbons), 135.8 (d, $^{1}J_{C-P}$= 11.0 Hz, *C*, Ar), 136.4 (d, $^{1}J_{C-P}$= 11.0 Hz, *C*, Ar), 146.3 ($^{1}J_{C-P}$= 22.0 Hz, *C*, Ar), 150.47 (*C*, Ar). MS HR-ESI [found 449.1649 $C_{28}H_{24}N_3OP$ $(M)^+$ requires 449.1652].

3.3.4.3. General procedure for the synthesis of ligands L9 and L10

To a suspension of **8** (0.112 g, 0.25 mmol) in CH_2Cl_2 (1 mL), were added 2,6-lutidine (0.06 mL, 0.5 mmol) and the corresponding silyl triflate (0.3 mmol), under Ar at 0 ºC. The resulting solution was then stirred 2 h at room temperature. After that time, a saturated solution of $NaHCO_3$ (2.5 ml) was added, followed by extraction with CH_2Cl_2 (3x2.5 mL). The combined organic phases were washed with brine (2.5 mL), dried over $MgSO_4$, concentrated, and purified with flash column chromatography (neutral SiO_2 *ca* 10 cm × 2.5 cm, 4:1 petroleum ether-EtOAc) to obtain the corresponding ligands **L9** and **L10**.

(*R*)-1-benzyl-4-((2-(diphenylphosphaneyl)phenyl)((triiso-propylsilyl)oxy)-methyl)-1H-1,2,3-triazole (L9). Reaction carried out using triisopropylsilyl trifluoromethanesulfonate (0.08 mL, 0.3 mmol). Pale-yellow oil (198 mg, 91% yield). ^{31}P NMR (162 MHz, $CDCl_3$) δ: -19.7. ^{1}H NMR (400 MHz, $CDCl_3$) δ: 0.91–0.94 (m, 18H, C*H*$_3$, *i*-Pr), 1.07 (m, 3H, C*H*, *i*-Pr), 5.13 (s, 2H, C*H*$_2$Ph), 6.72 (s, 1H, C*H*=N, trz), 6.92–7.02 (m, 6H, C*H*O, C*H*=, Ar), 7.13–7.19 (m, 6H, C*H*=, Ar), 7.28–7.30 (m, 6H, C*H*=, Ar), 7.40 (t, 1H, $^3J_{H\text{-}H}$= 7.3 Hz, C*H*=, Ar), 7.99-8.03 (m, 1H, C*H*=, Ar). ^{13}C NMR (100 MHz, $CDCl_3$) δ: 12.2 (*C*H, *i*-Pr), 17.9 (*C*H$_3$, *i*-Pr), 53.5 (*C*H$_2$Ph), 66.5 (d, $^3J_{C\text{-}P}$= 30.2 Hz, *C*H-O), 121.7 (*C*H=N, trz), 126.7–134.8 (aromatic carbons), 135.9 (d, $^1J_{C\text{-}P}$= 11.0 Hz, *C*=, Ar), 137.1 (d, $^1J_{C\text{-}P}$= 11.0 Hz *C*=, Ar), 148.7 ($^1J_{C\text{-}P}$= 22.0 Hz, *C*=, Ar), 151.3 (*C*=, Ar). MS HR-ESI [found 605.2983 $C_{37}H_{44}N_3OPSi$ $(M)^+$ requires 605.2986].

(*R*)-1-benzyl-4-(((tert-butyldimethylsilyl)oxy)(2-(diphenyl-phosphaneyl)-phenyl)methyl)-1H-1,2,3-triazole (L10). Reaction carried out using *t*-butyldimethylsilyl trifluoromethanesulfonate (0.07 mL, 0.3 mmol). Pale-yellow oil (118 mg, 78% yield). ^{31}P NMR (162 MHz, $CDCl_3$) δ: -19.3. ^{1}H NMR (400 MHz, $CDCl_3$) δ: -0.03 (s, 3H, C*H*$_3$, OTBS), -0.00 (s, 3H, C*H*$_3$, OTBS), 0.85 (s, 9H, *t*-Bu, OTBS), 5.13 (d, 1H, $^2J_{H\text{-}H}$= 14.8 Hz, C*H*$_2$Ph), 5.22 (d, 1H, $^2J_{H\text{-}H}$= 14.8 Hz, C*H*$_2$Ph), 6.70 (s, 1H, C*H*=N, trz), 6.88 (d, 1H, $^3J_{P\text{-}H}$= 7.41, C*H*OH), 6.92–6.96 (m, 1H, C*H*=, Ar), 7.04–7.10 (m, 4H, C*H*=, Ar), 7.15–7.24 (m, 6H, C*H*=, Ar), 7.30–7.32 (m, 6H, C*H*=, Ar), 7.41 (t, 1H, $^3J_{H\text{-}H}$= 7.6 Hz, C*H*=, Ar), 7.90–7.93 (m, 1H, C*H*=, Ar). ^{13}C NMR (100 MHz, $CDCl_3$) δ: 17.2 (*C*H$_3$, OTBS), 24.8 (*t*-Bu, OTBS), 52.3 (*C*H$_2$Ph), 65.9 (d, $^3J_{C\text{-}P}$= 29.2 Hz, *C*H-O), 120.8 (*C*H=N, trz), 125.7–133.7 (aromatic carbons), 134.8 (d, $^1J_{C\text{-}P}$= 11.0 Hz, *C*=, Ar), 136.1 (d, $^1J_{C\text{-}P}$= 11.0 Hz *C*=, Ar), 147.0 ($^1J_{C\text{-}P}$= 22.0 Hz, *C*=, Ar), 150.3 (*C*=, Ar). MS HR-ESI [found 563.2513 $C_{34}H_{38}N_3OPSi$ $(M)^+$ requires 563.2517].

3.3.4.4. General procedure for the preparation of [Ir(cod)(L9-10)]BAr$_F$ catalyst precursors

The corresponding ligand (0.037 mmol) was dissolved in CH_2Cl_2 (2 mL) and [Ir(μ-Cl)(cod)]$_2$ (13.5 mg, 0.02 mmol) was added. The reaction mixture was stirred at 45 °C for 1 h. After 5 min at room temperature, $NaBAr_F$ (35 mg, 0.04 mmol) and degassed

water (2 mL) were added and the reaction mixture was stirred vigorously for 30 min at room temperature. The phases were separated and the aqueous phase was extracted twice with CH_2Cl_2. The combined organic phases were dried with $MgSO_4$, evaporated in vacuo and purified by flash column chromatography (neutral SiO_2 *ca* 10 cm × 2 cm, 100% CH_2Cl_2).

[Ir(cod)(L9)]BAr$_F$. Reaction carried out using **L9** (22.4 mg, 0.037 mmol). Red-orange solid (60 mg, 89% yield). ^{31}P NMR (162 MHz, $CDCl_3$) δ: -5.9. ^{1}H NMR (400 MHz, $CDCl_3$) δ: 0.93–0.95 (m, 18H, C*H*$_3$, *i*-Pr), 1.06–1.11 (m, 3H, C*H*, *i*-Pr), 1.81 (m, 1H, C*H*$_2$, cod), 1.95–1.96 (m, 1H, C*H*$_2$, cod), 2.09–2.24 (m, 4H, C*H*$_2$, cod), 2.37–2.44 (m, 2H, C*H*$_2$, cod), 3.21 (m, 1H, C*H*, cod), 3.75 (m, 1H, C*H*, cod), 4.46 (m, 1H, C*H*, cod), 5.24 (d, 1H, $^2J_{H\text{-}H}$= 13.4 Hz, C*H*$_2$Ph), 5.34 (d, 1H, $^2J_{H\text{-}H}$= 13.4 Hz, C*H*$_2$Ph), 5.68 (m, 1H, C*H*, cod), 6.92 (d, 1H, $^3J_{H\text{-}H}$= 7.7 Hz, C*H*=N, trz), 7.03 (t, 1H, $^3J_{H\text{-}H}$= 8.5 Hz, C*H*=, Ar), 7.25–7.52 (m, 22H, C*H*O, C*H*=, Ar), 7.71 (s, 8H, C*H*=, Ar), 7.94–7.97 (m, 1H, C*H*=, Ar). ^{13}C NMR (100 MHz, $CDCl_3$) δ: 11.8 (*C*H, *i*-Pr), 17.7 (*C*H$_3$, *i*-Pr), 29.5 (*C*H$_2$, cod), 30.6 (*C*H$_2$, cod), 31.4 (*C*H$_2$, cod), 33.5 (*C*H$_2$, cod), 56.0 (*C*H$_2$Ph), 67.6 (*C*H, cod), 68.1 (*C*H, cod), 68.8 (d, $^3J_{C\text{-}P}$= 15.1 Hz, *C*HO), 91.2 (d, $^3J_{C\text{-}P}$=12.3, *C*H, cod), 95.0 (d, $^3J_{C\text{-}P}$=12.3, *C*H, cod), 117.4–135.9 (aromatic carbons), 127.8 (*C*H=N, trz), 145.7 (d, $^1J_{C\text{-}P}$= 13.0 Hz, *C*=, Ar), 154.5 (*C*=, Ar), 161.7 (q, $^1J_{C\text{-}B}$= 50.0 Hz, *C*=, Ar). MS HR-ESI [found 906.2375 $C_{45}H_{56}IrN_3OPSi$ $(M)^+$ requires 906.2382].

Ir(cod)(L10)]BAr$_F$. Reaction carried out using **L10** (20.8 mg, 0.037 mmol). Red-orange solid (57.5 mg, 90% yield). ^{31}P NMR (162 MHz, $CDCl_3$) δ: 6.5. ^{1}H NMR (400 MHz, $CDCl_3$) δ: -0.01 (s, 3H, C*H*$_3$, OTBS), 0.11 (s, 3H, C*H*$_3$, OTBS), 0.90 (s, 9H, *t*-Bu, OTBS), 1.79–1.84 (m, 1H, C*H*$_2$, cod), 1.96–1.99 (m, 1H, C*H*$_2$, cod), 2.16–2.29 (m, 4H, C*H*$_2$, cod), 2.34–2.47 (m, 2H, C*H*$_2$, cod), 3.22–3.26 (m, 1H, C*H*, cod), 3.83–3.87 (m, 1H, C*H*, cod), 4.45–4.49 (m, 1H, C*H*, cod), 5.24 (s, 2H, C*H*$_2$Ph), 5.55–5.67 (m, 1H, C*H*, cod), 6.90 (d, 1H, $^3J_{H\text{-}H}$= 7.7 Hz, C*H*=N, trz), 7.04 (t, 1H, $^3J_{H\text{-}H}$= 9.6 Hz, C*H*=, Ar), 7.23–7.57 (m, 22H, C*H*O, C*H*=, Ar), 7.73 (s, 8H, C*H*=, Ar), 7.92–7.95 (m, 1H, C*H*=, Ar). ^{13}C NMR (100 MHz, $CDCl_3$) δ: -5.23 (*C*H$_3$, OTBS), -5.11 (*C*H$_3$, OTBS), 25.5 (*t*-Bu, OTBS), 29.2 (*C*H$_2$, cod), 29.7 (*C*H$_2$, cod), 31.1 (*C*H$_2$, cod), 34.0 (*C*H$_2$, cod), 55.9 (*C*H$_2$Ph), 67.3 (*C*H, cod), 68.2 (*C*H, cod), 69.1 (d, $^3J_{C\text{-}P}$= 10.5 Hz, *C*HOH), 91.1 (d, $^3J_{C\text{-}P}$=11.0, *C*H, cod), 96.1 (d, $^3J_{C\text{-}P}$=11.0, *C*H, cod), 117.3–136.5 (aromatic carbons), 127.9 (*C*H=N, trz), 145.5 (d, $^1J_{C\text{-}P}$= 14.3 Hz, *C*=, Ar), 154.3 (*C*=, Ar), 161.6 (q, $^1J_{C\text{-}B}$= 50.0 Hz, *C*=, Ar). MS HR-ESI [found 864.3081 $C_{42}H_{50}IrN_3OPSi$ $(M)^+$ requires 864.3085].

3.3.4.5. General procedure for the preparation of exocyclic olefins S125–S129 and S132–134

According to the procedure reported by Zhang et al.,[4a] to a suspension of the substituted benzyltriphenylphosphonium chloride (15.14 mmol) in THF (40 ml), *n*-BuLi (6.06 mL, 2.5 M in hexanes, 15.14 mmol) was added dropwise. After stirring at room

temperature for 2 h, a solution of the corresponding ketone (7.57 mmol) in THF (10 mL) was added. The reaction mixture was stirred at reflux for 18 h. After that, the solution was cooled to room temperature, quenched with water (20 mL) and extracted with EtOAc (3x30 mL). Then, the organic layers were combined, washed with brine (10 mL) and dried with anhydrous $MgSO_4$. The solution was filtered and concentrated *in vacuo*. The crude mixture containing a mixture of *Z*- and *E*-olefins was then purified with column chromatography (SiO_2, 100% petroleum ether or 95:5 petroleum ether-EtOAc) to yield the pure olefin.

(*E*)-1-(3-Methylbenzylidene)-1,2,3,4-tetrahydronaphthalene (S125). Prepared using 3,4-dihydronaphthalen-1(2*H*)-one (458 mg, 3.1 mmol). White solid (147 mg, 20% yield). ^{1}H NMR (400 MHz, $CDCl_3$), δ: 1.84–1.87 (m, 2H), 2.40 (s, 3H), 2.81–2.88 (m, 4H), 7.03–7.15 (m, 3H), 7.19–7.23 (m, 4H), 7.25–7.28 (m, 1H), 7.70–7.73 (m, 1H). ^{13}C NMR (100.6 MHz, $CDCl_3$), δ: 21.6, 23.7, 28.0, 30.3, 123.8, 124.4, 126.2, 126.5, 127.2, 127.3, 128.1, 129.0, 130.2, 136.5, 137.2, 137.7, 137.9, 138.2.

(*E*)-1-Benzylidene-5-bromo-1,2,3,4-tetrahydronaphthalene (S126). Prepared using 5-bromo-3,4-dihydronaphthalen-1(2*H*)-one (812 mg, 3.6 mmol). White solid (162 mg, 15% yield). ^{1}H NMR (400 MHz, $CDCl_3$), δ: 1.85–1.88 (m, 2H), 2.72–2.76 (m, 2H), 2.86–2.89 (m, 2H), 7.03 (s, 1H), 7.08 (td, $^3J_{H\text{-}H}$= 7.9, 0.6 Hz, 1H), 7.21-7.28 (m, 1H), 7.33-7.40 (m, 4H), 7.49 (d, $^3J_{H\text{-}H}$= 7.9 Hz, 1H), 7.64 (d, $^3J_{H\text{-}H}$= 7.9 Hz, 1H). ^{13}C NMR (100.6 MHz, $CDCl_3$), δ: 23.6, 27.1, 30.7, 123.9, 124.8, 125.7, 126.7, 127.1, 2x128.2, 2x129.4, 131.4, 136.8, 137.5, 137.9, 139.3.

(*E*)-1-Benzylidene-5-methoxy-1,2,3,4-tetrahydronaphthalene (S127). Prepared using 5-methoxy-3,4-dihydronaphthalen-1(2*H*)-one (671 mg, 3.8 mmol). Colorless oil, 600 mg (63% yield). ^{1}H NMR (400 MHz, $CDCl_3$), δ: 1.83–1.86 (m, 2H), 2.76–2.78 (m, 4H), 3.86 (s, 3H), 6.78 (d, $^3J_{H\text{-}H}$= 7.8 Hz, 1H), 7.09 (s, 1H), 7.20–7.26 (m, 2H), 7.34-7.39 (m, 5H).^{13}C NMR (100.6 MHz, $CDCl_3$), δ: 23.3, 23.4, 27.3, 55.4, 108.6, 116.8, 123.8, 126.2, 126.4, 126.6, 2x128.1, 2x129.4, 137.6, 137.9, 138.3, 157.2.

(*E*)-1-Benzylidene-6-bromo-1,2,3,4-tetrahydronaphthalene (S128). Prepared using 6-bromo-3,4-dihydronaphthalen-1(2*H*)-one (472 mg, 2 mmol). White solid (21 mg, 4% yield). ^{1}H NMR (400 MHz, $CDCl_3$), δ: 1.80–1.83 (m, 2H), 2.76–2.82 (m, 4H), 7.02 (s, 1H), 7.25-7.37 (m, 7H), 7.56 (d, $^3J_{H\text{-}H}$= 9.7 Hz, 1H).^{13}C NMR (100.6 MHz, $CDCl_3$), δ: 23.3, 27.7, 30.1, 121.1, 124.2, 126.0, 126.6, 3x128.2, 2x129.2, 129.4, 131.6, 135.4, 136.3, 137.8, 139.9.

(*E*)-1-Benzylidene-7-bromo-1,2,3,4-tetrahydronaphthalene (S129). Prepared using 7-bromo-3,4-dihydronaphthalen-1(2*H*)-one (376 mg, 1.7 mmol). White solid (15 mg, 3% yield). ^{1}H NMR (400 MHz, $CDCl_3$), δ: 1.80–1.83 (m, 2H), 2.75–2.79 (m, 4H), 6.98-7.01 (m, 2H), 7.25-7.29 (m, 2H), 7.36-7.38 (m, 4H), 7.82-7.83 (m, 1H).

^{13}C NMR (100.6 MHz, $CDCl_3$), δ: 23.4, 27.6, 29.7, 119.9, 124.9, 126.7, 127.2, 2x128.2, 2x129.4, 130.0, 130.6, 136.1, 136.7, 137.7, 138.5.

(*E*)-1-Benzylidene-7-methoxy-1,2,3,4-tetrahydronaphthalene (S130). Prepared using 7-methoxy-3,4-dihydronaphthalen-1(2*H*)-one (267 mg, 1.5 mmol). Colorless oil (38 mg, 10% yield). ^{1}H NMR (400 MHz, $CDCl_3$), δ: 1.81–1.84 (m, 2H), 2.75–2.80 (m, 4H), 3.85 (s, 3H), 6.78–6.81 (m, 1H), 7.02–7.06 (m, 2H), 7.22–7.26 (m, 3H), 7.35–7.39 (m, 3H). ^{13}C NMR (100.6 MHz, $CDCl_3$), δ: 23.9, 27.9, 29.4, 55.4, 108.9, 113.8, 123.8, 126.4, 2x128.1, 2x129.4, 129.9, 130.4, 137.2, 137.5, 138.1, 157.9.

(*Z*)-1-(4-Methylbenzylidene)-2,3-dihydro-1H-indene (S132). Prepared using 2,3-dihydro-1*H*-inden-1-one (1 g, 7.57 mmol). Colorless oil (100 mg, 6% yield). ^{1}H NMR (400 MHz, $CDCl_3$), δ: 2.47 (s, 3H), 2.98-3.00 (m, 2H), 3.05-3.09 (m, 2H), 6.68 (s, 1H), 7.33 (t, $^3J_{H\text{-}H}$= 7.1 Hz, 1H), 7.20-7.25 (m, 3H), 7.33-7.40 (m, 4H). ^{13}C NMR (100.6 MHz, $CDCl_3$), δ: 21.4, 30.2, 34.2, 121.6, 124.4, 125.3, 125.8, 128.1, 2x128.5, 2x129.1, 135.4, 136.3, 139.8, 142.9, 148.7.

(*Z*)-1-Benzylidene-1,2,3,4-tetrahydronaphthalene (S133). Prepared using 3,4-dihydronaphthalen-1(2*H*)-one (1.1 g, 7.57 mmol). Colorless oil (21 mg, 1% yield). ^{1}H NMR (400 MHz, $CDCl_3$), δ: 2.01-2.06 (m, 2H), 2.53 (t, $^3J_{H\text{-}H}$= 6.2 Hz, 2H), 2.90 (t, $^3J_{H\text{-}H}$= 6.2 Hz, 2H), 6.45 (s, 1H), 6.83 (t, $^3J_{H\text{-}H}$= 7.2 Hz, 1H), 7.08-7.26 (m, 8H). ^{13}C NMR (100.6 MHz, $CDCl_3$), δ: 24.1, 29.5, 34.9, 124.4, 124.5, 126.2, 127.3, 2x128.2, 128.7, 128.9, 2x129.0, 135.1, 138.0, 138.6, 138.8.

(*Z*)-1-(4-chlorobenzylidene)-1,2,3,4-tetrahydronaphthalene (S134). Prepared using 3,4-dihydronaphthalen-1(2*H*)-one (536 mg, 3.6 mmol). Colorless oil (30 mg, 1% yield). ^{1}H NMR (400 MHz, $CDCl_3$), δ: 1.98-2.05 (m, 2H), 2.52 (t, $^3J_{H\text{-}H}$= 6.7 Hz, 2H), 2.89 (t, $^3J_{H\text{-}H}$= 6.7 Hz, 2H), 6.37 (s, 1H), 6.84-6.88 (m, 1H), 7.11-7.19 (m, 7H). ^{13}C NMR (100.6 MHz, $CDCl_3$), δ: 23.9, 29.4, 34.8, 123.1, 124.7, 127.6, 2x128.3, 128.8, 128.9, 2x130.3, 131.8, 134.7, 137.1, 138.9, 139.0.

3.3.4.6. General procedure for the preparation of exocyclic olefin S131

Following a modified procedure by Toste et al.,[16] into a suspension of ethoxymethyl phosphonium chloride[17] (3.3 g, 9.4 mmol) in THF (75 mL) *n*-BuLi (3.8 mL, 2.5M in hexanes, 9.4 mmol) was added dropwise at 0 ºC. After 1h stirring at room temperature a solution of 1-benzosuberone (1 mL, 6.2 mmol) in THF (10 mL) was added dropwise and left overnight at the same temperature. The reaction was then quenched with water (50 mL) and was extracted with Et_2O (3x20 mL). The organic layer was then washed with brine, dried with $MgSO_4$, filtered and concentrated *in vacuo*. The crude was dissolved in hexanes to remove the excess of triphenylphosphine. After filtration the crude product was used without further purification.

To the crude product (6.2 mmol) in THF (10 mL) a solution of 2M HCl (5 mL) was added and refluxed for 5 h. Upon completion, the crude solution was poured into water (20 mL) and extracted with Et_2O (3x10 mL) and washed with a saturated solution of $NaHCO_3$ (3x10 mL). The organic extracts were washed with brine, dried with $MgSO_4$ and concentrated *in vacuo*. The crude product was purified by column chromatography (SiO_2, 95:5 petroleum ether-EtOAc) to yield the corresponding aldehyde.

In a solution of 6,7,8,9-tetrahydro-5*H*-benzo[7]annulene-5-carbaldehyde (100 mg, 0.6 mmol) in THF (2 mL), PhMgBr (0.4 mL, 3.0M in Et_2O, 0.86 mmol) was added dropwise at 0 ºC. After completion, the reaction was quenched with a saturated solution of NH_4Cl (5 mL), extracted with Et_2O (3x10 mL) and the organic layers dried with $MgSO_4$ and concentrated *in vacuo*. The reaction crude was used in the next step without further purification.

The crude product (0.6 mmol) was dissolved in toluene (2 mL) and *p*-toluensulfonic acid monohydride was added (5 mg). After refluxing overnight, the reaction crude was poured into a mixture of water (10 mL) and Et_2O (10 mL), washed with $NaHCO_3$ (5 mL), dried with $MgSO_4$ and concentrated *in vacuo*. The crude product was purified by column chromatography (SiO_2, 100% petroleum ether) to yield the product as a mixture of *E*/*Z* isomers that were isolated by means of semipreparative HPLC (Chiralcel OD-H column).

6,7,8,9-Tetrahydro-5H-benzo[7]annulene-5-carbaldehyde. Yellow oil (500 mg, 46% yield over 2 steps). ^{1}H NMR (400 MHz, $CDCl_3$), δ: 1.46–1.49 (m, 1H), 1.68–1.72 (m, 2H), 1.80–1.86 (m, 2H), 2.03–2.07 (m, 1H), 2.61–2.69 (m, 2H), 3.60 (dd, $^3J_{H\text{-}H}$= 6.7, 2.3 Hz, 1H), 6.97–6.99 (m, 1H), 7.07–7.13 (m, 3H), 9.82 (s, 1H). ^{13}C NMR (100.6 MHz, $CDCl_3$), δ: 26.9, 27.7, 28.0, 35.9, 58.6, 126.5, 127.6, 129.5, 130.1, 138.0, 143.5, 202.8.

(*E*)-5-Benzylidene-6,7,8,9-tetrahydro-5H-benzo[7]annulene (S131). Colorless oil (34 mg, 25% yield over 2 steps). ^{1}H NMR (400 MHz, $CDCl_3$), δ: 1.81–1.83 (m, 2H), 1.88–1.90 (m, 2H), 2.60–2.63 (m, 2H), 2.81–2.84 (m, 2H), 6.54 (s, 1H), 7.14-7.43 (m, 9H). ^{13}C NMR (100.6 MHz, $CDCl_3$), δ: 27.5, 29.3, 30.9, 35.5, 126.3, 126.5, 127.1, 127.8, 128.3, 128.7, 2x128.8, 2x128.9, 138.1, 140.2, 145.6, 145.7.

3.3.4.7. General procedure for the asymmetric hydrogenation

The alkene (0.125 mmol) and the corresponding catalyst precursor [Ir(cod)(**L9**–**L10**)]BAr_F (1 mol %) were dissolved in the corresponding solvent (1 mL) and placed in a high-pressure autoclave. The autoclave was purged 4 times with hydrogen. Then, it was pressurized at the desired pressure. After 4 h, the autoclave was depressurized and the solvent evaporated off. The residue was dissolved in Et_2O (1.5 ml) and filtered through a short plug of silica. Conversions were determined by ^{1}H NMR and the enantiomeric excesses were determined by GC or HPLC .

3.3.4.8. Computational details

The calculations were carried out using B3LYP[18]-D3[19] functional as implemented in Gaussian 09.[20] For the geometry optimizations, the LANL2DZ[21] pseudopotential was used for iridium, and the 6-31G*[22] basis set was used for all other atoms. Implicit solvation using PCM[23] model with the parameters for dichloromethane was included in the geometry optimization. To obtain better accuracy, single-point calculations were carried out on the basis of the optimized geometries with the same basis set for iridium and the 6-311+G**[24] basis set for the other atoms. The reported energies are Gibbs free energies in solution. NCI-plot method was used to study the non-covalent interactions. The method is capable of mapping real-space regions where non-covalent interactions are important and is based exclusively on the electron density and its gradient. The information provided by NCI plots is essentially qualitative. Promolecular approximation using xyz files was used to perform these calculations.

3.3.5. References

[1] (a) *Comprehensive Asymmetric Catalysis*, (Eds. Jacobsen, E. N.; Pfaltz, A.; Yamamoto, H.), Springer–Verlag, Berlin, **1999**. (b) *Catalytic Asymmetric Synthesis*, *3rd ed.,* (Ed.: Ojima, I.), John Wiley & Sons, Inc., Hoboken, **2010**. (c) *Asymmetric Catalysis on Industrial Scale: Challenges, Approaches and Solutions*, *2nd ed.*, (Eds.: Blaser, H.–U.; Federsel, H.–J.), Wiley–VCH, Weinheim, **2010**. (d) Busacca, C. A.; Fandrick, D. R.; Song, J. J.; Senanayake, C. H. The Growing Impact of Catalysis in the Pharmaceutical Industry. *Adv. Synth. Catal.* **2011**, *353*, 1825–1864. (e) Ager, D. J.; de Vries, A. H. M.; de Vries, J. G. Asymmetric homogeneous hydrogenations at scale. *Chem. Soc. Rev*., **2012**, *41*, 3340–3380. (f) *Metal–catalyzed Asymmetric Hydrogenation. Evolution and Prospect* in Advances in Catalysis (Eds.: Diéguez, M.; Pizzano, A.), Elsevier, Oxford, Vol. 68, **2021**.

[2] Stoffels, M. A.; Klauck, F. J. R.; Hamadi, T.; Glorius, F.; Leker, J. Technology Trends of Catalysts in Hydrogenation Reactions: A Patent Landscape Analysis. *Adv. Synth. Catal.* **2020**, *362*, 1258–1274.

[3] See for instance: (a) Shao, S.–Y.; Wang, C.; Han, S.–W.; Suna, M.–H.; Li, S. Phenanthrenequinone enantiomers with cytotoxic activities from the tubers of *Pleione bulbocodioides***.** *Org. Biomol. Chem*. **2019**, *17*, 567–572. (b) Amberg, W.; Lange, U. E. W.; Ochse, M.; Pohlki, F.; Behl, B.; Relo, A. L.; Hornberger, W.; Hoft, C.; Mezler, M.; Sydor, J.; Wang, Y.; Zhao, H.; Brewer, J. T.; Dietrich, J.; Li, H.; Akritopoulou–Zanze, I.; Lao, Y.; Hannick, S. M.; Ku, Y.–Y.; Vasudevan, A. Discovery of Novel Aminotetralines and Aminochromanes as Selective and Competitive Glycine Transporter 1 (GlyT1) Inhibitors. *J. Med. Chem*. **2018**, *61*, 7503–7524. (c) Donde, Y.; Nguyen, J. H. WO2015048553A1, **2015**. (d) Pohlki, F.; Lange, U.; Ochse, M.; Behi, B.; Hutchins, C. W. US2012040948A1, **2012**. (e) Sock, H. T.; Teerhuis, N. M.; Veeneman, G. H. US20100240748A1, **2010**. (f) Lansbury, P. T.; Justman, C. J. WO2009036275A1, **2009**. (g) Yoshikawa, K.; Suzuki, K.; Umeyama, A.; Arihara, S. Abietane Diterpenoids from the Barks of *Cryptomeria japonica*. *Chem. Pharm. Bull*. **2006**, *54*, 574–578. (h) Numazawa, M.; Ando, M.; Watari, Y.; Tominaga, T.; Hayata, Y.; Yoshimura, A. Structure–activity relationships of 2–, 4–, or 6–substituted estrogens as aromatase inhibitors. *J. Steroid Biochem. Mol. Biol.* **2005**, *96*, 51–58. (i) Kolanos, R.; Siripurapu, U.; Pullagurla, M.; Riaz, M.; Setola, V.; Roth, B. L.; Dukata, M.; Glennona, R. A. Binding of isotryptamines and indenes at h5–HT_6 serotonin receptors. *Bioorg. Med. Chem. Lett*. **2005**, *15*, 1987–1991.

[4] (a) Xia, J.; Yang, G.; Zhuge, R.; Liu, Y.; Zhang, W. Iridium–Catalyzed Asymmetric Hydrogenation of Unfunctionalized Exocyclic C=C Bonds. *Chem. Eur. J.* **2016**, *22*, 18354–18357. (b) Biosca, M.; Magre, M.; Coll, M.; Pàmies, O.; Diéguez, M. Alternatives to Phosphinooxazoline (*t*–BuPHOX) Ligands in the Metal–Catalyzed Hydrogenation of Minimally Functionalized Olefins and Cyclic β–Enamides. *Adv. Synth. Catal.* **2017**, *359*, 2801–2814. (c) Biosca, M.; Magre, M.; Pàmies, O.; Diéguez, M. Asymmetric Hydrogenation of Disubstituted, Trisubstituted, and Tetrasubstituted Minimally Functionalized Olefins and Cyclic β–Enamides with Easily Accessible Ir–P,Oxazoline Catalysts. *ACS Catal*. **2018**, *8*, 10316–10320. (d) Biosca, M.; de la Cruz–Sánchez, P.; Faiges, J.; Margalef, J.; Salomó, E.; Riera, A.; Verdaguer, X.; Ferré, J.; Maseras, F.; Besora, M.; Pàmies, O.; Diéguez, M. P–Stereogenic Ir–MaxPHOX: A Step toward Privileged Catalysts for Asymmetric Hydrogenation of Nonchelating Olefins. *ACS Catal.* **2023**, *13*, 5, 3020–3035.

[5] See for instance: (a) Tian, F.; Yao, D.; Liu, Y.; Xie, F.; Zhang, W. Iridium–Catalyzed Highly Enantioselective Hydrogenation of Exocyclic α,β–Unsaturated Carbonyl Compounds. *Adv. Synth. Catal*. **2010**, *352*, 1841–1845. (b) Liu, X.; Han, Z.; Wang, Z.; Ding, K. SpinPhox/Iridium(I)–Catalyzed Asymmetric Hydrogenation of Cyclic α–Alkylidene Carbonyl Compounds. *Angew. Chem. Int. Ed*. **2014**, *53*, 1978–1982; *Angew. Chem*. **2014**, *126*, 2009–2013. (c) Biosca, M.; Pàmies, O.; Diéguez, M. Giving a Second Chance to Ir/Sulfoximine–Based Catalysts for the Asymmetric Hydrogenation of Olefins Containing Poorly Coordinative Groups. *J. Org. Chem*. **2019**, *84*, 8259–8266. (d) Margalef, J.; Biosca, M.; Cruz–Sánchez, P.; Caldentey, X.; Rodríguez–Escrich, C.; Pàmies, O.; Pericàs, M. A.; Diéguez, M. Indene Derived Phosphorus–Thioether Ligands for the Ir–Catalyzed Asymmetric Hydrogenation of Olefins with Diverse Substitution Patterns and Different Functional Groups. *Adv. Synth. Catal.* **2021**, *363*, 4561–4574. (e) Pàmies, O.; Zheng, J.; Faiges, J.; Andersson, P. G. Asymmetric hydrogenation of unfunctionalized olefins or with poorly coordinative groups. *Adv. Catal.* **2021**, *68*, 135–203.

[6] Biosca, M.; de la Cruz–Sánchez, P.; Tarr, D.; Llanes, P.; Karlsson, E. A.; Margalef, J.; Pàmies, O.; Pericàs, M. A.; Diéguez, M. Filling the gaps in the challenging asymmetric hydrogenation of exocyclic benzofused–based alkenes with Ir–P,N catalysts. *Adv. Synth. Catal.* **2022**, *365*, 167–177

[7] Drury III, W. J.; Zimmermann, N.; Keenan, M.; Hayashi, M.; Kaiser, S.; Goddard, R.; Pfaltz, A. Synthesis of Versatile Chiral N,P Ligands Derived from Pyridine and Quinoline. *Angew. Chem. Int. Ed*. **2004**, *43*, 70–74. Angew. Chem. **2004**, *116*, 72–76.

[8] In addition, the introduction of a triazole instead of the commonly used oxazoline group made the synthetic route more straightforward. Thus, for instance, the modification of the procedure in similar phosphine–oxazoline with a methylene linker developed by Hou, Wu and coworkers would require 2–3 more additional steps making the synthesis less appealing. Wu, W.–Q.; Peng, Q.; Dong, D.–X.; Hou, X.–L.; Wu, Y.–D. A Dramatic Switch of Enantioselectivity in Asymmetric Heck Reaction by Benzylic Substituents of Ligands. *J. Am. Chem*. *Soc*. **2008**, *130*, 9717–9725.

[9] Hempel, C.; Maichle–Mössmer, C.; Pericàs, M. A.; Nachtsheim, B. J. Modular Synthesis of Triazole–Based Chiral Iodoarenes for Enantioselective Spirocyclizations. *Adv. Synth. Catal.* **2017**, *359*, 2931–2941.

[10] Verendel, J. J.; Pàmies, O.; Diéguez, M.; Andersson, P. G. Asymmetric Hydrogenation of Olefins Using Chiral Crabtree–type Catalysts: Scope and Limitations. *Chem. Rev.* **2014**, *114*, 2130–2169.

[11] Mazuela, J.; Norrby, P.–O.; Andersson, P. G.; Pàmies, O.; Diéguez, M. Pyranoside Phosphite–Oxazoline Ligands for the Highly Versatile and Enantioselective Ir–Catalyzed Hydrogenation of Minimally Functionalized Olefins. A Combined Theoretical and Experimental Study**.** *J. Am. Chem. Soc*. **2011**, *133*, 13634–13645.

[12] (a) Brandt, P.; Hedberg, C.; Andersson, P. G. New Mechanistic Insights into the Iridium–Phosphanooxazoline–Catalyzed Hydrogenation of Unfunctionalized Olefins: A DFT and Kinetic Study. *Chem. Eur. J.* **2003**, *9*, 339−347. (b) Fan, Y.; Cui, X.; Burgess, K.; Hall, M. B. Electronic Effects Steer the Mechanism of Asymmetric Hydrogenations of Unfunctionalized Aryl–Substituted Alkenes. *J. Am. Chem. Soc.* **2004**, *126*, 16688−16689. (c) Cui, X.; Fan, Y.; Hall, M. B.; Burgess, K. Mechanistic Insights into Iridium–Catalyzed Asymmetric Hydrogenation of Dienes. *Chem. – Eur. J.* **2005**, *11*, 6859−6868. (d) Church, T. L.; Rasmussen, T.; Andersson, P. G. Enantioselectivity in the Iridium–Catalyzed Hydrogenation of Unfunctionalized Olefins. *Organometallics* **2010**, *29*, 6769−6781. (e) Hopmann, K. H.; Bayer, A. On the Mechanism of Iridium–Catalyzed Asymmetric Hydrogenation of Imines and Alkenes: A Theoretical Study. *Organometallics* **2011**, *30*, 2483−2497. (f) Gruber, S.; Pfaltz, A. Asymmetric Hydrogenation with Iridium C,N and N,P Ligand Complexes: Characterization of Dihydride Intermediates with a Coordinated Alkene. *Angew. Chem. Int. Ed.* **2014**, *53*, 1896−1900. *Angew. Chem*. **2014**, *126*, 1927−1931.

[13] Aguado–Ullate, S.; Urbano–Cuadrado, M.; Villalba, I.; Pires, E.; García, J. I.; Bo, C.; Carbó, J. J. Predicting the Enantioselectivity of the Copper–Catalysed Cyclopropanation of Alkenes by Using Quantitative Quadrant–Diagram Representations of the Catalysts. *Chem. Eur. J.* **2012**, *18*, 14026–14036.

[14] For the **TS_E** the two CH−−−N interactions are located between the N of the triazole and the phenyl substituent of the substrate and the same N with one of the methylenic hydrogens of the tetrahydronaphthalene moiety. The T–shaped π–π interaction is found between the substrate phenyl ring and the benzyl substituent of the triazole.

[15] Decribed in the Experimental Section and Supporting Information of section 3.2.

[16] Horino, Y.; Yakamoto, T.; Ueda, K.; Kuroda, S.; Toste, F. D. Au(I)–Catalyzed Cycloisomerizations Terminated by sp^3 C–H Bond Insertion. *J. Am. Chem. Soc*. **2009**, *131*, 2809–2811.

[17] Cheema, Z. M.; Gondal, H. Y.; Siddiqui, H.; Choudhary, M. I. Solvent free synthesis of 1–alkoxyphosphonium chlorides for stereoselective multipurpose vinyl ethers. *Phosphorus Sulfur Silicon Relat. Elem.* **2019**, *195*, 37–42.

[18] (a) Becke, A. D. Density–functional thermochemistry. III. The role of exact Exchange. *J. Chem. Phys.* **1993**, *98*, 5648−5652. (b) Stephens, P. J.; Devlin, F. J.; Chabalowski, C. F.; Frisch, M. J. Ab Initio Calculation of Vibrational Absorption and Circular Dichroism Spectra Using Density Functional Force Fields. *J. Phys. Chem.* **1994**, *98*, 11623−11627.

[19] Grimme, S.; Antony, J.; Ehrlich, S.; Krieg, H. A consistent and accurate ab initio parametrization of density functional dispersion correction (DFT–D) for the 94 elements H–Pu. *J. Chem. Phys.* **2010**, *132*, 154104.

[20] Frisch, M. J.; Trucks, G. W.; Schlegel, H. B.; Scuseria, G. E.; Robb, M. A.; Cheeseman, J. R.; Scalmani, G.; Barone, V.; Petersson, G. A.; Nakatsuji, H.; Li, X.; Caricato, M.; Marenich, A. V.; Bloino, J.; Janesko, B.G.; Gomperts, R.; Mennucci, B.; Hratchian, H.P.; Ortiz, J. V.; Izmaylov, A. F.; Sonnenberg, J. L.; Williams–Young, D.; Ding, F.; Lipparini, F.; Egidi, F.; Goings, J.; Peng, B.; Petrone, A.; Henderson, T.; Ranasinghe, D.; Zakrzewski, V. G.; Gao, J.; Rega, N.; Zheng, G.; Liang, W.; Hada, M.; Ehara, M.; Toyota, K.; Fukuda, R.; Hasegawa, J.; Ishida, M.; Nakajima, T.; Honda, Y.; Kitao, O.; Nakai, H.; Vreven, T.; Throssell, K.; Montgomery, J. A.; Peralta, J. E.; Ogliaro, F.; Bearpark, M. J.; Heyd, J. J.; Brothers, E. N.; Kudin, K. N.; Staroverov, V. N.; Keith, T. A.; Kobayashi, R.; Normand, J.; Raghavachari, K.; Rendell, A. P.; Burant, J. C.; Iyengar, S. S.; Tomasi, J.; Cossi, M.; Millam, J. M.; Klene, M.; Adamo, C.; Cammi, R.; Ochterski, J. W.; Martin, R. L.; Morokuma, K.; Farkas, O.; Foresman, J. B.; Fox, D. J. Gaussian 09, Revision A.03; Gaussian, Inc.: Wallingford CT, 2016.

[21] (a) Hay, P. J.; Wadt, W. R. Ab initio effective core potentials for molecular calculations. Potentials for the transition metal atoms Sc to Hg. *J. Chem. Phys.* **1985**, *82*, 270−283. (b) Hay, P. J.; Wadt, W. R. Ab initio effective core potentials for molecular calculations. Potentials for K to Au including the outermost core orbitals. *J. Chem. Phys.* **1985**, *82*, 299−310.

[22] (a) Hehre, W. J.; Ditchfield, R.; Pople, J. A. Self–Consistent Molecular Orbital Methods. XII. Further Extensions of Gaussian–Type Basis Sets for Use in Molecular Orbital Studies of Organic Molecules. *J. Chem. Phys*. **1972**, *56*, 2257−2261. (b) Hariharan, P. C.; Pople, J. A. The Influence of Polarization Functions on Molecular Orbital Hydrogenation Energies. *Theor. Chim. Acta* **1973**, *28*, 213−222. (c) Francl, M. M.; Pietro, W. J.; Hehre, W. J.; Binkley, J. S.; Gordon, M. S.; Defrees, D. J.; Pople, J. A. Self–Consistent Molecular Orbital Methods. XXIII. A Polarization–Type Basis Set for Second–Row Elements. *J. Chem. Phys*. **1982**, *77*, 3654−3665.

[23] Tomasi, J.; Mennucci, B.; Cammi, R. Quantum Mechanical Continuum Solvation Models. *Chem. Rev.* **2005**, *105*, 2999−3094.

[24] (a) Krishnan, R.; Binkley, J. S.; Seeger, R. Pople, J. A. Self–consistent molecular orbital methods. XX. A basis set for correlated wave functions. *J. Chem. Phys.* **1980**, *72*, 650−654. (b) McLean, A. D.; Chandler, G. S. Contracted Gaussian basis sets for molecular calculations. I. Second row atoms, *Z*=11–18. *J. Chem. Phys.* **1980**, *72*, 5639−5648.

3.4. Indene-based phosphorus-thioether ligands for the Ir-catalyzed asymmetric hydrogenation of olefins with diverse functional groups and substitution patterns

3.4.1. Introduction

As previously commented in Section 3.2 the bottleneck in finding the best Ir-catalyst is the identification of the right ligand.[1] The ligand libraries in our group were designed not only to maximize performance but also to develop ligands with industrial applicability in mind, which require few synthetic steps, are prepared from inexpensive starting materials, are air-stable, and easy to manipulate. In this respect, our group reported the first successful use of non-N-donor P-thioether heterodonor ligands for the Ir-catalyzed asymmetric hydrogenation of non-chelating olefins. These P-thioether ligands provide enantioselectivities comparable to the best ones reported with Ir-P,N catalysts.[2] The thioether moiety imparts higher stability with respect to commonly used oxazolines, and involves the introduction of an additional chiral center close to the metal with a different steric environment around the metal center than that exerted by the oxazoline group.[2f,3]

To continue the improvement of Ir-catalysts with air-stable and readily available ligands, in this section we disclose the study of a simple but modular P,S-ligand family (Figure 3.4.1, ligands **L11**–**L18a**–**f**) for the asymmetric hydrogenation of olefins.[4] These ligands are easily synthesized in only three steps from unexpensive indene (c.a. 20 USD/kg).[5] The substrates studied cover different substitution patterns with different functional groups, ranging from non-chelating olefins, through olefins with poorly coordinative groups to olefins with a coordinative functional group that can also anchor the substrate to the metal.

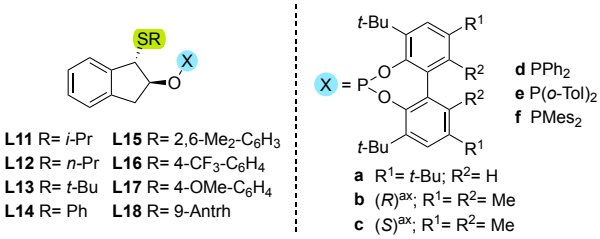

Figure 3.4.1. Readily available phosphite/phosphinite-thioether ligands **L11**–**L18a**–**f**.

3.4.2. Results and discussion

3.4.2.1. Synthesis of the Ir-catalyst precursors

The catalyst precursors were prepared in a two-step, one pot procedure. First, 0.5 equivalent of [Ir(μ-Cl)(cod)]$_2$ reacts with one equivalent of the appropriate P,S-ligand

(**L11**–**L18a**–**f**). Then, Cl^-/BAr_F^- counterion exchange was performed by reaction with sodium tetrakis[3,5-bis(trifluoromethyl)phenyl]borate ($NaBAr_F$; 1 equiv) in the presence of water (Scheme 3.4.1). The Ir-catalyst precursors were isolated in pure form as air-stable red-orange solids in high yields (typically above 90%) after a simple extraction workup. Advantageously, no further purification was required.

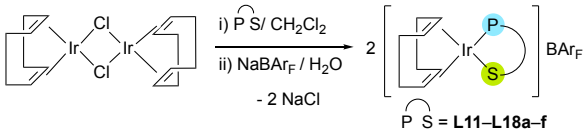

Scheme 3.4.1. Synthesis of [Ir(cod)(P-S)]BAr_F (P-S= **L11**–**L18a**–**f**): (i) [Ir(μ-Cl)(cod)]$_2$, CH_2Cl_2, reflux, 1 h; (ii) $NaBAr_F$, H_2O, rt, 30 min.

The HRMS-ESI spectra of these materials were in agreement with the assigned structures showing the heaviest ions at m/z values corresponding to the loss of the BAr_F anion from the molecular species. The complexes were also characterized by ^{31}P, ^1H and ^{13}C NMR spectroscopy. The spectral assignments were made using ^1H–^1H and ^{13}C–^1H correlation measurements, which were in agreement with what expected for these C_1-symmetric iridium complexes. Variable-temperature (VT) NMR spectra in CD_2Cl_2 (+35 to –85 °C) indicated that only one isomer was present, except for ligands **L13** that showed two isomers in solution, and for ligands **L11d**–**e**, **L15d** and **L16b** that depicted broad NMR signals, which may be indicative of rapid exchange between the two possible diastereomers formed upon coordination of the thioether moiety to the metal atom (note that the coordinated S atom is a stereogenic center), to the interconversion of the different conformers of the six-membered chelate ring or to both phenomena taking simultaneously place. To provide some light on the origin of these isomers, DFT calculations for [Ir(cod)**L13e**]BAr_F were performed (Figure 3.4.3). The population of isomers obtained by DFT calculation agree to that found by NMR spectroscopy. These DFT calculation also indicates that both isomers arise from the different coordination of the thioether group and different conformers of the chelate-ring. Thus, the major diastereoisomer shows an *R*-configuration of the S atom with a chair conformation of the chelate ring (Figure 3.4.2). On the other hand, the minor isomer adopts an *S*-configuration of the S atom with a boat conformation of the chelate ring (Figure 3.4.2). Unfortunately due to signal overlap in the ^1H-NMR spectrum, these studies could not be validated by NOE experiments.

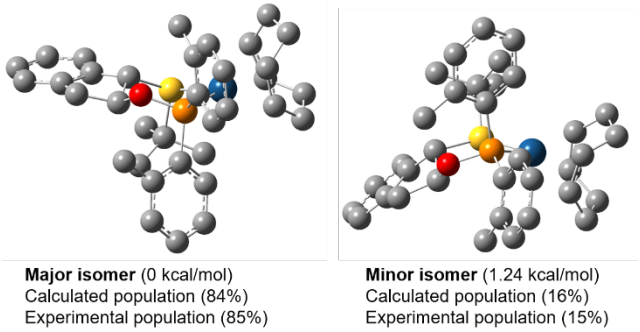

Figure 3.4.2. DFT-calculated structures for [Ir(cod)**L13e**]BAr_F complex. Hydrogen atoms have been omitted for simplicity.

3.4.2.2. Catalytic experiments

3.4.2.2.1. Substrate scope. *1,1-Di- and trisubstituted non-chelating olefins*

In a first set of experiments we evaluated the efficientcy of phosphite/phosphinite-thioether ligands **L11**–**L18a**–**f** in the asymmetric hydrogenation of 1,1'-di- and trisubstituted olefins lacking any extra functional group. Initially, we screened the ligand library in the reduction of the benchmark (*E*)-1-(but-2-en-2-yl)-4-methoxybenzene (**S15**) for trisubstituted olefins and (3,3-dimethylbut-1-en-2-yl)benzene (**S14**) for 1,1-disubstituted ones. To compare our results with the state of the art, we used the same optimal reaction conditions found in previous studies with other Ir-P,S catalytic systems.[2a] The results, which are shown in Table 3.4.2, indicated that enantioselectivity for both substrates is highly dependent on the thioether substituent and the nature of the P-donor group. In general, results indicated that the presence of a bulky aryl thioether moiety (e.g. 2,6-dimethylphenyl and 9-anthryl groups, ligands **L15** and **L18**, respectively) is needed to maximize enantioselectivity. Similarly, the use of ligands containing a chiral biaryl phosphite group (**b** or **c**) or a *o*-tolyl phosphinite moiety (**e**) had a positive effect on enantioselectivity. Nevertheless, each substrate requires a different combination of ligand parameters. Thus, while for the (*E*)-trisubstituted substrate **S15** the best enantioselectivities were achieved with with Ir/**L18e** containing a 9-anthryl thioether group and a *o*-tolyl phosphinite moiety (entry 20, 70% ee), precatalyst Ir/**L15c**, containing a 2,6-dimethylphenyl thioether group and a (*S*)-biaryl phosphite moiety, was the best for disubstituted substrate **S14** (entry 12, 97% ee). This latter result is comparable to the best reported in the literature for this class of substrate.[2a,6,7]

Table 3.4.1. Asymmetric hydrogenation of substrates **S14** and **S15** using [Ir(cod)(**L11**–**L18a**–**f**)]BAr_F catalyst precursors.[a]

		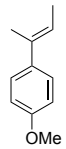 OMe **S15**	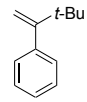 **S14**			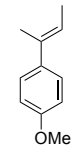 OMe **S15**	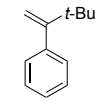 **S14**
Entry	Ligand	% ee[b,c]	% ee[b,c]	Entry	Ligand	% ee[b,c]	% ee[b,c]
1	**L11a**	5 (*R*)	24 (*S*)	11	**L15b**	38 (*S*)	66 (*S*)
2	**L11b**	48 (*R*)	82 (*S*)	12	**L15c**	11 (*S*)	97 (*R*)[d]
3	**L11c**	35 (*S*)	60 (*R*)	13	**L15d**	56 (*S*)	90 (*R*)
4	**L11d**	21 (*S*)	15 (*S*)	14	**L15e**	60 (*S*)	87 (*R*)
5	**L11e**	33 (*S*)	9 (*S*)	15	**L16b**	17 (*S*)	41 (*S*)
6	**L11f**	18 (*S*)	13 (*S*)	16	**L17b**	29 (*S*)	54 (*S*)
7	**L12b**	54 (*R*)	80 (*S*)	17	**L18b**	39 (*S*)	56 (*S*)
8	**L13b**	61 (*S*)	50 (*S*)	18	**L18c**	5 (*R*)	86 (*R*)
9	**L13e**	41 (*S*)	77 (*R*)	19	**L18d**	62 (*S*)	92 (*R*)
10	**L14b**	33 (*S*)	56 (*S*)	20	**L18e**	70 (*S*)	94 (*R*)

[a] Reactions conditions: Substrate (0.5 mmol), Ir-catalyst precursor (2 mol%), H_2 (100 bar for **S15** and 1 bar for **S14**), CH_2Cl_2 (2 mL), rt. Full conversions were achieved in all cases unless otherwise stated. [b] Conversion measured by ^1H NMR spectroscopic analysis after 4 h. [c] Enantiomeric excesses determined by GC analysis. [d] The reaction using 1,2-propylene carbonate (PC) as solvent yielded the hydrogenation product in 96% ee.

We next studied if the high enantioselectivity attained for **S14** could be maintained when using other 1,1'-disubstituted substrates. It is to note that the excellent enantioselectivities were attained for a range of α-*tert*-butylstyrenes **S18**–**S24** (Figure 3.4.3), independently of the electronic and steric properties of the substituents in the aryl moiety of the substrate (ee's up to 98%). Enantioselectivities were maintained when dichloromethane was replaced by the environmentally friendly solvent 1,2-propylene carbonate (Table 3.4.1, entry 12 and Figure 3.4.3).[8]

Like in other cases reported in the literature, the hydrogenation of the α-alkylstyrene derivative **S25** proceeded with a lower enantioselectivity than that of the analogue **S15**.[7] This result is in agreement with a competing isomerization pathway that was corroborated by studying the incorporation of deuterium in **S25** (Scheme 3.4.2).[9] It was found that deuterium was not only inserted in the double bond but also at the allylic position.

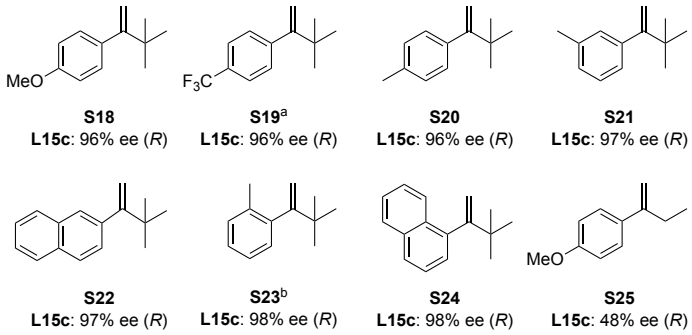

Figure 3.4.3. Substrate scope of the asymmetric hydrogenation of 1,1'-disubstituted olefins **S18**–**S25** with [Ir(cod)(**L11**–**L18a**–**f**)]BAr_F catalyst precursors. Reaction conditions: catalyst precursor (2 mol%), CH_2Cl_2, H_2 (1 bar), rt, 4 h. Full conversions were achieved in all cases. [a] The reaction using 1,2-propylene carbonate as solvent yielded the hydrogenation product in 96% ee. [b] The reaction using 1,2-propylene carbonate as solvent yielded the hydrogenation product in 98% ee.

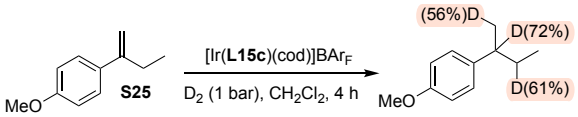

Scheme 3.4.2. Deuterium labeling study of substrate **S25** with [Ir(cod)(**L15c**)]BAr_F catalyst precursor. The percentages of incorporation of deuterium in different positions are shown in brackets.

3.4.2.2.2. Substrate scope. *Trisubstituted olefins with poorly coordinative neighboring groups*

We then moved on to asymmetric hydrogenation of key olefins with with relevant poorly coordinative groups. We first tested the efficiency of phosphite/phosphinite-thioether ligands **L11**–**L18a**–**f** with two ester substrates with different structural diversity: the α,β-unsaturated acyclic ester **S135** ((*E*)-3-phenylbut-2-enoate) and the α,β-unsaturated lactone with an exocyclic double bond **S64** ((*E*)-3-benzylidenetetrahydro-2H-pyran-2-one). The hydrogenation of substrates like **S64,** although less studied,[10] is important because it gives access to cyclic carbonyl compounds with an α-chiral center.[11] The results (Table 3.4.2) indicated that although the configuration of the phosphite moiety affects enantioselectivity (being better with an *S*-configuration for **S135** and the *R*-configuration for **S64**), the best enantioselectivities were achieved with the *o*-tolyl phosphinite moiety (e) for both substrates. In addition, a bulky thioether moiety is needed to maximize enantioselectivity, although each substrate requires a different thioether substituent. Thus, while for the α,β-unsaturated acyclic ester **S135** the highest enantioselectivity was achieved with Ir/**L18e** containing an anthracyl thioether group (entry 19, ee up to

94%), precatalyst Ir/**L13e**, containing a *tert*-butyl thioether group, was the best for cyclic substrate **S64** (entry 8, 94% ee). Again, the results were maintained by using 1,2-propylene carbonate as solvent (entries 21 and 23).

Table 3.4.2. Ir-catalyzed asymmetric hydrogenation of **S135** and **S64** using **L11**–**L18a**–**f**.[a]

		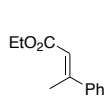 **S135**	 **S64**			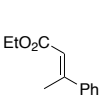 **S135**	 **S64**
Entry	Ligand	% ee[b]	% ee[b]	Entry	Ligand	% ee[b]	% ee[b]
1	**L11a**	20 (*S*)	17 (*S*)	12	**L15d**	77 (S)	40 (*S*)
2	**L11b**	7 (*S*)	28 (*S*)	14	**L16b**	19 (*S*)	22 (*S*)
3	**L11c**	25 (*S*)	2 (*R*)	15	**L17b**	20 (*S*)	21 (*S*)
4	**L11d**	30 (*S*)	32 (*S*)	16	**L18b**	26 (*S*)	19 (*S*)
5	**L11e**	11 (*S*)	38 (*S*)	17	**L18c**	49 (*S*)	6 (*R*)[c]
6	**L12b**	11 (*S*)	21 (*S*)	18	**L18d**	90 (*S*)	48 (*S*)
7	**L13b**	13 (*S*)	25 (*S*)	19	**L18e**	94 (*S*)	62 (S)
8	**L13e**	86 (*S*)	94 (*S*)	20[d]	**L13e**	85 (*S*)	94 (*S*)[e]
9	**L14b**	21 (*S*)	28 (*S*)	21[d]	**L18e**	94 (*S*)	62 (*S*)[f]
10	**L15b**	22 (*S*)	29 (*S*)	22[g]	**L13e**	86 (*S*)	94 (*S*)
11	**L15c**	43 (*S*)	3 (*S*)	23[g]	**L18e**	93 (*S*)	61 (*S*)

[a] Reaction conditions: substrate (0.5 mmol), Ir-catalyst precursor (2 mol%), H_2 (100 bar), CH_2Cl_2 (2 mL), rt for 4 h (substrate **S135**) or 20 h (substrate **S64**). Full conversions were achieved in all cases unless otherwise stated. [b] Enantiomeric excesses determined by HPLC analysis. [c] 27% conversion. [d] Reactions carried out using 0.5 mol% of catalyst precursors. [e] Reaction carried out during 32 h. [f] 98% conversion after 32 h. [g] Reactions carried out using 1,2-propylene carbonate as solvent.

Encouraged by these results, we investigated Ir/**L8e** and Ir/**L3e** in the reduction of a range of acyclic (**S136**–**S141**) and cyclic α,β-unsaturated esters (**S3**–**S13**) with different substitution patterns and geometries (Figure 3.4.4). Advantageously, for acyclic α,β-unsaturated esters **S136**–**S141**, the enantioselectivities were quite independent of the steric nature of the alkyl substituent in the substrate (**S135** and **S138**–**S140**, ee's up to 98%) and the electronic properties of the phenyl ring (**S135** and **S136**–**S137**, ee's up to 95%). The Ir/**L8e** catalytic system also provided high enantioselectivities independently of the geometry of the olefin substrate. Thus, high enantioselectivities were also attained in the reduction of the more challenging *Z*-analogue ((*E*)-**S140** vs (*Z*)-**S140**). Interestingly, the hydrogenation of acyclic ester **S141** containing substituents at both α and β positions also provided 98% of enantioselectivity. The scope was then extended to other cyclic α,β-unsaturated esters

(lactones, **S65**–**S69**). Remarkably, with Ir/**L13e** all α,β-unsaturated lactones with an exocyclic double bond were reduced with comparable high enantioselectivities (ee's up to 98 %) regardless of the substitution pattern on the aryl moiety.

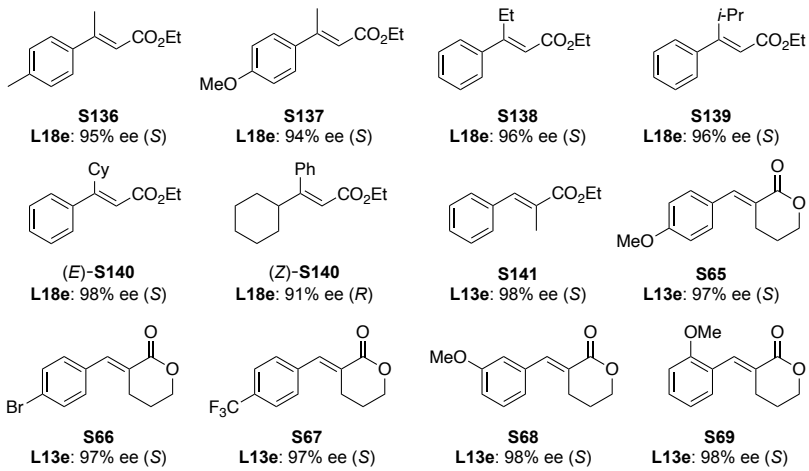

S136
L18e: 95% ee (*S*)

S137
L18e: 94% ee (*S*)

S138
L18e: 96% ee (*S*)

S139
L18e: 96% ee (*S*)

(*E*)-**S140**
L18e: 98% ee (*S*)

(*Z*)-**S140**
L18e: 91% ee (*R*)

S141
L13e: 98% ee (*S*)

S65
L13e: 97% ee (*S*)

S66
L13e: 97% ee (*S*)

S67
L13e: 97% ee (*S*)

S68
L13e: 98% ee (*S*)

S69
L13e: 98% ee (*S*)

Figure 3.4.4. Substrate scope of the asymmetric hydrogenation of trisubstituted acyclic (**S136**–**S141**) and cyclic (**S65**–**S69**) α,β-unsaturated esters with [Ir(cod)(**L11**–**L18a**–**f**)]BAr_F catalyst precursors. Reaction conditions: catalyst precursor (2 mol%), CH_2Cl_2, rt, H_2 (100 bar), 4 h for **S136**–**S141** or 20 h for **S65**–**S69**. Full conversions were achieved in all cases.

We then tested whether high enantioselectivities could also be achieved with olefins containing relevant, poorly coordinative groups other than the alkoxycarbonyl. For that purpose, we selected representative sets of substrates and found that enantioselectivities were also high for a range of α,β-unsaturated ketones (**S44**–**S51** and **S62**), lactams (**S76**–**S79** and **S142**) and the α,β-unsaturated amide **S143**. The results of these asymmetric hydrogenation reactions are shown in Figure 3.4.5. We again found that the ligand components must be selected for each particular substrate type in order to obtain the highest enantioselectivity. Up to 87% enantiomeric excess could be obtained for a range of α,β-unsaturated ketones (**S44**–**S51** and **S62**) independently of the nature of the alkyl substituent and the electronic nature of the phenyl ring, with the Ir/**L13e** catalytic system. In addition, higher enantioselectivities of up to 92% ee were achieved with more challenging β,β-disubstituted enones **S50** and **S51**, even in the reduction of substrate **S50** containing two β,β-substituents with different size.[12] Like lactone **S64**, cyclic α,β-unsaturated ketone **S62** and lactams **S76**–**S79** and **S142** are challenging substrates whose hydrogenation has been usually overlooked[10a,e,j,13] despite these frameworks being part of several natural products and have numerous synthetic utilities.[11f, 14] For the challenging cyclic ketone **S62** enantioselectivity was as high as 88%. Rh/Ru-catalysts have usually failed in affording high enantioselectivities for lactams. A possible reason is the exocyclic nature of the double bond, which cannot rotate towards the carbonyl oxygen, and this hampers the

chelation of such substrates to the metal. Gratifyingly, high asymmetric induction (up to 99% ee) was also achieved in the reduction of several valuable lactams **S76**–**S79** and **S142** but, unlike ketones, using the Ir/**L18e** catalytic system. Other challenging substrates are α,β-unsaturated amides,10[e,h,15] which can give access to important subunits in natural products. Ir/**L18e** catalyst was also able to reduce substrate **S143** yielding the corresponding amide with an α-stereogenic center with 84% ee.

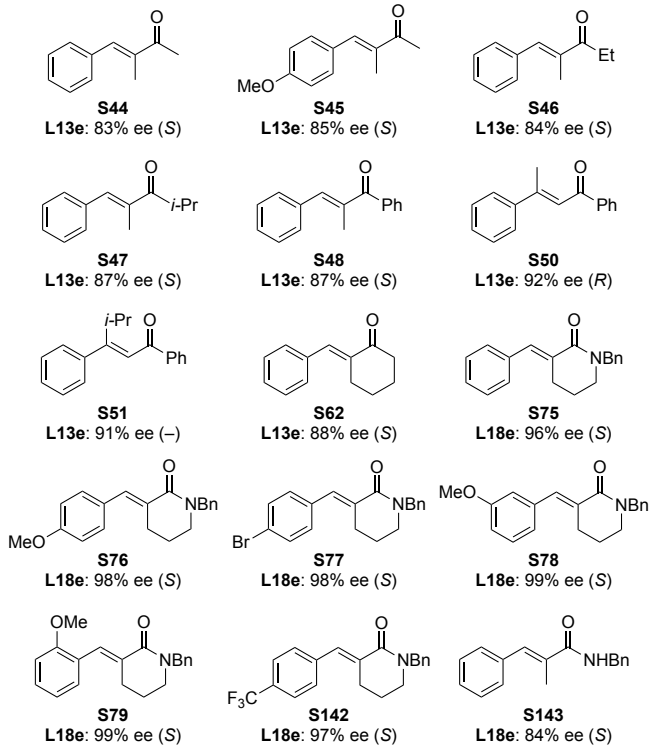

Figure 3.4.5. Substrate scope of the asymmetric hydrogenation of trisubstituted acyclic and cyclic α,β-unsaturated enones **S44**–**S51** and **S62**, lactams **S76**–**S79** and **S142** and amide **S143** with [Ir(cod)(**L11**–**L18a**–**f**)]BAr_F catalyst precursors. Reaction conditions: catalyst precursor (2 mol%), CH_2Cl_2, rt, H_2 (100 bar), 4 h for **S44**–**S51** and **S62** or 20 h for **S76**–**S79** and **S142**–**S143**. Full conversions were attained in all cases.

3.4.2.2.3. Substrate scope. *1,1-Di- and trisubstituted olefins with coordinating neighboring groups*

To further establish the potential of the P,S-ligands **L11**–**L18a**–**f** we studied the asymmetric hydrogenation of substrates bearing coordinating polar groups. We first considered the reduction of challenging tri- and di-substituted enol phosphinates (**S58**–**S59**, **S55** and **S60**–**S61**, Figure 3.4.6). The hydrogenation of both types of substrates opens up an interesting route for obtaining chiral organophosphinates, which can be easily transformed into high-value compounds such as alcohols (an alternative route to

the hydrogenation of ketones) and phosphines.[16] The Ir/**L18e** catalytic system can hydrogenate trisubstituted enol phosphinates (**S58**–**S59** and **S55**) in high enantioselectivities (ee's up to 94%). Remarkably, high enantioselectivities (ee's up to 97%) can also be achieved in the reduction of 1,1'-disubstituted enol phosphinates **S60** and **S61** but, unlike trisubstituted enol phosphinates, using the Ir/**L11f** catalytic system. Among these results it should be noted that the efficient reduction of purely alkyl-substituted enol phosphinates (tri- and disubstituted substrates **S59** and **S60**, respectively) is a plausible alternative to the asymmetric hydrogenation of prochiral alkyl-alkyl ketones to chiral alcohols by Rh/Ru-catalysts, which remains a challenging reaction due to the difficulty in differentiating enantiofaces involving two alkyl groups.[17]

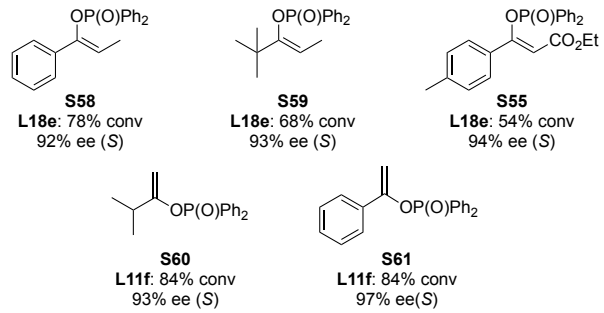

Figure 3.4.6. Asymmetric hydrogenation of tri- and 1,1'-disubstituted enol phosphinates **S58**–**S59**, **S55** and **S60**–**S61** with [Ir(cod)(**L11**–**L18a**–**f**)]BAr_F catalyst precursors. Reaction conditions: catalyst precursor (2 mol%), CH_2Cl_2, H_2 (100 bar for **S58**–**S59** and **S55** and 50 bar for **S60**–**S61**), rt, 4 h.

Finally, we focused on the reduction of cyclic β-enamides, which is another challenging type of chelating olefins. As we saw in Section 3.1, while the enantioselective reduction of α-enamides can be carried out with success,[18] the asymmetric hydrogenation of β-enamides remains a puzzling transformation, albeit the corresponding reduction products are key units in biologically active natural products and drugs such as rotigotine,[19] alnespirone[20] and robalzotan.[21] Most of the currently available catalysts, predominantly based on Rh and Ru, provide unsatisfactory enantioselectivities in reducing cyclic β-enamides.[22] More recently, it has been shown that Ir-P,X (X= N or S) catalysts can reduce cyclic β-enamides with higher enantioselectivities than the Rh/Ru-catalysts.[23] We first studied the reduction of the benchmark *N*-(3,4-dihydronaphthalen-2-yl)acetamide **S8** (Table 3.4.3) under previously reported conditions.[23c] Like for disubstituted olefins **S14** and **S18**–**S24**, the presence of a phosphite group instead of a phosphinite moiety had a positive effect on the enantioselectivity (entries 2 and 11 vs 4 and 13). Regarding the effect of the thioether group, the bulkiness of the moiety and its electronic nature had an important role on the enantioselectivity. The presence of an electron-poor thioether group worsened enantioselectivity (entry 14 (**L16b**) vs 15 (**L17b**)). The bulkiness of the

thioether substituents has a different effect depending on the configuration of the phosphite group. While for ligands with less bulky thioether substituents the presence of (*R*)-biaryl phosphite moieties resulted in a matched combination (**L11b**–**c**, entry 2 vs 3), for ligands containing bulkier thioether substituents, the best enantioselectivity was achieved with (*S*)-biaryl phosphite moieties (**L15** and **L18**, entries 10 and 16 vs 11 and 17). As expected, the highest enantioselectivity of the series (entry 6, 91% ee) is therefore provided with ligand **L12b**, which contains the optimal bulkiness of the thioether substituent in combination with the optimal configuration of the phosphite moiety. Advantageously, high enantioselectivities were still attained by lowering the hydrogen pressure to 10 bar of H_2 (entry 20). We were also pleased to find out that the enantioselectivity using 1,2-propylene carbonate remained as high as those observed with dichloromethane.

Table 3.4.3. Ir-catalyzed asymmetric hydrogenation of **S8** using **L11**–**L18a**–**f**.[a]

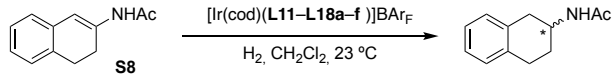

Entry	Ligand	% Conv[b]	% ee[b]	Entry	Ligand	% Conv[b]	% ee[b]
1	**L11a**	20	33 (*S*)	11	**L15c**	100	77 (*R*)
2	**L11b**	35	88 (*S*)	12	**L15d**	41	70 (*R*)
3	**L11c**	18	39 (*R*)	13	**L15e**	62	63 (*R*)
4	**L11d**	70	64 (*S*)	14	**L16b**	34	21 (*S*)
5	**L11e**	100	83 (*S*)	15	**L17b**	57	73 (*S*)
6	**L12b**	85	91 (*S*)	16	**L18b**	100	30 (*S*)
7	**L13b**	70	61 (*S*)	17	**L18c**	100	74 (*R*)
8	**L13e**	80	17 (*R*)	18	**L18d**	100	21 (*R*)
9	**L14b**	50	57 (*S*)	19	**L18e**	100	65 (*R*)
10	**L15b**	100	66 (*S*)	20[c,d]	**L12b**	98	92 (*S*)

[a] Reaction conditions: Substrate (0.5 mmol), Ir-catalyst precursor (1 mol%), H_2 (50 bar), CH_2Cl_2 (2 mL), rt, 18 h. [b] Conversion measured by ^{1}H-NMR and enantiomeric excesses determined by HPLC. [c] Reaction carried out using 10 bar of H_2 for 24 h. [d] Reaction carried out using PC as solvent; 86% conv, 91% ee (*S*).

We subsequently tested the scope of the Ir/**L12b** catalytic system in the reduction of a range of cyclic β-enamides derived from tetralones (substrates **S144**–**S149**, Figure 3.4.7). The high catalytic performance of this catalyst was maintained independently of the different substitution pattern of the 3,4-dihydronaphthalene core (92-94% ee). In addition, it could also effectively hydrogenate enamide **S149**, derived from 3-chromanone, in high enantioselectivity (95% ee). Among all these results, it is to note

the high enantioselectivity achieved in the asymmetric hydrogenation of **S148** and **S149**, whose hydrogenated products are key intermediates for the synthesis of rotigotine and alnespirone. The former is a dopamine agonist used for the treatment of Parkinson's disease,[19] while alnespirone is a selective 5-HT1A receptor with antidepressant and anxiolytic properties[20].

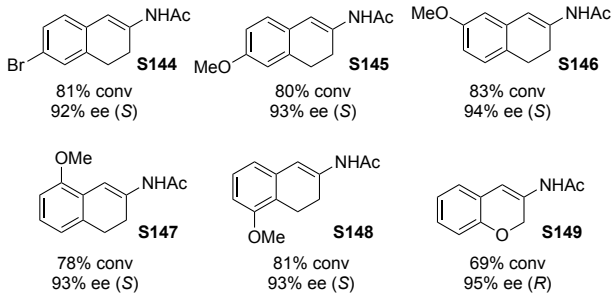

Figure 3.4.7. Asymmetric hydrogenation of chelating olefins **S144**–**S149** with [Ir(cod)(**L12b**)]BAr_F catalyst precursors. Reaction conditions: catalyst precursor (2 mol%), CH_2Cl_2, H_2 (50 bar), rt, 18 h.

3.4.3. Conclusions

The asymmetric hydrogenation of diversely substituted olefins bearing variably coordinating functional groups is in no case a problem that can be addressed with a single catalyst. Bearing this consideration in mind, the design of modular, easy-to-assemble ligands that can adapt to manifold substrates becomes a fundamental task towards the development of efficient and widely applicable asymmetric hydrogenation methodologies. In an effort towards this end, we have shown the utility of an indene-based phosphite/phosphinite-thioether ligand library for the Ir-catalyzed asymmetric hydrogenation of a broad range of substrates (50 olefins in total). The high modularity of these ligands helped us to identify highly enantioselective catalysts for asymmetric hydrogenation of substrates covering different substitution patterns with different functional groups and coordination abilities, ranging from non-chelating olefins, through olefins with poorly coordinative groups, to olefins with coordinative functional groups. Enantioselectivities up to 98% ee were also achieved for other challenging substrates such as non-chelating 1,1'-disubstituted olefin. Also, a range of α,β-unsaturated esters, ketones, even the much less studied lactones and lactams, and α,β-unsaturated amides were hydrogenated with enantioselectivities up to 99%. Vinyl phosphonates and β-cyclic enamides were also reduced successfully obtaining ee's up to 97%. Usefully, environmentally friendly 1,2-propylene carbonate can be used with no loss of enantioselectivity. These results open up the use of air stable, readily available and modular ligands to advance in the asymmetric hydrogenation of a broad type of

substrates with diverse functional groups with different coordination abilities and with different substitution patterns.

3.4.4. Experimental section

3.4.4.1. General considerations

All reactions were carried out using standard Schlenk techniques under an argon atmosphere. Solvents were purified and dried by standard procedures. Phosphorochloridites are easily prepared in one step from the corresponding biaryls.[24] Phosphite/phosphinite-thioether ligands **L11**–**L18a**–**f** were prepared as previously reported.[5] Substrates **S8**,[25] **S14**,[37] **S15**,[26] **S18**–**S24**,[37] **S25**,[27] **S44**,[28] **S45**–**S48**,[10g] **S50**,[29] **S51**,[10f] **S55**,[16b] **S58**–**S59**,[16b] **S62**,[30] **S64**,[10a] **S65**,[31] **S66**,[32] **S67**–**S68**,[31] **S69**,[32] **S75**,[33] **S76**–**S79**,[34] **S135**–**S137**,[35] **S138**–**S140**,[10c] **S141**,[36] **S143**,[37] **S144**–**S145**,[22j] **S146**,[38] **S147**,[22j] **S148**[22i] and **S149**[22a] were prepared following the reported procedures. ^{1}H, ^{13}C and ^{31}P NMR spectra were recorded using a 400 MHz spectrometer. Chemical shifts are relative to that of $SiMe_4$ (^{1}H and ^{13}C) as internal standard or H_3PO_4 (^{31}P) as external standard. ^{1}H, ^{13}C and ^{31}P assignments were made on the basis of ^{1}H-^{1}H gCOSY, ^{1}H-^{13}C gHSQC and ^{1}H-^{31}P gHMBC experiments. For characterization and ee determination details, copies of the NMR spectra, copies of GC or HPLC traces as well as for DFT details see Supporting Information.

3.4.4.2. General procedure for the preparation of [Ir(cod)(L1-L8a-f)]BAr$_F$

The corresponding ligand (0.037 mmol) was dissolved in CH_2Cl_2 (2 mL) and [Ir(μ-Cl)(cod)]$_2$ (12.5 mg, 0.0185 mmol) was added. The reaction mixture was refluxed at 50 ºC for 1 h. After 5 min at room temperature, $NaBAr_F$ (38.6 mg, 0.041 mmol) and water (2 mL) were added and the reaction mixture was stirred vigorously for 30 min at room temperature. The phases were separated and the aqueous phase was extracted twice with CH_2Cl_2. The combined organic phases were dried with $MgSO_4$, filtered through a plug of celite and the solvent was evaporated to give the product as red-orange solids.

[Ir(cod)(L11a)]BAr$_F$: Yield: 67 mg (92%). ^{31}P NMR (161.9 MHz, $CDCl_3$), δ= 114.1 (s). ^{1}H NMR (400 MHz, $CDCl_3$), δ= 1.36 (s, 9H, CH_3, *t*-Bu), 1.37 (s, 9H, CH_3, *t*-Bu), 1.49 (s, 9H, CH_3, *t*-Bu), 1.55 (s, 9H, CH_3, *t*-Bu), 1.63 (d, 6H, CH_3, *i*-Pr, $^{3}J_{H-H}$= 6.8 Hz), 1.91-2.10 (m, 5H, CH_2, cod), 2.22-2.27 (m, 3H, CH_2, cod), 3.02 (dd, 1H, CH_2, $^{2}J_{H-H}$= 14.8 Hz, $^{3}J_{H-H}$= 9.6 Hz), 3.26 (dd, 1H, CH_2, $^{2}J_{H-H}$= 15.2 Hz, $^{3}J_{H-H}$= 7.6 Hz), 3.68-3.75 (m, 1H, CH, *i*-Pr), 4.25 (d, 1H, CH-S, $^{3}J_{H-H}$= 18.8 Hz), 4.47 (b, 1H, CH=, cod), 4.76 (b, 1H, CH=, cod), 4.98-5.07 (m, 1H, CH-OP), 5.09 (b, 1H, CH= cod), 5.43 (b, 1H, CH=, cod), 7.16-7.71 (m, 20H, CH=). ^{13}C NMR (100.6 MHz, $CDCl_3$), δ= 24.6 (CH_3, *i*-Pr), 25.6 (CH_3, *i*-Pr), 28.4 (b, CH_2, cod), 29.9 (CH_2, cod), 30.9 (b, CH_2, cod), 31.3 (CH_3, ^{t}Bu), 31.5 (CH_3, *t*-Bu), 31.8 (CH_3, *t*-Bu), 33.6 (b, CH_2, cod), 35.0 (C, *t*-Bu), 35.5 (C, *t*-Bu), 35.6 (C, *t*-Bu), 37.5 (d, CH_2, $^{3}J_{C-P}$= 7.6 Hz), 48.3 (b, CH, *i*-Pr), 55.0 (CH-S), 75.7 (b, CH=, cod),

78.4 (b, CH=, cod), 82.5 (CH-OP), 100.8 (b, CH=, cod), 104.3 (b, CH=, cod), 117.6-149.1 (aromatic carbons), 161.9 (q, C-B, BAr_F, $^1J_{C-B}$= 49.7 Hz). MS HR-ESI [found 947.4136 $C_{48}H_{67}IrO_3PS$ $(M)^+$ requires 947.4172].

[Ir(cod)(L11b)]BAr_F: Yield: 60 mg (93%). ^{31}P NMR (161.9 MHz, $CDCl_3$), δ= 108.8 (s). ^{1}H NMR (400 MHz, $CDCl_3$), δ= 1.03 (d, 3H, CH_3, *i*-Pr, $^3J_{H-H}$= 6.4 Hz), 1.41 (s, 9H, CH_3, *t*-Bu), 1.50 (d, 3H, CH_3, *i*-Pr, $^3J_{H-H}$= 6.8 Hz), 1.54 (s, 9H, CH_3, *t*-Bu), 1.78 (s, 3H, CH_3), 1.79 (s, 3H, CH_3), 1.93-2.15 (m, 6H, CH_2, cod), 2.25 (b, 2H, CH_2, cod), 2.27 (s, 6H, CH_3), 2.89 (dd, 1H, CH_2, $^2J_{H-H}$= 15.2 Hz, $^3J_{H-H}$= 8.8 Hz), 3.35 (dd, 1H, CH_2, $^2J_{H-H}$= 15.6 Hz, $^3J_{H-H}$= 8.4 Hz), 3.61-3.77 (m, 1H, CH, *i*-Pr), 3.86 (b, 1H, CH=, cod), 4.53 (d, 1H, CH-S, $^3J_{H-H}$= 11.2 Hz), 4.97 (b, 1H, CH=, cod), 5.06-5.13 (m, 2H, CH-OP, CH=, cod), 5.37 (b, 1H, CH=, cod), 7.20-7.70 (m, 18H, CH=). ^{13}C NMR (100.6 MHz, $CDCl_3$), δ= 16.5 (CH_3), 16.8 (CH_3), 20.3 (CH_3), 20.4 (CH_3), 24.7 (CH_3, *i*-Pr), 24.9 (CH_3, *i*-Pr), 28.9 (CH_2, cod), 30.0 (CH_2, cod), 31.8 (CH_3, *t*-Bu), 32.1 (CH_3, *t*-Bu), 32.3 (CH_2, cod), 32.5 (d, CH_2, cod, J_{C-P}= 4.6 Hz), 34.7 (C, *t*-Bu), 34.8 (C, *t*-Bu), 38.2 (d, CH_2, $^3J_{C-P}$= 6.8 Hz), 44.7 (CH, *i*-Pr), 55.1 (CH-S), 71.9 (CH=, cod), 79.2 (CH-OP), 81.5 (CH=, cod), 98.0 (d, CH=, cod, J_{C-P}= 16.9 Hz), 106.7 (d, CH=, cod, J_{C-P}= 13.2 Hz), 117.4-145.0 (aromatic carbons), 161.7 (q, C-B, BAr_F, $^1J_{C-B}$= 49.7 Hz). MS HR-ESI [found 891.3519, $C_{44}H_{59}IrO_3PS$ $(M)^+$ requires 891.3546].

[Ir(cod)(L11c)]BAr_F: Yield: 62 mg (95%). ^{31}P NMR (161.9 MHz, $CDCl_3$), δ= 111.1 (s). ^{1}H NMR (400 MHz, $CDCl_3$), δ= 1.43 (s, 9H, CH_3, *t*-Bu), 1.56 (s, 9H, CH_3, *t*-Bu), 1.60 (d, 3H, CH_3, *i*-Pr, $^3J_{H-H}$= 6.8 Hz), 1.63 (d, 3H, CH_3, *i*-Pr, $^3J_{H-H}$= 6.8 Hz), 1.77 (s, 3H, CH_3), 1.82 (s, 3H, CH_3), 1.82-1.91 (m, 2H, CH_2, cod), 2.03-2.15 (m, 4H, CH_2, cod), 2.22 (b, 2H, CH_2, cod), 2.28 (s, 6H, CH_3), 3.09 (dd, 1H, CH_2, $^2J_{H-H}$= 15.2 Hz, $^3J_{H-H}$= 9.2 Hz), 3.28 (dd, 1H, CH_2, $^2J_{H-H}$= 15.6 Hz, $^3J_{H-H}$= 8.0 Hz), 3.63-3.70 (m, 1H, CH, *i*-Pr), 3.85 (b, 1H, CH=, cod), 4.22 (d, 1H, CH-S, $^3J_{H-H}$= 8.8 Hz), 4.86 (b, 1H, CH=, cod), 4.92-4.98 (m, 1H, CH-OP), 5.03 (b, 1H, CH= cod), 5.41 (b, 1H, CH=, cod), 7.22-7.72 (m, 18H, CH=). ^{13}C NMR (100.6 MHz, $CDCl_3$), δ= 16.5 (CH_3), 20.3 (CH_3), 24.0 (CH_3, *i*-Pr), 25.6 (CH_3, *i*-Pr), 28.1 (CH_2, cod), 29.7 (CH_2, cod), 30.6 (CH_2, cod), 31.2 (CH_3, *t*-Bu), 32.0 (CH_3, *t*-Bu), 33.3 (d, CH_2, cod, J_{C-P}= 4.0 Hz), 34.7 (C, *t*-Bu), 37.4 (d, CH_2, $^3J_{C-P}$= 8.9 Hz), 48.2 (CH, *i*-Pr), 54.4 (CH-S), 72.5 (CH=, cod), 79.9 (CH=, cod), 83.0 (d, CH-OP, $^3J_{C-P}$= 5.5 Hz), 99.3 (d, CH=, cod, J_{C-P}= 17.2 Hz), 104.6 (d, CH=, cod, J_{C-P}= 10.8 Hz), 117.4-144.7 (aromatic carbons), 161.7 (q, C-B, BAr_F, $^1J_{C-B}$= 50.0 Hz). MS HR-ESI [found 891.3518, $C_{44}H_{59}IrO_3PS$ $(M)^+$ requires 891.3546].

[Ir(cod)(L11d)]BAr_F: Yield: 54 mg (93%). ^{31}P NMR (161.9 MHz, $CDCl_3$), δ= 107.7 (s). ^{1}H NMR (400 MHz, $CDCl_3$), δ= 1.37 (d, 6H, CH_3, *i*-Pr, $^3J_{H-H}$= 6.8 Hz), 1.95 -2.15 (m, 8H, CH_2, cod), 2.72 (b, 1H, CH, *i*-Pr), 3.34 (dd, 1H, CH_2, $^2J_{H-H}$= 15.2 Hz, $^3J_{H-H}$= 9.5 Hz), 3.52-3.57 (m, 2H, CH_2, CH= cod), 3.83 (b, 1H, CH=, cod), 4.20 (b, 1H, CH-S), 4.96 (b, 1H, CH=, cod), 5.11 (b, 1H, CH-OP), 5.23 (b, 1H, CH=, cod), 7.32-7.74 (m, 26H, CH=). ^{13}C NMR (100.6 MHz, $CDCl_3$), δ= 24.5 (CH_3, *i*-Pr), 24.8 (CH_3, *i*-Pr), 29.5 (CH_2, cod), 30.5

(CH_2, cod), 31.9 (CH_2, cod), 32.7 (CH_2, cod), 38.0 (d, CH_2, $^3J_{C-P}$= 10.6 Hz), 48.5 (b, CH, *i*-Pr), 57.2 (CH-S), 98.2 (b, CH=, cod), 101.0 (bs, CH=, cod), 117.7-136.9 (aromatic carbons), 161.8 (q, C-B, BAr_F, $^1J_{C-B}$= 49.7 Hz). MS HR-ESI [found 693.1915, $C_{32}H_{37}IrOPS$ $(M)^+$ requires 693.1926].

[Ir(cod)(L11e)]BAr_F: Yield: 54 mg (92%). ^{31}P NMR (161.9 MHz, $CDCl_3$), δ= 116.0 (s). ^1H NMR (400 MHz, $CDCl_3$), δ= 1.42 (m, 6H, CH_3, *i*-Pr and CH_3, *o*-Tol), 1.57 (s, 3H, CH_3, *o*-Tol), 1.63 (d, 3H, CH_3, *i*-Pr, $^3J_{H-H}$= 5.2 Hz), 1.78 (b, CH_2, cod), 2.05-2.36 (m, 6H, CH_2, cod), 2.85 (b, 1H, CH=, cod), 2.97 (b, 1H, CH, *i*-Pr), 3.18-3.24 (m, 1H, CH_2), 3.41-3.44 (m, 1H, CH_2), 3.82 (b, 1H, CH=, cod), 3.92 (b, 1H, CH-S), 3.99 (b, 1H, CH=, cod), 4.62-4.83 (b, 1H, CH=, cod), 5.09 (b, 1H, CH-OP), 5.35 (b, 1H, CH=, cod), 6.52-8.34 (m, 24H, CH=). ^{13}C NMR (100.6 MHz, $CDCl_3$): δ= 21.5 (CH_3, *o*-Tol), 22.2 (CH_3, *o*-Tol), 24.2 (CH_3, *i*-Pr), 24.4 (CH_3, *i*-Pr), 27.5 (CH_2, cod), 29.8 (CH_2, cod), 32.2 (CH_2, cod), 34.2 (CH_2, cod), 37.5 (CH_2), 49.8 (b, CH, *i*-Pr), 57.6 (CH-S), 75.9 (CH=, cod), 77.2 (b, CH-OP), 87.4 (b, CH=, cod), 93.6 (b, CH=, cod), 101.0 (b, CH=, cod), 117.4-143.1 (aromatic carbons), 161.7 (q, C-B, BAr_F, $^1J_{C-B}$= 49.7 Hz). MS HR-ESI [found 721.2243, $C_{34}H_{41}IrOPS$ $(M)^+$ requires 721.2240].

[Ir(cod)(L12b)]BAr_F: Yield: 62 mg (93%). ^{31}P NMR (161.9 MHz, $CDCl_3$), δ= 107.9 (s). ^1H NMR (400 MHz, $CDCl_3$): δ= 0.98 (t, 3H, CH_3, Pr, $^3J_{H-H}$= 6.8 Hz), 1.42 (s, 9H, CH_3, *t*-Bu), 1.55 (s, 9H, CH_3, *t*-Bu), 1.57-1.67 (m, 2H, CH_2, Pr), 1.78 (s, 3H, CH_3), 1.82 (s, 3H, CH_3), 1.94-1.99 (m, 2H, CH_2, cod), 2.04 (m, 2H, CH_2, cod), 2.18 (m, 2H, CH_2, cod), 2.22-2.30 (m, 2H, CH_2, cod), 2.28 (s, 3H, CH_3), 2.29 (s, 3H, CH_3), 2.77-2.81 (m, 2H, CH_2, Pr), 2.95 (dd, 1H, CH_2, $^2J_{H-H}$= 15.2 Hz, $^3J_{H-H}$= 9.2 Hz), 3.34 (dd, 1H, CH_2, $^2J_{H-H}$= 15.6 Hz, $^3J_{H-H}$= 7.6 Hz), 3.44 (b, 1H, CH=, cod), 4.43 (d, 1H, CH-S, $^3J_{H-H}$= 8.8 Hz), 4.93-5.01 (m, 2H, CH-OP and CH= cod), 5.05-5.09 (m, 1H, CH=, cod), 5.31 (b, 1H, CH=, cod), 7.22-7.70 (m, 18H, CH=). ^{13}C NMR (100.6 MHz, $CDCl_3$): δ= 13.2 (CH_3, Pr), 16.5 (CH_3), 16.7 (CH_3), 20.3 (CH_3), 20.4 (CH_3), 21.8 (CH_2, Pr), 29.2 (CH_2, cod), 29.6 (CH_2, cod), 31.9 (CH_3, *t*-Bu, CH_2, cod), 32.3 (CH_3, *t*-Bu), 33.1 (CH_2, cod), 35.0 (C, *t*-Bu), 37.3 (CH_2, Pr), 38.1 (d, CH_2, $^3J_{C-P}$= 6.8 Hz), 53.8 (CH-S), 70.9 (CH=, cod), 79.3 (CH-OP), 82.1 (CH=, cod), 98.5 (d, CH=, cod, J_{C-P}= 17.5 Hz), 108.8 (d, CH=, cod, J_{C-P}= 14.6 Hz), 117.4-137.0 (aromatic carbons), 161.7 (q, C-B, BAr_F, $^1J_{C-B}$= 50.5 Hz). MS HR-ESI [found 889.3509, $C_{44}H_{59}IrO_3PS$ $(M)^+$ requires 889.3523].

[Ir(cod)(L13b)]BAr_F: Yield: 60.2 mg (92%). Major isomer (65%): ^{31}P NMR (161.9 MHz, $CDCl_3$), δ= 107.7 (s). ^1H NMR (400 MHz, $CDCl_3$), δ= 1.37 (s, 9H, CH_3, *t*-Bu), 1.45 (s, 9H, CH_3, *t*-Bu), 1.55 (s, 9H, CH_3, *t*-Bu), 1.77 (s, 3H, CH_3), 1.80 (s, 3H, CH_3), 2.00-2.40 (m, 8H, CH_2, cod), 2.26 (s, 3H, CH_3), 2.28 (s, 3H, CH_3), 2.82 (m, 1H, CH_2), 3.41 (m, 1H, CH_2), 3.79 (m, 1H, CH=, cod), 4.78 (m, 1H, CH-S), 4.95 (m, 1H, CH=, cod), 5.24 (m, 1H, CH=, cod), 5.48 (m, 1H, CH=, cod), 5.67 (m, 1H, CH-OP), 7.20-7.80 (m, 18H, CH=). ^{13}C NMR (100.6 MHz, $CDCl_3$), δ= 16.5 (CH_3), 16.7 (CH_3), 20.3 (b, CH_3), 28.4-33.0 (CH_2, cod), 31.6-34.0 (CH_3, *t*-Bu), 34.5-35.2 (C, *t*-Bu), 38.4 (CH_2), 58.9 (CH-

S), 68.9 (CH=, cod), 79.4 (CH=, cod), 81.0 (CH-OP), 99.4 (d, CH=, cod, J_{C-P}= 14.3 Hz), 110.5 (d, CH=, cod, J_{C-P}= 18.2 Hz), 117.4-135.9 (aromatic carbons), 161.6 (q, C-B, BAr_F, $^1J_{C-B}$= 49.7 Hz). Minor isomer (35%): ^{31}P NMR (161.9 MHz, $CDCl_3$), δ= 105.6 (s). ^{1}H NMR (400 MHz, $CDCl_3$), δ= 1.41 (s, 9H, CH_3, *t*-Bu), 1.48 (s, 9H, CH_3, *t*-Bu), 1.58 (s, 9H, CH_3, *t*-Bu), 1.77 (s, 3H, CH_3), 1.80 (s, 3H, CH_3), 2.00-2.40 (m, 8H, CH_2, cod), 3.12 (s, 3H, CH_3), 3.27 (s, 3H, CH_3), 3.12 (m, 1H, CH_2), 3.27 (m, 1H, CH_2), 4.12 (m, 1H, CH-S), 4.48 (m, 1H, CH=, cod), 4.56 (m, 1H, CH=, cod), 4.94 (m, 1H, CH-OP), 5.48 (m, 1H, CH=, cod), 6.02 (m, 1H, CH=, cod), 7.20-7.80 (m, 18H, CH=). ^{13}C NMR (100.6 MHz, $CDCl_3$), δ= 16.5 (CH_3), 16.7 (CH_3), 20.3 (b, CH_3), 28.4-33.0 (CH_2, cod), 31.6-34.0 (CH_3, *t*-Bu), 34.5-35.2 (C, *t*-Bu), 36.5 (CH_2), 49.9 (CH-S), 68.9 (CH=, cod), 81.3 (CH-OP), 82.9 (CH=, cod), 93.5 (b, CH=, cod), 95.7 (b, CH=, cod), 117.4-135.9 (aromatic carbons), 161.6 (q, C-B, BAr_F, $^1J_{C-B}$= 49.7 Hz). MS HR-ESI [found 905.3711, $C_{45}H_{61}IrO_3PS$ $(M)^+$ requires 905.3703].

[Ir(cod)(L13e)]BAr_F: Yield: 52.6 mg (89%). Major isomer (85%): ^{31}P NMR (161.9 MHz, $CDCl_3$), δ= 116.0 (s). ^{1}H NMR (400 MHz, $CDCl_3$): δ= 1.37 (s, 9H, CH_3, *t*-Bu), 1.70-2.40 (m, 8H, CH_2, cod), 2.27 (s, 3H, CH_3, *o*-Tol), 2.72 (s, 3H, CH_3, *o*-Tol), 2.92 (b, 1H, CH=, cod), 3.28 (dd, 1H, CH_2, $^2J_{H-H}$= 14.8 Hz, $^3J_{H-H}$= 7.6 Hz), 3.42 (dd, 1H, CH_2, $^2J_{H-H}$= 14.8 Hz, $^3J_{H-H}$= 9.6 Hz), 3.93 (b, 1H, CH=, cod), 4.21 (d, 1H, CH-S, $^3J_{H-H}$= 9.6 Hz), 4.82 (b, 1H, CH=, cod), 5.08 (m, 1H, CH-OP), 5.47 (b, 1H, CH=, cod), 6.42 (m, 1H, CH=), 7.00-7.80 (m, 22H, CH=), 8.24 (dd, 1H, $^3J_{H-H}$= 17.6 Hz, $^3J_{H-H}$= 7.2 Hz). ^{13}C NMR (100.6 MHz, $CDCl_3$), δ= 22.4 (CH_3, *o*-Tol), 22.5 (CH_3, *o*-Tol), 27.3 (CH_2, cod), 29.7 (CH_2, cod), 30.0 (CH_2, cod), 31.5 (CH_2, cod), 31.9 (CH_3, *t*-Bu), 34.0 (C, *t*-Bu), 37.5 (d, CH_2, $^3J_{C-P}$= 4.2 Hz), 52.5 (CH-S), 74.4 (CH=, cod), 76.6 (CH=, cod), 87.4 (CH-OP), 93.6 (d, CH=, cod, J_{C-P}= 15.2 Hz), 104.0 (d, CH=, cod, J_{C-P}= 16.0 Hz), 117.4-142.9 (aromatic carbons), 161.6 (q, C-B, BAr_F, $^1J_{C-B}$= 48.8 Hz). Minor isomer (15%): ^{31}P NMR (161.9 MHz, $CDCl_3$), δ= 115.6 (s). ^{1}H NMR (400 MHz, $CDCl_3$), δ= 1.56 (s, 9H, CH_3, *t*-Bu), 1.70-2.40 (m, 8H, CH_2, cod), 2.29 (s, 3H, CH_3, *o*-Tol), 2.60 (s, 3H, CH_3, *o*-Tol), 2.92 (b, 1H, CH=, cod), 3.12 (dd, 1H, CH_2, $^2J_{H-H}$= 15.2 Hz, $^3J_{H-H}$= 8.0 Hz), 3.42 (m, 1H, CH_2), 3.57 (m, 1H, CH=, cod), 4.24 (b, 1H, CH-S), 4.76 (b, 1H, CH=, cod), 5.09 (m, 1H, CH-OP), 5.29 (b, 1H, CH=, cod), 6.60 (m, 1H, CH=), 7.00-7.80 (m, 22H, CH=), 8.65 (dd, 1H, $^3J_{H-H}$= 17.6 Hz, $^3J_{H-H}$= 7.2 Hz). ^{13}C NMR (100.6 MHz, $CDCl_3$), δ= 22.2 (CH_3, *o*-Tol), 22.7 (CH_3, *o*-Tol), 27.0 (CH_2, cod), 29.3 (CH_2, cod), 29.5 (CH_2, cod), 30.0 (CH_2, cod), 31.5 (CH_3, *t*-Bu), 34.5 (C, *t*-Bu), 37.0 (b, CH_2), 52.9 (CH-S), 70.6 (CH=, cod), 76.0 (CH=, cod), 86.4 (CH-OP), 94.2 (b, CH=, cod), 103.8 (b, CH=, cod), 117.4-142.9 (aromatic carbons), 161.6 (q, C-B, BAr_F, $^1J_{C-B}$= 48.8 Hz). MS HR-ESI [found 735.2398, $C_{35}H_{43}IrOPS$ $(M)^+$ requires 735.2396].

[Ir(cod)(L14b)]BAr_F: Yield: 61 mg (93%). ^{31}P NMR (161.9 MHz, $CDCl_3$), δ= 104.4 (s). ^{1}H NMR (400 MHz, $CDCl_3$), δ= 1.49 (s, 9H, CH_3, *t*-Bu), 1.59 (s, 9H, CH_3, *t*-Bu), 1.63-1.91 (m, 4H, CH_2, cod), 1.75 (s, 3H, CH_3), 1.85 (s, 3H, CH_3), 2.12-2.36 (m, 4H,

CH_2, cod), 2.29 (s, 6H, CH_3), 2.89 (b, 1H, CH=, cod), 3.00 (dd, 1H, CH_2, $^2J_{H-H}$= 14.8 Hz, $^3J_{H-H}$= 9.6 Hz), 3.37 (dd, 1H, CH_2, $^2J_{H-H}$= 15.6 Hz, $^3J_{H-H}$= 8.0 Hz), 4.19 (m, 1H, CH=, cod), 4.67 (m, 1H, CH=, cod), 4.81-4.91 (m, 1H, CH-OP), 5.17 (b, 1H, CH=, cod), 5.21 (d, 1H, CH-S, $^3J_{H-H}$= 9.6 Hz), 6.23-7.74 (m, 23H, CH=). ^{13}C NMR (100.6 MHz, $CDCl_3$), δ= 16.4 (CH_3), 16.6 (CH_3), 20.2 (CH_3), 20.5 (CH_3), 26.4 (CH_2, cod), 29.9 (CH_2, cod), 31.1 (CH_2, cod), 31.8 (CH_3, *t*-Bu), 32.8 (CH_3, *t*-Bu), 34.7 (CH_2, cod), 35.0 (C, *t*-Bu), 35.2 (C, *t*-Bu), 37.8 (d, CH_2, $^3J_{C-P}$= 7.4 Hz), 55.9 (CH-S), 67.9 (CH=, cod), 78.6 (CH=, cod), 79.4 (CH-OP), 101.2 (d, CH=, cod, J_{C-P}= 14.5 Hz), 106.0 (d, CH=, cod, J_{C-P}= 15.3 Hz), 117.4-143.6 (aromatic carbons), 161.7 (q, C-B, BAr_F, $^1J_{C-B}$= 50.4 Hz). MS HR-ESI [found 923.3367, $C_{47}H_{57}IrO_3PS$ $(M)^+$ requires 923.3366].

[Ir(cod)(L15b)]BAr_F: Yield: 64 mg (95%). ^{31}P NMR (161.9 MHz, $CDCl_3$), δ= 104.1 (s). ^{1}H NMR (400 MHz, $CDCl_3$), δ= 1.47 (s, 9H, CH_3, *t*-Bu), 1.60 (s, 9H, CH_3, *t*-Bu), 1.65-1.84 (m, 4H, CH_2, cod), 1.76 (s, 3H, CH_3), 1.86 (s, 3H, CH_3), 2.13-2.38 (m, 4H, CH_2, cod), 2.29 (s, 3H, CH_3), 2.30 (s, 3H, CH_3), 2.56 (s, 3H, CH_3), 2.72 (m, 1H, CH=, cod), 2.95 (dd, 1H, CH_2, $^2J_{H-H}$= 15.2 Hz, $^3J_{H-H}$= 9.6 Hz), 3.08 (s, 3H, CH_3), 3.38 (dd, 1H, CH_2, $^2J_{H-H}$= 15.2 Hz, $^3J_{H-H}$= 7.6 Hz), 3.92 (m, 1H, CH=, cod), 4.72 (m, 1H, CH=, cod), 4.89 (m, 1H, CH-OP), 5.12 (d, 1H, CH-S, $^3J_{H-H}$= 8.8 Hz), 5.18 (b, 1H, CH=, cod), 6.08-7.70 (m, 21H, CH=). ^{13}C NMR (100.6 MHz, $CDCl_3$), δ= 16.4 (CH_3), 16.6 (CH_3), 20.3 (CH_3), 20.5 (CH_3), 22.8 (CH_3), 22.9 (CH_3), 25.7 (CH_2, cod), 30.5 (CH_2, cod), 31.0 (CH_2, cod), 31.8 (CH_3, *t*-Bu), 32.7 (CH_3, *t*-Bu), 35.0 (CH_2, cod), 35.2 (C, *t*-Bu), 37.8 (d, CH_2, $^3J_{C-P}$= 7.6 Hz), 53.7 (CH-S), 66.2 (CH=, cod), 77.7 (CH=, cod), 80.0 (CH-OP), 102.1 (d, CH=, cod, J_{C-P} =13.8 Hz), 104.6 (d, CH=, cod, J_{C-P}= 16.1 Hz), 117.4-143.8 (aromatic carbons), 161.7 (q, C-B, BAr_F, $^1J_{C-B}$= 49.7 Hz). MS HR-ESI [found 951.3674, $C_{49}H_{61}IrO_3PS$ $(M)^+$ requires 951.3679].

[Ir(cod)(L15c)]BAr_F: Yield: 63 mg (94%). ^{31}P NMR (161.9 MHz, $CDCl_3$), δ= 108.7 (s). ^{1}H NMR (400 MHz, $CDCl_3$), δ= 1.41 (s, 9H, CH_3, *t*-Bu), 1.59 (s, 9H, CH_3, *t*-Bu), 1.71-1.89 (m, 4H, CH_2, cod), 1.71 (s, 3H, CH_3), 1.73 (s, 3H, CH_3), 1.97-2.20 (m, 4H, CH_2, cod), 2.21 (s, 3H, CH_3), 2.22 (s, 3H, CH_3), 2.24 (s, 3H, CH_3), 2.75 (s, 3H, CH_3), 2.99-3.08 (m, 2H, CH_2 and CH= cod), 3.31 (dd, 1H, CH_2, $^2J_{H-H}$= 15.6 Hz, $^3J_{H-H}$= 8.4 Hz), 4.26 (m, 1H, CH=, cod), 4.67 (m, 1H, CH=, cod), 4.74 (m, 1H, CH=, cod), 4.80 (d, 1H, CH-S, $^3J_{H-H}$ =8.8 Hz), 5.31-5.35 (m, 1H, CH-OP), 5.88-7.63 (m, 21H, CH=). ^{13}C NMR (100.6 MHz, $CDCl_3$), δ= 16.7 (CH_3), 16.8 (CH_3), 20.5 (CH_3), 20.7 (CH_3), 23.5 (CH_3), 24.3 (CH_3), 27.6 (CH_2, cod), 29.9 (d, CH_2, cod, J_{C-P}= 10.0 Hz), 31.8 (CH_3, *t*-Bu), 32.1 (CH_2, cod), 32.9 (CH_3, *t*-Bu), 34.2 (CH_2, cod), 35.1 (C, *t*-Bu), 35.5 (C, *t*-Bu), 37.5 (d, CH_2, $^3J_{C-P}$= 9.2 Hz), 56.4 (CH-S), 67.3 (CH=, cod), 77.4 (CH=, cod), 86.3 (d, CH-OP, $^2J_{C-P}$= 6.0 Hz), 103.4 (d, CH=, cod, J_{C-P}= 14.8 Hz), 104.7 (d, CH=, cod, J_{C-P}= 13.9 Hz), 117.7-144.7 (aromatic carbons), 161.9 (q, C-B, BAr_F, $^1J_{C-B}$= 50.1 Hz). MS HR-ESI [found 951.3641, $C_{49}H_{61}IrO_3PS$ $(M)^+$ requires 951.3679].

[Ir(cod)(L15d)]BAr$_F$: Yield: 55 mg (92%). ^{31}P NMR (161.9 MHz, $CDCl_3$), δ= 114.3 (s). ^{1}H NMR (400 MHz, $CDCl_3$), δ= 1.75-1.86 (m, 2H, CH_2, cod), 1.93-2.01 (m, 2H, CH_2, cod), 2.10-2.15 (m, 1H, CH_2, cod), 2.20-2.40 (m, 3H, CH_2, cod), 2.57 (s, 3H, CH_3), 3.02 (s, 3H, CH_3), 3.07 (dd, 1H, CH_2, $^2J_{H-H}$= 15.6 Hz, $^3J_{H-H}$= 9.6 Hz), 3.19 (dd, 1H, CH_2, $^2J_{H-H}$= 15.6 Hz, $^3J_{H-H}$= 8.0 Hz), 3.27 (m, 1H, CH=, cod), 3.41 (m, 1H, CH=, cod), 3.88 (m, 1H, CH=, cod), 4.49-4.58 (m, 1H, CH-OP), 5.05 (d, 1H, CH-S, $^3J_{H-H}$= 8.4 Hz), 5.11 (m, 1H, CH=, cod), 6.09-7.94 (m, 29H, CH=). ^{13}C NMR (100.6 MHz, $CDCl_3$), δ= 23.2 (CH_3), 23.6 (CH_3), 27.3 (CH_2, cod), 30.7 (CH_2, cod), 31.0 (CH_2, cod), 33.6 (CH_2, cod), 38.3 (d, CH_2, $^3J_{C-P}$= 7.6 Hz), 52.9 (CH-S), 69.3 (CH=, cod), 74.9 (CH=, cod), 82.5 (CH-OP), 97.2 (d, CH=, cod, J_{C-P}= 10.0 Hz), 98.6 (d, CH=, cod, J_{C-P}= 13.0 Hz), 117.4-143.2 (aromatic carbons), 161.7 (q, C-B, BAr_F, $^1J_{C-B}$= 49.7 Hz). MS HR-ESI [found 755.2085, $C_{37}H_{39}IrOPS$ $(M)^+$ requires 755.2083].

[Ir(cod)(L15e)]BAr$_F$: Yield: 56 mg (96%). ^{31}P NMR (161.9 MHz, $CDCl_3$), δ= 118.2 (s). ^{1}H NMR (400 MHz, $CDCl_3$), δ= 1.68-1.85 (m, 2H, CH_2, cod), 1.95-2.19 (m, 2H, CH_2, cod), 2.23 (s, 3H, CH_3), 2.25-2.47 (m, 4H, CH_2, cod), 2.53 (s, 3H, CH_3), 2.92 (s, 4H, CH=, cod and CH_3), 3.03 (dd, 1H, CH_2, $^2J_{H-H}$= 15.6 Hz, $^3J_{H-H}$= 9.6 Hz), 3.15 (s, 3H, CH_3), 3.15-3.20 (m, 2H, CH= cod, CH_2), 3.75 (m, 1H, CH=, cod), 4.32-4.42 (m, 1H, CH-OP), 5.08 (b, 1H, CH=, cod), 5.24 (d, 1H, CH-S, $^3J_{H-H}$= 8.4 Hz), 5.89-9.06 (m, 27H, CH=). ^{13}C NMR (100.6 MHz, $CDCl_3$), δ= 21.8 (CH_3), 22.3 (d, CH_3, $^3J_{C-P}$= 6.9 Hz), 23.1 (CH_3), 26.7 (CH_2, cod), 29.9 (CH_2, cod), 31.7 (CH_2, cod), 34.3 (CH_2, cod), 38.3 (d, CH_2, $^3J_{C-P}$= 7.6 Hz), 52.0 (CH-S), 67.9 (CH=, cod), 77.2 (CH=, cod), 81.4 (CH-OP), 96.5 (d, CH=, cod, J_{C-P} =9.2 Hz), 96.8 (d, CH=, cod, J_{C-P}= 13.8 Hz), 117.4-143.5 (aromatic carbons), 161.7 (q, C-B, BAr_F, $^1J_{C-B}$= 49.7 Hz). MS HR-ESI [found 783.2401, $C_{39}H_{43}IrOPS$ $(M)^+$ requires 783.2396].

[Ir(cod)(L16b)]BAr$_F$: Yield: 69 mg (97%). ^{31}P NMR (161.9 MHz, $CDCl_3$), δ= 104.1 (s). ^{1}H NMR (400 MHz, $CDCl_3$), δ= 1.49 (s, 9H, CH_3, ^{t}Bu), 1.58 (s, 9H, CH_3, ^{t}Bu), 1.64-1.71 (m, 4H, CH_2, cod), 1.76 (s, 3H, CH_3), 1.85 (s, 3H, CH_3), 2.08-2.22 (m, 4H, CH_2, cod), 2.29 (s, 6H, CH_3), 2.99-3.05 (m, 2H, CH_2 and CH=, cod), 3.39 (dd, 1H, CH_2, $^2J_{H-H}$= 15.2 Hz, $^3J_{H-H}$= 7.6 Hz), 4.10 (m, 1H, CH=, cod), 4.76 (b, 1H, CH=, cod), 4.84-4.92 (m, 1H, CH-OP), 5.13 (b, 1H, CH=, cod), 5.23 (d, 1H, CH-S, $^3J_{H-H}$= 9.2 Hz), 6.23-7.89 (m, 22H, CH=). ^{13}C NMR (100.6 MHz, $CDCl_3$), δ= 16.4 (CH_3), 16.6 (CH_3), 20.2 (CH_3), 20.4 (CH_3), 26.6 (CH_2, cod), 29.8 (CH_2, cod), 31.2 (CH_2, cod), 31.8 (CH_3, ^{t}Bu), 32.8 (CH_3, ^{t}Bu), 34.5 (CH_2, cod), 35.0 (C, ^{t}Bu), 35.2 (C, ^{t}Bu), 37.7 (CH_2), 56.1 (CH-S), 68.9 (CH=, cod), 79.3 (CH=, cod), 79.7 (CH-OP), 100.9 (d, CH=, cod, J_{C-P}= 13.7 Hz), 105.4 (d, CH=, cod, J_{C-P}= 15.3 Hz), 117.4-143.5 (aromatic carbons), 161.7 (q, C-B, BAr_F, $^1J_{C-B}$= 49.7 Hz). MS HR-ESI [found 991.3222, $C_{48}H_{56}F_3IrO_3PS$ $(M)^+$ requires 991.3240].

[Ir(cod)(L17b)]BAr$_F$: Yield: 64 mg (95%). ^{31}P NMR (161.9 MHz, $CDCl_3$), δ= 104.7 (s). ^{1}H NMR (400 MHz, $CDCl_3$), δ= 1.49 (s, 9H, CH_3, ^{t}Bu), 1.58 (s, 9H, CH_3, ^{t}Bu), 1.63-1.94 (m, 4H, CH_2, cod), 1.75 (s, 3H, CH_3), 1.85 (s, 3H, CH_3), 2.07-2.37 (m, 4H, CH_2,

cod), 2.29 (s, 6H, CH_3), 2.86 (m, 1H, CH=, cod), 2.98 (dd, 1H, CH_2, $^2J_{H-H}$= 15.2 Hz, $^3J_{H-H}$= 9.6 Hz), 3.36 (dd, 1H, CH_2, $^2J_{H-H}$= 15.2 Hz, $^3J_{H-H}$= 8.0 Hz), 3.84 (s, 3H, CH_3, MeO), 4.30-4.33 (m, 1H, CH=, cod), 4.67 (b, 1H, CH=, cod), 4.79-4.88 (m, 1H, CH-OP), 5.12 (d, 1H, CH-S, $^3J_{H-H}$= 9.2 Hz), 5.16 (b, 1H, CH=, cod), 6.31-7.71 (m, 22H, CH=). ^{13}C NMR (100.6 MHz, $CDCl_3$), δ= 16.4 (CH_3), 16.6 (CH_3), 20.2 (CH_3), 20.5 (CH_3), 26.3 (CH_2, cod), 30.0 (CH_2, cod), 31.0 (CH_2, cod), 31.8 (CH_3, ^{t}Bu), 32.8 (CH_3, ^{t}Bu), 34.9 (CH_2, cod), 35.0 (C, ^{t}Bu), 35.2 (C, ^{t}Bu), 37.8 (d, CH_2, $^3J_{C-P}$= 8.1 Hz), 55.6 (CH_3, MeO), 56.2 (CH-S), 67.7 (CH=, cod), 78.5 (CH=, cod), 79.4 (CH-OP), 101.3 (d, CH=, cod, J_{C-P}= 14.4 Hz), 106.0 (d, CH=, cod, J_{C-P}= 16.3 Hz), 116.2-163.4 (aromatic carbons), 161.7 (q, C-B, BAr_F, $^1J_{C-B}$= 50.5 Hz). MS HR-ESI [found 955.3512, $C_{48}H_{56}F_3IrO_3PS$ $(M)^+$ requires 955.3501].

[Ir(cod)(L18b)]BAr_F: Yield: 57.1 mg (89%). ^{31}P NMR (161.9 MHz, $CDCl_3$), δ=104.4 (s). ^{1}H NMR (400 MHz, $CDCl_3$), δ=1.14-1.17 (m, 2H, CH_2, cod), 1.66 (s, 9H, CH_3, ^{t}Bu), 1.69 (s, 9H, CH_3, ^{t}Bu), 1.73-1.82 (m, 2H, CH_2, cod), 1.79 (s, 3H, CH_3), 1.90 (s, 3H, CH_3), 2.09-2.26 (m, 2H, CH_2, cod), 2.31 (s, 3H, CH_3), 2.32 (s, 3H, CH_3), 2.78 (m, 1H, CH=, cod), 2.93 (dd, 1H, CH^2, $^2J_{H-H}$= 15.2 Hz, $^3JH_{-H}$= 9.2 Hz), 3.39 (dd, 1H, CH_2, $^2J_{H-H}$= 15.6 Hz, $^3J_{H-H}$= 8.0 Hz), 3.53 (m, 1H, CH=, cod), 4.83 (b, 1H, CH=, cod), 4.99-5.03 (m, 1H, CH-OP), 5.35 (d, 1H, CH-S, $^3J_{H-H}$= 9.2 Hz), 5.37 (b, 1H, CH=, cod), 5.50-9.47 (m, 27H, CH=). ^{13}C NMR (100.6 MHz, $CDCl_3$), δ=16.5 (CH_3), 16.7 (CH_3), 20.3 (CH_3), 20.6 (CH_3), 24.9 (CH_2, cod), 30.3 (CH_2, cod), 31.0 (CH_2, cod), 31.9 (CH_3, ^{t}Bu), 32.8 (CH_3, ^{t}Bu), 35.1 (CH_2, cod and C, ^{t}Bu), 35.3 (C, ^{t}Bu), 37.7 (CH2), 54.5 (CH-S), 65.8 (CH=, cod), 78.3 (CH=, cod), 79.9 (CH-OP), 103.1 (CH=, cod, J_{C-P}= 13.7 Hz), 105.6 (CH=, cod, J_{C-P}= 16.0 Hz), 117.4-143.9 (aromatic carbons), 161.7 (q, C-B, BAr_F, $^1J_{C-B}$= 49.8 Hz). MS HR-ESI [found 1025.3706, $C_{55}H_{61}IrO_3PS$ $(M)^+$ requires 1025.3703].

[Ir(cod)(L18c)]BAr_F: Yield: 35 mg (24%). ^{31}P NMR (161.9 MHz, $CDCl_3$), δ= 106.0 (s). ^{1}H NMR (400 MHz, $CDCl_3$), δ= 1.53-1.61 (m, 1H, CH_2, cod), 1.56 (s, 9H, CH_3, ^{t}Bu), 1.75-2.09 (m, 6H, CH_2, cod), 1.80 (s, 3H, CH_3), 1.81 (s, 12H, ^{t}Bu and CH_3), 2.30 (s, 3H, CH_3), 2.32-2.36 (m, 1H, CH_2, cod), 3.01 (m, 1H, CH_2), 3.14 (m, 1H, CH=, cod), 3.26 (m, 1H, CH_2), 4.46 (m, 1H, CH=, cod), 4.87 (m, 1H, CH=, cod), 4.96 (m, 1H, CH=, cod), 5.14 (d, 1H, CH-S, $^3J_{H-H}$= 8.3 Hz), 5.39 (d, 1H, CH=, $^3J_{H-H}$= 7.8 Hz), 5.55 (m, 1H, CH-OP), 6.39-9.09 (m, 27H, CH=). ^{13}C NMR (100.6 MHz, $CDCl_3$), δ= 16.5 (CH_3), 16.6 (CH_3), 20.3 (CH_3), 20.4 (CH_3), 26.6 (CH_2, cod), 30.0 (CH_2, cod), 31.7 (CH_3, ^{t}Bu), 32.7 (CH_3, ^{t}Bu), 33.0 (CH_2, cod), 34.6 (CH_2, cod), 34.9 (C, ^{t}Bu), 35.2 (C, ^{t}Bu), 37.7 (CH_2-O), 53.4 (CH-S), 66.8 (CH=, cod), 78.5 (CH=, cod), 84.1 (CH-OP), 102.2 (b, CH=, cod), 106.6 (b, CH=, cod), 117.4-144.7 (aromatic carbons), 161.1 (q, C-B, BAr_F, $^1J_{C-B}$= 51.9 Hz). MS HR-ESI [found 1025.3706, $C_{55}H_{61}IrO_3PS$ $(M)^+$ requires 1025.3703].

[Ir(cod)(L18d)]BAr_F: Yield: 75 mg (60%). ^{31}P NMR (161.9 MHz, $CDCl_3$), δ= 115.0 (s). ^{1}H NMR (400 MHz, $CDCl_3$), δ= 1.44-1.54 (m, 2H, CH_2, cod), 1.78-1.89 (m, 2H, CH_2, cod), 1.97-2.03 (m, 2H, CH_2, cod), 2.22-2.37 (m, 2H, CH_2, cod), 3.09 (m, 1H, CH_2),

3.25 (m, 1H, CH_2), 3.37 (m, 1H, CH=, cod), 3.54 (m, 2H, CH=, cod), 4.78 (m, 1H, CH=, cod), 5.17 (m, 1H, CH-OP), 5.25 (d, 1H, CH-S, $^3J_{H-H}$= 8.7 Hz), 5.49 (d, 1H, CH=, $^3J_{H-H}$= 7.8 Hz), 6.58-9.05 (m, 34H, CH=). ^{13}C NMR (100.6 MHz, $CDCl_3$), δ= 27.4 (CH_2, cod), 30.3 (CH_2, cod), 31.3 (CH_2, cod), 32.8 (CH_2, cod), 38.3 (CH_2), 54.2 (CH-S), 70.7 (CH=, cod), 74.1 (CH=, cod), 83.2 (CH-OP), 97.8 (d, CH=, cod, J_{C-P}= 10.6 Hz), 99.9 (d, CH=, cod, J_{C-P}= 12.4 Hz), 117.4-137.8 (aromatic carbons), 161.7 (q, C-B, BAr_F, $^1J_{C-B}$= 49.9 Hz). MS HR-ESI [found 827.2087, $C_{43}H_{39}IrOPS$ $(M)^+$ requires 827.2083].

[Ir(cod)(L18e)]BAr_F: Yield: 55 mg (43%). ^{31}P NMR (161.9 MHz, $CDCl_3$), δ= 119.4 (s). ^{1}H NMR (400 MHz, $CDCl_3$), δ= 1.42-1.47 (m, 2H, CH_2, cod), 1.64-1.76 (m, 1H, CH_2, cod), 1.79-2.00 (m, 3H, CH_2, cod), 2.08-2.16 (m, 1H, CH_2, cod), 2.26 (s, 3H, CH_3, *o*-Tol), 2.31-2.39 (m, 2H, CH_2, cod), 2.97 (m, 1H, CH=, cod), 2.99 (m, 1H, CH_2), 3.11 (m, 1H, CH_2), 3.13 (m, 1H, CH=, cod), 3.26 (s, 3H, CH_3, *o*-Tol), 3.43 (m, 1H, CH=, cod), 4.50 (m, 1H, CH-OP), 5.07 (d, 1H, CH=, $^3J_{H-H}$= 7.8 Hz), 5.21 (m, 1H, CH=, cod), 5.51 (d, 1H, CH-S, $^3J_{H-H}$= 9.0 Hz), 6.49-9.49 (m, 32H, CH=). ^{13}C NMR (100.6 MHz, $CDCl_3$), δ= 21.8 (CH_3, *o*-Tol), 22.2 (CH_3, *o*-Tol), 26.3 (CH_2, cod), 29.9 (CH_2, cod), 31.4 (CH_2, cod), 34.1 (CH_2, cod), 38.3 (CH_2-O), 53.4 (CH-S), 67.8 (CH=, cod), 77.2 (CH=, cod), 81.3 (CH-OP), 97.9 (d, CH=, cod, J_{C-P}= 9.9 Hz), 98.4 (d, CH=, cod, J_{C-P}= 12.4 Hz), 117.4-142.9 (aromatic carbons), 161.66 (q, C-B, BAr_F, $^1J_{C-B}$= 50.0 Hz). MS HR-ESI [found 855.2399, $C_{45}H_{43}IrOPS$ $(M)^+$ requires 855.2396].

3.4.4.3. Preparation of exocyclic lactam S142

Lactam **S142** was prepared from 1-acetylpiperidin-2-one in two steps following an already reported procedure.[10a] A mixture of *N*-acetyl-2-pyrrolidinone (6 mmol, 847 mg) and THF (12 mL) was cooled to 0 °C. NaH (60% in mineral oil) (12 mmol, 480 mg) was then added, followed by addition of the corresponding aldehyde (3 mmol). The reaction was stirred at 0 °C for 1 h followed by warming to room temperature and stirring for 2 h. After quenching carefully with methanol at 0 °C, the solvent was removed under reduced pressure. The residue was diluted with water and extracted with ethyl acetate (3x10 mL). The organic extracts were washed with brine and dried over anhydrous Na_2SO_4. The solvent was removed under reduced pressure and the residue was dissolved in a small amount of ethyl acetate. Addition of petroleum ether resulted in precipitation of the unprotected lactam. The resulting solid was washed with petroleum ether and used without further purification.

(*E*)-3-(4-(Trifluoromethyl)benzylidene)piperidin-2-one.[10e] Brown solid, 49% yield (372 mg). ^{1}H NMR (400 MHz, $CDCl_3$), δ: 1.82-1.88 (m, 2H), 2.72-2.79 (m, 2H), 3.42 (t, *J* = 5.8 Hz, 2H), 6.85 (bs, 1H), 7.43 (d, *J* = 8.0 Hz, 2H), 7.60 (d, *J* = 8.0 Hz, 2H), 7.79 (s, 1H).

To a stirred solution of the corresponding (*E*)-3-aryl-pyrrolidin-2-one (1.0 mmol) in anhydrous THF (5 mL) over an ice bath, was added a suspension of sodium hydride

(60% in mineral oil) (1.1 mmol, 43.9 mg). The mixture was stirred for 30 min at 0 °C and benzyl bromide (1.65 mmol, 133 µl) was then added dropwise. The reaction mixture was allowed to warm to room temperature and was stirred for a further 3 h. The solvent was evaporated in vacuo and the residue was extracted with ethyl acetate (3x10 mL). The organic phase was washed several times with brine, dried and evaporated. The residue was purified by column chromatography (silica gel, petroleum/ethyl acetate, 1:1) to afford the corresponding protected lactam.

(*E*)-1-Benzyl-3-(4-(trifluoromethyl)benzylidene)piperidin-2-one (S142). White solid, 54% yield (186 mg). ^{1}H NMR (401 MHz, $CDCl_3$), δ: 1.73-1.79 (m, 2H), 2.68-2.72 (m, 2H), 3.28-3.31 (m, 2H), 4.66 (s, 2H), 7.31-7.08 (m, 5H), 7.39 (d, *J* = 8.1 Hz, 2H), 7.56 (d, *J* = 8.1 Hz, 2H), 7.83 (s, 1H). ^{13}C NMR (401 MHz, $CDCl_3$), δ: 22.9. 26.5, 47.2, 51.4, 122.7 (q, *J* = 268.3), 125.2 (q, *J* = 3.0 Hz), 127.5, 129.8, 132.1, 134.0, 137.1, 139.8, 164.6.

3.4.4.4. General procedure for the hydrogenation of non-chelating olefins and olefins with a polar neighbouring group

The alkene (0.5 mmol) and the corresponding catalyst precursor [Ir(cod)(**L**)]BAr_F (2 mol %) were dissolved in the corresponding solvent (2 mL) and placed in a high-pressure autoclave. The autoclave was purged 4 times with hydrogen. Then, it was pressurized at the desired pressure. After the desired reaction time, the autoclave was depressurized and the solvent evaporated off. The residue was dissolved in Et_2O (1.5 ml) and filtered through a short plug of celite. The enantiomeric excess was determined by chiral GC or chiral HPLC and conversions were determined by ^{1}H NMR.

3.3.4.5. General procedure for the hydrogenation of cyclic β-enamides

The enamide (0.25 mmol) and the corresponding catalyst precursor [Ir(cod)(**L**)]BAr_F (1 mol%) were dissolved in in the corresponding solvent (1 mL) and placed in a high-pressure autoclave, which was purged four times with hydrogen. It was then pressurized at the desired pressure. After the desired reaction time, the autoclave was depressurized and the solvent evaporated off. The residue was dissolved in Et_2O (1.5 ml) and filtered through a short celite plug. The enantiomeric excess was determined by chiral HPLC and conversions were determined by ^{1}H NMR.

3.3.4.6. Computational details

All calculations were performed using the Gaussian 16 program.[39] Optimizations of [Ir(cod)**L13e**]BAr_F complexes were performed employing the B3LYP-D3[40] density functionaland the 6-31G(d)[41] basis set for all elements except for Ir for which SDD[42] was used. Solvation correction was applied in the course of the optimizations using the PCM model with the default parameters for dichloromethane.[43] The complexes were treated with charge +1 and in the singlet state. No symmetry constraints were applied.

The energies were further refined by performing single-point calculations using the above-mentioned parameters, with the exception that the density functional used was PBE-D2[44],[45] and the basis set was 6-311+G**[46] for all elements except for iridium. All energies reported are Gibbs free energies at 298.15 K and calculated as $\Delta G_{reported} = \Delta G_{B3LYP/6\text{-}31G(d)} + (\Delta E_{PBE\text{-}D2/6\text{-}311+G(d,p)} - \Delta E_{B3LYP/6\text{-}31G(d)})$.

3.3.5. References

[1] (a) Pfaltz, A.; Drury III, W. J. Design of chiral ligands for asymmetric catalysis: From C2–symmetric P,P– and N,N–ligands to sterically and electronically nonsymmetrical P,N–ligands. *PNAS*, **2004**, *101*, 5723–5726. (b) Yoon, T. P.; Jacobsen, E. N. Privileged chiral catalysts. *Science* **2003**, *299*, 1691–1693. (c) Sommer, W.; Weibel, D. *Asymmetric Catalysis, Privileged Ligands and Complexes*, Sigma Aldrich's Chemfiles, **2008**, *2***,** 1–91. (d) Zhou, Q., Ed. *Privileged Chiral Ligands and Catalysts*, John Wiley& Sons Inc.: New York, **2011**. (e) Diéguez, M., Ed. *Chiral ligands. Evolution of ligand libraries for asymmetric Catalysis*, CRC Press: Boca Raton, **2021**.

[2] (a) Coll, M.; Pàmies, O.; Diéguez, M. Thioether–phosphite: new ligands for the highly enantioselective Ir–catalyzed hydrogenation of minimally functionalized olefins. *Chem. Commun.* **2011**, *47*, 9215–9217. (b) Coll, M.; Pàmies, O.; Diéguez, M. A Modular Furanoside Thioether–Phosphite/Phosphinite/ Phosphine Ligand Library for Asymmetric Iridium–Catalyzed Hydrogenation of Minimally Functionalized Olefins: Scope and Limitations. *Adv. Synth. Catal.* **2013**, *355*, 143–160. (c) Margalef, J.; Caldentey, X.; Karlsson, E. A.; Coll, M.; Mazuela, J.; Pàmies, O.; Diéguez, M.; Pericàs, M. A. A Theoretically–Guided Optimization of a New Family of Modular P,S–Ligands for Iridium–Catalyzed Hydrogenation of Minimally Functionalized Olefins. *Chem. Eur. J.* **2014**, *20*, 12201–12214. (d) Borràs, C.; Biosca, M.; Pàmies, O.; Diéguez, M. Iridium–Catalyzed Asymmetric Hydrogenation with Simple Cyclohexane–Based P/S Ligands: *In Situ* HP–NMR and DFT Calculations for the Characterization of Reaction Intermediates. *Organometallics* **2015**, *34*, 5321–5334. (e) Biosca, M.; Coll, M.; Lagarde, F.; Brémond, E.; Routaboul, L.; Manoury, E.; Pàmies, O.; Poli, R.; Diéguez, M. Chiral ferrocene–based P,S ligands for Ir–catalyzed hydrogenation of minimally functionalized olefins. Scope and limitations. *Tetrahedron* **2016**, *72*, 2623–2631. (f) Margalef, J.; Pàmies, O.; Pericàs, M. A.; Diéguez, M. Evolution of phosphorus–thioether ligands for asymmetric catalysis. *Chem. Comm.* **2020**, *56*, 10795–10808. (g) Faiges, J.; Borràs, C.; Pastor, I. M.; Pàmies, O.; Besora, M.; Diéguez, M. Density Functional Theory–Inspired Design of Ir/P,S–Catalysts for Asymmetric Hydrogenation of Olefins. *Organometallics* **2021,** *40*, 20, 3424–3435.

[3] (a) Masdeu–Bultó, A. M.; Diéguez, M.; Martin, E.; Gómez, M. Chiral thioether ligands: coordination chemistry and asymmetric catalysis. *Coord. Chem. Rev.* **2003**, *242*, 159–201. (b) Mellah, M.; Voituriez, A.; Schultz, E. Chiral Sulfur Ligands for Asymmetric Catalysis. *Chem. Rev.* **2007**, *107*, 5133–5209. (c) Pellissier, H. Chiral sulfur–containing ligands for asymmetric catalysis. *Tetrahedron*, **2007**, *63*, 1297–1330. (d) Lam, F. L.; Kwong, F. Y.; Chan, A. S. C. Recent developments on chiral P,S–type ligands and their applications in asymmetric catalysis**.** *Chem. Commun.* **2010**, *46*, 4649–4667. (e) Carretero, J. C.; Adrio, J.; Rivero, M. R. In *Chiral Ferrocene in Asymmetric Catalysis*, (Ed.: L.–X. Dai, X.–L. Hou), *Sulfur– and Selenium–Containing Ferrocenyl Ligands in Chiral Ferrocenes in Asymmetric Catalysis*, Wiley–VCH, Weiheim, **2010**, pp. 257–282. (f) Gómez, R.; Carretero, J. C. Chiral thioether–based catalysts in asymmetric synthesis: recent advances. *Chem. Commun.* **2011**, *47*, 2207–2211.

[4] Margalef, J.; Biosca, M.; de la Cruz–Sánchez, P.; Caldentey, X.; Rodríguez–Escrich, C.; Pàmies, O.; Pericàs, M. A.; Diéguez, M. Indene Derived Phosphorus–Thioether Ligands for the Ir–Catalyzed

Asymmetric Hydrogenation of Olefins with Diverse Substitution Patterns and Different Functional Groups. *Adv. Synth. Catal.* **2021**, *363*, 4561–4574.

[5] These ligands have been recently successfully applied in the Pd–catalyzed allylic substitution reactions, see: Biosca, M.; Margalef, J.; Caldentey, X.; Besora, M.; Rodríguez–Escrich, C.; Saltó, J.; Cambeiro, X. C.; Maseras, F.; Pàmies, O.; Diéguez, M.; Pericàs, M. A. Computationally Guided Design of a Readily Assembled Phosphite–Thioether Ligand for a Broad Range of Pd–Catalyzed Asymmetric Allylic Substitutions. *ACS Catal.* **2018**, *8*, 3587−3601.

[6] Verendel, J. J.; Pàmies, O.; Diéguez, M.; Andersson, P. G. Asymmetric Hydrogenation of Olefins Using Chiral Crabtree–type Catalysts: Scope and Limitations. *Chem. Rev.* **2014**, *114*, 2130−2169.

[7] Pàmies, O.; Andersson, P.G.; Diéguez, M. Asymmetric Hydrogenation of Minimally Functionalised Terminal Olefins: An Alternative Sustainable and Direct Strategy for Preparing Enantioenriched Hydrocarbons. *Chem. Eur. J.* **2010**, *16*, 14232–14240.

[8] PC is a noncorrosive, nontoxic, and biodegradable environmentally friendly alternative to standard polar and aromatic solvents. See for instance: a) Bayardon, J.; Holz, J.; Schäffner, B.; Andrushko, V.; Verevkin, S. P.; Preetz, A.; Börner, A. Propylene Carbonate as a Solvent for Asymmetric Hydrogenations. *Angew. Chem., Int. Ed.* **2007**, *46*, 5971–5974. (b) Schäffner, B.; Holz, J.; Verevkin, S. P.; Börner, A. Organic carbonates as alternative solvents for palladium-catalyzed substitution reactions. *ChemSusChem* **2008**, *1*, 249–253. (c) Schäffner, B.; Schäffner, B.; Verevkin, S. P.; Börner, A. Organic carbonates as solvents in synthesis and catalysis. *Chem. Rev.* **2010**, *110*, 4554–4581.

[9] The isomerization process has been suggested to proceed via either protonation of the double bond at the terminal position, which gives a stabilized carbocation or the formation of Ir−π−allyl intermediates. See for instance: (a) Perry, M. C.; Cui, X.; Powell, M. T.; Hou, D.–R.; Reibenspies, J. H.; Burgess, K. Optically Active Iridium Imidazol–2–ylidene–oxazoline Complexes: Preparation and Use in Asymmetric Hydrogenation of Arylalkenes. *J. Am. Chem. Soc.* **2003**, *125*, 113–123. (b) Brown, J. M.; Derome, A. E.; Hughes, G. D.; Monaghan, P. K. Homogeneous Hydrogenation With Iridium Complexes. Evidence for Polyhydride Intermediates in the Reduction of α–Pinene**.** *Aust. J. Chem.* **1992**, *45*, 143–153.

[10] (a) Tian, F.; Yao, D.; Liu, Y.; Xie, F. Iridium–Catalyzed Highly Enantioselective Hydrogenation of Exocyclic α,β–Unsaturated Carbonyl Compounds. *Adv. Synth. Catal.* **2010**, *352*, 1841–1845. (b) Rageot, D.; Woodmansee, D. H.; Pugin, B.; Pfaltz, A. Proline–Based P,O Ligand/Iridium Complexes as Highly Selective Catalysts: Asymmetric Hydrogenation of Trisubstituted Alkenes. *Angew. Chem. Int. Ed.* **2011**, *50*, 9598–9601; *Angew. Chem.* **2011**, *123*, 9772–9775. (c) Li, J. Q.; Quan, X.; Andersson, P. G. Highly Enantioselective Iridium–Catalyzed Hydrogenation of α,β–Unsaturated Esters. *Chem. Eur. J.* **2012**, *18*, 10609–10616. (d) Woodmansee, D. H.; Müller, M. A.; Tröndlin, L.; Hörmann, E.; Pfaltz, A. Asymmetric Hydrogenation of α,β–Unsaturated Carboxylic Esters with Chiral Iridium N,P Ligand Complexes. *Chem. Eur. J.* **2012**, *18*, 13780–13786. (e) Liu, X.; Han, Z.; Wang, Z.; Ding, K. SpinPhox/Iridium(I)–Catalyzed Asymmetric Hydrogenation of Cyclic α–Alkylidene Carbonyl Compounds. *Angew. Chem. Int. Ed.* **2014**, *53*, 1978–1982. (f) Lu, S.–M.; Bolm, C. Highly Chemo– and Enantioselective Hydrogenation of Linear α,β–Unsaturated Ketones. *Chem. Eur. J.* **2008**, *14*, 7513–7516. (g) Lu, S. M.; Bolm, C. Highly Enantioselective Synthesis of Optically Active Ketones by Iridium–Catalyzed Asymmetric Hydrogenation. *Angew. Chem. Int. Ed.* **2008**, *47*, 8920–8923; *Angew. Chem.* **2008**, *120*, 9052–9055. (h) Lu, W.–J.; Chen, Y.–W.; Hou, X.–L. Iridium–Catalyzed Highly Enantioselective Hydrogenation of the C=C Bond of α, β–Unsaturated Ketones. *Angew. Chem. Int. Ed.* **2008**, *47*, 10133–10136; *Angew. Chem.* **2008**, *120*, 10287–10290. (i) Shang, J.; Han, Z.; Li, Y.; Wang, Z.; Ding, K. Highly enantioselective asymmetric hydrogenation of

(*E*)–β,β–disubstituted α,β–unsaturated Weinreb amides catalyzed by Ir(i) complexes of SpinPhox ligands. *Chem. Commun.* **2012**, *48*, 5172–5174. (j) Maurer, F.; Huch, V.; Ullrich, A.; Kazmaier, U. Development of Catalysts for the Stereoselective Hydrogenation of α,β–Unsaturated Ketones. *J. Org. Chem.* **2012**, *77*, 5139–5143. (k) Biosca, M.; Pàmies, O.; Diéguez, M. Giving a Second Chance to Ir/Sulfoximine–Based Catalysts for the Asymmetric Hydrogenation of Olefins Containing Poorly Coordinative Groups. *J. Org. Chem.* **2019**, *84*, 8259–8266.

[11] (a) *Comprehensive Asymmetric Catalysis*, (Eds. Jacobsen, E. N.; Pfaltz, A.; Yamamoto, H.), Springer–Verlag, Berlin, **1999**. (b) *Catalytic Asymmetric Synthesis*, *3rd ed.,* (Ed.: Ojima, I.), John Wiley & Sons, Inc., Hoboken, **2010**. (c) *Asymmetric Catalysis on Industrial Scale: Challenges, Approaches and Solutions*, *2nd ed.*, (Eds.: Blaser, H.–U.; Federsel, H.–J.), Wiley–VCH, Weinheim, **2010**. (d) Busacca, C. A.; Fandrick, D. R.; Song, J. J.; Senanayake, C. H. The Growing Impact of Catalysis in the Pharmaceutical Industry. *Adv. Synth. Catal.* **2011**, *353*, 1825–1864. (e) Ager, D. J.; de Vries, A. H. M.; de Vries, J. G. Asymmetric homogeneous hydrogenations at scale. *Chem. Soc. Rev*., **2012**, *41*, 3340–3380. (f) *Metal–catalyzed Asymmetric Hydrogenation. Evolution and Prospect* in Advances in Catalysis (Eds.: Diéguez, M.; Pizzano, A.), Elsevier, Oxford, Vol. 68, **2021**.

[12] For the reduction of α,β–unsaturated ketones the efficiency of most of Ir/P,N catalysts reported depended highly on the substitution pattern of the enone and the steric constrains of the olefin substituents. In addition, excellent enantioselectivities were mainly obtained for β,β'–disubstituted enones containing two large substituents. See, for instance ref. 10k.

[13] (a) Yue, T.–Y.; Nugent, W. A. Enantioselective Hydrogenation of 3–Alkylidenelactams: High–Throughput Screening Provides a Surprising Solution. *J. Am. Chem. Soc.* **2002**, *124*, 13692–13963. (b) Li, Q.; Wan, P.; He, Y.; Zhou, Y.; Li, L.; Chen, B.; Duan, K.; Cao, R.; Zhou, Z.; Qiu, L. Enantioselective Hydrogenation of the Double Bond of Exocyclic α,β–Unsaturated Carbonyl Compounds Catalyzed by Iridium/H_8–BINOL–Derived Phosphine–Oxazoline Complexes. *Asian J. Org. Chem.* **2014**, *3*, 774–783.

[14] Duggan, M. E.; Naylor–Olsen, A. M.; Perkins, J. J.; Anderson, P. S.; Chang, C. T.–C.; Cook, J. J.; Gould, R. J.; Ihle, N. C.; Hartman, G. D.; Lynch, J. J.; Lynch, R. J.; Manno, P. D.; Schaffer, L. W.; Smith, R. L. Non–Peptide Fibrinogen Receptor Antagonists. 7. Design and Synthesis of a Potent, Orally Active Fibrinogen Receptor Antagonist. *J. Med. Chem.* **1995**, *38*, 3332–3341.

[15] (a) Lu, W.-J.; Hou, X.-L. Highly Enantioselective Construction of the α–Chiral Center of Amides *via* Iridium–Catalyzed Hydrogenation of α,β–Unsaturated Amides. *Adv. Synth. Catal.* **2009**, *351*, 1224–1228. b) Ref. 10i. (c) Ref. 10a. (d) Ref. 10c.

[16] See for instance: (a) Cheruku, P.; Gohil, S.; Andersson, P. G. Asymmetric hydrogenation of enol phosphinates by iridium catalysts having N,P ligands. *Org. Lett.* **2007**, *9*, 1659–1661. (b) Cheruku, P.; Diesen, J.; Andersson, P. G. Asymmetric Hydrogenation of Di and Trisubstituted Enol Phosphinates with N,P– Ligated Iridium Complexes. *J. Am. Chem. Soc.* **2008**, *130*, 5595–5599.

[17] Ohkuma, T.; Noyori, R. In *Handbook of Homogeneous Hydrogenation*, *Vol. 3* (Eds.: J. G. de Vries, C. J. Elsevier), Wiley–VCH: Weinheim, Germany, **2007**, pp. 1105–1163.

[18] (a) Genêt, J. P. In *Modern Reduction Methods*; Andersson, P. G., Munslow, I. J., Eds; Wiley–VCH, Weinheim, **2008**, pp 3–38. (b) Tang, W.; Zhang, X. New Chiral Phosphorus Ligands for Enantioselective Hydrogenation. *Chem. Rev.* **2003**, *103*, 3029–3069. (c) Chi, Y.; Tang, W.; Zhang, X. In *Modern Rhodium–Catalyzed Organic Reactions*; Evans, P. A., Ed; Wiley–VCH: Weinheim, **2005**, pp 1–31. (d) Kitamura, M., Noyori, R. In *Ruthenium in Organic Synthesis*; Murahashi, S.–I., Ed.; Wiley–VCH: Weinheim, **2004**, pp 3–52. (e) Weiner, B.; Szymanski, W.; Janssen, D. B.; Minnaard, A. J.; Feringa, B. L. Recent Advances in the Catalytic Asymmetric Synthesis of Beta–amino Acids. *Chem. Soc. Rev.* **2010**, *39*, 1656–1691. (f) Xie, J.–H.; Zhu, S.–F.; Zhou, Q.–L. Transition Metal–

Catalyzed Enantioselective Hydrogenation of Enamines and Imines. *Chem. Rev.* **2011**, *111*, 1713–1760. (g) Etayo, P.; Vidal–Ferran, A. Rhodium–catalysed asymmetric hydrogenation as a valuable synthetic tool for the preparation of chiral drugs. *Chem. Soc. Rev.* **2013**, *42*, 728–754.

[19] Pham, D. Q.; Nogid, A. Rotigotine transdermal system for the treatment of Parkinson's disease. *Clin. Ther.* **2008**, *30*, 813–824.

[20] Astier, B.; Señas, L. L.; Soulière, F.; Schmitt, P.; Urbain, N.; Rentero, N.; Bert, L.; Denoroy, L.; Renaud, B.; Lesourd, M.; Muñoz, C.; Chouvet, G. In vivo comparison of two 5–HT_{1A} receptors agonists alnespirone (S–20499) and buspirone on locus coeruleus neuronal activity. *Eur. J. Pharmacol.* **2003**, *459*, 17–26.

[21] Ross, S. B.; Thorberg, S.–O.; Jerning, E.; Mohell, N.; Stenfors, C.; Wallsten, C.; Milchert, I. G.; Ojteg, G. A. Robalzotan (NAD–299), a Novel Selective 5–HT $_{1A}$ Receptor Antagonist. *CNS Drug Rev.* **1999**, *5*, 213–232.

[22] For selected examples: (a) Renaud, J. L.; Dupau, P.; Hay, A.–E.; Guingouain, M.; Dixneouf, P. H.; Bruneau, C. Ruthenium–Catalysed Enantioselective Hydrogenation of Trisubstituted Enamides Derived from 2–Tetralone and 3–Chromanone: Influence of Substitution on the Amide Arm and the Aromatic Ring. *Adv. Synth. Catal.* **2003**, *345*, 230–238. (b) Hoen, R.; van den Berg, M.; Bernsmann, H.; Minnaard, A. J.; de Vries, J. G.; Feringa, B. L. Catechol–Based Phosphoramidites: A New Class of Chiral Ligands for Rhodium–Catalyzed Asymmetric Hydrogenations. *Org. Lett.* **2004**, *6*, 1433–1436;ı. (c) Jiang, X.–B.; Lefort, L.; Goudriaan, P. E.; de Vries, A. H. M.; van Leeuwen, P. W. N. M.; Reek, J. N. H. Screening of a Supramolecular Catalyst Library in the Search for Selective Catalysts for the Asymmetric Hydrogenation of a Difficult Enamide Substrate. *Angew. Chem. Int. Ed.* **2006**, *45*, 1223–1227; *Angew. Chem.* **2006**, *118*, 1245–1249. (d) Sandee, A. J.; van der Burg, A. M.; Reek, J. N. H. UREAphos: supramolecular bidentate ligands for asymmetric hydrogenation. *Chem. Commun.* **2007**, 864–866. (e) Revés, M.; Ferrer, C.; León, T.; Doran, S.; Etayo, P.; Vidal–Ferran, A.; Riera, A.; Verdaguer, X. Primary and Secondary Aminophosphines as Novel P–Stereogenic Building Blocks for Ligand Synthesis. *Angew. Chem. Int. Ed.* **2010**, *49*, 9452–9455; *Angew. Chem.* **2010**, *122*, 9642–9645. (f) Wu, Z.; Ayad, T.; Ratovelomanana–Vidal, V. Efficient Enantioselective Synthesis of 3–Aminochroman Derivatives Through Ruthenium–Synphos Catalyzed Asymmetric Hydrogenation. *Org. Lett.* **2011**, *13*, 3782–3785. (g) Pignataro, L.; Boghi, M.; Civera, M.; Carboni, S.; Piarulli, U.; Gennari, C. Rhodium–Catalyzed Asymmetric Hydrogenation of Olefins with PhthalaPhos, a New Class of Chiral Supramolecular Ligands. *Chem. Eur. J.* **2012**, *18*, 1383–1400. (h) Frank, D. J.; Franzke, A.; Pfaltz, A. Asymmetric Hydrogenation Using Rhodium Complexes Generated from Mixtures of Monodentate Neutral and Anionic Phosphorus Ligands. *Chem. Eur. J.* **2013**, *19*, 2405–2415. (i) Bravo, M. J.; Ceder, R. M.; Muller, G.; Rocamora, M. New Enantiopure P,P–Bidentate Bis(diamidophosphite) Ligands. Application in Asymmetric Rhodium–Catalyzed Hydrogenation. *Organometallics* **2013**, *32*, 2632–2642. (j) Arribas, I.; Rubio, M.; Kleman, P.; Pizzano, A. Rhodium Phosphine–Phosphite Catalysts in the Hydrogenation of Challenging *N*–(3,4–dihydronaphthalen–2–yl) Amide Derivatives. *J. Org. Chem.* **2013**, *78*, 3997–4005. (k) Liu, G.; Liu, X.; Cai, Z.; Jiao, G.; Xu, G.; Tang, W. Design of Phosphorus Ligands with Deep Chiral Pockets: Practical Synthesis of Chiral β–Arylamines by Asymmetric Hydrogenation. *Angew. Chem. Int. Ed.* **2013**, *52*, 4235–4238; *Angew. Chem.* **2013**, *125*, 4329–4332.

[23] (a) Salomó, E.; Orgué, S.; Riera, A.; Verdaguer, X. Highly Enantioselective Iridium-Catalyzed Hydrogenation of Cyclic Enamides. *Angew. Chem. Int. Ed.* **2016**, *55*, 7988–7992. (b) Magre, M.; Pàmies, O.; Diéguez, M. PHOX–Based Phosphite–Oxazoline Ligands for the Enantioselective Ir–Catalyzed Hydrogenation of Cyclic β–Enamides. *ACS Catal.* **2016**, *6*, 5186–5190. (c) Margalef, J.; Pàmies, O.; Diéguez, M. Phosphite–Thiother Ligands Derived from Carbohydrates allow the

Enantioswitchable Hydrogenation of Cyclic β–Enamides by using either Rh or Ir Catalysts. *Chem. Eur. J.* **2018**, *23*, 813–822.

[24] Buisman, G. J. H. Kamer, P. C. J.; van Leeuwen, P. W. N. M. Rhodium catalysed asymmetric hydroformylation with chiral diphosphite ligands. *Tetrahedron: Asymmetry* **1993**, *4*, 1625–1634.

[25] Dupau, P.; Le Gendre, P.; Bruneau, C.; Dixneuf, P. H. Optically Active Amine Derivatives: Ruthenium–Catalyzed Enantioselective Hydrogenation of Enamides. *Synlett* **1999**, *1999*, 1832–1834.

[26] Yanagisawa, A.; Nezu, T.; Mohri, S.–I. Brønsted Acid–Promoted Hydrocyanation of Arylalkenes. *Org. Lett*. **2009**, *11*, 5286–5289.

[27] McIntyre, S.; Hörmann, E.; Menges, F.; Smidt, S. P.; Pfaltz, A. Iridium–Catalyzed Enantioselective Hydrogenation of Terminal Alkenes. *Adv. Synth. Catal.* **2005**, *347*, 282−288.

[28] Too, P. C.; Noji, T.; Lim, Y. J.; Li, X.; Chiba, S. Rhodium(III)–Catalyzed Synthesis of Pyridines from α,β–Unsaturated Ketoximes and Internal Alkynes. *Synlett* **2011**, *19*, 2789–2794.

[29] Deng, K.; Huai, Q.–Y.; Shen, Z.–L.; Li, H.–J.; Liu, C.; Wu, C.–Y. Rearrangement of Dypnones to 1,3,5–Triarylbenzenes. *Org. Lett.* **2015**, *17*, 1473–1476.

[30] Galambos, J.; Wágner, G.; Nógrádi, K.; Bielik, A.; Molnár, L.; Bobok, A.; Horváth, A.; Kiss, B.; Kolok, S.; Nagy, J.; Kurkó, D.; Bakk, M. L.; Vastag, M.; Sághy, K.; Gyertyán, I.; Gál, K.; Greiner, I.; Szombathelyi, Z.; Keserű, G. M.; Domány, G. Carbamoyloximes as novel non–competitive mGlu5 receptor antagonists. *Bioorg. Med. Chem. Lett*. **2010**, *20*, 4371–4375.

[31] Yang, J.; Li, X.; You, C.; Li, S.; Guan, Y.–Q.; Lv, H.; Zhang, X. Rhodium–catalyzed asymmetric hydrogenation of exocyclic α,β–unsaturated carbonyl compounds. *Org. Biomol. Chem.* **2020**, *18*, 856–859.

[32] Wu, Y.–L.; Gao, Y.–Q.; Wang, D.–L.; Zhong, C.–Q.; Feng, J.–T.; Zhang, X. Bioactivity–guided mixed synthesis and evaluation of α–alkenyl–γ and δ–lactone derivatives as potential fungicidal agents. *RSC Adv.* **2017**, *7*, 56496–56508.

[33] Hatch, L. F.; Patton, T. L. Allylic Chlorides. XXI. 3–Chloro–2–phenyl–1–propene. *J. Am. Chem. Soc.* **1954**, *76*, 2705–2707.

[34] Decribed in the Experimental Section and Supporting Information of Section 3.2.

[35] Chen, X.; Yang, H.; Ge, Y.; Feng, L.; Jia, J.; Wang, J. Synthesis, X–ray crystal structure and optical properties of novel 2–aryl–3–ethoxycarbonyl–4–phenylpyrido[1,2–a]benzimidazoles. *Luminescence* **2012**, *27*, 382–389.

[36] Sugimoto, K.; Oshiro, M.; Hada, R.; Matsuya, Y. 2,2–Biphenol/$B(OH)_3$ Catalyst System for Nazarov Cyclization. *Chem. Pharm. Bull.* **2019**, *67*, 1019–1022.

[37] Biosca, M.; Paptchikhine, A.; Pamies, O.; Andersson, P. G.; Diéguez, M. Extending the Substrate Scope of Bicyclic P–Oxazoline/Thiazole Ligands for Ir–Catalyzed Hydrogenation of Unfunctionalized Olefins by Introducing a Biaryl Phosphoroamidite Group. *Chem. Eur. J.* **2015**, *21*, 3455−3464.

[38] Pautigny, C.; Debouit, C.; Vayron, P.; Ayad, T. Ratovelomanana–Vidal, V. Asymmetric hydrogenation of trisubstituted *N*–acetyl enamides derived from 2–tetralones using ruthenium–SYNPHOS catalysts: a practical synthetic approach to the preparation of $β_3$–adrenergic agonist SR58611A. *Tetrahedron: Asymmetry* **2010**, *21*, 1382–1388.

[39] Frisch, M. J.; Trucks, G. W.; Schlegel, H. B.; Scuseria, G. E.; Robb, M. A.; Cheeseman, J. R.; Scalmani, G.; Barone, V.; Petersson, G. A.; Nakatsuji, H.; Li, X.; Caricato, M.; Marenich, A.; Bloino, J.; Janesko,B.G.;Gomperts,R.;Mennucci,B.;Hratchian,H.P.;Ortiz,J. V.; Izmaylov, A. F.; Sonnenberg, J. L.; Williams–Young, D.; Ding, F.; Lipparini, F.; Egidi, F.; Goings, J.; Peng, B.; Petrone, A.; Henderson, T.; Ranasinghe, D.; Zakrzewski, V. G.; Gao, J.; Rega, N.; Zheng, G.; Liang, W.; Hada, M.; Ehara, M.; Toyota, K.; Fukuda, R.; Hasegawa, J.; Ishida, M.; Nakajima, T.; Honda, Y.; Kitao,

O.; Nakai, H.; Vreven, T.; Throssell, K.; Montgomery, J. A., Jr.; Peralta, J. E.; Ogliaro, F.; Bearpark, M.; Heyd, J. J.; Brothers, E.; Kudin, K. N.; Staroverov, V. N.; Keith, T.; Kobayashi, R.; Normand, J.; Raghavachari, K.; Rendell, A.; Burant, J. C.; Iyengar, S. S.; Tomasi, J.; Cossi, M.; Millam, J. M.; Klene, M.; Adamo, C.; Cammi, R.; Ochterski, J. W.; Martin, R. L.; Morokuma, K.; Farkas, O.; Foresman, J. B.; Fox, D. J. Gaussian 09, Revision A.02; Gaussian, Inc.: Wallingford CT, 2016.

[40] (a) Lee, C.; Yang, W.; Parr, R. G. Development of the Colle–Salvetti correlation–energy formula into a functional of the electron density. *Phys. Rev. B* **1988**, *37*, 785–789.(b) Becke, A. D. Density–functional thermochemistry. III. The role of exact Exchange. *J. Chem. Phys.* **1993**, *98*, 5648−5652. (c) Grimme, S.; Antony, J.; Ehrlich, S.; Krieg, H. A consistent and accurate ab initio parametrization of density functional dispersion correction (DFT–D) for the 94 elements H–Pu. *J. Chem. Phys.* **2010**, *132*, 154104. (d) Grimme, S.; Ehrlich, S.; Goerigk, L. Effect of the damping function in dispersion corrected density functional theory. *J. Comput. Chem.* **2011**, *32*, 1456–1465. (e) Kruse, H.; Goerigk, L.; Grimme, S. Why the Standard B3LYP/6–31G* Model Chemistry Should Not Be Used in DFT Calculations of Molecular Thermochemistry: Understanding and Correcting the Problem. *J. Org. Chem.* **2012**, *77*, 10824–10834.

[41] (a) Hehre, W. J.; Ditchfeld, R.; Pople, J. A. Self—Consistent Molecular Orbital Methods. XII. Further Extensions of Gaussian—Type Basis Sets for Use in Molecular Orbital Studies of Organic Molecules. *J. Chem. Phys.* **1972**, *56*, 2257–2261. (b) Hariharan, P. C.; Pople, J. A. The influence of polarization functions on molecular orbital hydrogenation energies. *Theor. Chim. Acta* **1973**, *28*, 213–222. (c) Francl, M. M.; Pietro, W. J.; Hehre W. J.; Binkley, J. S.; Gordon, M. S.; Defrees, D. J.; Pople, J. A. Self-consistent molecular orbital methods. XXIII. A polarization-type basis set for second-row elements. *J. Chem. Phys.* **1982**, *77*, 3654–3665.

[42] Andrae, D.; Häußermann. U.; Dolg, M.; Stoll, H., Preuß, H. Energy–adjusted*ab initio* pseudopotentials for the second and third row transition elements. *Theor. Chim. Acta* **1990**, *77*, 123–141.

[43] (a) Miertus, S.; Tomasi, J. Approximate evaluations of the electrostatic free energy and internal energy changes in solution processes. *Chem. Phys.* **1982**, *65*, 239−245. (b) Mennucci, B.; Tomasi, J. Continuum solvation models: A new approach to the problem of solute's charge distribution and cavity boundaries. *J. Chem. Phys.* **1997**, *106*, 5151−5158. (c) Cossi, M.; Barone, V.; Mennucci, B.; Tomasi, J. Ab initio study of ionic solutions by a polarizable continuum dielectric model. *Chem. Phys. Lett.* **1998**, *286*, 253−260.

[44] Hopmann et. al. showed that the PBE–D2 density funcional was among the most accurate computational methods for computing free energies on iridium–based catalytic systems. See: Hopmann, K. H. How Accurate is DFT for Iridium–Mediated Chemistry? *Organometallics* **2016**, *35*, 3795–3807.

[45] (a) Perdew, J. P.; Burke, M.; Ernzerhof, K. Generalized Gradient Approximation Made Simple. *Phys. Rev. Lett.* **1996**, *77*, 3865−3868. (b) Perdew, J. P.; Burke, K.; Ernzerhof, M. Generalized Gradient Approximation Made Simple. *Phys. Rev. Lett.* **1997**, *78*, 1396.

[46] (a) Krishnan, R.; Binkley, J. S.; Seeger, R.; Pople, J. A. Self–consistent molecular orbital methods. XX. A basis set for correlated wave functions. *J. Chem. Phys.* **1980**, *72*, 650−654. (b) McLean, A. D.; Chandler, G. S. Contracted Gaussian basis sets for molecular calculations. I. Second row atoms, *Z*=11–18. *J. Chem. Phys.* **1980**, *72*, 5639−5648.

3.5. Ir/thioether–carbene, –phosphinite and –phosphite complexes for asymmetric hydrogenation. A case for comparison

3.5.1. Introduction

In the last two decades, *N*-heterocyclic carbenes have emerged as powerful alternatives for phosphine ligands[1] in catalysis thanks to their strong σ-donor ability, air stability and robustness.[2] In this respect, in 2001, Burgess' group reported for the first time that NHC-oxazoline based Ir-catalysts can also be applied in the asymmetric hydrogenation of unfunctionalized olefins with results comparable to the commonly used Ir-P,N catalysts.[1a,b] However, these catalysts afforded high enantioselectivities (up to 98% ee) in a limited group of unfunctionalized olefins, mainly trisubstituted and for the more challenging disubstituted olefins only one example was reported with low enantioselectivity. Since then, a few more carbene-N ligands have been developed but with less success,[1c-g] except for the family of Ir-NHC-pyridine catalysts[1h] developed in Pfaltz's group that showed similar enantioselectivities to the Burgess ones. Some Ir/carbene-phosphorus catalysts have also been tested but with low success.[3] However, the combination of the carbene moiety to other heteroatom donor groups have not been applied to asymmetric hydrogenation of unfunctionalized olefins.

In 2011, our group reported the first application of P-thioether ligands in AH of unfunctionalized olefins[4a,b] and further improvements with new generations of P-thiother ligands.[4c-i] Their corresponding Ir-complexes efficiently catalyzed the hydrogenation of 40 cases including a large range of *E*- and *Z*-trisubstituted olefins and the more challenging disubstituted olefins. The results were comparable to the best ones catalytic systems found in the literature. In addition, more recently we found that some of these Ir-based P-thioether catalysts could also efficiently reduce cyclic β-enamides.[4f,5]

Inspired by the pioneering work on the asymmetric hydrogenation of unfunctionalized olefins using NHC-based ligands and the success of thioether-containing ligands in the asymmetric hydrogenation,[6] in this section, we report a combination of these scaffolds as a logical field for investigation. Consequently, we here report the first examples of mixed thioether-carbene compounds, **L19**H·Br and **L20**H·Br (Figure 3.5.1) for the asymmetric hydrogenation of unfunctionalized olefins and cyclic β-enamides.[7] These ligands combine the advantages of thioether and NHC moieties. For comparison, we also synthesized their related thioether-phosphite **L21**–**L22a**–**b** and thioether-phosphinite **L21**–**L22c**–**e** ligands. For the purpose of this work, only two thioether substituents, phenyl and 2,6-dimethylphenyl, were used because previous work with Ir/P-thioether catalysts showed that these two substituents made it possible to achieve high enantioselectivities.[5d-f]

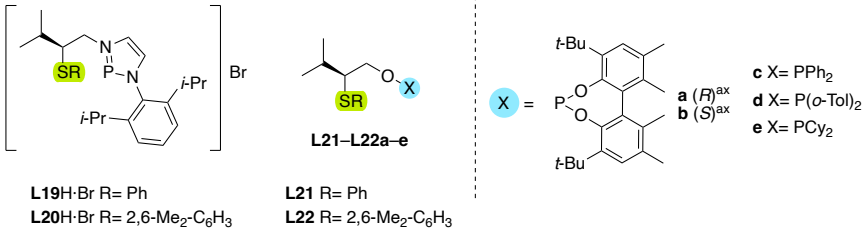

Figure 3.5.1. Thioether-carbene (**L19**–**L20**H·Br) and thioether-phosphite/phosphinite (**L21**–**L22a**–**e**) compounds.

3.5.2. Results and discussion

3.5.2.1. Preparation of [Ir(cod)(L1–L4)]BAr$_F$ catalyst precursors

The preparation of novel thioether-imidazolium salts (**L19**–**L20**H·Br) and thioether-phosphite/phosphinite ligands (**L21**–**L22a**–**e**) was carried out from readily available Evan's *N*-acyl carboximide **11**[8] as depicted in Scheme 3.5.1. The stereospecific introduction of the thioether group was carried out after selective α-bromation of **11** using *N*-bromosuccinimide (NBS) and dibutylboryl triflate (step i),[9] followed by treatment with the corresponding *insitu* formed thiolate (step ii)[10]. The resulting compounds were then treated with lithium borohydride to yield the desired hydroxyl-thioether compounds **12** and **13** (step iii).[10] From this point the synthesis followed two different pathways depending on the type of ligand. For the preparation of the thioether-imidazolium salts (**L19**–**L20**H·Br), compounds **12** and **13** were treated with tetrabromomethane and triphenylphosphine to yield thioether-bromine intermediates (step iv).[11] Reaction of the latter with 1-(2,6-diisopropylphenyl)-1*H*-imidazole[12] gave access to the desired thioether-imidazolium ligand precursors **L19**–**L20**H·Br (step v). For the synthesis of the thioether-phosphite/phosphinite ligands **L21**–**L22c**–**e**, hydroxyl-thioethers **12** and **13** were treated with the corresponding phosphorochloridite (step vi) or chlorophosphine (step vii). Thioether-imidazolium salts (**L19**–**L20**H·Br) and thioether-phosphite ligands (**L21**–**L22a**–**e**) were isolated as air stable solids whereas the thioether-phosphinite ligands (**L21**–**L22c**–**e**) were isolated as oils that needed to be stored under argon or at low temperature, since they slowly decompose in air at room temperature. In this case, they were immediately used for preparing the Ir-catalyst precursors.[13]

For the preparation of the Ir-catalyst precursors containing the thioether-carbene ligands ([Ir(cod)(**L19**–**L20**)]BAr$_F$), the imidazolium salts were first treated with Ag_2O to form the corresponding silver-carbene complexes (step viii). Then, transmetallation of the latter Ag-complexes with 0.5 equivalent of [Ir(μ-Cl)cod]$_2$ followed by in situ Cl^-/BAr$_F^-$ counterion exchange led to the desired [Ir(cod)(**L19**–**L20**)]BAr$_F$ (step ix). For the preparation of the Ir-catalyst precursors containing the thioether-phosphite/phosphinite

ligands ([Ir(cod)(**L21**–**L22a**–**e**)]BAr_F), the corresponding ligands were directly coordinated to Ir by reaction with 0.5 equivalent of [Ir(μ-Cl)cod]$_2$ followed by in situ Cl^-/BAr_F^- counterion exchange (step x). All complexes, even the phosphinite-based ones, were isolated as air-stable orange solids in pure form. The HRMS-ESI spectra were in agreement with the assigned structures, displaying the heaviest ions at m/z which correspond to the loss of the BAr_F anion from the molecular species. NMR spectra showed the expected pattern for these C_1-complexes (see experimental and Supporting Information for characterization details).[14]

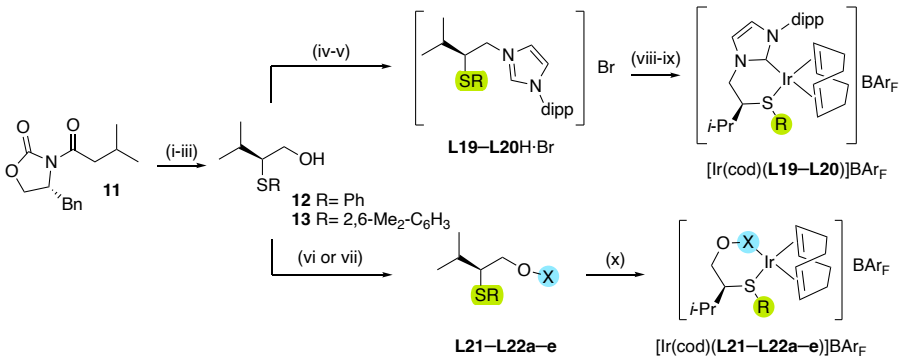

Scheme 3.5.1. Preparation of [Ir(cod)(**L19–L22**)]BAr_F catalyst precursors. (i) DIPEA, *n*-Bu_2BOTf, NBS, CH_2Cl_2, -78 °C, 3 h; (ii) RSH, DBU, THF, -10 °C during 1.5 h and then 2.5 h at rt; (iii) $LiBH_4$, H_2O, THF, rt, 16 h; (iv) CBr_4, PPh_3, CH_2Cl_2, 0 °C, 16 h; (v) 1-(2,6-diisopropylphenyl)-1H-imidazole, CH_3CN, reflux, 1.5 d; (vi) $ClP(OR')_2$ (OR'$_2$= **a**–**b**), Py, toluene, 80 °C, 16 h; (vii) $ClPX_2$ (X= c–e), NEt_3, DMAP, toluene, rt, 20 min; (viii) Ag_2O, CH_2Cl_2, 16 h; (ix) [Ir(μ-Cl)(cod)]$_2$, CH_2Cl_2, rt, 4.5 h then $NaBAr_F$, rt, 1 h. (x) [Ir(μ-Cl)(cod)]$_2$, CH_2Cl_2, 50 °C, 1 h then $NaBAr_F$, H_2O, rt, 30 min.

3.5.2.2. Catalytic experiments

3.5.2.2.1. Asymmetric hydrogenation of trisubstituted unfunctionalized olefins

To first evaluate de potential of the new catalyst precursors [Ir(cod)(**L1**–**L4**)]BAr_F in the asymmetric hydrogenation of trisubstituted olefins a comparative study using substrates **S27**, **S44**, **S64**, **S135** and **S58** was performed (Table 3.5.1). These substrates were chosen because they represent different substitution patterns with different functional groups with increasing coordinating abilities. They cover from olefin **S27** without a coordinative functional group, to olefin **S58**, which has a coordinative functional group that can also anchor the substrate to the metal. Note that substrates **S44**, **S64** and **S135**, which contain neighbouring polar groups, typically do not coordinate in Rh- and Ir-complexes.[15] To compare with the state of the art, we used the same optimal reaction conditions found in previous studies with other Ir/P-S systems.[4d]

The results indicate that the Ir/thioether-carbene catalysts are typically less active than the phosphite and phosphinite analogues, except in the hydrogenation of enol phosphonate **S27**. These results can be correlated with the fact that the presence of the bulky dipp group at the *N*-heterocylic carbene moiety gives the Ir/thioether-carbene catalytic system a higher sterical congestion around the metal center than in the case of the phosphite and phosphinite analogues. Such a steric hindrance hampers the olefin coordination which, at the same time, triggers the deactivation of the Ir-catalyst probably due to the formation of inactive trimeric species (see reactivity studies below).[16] Catalyst deactivation can be avoided in the presence of a good coordinating functional group like for the hydrogenation of **S27**.

Regarding the enantiomeric outcome of the reactions, the use of catalyst precursors with the carbene moiety sharply reduces the enantioselectivity compared with the use of thioether-phosphite/phosphinite analogues. This decrease in enantioselectivity is large for substrates with poorly coordinative or non-coordinative groups (**S27**, **S44**, **S64**, **S135** and **S58**) but less pronounced for the hydrogenation of **S58**. Results also indicate that each substrate requires a different catalyst to maximize the enantioselectivity. The highest enantioselectivities were typically achieved with catalyst precursors with a thioether-phosphinite ligand (ee's between 82-93%), except for **S135** for which ee's were best using phosphite-based catalyst precursor [Ir(cod)(**L22b**)]BAr_F (ee's up to 97% ee).

3.5.2.2.2. Asymmetric hydrogenation of 1,1-disubstituted unfunctionalized olefins

We then focused on the asymmetric hydrogenation of 1,1-disubstituted olefins (substrates **S25**, **S14, S53** and **S61**, Table 3.5.2). These substrates are less hindered than the trisubstituted olefins, so they are more easily hydrogenated but, in turn, face-selectivity is more difficult to control. Substrates were chosen because, again, they have different functional groups with increasing coordinating abilities, from non-coordinative **S25** and **S14** to coordinative olefin **S61**. Again we used the same optimal reaction conditions found in previous studies with Ir/P-S catalysts. Thus, substrates **S25**, **S14, S53** were reduced at 1 bar of hydrogen while 50 bars were required for **S61**. In contrast to the results reported above, full conversions were achieved with carbene-based catalytic systems, except for the more sterically hindered substrate **S14**. These results are in line with the formation of inactive species when attempting to hydrogenate **S14** with Ir-**L19**/**L20** catalysts. Agreeing with previous results, the use of phosphite and phosphinite-based catalytic systems (Ir-**L21**/**L22**) provided higher enantioselectivities than Ir-**L19**/**L20** catalytic systems, and the decrease in enantioselectivity with carbene-based catalysts is less pronounced for the hydrogenation of **S61**, with a good coordinative functional group. Again, the correct choice of the catalyst is necessary to maximize enantioselectivities for each substrate type. It is to note the excellent enantioselectivities,

Table 3.5.1. Asymmetric hydrogenation of trisubstituted olefins **S27**, **S44**, **S64**, **S135** and **S58** using [Ir(cod)(**L19–L22**)]BAr_F catalyst precursors.[a]

		S27		**S44**		**S64**		**S135**		**S58**	
Entry	L	% Conv[b]	% ee[c]	% Conv[b]	% ee[c]	% Conv[b]	% ee[c]	% Conv[b]	% ee[c]	% Conv[b]	% ee[c]
1	**L19**	15	2 (*R*)	10	9 (*R*)	20	25 (*R*)	20	20 (*R*)	100	75 (*S*)
2	**L20**	25	4 (*S*)	25	5 (*S*)	30	8 (*S*)	10	28 (*R*)	95	70 (*S*)
3	**L21a**	100	48 (*S*)	80	20 (*R*)	90	80 (*S*)	90	68 (*R*)	25	72 (*S*)
4	**L21b**	85	36 (*S*)	70	60 (*S*)	80	50 (*S*)	100	75 (*S*)	25	9 (*S*)
5	**L21c**	95	61 (*S*)	95	82 (*S*)	100	31 (*S*)	100	70 (*S*)	86	85 (*S*)
6	**L22a**	100	43 (*S*)	95	56 (*R*)	95	13 (*S*)	100	83 (*R*)	15	30 (*R*)
7	**L22b**	95	39 (*S*)	10	65 (*S*)	75	6 (*S*)	100	97 (*S*)	30	17 (*S*)
8	**L22c**	100	90 (*S*)	98	38 (*S*)	100	75 (*S*)	100	85 (*S*)	100	85 (*S*)
9	**L22d**	100	91 (*S*)	100	45 (*S*)	100	89 (*S*)	100	47 (*S*)	95	75 (*S*)
10	**L22e**	100	89 (*S*)	100	55 (*S*)	100	93 (*S*)	95	66 (*S*)	70	10 (*S*)

[a] Reaction conditions: substrate (0.5 mmol), Ir-catalyst precursor (1 mol%), H_2 (100 bar). [b] Conversions determined by ^{1}H-NMR. [c] Enantiomeric excesses determined by chiral HPLC or GC.

comparable to the best one reported, achieved with phosphite-based catalysts in the hydrogenation of **S14** and **S61** (ee's >97%).[17]

Table 2. Asymmetric hydrogenation of 1,1'-disusbtitued olefins **S25**, **S18, S53** and **S61** using [Ir(cod)(**L19**–**L22**)]BArF catalyst precursors.[a]

		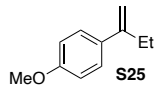 **S25**	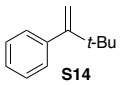 **S14**	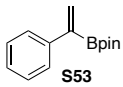 **S53**	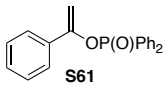 **S61**
Entry	L	% ee[c]	% ee[c]	% ee[c]	% ee[c]
1	**L19**	2 (*S*)	-[f]	10 (*R*)	91 (*S*)
2	**L20**	3 (*R*)	-[f]	9 (*R*)	61 (*S*)
3	**L21a**	7 (*S*)[d]	15 (*R*)	44 (*S*)	94 (*S*)
4	**L21b**	46 (*R*)	91 (*R*)	1 (*S*)	98 (*S*)
5	**L21c**	38 (*R*)	80 (*R*)	74 (*R*)	3 (*S*)
6	**L22a**	25 (*S*)[e]	56 (S)	33 (*S*)	21 (*R*)
7	**L22b**	50 (*R*)	97 (*R*)	53 (*R*)	51 (*S*)
8	**L22c**	60 (*R*)	88 (*R*)	68 (*R*)	70 (*S*)[g]
9	**L22d**	60 (*R*)	91 (*R*)	44 (*R*)	85 (*S*)
10	**L22e**	52 (*R*)	65 (*R*)	54 (*R*)	70 (*S*)[g]

[a] Reaction conditions: substrate (0.5 mmol), Ir-catalyst precursor (1 mol%), H_2 (1 bar for **S25**, **S18, S53** or 50 bar for **S61**). Full conversions obtained unless otherwise noted. [b] Conversions determined by ^{1}H-NMR. [c] Enantiomeric excesses determined by chiral HPLC or GC. [d] 90% conversion. [e] 80% conversion. [f] <5% conversion. [g] 95% conversion.

Like other cases reported in the literature, the hydrogenation of the α-alkylstyrene derivative **S25** proceeded with a much lower enantioselectivity than the analogue **S14**.[17a] This can be due to the fact that either hydrogenation competes with isomerization or that face selectivity is not successfully controlled. To find the explanation, we studied the reduction of **S25** using deuterium, with Ir/S-carbene (**L20**), Ir/S-phosphite (**L22b**) and Ir/S-phosphinite (**L22c**) as catalyst precursors (Scheme 3.5.2). With the Ir/S-phosphite/phosphinite catalyst systems, deuterium was found not only found at the double bond but also at the allylic position. This suggests that the isomerization process[18] is responsible for the low enantioselectivity achieved. On the other hand, isomerization was hardly seen with the Ir/S-carbene catalyst **L20**, which suggest that the low enantioselectivity is due to face-selectivity issues.

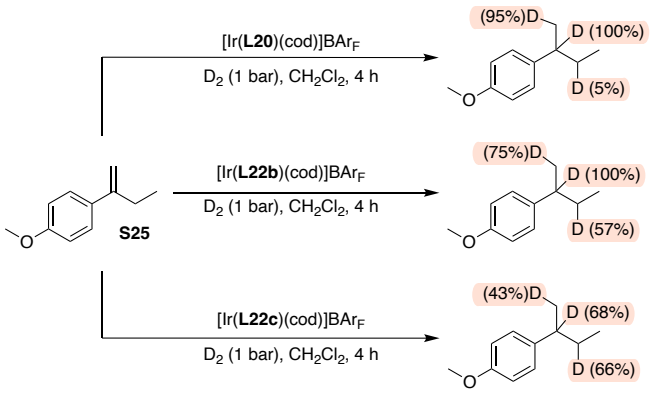

Scheme 3.5.2. Deuterium labeling studies of substrate **S25** with Ir/**L20**, Ir/**L22b** and Ir/**L22c** catalysts precursors. The percentage of addition of deuterium is illustrated in brackets.

3.5.2.2.3. Asymmetric hydrogenation of cyclic β-enamides

Finally, we studied the asymmetric hydrogenation of cyclic β-enamides which are a challenging class of functionalized substrates. As discussed in the previous section, the selective reduction of these substrates is highly desirable because their hydrogenated products (rotigotine, robalzotan and alnespirone) have important therapeutic properties.[19] Only a few examples are able to hydrogenate a broad range of these substrates in high enantioselectivities. Most of the catalysts, predominantly based on Rh and Ru, provide unsatisfactory enantioselectivities in reducing cyclic β-enamides.[20] We therefore, following the steps of the previous capter, studied first the Ir-catalyzed asymmetric hydrogenation of the benchmark *N*-(3,4-dihydronaphthalen-2-yl)acetamide **S8** under previously reported conditions.[5] The results are shown in Table 3.5.3. Gratifyingly, we found enantioselectivities as high as 96% ee using Ir/phosphinite-thioether **L22d** catalytic system (entry 10). Again P-thioether containing catalysts had a higher catalytic performance than the carbene-thioether based catalysts, being the best results with phosphinite-based catalysts.

We further studied Ir/**L22d** in the reduction of a range of substituted cyclic β-enamides, which contemplate all possible monosubstitution patterns (Figure 3.5.2). We were pleased to see that they were all hydrogenated in enantioselectivities (ee's up to 97%) comparable to those achieved with substrate **S8**. Among them, it is to note the high enantioselectivity obtained in the asymmetric hydrogenation of **S148** whose hydrogenated product is a key intermediate for the synthesis of rotigotine.

Table 3.5.3. Ir-catalyzed asymmetric hydrogenation of **S8** using **L19**–**L22a**–**e**.[a]

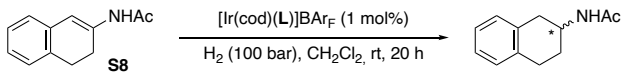

Entry	Ligand	% Conv[b]	% ee[b]
1	**L19**	30	72 (*R*)
2	**L20**	25	69 (*R*)
3	**L21a**	100	69 (*R*)
4	**L21b**	90	57 (*S*)
5	**L21c**	95	92 (*R*)
6	**L22a**	80	61 (*S*)
7	**L22b**	100	80 (*R*)
8	**L22c**	100	85 (*R*)
9	**L22d**	100	96 (*R*)
10	**L22e**	100	88 (*R*)

[a] Reaction conditions: Substrate (0.25 mmol), Ir-catalyst precursor (1 mol%), H_2 (50 bar), CH_2Cl_2 (1 mL), rt, 20 h. [b] Conversion measured by ^{1}H-NMR and enantiomeric excesses determined by HPLC.

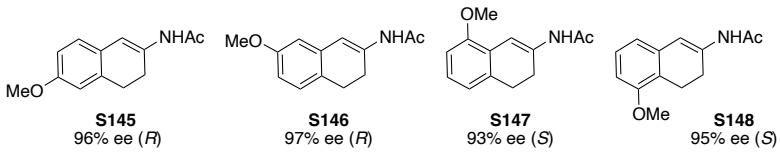

Figure 3.5.2. Hydrogenation results for the asymmetric hydrogenation of cyclic β-enamides. Typical reaction conditions: 1 mol% of [Ir(cod)(**L**)]BAr_F, 100 bar, CH_2Cl_2, rt for 20 h. Full conversions obtained in all cases.

3.5.2.3. Reactivity studies of [Ir(cod)(L)]BAr_F towards H_2

We investigated the reactivity of the iridium catalyst precursors with hydrogen. For comparison purposes we considered compounds [Ir(cod)(L)]BAr_F containing the thioether-carbene ligand **L20**, the thioether-phosphite ligand **L22b** and the thioether-phosphinite ligand **L22d** as models. As expected, the oxidative addition of H_2 to the [Ir(cod)(**L20**)]BAr_F is more favored than with the analogous phosphinite- and phosphite-based compounds. When the temperature was above - 78°C the formation of the stable and catalytically inactive trinuclear iridium hydrido species [$Ir_3(\mu_3$-H)$(H)_6$(C-S)$_3$]$(BAr_F)_2$ **16** was observed (Figure 3.5.3).[21] This behavior is in agreement with our previous catalytic results where Ir/thioether-carbene catalyst precursors had low activities in the reduction of tri- and bulky di-substituted olefins with non-coordinative groups. Therefore, in the absence of a coordinative substrate, the Ir-based-

carbene catalyst precursors are prone to the formation of these inactive trinuclear hydrido species.

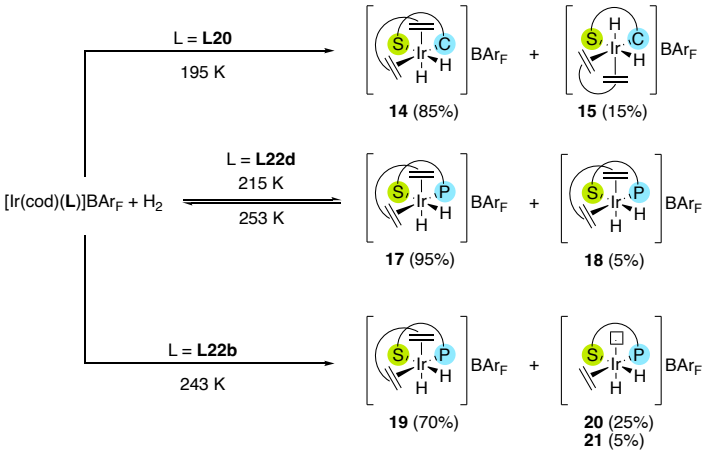

Scheme 3.5.3. Reactivity of [Ir(cod)(**L**)]BAr_F complexes (L= **L20**, **L22b** and **L22b**) with H_2

Table 3.5.4. ^{1}H NMR data at the hydride region of dihydride species **14**, **15**, **17**–**21**.

Compound	H (*trans* to olefin)	H (*trans* to sulfur)
[Ir(H)$_2$(cod)(**L20**)]BAr_F (**14**)	-14.44 (s)	-15.07 (s)
[Ir(H)$_2$(cod)(**L20**)]BAr_F (**15**)	-12.56 (s)	-12.87 (s)
[Ir(H)$_2$(cod)(**L22d**)]BAr_F (**17**)	-12.06 (d, $^2J_{P-H}$= 16.8 Hz)	-15.47 (d, $^2J_{P-H}$= 14.8 Hz)
[Ir(H)$_2$(cod)(**L22d**)]BAr_F (**18**)	-12.92 (d, $^2J_{P-H}$= 15.8 Hz)	-16.63 (d, $^2J_{P-H}$= 15.4 Hz)
[Ir(H)$_2$(cod)(**L22b**)]BAr_F (**19**)	-11.98 (d, $^2J_{P-H}$= 19.2 Hz)	-15.37 (s)
[Ir(H)$_2$(coe)(**L22b**)]BAr_F (**20**)	-27.53 (dd, $^2J_{P-H}$= 28.1 Hz; $^3J_{H-H}$= 6.0 Hz)	-15.93 (dd, $^2J_{P-H}$= 20 Hz; $^3J_{H-H}$= 6.0 Hz)
[Ir(H)$_2$(coe)(**L22b**)]BAr_F (**21**)	-27.68 (dd, $^2J_{P-H}$= 34.0 Hz; $^3J_{H-H}$= 6.4 Hz)	-16.06 (dd, $^2J_{P-H}$= 20 .8 Hz; $^3J_{H-H}$= 6.4 Hz)

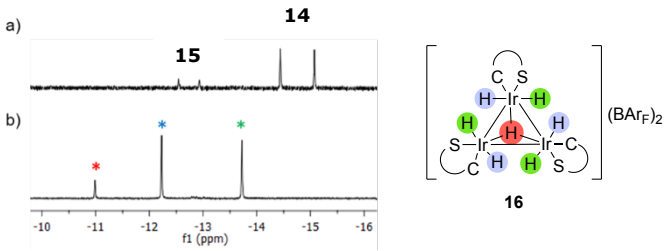

Figure 3.5.3. ^{1}H-NMR in the hydride region for (a) dihydride species [Ir(H)$_2$(cod)(**L20**)]BAr$_F$ **14** an **15** and (b) trinuclear iridium hydrido species [Ir$_3$(μ_3-H)(H)$_6$(C-S)$_3$](BAr$_F$)$_2$ **16**.

The 3D structures of dihydrides **14** and **15** have been elucidated by DFT calculations and NMR studies (see Supporting Information for the NMR copies and DFT details). Figure 3.5.4 shows the 3D structures of the two most stable dihydrides. The population of these two dihydridre species obtained by DFT calculation is in good agreement with the experimental ^{1}H-NMR population. The most stable dihydride species **14** has the hydride *trans* to the olefin pointing down, an *S* configuration of the thioether group and a boat-like conformation for the six-membered chelate ring with the methylenic group of the ligand backbone pointing up (Figure 3.5.4a). [22] In agreement with this assignment, the hydride *trans* to the olefin of complex **15** showed NOE contacts with the methinic proton of the ligand backbone and also with one of the methyls of the 2,6-dimethylphenyl thioether group. The minor species **15** corresponds to the dihydride species in which the hydride *trans* to the olefin is pointing up, the S atom has an *S* configuration and the chelate ring adopts a boat-like conformation with the methylenic group of the ligand backbone pointing down (Figure 3.5.4b).

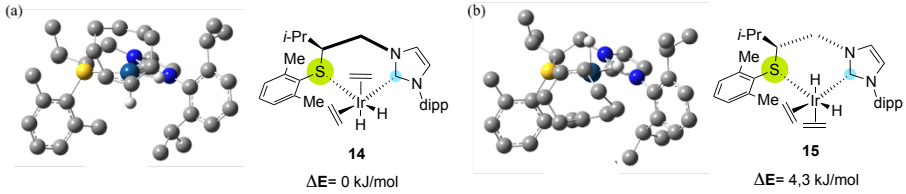

Figure 3.5.4. Calculated structures (hydrogen atoms, except metal hydrides, and BAr$_F$ anion have been omitted for clarity) and energies of [Ir(H)$_2$(cod)(**L20**)]BAr$_F$ complexes (a) **14** and (b) **15**.

The oxidative addition of H_2 to phosphinite-based [Ir(cod)(**L22d**)]BAr$_F$ needed to be carried out at 215 K, since it did not took place at lower temperature. Bubbling H_2 to [Ir(cod)(**L22d**)]BAr$_F$ led to an equilibrium between the starting complex [Ir(cod)(**L22d**)]BAr$_F$ and two dihydride species [Ir(H)$_2$(cod)(**L22d**)]BAr$_F$ (**17** and **18**, Scheme 3.5.3). The dihydride species **17** and **18** are not stable upon raising the temperature and, therefore, the equilibrium shifts back to the starting complex [Ir(cod)(**L22d**)]BAr$_F$ at 253 K. In contrast to the carbene-based catalyst precursor, the

analogous inactive trinuclear iridium hydrido species **17** were not detected. Dihydride compounds **17** and **18** showed small phosphorus-hydride coupling constants ($^2J_{P\text{-}H} \leq$ 16.8 Hz; Table 3.5.4). This indicates that both hydrides are *cis* to the phosphorus atom. DFT calculations and NOESY experiments showed that isomer **17** corresponds to the dihydride complex in which the hydride *trans* to the olefin is pointing down with an *S* configuration at the S atom and a boat-like conformation with the methylenic group of the ligand backbone pointing down (Figure 3.5.5a). The minor isomer **18** only differs from **17** in the fact that the methylenic group of the ligand backbone points down (Figure 3.5.5b). Therefore, this minor intermediate adopts the same 3D structure as the major dihydride species **14**, formed after the oxidative addition of the carbene-based catalyst precursor.

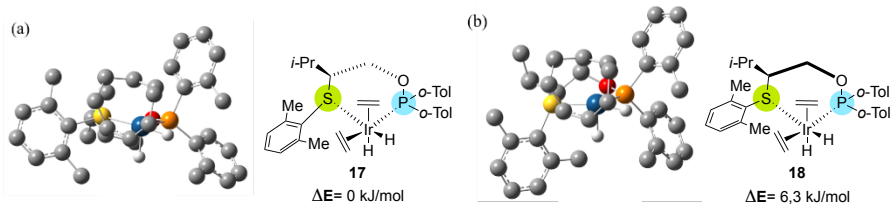

Figure S3.5.5. Calculated structures (hydrogen atoms, except metal hydrides, and BAr_F anion have been omitted for clarity) and energies of $[Ir(H)_2(cod)(\mathbf{L22d})]BAr_F$ complexes (a) **17** and (b) **18**.

As expected for compound $[Ir(cod)(\mathbf{L22b})]BAr_F$, that contains the ligand with the stronger π-acceptor ability, its oxidative addition required to bubble H_2 at the highest temperature, 243 K, to drive the equilibrium to the dihydride species. At this temperature, three dihydride species **19**–**21** in a 70:25:5 ratio were observed (Scheme 3.5.3). Major species **19** corresponds to the dihydride complex $[Ir(H)_2(cod)(\mathbf{L22b})]BAr_F$ in which both hydrides are *cis* to the phosphite group ($^2J_{P\text{-}H} \leq$ 19.2 Hz; Table 3.5.4). Similarly to that observed for the analogue complex **17**, the hydride *trans* to the olefin shows NOE interactions with the methylenic protons of the ligand backbone and also with one of the methyls of the 2,6-dimethylphenyl thioether group (Figure 3.5.6). These NOE contacts indicated that the dihydride complex **19** has the same structure as the major isomer **17**, with the hydride *trans* to the olefin pointing down, an *S* configuration at the S atom and a boat-like conformation with the methylenic group of the ligand backbone pointing down (Figure 3.5.6). DFT calculations not only corroborated the structure of **19**, which is the most stable dihydride, but was also in full agreement with the presence of a single $[Ir(H)_2(\mathbf{L22b})(cod)]BAr_F$ complex since the other calculated isomers were of much higher energy (ΔE ≥ 28 kJ/mol).

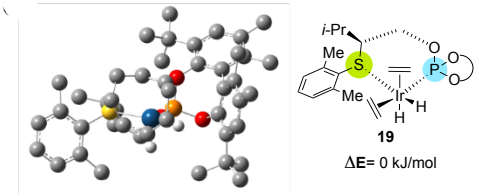

Figure 3.5.6. Calculated structure for $[Ir(H)_2(cod)(\mathbf{L22b})]BAr_F$ complex **19** (hydrogen atoms, except metal hydrides, and the BAr_F anion have been omitted for clarity).

Minor species **20** and **21** not only show that the hydrides are *cis* to the P-atom atom ($^2J_{P\text{-}H} \leq 28$ Hz; Table 4) but also a very distinct chemical shift for one of the hydrides that appears at high chemical shift (c.a. -27.5 ppm). This is characteristic of a hydride ligand positioned *trans* to a vacant site or to a coordination site involved in a C-H agostic interaction.[23] These species have been therefore assigned to the elusive dihydride intermediate species $[Ir(H)_2(coe)(\mathbf{L22b})]BAr_F$. This indicates that at this temperature not only the oxidative addition of H_2 to $[Ir(cod)(\mathbf{L22b})]BAr_F$ takes place but also the partial hydrogenation of the coordinated cyclooctadiene.

To summarize, the species resulting of the reactivity of the Ir-catalyst precursors towards H_2 depend on the type of ligand in agreement with the catalytic results, where each substrate type requires a different catalyst for maximum catalytic performance. Thus, although the reactivity of carbene-based catalysts with H_2 is more favored than with the analogous P-based catalysts, they are prone to form inactive trinuclear hydrido species that explain their lower activities when hydrogenating tri- and bulky disubstituted olefins with non-coordinative groups. On the other hand, the reactivities with H_2 have in common the formation, for each catalytic precursor, of cis-dihydride intermediates (two for carbene/phosphinite-containing ligands and three for the phosphite-containing ligand) in different ratios, one in major proportion. In all of them the configuration of the thioether moiety is the same. However, while for the phosphinite/phosphite-containing ligands the major species have the same 3D structures, for the carbene-based precursor the major species shows a different disposition of the six-membered chelate ring with the same disposition of the hydride ligands, which is the same 3D structure of the minor isomer for the phosphinite-based compound. In addition, for the phosphite-containing ligand we detected the presence of two *cis*-dihydride intermediates with one of the hydride ligand in *trans* to a vacant side and with the partial hydrogenation of the cyclooctadiene.

3.5.3. Conclusions

We studied for the first time the potential of novel and simple Ir/thioether-NHC complexes, with a six-membered chelate, in the asymmetric hydrogenation of non-chelating olefins and cyclic β-enamides. For comparison, we also prepared and applied the analogues thioether–phosphinite/phosphite complexes. All these complexes are

solid, air stable and easy to synthesize by a simple and efficient synthetic route. We found that the efficiency of the new Ir/thioether-carbene catalyst precursors varies with the type of olefin. Thus, while the Ir/thioether-carbene catalyst precursors provide lower catalytic performance than their related Ir/thioether-P complexes in the hydrogenation of olefins lacking a coordinating group, for the reduction of chelating olefins (e.g. tri- and disubstituted enol phosphonate derivatives) the catalysts had similar good performance. We have also found that the low activities in the hydrogenation of non-chelating tri- and bulky disubstituted olefins with carbene-based catalysts is due to the high steric constrains imposed by the thioether-carbene design, which favors the formation of inactive trinuclear species. This behavior agrees with the reactivity study of the iridium-containing S-carbene/phosphinite/phosphite catalyst precursors toward H_2 that shows the formation of inactive trinuclear hydrido species in the case of the carbene-based catalysts. Interestingly, in the hydrogenation of challenging 1,1'-disubstituted olefins, the deuterogenation studies indicate that carbene-based catalyst favors the hydrogenation vs the competing isomerization process, which is one important problem in the reduction of this type of olefins. It is also interesting to note the discovery of simple-to-synthesize Ir/thioether-P complexes containing a simple backbone that gave high enantioselectivities for some tri- and the challenging 1,1'-disubstituted olefins and cyclic β-enamides (ee's up to 98%).

Finally, we want to stress the high potential of thioether-carbene ligands. Although the enantioselectivities achieved with these ligands are not as high as those obtained with their phosphite/phosphinite analogues, their promising results in the reduction of chelating substrates (ee values up to 91%, including the challenging cyclic β-enamides) together with their potential modularity make thioether/carbene-based ligands an interesting field for future research.

3.5.4. Experimental section

3.5.4.1. General considerations

All reactions were carried out using standard Schlenk techniques under an argon atmosphere. Commercial chemicals were used as received. Solvents were dried by means of standard procedures and stored under argon. ^{1}H, $^{13}C\{^{1}H\}$ and $^{31}P\{^{1}H\}$ NMR spectra were recorded using a Varian Mercury-400 MHz spectrometer. Chemical shifts are relative to that of $SiMe_4$ (^{1}H and $^{13}C\{^{1}H\}$) as an internal standard or H_3PO_4 (^{31}P) as an external standard. ^{1}H and ^{13}C assignments were made on the basis of ^{1}H-^{1}H gCOSY, ^{1}H-^{13}C gHSQC and NOESY experiments. The compounds **11**,[8] **12**,[9] 1-(2,6-diisopropylphenyl)-1*H*-imidazole,[12] (*R*)-4-benzyl-3-((*S*)-2-bromo-3-methylbutanoyl) oxazolidin-2-one[9], (*S*)-(1-bromo-3-methylbutan-2-yl)(phenyl)sulfane,[11] phosphoro-chloridites[24] and susbtrates **S8**,[25] **S14**,[26], **S25**,[27] **S44**,[28] **S53**,[29] **S58**,[30] **S61**[30], **S64**,[31] **S135**,[32] **S145**,[20j] **S146**,[33] **S147**[20j] and **S148**[20a] were prepared in accordance with the

corresponding methods published in the literature. For characterization and ee determination details, copies of the NMR spectra as well as for DFT details see Supporting Information.

3.5.4.2. General procedure for the synthesis of (*S*)-2-((2,6-dimethylphenyl)thio)-3-methylbutan-1-ol (13)

Hydroxyl-thioether derivative **13** was prepared in two steps from (*R*)-4-benzyl-3-((*S*)-2-bromo-3-methylbutanoyl) oxazolidin-2-one steps following an already reported procedure.[9] DBU (15.6 mmol) was added to a cooled solution (-10 °C) of 2,6-dimethylphenyl)thiol (2 mL, 15.6 mmol) in anhydrous THF (3 M). After 20 min a white suspension was formed. To the suspension, a THF (90 mL) solution of (*R*)-4-benzyl-3-((*S*)-2-bromo-3-methylbutanoyl)oxazolidin-2-one (4.0 g, 13 mmol) was added and the reaction was stirred for an additional 90 min at -10 °C. Then, it was stirred for 2.5 h at room temperature. After that, the reaction mixture was quenched with water (25 mL), extracted with diethyl ether (3 x 25mL) and then the organic phase was washed with water (25 mL) and brine (25 mL). The diethyl ether solution was dried with $MgSO_4$, filtered and concentrated under vacuum. For purification column chromatography was needed (SiO_2, hexane/ethyl acetate – 90:10). Yield: 3.2 g (68%) as a colourless oil. ^{1}H NMR (400 MHz, $CDCl_3$) *δ*: 1.03 (d, 3H, $^3J_{H-H}$= 6.8 Hz, CH_3, *i*-Pr), 1.23 (d, 3H, $^3J_{H-H}$= 6.8 Hz, CH_3, *i*-Pr), 2.27 (m, 1H, CH, *i*-Pr), 2.44 (s, 6H, CH_3, Ar), 2.54 (dd, 1H, $^2J_{H-H}$= 13.4 Hz, $^3J_{H-H}$= 9.9 Hz, CH_2-Ph), 3.14 (dd, 1H, $^2J_{H-H}$= 13.4 Hz, $^3J_{H-H}$= 3.6 Hz, CH_2-Ph), 3.44 (t, 1H, $^2J_{H-H}$= 8.3 Hz, CH_2-O), 3.80 (dd, 1H, $^2J_{H-H}$= 8.3 Hz, $^3J_{H-H}$= 1.8 Hz, CH_2-O), 4.20 (m, 1H, CH-N), 4.91 (d, 1H, $^3J_{H-H}$= 9.3 Hz, CH-S), 6.96-7.25 (m, 8H, CH=). ^{13}C NMR (100.6 MHz, $CDCl_3$) *δ*: 20.1 (CH_3, *i*-Pr), 21.1 (CH_3, *i*-Pr), 21.9 (CH_3, Ar), 30.5 (CH, *i*-Pr), 37.8 (CH_2-Ph), 52.1 (CH-S), 56.4 (CH-N), 65.8 (CH_2-O), 127.3-173.3 (aromatic carbons). Anal. calcd. (%) for $C_{23}H_{27}NO_3S$: C 69.49, H 6.85, N 3.52, S 8.06; found: C 69.17, H 6.81, N 3.49, S 8.01. MS HR-ESI [found 420.1601, $C_{23}H_{27}NO_3S$ $(M+Na)^+$ requires 420.1604].

To a solution of (*R*)-4-Benzyl-3-((*S*)-2-((2,6-dimethylphenyl)thio)-3-methylbutan-oyl)oxazolidin-2-one (1.0 g, 1 mmol) in anhydrous THF (8 mL) a solution of $LiBH_4$ (2 mmol, 2.0 M in THF) and H_2O (90 µL, 2 mmol) were added and stirred overnight at room temperature. The solution was quenched with HCl 1 M, until no gas release is observed, and diluted with ethyl acetate (15 mL). The organic layer was washed with HCl 1 M (20 mL), water (20 mL) and brine (20 mL). Afterwards it was dried over $MgSO_4$, filtered and concentrated under vacuum. For purification column chromatography was needed (SiO_2, hexane/ethyl acetate – 90:10). Yield: 240 mg (85%) as a pale yellow oil. ^{1}H NMR (400 MHz, $CDCl_3$) *δ:* 1.11 (d, 3H, $^3J_{H-H}$= 6.8 Hz, CH_3, *i*-Pr), 1.13 (d, 3H, $^3J_{H-H}$= 6.8 Hz, CH_3, *i*-Pr), 1.91 (m, 1H, OH), 2.07 (m, 1H, CH, *i*-Pr), 2.54 (s, 6H, CH_3, Ar), 2.82 (m, 1H, CH- S), 3.57 (m, 2H, CH_2-OH), 7.08-7.12 (m, 3H, CH=). ^{13}C NMR (100.6 MHz, $CDCl_3$) *δ:* 19.8 (CH_3, *i*-Pr), 20.1 (CH_3, *i*-Pr), 22.3 (2 CH_3, Ar), 29.5 (CH, *i*-Pr), 58.8 (CH-

S), 62.4 (CH_2-OH), 128.3-143.3 (aromatic carbons). Anal. calcd. (%) for $C_{13}H_{20}OS$: C 69.59, H 8.99, S 14.29; found: C 69.16, H 8.93, S 14.18. MS HR-ESI [found 247.1122, $C_{13}H_{20}OS$ $(M+Na)^+$ requires 247.1127].

3.5.4.3. General procedure for the preparation of thioether–imidazolium derivatives L19H·Br–L20H·Br

Thioether–imidazolium derivatives **L1**H·Br–**L2**H·Br were prepared in two steps from **12**–**13** following an already reported procedure.[11] To a solution of the corresponding thioether-alcohol **13** (3.1 eq) in dry DCM (6 mL), tetrabromomethane (1.2 g, 3.7 mmol) and triphenylphosphine (0.98 g, 3.7 mmol) were added. Then, it was stirred overnight at 0 ºC. The reaction mixture was then diluted with DCM (15 mL) and washed with water (15 mL) and brine (15 mL). The thioether-bromine compounds were further purified by column chromatography (SiO_2, hexane/ethyl acetate – 80:20).

***(S)*-(1-Bromo-3-methylbutan-2-yl)(2,6-dimethylphenyl)sulfane**: Yield: 695 mg (77%) as a pale yellow oil. ^{1}H NMR (400 MHz, $CDCl_3$) δ: 0.84 (d, 3H, $^3J_{H-H}$= 6.8 Hz, CH_3, *i*-Pr), 0.94 (d, 3H, $^3J_{H-H}$= 6.8 Hz, CH_3, *i*-Pr), 2.08 (m, 1H, CH, *i*-Pr), 2.46 (s, 6H, CH_3, Ar), 3.05 (m, 2H, CH_2-Br), 3.97 (m, 1H, CH-S), 7.00-7.04 (m, 3H, CH=). ^{13}C NMR (100.6 MHz, $CDCl_3$) δ: 15.5 (CH_3, *i*-Pr), 20.7 (CH_3, *i*-Pr), 21.1 ($2CH_3$, Ar), 30.5 (CH, *i*-Pr), 40.6 (CH_2-Br), 62.7 (CH-S), 127.2-141.8 (aromatic carbons). Anal. calcd. (%) for $C_{13}H_{19}BrS$: C 54.36, H 6.67, S 11.16; found: C 54.06, H 6.64, S 11.08. MS HR-ESI [found 309.0279, $C_{13}H_{19}BrS$ $(M+Na)^+$ requires 309.0283].

To a solution of the corresponding thioether-bromine compounds (1 eq) in anhydrous acetonitrile (3 mL), 1-(2,6-diisopropylphenyl)-1*H*-imidazole (1.2 eq) was added. The mixture was refluxed for 1.5 days after that the solution was cooled to room temperature and the solvent was evaporated and purified by flash chromatography (SiO_2, DCM/MeOH – 20:1 → 10:1).

L19H·Br: Yield: 230 mg (42%, reaction carried out using 1.1 mmol of (*S*)-(1-bromo-3-methylbutan-2-yl)(phenyl)sulfane as dark orange oil. ^{1}H NMR ($CDCl_3$) δ: 1.01 (m, 3H, CH_3 *i*-Pr-Ar), 1.08 (m, 3H, CH_3, *i*-Pr -Ar), 1.10 (m, 3H, CH_3, *i*-Pr-Ar), 1.13 (m, 3H, CH_3, *i*-Pr -Ar), 1.15 (m, 3H CH_3, *i*-Pr), 1.17 (m, 3H, CH_3, *i*-Pr), 2.15 (m, 2H, CH, *i*-Pr -Ar), 2.38 (m, 1H, CH, *i*-Pr), 3.81 (m, 1H, CH-S), 4.63 (dd, 1H, $^2J_{H-H}$= 14.0 Hz, $^3J_{H-H}$= 11.3 Hz, CH_2-N), 5.40 (dd, 1H, $^2J_{H-H}$= 14.0 Hz, $^3J_{H-H}$= 3.6 Hz, CH_2-N), 7.15 (ps, 1H, CH=, NHC), 7.20-7.35 (m, 7H, CH=), 7.52 (t, 1H, $^3J_{H-H}$= 7,5 Hz, CH=), 8.43 (ps, 1H, CH=, NHC), 10.10 (s, 1H, CH=, NHC). ^{13}C NMR (100.6 MHz, $CDCl_3$) δ: 18.3 (CH_3, *i*-Pr -Ar), 20.7 (CH_3, *i*-Pr -Ar), 24.1 (CH_3, *i*-Pr), 24.2 (CH_3, *i*-Pr -Ar), 24.2 (CH_3, *i*-Pr), 24.4 (CH_3, *i*-Pr -Ar), 28.6 (CH, *i*-Pr -Ar), 28.6 (CH, *i*-Pr -Ar), 31.6 (CH, *i*-Pr), 53.2 (CH_2-N), 57.9 (CH-S), 123.5 (CH=, NHC), 124.5 (CH=, NHC), 124.7-145.5 (aromatic carbons), 138.7 (CH=, NHC). Anal. calcd. (%) for $C_{26}H_{35}BrN_2S$: C 64.05, H 7.24, N 5.75, S 6.58; found:

C 63.81, H 7.20, N 5.71, S 6.53. MS HR-ESI [found 407.2507, $C_{26}H_{35}N_2S$ $(M)^+$ requires 407.2515].

L20H·Br: Yield: 600 mg (46%, reaction carried out using 2.4 mmol of (*S*)-(1-bromo-3-methylbutan-2-yl)(2,6-dimethylphenyl)sulfane as light brown foam. ^{1}H NMR ($CDCl_3$) *δ*: 1.05 (m, 3H, CH_3, *i*-Pr), 1.07 (m, 3H, CH_3, *i*-Pr), 1.10 (m, 3H, CH_3, *i*-Pr -Ar), 1.12 (m, 3H, CH_3, *i*-Pr -Ar), 1.17 (m, 3H, CH_3, *i*-Pr -Ar), 1.18 (m, 3H, CH_3, *i*-Pr -Ar), 1.81 (m, 1H, CH, *i*-Pr), 2.23 (m, 1H, CH, *i*-Pr -Ar), 2.30 (m, 1H, CH, *i*-Pr -Ar), 2.40 (s, 6H, CH_3, Ar), 3.31 (m, 1H, CH-S), 4.42 (dd, 1H, $^2J_{H\text{-}H}$= 14.3 Hz, $^3J_{H\text{-}H}$= 9.3 Hz, CH_2-N), 5.29 (dd, 1H, $^2J_{H\text{-}H}$= 14.3 Hz, $^3J_{H\text{-}H}$= 4.3 Hz, CH_2-N), 7.03-7.09 (m, 3H, CH=) 7.15 (ps, 1H, CH=, NHC), 7.20-7.25 (m, 2H, CH=), 7.47 (m, 1H, CH=), 7.89 (ps, 1H, CH=, NHC), 10.36 (s, 1H, CH=N, NHC). ^{13}C NMR (100.6 MHz, $CDCl_3$) *δ*: 18.8 (CH_3, *i*-Pr), 19.5 (CH_3, *i*-Pr), 22.1 (CH_3, Ar), 24.3 (CH_3, Ar), 24.3 (CH_3, *i*-Pr -Ar), 24.4 (CH_3, *i*-Pr -Ar), 24.4 (CH_3 *i*-Pr -Ar), 24.4 (CH_3, *i*-Pr -Ar), 28.7 (CH, *i*-Pr -Ar) 28.7 (CH, *i*-Pr -Ar), 30.7 (CH, *i*-Pr), 51.4 (CH_2-N), 55.1 (CH-S), 123.8 (CH=, NHC), 123.9 (CH=, NHC), 124.6-145.5 (aromatic carbons), 139.0 (CH=, NHC). Anal. calcd. (%) for $C_{28}H_{39}BrN_2S$: C 65.23, H 7.62, N 5.43, S 6.22; found: C 64.95, H 7.60, N 5.40, S 6.18. MS HR-ESI [found 435.2822, $C_{28}H_{39}N_2S$ $(M)^+$ requires 435.2828].

3.5.4.4. General procedure for the preparation of thiother-phosphite ligands L21–L22a–b

The corresponding phosphorochloridite (0.55 mmol) produced *in situ* was dissolved in toluene (5 mL) and pyridine (1.9 mmol, 0.15 mL) was added. Then, the corresponding hydroxyl-thioether (0.5 mmol) compound was azeotropically dried with toluene (3x1 mL) and dissolved in toluene (5 mL) to which pyridine (1.9 mmol, 0,15 mL) was added. The solution was transferred slowly at 0 ºC to the phosphorochloridite solution. The reaction mixture was stirred overnight at 80 ºC, and the pyridine salts were removed by filtration. The evaporation of the solvent yielded a white foam, which was purified by flash chromatography in alumina (100:1 - toluene/NEt_3) to produce the corresponding ligand as a white solid.

L21a: Yield: 208 mg (72%). ^{31}P (161.9 MHz, C_6D_6), *δ*: 128.8. ^{1}H (400 MHz, C_6D_6), *δ*: 0.90 (m, 3H, CH_3, *i*-Pr), 1.03 (m, 3H, CH_3, *i*-Pr), 1.51 (s, 9H, CH_3, *t*-Bu), 1.51 (s, 9H, CH_3, *t*-Bu), 1.64 (s, 3H, CH_3), 1.67 (s, 3H, CH_3), 2.01 (s, 6H, CH_3), 2.36 (m, 1H, CH, *i*-Pr), 3.28 (m, 1H, CH-S), 3.68 (m, 1H, CH_2-O), 4.12 (m, 1H, CH_2-O), 6.75-7.27 (m, 7H, CH=). ^{13}C (100.6 MHz, C_6D_6), *δ*: 16.1 (CH_3), 16.4 (CH_3), 16.8 (CH_3) 20.0 (CH_3), 20.1 (CH_3, *i*-Pr), 20.6 (CH_3, *i*-Pr), 27.4 (CH, *i*-Pr), 30.9 (CH_3, *t*-Bu), 31.2 (CH_3, *t*-Bu), 34.5 (C, *t*-Bu), 34.5 (C, *t*-Bu), 56.2 (CH-S), 64.8 (CH_2-O), 125.9-145.7 (aromatic carbons). Anal. calcd. (%) for $C_{35}H_{47}O_3PS$: C 72.63, H 8.19, S 5.54; found: C 72.76, H 8.18, S 5.50. MS HR-ESI [found 601.2875, C35H47O3PS $(M+Na)^+$ requires 601.2876].

L21b: Yield: 176 mg (61%). ^{31}P (161.9 MHz, C_6D_6), *δ*: 127.7. ^{1}H (400 MHz, C_6D_6), *δ*: 0.89 (m, 3H, CH_3, *i*-Pr), 1.03 (m, 3H, CH_3, *i*-Pr), 1.38 (s, 9H, CH_3, *t*-Bu), 1.52 (s, 9H, CH_3, *t*-Bu), 1.62 (s, 3H, CH_3), 1.75 (s, 3H, CH_3), 2.01 (s, 3H, CH_3), 2.07 (s, 3H, CH_3), 2.32 (m, 1H, CH, *i*-Pr), 3.19 (m, 1H, CH-S), 3.43 (m, 1H, CH_2-O), 4.27 (m, 1H, CH_2-O), 6.93-7.31 (m, 7H, CH=). ^{13}C (100.6 MHz, C_6D_6), *δ*: 16.1 (CH_3), 16.3 (CH_3), 16.6 (CH_3), 20.0 (CH_3, *i*-Pr), 20.5 (CH_3), 27.4 (CH, *i*-Pr), 30.6 (CH_3, *t*-Bu), 31.2 (CH_3, *t*-Bu), 34.4 (C, *t*-Bu), 34.5 (C, *t*-Bu), 56.9 (CH-S), 64.0 (CH_2-O), 126.8-146.4 (aromatic carbons). Anal. calcd. (%) for $C_{35}H_{47}O_3PS$: C 72.63, H 8.19, S 5.54; found: C 72.68, H 8.18, S 5.51. MS HR-ESI [found 601.2873, $C_{35}H_{47}O_3PS$ $(M+Na)^+$ requires 601.2876].

L22a: Yield: 171 mg (56%). ^{31}P (161.9 MHz, C_6D_6), *δ*: 126.9. ^{1}H (400 MHz, C_6D_6), *δ*: 1.37 (m, 3H, CH_3, *i*-Pr), 1.51 (m, 3H, CH_3, *i*-Pr), 1.77 (s, 9H, CH_3, *t*-Bu), 1.87 (s, 9H, CH_3, *t*-Bu), 1.98 (s, 3H, CH_3), 2.10 (s, 3H, CH_3), 2.37 (s, 3H, CH_3), 2.48 (s, 3H, CH_3), 2.71 (s, 6H, CH_3), 2.80 (m, 1H, CH, *i*-Pr), 3.44 (m, 1H, CH-S), 3.99 (m, 1H, CH_2-O), 4.37 (m, 1H, CH_2-O), 7.18-7.54 (m, 5H, CH=). ^{13}C (100.6 MHz, C_6D_6), *δ*: 16.4 (CH_3, *i*-Pr), 16.7 (CH_3), 20.3 (CH_3, *i*-Pr), 20.5 (CH_3), 20.8 (CH_3), 22.1 (2xCH_3), 28.2 (CH, *i*-Pr), 31.2 (CH_3, *t*-Bu), 31.3 (CH_3, *t*-Bu), 34.7 (C, *t*-Bu), 34.9 (C, *t*-Bu), 56.4 (CH-S), 64.2 (CH_2-O), 127.7-146.0 (aromatic carbons). Anal. calcd. (%) for $C_{37}H_{51}O_3PS$: C 73.23, H 8.47, S 5.28; found: C 73.32, H 8.46, S 5.26. MS HR-ESI [found 629.3184, $C_{37}H_{51}O_3PS$ $(M+Na)^+$ requires 629.3189].

L22b: Yield: 144 mg (47%). ^{31}P (161.9 MHz, C_6D_6), *δ*: 122.9. ^{1}H (400 MHz, C_6D_6), *δ*: 0.98 (m, 3H, CH_3, *i*-Pr), 1.15 (m, 3H, CH_3, *i*-Pr), 1.23 (s, 9H, CH_3, *t*-Bu), 1.51 (s, 9H, CH_3, *t*-Bu), 1.61 (s, 3H, CH_3), 1.77 (s, 3H, CH_3), 2.00 (s, 3H, CH_3), 2.13 (s, 3H, CH_3), 2.28 (s, 6H, CH_3), 2.44 (m, 1H, CH, *i*-Pr), 3.04 (m, 1H, CH-S), 3.16 (m, 1H, CH_2-O), 4.36 (m, 1H, CH_2-O), 6.91-7.16 (m, 5H, CH=). ^{13}C (100.6, MHz, C_6D_6), *δ*: 15.2 (CH_3, *i*-Pr), 15.3 (CH_3), 15.6 (CH_3), 19.3 (CH_3, *i*-Pr), 19.6 (CH_3), 19.7 (CH_3), 21.1 (2xCH_3), 26.7 (CH, *i*-Pr), 29.3 (CH_3, *t*-Bu), 30.6 (CH_3, *t*-Bu), 33.5 (C, *t*-Bu), 33.8 (C, *t*-Bu), 54.1 (CH-S), 62.8 (CH_2-O), 124.4-144.9 (aromatic carbons). Anal. calcd. (%) for $C_{37}H_{51}O_3PS$: C 73.23, H 8.47, S 5.28; found: C 73.41, H 8.46, S 5.23. MS HR-ESI [found 629.3188, $C_{37}H_{51}O_3PS$ $(M+Na)^+$ requires 629.3189].

3.5.4.5. General procedure for the preparation of thioether-phosphinite ligands L21–L22c–e

The corresponding hydroxyl-thioether (0.5 mmol) and DMAP (0.055 mmol, 6.7 mg) were dissolved in toluene (1 mL), and triethylamine was added (0.65 mmol, 0.09 mL) at r.t. Followed by the addition of the corresponding chlorophosphine (0.55 mmol) via syringe. The reaction was stirred 20 min at r.t. The solvent was removed *in vacuo*, and the product was purified by flash chromatography on alumina (100:1 - toluene/NEt_3) to produce the corresponding ligands as colorless oils.

L21c: Yield: 118 mg (62%). ^{31}P NMR (161.9 MHz, C_6D_6), *δ*: 114.5. ^{1}H (400 MHz, C_6D_6), *δ*: 0.91 (m, 3H, CH_3, *i*-Pr), 0.98 (m, 3H, CH_3, *i*-Pr), 2.20 (m, 1H, CH- *i*-Pr), 3.24 (m, 1H, CH-S), 4.01 (m, 2H, CH_2-O), 6.85-7.57 (m, 15H, CH=). ^{13}C (100.6 MHz, C_6D_6), *δ*: 18.6 (CH_3, *i*-Pr), 21.2 (CH_3, *i*-Pr), 29.5 (CH- *i*-Pr), 58.0 (d, CH-S, $J_{C\text{-}P}$= 19.1 Hz), 71.1 (d, CH_2-O, $J_{C\text{-}P}$= 19.1 Hz), 126.0-143.2 (aromatic carbons). Anal. calcd. (%) for $C_{23}H_{25}OPS$: C 72.61, H 6.62, S 8.43; found: C 72.74, H 6.63, S 8.37. MS HR-ESI [found 403.1261, $C_{23}H_{25}OPS$ $(M+Na)^+$ requires 403.1256].

L22c: Yield: 87 mg (43%). ^{31}P NMR (161.9 MHz, C_6D_6), *δ*: 114.7. ^{1}H (400 MHz, C_6D_6), *δ*: 0.97 (m, 3H, CH_3, *i*-Pr), 1.02 (m, 3H, CH_3, *i*-Pr), 2.24 (m, 1H, CH- *i*-Pr), 2.42 (s, 6H, CH_3), 3.03 (m, 1H, CH-S), 3.81 (m, 1H, CH_2-O), 3.99 (m, 1H, CH_2-O), 6.87-7.48 (m, 13H, CH=). ^{13}C (100.6 MHz, C_6D_6), *δ*: 17.8 (CH_3, *i*-Pr), 20.2 (CH_3, *i*-Pr), 22.1 (2xCH_3), 28.9 (CH- *i*-Pr), 56.3 (CH-S), 69.8 (CH_2-O), 125.3-143.3 (aromatic carbons). Anal. calcd. (%) for $C_{25}H_{29}OPS$: C 73.50, H 7.16, S 7.85; found: C 73.72, H 7.15, S 7.72. MS HR-ESI [found 431.1572, $C_{25}H_{29}OPS$ $(M+Na)^+$ requires 431.1569].

L22d: Yield: 152 mg (70%). ^{31}P (161.9 MHz, C_6D_6), *δ*: 101.7. ^{1}H (400 MHz, C_6D_6), *δ*: 0.98 (m, 3H, CH_3, *i*-Pr), 1.03 (m, 3H, CH_3, *i*-Pr), 2.23 (s, 3H, CH_3, *o*-Tol), 2.25 (m, 4H, CH_3, *o*-Tol and CH- *i*-Pr), 2.40 (s, 6H, CH_3), 3.02 (m, 1H, CH-S), 3.78 (m, 1H, CH_2-O), 4.03 (m, 1H, CH_2-O), 6.84-7.12 (m, 9H, CH=), 7.48 (m, 1H, CH=), 7.60 (m, 1H, CH=). ^{13}C (100.6 MHz, C_6D_6), *δ*: 17.5 (CH_3, *i*-Pr), 20.05 (CH_3, *o*-Tol), 20.1 (CH_3, *o*-Tol), 20.3 (CH_3, *i*-Pr), 22.1 (2xCH_3), 28.8 (CH, *i*-Pr), 56.5 (CH-S), 70.1 (CH_2-O), 125.9-147.3 (aromatic carbons). Anal. calcd. (%) for $C_{27}H_{33}OPS$: C 74.28, H 7.62, S 7.34; found: C 74.53, H 7.64, S 7.23. MS HR-ESI [found 459.1881, $C_{27}H_{33}OPS$ $(M+Na)^+$ requires 459.1882].

L22e: Yield: 146 mg (69%). ^{31}P NMR (C_6D_6), δ: 101.7. ^{1}H NMR (C_6D_6), δ: 0.98 (m, 3H, CH_3, *i*-Pr), 1.03 (m, 3H, CH_3, *i*-Pr), 1.22-1.82 (m, 22H, CH, Cy), 2.29 (m, 1H, CH, CH- *i*-Pr), 2.50 (s, 6H, CH_3-Ar), 3.07 (m, 1H, CH-S), 3.66 (m, 1H, CH_2-O), 3.93 (m, 1H, CH_2-O), 6.90-7.12 (m, 3H, CH=). ^{13}C NMR (C_6D_6), δ: 17.7 (CH_3, *i*-Pr), 20.3 (CH_3, *i*-Pr), 22.1 (CH_3-Ar), 25.3-28.9 (CH_2, Cy), 35.6 (d, $^{1}J_{C\text{-}P}$= 20.2 Hz, CH, Cy), 36.2 (d, $^{1}J_{C\text{-}P}$= 20.2 Hz, CH, Cy), 56.6 (CH-S), 72.6 (CH_2-O), 132.6-143.1 (aromatic carbons).

3.5.4.6. General procedure for the preparation of [Ir(cod)(L19–L20a–e)]BAr$_F$

Catalyst precursors [Ir(cod)(**L19–L20**)]BAr_F were prepared in two steps from **L19**H·Br–**L20**H·Br. Ag_2O (55.6 mg. 0.24 mmol) was added into a solution of the corresponding imidazolium salt derivative (0.48 mmol) in dichloromethane (30 mL) and kept in the dark with vigorous stirring overnight. After that, the reaction crude was passed through a dry celite plug and evaporated affording the silver carbene complexes Ag**L19**$_2$·$AgBr_2$ and Ag**L20**$_2$·$AgBr_2$ as a dark brown foam.

Ag**L19**$_2$·AgBr$_2$: Yield: 104.2 mg (63%). ^{1}H NMR (400 MHz, $CDCl_3$), δ: 1.06-1.20 (m, 18H, CH_3, *i*-Pr -Ar and CH_3, *i*-Pr), 2.10 (m, 1H, CH, *i*-Pr), 2.21 (m, 1H, CH, *i*-Pr -Ar), 2.51 (m, 1H, CH, *i*-Pr -Ar), 3.50 (m, 1H, CH-S), 4.20 (m, 1H, CH_2-N), 4.59 (m, 1H, CH_2-N), 6.94-7.47 (m, 10H, CH=). Anal. calcd. (%) for $C_{52}H_{70}Ag_2Br_2N_4S_2$: C 52.45, H 5.93, N 4.70, S 5.38; found: C 52.27, H 5.91, N 4.68, S 5.32. MS HR-ESI [found 919.3919, $C_{52}H_{68}AgN_4S_2$ (M-$AgBr_2$)$^+$ requires 919.3931].

Ag**L20**$_2$·AgBr$_2$: Yield: 120 mg (70%). ^{1}H NMR (400 MHz, $CDCl_3$), δ: 1.44 (m, 18H, CH_3, *i*-Pr and CH_3, *i*-Pr -Ar), 2.08 (m, 1H, CH, *i*-Pr), 2.61 (m, 2H, CH, *i*-Pr -Ar), 2.75 (s, 6H, CH_3, Ar), 3.54 (m, 1H, CH-S), 4.21 (m, 1H, CH_2-N), 4.84 (m, 1H, CH_2-N), 7.20-7.72 (m, 8H, CH=). Anal. calcd. (%) for $C_{56}H_{78}Ag_2Br_2N_4S_2$: C 53.92, H 6.31, N 4.49, S 5.148; found: C 53.67, H 6.28, N 4.46, S 5.10. MS HR-ESI [found 975.4559, $C_{56}H_{76}AgN_4S_2$ (M-$AgBr_2$)$^+$ requires 975.4564].

Into a solution of the corresponding silver carbene (0.074 mmol) and dichloromethane (5 mL), [Ir(μ-Cl)(cod)]$_2$ (0.037 mmol, 25 mg) was added and stirred for 4.5 h in the dark. Subsequently, $NaBAr_F$ (0.080 mmol, 77.2 mg) was added and stirred for an additional hour at r.t. Then, the solvent is evaporated in vacuo and the crude product purified via column chromatography with neutral silica (75:25 – dichloromethane/hexane) to yield the corresponding complexes as orange solids.

[Ir(cod)(L19)]BAr$_F$: Yield: 38 mg (46%). ^{1}H NMR (400 MHz, $CDCl_3$), δ: 1.00 (m, 3H, CH_3, *i*-Pr -Ar), 1.04 (m, 6H, CH_3, *i*-Pr), 1.08 (m, 3H, CH_3, *i*-Pr -Ar), 1.10 (m, 3H, CH_3, *i*-Pr -Ar), 1.43 (m, 3H, CH_3, *i*-Pr -Ar), 1.60-1.88 (m, 8H, CH_2, cod), 1.99 (m, 1H, CH, *i*-Pr) 2.31 (m, 1H, CH, *i*-Pr -Ar), 2.40 (m, 1H, CH, *i*-Pr -Ar), 3.21 (m, 1H, CH-S), 3.67 (b, 2H, CH=, cod), 3.85 (b, 1H, CH=, cod), 4.12 (b, 1H, CH=, cod), 4.57 (dd, 1H, $^2J_{H\text{-}H}$= 14.2 Hz, $^3J_{H\text{-}H}$= 6.3 Hz, CH_2-N), 4.82 (m, 1H, CH_2-N), 6.99 (d, 1H, $^3J_{H\text{-}H}$= 2.9 Hz, CH=, NHC), 7.13 (d, 1H, $^3J_{H\text{-}H}$= 2.9 Hz, CH=, NHC), 7.25-7.75 (m, 20H, CH=). ^{13}C NMR (100.6 MHz, $CDCl_3$), δ: 19.8 (CH_3, *i*-Pr), 20.4 (CH_3, *i*-Pr), 22.6 (CH_3, *i*-Pr -Ar), 23.4 (CH_3, *i*-Pr -Ar), 24.0 (CH_3, *i*-Pr,-Ar), 25.1 (CH_3, *i*-Pr -Ar), 25.3 (CH, *i*-Pr), 28.7 (CH, *i*-Pr -Ar), 29.3 (CH, *i*-Pr), 29.7 (2xCH_2, cod), 31.1 (CH_2, cod), 31.9 (CH_2, cod), 54.7 (CH_2-N), 57.9 (CH-S), 71.5 (CH=, cod), 83.3 (CH=, cod), 83.9 (CH=, cod), 122.2 (CH=, NHC), 125.9 (CH=, NHC), 117.5-145.9 (aromatic carbons), 161.4 (q, C, $^1J_{C\text{-}B}$= 49.6 Hz, BAr_F), 169.6 (C, NHC). Anal. calcd. (%) for $C_{66}H_{58}BF_{24}IrN_2S$: C 50.46, H 3.78, N 1.78, S 2.04; found: C 50.31, H 3.70, N 1.75, S 2.02. MS HR-ESI [found 707.2986, $C_{34}H_{46}IrN_2S$ (M-BAr_F)$^+$ requires 707.3005].

[Ir(cod)(L20)]BAr$_F$: Yield: 50 mg (42%). ^{1}H NMR (400 MHz, $CDCl_3$), δ: 0.85 (m, 3H, CH_3, *i*-Pr -Ar), 0.92 (m, 3H, CH_3, *i*-Pr -Ar), 0.94 (m, 3H, CH_3, *i*-Pr), 1.09 (m, 6H, CH_3, *i*-Pr -Ar), 1.50 (m, 3H, CH_3, *i*-Pr -Ar), 1.68 (m, 2H, CH_2, cod), 1.90 (m, 3H, CH_2, cod), 2.12 (m, 3H, CH_2, cod) 2.33 (m, 2H, CH, *i*-Pr -Ar), 2.47 (s, 3H, CH_3, Ar), 2.53 (m, 1H, CH, *i*-Pr), 2.67 (s, 3H, CH_3, Ar), 2.77 (m, 2H, CH-S an CH=, cod), 2.94 (m, 1H,

CH=, cod), 3.96 (m, 1H, CH=, cod), 4.22 (m, 1H, CH=, cod), 4.42 (dd, 1H, $^2J_{H-H}$= 14.6 Hz, $^3J_{H-H}$= 2.6 Hz, CH_2-N), 5.02 (dd, 1H, $^2J_{H-H}$= 14.6 Hz, $^3J_{H-H}$= 3.5 Hz, CH_2-N), 6.89 (s, 1H, CH=, NHC), 6.97 (s, 1H, CH=, NHC), 7.09-7.64 (m, 18H, CH=). ^{13}C NMR (100.6 MHz, $CDCl_3$), *δ*: 20.6 (CH_3, *i*-Pr), 21.1 (CH_3, *i*-Pr -Ar), 21.9 (CH_3, Ar), 22.3 (CH_3, Ar), 22.7 (CH_3, *i*-Pr -Ar), 24.2 (CH_3, *i*-Pr), 24.9 (CH_3, *i*-Pr -Ar), 25.9 (CH_3, *i*-Pr -Ar), 28.4 (CH, *i*-Pr -Ar), 28.5 (CH, *i*-Pr -Ar) 29.3 (CH, *i*-Pr), 31.2 (CH_2, cod), 31.5 (CH_2, cod) 32.9 (CH_2, cod), 36.5 (CH_2, cod), 55.0 (CH_2-N), 55.1 (CH-S), 68.2 (CH=, cod), 72.3 (CH=, cod), 83.3 (CH=, cod), 84.9 (CH=, cod), 123.2 (CH=, NHC), 125.9 (CH=, NHC), 117.4-145.7 (aromatic carbons), 161.7 (q, C, $^1J_{C-B}$= 49.6 Hz, BAr_F), 168.5 (C, NHC). Anal. calcd. (%) for $C_{68}H_{62}BF_{24}IrN_2S$: C 51.10, H 3.91, N 1.75, S 2.00; found: C 51.01, H 3.89, N 1.73, S 1.98. MS HR-ESI [found 735.3324, $C_{36}H_{50}IrN_2S$ $(M\text{-}BAr_F)^+$ requires 735.3318].

3.5.4.7. General procedure for the preparation of [Ir(cod)(L21–L22a)]BAr_F

The corresponding ligand (0.074 mmol) was dissolved in CH_2Cl_2 (5 mL) and [Ir(μ-Cl)(cod)]$_2$ (0.037 mmol, 25 mg) was added. The reaction mixture was refluxed at 50 ºC for 1 hour. After 5 min at room temperature, $NaBAr_F$ (0.080 mmol, 77.2 mg) and water (5 mL) were added and the reaction mixture was stirred vigorously for 30 min at r.t. The phases were separated and the aqueous phase was extracted twice with CH_2Cl_2. The combined organic phases were dried with $MgSO_4$ and purified, if necessary, with neutral silica resulting in orange solids.

[Ir(cod)(L21a)]BAr_F: Yield 110 mg (87%). ^{31}P NMR (161.9 MHz, $CDCl_3$), *δ*: 96.4. ^{1}H NMR (400 MHz, $CDCl_3$), *δ*: 1.01 (d, 3H, CH_3, *i*-Pr, $^3J_{H-H}$= 6.6 Hz), 1.11 (d, 3H, CH_3, *i*-Pr, $^3J_{H-H}$= 6.6 Hz) 1.47 (s, 9H, CH_3, *t*-Bu) 1.75 (s, 9H, CH_3, *t*-Bu), 1.81 (s, 3H, CH_3), 1.85 (s, 3H, CH_3), 1.98 (b, 4H, CH_2, cod), 2.20 (m, 5H, CH, *i*-Pr and CH_2, cod), 2.27 (m, 6H, $2CH_3$), 3.05 (b, 1H, CH=, cod), 3.26 (b, 1H, CH=, cod) 4.34 (b, 1H, CH=, cod), 4.56 (m, 2H, CH_2-O and CH-S), 4.95 (m, 2H, CH_2-O and CH=, cod), 7.22-7.71 (m, 19H, CH=). ^{13}C NMR (100.6 MHz, $CDCl_3$), *δ*: 14.5 (CH_3), 14.6 (CH_3), 17.3 (CH_3, *i*-Pr), 18.3 (CH_3), 18.5 (CH_3), 18.9 (CH_3, *i*-Pr), 25.7 (CH_2, cod), 27.0 (CH, *i*-Pr), 27.5 (CH_2, cod), 29.6 (CH_3, *t*-Bu), 30.2 (d, CH_2, cod, $^2J_{C-P}$ =3.8 Hz), 30.6 (CH_3, *t*-Bu), 31.4 (CH_2, cod, J_{C-P} =3.8 Hz), 32.9 (C, *t*-Bu), 33.2 (C, *t*-Bu), 60.6 (CH=, cod), 66.9 (CH=, cod), 67.8 (CH_2-O), 75.5 (CH-S), 100.0 (CH=, cod, J_{C-P}= 14.9 Hz), 104.3 (CH=, cod, J_{C-P}= 14.9 Hz), 115.5-141.9 (aromatic carbons) 159.7 (q, C-B, BAr_F J_{C-B}= 49.7Hz). Anal. calcd. (%) for $C_{75}H_{71}BF_{24}IrO_3PS$: C 51.67, H 4.11, S 1.84; found: C 51.49, H 4.07, S 1.81. MS HR-ESI [found 879.3557, $C_{43}H_{59}IrO_3PS$ $(M\text{-}BAr_F)^+$ requires 879.3546].

[Ir(cod)(L21b)]BAr_F; Yield 102 mg (72%). ^{31}P NMR (161.9 MHz, $CDCl_3$), *δ*: 98.2. ^{1}H NMR (400 MHz, $CDCl_3$), *δ*: 0.89 (d, 3H, $^3J_{H-H}$= 6.6 Hz, CH_3, *i*-Pr), 1.02 (d, 3H, $^3J_{H-H}$= 6.6 Hz, CH_3, *i*-Pr) 1.43 (s, 9H, CH_3, *t*-Bu) 1.63 (s, 9H, CH_3, *t*-Bu), 1.78 (b, 7H, CH_3 and

CH, *i*-Pr), 1.95 (m, 6H, CH_2, cod), 2.18 (m, 2H, CH_2, cod), 2.27 (m, 6H, CH_3), 3.02 (b, 1H, CH=, cod), 3.41 (b, 1H, CH=, cod) 4.33 (m, 1H, CH_2-O), 4.67 (m, 3H, CH_2-O, CH-S and CH=, cod), 5.09 (b, 1H, CH=, cod) 7.23-7.71 (m, 19H, CH=). ^{13}C NMR (100.6 MHz, $CDCl_3$) *δ*: 14.4 (CH_3), 14.4 (CH_3), 14.6 (CH_3, *i*-Pr), 18.3 (CH_3), 18.5 (CH_3, *i*-Pr), 25.8 (CH_2, cod), 26.6 (CH_2, cod), 27.3 (CH, *i*-Pr), 27.8 (CH_3r), 29.7 (CH_3, *t*-Bu), 30.4 (d, $^2J_{C\text{-}P}$ =3,8 Hz CH_2, cod), 30.6 (CH_3, *t*-Bu), 31.4 (d, $J_{C\text{-}P}$ =3,8 Hz, CH_2, cod), 32.9 (C, *t*-Bu), 33.1 (C, *t*-Bu), 54.8 (CH=, cod), 65.1 (CH=, cod), 65.4 (CH_2-O), 76.9 (CH-S), 102.9 (d, $J_{C\text{-}P}$= 14.9 Hz, CH=, cod), 104.1 (d, $J_{C\text{-}P}$= 14.9 Hz, CH=, cod), 115.5-142.4 (aromatic carbons), 159.7 (q, C-B, BAr_F $J_{C\text{-}B}$= 49.7Hz). Anal. calcd. (%) for $C_{75}H_{71}BF_{24}IrO_3PS$: C 51.67, H 4.11, S 1.84; found: C 51.52, H 4.09, S 1.82. MS HR-ESI [found 879.3542, $C_{43}H_{59}IrO_3PS$ $(M\text{-}BAr_F)^+$ requires 879.3546].

[Ir(cod)(L21c)]BAr_F: Yield: 99 mg (87%). ^{31}P NMR (161.9 MHz, $CDCl_3$), *δ*: 103.7. ^{1}H NMR (400 MHz, $CDCl_3$), *δ*: 0.91 (d, 3H, $^3J_{H\text{-}H}$= 6.8 Hz, CH_3, *i*-Pr), 1.01 (d, 3H, $^3J_{H\text{-}H}$= 6.8 Hz, CH_3, *i*-Pr,), 1.95 (m, 5H, CH, *i*-Pr and CH_2, cod), 2.28 (m, 4H, CH_2, cod), 3.28 (b, 1H, CH=, cod), 3.36 (m, 1H, CH-S), 3.55 (b, 1H, CH=, cod), 4.33 (m, 2H, CH_2-O and CH=, cod) 4.61 (m, 1H, CH_2-O), 4.98 (b, 1H, CH=, cod), 7.26-7.73 (m, 27H, CH=). ^{13}C NMR (100.6 MHz, $CDCl_3$), *δ*: 17.5 (CH_3, *i*-Pr), 20.4 (CH_3, *i*-Pr), 28.8 (d, $J_{C\text{-}P}$= 2.0 Hz, CH_2, cod), 29.0 (d, $J_{C\text{-}P}$= 2.0 Hz, CH_2, cod), 29.6 (CH_2, cod), 30.3 (CH, *i*-Pr), 32.2 (d, $J_{C\text{-}P}$= 6.9 Hz, CH_2, cod,), 59.0 (CH-S), 68.9 (CH_2-O), 73.2 (CH=, cod), 73.3 (CH=, cod), 99.7 (d, $J_{C\text{-}P}$= 11.4 Hz, CH=, cod), 100.6 (d, $J_{C\text{-}P}$= 11.9 Hz, CH=, cod), 117.4-134.8 (aromatic carbons), 161.6 (q, C-B, BAr_F, $^1J_{C\text{-}B}$= 49.9 Hz). Anal. calcd. (%) for $C_{63}H_{49}BF_{24}IrOPS$: C 49.01, H 3.20, S 2.07; found: C 48.88, H 3.17, S 2.05. MS HR-ESI [found 681.1932, $C_{31}H_{37}IrOPS$ $(M\text{-}BAr_F)^+$ requires 681.1926].

[Ir(cod)(L22a)]BAr_F: Yield: 56 mg (42%). ^{31}P NMR (161.9 MHz, $CDCl_3$), *δ*: 97.5. ^{1}H NMR (400 MHz, $CDCl_3$), *δ*: 0.95 (m, 3H, CH_3, *i*-Pr), 1.01 (m, 3H, CH_3, *i*-Pr), 1.44 (s, 9H, CH_3, *t*-Bu), 1.63 (s, 9H, CH_3, *t*-Bu), 1.73 (s, 3H, CH_3), 1.81 (s, 3H, CH_3), 1.84-2.16 (m, 9H, CH, *i*-Pr and CH_2, cod), 2.26 (s, 3H, CH_3), 2.28 (s, 3H, CH_3), 2.54 (s, 3H, CH_3), 2.85 (m, 4H, CH_3 and CH=, cod), 3.30 (m, 1H, CH-S), 3.91 (m, 1H, CH=, cod), 4.49 (m, 2H, CH_2-O and CH=, cod), 4.78 (m, 1H, CH_2-O), 4.93 (m, 1H, CH=, cod), 7.16-7.70 (m, 17H, CH=). ^{13}C NMR (100.6 MHz, $CDCl_3$), *δ*: 16.3 (CH_3, *i*-Pr), 16.5 (CH_3, *i*-Pr), 17.9 (CH_3), 20.3 (CH_3), 20.4 (CH_3), 22.1 (CH_3), 22.6 (CH_3), 22.9 (CH_3), 27.0 (CH_2, cod), 29.5-29.7 (2xCH_2, cod), 30.9 (CH, *i*-Pr), 31.5 (CH_3, *t*-Bu), 32.6 (CH_3, *t*-Bu), 33.7 (CH_2, cod), 34.8 (C, *t*-Bu), 35.2 (C, *t*-Bu), 57.6 (CH-S), 66.6 (CH_2-O), 67.0 (CH=, cod), 75.9 (CH=, cod), 102.8 (d, $J_{C\text{-}P}$= 13.7 Hz CH=, cod), 106.1 (d, $J_{C\text{-}P}$= 14.2 Hz, CH=, cod), 117.4-143.5 (aromatic carbons), 161.4 (q, $^1J_{C\text{-}B}$= 49.9 Hz, C-B, BAr_F). Anal. calcd. (%) for $C_{77}H_{75}BF_{24}IrO_3PS$: C 52.24, H 4.27, S 1.81; found: C 52.01, H 4.24, S 1.79. MS HR-ESI [found 907.3865, $C_{45}H_{63}IrO_3PS$ $(M\text{-}BAr_F)^+$ requires 907.3859].

[Ir(cod)(L22b)]BAr_F: Yield: 77 mg (59%). ^{31}P NMR (161.9 MHz, $CDCl_3$), *δ*: 96.3. ^{1}H NMR (400 MHz, $CDCl_3$), *δ*: 0.90 (m, 6H, CH_3, *i*-Pr), 1.46 (s, 9H, CH_3, *t*-Bu), 1.62 (s,

9H, CH_3, *t*-Bu), 1.72 (s, 3H, CH_3), 1.74 (s, 3H, CH_3), 1.90-2.15 (m, 7H, CH_2, cod), 2.24 (s, 6H, CH_3), 2.34 (m, 2H, CH, *i*-Pr and CH_2, cod), 2.62 (s, 3H, CH_3), 2.73 (s, 3H, CH_3), 3.10 (m, 1H, CH=, cod), 3.35 (m, 1H, CH-S), 4.48 (m, 2H, CH_2-O and CH=, cod), 4.60 (m, 2H, CH_2-O and CH=, cod), 4.77 (m, 1H, CH=, cod), 7.17-7.70 (m, 17H, CH=). ^{13}C NMR (100.6 MHz, $CDCl_3$), *δ*: 16.4 (CH_3, *i*-Pr), 16.6 (CH_3, *i*-Pr), 20.3 (CH_3), 20.4 (CH_3), 20.6 (CH_3), 22.6 (CH_3), 23.5 ($2CH_3$), 26.6 (CH_2, cod), 29.6 (CH, *i*-Pr), 29.7 (CH_2, cod) 30.2 (CH_2, cod), 31.0 (CH_2, cod), 31.8 (CH_3, *t*-Bu), 32.2 (CH_3, *t*-Bu), 34.9 (C, *t*-Bu), 35.0 (C, *t*-Bu), 54.9 (CH-S), 64.8 (CH=, cod), 66.9 (CH_2-O), 77.7 (CH=, cod), 101.7 (d, $J_{C\text{-}P}$= 13.4 Hz, CH=, cod), 107.1 (d, $J_{C\text{-}P}$= 11.5 Hz, CH=, cod), 110.0-143.2 (aromatic carbons), 161.4 (q, $^1J_{C\text{-}B}$= 49.9 Hz, C-B, BAr_F). Anal. calcd. (%) for $C_{77}H_{75}BF_{24}IrO_3PS$: C 52.24, H 4.27, S 1.81; found: C 51.99, H 4.25, S 1.79. MS HR-ESI [found 907.3862, $C_{45}H_{63}IrO_3PS$ $(M\text{-}BAr_F)^+$ requires 907.3859].

[Ir(cod)(L22c)]BAr$_F$: Yield: 47 mg (41%). Major isomer (53%): ^{31}P NMR ($CDCl_3$) *δ*: 107.7. ^{1}H NMR ($CDCl_3$) *δ*: 0.96 (m, 6H, CH_3, *i*-Pr), 1.75-2.33 (m, 9H, CH_2, cod and CH, *i*-Pr), 2.55 (s, 3H, CH_3-Ar), 2.60 (s, 3H, CH_3-Ar), 3.10 (m, 1H, CH=, cod), 3.43 (b, 1H, CH=, cod), 3.56 (m, 1H, CH-S), 3.79 (m, 1H, CH_2-O), 4.45 (m, 1H, CH_2-O), 4.56 (b, 1H, CH=, cod), 5.09 (b, 1H, CH=, cod), 6.92-7.97 (m, 25H, CH=). ^{13}C NMR ($CDCl_3$) *δ*: 14.1 (CH_3, *i*-Pr), 16.3 (CH_3, *i*-Pr), 20.6 (CH_3-Ar), 20.8 (CH_3-Ar), 22.4-36.4 (CH_2, cod), 33.1 (CH, *i*-Pr), 54.9 (CH-S), 66.0 (CH_2-O), 75.4 (CH=, cod), 81.9 (CH=, cod), 95.6 (d, $J_{C\text{-}P}$= 13.9 Hz, CH=, cod), 99.4 (d, $J_{C\text{-}P}$= 14.6 Hz, , CH=, cod), 117.4-155.3 (aromatic carbons), 161.4 (q, $^1J_{C\text{-}B}$= 49.9 Hz, C-B, BAr_F). Minor isomer (47%): ^{31}P NMR ($CDCl_3$) *δ*: 85.6. ^{1}H NMR ($CDCl_3$) *δ*: 1.38 (m, 3H, CH_3, *i*-Pr), 1.75-2.33 (m, 8H, CH-S, CH_2, cod and CH, *i*-Pr), 2.89 (m, 2H, CH_2, cod), 2.99 (s, 6H, CH_3-Ar), 3.43 (b, 2H, CH=, cod), 3.69 (m, 1H, CH=, cod), 3.79 (m, 1H, CH_2-O), 4.62 (m, 1H, CH_2-O), 5.09 (m, 1H, CH=, cod), 6.92-7.97 (m, 20H, CH=). ^{13}C NMR ($CDCl_3$) *δ*: 20.2 (CH_3, *i*-Pr), 22.2 (CH_3, *i*-Pr), 23.8 (CH_3-Ar), 22.2 (CH_3-Ar), 31.7 (CH- *i*-Pr), 22.6-36.4 (CH_2, cod), 55.1 (CH-S), 66.2 (CH_2-O), 68.02 (CH=, cod), 91.8 (CH=, cod), 98.5 (d, $J_{C\text{-}P}$= 13.0 Hz CH=, cod), 103.0 (d, $J_{C\text{-}P}$= 9.47 Hz, CH=, cod), 117.4-155.3 (aromatic carbons), 161.4 (q, $^1J_{C\text{-}B}$= 49.9 Hz, C-B, BAr_F). Anal. calcd. (%) for $C_{65}H_{53}BF_{24}IrOPS$: C 49.66, H 3.40, S 2.03; found: C 49.71, H 3.42, S 2.01. MS HR-ESI [found 709.2245, $C_{33}H_{41}IrOPS$ $(M\text{-}BAr_F)^+$ requires 709.2239].

[Ir(cod)(L22d)]BAr$_F$: Yield: 90 mg (77%). ^{31}P NMR (161.9 MHz, $CDCl_3$), *δ*: 110.7. ^{1}H NMR (400 MHz, $CDCl_3$), *δ*: 0.72 (m, 3H, CH_3, *i*-Pr), 0.87 (m, 3H, CH_3, *i*-Pr), 1.44 (m, 1H, CH, *i*-Pr), 1.85-2.00 (m, 6H, CH_2, cod), 2.12 (s, 3H, CH_3, *o*-Tol), 2.18-2.85 (m, 2H, CH_2, cod), 2.55 (s, 3H, CH_3, *o*-Tol), 2.72 (m, 1H, CH=, cod), 2.88 (s, 3H, CH_3), 2.97 (s, 3H, CH_3), 3.17 (m, 1H, CH=, cod), 3.70 (m, 1H, CH=, cod), 3.78 (b, 2H, CH_2-O and CH-S), 4.54 (m, 1H, CH_2-O), 4.87 (m, 1H, CH=, cod), 6.68-8.95 (m, 23H, CH=). ^{13}C NMR (100.6 MHz, $CDCl_3$), *δ*: 16.2 (CH_3, *i*-Pr), 20.2 (CH_3, *i*-Pr), 21.6 (CH_3, *o*-Tol), 22.2 (CH_3, *o*-Tol), 22.3 (CH_3); 23.0 (CH_3), 27.6 (CH, *i*-Pr) 28.7 (CH_2, cod), 30.6 (CH_2, cod), 30.9 (CH_2, cod), 33.3 (CH_2, cod), 54.7 (CH-S), 66.2 (CH_2-O), 67.6 (CH=, cod), 76.1

(CH=, cod), 97.1 (d, $J_{C\text{-}P}$= 9.2 Hz, CH=, cod), 98.4 (d, $J_{C\text{-}P}$= 11.5 Hz, CH=, cod), 117.4-143.2 (aromatic carbons), 161.9 (q, $^{1}J_{C\text{-}B}$= 49.9 Hz, C-B, BAr_F). Anal. calcd. (%) for $C_{67}H_{57}BF_{24}IrOPS$: C 50.29, H 3.59, S 2.00; found: C 50.34, H 3.58, S 1.98. MS HR-ESI [found 737.2554, $C_{35}H_{45}IrOPS$ $(M\text{-}BAr_F)^+$ requires 737.2552].

[Ir(cod)(L22e)]BAr_F: Yield: 45 mg (39%). ^{31}P NMR (161.9 MHz, $CDCl_3$), δ: 129.7. ^{1}H NMR (400 MHz, $CDCl_3$), δ: 1.11 (m, 3H, CH_3, *i*-Pr), 1.20 (m, 3H, CH_3, *i*-Pr), 1.47-2.56 (m, 31 H, CH, Cy, CH_2, Cy, CH, *i*-Pr r and CH_2, cod), 2.80 (s, 3H, CH_3), 2.93 (s, 3H, CH_3), 3.13 (m, 1H, CH-S), 3.77 (m, 1H, CH=, cod), 4.01 (m, 1H, CH=, cod), 4.24 (m, 1H, CH=, cod), 4.59 (m, 2H, CH_2-O), 4.75 (m, 1H, CH=, cod), 7.33-7.92 (m, 15H, CH=). ^{13}C NMR (100.6 MHZ, $CDCl_3$), δ: 19.1 (CH_3, *i*-Pr), 20.9 (CH_3, *i*-Pr), 22.2 (CH_3), 23.0 (CH_3), 25.8-34.0 (CH_2, Cy andCH, *i*-Pr and CH_2, cod,), 40.0 (d, $^{1}J_{C\text{-}P}$= 29.9 Hz, CH, Cy), 41.5 (d, $^{1}J_{C\text{-}P}$= 30.0 Hz, CH, *i*-Pr), 57.8 (CH-S), 66.3 (CH=, cod), 70.0 (CH=, cod), 71.3 (CH_2-O), 94.9 (d, $J_{C\text{-}P}$= 10.2 Hz, CH=, cod), 96.9 (d, $J_{C\text{-}P}$= 10.2 Hz, CH=, cod), 117.4-142.2 (aromatic carbons), 161.9 (q, $^{1}J_{C\text{-}B}$= 49.9 Hz, C-B, BAr_F). Anal. calcd. (%) for $C_{65}H_{65}BF_{24}IrOPS$: C 49.28, H 4.14, S 2.02; found: C 49.17, H 4.11, S 1.99. MS HR-ESI [found 721.3180, $C_{33}H_{53}IrOPS$ $(M\text{-}BAr_F)^+$ requires 721.3178].

3.5.4.8. General procedure for the asymmetric hydrogenation

The alkene (0.5 mmol) and Ir complex (1 mol %) were dissolved in CH_2Cl_2 (2 mL) and placed in a high-pressure autoclave. The autoclave was purged 4 times with hydrogen. Then, it was pressurized at the desired pressure. After the desired reaction time, the autoclave was depressurized and the solvent evaporated off. The residue was dissolved in Et_2O (1.5 mL) and filtered through a short plug of celite. The enantiomeric excess was determined by chiral GC or chiral HPLC and conversions were determined by ^{1}H NMR.

3.5.4.9. Reactivity studies of [Ir(cod)(L)]BAr_F towards H_2

In a typical experiment hydrogen was bubbled through a CD_2Cl_2 solution of the desired [Ir(cod)(L)]BAr_F catalyst precursor (5 mmol) to the desired temperature for 15-30 min. The reaction mixture was analyzed by NMR spectroscopy at the desired temperature. All attempts to isolate the *cis*-dihydride iridium complexes **14**, **15**, **17**, **18** and **19** were unsuccessful even at -70 ºC under a hydrogen atmosphere.

3.5.4.10. Computational details

The geometries of all intermediates were optimized using the Gaussian 09 program,[34] employing the B3LYP-D3[35] density functional and the LANL2DZ[36] basis set for iridium and the 6-31G*[37] basis set for all other elements.[38] Solvation correction was applied in the course of the optimizations using PCM model with the default parameters for dichloromethane.[39] The complexes were treated with charge +1 and in the single state. No symmetry constraints were applied. All energies reported are Gibbs free energies.

3.5.5. References

[1] (a) Powell, M. T.; Hou, D.–R.; Perry, M. C.; Cui, X.; Burgess, K. Chiral Imidazolylidine Ligands for Asymmetric Hydrogenation of Aryl Alkenes. *J. Am. Chem. Soc.* **2001**, *123*, 8878–8879. (b) Perry, M. C.; Cui, X.; Powell, M. T.; Hou, D.–R.; Reibenspies, J. H.; Burgess, K. Optically Active Iridium Imidazol–2–ylidene–oxazoline Complexes: Preparation and Use in Asymmetric Hydrogenation of Arylalkenes. *J. Am. Chem. Soc.* **2003**, *125*, 113–123. (c) Bolm, C.; Focken, T.; Raabe, G. Synthesis of iridium complexes with novel planar chiral chelating imidazolylidene ligands. *Tetrahedron: Asymmetry* **2003**, *14*, 1733–1746. (d) Källström, K.; Andersson, P. G. Asymmetric Hydrogenation of Tri–substituted Alkenes with Ir–NHC–thiazole Complexes. *Tetrahedron Lett.* **2006**, *47*, 7477–7480. (e) Nanchen, S.; Pfaltz, A. Synthesis and Application of Chiral N-Heterocyclic Carbene–Oxazoline Ligands: Iridium-Catalyzed Enantioselective Hydrogenation. *Chem. Eur. J.* **2006**, *12*, 4550–4558. (f) Chen, D.; Banphavichit, V.; Reibenspies, J.; Burgess, K. New Optically Active N–Heterocyclic Carbene Complexes for Hydrogenation: A Tale with an Atropisomeric Twist. *Organometallics* **2007**, *26*, 855–859. (g) Khumsubdee, S.; Fan, Y.; Burgess, K. A Comparison between Oxazoline–imidazolinylidene, –imidazolylidine, –benzimidazolylidene Hydrogenation Catalysts. *J. Org. Chem.* **2013**, *78*, 9969–9974. (h) Schumacher, A.; Bernasconi, M.; Pfaltz, A. Chiral N-Heterocyclic Carbene/Pyridine Ligands for the Iridium-Catalyzed Asymmetric Hydrogenation of Olefins. *Angew. Chem. Int. Ed.* **2013**, *52*, 7422–7425.

[2] (a) Bourissou, D.; Guerret, O.; Gabbai, F. P.; Bertrand, G. Stable Carbenes. *Chem. Rev.* **2000**, *100*, 39–92. (b) Arduengo, A. J.; Bertrand, G. Carbenes Introduction. *Chem. Rev.* **2009**, *109*, 3209–3210 (thematic issue). (c) Mercs, L.; Albrecht, M. Beyond Catalysis: N–Heterocyclic Carbene Complexes as Components for Medicinal, Luminescent, and Functional Materials Applications. *Chem. Soc. Rev.* **2010**, *39*, 1903–1912. (d) Herrmann, W. A. N–Heterocyclic Carbenes: a New Concept in Organometallic Catalysis. *Angew. Chem. Int. Ed.* **2002**, *41*, 1290–1309. (e) Díez–González; S.; Marion, N.; Nolan, S. P. N–Heterocyclic Carbenes in Late Transition Metal Catalysis. *Chem. Rev.* **2009**, *109*, 3612–3676. (f) Hahn, F. E.; Jahnke, M. C. Heterocyclic Carbenes: Synthesis and Coordination Chemistry. *Angew. Chem. Int. Ed.* **2008**, *47*, 3122–3172. (g) Peris, E. Smart N–Heterocyclic Carbene Ligands in Catalysis. *Chem. Rev.* **2018**, *118*, 9988–10031. (h) Glorious, F. N–Heterocyclic Carbenes in Transition Metal Catalysis, in *Topics in Organometallic Chemistry*, Springer, Berlin, **2007**. (i) Cazin, C. S. J. N–Heterocyclic Carbenes in Transition Metal Catalysis and Organocatalysis, Springer, Berlin, **2011**. (j) Díez–González, S. N–Heterocyclic Carbenes: from Laboratory Curiosities to Efficient Synthetic Tools, RSC Publishing, Cambridge, **2011**. (k) Huynh, H. V. *The Organometallic Chemistry of N–heterocyclic Carbenes,* Wiley, Chichester, **2017**. (l) Fliedel, C.; Labande, A.; Manoury, E.; Poli, R. Chiral N–heterocyclic Carbene Ligands with Additional Chelating Group(s) Applied to Homogeneous Metal–mediated Asymmetric Catalysis. *Coord. Chem. Rev.* **2019**, *394*, 65–103. (m) Krishnan, D.; Wu, M.; Chiang, M.; Li, Y.; Leung, P.–H.; Pullarkat, S. A. N–Heterocyclic Carbene C,S Palladium(II) η–Allyl Complexes: Synthesis, Characterization, and Catalytic Application In Allylic Amination Reactions. *Organometallics*, **2013**, *32*, 2389–2397. (n) Krishnan, D.; Pullarkat, S. A.; Wu, M.; Li, Y.; Leung, P.–H. Synthesis, Structural Characterisation and Stereochemical Investigation of Chiral Sulfur–Functionalised N–Heterocyclic Carbene Complexes of Palladium and Platinum. *Chem. Eur. J.* **2013**, *19*, 5468–5475. (o) Hopkinson, M. N.; Richter, C.; Scheler, M.; Glorius. F. An Overview of N–heterocyclic Carbenes. *Nature* **2014**, *510*, 485–496. (p) Janssen–Mueller, D.; Schlepphortst, C.; Glorius, F. Privileged Chiral N–heterocyclic Carbene Ligands for Asymmetric Transition–metal Catalysis. *Chem. Soc. Rev. 2017*, *46* , 4845–4854.

[3] (a) Focken, T.; Raabe, G.; Bolm, C. Synthesis of Iridium Complexes with New Planar Chiral Chelating Phosphinyl–imidazolylidene Ligands and Their Application in Asymmetric Hydrogenation. *Tetrahedron: Asymmetry* **2004**, *15*, 1693–1706. (b) Nanchen, S.; Pfaltz, A. Chiral Phosphino- and (Phosphinooxy)-Substituted N-Heterocyclic Carbene Ligands and Their Application in Iridium-Catalyzed Asymmetric Hydrogenation. *Helv. Chim. Acta* **2006**, *89*, 1559–1573. (c) Gu, P.; Zhang, J.; Xu, Q.; Shi, M. Synthesis of Iridium and Rhodium Complexes with New Chiral Phosphine–NHC Ligands Based on 1,1′–Binaphthyl Framework and Their Application in Asymmetric Hydrogenation. *Dalton Trans.* **2013**, *42*, 13599–13606.

[4] (a) Coll, M.; Pàmies, O.; Diéguez, M. Thioether–phosphite: new ligands for the highly enantioselective Ir–catalyzed hydrogenation of minimally functionalized olefins. *Chem. Commun.* **2011**, *47*, 9215–9217. (b) Coll, M.; Pàmies, O.; Diéguez, M. A Modular Furanoside Thioether–Phosphite/Phosphinite/ Phosphine Ligand Library for Asymmetric Iridium–Catalyzed Hydrogenation of Minimally Functionalized Olefins: Scope and Limitations. *Adv. Synth. Catal.* **2013**, *355*, 143–160. (c) Margalef, J.; Caldentey, X.; Karlsson, E. A.; Coll, M.; Mazuela, J.; Pàmies, O.; Diéguez, M.; Pericàs, M. A. A Theoretically–Guided Optimization of a New Family of Modular P,S–Ligands for Iridium–Catalyzed Hydrogenation of Minimally Functionalized Olefins. *Chem. Eur. J.* **2014**, *20*, 12201–12214. (d) Borràs, C.; Biosca, M.; Pàmies, O.; Diéguez, M. Iridium–Catalyzed Asymmetric Hydrogenation with Simple Cyclohexane–Based P/S Ligands: *In Situ* HP–NMR and DFT Calculations for the Characterization of Reaction Intermediates. *Organometallics* **2015**, *34*, 5321–5334; (e) Biosca, M.; Coll, M.; Lagarde, F.; Brémond, E.; Routaboul, L.; Manoury, E.; Pàmies, O.; Poli, R.; Diéguez, M. Chiral ferrocene–based P,S ligands for Ir–catalyzed hydrogenation of minimally functionalized olefins. Scope and limitations. *Tetrahedron* **2016**, *72*, 2623–2631; (f) Margalef, J.; Borràs, C.; Alegre, S.; Alberico, E.; Pàmies, O.; Diéguez, M. Phosphite-thioether/selenoether Ligands from Carbohydrates: An Easily Accessible Ligand Library for the Asymmetric Hydrogenation of Functionalized and Unfunctionalized Olefins. *ChemCatChem* **2019**, *11*, 2142–2168. (g) Margalef, J.; Pàmies, O.; Pericàs, M. A.; Diéguez, M. Evolution of phosphorus–thioether ligands for asymmetric catalysis. *Chem. Comm.* **2020**, *56*, 10795–10808. (h) Faiges, J.; Borràs, C.; Pastor, I. M.; Pàmies, O.; Besora, M.; Diéguez, M. Density Functional Theory–Inspired Design of Ir/P,S–Catalysts for Asymmetric Hydrogenation of Olefins. *Organometallics* **2021,** *40*, 20, 3424–3435. (i) Margalef, J.; Biosca, M.; de la Cruz–Sánchez, P.; Caldentey, X.; Rodríguez–Escrich, C.; Pàmies, O.; Pericàs, M. A.; Diéguez, M. Indene Derived Phosphorus–Thioether Ligands for the Ir–Catalyzed Asymmetric Hydrogenation of Olefins with Diverse Substitution Patterns and Different Functional Groups. *Adv. Synth. Catal.* **2021**, *363*, 4561–4574.

[5] Margalef, J.; Pàmies, O.; Diéguez, M. Phosphite-Thiother Ligands Derived from Carbohydrates allow the Enantioswitchable Hydrogenation of Cyclic β-Enamides by using either Rh or Ir Catalysts. *Chem. Eur. J.* **2018**, *23*, 813–822.

[6] Thioether–P ligands also early showed promising results in the asymmetric hydrogenation of functionalized olefins (mainly dehydroamino acids). See for example: (a) Hauptman, E.; Fagan, P. J.; Marshall, W. Synthesis of Novel (P,S) Ligands Based on Chiral Nonracemic Episulfides. Use in Asymmetric Hydrogenation. *Organometallics* **1999**, *18*, 2061–2073. (b) Evans, D. A.; Michael, F. E.; Tedrow, J. S.; Campos, K. R. Application of Chiral Mixed Phosphorus/Sulfur Ligands to Enantioselective Rhodium–Catalyzed Dehydroamino Acid Hydrogenation and Ketone Hydrosilylation Processes. *J. Am. Chem. Soc.* **2003**, *125*, 3534–3543. (c) Molander, G. A.; Burke, J. P.; Carroll, P. J. Synthesis and Application of Chiral Cyclopropane–Based Ligands in Palladium–Catalyzed Allylic Alkylation. *J. Org. Chem.* **2004**, *69*, 8062–8069. (d) Guimet, E.; Diéguez, M.; Ruiz, A.; Claver, C.

Asymmetric Hydrogenation of Prochiral Olefins Catalysed by Furanoside Thioether–phosphinite Rh(I) and Ir(I) Complexes. *Dalton Trans.* **2005**, 2557–2562.

[7] De La Cruz–Sánchez, P.; Faiges, J.; Mazloomi, Z.; Borràs, C.; Biosca, M.; Pàmies, O.; Diéguez, M. Ir/Thioether−Carbene, −Phosphinite, and −Phosphite Complexes for Asymmetric Hydrogenation. A Case for Comparison. *Organometallics* **2019**, *38*, 4193−4205.

[8] Ohtaka, J.; Hamajima, A.; Nemoto, T.; Hamada, Y. Efficient Diastereoselective Synthesis of (2*R*,3*R*,4*R*)−2−Amino−3−hydroxy−4,5−dimethylhexanoic Acid, the Lactone Linkage Unit of Homophymine A. *Chem. Pharm. Bull.* 2013, *61*, 245–250.

[9] Evans, D. A.; Britton, T. C.; Ellman, J. A.; Dorow, R. L. The Asymmetric Synthesis of .Alpha.–Amino Acids. Electrophilic Azidation of Chiral Imide Enolates, a Practical Approach to the Synthesis of (*R*)–and (*S*)–.Alpha.–Azido Carboxylic Acids. *J. Am. Chem. Soc.* 1990, *112*, 4011–4030.

[10] Evans, D. A.; Campos, K. R.; Tedrow, J. S.; Michael, F. E.; Gagné, M. R. Application of Chiral Mixed Phosphorus/Sulfur Ligands to Palladium–Catalyzed Allylic Substitutions. *J. Am. Chem. Soc.* 2000, *122*, 7905–7920.

[11] Iglesias–Sigüenza, J.; Ros, A.; Díez, E.; Magriz, A.; Vázquez, A.; Álvarez, E.; Fernández, R.; Lassaletta, J. M. C_2 –Symmetric S/C/S Ligands Based on N–Heterocyclic Carbenes: a New Ligand Architecture for Asymmetric Catalysis. *Dalton Trans.* **2009**, 8485–8488.

[12] Kumar, M. R.; Park, K.; Lee, S. Synthesis of Amido-N-imidazolium Salts and their Applications as Ligands in Suzuki–Miyaura Reactions: Coupling of Hetero- aromatic Halides and the Synthesis of Milrinone and Irbesartan. *Adv. Synth. Catal.* **2010**, *352*, 3255–3266.

[13] The decomposition is especially fast for ligand **L4e** for which it has been not possible to obtain a pure sample. Fortunately, we were able to remove these impurities during the preparation of the corresponding Ir–catalyst precursor that could be obtained in pure form.

[14] The [Ir(cod)(**L22c**)]BAr_F complex shows two set of NMR signals. The 2D–DOSY experiments showed that the two species have the same diffusion coefficient (see the Supporting Information), which agree with a mixture of two isomers in solution.

[15] Zhu, Y.; Burgess, K. Filling Gaps in Asymmetric Hydrogenation Methods for Acyclic Stereocontrol: Application to Chirons for Polyketide–Derived Natural Products. *Acc. Chem. Res.* **2012**, *45*, 1623–1636.

[16] Crabtree, R. H. Iridium Compounds in Catalysis. *Acc. Chem. Res.* **1979**, *12*, 331–337.

[17] (a) Pàmies, O.; Andersson, P.G.; Diéguez, M. Asymmetric Hydrogenation of Minimally Functionalised Terminal Olefins: An Alternative Sustainable and Direct Strategy for Preparing Enantioenriched Hydrocarbons. *Chem. Eur. J.* **2010**, *16*, 14232–14240. (b) Pàmies, O.; Magre, M.; Diéguez, M. Extending the Substrate Scope for the Asymmetric Iridium-Catalyzed Hydrogenation of Minimally Functionalized Olefins by Using Biaryl Phosphite-Based Modular Ligand Libraries. *Chem. Rec.* **2016**, *16*, 1578–1590. (c) Mazuela, J.; Norrby, P.–O.; Andersson, P. G.: Pàmies, O.; Diéguez, M. Pyranoside Phosphite–Oxazoline Ligands for the Highly Versatile and Enantioselective Ir–Catalyzed Hydrogenation of Minimally Functionalized Olefins. A Combined Theoretical and Experimental Study. *J. Am. Chem. Soc.* **2011**, *133*, 13634–13635. (d) Biosca, M.; Magre, M.; Coll, M.; Pàmies, O.; Diéguez, M. Alternatives to Phosphinooxazoline (t-BuPHOX) Ligands in the Metal-Catalyzed Hydrogenation of Minimally Functionalized Olefins and Cyclic β-Enamide. *Adv. Synth. Catal.* **2017**, *359*, 2801–2814.

[18] It has been suggested that this isomerization process can proceed either via the formation of Ir–η–allyl intermediates or via protonation of the double bond at the terminal position, which gives a stabilized carbocation. See refs. 1b and Brown, J. M.; Derome, A. E.; Hughes, G. D.; Monaghan, P.

K. Homogeneous Hydrogenation With Iridium Complexes. Evidence for Polyhydride Intermediates in the Reduction of α–Pinene. *Aust. J. Chem*. **1992**, *45*, 143–153.

[19] (a) Pharm, D. Q.; Nogid, A. Rotigotine Transdermal System for the Treatment of Parkinson's Disease. *Clin. Ther.* **2008**, *30*, 813–824 (Rotigotine). (b) Osende, J. I.; Shimbo, D.; Fuster, V.; Dubar, M.; Badimon, J. J. Antithrombotic Effects of S 18886, a Novel Orally Active Thromboxane A2 Receptor Antagonist. *J. Thromb. Haemost.* **2004**, *2*, 492–497 (Terutroban). (c) Ross, S. B.; Thorberg, S.–O.; Jerning, E.; Mohell, N.; Stenfors, C.; Wallsten, C.; Milchert, I. G.; Ojteg, G. A. Robalzotan (NAD–299), a Novel Selective 5–HT1A Receptor Antagonist. *CNS Drug Rev.* **1999**, *5*, 213–232 (Robalzotan). (d) Astier, B.; Lambás Señas, L.; Soulière, F.; Schmitt, P.; Urbain, N.; Rentero, N.; Bert, L.; Denoroy, L.; Renaud, B.; Lesourd, M.; Muñoz, C.; Chouvet, G. In Vivo Comparison of Two 5–HT1A Receptors Agonists Alnespirone (S–20499) and Buspirone on Locus Coeruleus Neuronal Activity. *Eur. J. Pharmacol.* **2003**, *459*, 17–26 (Alnespirone).

[20] (a) Renaud, J. L.; Dupau, P.; Hay, A.–E.; Guingouain, M.; Dixneouf, P. H.; Bruneau, C. Ruthenium-Catalysed Enantioselective Hydrogenation of Trisubstituted Enamides Derived from 2-Tetralone and 3-Chromanone: Influence of Substitution on the Amide Arm and the Aromatic Ring. *Adv. Synth. Catal.* **2003**, *345*, 230–238. (b) Hoen, R.; van den Berg, M.; Bernsmann, H.; Minnaard, A. J.; de Vries, J. G.; Feringa, B. L. Catechol–Based Phosphoramidites: A New Class of Chiral Ligands for Rhodium–Catalyzed Asymmetric Hydrogenations. *Org. Lett.* **2004**, *6*, 1433–1436. (c) Jiang, X.–B.; Lefort, L.; Goudriaan, P. E.; de Vries, A. H. M.; van Leeuwen, P. W. N. M.; Reek, J. N. H. Screening of a Supramolecular Catalyst Library in the Search for Selective Catalysts for the Asymmetric Hydrogenation of a Difficult Enamide Substrate. *Angew. Chem. Int. Ed.* **2006**, 45, 1223–1227. (d) Sandee, A. J.; van der Burg, A. M.; Reek, J. N. H. UREAphos: Supramolecular Bidentate Ligands for Asymmetric Hydrogenation. *Chem. Commun.* **2007**, 864–866. (e) Revés, M.; Ferrer, C.; León, T.; Doran, S.; Etayo, P.; Vidal–Ferran, A.; Riera, A.; Verdaguer, X. Primary and Secondary Aminophosphines as Novel P-Stereogenic Building Blocks for Ligand Synthesis. *Angew. Chem. Int. Ed.* **2010**, *49*, 9452–9455. (f) Wu, Z.; Ayad, T.; Ratovelomanana–Vidal, V. Efficient Enantioselective Synthesis of 3–Aminochroman Derivatives Through Ruthenium–Synphos Catalyzed Asymmetric Hydrogenation. *Org. Lett.* **2011**, *13*, 3782–3785. (g) Pignataro, L.; Boghi, M.; Civera, M.; Carboni, S.; Piarulli, U.; Gennari, C. Rhodium-Catalyzed Asymmetric Hydrogenation of Olefins with PhthalaPhos, a New Class of Chiral Supramolecular Ligands. *Chem. Eur. J.* **2012**, *18*, 1383–1400. (h) Frank, D. J.; Franzke, A.; Pfaltz, A. Asymmetric Hydrogenation Using Rhodium Complexes Generated from Mixtures of Monodentate Neutral and Anionic Phosphorus Ligands. *Chem. Eur. J.* **2013**, *19*, 2405–2415. (i) Bravo, M. J.; Ceder, R. M.; Muller, G.; Rocamora, M. New Enantiopure P,P–Bidentate Bis(diamidophosphite) Ligands. Application in Asymmetric Rhodium–Catalyzed Hydrogenation. *Organometallics* **2013**, *32*, 2632–2642. (j) Arribas, I.; Rubio, M.; Kleman, P.; Pizzano, A. Rhodium Phosphine–Phosphite Catalysts in the Hydrogenation of Challenging N–(3,4–dihydronaphthalen–2–yl) Amide Derivatives. *J. Org. Chem.* **2013**, *78*, 3997–4005. (k) Liu, G.; Liu, X.; Cai, Z.; Jiao, G.; Xu, G.; Tang, W. Design of Phosphorus Ligands with Deep Chiral Pockets: Practical Synthesis of Chiral β-Arylamines by Asymmetric Hydrogenation. *Angew. Chem. Int. Ed.* **2013**, *52*, 4235–4238.

[21] (a) Chodosh, D. F.; Crabtree, R. H.; Felkin, H.; Morris, G. E. A Tri–coordinate Hydrogen Ligand in a Trinuclear Iridium Cluster. *J. Organomet. Chem.* **1978**, *161*, C67–C70. (b) Smidt, S. P.; Pfaltz, A.; Martínez–Viviente, E.; Pregosin, P. S.; Albinati, A. X–ray and NOE Studies on Trinuclear Iridium Hydride Phosphino Oxazoline (PHOX) Complexes. *Organometallics* **2003**, *22*, 1000–1009.

[22] The stereochemical description of the different dihydrido species is based on the location of the S–C and S–P ligands at the back of the octahedral.

[23] Gruber, S.; Pfaltz, A. Asymmetric Hydrogenation with Iridium C,N and N,P Ligand Complexes: Characterization of Dihydride Intermediates with a Coordinated Alkene. *Angew. Chem. Int. Ed.* **2014**, *53*, 1896–1900.

[24] Buisman, G. J. H.; Kamer, P. C. J.; van Leeuwen, P. W. N. M. Rhodium Catalysed Asymmetric Hydroformylation with Chiral Diphosphite Ligands. *Tetrahedron: Asymmetry* **1993**, *4*, 1625–1634.

[25] Dupau, P.; Le Gendre, P.; Bruneau, C.; Dixneuf, P. H. Optically Active Amine Derivatives: Ruthenium–Catalyzed Enantioselective Hydrogenation of Enamides. *Synlett* **1999**, *1999*, 1832–1834.

[26]Biosca, M.; Paptchikhine, A.; Pamies, O.; Andersson, P. G.; Dieguez, M. Extending the Substrate Scope of Bicyclic P–Oxazoline/Thiazole Ligands for Ir–Catalyzed Hydrogenation of Unfunctionalized Olefins by Introducing a Biaryl Phosphoroamidite Group. *Chem. Eur. J.* **2015**, *21*, 3455−3464.

[27] McIntyre, S.; Hörmann, E.; Menges, F.; Smidt, S. P.; Pfaltz, A. Iridium–Catalyzed Enantioselective Hydrogenation of Terminal Alkenes. *Adv. Synth. Catal.* **2005**, *347*, 282−288.

[28] Too, P. C.; Noji, T.; Lim, Y. J.; Li, X.; Chiba, S. Rhodium(III)–Catalyzed Synthesis of Pyridines from α,β–Unsaturated Ketoximes and Internal Alkynes. *Synlett* **2011**, *19*, 2789–2794.

[29] (a) Paptchikhine, A.; Cheruku, P.; Engman, M.; Andersson, P. G. Iridium–catalyzed enantioselective hydrogenation of vinyl boronates. *Chem. Commun.* **2009**, 5996−5998. (b) Ganic, A.; Pfaltz, A. Iridium–Catalyzed Enantioselective Hydrogenation of Alkenylboronic Esters. *Chem. Eur. J.* **2012**, *18*, 6724−6728.

[30] (a) Cheruku, P.; Gohil, S.; Andersson, P. G. Asymmetric hydrogenation of enol phosphinates by iridium catalysts having N,P ligands. *Org. Lett.* **2007**, *9*, 1659− 1661. (b) Cheruku, P.; Diesen, J.; Andersson, P. G. Asymmetric Hydrogenation of Di and Trisubstituted Enol Phosphinates with N,P–Ligated Iridium Complexes. *J. Am. Chem. Soc.* **2008**, *130*, 5595−5599.

[31] Tian, F.; Yao, D.; Liu, Y.; Xie, F. Iridium–Catalyzed Highly Enantioselective Hydrogenation of Exocyclic α,β–Unsaturated Carbonyl Compounds. *Adv. Synth. Catal.* **2010**, *352*, 1841–1845.

[32] Chen, X.; Yang, H.; Ge, Y.; Feng, L.; Jia, J.; Wang, J. Synthesis, X–ray crystal structure and optical properties of novel 2–aryl–3–ethoxycarbonyl–4–phenylpyrido[1,2–a]benzimidazoles. *Luminescence* **2012**, *27*, 382–389.

[33] Pautigny, C.; Debouit, C.; Vayron, P.; Ayad, T. Ratovelomanana–Vidal, V. Asymmetric hydrogenation of trisubstituted *N*–acetyl enamides derived from 2–tetralones using ruthenium–SYNPHOS catalysts: a practical synthetic approach to the preparation of β_3–adrenergic agonist SR58611A. *Tetrahedron: Asymmetry* **2010**, *21*, 1382–1388.

[34] Frisch, M. J.; Trucks, G. W.; Schlegel, H. B.; Scuseria, G. E.; Robb, M. A.; Cheeseman, J. R.; Scalmani, G.; Barone, V.; Mennucci, B.; Petersson, G. A.; Nakatsuji, H.; Caricato, M.; Li, X.; Hratchian, H. P.; Izmaylov, A. F.; Bloino, J.; Zheng, G.; Sonnenberg, J. L.; Hada, M.; Ehara, M.; Toyota, K.; Fukuda, R.; Hasegawa, J.; Ishida, M.; Nakajima, T.; Honda, Y.; Kitao, O.; Nakai, H.; Vreven, T.; Montgomery, J. A., Jr.; Peralta, J. E.; Ogliaro, F.; Bearpark, M.; Heyd, J. J.; Brothers, E.; Kudin, K. N.; Staroverov, V. N.; Kobayashi, R.; Normand, J.; Raghavachari, K.; Rendell, A.; Burant, J. C.; Iyengar, S. S.; Tomasi, J.; Cossi, M.; Rega, N.; Millam, J. M.; Klene, M.; Knox, J. E.; Cross, J. B.; Bakken, V.; Adamo, C.; Jaramillo, J.; Gomperts, R.; Stratmann, R. E.; Yazyev, O.; Austin, A. J.; Cammi, R.; Pomelli, C.; Ochterski, J. W.; Martin, R. L.; Morokuma, K.; Zakrzewski, V. G.; Voth, G. A.; Salvador, P.; Dannenberg, J. J.; Dapprich, S.; Daniels, A. D.; Farkas, O.; Foresman, J. B.; Ortiz, J. V.; Cioslowski, J.; Fox, D. J. Gaussian 09, Revision A.02; Gaussian: Wallingford, CT, 2009.

[35] (a) Lee, C.; Yang, W.; Parr, R. G. Development of the Colle–Salvetti Correlation–Energy Formula into a Functional of the Electron Density. *Phys. Rev. B: Condens. Matter Mater. Phys.* **1988**, *37*,

785−789. (b) Becke, A. D. Density–Functional Thermochemistry. III. The Role of Exact Exchange. *J. Chem. Phys.* **1993**, *98*, 5648−5652.

[36] Hay, P. J.; Wadt, W. R. Ab initio Effective Core Potentials for Molecular Calculations. Potentials for K to Au Including the Outermost Core Orbitals. *J. Chem. Phys.* **1985**, *82*, 299−310.

[37] (a) Hehre, W. J.; Ditchfield, R.; Pople, J. A. Self–Consistent Molecular Orbital Methods. XII. Further Extensions of Gaussian Type Basis Sets for Use in Molecular Orbital Studies of Organic Molecules. *J. Chem. Phys.* **1972**, *56*, 2257−2261. (b) Hariharan, P. C.; Pople, J. A. The Influence of Polarization Functions on Molecular Orbital Hydrogenation Energies. *Theor. Chim. Acta* **1973**, *28*, 213−222. (c) Francl, M. M.; Pietro, W. J.; Hehre, W. J.; Binkley, J. S.; Gordon, M. S.; Defrees, D. J.; Pople, J. A. Self–Consistent Molecular Orbital Methods. XXIII. A Polarization–type Basis Set for Second–row Elements. *J. Chem. Phys.* **1982**, *77*, 3654−3665.

[38] (a) Miertus, S.; Tomasi, J. Approximate Evaluations of the Electrostatic Free Energy and Internal Energy Changes in Solution *Processes. Chem. Phys.* **1982**, *65*, 239−245. (b) Mennucci, B.; Tomasi, J. Continuum Solvation Models: A New Approach to the Problem of Solute's Charge Distribution and Cavity Boundaries. *J. Chem. Phys.* **1997**, *106*, 5151−5158. (c) Cossi, M.; Barone, V.; Mennucci, B.; Tomasi, J. Ab initio Study of Ionic Solutions by a Polarizable Continuum Dielectric Model. *Chem. Phys. Lett.* **1998**, *286*, 253−260.

[39] (a) Krishnan, R.; Binkley, J. S.; Seeger, R.; Pople, J. A. Self–Consistent Molecular Orbital Methods. XX. A Basis Set for Correlated Wave Functions. *J. Chem. Phys.* **1980**, *72*, 650−654. (b) McLean, A. D.; Chandler, G. S. Contracted Gaussian Basis Sets for Molecular Calculations. I. Second Row Atoms, Z = 11−18. *J. Chem. Phys.* **1980**, *72*, 5639−5648.

UNIVERSITAT ROVIRA I VIRGILI
DEVELOPMENT OF CHIRAL METAL-CATALYSTS FOR THE SELECTIVE FORMATION OF C-H, C-C AND C-X BONDS. FROM DESIGN TO APPLICATION
Pol De La Cruz Sanchez Badia

3.6. Chiral ferrocene-based thioether-carbene ligands for the Ir-catalyzed hydrogenation of non-chelating olefins

3.6.1. Introduction

In the field of asymmetric catalysis, chiral ferrocene-based ligands have been successfully employed for over three decades.[1] They are particularly interesting because of the facile introduction of different types of chirality simultaneously (planar and central), their particular stereoelectronic properties and their high stability. The advantages of the structure of these ligands led them to be merged with a wide variety of donor groups and their combination with *N*-heterocyclic carbenes has been widely used in several asymmetric transformations in recent years.[2] However, despite chiral ferrocenes gained recognition as privileged ligands for enantioselective catalysis, their application in the Ir-catalyzed hydrogenation of non-chelating alkenes has been very limited.[3] Furthermore, and to the best of our knowledge, the combination of thioether-carbene ligands with a chiral ferrocene-based scaffold is unexplored for this reaction, largely because the attempts of coordinating the thioether-carbene ligands to iridium in a chelate form have been unsuccessful.[4]

Following the promising results obtained in the previous section with the first family of thioether-carbene ligands applied in the Ir-catalyzed asymmetric hydrogenation of olefins and having unravelled the causes of the unsatisfactory activities, we here in explore if the combination of the chiral ferrocene scaffold with thioether-carbene moieties would improve previous results obtained in the group (Section 3.5).[5] The hypothesis was that by taking advantage of the ferrocene's group structure, the Ir metallocycle would form a 7-membered ring, thus reducing the steric congestion around the metal centre, which should results in high activities and hopefully higher enantioselectivities.

To this end, in this section we describe a novel family of modular ferrocene-based thioether-carbene ligands **L23**–**L30**H·Cl (Figure 3.6.1) for the Ir-catalyzed hydrogenation of non-chelating alkenes and alkenes bearing neighbouring polar groups. The selection of chiral ligands contemplates systematic variations of the electronic and steric properties of the thioether moiety (**L23**–**L27**H·Cl) and of the substituent in the nitrogen of the imidazole group (**L28**–**L30**H·Cl), as well as the replacement of the benzimidazole by a simpler imidazole moiety (**L23**–**L28**H·Cl vs. **L29**–**L30**H·Cl).

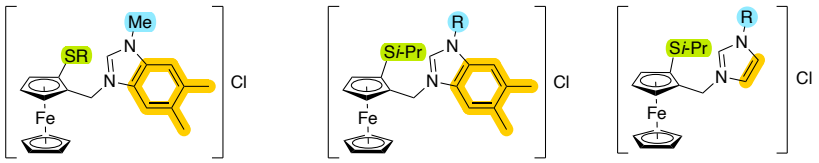

L23H·Cl R= Me **L26**H·Cl R= Ph
L24H·Cl R= Et **L27**H·Cl R= 2,6-Me_2-C_6H_3
L25H·Cl R= *i*-Pr

L28H·Cl R= CH_2Me_5-C_6

L29H·Cl R= Dipp
L30H·Cl R= Mes

Figure 3.6.1. Ferrocene-based thioether-carbene **L23**–**L30**H·Cl.

3.6.2. Results and discussion

3.6.2.1. Preparation of [Ir(cod)(L23–L30)]BAr_F catalyst precursors

The synthesis of ligands **L23**–**L30**H·Cl was carried out in a simple multistep sequence from commercially available (dimethylaminomethyl)ferrocene (Schemes 3.6.1 and 3.6.2). This ferrocene derivative is significantly cheaper that the more widely used Ugi's amine,[1] however the introduction of an enantiomeric resolution step in our synthesis will be needed in order to access both enantiomers of the newly designed ligands. In the first step of the synthesis, the racemic thioether(dimethylaminomethyl)-ferrocene derivatives **22**–**26** were obtained selectively via electrophilic aromatic substitution of the ferrocene using with aryl/alkyl disulfides (step i).[6] At this point of the synthesis we performed the enantiomeric resolution of both of the ferrocene enantiomers employing a classic methodology utilizing ephedrine[7] as the chiral auxiliary (steps ii-iii), which gave access to both diastereoisomers in high yields in a 1:1 ratio that were isolated by means of column chromatography. The transformation of the resulting compounds into the corresponding acetoxy methyl derivates **32**–**36** was performed easily by reacting them with acetic anhydride (step iv).[8] This was followed by the straightforward saponification the thioether-acetate species, yielding thioether-hydroxyl compounds **37**–**41** in pure form (step v).[8a,9] The configuration of the ferrocene moiety was confirmed by X-ray diffraction of hydroxyl-thioether compound **37** (Supporting Information for more details) and assigned by analogy to the rest of the compounds. Alternatively, we were also able to resolve racemates of compounds **22**–**26**, **32**–**36** and **37**–**41** with the use of semipreparative Supercritical Fluid Chromatography (SFC) which gave access to both enantiomers of these intermediates. SFC allows access to the enantiopure intermediates easily and reduce the environmental cost of the synthesis pathway at the same time.[10] However, to simplify the ligand synthesis and posterior screening we selected the R_{Fc} enantiomer of the hydroxyl-thioether derivatives **37**–**41** to carry on the posterior steps of the synthesis of the catalyst precursors.

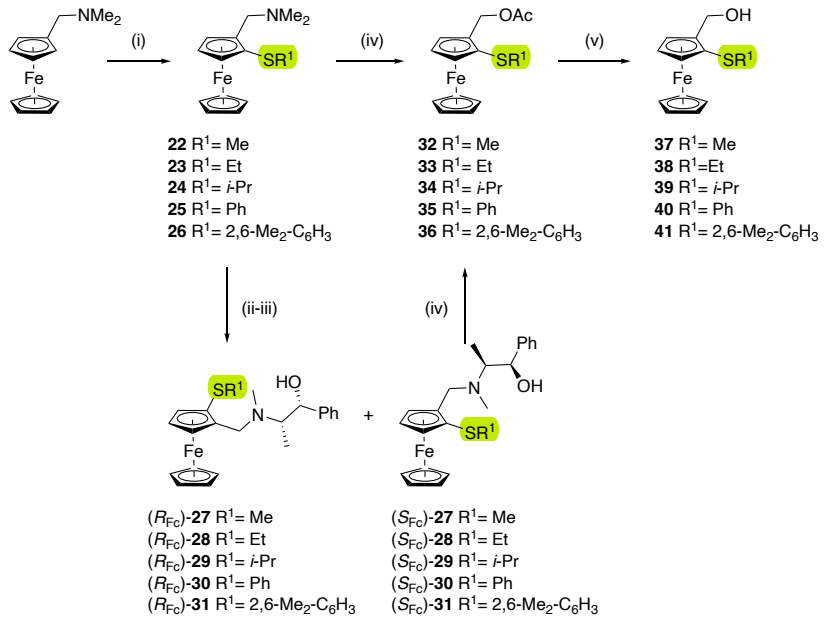

Scheme 3.6.1. Preparation of enantiopure ferrocene-based hydroxyl-thioether intermediates **37**–**38**. (i) *n*-BuLi, R^1SSR^1, 0 ºC to rt, 16 h; (ii) MeI, Et_2O, rt, 1h; (iii) (1*R*,2*S*)-(-)-ephedrine, toluene, reflux, 16 h (iv) Ac_2O, 120 ºC, 16 h; (v) K_2CO_3, MeOH, rt, 16 h.

Initially, for the preparation of the thioether-benzimidazolium/imidazolium salts we reacted the hydroxyl-thioether compounds **37**–**38** with $HBF_4{\cdot}Et_2O$ and the corresponding benzimidazoles/imidazoles, following an already reported procedure.[11] However, this procedure did not work well on our hands. Thus, we were only able to isolate in moderate yields benzimidazolium salts **L26**H·BF_4 and **L28**H·BF_4 (see Supporting Information). In addition, the subsequent attempts to coordinate them to iridium were unsuccessful.

We then turned our attention to the preparation of the chlorine salts **L23**–**L30**H·Cl. In a one-pot two-steps, the reaction of acetic acid and the hydroxyl-thioether compounds **37**–**41** with the corresponding benzimidazoles/imidazoles, followed by the subsequent OAc^-/Cl^- anion exchange with LiCl yielded the thioether-benzimidazolium/imidazolium salts **L23**–**L30**H·Cl in high yields as orange or orange-yellow solids (Scheme 3.6.2, steps i and ii).

Finally, the Ir-catalyst precursors [Ir(cod)(**L23**–**L30**)]BAr_F containing the thioether-carbene ligands were prepared by treatment of the imidazolium salts **L23**–**L30**H·Cl with Ag_2O to form the corresponding silver-carbene complexes (step iii). Immediately after, transmetallation of the Ag-complexes with 0.5 equivalent of [Ir(μ-Cl)cod]$_2$ followed by in situ Cl^-/BAr_F^- counterion exchange led to the desired [Ir(cod)(**L23**–**L30**)]BAr_F complexes(step iv).

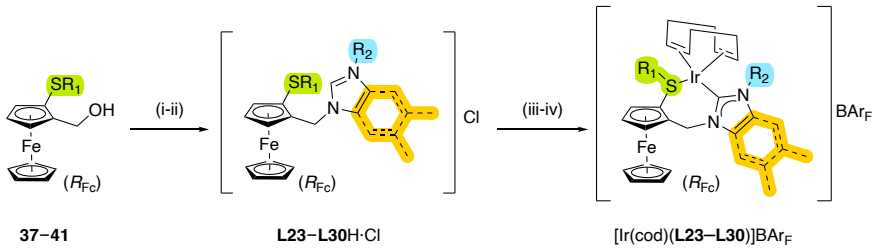

37–41 **L23–L30**H·Cl [Ir(cod)(**L23–L30**)]BAr_F

Scheme 3.6.2. Preparation of [Ir(cod)(**L23**–**L30**)]BAr_F catalyst precursors. (i) 5,6-Me_2-BnImid or imidazolyl derivates, AcOH, 60 ºC, 16 h; (ii) LiCl, EtOH, rt, 2 h; (iii) Ag_2O, CH_2Cl_2, 16 h; (iv) [Ir(μ-Cl)(cod)]$_2$, CH_2Cl_2, rt, 4.5 h then $NaBAr_F$, rt, 1 h.

All complexes were isolated as air-stable deep-red solids in pure form and were characterized by ^{1}H ,^{13}C NMR spectroscopy and HRMS-ESI spectrometry. The spectral assignments were made using ^{1}H–^{1}H and ^{13}C–^{1}H correlation measurements, which agreed with what expected for these C_1-symmetric iridium complexes. Furthermore, crystals suitable for X-ray diffraction analysis of a racemic sample of [Ir(cod)(**L23**)]BAr_F complex were also obtained in order to determine the coordination mode of the newly designed ligands (Figure 3.6.2). The structure revealed that, in fact, the ligand coordinated as a chelate in contrast to previous reports in which the thioether moiety did not coordinate to the metal center resulting in a biscarbene complex.[4] In the crystal structure presented, the seven-membered chelate ring adopted a twist-boat conformation, with the thioether substituent in an axial position and the sulfur in an (*R*)-configuration.

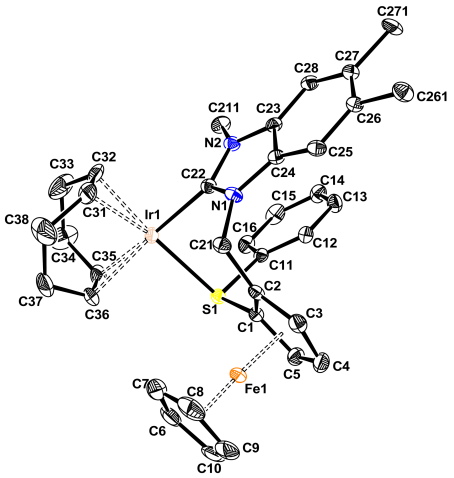

Figure 3.6.2. X-ray structure of [Ir(cod)(**L23**)]BAr_F (the hydrogen atoms and BAr_F anion have been omitted for clarity).

3.6.2.2. Catalytic experiments

3.6.2.2.1. Asymmetric hydrogenation of trisubstituted olefins

In order to evaluate the efficiency of ferrocene-based thioether-carbene catalyst precursors [Ir(cod)(**L23**–**L30**)]BAr_F we initially applied them in the asymmetric hydrogenation of the non-chelating trisubstituted olefins **S27** and **S28**. We chose two substrates with different geometry features since the asymmetric hydrogenation is highly dependent of this parameter.[12] For comparison purposes we used the same reactions conditions for the hydrogenation as described in Section 3.5 (Table 3.6.1). The results indicate that, in all cases the hydrogenation of substrates **S27** and **S28** present full conversion. This in in agreement with our initial hypothesis which, with the modification of the side chain of the ligands we would expand the metallocycle of Ir-complexes from a 6-membered ring to a 7-membered ring, which reduces the congestion around the metal centre and prevents the formation of inactive trinuclear species, ensuring complete conversion.

Table 3.6.1. Asymmetric hydrogenation of olefins **S27** and **S28** with ([Ir(cod)(**L23**–**L30**)]BAr_F.[a]

		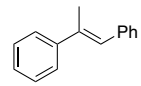 **S27**		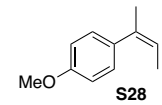 **S28**	
Entry	Ligand	% Conv[b]	% ee[c]	% Conv[b]	% ee[c]
1	**L23**	100	44 (*S*)	100	30 (*S*)
2	**L24**	100	51 (*S*)	100	30 (*R*)
3	**L25**	100	62 (*S*)	100	44 (*R*)
4	**L26**	100	65 (*S*)	100	5 (*R*)
5	**L27**	100	5 (*S*)	100	–
6	**L28**	100	63 (*S*)	100	6 (*R*)
7	**L29**	100	31 (*S*)	100	12 (*R*)
8	**L30**	100	22 (*S*)	100	20 (*R*)

[a] Reaction conditions: substrate (0.5 mol), Ir-catalyst precursor (1 mol%), H_2 (100 bar). [b] Conversions determined by ^{1}H-NMR. [c] Enantiomeric excesses determined by chiral HPLC or GC.

Unfortunately, enantioselectivities for trisubstituted olefins **S27** and **S28** were not as high as those previously reported in the literature.[12] However, for **S27** ee's substantially increased in comparison to previous catalytic systems described in Section 3.5 (max. 4% ee). For trisubstituted olefin **S27**, the highest enantioselectivities were obtained with benzimidazole-based ligands with bulky substituents in the thioether moiety (entries 3, 4 and 6, Table 3.6.1) reaching up to 65% ee with catalytic system Ir/**L23**

bearing a phenyl in the thioether moiety. In line with previous reports, the hydrogenation of *Z*-trisubstituted alkene **S28** led to lower enantioselectivities. Highest ee's were obtained with benzimidazole-based ligands, specifically with system Ir/**L25** with a *i*-Pr substituent on the thioether moiety (entry 3, 44% ee).

Encouraged with the results we investigated other trisubstituted olefins bearing polar neighbouring groups (**S44**, **S64** and **S135**) and the more challenging cyclic β-enamide **S8**. The results are summarized in Table 3.6.2. We found that, to obtain the highest enantioselectivities, the ligand parameters must be carefully selected.

Table 3.6.2. Asymmetric hydrogenation of olefins **S44**, **S64**, **S135**, **S58** and **S8** with ([Ir(cod)(**L23**–**L30**)]BAr$_F$.[a]

Entry	Ligand	Substrate	% Conv[b]	% ee[c]
1	**L25**	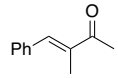 **S44**	100	33 (*R*)
2	**L25**	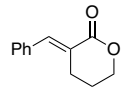 **S64**	100	99 (*R*)[d]
3	**L30**	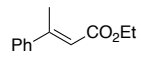 **S135**	100	98 (*S*)
4	**L28**	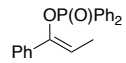 **S58**	100	81 (*S*)
5[e]	**L30**	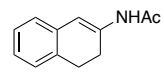 **S8**	100	33 (*R*)

[a] Reaction conditions: substrate (0.5 mol), Ir-catalyst precursor (1 mol%), H_2 (100 bar). [b] Conversions determined by ^{1}H-NMR. [c] Enantiomeric excesses determined by chiral HPLC or GC. [d] 99% ee using Ir/**L23**. [e] Reaction conditions: substrate (0.25 mmol), Ir-catalyst precursor (1 mol%), H_2 (50 bar), CH_2Cl_2 (1 mL), rt, 20 h.

We first started screening several α,β–unsaturated carbonylic species. Disappointingly, for enone **S44** only 33% ee was obtained using catalytic system Ir/**L25** (entry 1, Table 3.6.2). However, we were pleased to find out that high enantioselectivities were achieved for lactone **S64** and acyclic ester **S135** (ee's up to 99% and 98% respectively; entries 2 and 3, Table 3.6.2). While for lactone **S64** the best enantioselectivities were attained with 2,5-dimethyl-benzoimidazole containing catalytic systems Ir/**L23** or Ir/**L25**, the presence of a bulky mesityl imidazole group in the catalyst (Ir/**L30**) is crucial to obtain the highest

enantioselectivities Noteworthy, these results are comparable to the best ones reported in the literature for carbene-based ligands, since there are rather scarce examples of the hydrogenation of olefins with poorly coordinative groups using these ligand scaffold.[13]

Surpassing previous results using carbene-thioether catalysts, good enantioselectivities were also obtained for enol phosphinate **S58** using Ir/**L28** catalytic system bearing a benzimidazole group and a *i*-Pr thioether substituent (entry 4, 81% ee). Finally, the reduction of cyclic β-enamide **S8** did not occur in high enantioselectivities. The highest enantioselectivity was obtained with catalytic precursor Ir/**L30** (entry 5, 33% ee).

3.6.2.2.2. Asymmetric hydrogenation of 1,1-disubstituted olefins

Next, we screened the thioether carbene ligands **L23**–**L30** in the hydrogenation of the more challenging 1,1-disubstituted olefins. In the first set of experiments, we studied the reduction of benchmark substrate α-*tert*-butylstyrene **S14**. The results, reflected in Table 3.6.3, indicate that again full conversion was obtained in all cases. This is in contrast with the very low activities (<5%) presented in the previous section. On the other hand, in line with the results obtained with non-chelating trisubstituted alkenes, enantioselectivities remained moderate and were far away from the best ee's previously reported in the literature.[12] The highest enantioselectivities were reached again with a benzimidazole group in the carbene moiety, reaching 64% ee (entry 4, Table 3.6.3) with catalytic system Ir/**L26** with a phenyl substituent was present in the thioether moiety.

Then, we studied the reduction of 1,1-disubstituted alkenes **S53** and **S61** bearing polar neighbouring groups with catalytic systems [Ir(cod)(**L23**–**L30**)]BAr_F (Table 3.6.4). Again, selection of the optimal catalytic system is essential to maximize the enantioselectivity outcome of the reaction. The hydrogenation of alkenyl boronic ester **S53** proceeded with complete conversion, however only 33% ee was obtained with complex Ir/**L29** (entry 1, 30% ee). Moreover 1,1-disubstituted enol phosphinate **S61** yielded higher enantioselectivities with the same Ir/**L29** system (entry 2, 55% ee).

Table 3.6.3. Ir-catalyzed asymmetric hydrogenation of **S14** using [Ir(cod)(**L23**–**L30**)]BAr_F.[a]

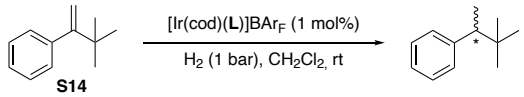

Entry	Ligand	% Conv[b]	% ee[b]
1	**L23**	100	50 (*R*)
2	**L24**	100	50 (*R*)
3	**L25**	100	50 (*R*)
4	**L26**	100	64 (*R*)
5	**L27**	100	45 (*R*)
6	**L28**	100	34 (*R*)
7	**L29**	100	46 (*R*)
8	**L30**	100	20 (*R*)

[a] Reaction conditions: substrate (0.5 mmol), Ir-catalyst precursor (1 mol%), H_2 (1 bar). [b] Conversions determined by ^{1}H-NMR. [c] Enantiomeric excesses determined by chiral GC.

Table 3.6.4. Asymmetric hydrogenation of olefins **S153** and **S61** with ([Ir(cod)(**L23**–**L30**)]BAr_F.[a]

Entry	Ligand	Substrate	% Conv[b]	% ee[c]
1	**L29**	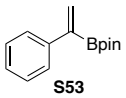 **S53**	100	30 (*S*)
2	**L29**	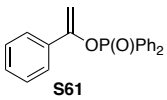 **S61**	100	55 (*R*)

[a] Reaction conditions: substrate (0.5 mmol), Ir-catalyst precursor (1 mol%), H_2 (1 bar for **S53** or 50 bar for **S61**). [b] Conversions determined by ^{1}H-NMR. [c] Enantiomeric excesses determined by chiral HPLC or GC.

3.6.2.2.3. Asymmetric hydrogenation of tetrasubstituted olefins

In order to test the limits of the substrate scope of non-chelating olefins that we can hydrogenate, we also investigated the reduction of the challenging cyclic and acyclic tetrasubstituted alkenes **S16** and **S112** (Table 3.6.5). We very pleased to see, that full conversions were obtained again in all cases, further demonstrating that the seven membered metallocycle is able to adapt to the steric demands of bulkier substrates. However, low enantioselectivities were obtained in both cases.

Table 3.6.5. Asymmetric hydrogenation of olefins **S112** and **S14** with ([Ir(cod)(**L23**–**L30**)]BAr_F. [a]

		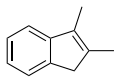 S112		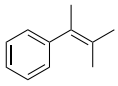 S16	
Entry	Ligand	% Conv[b]	% ee[c]	% Conv[b]	% ee[c]
1	**L23**	100	25 (*R,R*)	100	9 (*S*)
2	**L24**	100	22 (*R,R*)	100	3 (*S*)
3	**L25**	100	1 (S,*S*)	100	9 (*R*)
4	**L26**	100	7 (*R,R*)	100	1 (*S*)
5	**L27**	100	4 (S,*S*)	100	5 (*R*)
6	**L28**	100	36 (*R,R*)	100	4 (*S*)
7	**L29**	100	15 (*R,R)*	100	3 (*S*)
8	**L30**	100	20 (*R,R*)	100	8 (*S*)

[a] Reaction conditions: substrate (0.5 mol), Ir-catalyst precursor (1 mol%), H_2 (100 bar). [b] Conversions determined by ^{1}H-NMR. [c] Enantiomeric excesses determined by chiral GC.

3.6.2.3. Reactivity studies of [Ir(cod)(L)]BAr_F towards H_2

In order to further understand the effect of the ligand structure in the experimental results, we investigated the reactivity of several iridium catalyst precursors with hydrogen in the same fashion as in the previous section. We selected four [Ir(cod)(L)]BAr_F (L= **L23**, **L25**, **L27** and **L30**) catalytic systems containing a different combination of the benzimidazole/imidazole scaffold and the thioether moiety. The ligand selection can provide insight into their previously observed substantial effect on the enantioselectivity of the different substrates.

In all cases bubbling H_2 in a CD_2Cl_2 solution of the Ir catalyst precursors at 195 K for 10 min led to the formation of the corresponding dihydride species **42**–**48** (Scheme 3.6.3 and Table 3.6.6). The formation of catalytically inactive trinuclear iridium hydrido species $[Ir_3(\mu_3\text{-}H)(H)_6(C\text{-}S)_3](BAr_F)_2$ was not observed, in contrast with the thioether-carbene ligands discussed in Section 3.5.

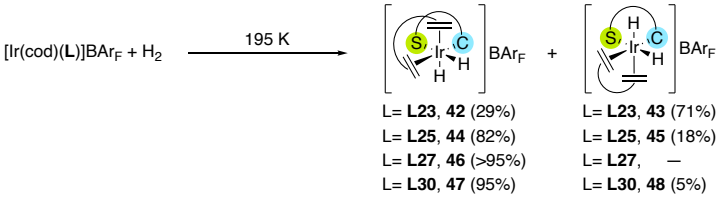

Scheme 3.6.3. Reactivity of [Ir(cod)(**L**)]BAr_F complexes (L= **L23**, **L25**, **L27** and **L30**) with H_2.

Table 3.6.6. ^{1}H NMR data at the hydride region of dihydride species **42–48**.

Compound	H (*trans* to olefin)	H (*trans* to S)
[Ir(H)$_2$(cod)(**L23**)]BAr$_F$ (**42**)	-13.4 (s)	-14.5 (s)
[Ir(H)$_2$(cod)(**L23**)]BAr$_F$ (**43**)	-13.8 (s)	-14.9 (s)
[Ir(H)$_2$(cod)(**L25**)]BAr$_F$ (**44**)	-13.5 (s)	-15.0 (s)
[Ir(H)$_2$(cod)(**L25**)]BAr$_F$ (**45**)	-13.0 (s)	-14.6 (s)
[Ir(H)$_2$(coe)(**L27**)]BAr$_F$ (**46**)	-14.4 (s)	-14.7 (s)
[Ir(H)$_2$(coe)(**L30**)]BAr$_F$ (**47**)	-14.0 (s)	-14.8 (s)
[Ir(H)$_2$(coe)(**L30**)]BAr$_F$ (**48**)	-14.5 (s)	-14.7 (s)

The 3D structures of dihydrides **42**–**48** were assigned by DFT calculations and in some cases further confirmed by NMR studies (see Supporting Information for the NMR copies and DFT details). In general, the calculated population of the different dihydrides matches well with the experimental population (see Supporting Information). Figure 3.6.3 shows the calculated structures of dihydride species **42**–**48**. In all cases, the calculated population of dihydrides matches well with the experimental ratio (see Supporting Information). Bubbling hydrogen to a solution of [Ir(cod)(**L23**)]BAr$_F$ led to the formation of dihydride complexes **42** and **43**. The major dihydride species **43** has the hydride *trans* to the olefin pointing up, an *S* configuration of the thioether group and a twist-boat-like conformation for the seven-membered chelate ring with the methylenic group of the ligand backbone pointing down (Figure 3.6.3a).[14] The minor species **42** corresponds to the dihydride species in which the hydride *trans* to the olefin is pointing down, the S atom has an *R* configuration and the chelate ring adopts a twist-boat-like conformation with the methylenic group of the ligand backbone pointing down (Figure 3.6.3a).

DFT calculations indicated that introducing a bulkier thioether favours the formation of dihydride species in which the hydride *trans* to the olefin is pointing down, the S atom has an *R* configuration and the chelate ring adopts a twist-boat-like conformation with the methylenic group of the ligand backbone pointing up (complexes **44** and **46**; Scheme 3.6.3 and Figure 3.6.3). Similarly, the introduction of more sterically hindered group at carbene N-substituent also favours the formation of dihydride species with the same spatial rearrangement than that of dihydride complexes **44** and **46**. Thus, bubbling hydrogen to a solution of [Ir(cod)(**L30**)]BAr$_F$, containing a ligand with a N-mesityl substituent in the carbene moiety, led to the preferentially formation of dihydride complex **47** (95% population vs 5% of dihydride **48**). The formation of complex **47** was further confirmed by NOE experiments. Thus, the apical hydride *trans*

to the olefin shows NOE interactions with the methyls at both the isopropyl thioether group and at the mesitylene moiety.

a)

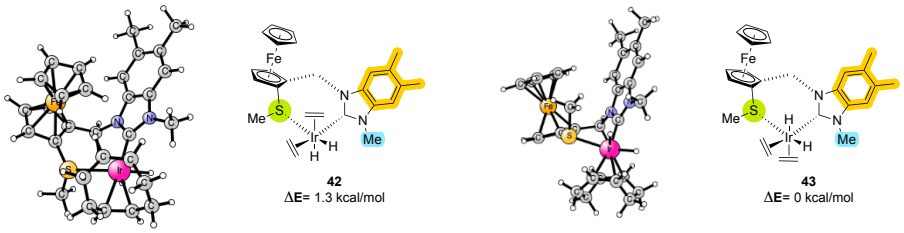

b)

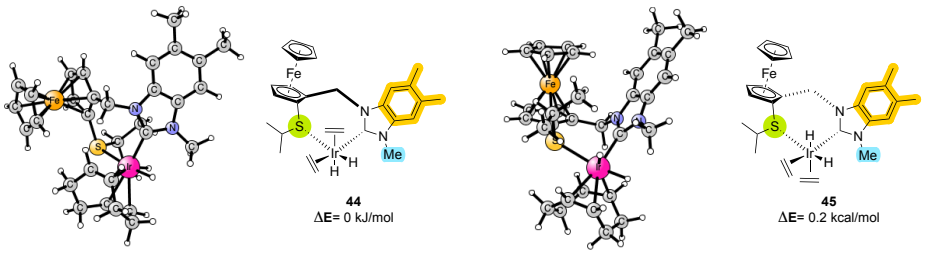

c)

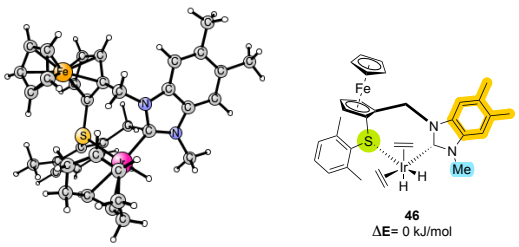

d)

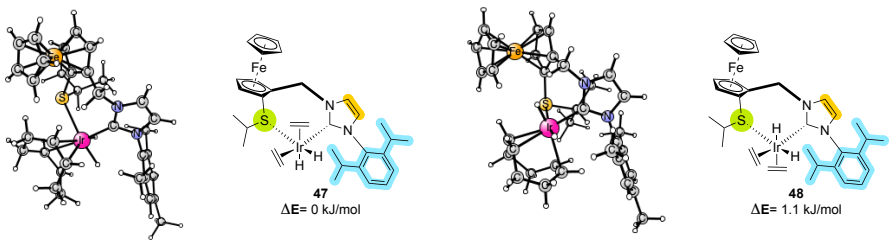

Figure 3.6.3. Calculated structures (BAr_F anion have been omitted for clarity) and energies of $[Ir(H)_2(cod)(\mathbf{L23})]BAr_F$ complexes (a) **42** and **43**; (b) **44** and **45**; (c) **46**; (d) **47** and **48**.

3.6.3. Conclusions

Continuing the efforts of the previous section we studied the potential of novel ferrocene-based Ir/thioether-NHC complexes, with a seven-membered chelate, in the asymmetric hydrogenation of non-chelating olefins and olefins with polar neighbouring groups. The newly prepared Ir-C,S catalyst precursors were easy to synthesize from racemic/readily available materials in simple elemental steps. The resulting complexes were deep red, air-stable and easy to manipulate solids. Satisfyingly, we could observe that the introduction of a extended chelate ring did improve the conversion issues we observed in other C,S ligand designs. In this case full conversion are observed in all cases, even with the most challenging and bulky tetrasubstituted olefins. Regarding the enantioselectivity outcome, moderate results are still obtained in the majority of the cases, however most of the substrates tested in this study yielded higher ee's than those reported in the previous section. It is to note the excellent enantioselectivities (up to 99% ee) obtained for lactones and acyclic esters with careful selection of the ligand parameters. These results open up for the future exploration of different substrates containing the ester moiety, with different geometries and substitution patterns, in order to demonstrate the high potential of these new ferrocene-based carbene-thioether Ir catalyst precursors. Similarly, to previous studies the reactivity with hydrogen of selected ligand scaffolds was tested as well. In contrast with other investigations, the presence of catalytically inactive trinuclear hydrido species was not detected. Furthermore, we could observe that, in agreement with experimental results, the reactivity of the Ir-catalyst precursors towards H_2 depend on the type of ligand. Suggesting that, each type of substrate would probably need a different ligand design that adapts to the steric and electronic demands of the olefin.

3.6.4. Experimental section

3.6.4.1. General considerations

All reactions were carried out using standard Schlenk techniques under an argon atmosphere. Commercial chemicals were used as received. Solvents were dried by means of standard procedures and stored under argon. ^{1}H, $^{13}C\{^{1}H\}$ and $^{31}P\{^{1}H\}$ NMR spectra were recorded using a Varian Mercury-400 MHz spectrometer. Chemical shifts are relative to that of $SiMe_4$ (^{1}H and $^{13}C\{^{1}H\}$) as an internal standard or H_3PO_4 (^{31}P) as an external standard. ^{1}H and ^{13}C assignments were made on the basis of ^{1}H-^{1}H gCOSY, ^{1}H-^{13}C gHSQC and NOESY experiments. The compounds **22**–**26**,[6] **32**–**36**,[6,8] **37**–**41**[8a,9] and benzimidazole and imidazole derivatives[15,16,17,18] were prepared in accordance with the corresponding methods published in the literature .For characterization and ee determination details, copies of the NMR spectra, X-ray data as well as for DFT details see Supporting Information.

3.6.4.2. General procedure for the preparation of thioether-(dimethylaminomethyl) ferrocene derivatives (22–26)

A slightly modified procedure from the literature was used to synthetise of the thioether-(dimethyaminoemthyl)ferrocene intermediates.[6]

To a solution of (dimethylaminomethyl)ferrocene (1 eq) in Et_2O (4 mL/mmol) at 0ºC, *n*-BuLi (2.5 M in hexanes, 1.15 eq) was added dropwise. After addition the solution was warmed up to room temperature and let react for 3 additional hours. Then the corresponding disulfide (1.5 eq) was added dropwise at 0 °C. If the disulfide derivative was a solid it was dissolved in the minimum amount of Et_2O before addition. The reaction was then stirred 16 h at room temperature. After reaction time was completed, the crude solution was quenched with brine (25 mL) and extracted with Et_2O (3 x 20 mL). Then the combined organic extracts were dried over $MgSO_4$, filtered and evaporated under reduced pressure. Further purification with column chromatography (SiO_2, cyclohexane/ethyl acetate/NEt_3 – 1:1:0.1) yielded the corresponding thioether-(dimethylaminomethyl)ferrocene derivatives in pure form. ^1H and ^{13}C NMR spectra of the compounds **22**–**26** agreed with those reported in the literature. Both enantiomers of intermediates **22**–**25** were isolated by means of preparative HPLC (*vide infra*).

22: Yield 3.3 g (56%) as a dark brown viscous oil (using 20.5 mmol of (dimethylaminomethyl)ferrocene). Chiralpak IG 3µm column (sCO_2/MeOH/DEA (90:10:0.1), flow 1.5mL/min, 254 nm). t_R 5.5 min (*S*); t_R 6.6 min (*R*).

23: Yield 3.8 g (62%) as a dark orange-brown solid (using 20.5 mmol of (dimethylaminomethyl) ferrocene). Chiralpak IG 3µm column (sCO_2/MeOH/DEA (90:10:0.1), flow 1.5mL/min, 254 nm). t_R 6.7 min (*S*); t_R 7.0 min (*R*).

24: Yield 3.8 g (59%) as a dark orange-brown solid (using 20.5 mmol of (dimethylaminomethyl) ferrocene). Chiralpak IG 3µm column (sCO_2/MeOH/DEA (90:10:0.1), flow 1.5mL/min, 254 nm). t_R 4.2 min (*S*); t_R 5.3 min (*R*).

25: Yield 4.9g (69%) as a dark orange-brown solid (using 20.5 mmol of (dimethylaminomethyl) ferrocene). Chiralpak IA 3µm column (sCO_2/MeOH/DEA (90:10:0.1), flow 1.5mL/min, 254 nm). t_R 5.1 min (*S*); t_R 6.8 min (*R*).

26: Yield 3.8 g (50%) as dark brown viscous oil (using 20.5 mmol of (dimethylaminomethyl) ferrocene). ^1H NMR ($CDCl_3$, 400 MHz), δ : 7.07-7.05 (3H, m, Ph), 4.34 (1H, m, subst. Cp), 4.12 (5H, s, Cp), 4.05 (2H, m, subst. Cp), 3.53 (1H, d, $^2J_{H\text{-}H}$= 13.1 Hz, CH_2), 3.32 (1H, d, $^2J_{H\text{-}H}$ =13.1 Hz, CH_2), 2.48 (6H, s, S(C$\underline{H}_3$)$_2$C$_6$H$_3$), 2.02 (3H, s, N(C$\underline{H}_3$)$_2$). ^{13}C NMR {^1H} ($CDCl_3$, 100 MHz), δ: 142.0 (quat. Ph), 134.1 (quat. Ph), 128.2 (Ph), 127.9 (quat. Ph), 84.5 (quat. Cp), 84.4 (quat. Cp), 71.2 (subst. Cp), 70.5 (Cp), 69.6 (subst. Cp), 66.6 (subst. Cp), 57.1 (CH_2), 44.8 (N($\underline{C}H_3$)$_2$), 22.4 (S(C$\underline{H}_3$)$_2$C$_6$H$_3$). HRMS (ESI) : 438.1564 (438.1554 calculated for $C_{24}H_{32}FeNOS$, M+H).

3.6.4.3. General procedure for the preparation of *N*-thioether-(ferrocenylmethyl)-(−)-ephedrine derivatives (27–31)

(i) In an open air flask, methyl iodide (9 eq) was added dropwise to a solution of the corresponding thioether-(dimethylaminomethyl)ferrocene compounds **22**–**26** (1 eq) in Et_2O (10 mL/mmol). After 1 h the yellowish solid formed was filtered through a sintered funnel and washed three times with Et_2O. After drying the formed solid in air, the resulting ammonium iodide salts were used in the next step directly without further purification.

(ii) (1*R*, 2*S*)-(**−**)-Ephedrine (3 eq) was added stepwise into a solution of the previous ammonium iodide salt in dry toluene (20 mL/mmol) and refluxed overnight. Then, the solution was cooled down to room temperature and K_2CO_3 (3 eq) was added. After stirring for a couple of minutes the crude was filtered and the clear deep orange solution evaporated *in vacuo.* Further purification with column chromatography (SiO_2, cyclohexane/ethyl acetate/NEt_3 – 1:1:0.1) yielded the two diastereoisomers of the corresponding thioether-*N*-(ferrocenylmethyl)-(**−**)-ephedrine derivatives in a 1:1 ratio.

27: Yield 516 mg (97%) 1:1 mixture of diastereoisomers as a dark brown oil (using 1.3 mmol of **22**). *Diast 1 (R_{Fc})* ^{1}H NMR ($CDCl_3$, 400 MHz), δ: 7.40-7.30 (4H, m, Ph), 7.28-7.22 (1H, m, Ph), 4.90 (1H, d, $^3J_{H-H}$= 4.2 Hz, CHPh), 4.35 (1H, m, subst. Cp), 4.29 (1H, m, subst. Cp), 4.19 (1H, t, $^3J_{H-H}$= 2.6 Hz, subst. Cp), 4.13 (5H, s, Cp), 3.92 (1H, d, $^2J_{H-H}$= 13.1 Hz, CH_2), 3.39 (1H, d, $^2J_{H-H}$= 13.1 Hz, CH_2), 2.94 (1H, qd, $^3J_{H-H}$= 6.9 Hz, $^3J_{H-H}$= 4.2 Hz, C<u>H</u>CH_3), 2.28 (3H, s, SC<u>H</u>$_3$), 2.20 (3H, s, NC<u>H</u>$_3$), 0.95 (3H, d, $^3J_{H-H}$= 6.9 Hz, CHC<u>H</u>$_3$). ^{13}C NMR {^{1}H} ($CDCl_3$, 100 MHz), δ: 142.2 (quat. Ph), 127.9 (Ph), 126.7 (Ph), 126.1 (Ph), 86.7 (quat. Cp), 83.7 (quat. Cp), 73.7 (<u>C</u>HPh), 71.8 (subst. Cp), 70.7 (subst. Cp), 69.9 (Cp), 67.3 (subst. Cp), 63.5 (<u>C</u>HCH_3), 52.8 (CH_2), 38.7 (N<u>C</u>H_3), 20.2 (S<u>C</u>H_3), 9.58 (CH<u>C</u>H_3). HRMS (ESI) : 410.1247 (410.1241 calculated for $C_{22}H_{28}FeNOS$, M+H). *Diast 2 (S_{Fc})* ^{1}H NMR ($CDCl_3$, 400 MHz), δ: 7.40-7.30 (4H, m, Ph), 7.29-7.23 (1H, m, Ph), 4.96 (1H, d, $^3J_{H-H}$= 4.4 Hz, CHPh), 4.36 (1H, m, subst. Cp), 4.29 (1H, m, subst. Cp), 4.18 (1H, t, $^3J_{H-H}$= 2.6 Hz, subst. Cp), 4.13 (5H, s, Cp), 3.96 (1H, d, $^2J_{H-H}$= 12.7 Hz, CH_2), 3.32 (1H, d, $^2J_{H-H}$= 12.7 Hz, CH_2), 2.94 (1H, m, C<u>H</u>CH_3), 2.30 (3H, s, SC<u>H</u>$_3$), 2.08 (3H, s, NC<u>H</u>$_3$), 0.96 (3H, d, $^3J_{H-H}$= 6.9 Hz, CHC<u>H</u>$_3$). ^{13}C NMR {^{1}H} ($CDCl_3$, 100 MHz), δ: 142.2 (quat. Ph), 127.9 (Ph), 126.8 (Ph), 126.2 (Ph), 86.3 (quat. Cp), 84.1 (quat. Cp), 73.2 (<u>C</u>HPh), 71.7 (subst. Cp), 70.7 (subst. Cp), 69.9 (Cp), 67.4 (subst. Cp), 63.2 (<u>C</u>HCH_3), 53.54 (NCH_2), 37.9 (N<u>C</u>H_3), 20.4 (S<u>C</u>H_3), 10.1 (CH<u>C</u>H_3). HRMS (ESI) : 410.1239 (15%, 410.1241 calculated for $C_{22}H_{28}FeNOS$, M+H).

28: Yield 484 mg (88%) 1:1 mixture of diastereoisomers as a dark brown solid (using 1.3 mmol of **23**). *Diast 1 (R_{Fc})* ^{1}H NMR ($CDCl_3$, 400 MHz), δ: 7.40-7.30 (4H, m, Ph), 7.28-7.22 (1H, m, Ph), 4.89 (1H, d, $^3J_{H-H}$= 4.2 Hz, CHPh), 4.38 (1H, m, subst. Cp), 4.30 (1H, m, subst. Cp), 4.20 (1H, t, $^3J_{H-H}$ = 2.6 Hz, subst. Cp), 4.13 (5H, s, Cp), 3.91 (1H,

d, $^2J_{H-H}$= 13.1 Hz, CH_2), 3.36 (1H, d, $^2J_{H-H}$= 13.1 Hz, C$\underline{H}_2$), 2.93 (1H, qd, $^3J_{H-H}$= 6.9 Hz, $^3J_{H-H}$= 4.2 Hz, C$\underline{H}CH_3$), 2.64 (2H, q, $^3J_{H-H}$= 7.4 Hz, SC$\underline{H}_2$), 2.20 (3H, s, NC$\underline{H}_3$), 1.24 (3H, t, $^3J_{H-H}$= 7.4 Hz, SCH_2 C$\underline{H}_3$), 0.96 (3H, d, $^3J_{H-H}$= 6.9Hz, CHC$\underline{H}_3$). ^{13}C NMR {^{1}H} ($CDCl_3$, 100 MHz), δ : 142.2 (quat. Ph), 127.9 (Ph), 126.7 (Ph), 126.1 (Ph), 86.5 (quat. Cp), 80.5 (quat. Cp), 74.1 (subst. Cp), 73.9 (C$\underline{H}$Ph), 70.9 (subst. Cp), 70.0 (Cp), 67.5 (subst. Cp), 63.19 (C$\underline{H}CH_3$), 52.7 (NCH_2), 38.8 (NC$\underline{H}_3$), 31.19 (SC$\underline{H}_2$), 14.8 ($SCH_2C\underline{H}_3$), 9.44 (CHC$\underline{H}_3$). HRMS (ESI) : 424.1402 (424.1397 calculated for $C_{23}H_{30}FeNOS$, M+H),. *Diast 2 (S_{Fc})* ^{1}H NMR ($CDCl_3$, 400 MHz), δ: 7.40-7.30 (4H, m, Ph), 7.30-7.22 (1H, m, Ph), 4.96 (1H, d, $^3J_{H-H}$= 4.3 Hz, CHPh), 4.39 (1H, m, subst. Cp), 4.31 (1H, m, subst. Cp), 4.20 (1H, t, $^2J_{H-H}$= 2.5 Hz, subst. Cp), 4.13 (5H, s, Cp), 3.97 (1H, d, $^2J_{H-H}$= 12.7 Hz, CH_2), 3.29 (1H, d, $^2J_{H-H}$= 12.7 Hz, C$\underline{H}_2$), 2.92 (1H, qd, $^3J_{H-H}$= 6.9 Hz, $^3J_{H-H}$= 4.3 Hz, C$\underline{H}CH_3$), 2.65 (2H, q, $^2J_{H-H}$= 7.4 Hz, SC$\underline{H}_2$), 2.08 (3H, s, NC$\underline{H}_3$), 1.26 (3H, t, $^3J_{H-H}$= 7.4Hz, SCH_2 C$\underline{H}_3$), 0.95 (3H, d, $^3J_{H-H}$= 6.9 Hz, CHC$\underline{H}_3$). ^{13}C NMR {^{1}H} ($CDCl_3$, 100 MHz), δ: 142.2 (quat. Ph), 127.9 (Ph), 126.8 (Ph), 126.2 (Ph), 86.8 (quat. Cp), 81.0 (quat. Cp), 74.0 (subst. Cp), 73.1 (C$\underline{H}$Ph), 71.0 (subst. Cp), 70.0 (Cp), 67.7 (subst. Cp), 63.3 (C$\underline{H}CH_3$), 53.4 (NCH_2), 38.0 (NC$\underline{H}_3$), 31.3 (SC$\underline{H}_2$), 14.9 ($SCH_2C\underline{H}_3$), 10.1 (CHC$\underline{H}_3$). HRMS (ESI) : 424.1402 (424.1397 calculated for $C_{23}H_{30}FeNOS$, M+H).

29: Yield 436 mg (83%) 1:1 mixture of diastereoisomers as a dark brown oil (using 1.2 mmol of **24**). *Diast 1 (R_{Fc})* ^{1}H NMR ($CDCl_3$, 400 MHz), δ: 7.40-7.30 (4H, m, Ph), 7.30-7.20 (1H, m, Ph), 4.90 (1H, d, $^3J_{H-H}$= 4.1 Hz, CHPh), 4.39 (1H, m, subst. Cp), 4.33 (1H, m, subst. Cp), 4.22 (1H, t, $^3J_{H-H}$= 2.7 Hz, subst. Cp), 4.13 (5H, s, Cp), 3.90 (1H, d, $^2J_{H-H}$= 13.2 Hz, CH_2), 3.37 (1H, d, $^2J_{H-H}$= 13.2 Hz, CH_2), 2.99 (1H, hept, $^3J_{H-H}$=6.7 Hz, CH of *i*-Pr), 2.93 (1H, m, C$\underline{H}CH_3$), 2.21 (3H, s, NC$\underline{H}_3$), 1.23 (6H, m, CH_3 of *i*-Pr), 0.97 (3H, d, $^3J_{H-H}$ =6.8Hz, CHC$\underline{H}_3$). ^{13}C NMR {^{1}H} ($CDCl_3$, 100 MHz), δ: 142.26 (quat. Ph), 127.9 (Ph), 126.8 (Ph), 126.1 (Ph), 88.2 (quat. Cp), 78.8 (quat. Cp), 75.5 (subst. Cp), 73.9 (C$\underline{H}$Ph), 71.2 (subst. Cp), 70.0 (Cp), 67.7 (subst. Cp), 63.5 (C$\underline{H}CH_3$), 52.8 (CH_2), 39.8 (CH of *i*-Pr), 38.9 (NCH_3), 23.6 (CH_3 of *i*-Pr), 22.8 (CH_3 of *i*-Pr), 9.3 (CHC$\underline{H}_3$). HRMS (ESI) : 438.1555 (438.1554 calculated for $C_{24}H_{32}FeNOS$, M+H). *Diast 2 (S_{Fc})* ^{1}H NMR ($CDCl_3$, 400 MHz) δ: 7.40-7.30 (4H, m, Ph), 7.30-7.22 (1H, m, Ph), 4.99 (1H, d, $^3J_{H-H}$= 4.2 Hz, CHPh), 4.41 (1H, br s, subst. Cp), 4.35 (1H, br s, subst. Cp), 4.22 (1H, m, subst. Cp), 4.12 (5H, s, Cp), 3.98 (1H, d, $^2J_{H-H}$=1 2.7 Hz, CH_2), 3.31 (1H, d, $^2J_{H-H}$= 12.7 Hz, CH_2), 2.98 (1H, hept, $^3J_{H-H}$= 6.7 Hz, CH of *i*-Pr), 2.90 (1H, m, C$\underline{H}CH_3$), 2.12 (3H, s, NC$\underline{H}_3$), 1.24 (6H, m, CH_3 of *i*-Pr), 0.95 (3H, d, $^3J_{H-H}$= 6.8 Hz, CHC$\underline{H}_3$). ^{13}C NMR {^{1}H} ($CDCl_3$, 100 MHz), δ: 142.2 (quat. Ph), 127.9 (Ph), 126.8 (Ph), 126.1 (Ph), 87.4 (quat. Cp), 79.3 (quat. Cp), 75.4 (subst. Cp), 73.0 (C$\underline{H}$Ph), 71.3 (subst. Cp), 70.1 (Cp), 67.9 (subst. Cp), 63.4 (C$\underline{H}CH_3$), 53.2 (CH_2), 39.8 (CH of *i*-Pr), 38.1 (NCH_3), 23.6 (CH_3 of *i*-Pr), 22.8 (CH_3 of *i*-Pr), 9.3 (CHC$\underline{H}_3$).HRMS (ESI) : 438.1564 (438.1554 calculated for $C_{24}H_{32}FeNOS$, M+H).

30: Yield 640 mg (97%) 1:1 mixture of diastereoisomers as a dark orange solid (using 1.4 mmol of **25**). *Diast 1 (R_{Fc})* ^{1}H NMR ($CDCl_3$, 400 MHz), δ: 7.35-7.05 (10H, m, Ph), 4.75 (1H, d, $^{3}J_{H-H}$ =3.9 Hz, CHPh), 4.53 (1H, m, subst. Cp), 4.48 (1H, m, subst. Cp), 4.38 (1H, t, $^{3}J_{H-H}$= 2.6 Hz, subst. Cp), 4.22 (5H, s, Cp), 3.88 (1H, d, $^{2}J_{H-H}$=13.3 Hz, CH_2), 3.43 (1H, d, $^{2}J_{H-H}$= 13.3 Hz, CH_2), 2.76 (1H, qd, $^{3}J_{H-H}$= 6.8 Hz, $^{3}J_{H-H}$= 3.9 Hz, C<u>H</u>CH_3), 2.04 (3H, s, NC<u>H</u>$_3$) 0.81 (3H, d, $^{3}J_{H-H}$= 6.8 Hz, CHC<u>H</u>$_3$). ^{13}C NMR {^{1}H} ($CDCl_3$, 100 MHz), δ: 142.2 (quat. Ph), 140.3 (quat. Ph), 128.6 (Ph), 127.8 (Ph), 126.6 (Ph), 126.1 (Ph), 125.7 (Ph), 124.9 (Ph), 85.6 (quat. Cp), 76.0 (quat. Cp), 76.0 (subst. Cp), 72.9 (<u>C</u>HPh), 71.9 (subst. Cp), 70.2 (Cp), 68.9 (subst. Cp), 63.5 (<u>C</u>HCH_3), 52.6 (CH_2), 38.4 (N<u>C</u>H_3), 9.9 (CH<u>C</u>H_3). HRMS (ESI) : 472.1389 (34%, 472.1397 calculated for $C_{27}H_{30}FeNOS$, M+H), 307.0246 (100%, 307.0244 calculated for $C_{17}H_{15}FeS$, M-(ephedrine)+H).

31: Yield 515 mg (86%) 1:1 mixture of diastereoisomers (using 1.2 mmol of **26**). *Diast 1 (R_{Fc})* ^{1}H NMR ($CDCl_3$, 400 MHz) δ: 7.35-7.22 (5H, m, Ph), 7.16-7.06 (3H, m, Ph), 4.78 (1H, d, $^{3}J_{H-H}$= 3.3Hz, CHPh), 4.27 (1H, m, subst Cp), 4.15 (5H, s, Cp), 4.10 (1H, m, subst Cp), 4.07 (1H, t, $^{3}J_{H-H}$= 2.5Hz, subst Cp), 3.71 (1H, d, $^{2}J_{H-H}$= 13.5Hz, CH_2), 3.60 (1H, d, $^{2}J_{H-H}$= 13.5Hz, CH_2), 2.89 (1H, qd, $^{3}J_{H-H}$= 7Hz, $^{3}J_{H-H}$= 4Hz, C<u>H</u>CH_3), 2.51 (6H, s, PhC<u>H</u>$_3$) 1.96 (3H, s, NC<u>H</u>$_3$) 0.88 (3H, d, $^{3}J_{H-H}$= 6.9Hz, CHC<u>H</u>3). ^{13}C NMR {^{1}H} ($CDCl_3$, 100 MHz), δ: 142.20 (quat. Ph), 141.96 (quat Ph), 133.96 (quat. Ph), 128.33 (Ph), 128.03 (Ph), 127.87 (Ph), 126.75 (Ph), 126.16 (Ph), 84.83 (quat Cp), 84.60 (quat. Cp), 73.15 (<u>C</u>HPh), 71.49 (subst. Cp), 70.52 (Cp), 69.94 (subst. Cp), 66.43 (subst. Cp), 62.98 (<u>C</u>HCH_3), 53.22 (CH_2), 38.05 ppm (N<u>C</u>H_3), 22.42 (S(C<u>H</u>$_3$)$_2$$C_6H_3$), (9.98 (CH<u>C</u>$H_3$). HRMS (ESI) : 438.1564 (438.1554 calculated for $C_{24}H_{32}FeNOS$, M+H). *Diast 2 (S_{Fc})* ^{1}H NMR ($CDCl_3$, 400 MHz) δ: 7.27-7.22 (4H, m, Ph), 7.18-7.14 (1H, m, Ph), 7.04-6.96 (3H, m, Ph), 4.70 (1H, d, $^{3}J_{H-H}$= 4.7 Hz, CHPh), 4.16-4.15 (1H, br s, subst. Cp), 4.35 (5H, s, Cp), 3.92 (1H, t, $^{3}J_{H-H}$= 2.5 Hz, subst. Cp), 3.90-3.89 (1H, br s, subst. Cp), 3.55 (1H, d, $^{2}J_{H-H}$= 13.3 Hz, CH_2), 3.61 (1H, d, $^{2}J_{H-H}$= 13.3 Hz, CH_2), 2.79-2.75 (1H, m, C<u>H</u>CH_3), 2.39 (3H, s, S(C<u>H</u>$_3$)$_2$$C_6H_3$), 1.82 (3H, s, NCH_3), 0.80 (3H, d, $^{3}J_{H-H}$= 6.8 Hz, CHC<u>H</u>$_3$). ^{13}C NMR {^{1}H} ($CDCl_3$, 100 MHz), δ: 142.2 (quat. Ph), 142.1 (Ph), 133.6 (quat. Ph), 128.3 (Ph), 128.1 (quat. Ph), 126.9 (Ph), 126.8 (quat. Ph), 126.3 (Ph), 85.6 (quat. Cp), 83.7 (quat. Cp), 73.4 (subst. Cp), 70.7 (<u>C</u>HPh), 70.5 (Cp), 69.6 (subst. Cp), 66.3 (subst. Cp), 62.9 (<u>C</u>HCH_3), 52.7 (CH_2), 38.2 (NCH_3), 22.3 (S(C<u>H</u>$_3$)$_2$$C_6H_3$), 9.9 (CH<u>C</u>$H_3$). HRMS (ESI) : 438.1564 (438.1554 calculated for $C_{24}H_{32}FeNOS$, M+H).

3.6.4.4. General procedure for the preparation of thioether-(acetoxymethyl) ferrocene derivatives (32–36)

The corresponding thioether-(dimethylaminomethyl)ferrocene (1 eq) derivatives **22–26** or thioether-*N*-(ferrocenylmethyl)-(**–**)-ephedrine (1 eq) derivatives **27–31** dissolved in freshly distilled acetic anhydride (0.65 mL/mmol) and 120 °C for 16 h. After

that, all volatiles were completely evaporated and the crude mixture was purified by flash chromatography (SiO_2, cyclohexane/ethyl acetate – 80:20) to yield the pure acetate derivative. ^1H and ^{13}C NMR spectra of the compounds agreed with those reported in the literature.[6,8] Both enantiomers of intermediates **32**–**35** were isolated by means of preparative HPLC (*vide infra*).

32: Yield 428 mg (82%) as a dark brown oil (using 1.64 mmol of **22**). Chiralpak IG 3µm column (sCO_2/MeOH (90:10), flow 1.5mL/min, 254 nm). t_R 2.9 min (*S*); t_R 3.1 min (*R*).

33: Yield 528 mg (96%) as a dark brown oil (using 1.73 mmol of **23**). Chiralpak IG 3µm column (sCO_2/MeOH (90:10), flow 1.5mL/min, 254 nm). t_R 2.4 min (*S*); t_R 2.8 min (*R*).

34: Yield 470 mg (90%) as a dark brown oil (using 1.57 mmol of **24**). Chiralpak IG 3µm column (sCO_2/MeOH (90:10), flow 1.5mL/min, 254 nm). t_R 1.9 min (*S*); t_R 2.3 min (*R*).

35: Yield 593 mg (91%) as a dark orange solid (using 1.62 mmol of **25**). Chiralpak IG 3µm column (sCO_2/MeOH (90:10), flow 1.5mL/min, 254 nm). t_R 5.4 min (*S*); t_R 7.7 min (*R*).

36: Yield 425 mg (98%) as a dark brown oil (using 1.08 mmol of **26**). ^1H NMR ($CDCl_3$, 400 MHz), δ: 7.07-6.99 (3H, m, Ph), 5.00 (1H, d, $^2J_{H-H}$= 12.0 Hz, CH_2), 4.93 (1H, d, $^2J_{H-H}$= 12.0 Hz, CH_2), 4.36 (1H, m, subst. Cp), 4.31 (1H, m, subst. Cp), 4.21 (5H, s, Cp), 4.16 (1H, m, sust. Cp), 2.45 (6H, s, $S(C\underline{H}_3)_2C_6H_3$), 1.78 (3H, s, $OC\underline{H}_3$). ^{13}C NMR {^1H} ($CDCl_3$, 100 MHz), δ: 170.8 (CO), 141.5 (quat. Ph), 134.3 (quat. Ph), 128.1 (Ph), 127.7 (quat. Ph), 83.5 (quat. Cp), 82.4 (quat. Cp), 73.8 (subst. Cp), 70.3 (Cp, subst. Cp), 67.9 (subst. Cp), 61.5 (CH_2), 22.3 ($S(C\underline{H}_3)_2C_6H_3$), 20.6 ($OC\underline{H}_3$). HRMS (ESI) : 394.0689 (394.0690 calculated for $C_{21}H_{22}FeO_2S$, M+H).

3.6.4.5. General procedure for the preparation of thioether-(hydroxymethyl) ferrocene derivatives (37–41)

The corresponding thioether-(acetoxymethyl)ferrocene derivatives **32**–**36** (1 eq) were dissolved in anhydrous methanol (1.5 mL/mmol) and anhydrous K_2CO_3 (10 eq) was added and the resulting suspension was stirred until it reached homogeneity. Then it was let react for an additional 16 h. The crude suspension was filtered through a celite plug and the volatiles evaporated under reduced pressure. The residue was redissolved in dichloromethane (20 mL) and washed with water (20 mL) the organic phase was dried with $MgSO_4$, filtered and evaporated under reduced pressure. This yielded a sufficiently pure alcohol to be used in the next steps without further purification, although in some cases we observed the presence of a minor amount of the previous acetate compound (>5%), flash column chromatography (SiO_2, cyclohexane/ethyl

acetate – 80:20) could be performed to obtain the pure alcohol. ^{1}H and ^{13}C NMR spectra of the compounds **37**–**41** agreed with those reported in the literature. Both enantiomers of intermediates **37**–**40** were isolated by means of preparative HPLC (*vide infra*).

37: Yield 331 mg (97%) as a dark brown solid (using 1.3 mmol of **32**). Chiralpak IG 3µm column (sCO_2/MeOH (90:10), flow 1.5mL/min, 254 nm). t_R 7.2 min (*S*); t_R 9.0 min (*R*).

38: Yield 315 mg (88%) as a dark brown solid (using 1.3 mmol of **33**). Chiralpak IG 3µm column (sCO_2/MeOH (90:10), flow 1.5mL/min, 254 nm). t_R 6.8 min (*S*); t_R 11.9 min (*R*).

39: Yield 290 mg (83%) as a dark brown oil (using 1.2 mmol of **34**). Chiralpak IG 3µm column (sCO_2/MeOH (90:10), flow 1.5mL/min, 254 nm). t_R 6.1 min (*S*); t_R 9.4 min (*R*).

40: Yield 440 mg (97%) as a dark orange solid (using 1.4 mmol of **35**). Chiralpak IC 3µm column (sCO_2/MeOH (90:10), flow 1.5mL/min, 254 nm). t_R 5.1 min (*S*); t_R 5.4 min (*R*).

41: Yield 383 mg (99%) (using 1.1 mmol of **36**). ^{1}H NMR ($CDCl_3$, 400 MHz) : 7.00 - 6.69 (3H, m, Ph), 4.39 (1H, d, $^{2}J_{H\text{-}H}$= 12.3Hz, CH_2), 4.27 (1H, m, subst. Cp), 4.22 (2H, m, CH_2 and subst. Cp), 4.14 (5H, s, Cp), 4.06 (1H, m, sust. Cp), 2.39 (6H, s, $S(C\underline{H}_3)_2C_6H_3$). ^{13}C NMR {^{1}H} ($CDCl_3$, 100 MHz) : 141.4 (quat. Ph), 135.1 (quat. Ph), 128.5 (Ph), 128.1 (quat. Ph), 88.9 (quat. Cp), 82.7 (quat. Cp), 73.1 (subst. Cp), 70.1 (Cp, subst. Cp), 69.3 (subst. Cp), 67.3 (CH_2), 59.8 ($S(C\underline{H}_3)_2C_6H_3$), 22.3 ($O\underline{C}H_3$). HRMS (ESI) : 352.0581 (352.0584 calculated for $C_{19}H_{20}FeOS$, M+H).

3.6.4.6. General procedure for the preparation of ferrocenyl thioether-imidazolium salt derivatives (L23–L30H·Cl)

The corresponding (R_{Fc})-thioether-(hydroxymethyl) ferrocene derivatives **37**–**41** (1 eq) were dissolved in dry AcOH (1 mL/mmol). Then the corresponding imidazole derivative (1.5 eq) was subsequently added. The reaction mixture was stirred overnight at 60º C. After that, the volatiles were evaporated *in vacuo* and the residue redissolved in EtOH (1.6 mL/mmol). Then, LiCl (3 eq) was added and stirred for 2 additional hours. When the reaction was finished the solvent was evaporated, redissolved in DCM, filtered through a celite plug and evaporated *in vacuo*. Column chromatography and recrystallization were necessary to obtain the pure imidazolium salt derivatives.

L23H·Cl: Yield 79 mg (99%) as an orange-brown solid (using 0.18 mmol of **37**). ^{1}H NMR ($CDCl_3$, 400 MHz), δ: 11.08 (1H, s, NCHN), 7.76 (1H, s, CH of benzimidazole), 7.34 (1H, s, CH of benzimidazole), 5.67 (1H, d, $^{2}J_{H\text{-}H}$= 14.4 Hz, CH_2), 5.54 (1H, d, $^{2}J_{H\text{-}H}$= 14.4 Hz, CH_2), 5.06 (1H, s, subst. Cp), 4.40 (1H, s, subst. Cp), 4.30 (1H, s, subst. Cp), 4.29 (5H, s, Cp), 4.17 (3H, s, NCH_3), 2.41 (6H, s, CH_3 of benzimidazole), 1.95

(3H, s, SCH_3). ^{13}C NMR {^1H} ($CDCl_3$, 100 MHz), δ: 142.3 (NCHN), 137.1 (quat. Ph), 137.0 (quat. Ph), 130.3 (quat. Ph), 125.3 (quat. Ph), 113.2 (CH of benzimidazole), 112.2 (CH of benzimidazole), 82.6 (quat. Cp), 81.8 (quat. Cp), 73.7 (subst. Cp), 71.2 (subst. Cp), 70.6 (Cp), 69.8 (subst. Cp), 45.1 (CH_2), 33.5 (NCH_3), 21.3 (SCH_3), 21.3 (CH_3 of benzimidazole) 21.3 (CH_3 of benzimidazole). HRMS (ESI) : 405.1090 (405.1088 calculated for $C_{22}H_{25}FeN_2S$, M-Cl).

L24H·Cl: Yield 50 mg (61%) as an orange-brown solid (using 0.18 mmol of **38**). ^1H NMR ($CDCl_3$, 400 MHz), δ: 11.43 (1H, s, NCHN), 7.76 (1H, s, CH of benzimidazole), 7.33 (1H, s, CH of benzimidazole), 5.61-5.53 (2H, m, CH_2), 5.19 (1H, s, subst. Cp), 4.44 (1H, s, subst. Cp), 4.35 (1H, s, subst. Cp), 4.22 (5H, s, Cp), 4.18 (3H, s, NCH_3), 2.44-2.43 (6H, m, CH_3 of benzimidazole), 2.23-2.10 (2H, m, $C\underline{H}_2CH_3$), 0.99 (3H, t, $^3J_{H-H}$= 7.23Hz, $CH_2C\underline{H}_3$). ^{13}C NMR {^1H} ($CDCl_3$, 100 MHz), δ: 142.9 (NCHN), 137.1 (quat. Ph), 136.9 (quat. Ph), 130.1 (quat. Ph), 129.3 (quat. Ph), 113.2 (CH of benzimidazole), 112.1 (CH of benzimidazole), 82.4 (subst. Cp), 79.9 (quat. Cp), 75.4 (subst. Cp), 71.8 (quat. Cp), 70.6 (Cp), 70.1 (subst. Cp), 45.1 (CH_2), 33.6 ($\underline{C}H_2CH_3$), 32.1 (NCH_3), 20.7 (CH_3 of benzimidazole) 20.6 (CH_3 of benzimidazole), 14.6 ($CH_2\underline{C}H_3$). HRMS (ESI) : 419.1250 (419.1244 calculated for $C_{23}H_{27}FeN_2S$, M-Cl).

L25H·Cl: Yield 60 mg (74%) as an orange-brown solid (using 0.17 mmol of **39**). ^1H NMR ($CDCl_3$, 400 MHz), δ: 11.37 (1H, s, NCHN), 7.71 (1H, s, CH of benzimidazole), 7.24 (1H, s, CH of benzimidazole), 5.57-5.60 (2H, m, CH_2), 5.26 (1H, s, subst. Cp), 4.45-4.44 (1H, m, subst. Cp), 4.37 (1H, s, subst. Cp), 4.18 (8H, s, Cp and NCH_3), 2.44-2.42 (6H, m, CH_3 of benzimidazole), 2.26-2.22 (1H, m, CH of *i*-Pr), 0.98 (3H, d, $^3J_{H-H}$= 6.7Hz, CH_3 of *i*-Pr), 0.86 (3H, d, $^3J_{H-H}$= 6.7Hz, CH_3 of *i*-Pr). ^{13}C NMR {^1H} ($CDCl_3$, 100 MHz), δ: 142.9 (NCHN), 137.1 (quat. Ph), 136.9 (quat. Ph), 130.1 (quat. Ph), 129.4 (quat. Ph), 113.2 (CH of benzimidazole), 112.2 (CH of benzimidazole), 82.8 (quat. Cp), 78.5 (quat. Cp), 76.5 (subst. Cp), 72.1 (subst. Cp), 70.5 (Cp), 70.3 (subst. Cp), 44.9 (CH_2), 40.3 (CH of *i*-Pr), 33.5 (NCH_3), 23.2 (CH_3 of *i*-Pr), 22.4 (CH_3 of *i*-Pr), 20.7 (CH_3 of benzimidazole) 20.6 (CH_3 of benzimidazole). HRMS (ESI) : 433.1410 (433.1401 calculated for $C_{24}H_{29}FeN_2S$, M-Cl).

L26H·Cl: Yield 56 mg (74%) as an orange-brown solid (using 0.15 mmol of **40**). ^1H NMR (CD_2Cl_2, 400 MHz), δ: 11.88 (1H, s, NCHN), 7.36 (1H, s, CH of benzimidazole), 7.09 (1H, s, CH of benzimidazole), 6.77-6.76 (3H, m, Ph), 6.50-6.48 (2H, m, Ph), 5.73 (1H, m, CH_2), 5.43-5.39 (1H, m, CH_2), 5.25 (1H, s, subst. Cp), 4.55-4.53 (2H, m, subst. Cp), 4.39 (5H, s, Cp), 3.85 (3H, s, NCH_3), 2.23 (3H, s, CH_3 of benzimidazole), 2.21 (3H, m, CH_3 of benzimidazole). ^{13}C NMR {^1H} (CD_2Cl_2, 100 MHz), δ: 143.0 (NCHN), 140.1 (quat. Ph), 137.1 (quat. Ph), 137.0 (quat. Ph), 130.3 (quat. Ph), 129.5 (quat. Ph), 128.5 (2xPh), 124.6 (Ph), 124.5 (2xPh), 113.3 (CH of benzimidazole), 112.1 (CH of benzimidazole), 83.9 (quat. Cp), 77.5 (subst. Cp), 75.7 (quat. Cp), 73.8 (subst. Cp), 73.8 (Cp), 70.9 (subst. Cp), 45.9 (CH_2), 33.7 (NCH_3), 20.7 (CH_3 of benzimidazole) 20.6

(CH_3 of benzimidazole). HRMS (ESI) : 467.1250 (467.1244 calculated for $C_{27}H_{27}FeN_2S$, M-Cl).

L27H·Cl: Yield 60 mg (80%) as an orange-brown solid (using 0.14 mmol of **41**). ^{1}H NMR ($CDCl_3$, 400 MHz), δ: 10.41 (1H, s, NCHN), 7.26 (1H, s, CH of benzimidazole), 7.15 (1H, s, CH of benzimidazole), 6.74-6.70 (1H, m, Ph), 6.63-6.61 (2H, m, Ph), 5.43 (2H, s, CH_2), 4.84 (1H, s, subst. Cp), 4.32 (1H, s, subst. Cp), 4.27 (1H, s, subst. Cp), 4.23 (5H, s, Cp), 3.96 (3H, s, NCH_3), 2.35 (3H, s, CH_3 of benzimidazole), 2.31 (3H, s, CH_3 of benzimidazole), 2.15 (6H, s, $S(C\underline{H}_3)_2C_6H_3$). ^{13}C NMR {^{1}H} ($CDCl_3$, 100 MHz), δ: 141.6 (NCHN), 140.8 (2xquat. Ph), 136.8 (quat. Ph), 136.6 (quat. of Ph), 133.7 (quat. Ph), 130.3 (quat. Ph), 129.2 (quat. Ph), 127.9 (Ph), 127.5 (Ph) 112.9 (CH of benzimidazole), 111.9 (CH of benzimidazole), 83.2 (quat. Cp), 79.5 (quat. Cp), 74.2 (subst. Cp), 71.2 (subst. Cp), 71.0 (Cp), 68.9 (subst. Cp), 46.0 (CH_2), 33.4 (NCH_3), 33.5 (NCH_3), 22.3 (CH_3 of benzimidazole), 20.6 ($S(\underline{C}H_3)_2C_6H_3$). HRMS (ESI) : 495.1560 (495.1557 calculated for $C_{29}H_{31}FeN_2S$, M-Cl).

L28H·Cl: Yield 86 mg (79%) as an orange-brown solid (using 0.17 mmol of **39**). ^{1}H NMR ($CDCl_3$, 400 MHz) : δ: 10.11 (1H, s, NCHN), 7.68 (1H, s, CH of benzimidazole), 7.06 (1H, s, CH of benzimidazole), 5.69-5.64 (3H, m, $C\underline{H}_2C(CH_3)_5$ and CH_2), 5.55-5.52 (1H, m, CH_2), 5.02 (1H, s, subst. Cp), 4.38 (1H, s, subst. Cp), 4.29 (1H, s, subst. Cp), 4.12 (5H, s, Cp), 2.37 (3H, s, CH_3 of benzimidazole), 2.28 (3H, s, CH_3 of benzimidazole), 2.24-2.16 (16H, s, $CH_2C(C\underline{H}_3)_5$ and CH of *i*-Pr), 0.91 (3H, d, $^3J_{H\text{-}H}$= 6.6Hz, CH_3 of *i*-Pr), 0.77 (3H, d, $^3J_{H\text{-}H}$= 6.6Hz, CH_3 of *i*-Pr).^{13}C NMR {^{1}H} ($CDCl_3$, 100 MHz), δ: 141.3 (NCHN), 137.0 (quat. Ph), 136.8 (quat. Ph), 136.7 (quat. Ph), 133.7 (2xquat. Ph), 133.5 (2xquat. Ph), 130.1 (quat. Ph), 129.6 (quat. Ph), 125.2 (quat. Ph), 113.4 (CH of benzimidazole), 113.0 (CH of benzimidazole), 82.8 (quat. Cp), 79.7 (quat. Cp), 76.1 (subst. Cp), 71.8 (subst. Cp), 70.5 (Cp), 69.8 (subst. Cp), 47.7 ($\underline{C}H_2C(CH_3)_5$), 45.2 ($CH_2$), 40.0 (CH of *i*-Pr), 23.0 (CH_3 of benzimidazole), 22.4 (CH_3 of benzimidazole), 20.8 (CH_3 of *i*-Pr), 20.6 (CH_3 of *i*-Pr), 17.2 ($CH_2C(\underline{C}H_3)_5$), 17.0 ($2xCH_2C(\underline{C}H_3)_5$), 16.9 ($2xCH_2C(\underline{C}H_3)_5$). HRMS (ESI) : 579.2489 (579.2496 calculated for $C_{35}H_{43}FeN_2S$, M-Cl).

L29H·Cl: Yield 58 mg (64%) as an orange-brown solid (using 0.17 mmol of **39**). ^{1}H NMR ($CDCl_3$, 400 MHz), δ: 10.54 (1H, s, NCHN), 7.62 (1H, s, CH of imidazole), 7.51-7.47 (1H, m, Ph), 7.28-7.26 (2H, m, Ph), 7.02 (1H, s, CH of imidazole), 6.19 (1H, d, $^2J_{H\text{-}H}$= 13.9 Hz, CH_2), 5.56 (1H, d, $^2J_{H\text{-}H}$= 13.9 Hz, CH_2), 5.07 (1H, s, subst. Cp), 4.48-4.47 (1H, m, subst. Cp), 4.35-4.34 (1H, m, subst. Cp), 4.26 (5H, s, Cp), 2.72-2.69 (1H, m, CH of *i*-Pr), 2.33-2.29 (1H, m, CH of *i*-Pr), 2.14-2.10 (1H, m, CH of *i*-Pr), 1.25-1.06 (18H, m, CH_3 of *i*-Pr). ^{13}C NMR {^{1}H} ($CDCl_3$, 100 MHz), δ: 145.3 (quat. Ph), 145.2 (quat. Ph), 138.7 (NCHN), 131.8 (Ph), 130.2 (quat. Ph), 124.6 (Ph), 124.5 (Ph), 123.3 (CH of imidazole), 122.3 (CH of imidazole), 81.8 (quat. Cp), 79.5 (quat. Cp), 75.8 (subst. Cp), 71.8 (subst. Cp), 70.9 (Cp), 69.9 (subst. Cp), 48.8 (CH_2), 40.3 (CH of *i*-Pr), 28.7 (CH of *i*-Pr), 28.7 (CH of *i*-Pr), 24.4 (CH_3 of *i*-Pr), 24.3 (CH_3 of *i*-Pr), 24.2 (CH_3

of *i*-Pr), 24.1 (CH_3 of *i*-Pr), 23.7 (CH_3 of *i*-Pr), 23.2 (CH_3 of *i*-Pr). HRMS (ESI) : 501.2030 (501.2027 calculated for $C_{29}H_{37}FeN_2S$, M-Cl).

L30H·Cl: Yield 75 mg (89%) as an orange-brown solid (using 0.17 mmol of **39**). ^{1}H NMR ($CDCl_3$, 400 MHz), δ: 10.45 (1H, s, NCHN), 7.51 (1H, s, CH of imidazole), 7.05 (1H, s, CH of imidazole), 6.94-6.93 (2H, m, Ph), 6.04-5.98 (1H, m, CH_2), 5.59-5.48 (1H, m, CH_2), 5.01 (1H, s, subst. Cp), 4.47-4.46 (1H, m, subst. Cp), 4.32 (1H, s, subst. Cp), 4.23 (5H, s, Cp), 2.66-2.63 (1H, m, CH of *i*-Pr), 2.28 (3H, s, CH_3 of Mes), 2.05 (3H, s, CH_3 of Mes), 1.96 (3H, s, CH_3 of Mes), 1.13 (3H, d, $^3J_{H-H}$= 6.6Hz, CH_3 of *i*-Pr), 1.08 (3H, d, $^3J_{H-H}$= 6.6Hz, CH_3 of *i*-Pr). ^{13}C NMR {^{1}H} ($CDCl_3$, 100 MHz), δ: 141.2 (NCHN), 138.5 (quat. Ph), 134.2 (quat. Ph), 134.1 (quat. Ph), 130.7 (quat. Ph), 129.8 (Ph), 122.3 (CH of imidazole), 122.1 (CH of imidazole), 81.8 (quat. Cp), 79.4 (quat. Cp), 75.9 (subst. Cp), 71.8 (subst. Cp), 70.8 (Cp), 69.9 (subst. Cp), 48.5 (CH_2), 40.3 (CH of *i*-Pr), 23.3 (CH_3 of *i*-Pr), 23.2 (CH_3 of *i*-Pr), 21.0 (CH_3 of Mes), 17.7 (CH_3 of Mes), 17.6 (CH_3 of Mes). HRMS (ESI) : 459.1549 (459.1557 calculated for $C_{26}H_{31}FeN_2S$, M-Cl).

3.6.4.7. General procedure for the preparation of [Ir(cod)(L23–L30)]Bar$_F$ thioether-carbene complexes

Ag_2O (0.5 eq) was added into a solution in the CH_2Cl_2 (50 mL/mmol) of the corresponding thioether-imidazolium salt derivatives **L23–L30**H·Cl (1 eq). The resulting solution was vigorously stirred overnight at room temperature in the absence of light. Then, the solution was filtered through a dry celite plug and evaporated. The resulting solid complex was used immediately in the next step without further purification since the product rapidly decomposes into solution in the presence of light.

The corresponding Ag**L23–L30**$_2$·$AgBr_2$ (1 eq) was dissolved in dry CH_2Cl_2 (50 mL/mmol) and [Ir(μ-Cl)(cod)]$_2$ (0.5 eq) and stirred 4.5h in the absence of light. The crude solution was passed through a dry celite plug to achieve a clear deep brownish-orange solution. The solution was evaporated in vacuo and redissolved in CH_2Cl_2 (50 mL/mmol), into this solution $NaBAr_F$ (1.1 eq) was added and let react for an additional hour. Then, the reaction crude was evaporated in vacuo and purified by flash chromatography (SiO_2, DCM/hexane– 80:20) leading to the pure Ir complexes.

[Ir(cod)(L23)]BAr$_F$: Yield 127 mg (45%) over 2 steps as an bright-red solid (using 0.28 mmol of **L23**H·Cl). ^{1}H NMR ($CDCl_3$, 400 MHz), δ: ^{1}H NMR ($CDCl_3$, 400 MHz) δ: 7.68 (8H, s, BAr_F), 7.49 (4H, s, BAr_F), 7.07 (1H, s, CH of benzimidazole), 7.06 (1H, s, CH of benzimidazole), 6.35 (1H, d, $^2J_{H-H}$= 15.6 Hz, CH_2), 5.02 (1H, d, $^2J_{H-H}$= 14.9 Hz, CH_2), 4.59-4.57 (1H, m, CH of cod), 4.51-4.50 (2H, m, subst. Cp an CH of cod), 4.41-4.40 (1H, m, CH of cod), 4.35 (5H, s, Cp), 4.28-4.25 (2H, m, subst. Cp), 4.14-4.09 (1H, m, CH of cod), 3.93 (3H, s, NCH_3), 2.39-2.35 (4H, m, CH_2 of cod), 2.30 (6H, s, CH_3 of benzimidazole), 2.18-2.15 (4H, m, CH_2 of cod), 2.08 (3H, s, SCH_3) . ^{13}C NMR {^{1}H}

($CDCl_3$, 100 MHz), δ: 182.2 (NCN), 161.6 (q, $^1J_{B-C}$= 50.0 Hz, BAr_F), 134.7 (BAr_F), 134.1 (quat. Ph), 133.8 (quat. Ph), 133.7 (quat. Ph), 131.2 (quat. Ph), 129.3-128.3 (m, CF_3), 125.8 (quat. Ph), 123.1 (quat. Ph), 120.4 (quat. Ph), 117.4 (BAr_F), 110.9 (CH of benzimidazole), 109.9 (CH of benzimidazole), 84.0 (CH of cod), 82.3 (CH of cod), 81.3 (quat. Cp), 81.1 (quat. Cp), 73.2 (CH of cod), 72.4 (CH of cod), 71.7 (subst. Cp), 70.9 (Cp), 70.5 (subst. Cp), 69.2 (subst. Cp), 46.1 (CH_2), 33.9 (NCH_3), 33.6 (CH_2 of cod), 31.3 (CH_2 of cod), 31.1 (CH_2 of cod), 29.9 (CH_2 of cod), 28.3 (SCH_3), 20.2 (CH_3 of benzimidazole), 20.1 (CH_3 of benzimidazole). HRMS (ESI) : 705.1581 (705.1578 calculated for $C_{30}H_{36}FeIrN_2S$, M-BAr_F).

[Ir(cod)(L24c)]BAr_F: Yield 63 mg (36%) over 2 steps as an bright-red solid (using 0.11 mmol of **L24**H·Cl). ^{1}H NMR ($CDCl_3$, 400 MHz), δ: 7.69 (8H, s, BAr_F), 7.49 (4H, s, BAr_F), 7.07 (1H, s, CH of benzimidazole), 7.05 (1H, s, CH of benzimidazole), 6.40 (1H, d, $^2J_{H-H}$= 15.6 Hz, CH_2), 5.01 (1H, d, $^2J_{H-H}$= 15.6 Hz, CH_2), 4.64-4.63 (1H, m, CH of cod), 4.58 (1H, s, subst. Cp), 4.49-4.45 (2H, m, CH of cod), 4.38 (1H, s, subst. Cp), 4.34 (5H, s, Cp), 4.29-4.28 (1H, m, subst. Cp), 4.09-4.08 (1H, m, CH of cod), 3.94 (3H, s, NCH_3), 2.45-2.08 (16H, m, CH_2 of cod, CH_3 of benzimidazole and $C\underline{H}_2CH_3$), 1.24-1.20 (3H, m, $CH_2C\underline{H}_3$). ^{13}C NMR {^{1}H} ($CDCl_3$, 100 MHz), δ: 182.5 (NCN), 161.5 (q, $^1J_{B-C}$= 50.7 Hz, BAr_F), 134.7 (BAr_F), 134.1 (quat. Ph), 133.6 (quat. Ph), 131.2 (quat. Ph), 128.9-128.6 (m, CF_3), 125.8 (quat. Ph), 123.1 (quat. Ph), 119.6 (quat. Ph), 117.4 (BAr_F), 110.9 (CH of benzimidazole), 109.9 (CH of benzimidazole), 84.5 (CH of cod), 81.9 (CH of cod), 80.6 (quat. Cp), 78.2 (quat. Cp), 77.2 (CH of cod), 75.0 (subst. Cp), 72.1 (subst. Cp), 71.9 (CH of cod), 71.1 (Cp), 69.2 (subst. Cp), 45.0 (CH_2), 42.2 ($\underline{C}H_2CH_3$), 34.3 (NCH_3), 34.0 (CH_2 of cod), 31.8 (CH_2 of cod), 30.8 (CH_2 of cod), 29.2 (CH_2 of cod), 20.2 (CH_3 of benzimidazole), 20.1 (CH_3 of benzimidazole), 14.01 ($CH_2\underline{C}H_3$). HRMS (ESI) : 719.1740 (719.1734 calculated for $C_{31}H_{38}FeIrN_2S$, M-BAr_F)

[Ir(cod)(L25)]BAr_F: Yield 67 mg (46%) over 2 steps as an bright-red solid (using 0.09 mmol of **L25**H·Cl). ^{1}H NMR ($CDCl_3$, 400 MHz), δ: ^{1}H NMR ($CDCl_3$, 400 MHz): 7.68 (8H, s, BAr_F), 7.49 (4H, s, BAr_F), 7.07-7.06 (2H, m, CH of benzimidazole), 6.45 (1H, d, $^2J_{H-H}$= 14.9 Hz, CH_2), 5.00 (1H, d, $^2J_{H-H}$= 14.9 Hz, CH_2), 4.72-4.66 (1H, m, CH of cod), 4.59-4.57 (1H, s, subst. Cp), 4.45-4.42 (3H, m, 2xCH of cod and subst. Cp), 4.35 (5H, s, Cp), 4.32-4.31 (1H, m, subst. Cp), 3.97-3.94 (4H, m, NCH_3 and CH of cod), 2.45-2.13 (13H, m, CH_2 of cod, CH_3 of benzimidazole and CH of *i*-Pr), 1.96-1.85 (2H, m, CH_2 of cod), 1.07 (3H, d, $^3J_{H-H}$= 6.8 Hz, CH_3 of *i*-Pr), 1.02 (3H, d, $^3J_{H-H}$= 6.8 Hz, CH_3 of *i*-Pr). ^{13}C NMR {^{1}H} ($CDCl_3$, 100 MHz), δ: 182.0 (NCN), 161.6 (q, $^1J_{B-C}$= 49.7 Hz, BAr_F), 134.7 (BAr_F), 134.7 (quat. Ph), 134.1 (quat. Ph), 133.6 (quat. Ph), 133.5 (quat. Ph), 131.2 (quat. Ph), 129.2-128.3 (m, CF_3), 125.8 (quat. Ph), 123.1 (quat. Ph), 120.4 (quat. Ph), 117.4 (BAr_F), 110.9 (CH of benzimidazole), 109.8 (CH of benzimidazole), 85.2 (CH of cod), 82.3 (CH of cod), 80.7 (quat. Cp), 77.2 (quat. Cp), 76.3 (CH of cod), 75.7 (subst. Cp), 72.6 (subst. Cp), 71.1 (Cp), 70.1 (subst. Cp), 68.8 (CH of cod), 50.0 (CH of *i*-Pr),

45.9 (CH_2), 35.1 (NCH_3), 34.2 (CH_2 of cod), 32.5 (CH_2 of cod), 30.0 (CH_2 of cod), 28.4 (CH_2 of cod), 22.9 (CH_3 of *i*-Pr), 22.6 (CH_3 of *i*-Pr), 20.2 (CH_3 of benzimidazole), 20.1 (CH_3 of benzimidazole). HRMS (ESI) : 733.1885 (733.1891 calculated for $C_{32}H_{40}FeIrN_2S$, M-BAr_F).

[Ir(cod)(L26)]BAr_F: Yield 45 mg (55%) over 2 steps as an bright-red solid (using 0.05 of **L26**H·Cl). ^{1}H NMR ($CDCl_3$, 400 MHz), δ: 7.72 (8H, s, BAr_F), 7.72 (4H, s, BAr_F), 7.16 (1H, t, $^3J_{H-H}$= 6.9 Hz, Ph), 7.12 (1H, s, CH of benzimidazole), 6.95 (2H, t, $^3J_{H-H}$= 6.9 Hz, Ph), 6.86 (1H, s, CH of benzimidazole), 6.47 (1H, d, $^2J_{H-H}$= 14.9 Hz, CH_2), 6.20 (2H, d, $^3J_{H-H}$= 6.9 Hz, Ph), 5.11 (1H, d, $^2J_{H-H}$= 14.9 Hz, CH_2), 4.92-4.86 (1H, m, CH of cod), 4.74-4.73 (1H, m, subst. Cp), 4.68-4.64 (1H, m, CH of cod), 4.47-4.40 (7H, m, subst. Cp, Cp and CH of cod), 4.35-4.34 (1H, m, CH of cod), 2.97 (3H, s, NCH_3), 2.40-2.36 (3H, m, CH_2 of cod), 2.33 (3H, s, CH_3 of benzimidazole), 2.29 (3H, s, CH_3 of benzimidazole), 2.27-2.22 (2H, m, CH_2 of cod), 2.17-2.00 (3H, m, CH_2 of cod). ^{13}C NMR {^{1}H} ($CDCl_3$, 100 MHz), δ: 180.2 (NCN), 161.7 (q, $^1J_{B-C}$= 49.7 Hz, BAr_F), 135.1 (quat. Ph), 134.7 (BAr_F), 133.9 (quat. Ph), 133.8 (quat. Ph), 133.6 (quat. Ph), 131.0 (quat. Ph), 129.7 (Ph), 129.0-128.3 (m, CF_3), 128.7 (Ph), 125.8 (quat. Ph), 125.4 (Ph), 123.17 (quat. Ph), 120.4 (quat. Ph), 117.4 (BAr_F), 110.4 (CH of benzimidazole), 109.8 (CH of benzimidazole), 84.2 (CH of cod), 82.3 (quat. Cp), 81.9 (CH of cod), 76.2 (CH of cod), 75.8 (subst.Cp), 74.8 (quat. Cp), 72.7 (subst. Cp), 71.4 (CH of cod), 71.2 (Cp), 70.2 (subst. Cp), 45.8 (CH_2), 34.2 (NCH_3), 32.5 (CH_2 of cod), 31.5 (CH_2 of cod), 31.0 (CH_2 of cod), 29.7 (CH_2 of cod), 20.2 (CH_3 of benzimidazole), 20.1 (CH_3 of benzimidazole). HRMS (ESI) : 767.1741 (767.1734 calculated for $C_{35}H_{38}FeIrN_2S$, M-BAr_F).

[Ir(cod)(L27)]BAr_F: Yield 37 mg (20%) over 2 steps as an orange-red solid (using 0.11 mmol of **L27**H·Cl). ^{1}H NMR ($CDCl_3$, 400 MHz): δ: 7.70 (8H, s, BAr_F), 7.49 (4H, s, BAr_F), 7.31 (1H, s, CH of benzimidazole), 7.27 (1H, s, CH of benzimidazole), 7.20-7.09 (3H, m, Ph), 5.36 (1H, d, $^2J_{H-H}$= 14.7 Hz, CH_2), 4.18 (1H, d, $^2J_{H-H}$= 14.7 Hz, CH_2), 4.39-4.32 (2H, m, subst. Cp and CH of cod), 4.27 (3H, s, NCH_3), 4.12-4.11 (2H, m, subst. Cp and CH of cod), 3.95 (1H, s, subst. Cp), 3.38-3.31 (6H, m, Cp and CH of cod), 2.95-2.93 (1H, m, CH of cod), 2.45 (3H, s, CH_3 of benzimidazole), 2.40 (3H, s, CH_3 of benzimidazole), 2.36-2.28 (3H, m, CH_2 of cod), 2.20-2.10 (8H, m, CH_2 of cod and $S(C\underline{H}_3)_2C_6H_3$), 1.23 (3H, s, $S(C\underline{H}_3)_2C_6H_3$). ^{13}C NMR {^{1}H} ($CDCl_3$, 100 MHz), δ: 178.2 (NCN), 161.6 (q, $^1J_{B-C}$= 50.3 Hz, BAr_F), 140.0 (quat. Ph), 134.7 (BAr_F), 134.4 (quat. Ph), 134.2 (quat. Ph), 133.9 (quat. Ph), 133.0 (quat. Ph), 131.3 (Ph), 129.4-128.36 (m, CF_3), 125.8 (quat. Ph), 123.1 (quat. Ph), 120.4 (quat. Ph), 117.4 (BAr_F), 111.4 (CH of benzimidazole), 110.7 (CH of benzimidazole), 87.3 (CH of cod), 86.0 (CH of cod), 84.9 (quat. Cp), 74.9 (quat. Cp), 72.7 (CH of cod), 71.8 (subst. Cp), 70.5 (Cp), 67.4 (subst. Cp), 67.0 (CH of cod), 43.2 (CH_2), 36.6 (CH_2 of cod), 35.4 (NCH_3), 34.0 (CH_2 of cod), 30.9 (CH_2 of cod), 29.6 ($S(\underline{C}H_3)_2C_6H_3$), 28.2 ($S(\underline{C}H_3)_2C_6H_3$), 25.7 ($CH_2$ of cod),

20.4 (CH_3 of benzimidazole), 20.3 (CH_3 of benzimidazole). HRMS (ESI) : 795.2046 (795.2047 calculated for $C_{37}H_{42}FeIrN_2S$, M-BAr_F).

[Ir(cod)(L28)]BAr_F: Yield 25 mg (19%) over 2 steps as an bright-red solid (using 0.08 mmol of **L28**H·Cl). ^{1}H NMR ($CDCl_3$, 400 MHz), δ: 7.71 (8H, s, BAr_F), 7.51 (4H, s, BAr_F), 6.96 (1H, s, CH of benzimidazole), 6.62 (1H, d, $^2J_{H-H}$= 14.6 Hz, CH_2), 5.36 (1H, d, $^2J_{H-H}$= 15.3 Hz, C$\underline{H}_2$C(CH_3)$_5$), 5.76 (1H, s, CH of benzimidazole), 5.43 (1H, d, $^2J_{H-H}$= 14.6 Hz, CH_2), 5.09 (1H, d, $^2J_{H-H}$= 15.3 Hz, C$\underline{H}_2$C(CH_3)$_5$), 4.80-4.75 (2H, m, subst. Cp and CH of cod), 4.47-4.43 (1H, s, subst. Cp), 4.41-4.32 (8H, m, subst. Cp, Cp and CH of cod), 2.60-2.50 (4H, m, CH_2 of cod), 2.46-2.39 (1H, m, CH of *i*-Pr), 2.34 (3H, s, $CH_2C(C\underline{H}_3)_5$), 2.30-2.26 (2H, m, CH_2 of cod), 2.24 (6H, s, $CH_2C(C\underline{H}_3)_5$), 2.19 (3H, s, CH of benzimidazole), 2.09 (6H, s, $CH_2C(C\underline{H}_3)_5$), 1.90 (3H, s, CH of benzimidazole), 1.89-1.70 (3H, m, CH_2 of cod), 1.32 (3H, d, $^3J_{H-H}$= 6.7 Hz, CH_3 of *i*-Pr), 1.02 (3H, d, $^3J_{H-H}$= 6.7 Hz, CH_3 of *i*-Pr). ^{13}C NMR {^{1}H} ($CDCl_3$, 100 MHz), δ: 182.5 (NCN), 161.6 (q, $^1J_{B-C}$= 50.3 Hz, BAr_F), 137.01 (quat. Ph), 134.8 (BAr_F), 133.7 (quat. Ph), 133.6 (quat. Ph), 133.5 (quat. Ph), 133.4 (quat. Ph), 133.1 (Ph), 129.0-128.3 (m, CF_3), 126.2 (quat. Ph), 125.8 (quat. Ph), 120.4 (quat. Ph), 117.4 (BAr_F), 112.8 (CH of benzimidazole), 109.6 (CH of benzimidazole), 84.6 (CH of cod), 81.4 (CH of cod), 80.8 (quat. Cp), 77.2 (quat. Cp), 77.0 (CH of cod), 75.7 (CH of cod), 72.6 (subst. Cp), 71.1 (Cp), 68.8 (subst. Cp), 68.8 (CH of cod), 50.3 ($C\underline{H}_2C(CH_3)_5$), 49.2 (CH of *i*-Pr), 46.1 (CH_2), 36.5 (CH_2 of cod), 33.7 (CH_2 of cod), 29.1 (CH_2 of cod), 27.2 (CH_2 of cod), 24.0 (CH_3 of *i*-Pr), 22.7 (CH_3 of *i*-Pr), 20.3 (CH_3 of benzimidazole), 20.0 (CH_3 of benzimidazole), 17.2 ($CH_2C(\underline{C}H_3)_5$), 16.8 (2x $CH_2C(\underline{C}H_3)_5$), 16.7 (2x $CH_2C(\underline{C}H_3)_5$). HRMS (ESI) : 879.2990 (879.2986 calculated for $C_{43}H_{54}FeIrN_2S$, M-BAr_F).

[Ir(cod)(L29)]BAr_F: Yield 99 mg (64%) over 2 steps as an bright-red solid (using 0.09 mmol of **L29**H·Cl). ^{1}H NMR ($CDCl_3$, 400 MHz) δ: 7.70 (8H, s, BAr_F), 7.51-7.47 (5H, s, BAr_F and Ph), 7.32-7.30 (1H, m, Ph), 7.20-7.18 (1H, m, Ph), 7.03 (1H, s, CH of imidazole), 6.84 (1H, s, CH of imidazole), 6.53 (1H, d, $^2J_{H-H}$= 15.1 Hz, CH_2), 4.73 (1H, d, $^2J_{H-H}$= 15.1 Hz, CH_2), 4.57-4.51 (3H, m, 2xsubst. and CH of cod), 4.35-4.34 (1H, s, subst. Cp), 4.32-4.30 (6H, m, Cp and CH of cod), 4.26-4.23 (1H, m, CH of cod), 3.30-3.24 (1H, m, CH of cod), 3.00-2.90 (1H, m, CH of *i*-Pr), 2.34-2.26 (1H, m, CH_2 of cod), 2.15-2.08 (4H, m, CH_2 of cod), 1.55-1.50 (5H, m, CH of *i*-Pr and CH_2 of cod), 1.40 (3H, d, $^3J_{H-H}$= 6.8 Hz, CH_3 of *i*-Pr), 1.31 (3H, d, $^3J_{H-H}$= 6.8 Hz, CH_3 of *i*-Pr), 1.08-0.98 (9H, m, CH_3 of *i*-Pr), 0.39 (3H, d, $^3J_{H-H}$= 6.4 Hz, CH_3 of *i*-Pr). ^{13}C NMR {^{1}H} ($CDCl_3$, 100 MHz), δ: 172.8 (NCN), 161.5 (q, $^1J_{B-C}$= 51.0 Hz, BAr_F), 147.1 (quat. Ph), 144.5 (quat. Ph), 134.7 (BAr_F), 133.9 (quat. Ph), 131.0 (Ph), 129.0-128.6 (m, CF_3), 127.5 (CH of imidazole), 125.8 (quat. Ph), 124.4 (Ph), 124.0 Ph), 123.1 8quat. Ph), 120.4 (quat. Ph), 120.2 (CH of imidazole) 117.4 (BAr_F), 81.9 (CH of cod), 81.5 (CH of cod), 79.5 (quat. Cp), 76.1 (quat. Cp), 74.7 (subst. Cp), 74.6 (CH of cod), 72.1 (subst. Cp), 71.7 (Cp), 70.7 (CH of cod), 68.7 (subst. Cp), 50.1 (CH_2), 45.8 (CH of *i*-Pr), 36.1 (CH_2 of

cod), 32.4 (CH_2 of cod), 30.1 (CH_2 of cod), 28.6 (CH of *i*-Pr), 28.2 (CH of *i*-Pr), 27.9 (CH_2 of cod), 26.3 (CH_3 of *i*-Pr), 25.3 (CH_3 of *i*-Pr), 24.2 (CH_3 of *i*-Pr), 23.0 (CH_3 of *i*-Pr), 22.9 (CH_3 of *i*-Pr), 19.4 (CH_3 of *i*-Pr). HRMS (ESI) : 801.2513 (801.2517 calculated for $C_{37}H_{48}FeIrN_2S$, M-BAr_F).

[Ir(cod)(L30)]BAr_F: Yield 38 mg (25%) over 2 steps as an bright-red solid (using 0.1 mmol of **L30**H·Cl). ^{1}H NMR ($CDCl_3$, 400 MHz), δ: 7.68 (8H, s, BAr_F), 7.50 (4H, s, BAr_F), 7.00 (2H, s, Ph), 6.90 (1H, s, CH of imidazole), 6.72 (1H, s, CH of imidazole) 6.63 (1H, d, $^2J_{H-H}$= 14.9 Hz, CH_2), 4.72 (1H, d, $^2J_{H-H}$= 14.9 Hz, CH_2), 4.54-4.52 (3H, m, subst. and 2xCH of cod), 4.34-4.33 (1H, s, subst. Cp), 4.30 (5H, m, Cp), 4.23 (2H, m, subst. Cp and CH of cod), 3.57-3.56 (1H, m , CH of cod), 2.83-2.80 (1H, m, CH of *i*-Pr), 2.32-2.37 (5H, m, CH_2 of cod and CH_3 of Mes), 2.17 (3H, s, CH_3 of Mes), 2.10-2.01 (4H, m, CH_2 of cod), 1.68 (3H, s, CH_3 of Mes), 1.48-1.40 (2H, m, CH_2 of cod), 1.35 (3H, d, $^3J_{H-H}$= 6.7 Hz, CH_3 of *i*-Pr), 0.78 (3H, d, $^3J_{H-H}$= 6.7 Hz, CH_3 of *i*-Pr). ^{13}C NMR {^{1}H} ($CDCl_3$, 100 MHz), δ: 172.8 (NCN), 161.6 (q, $^1J_{B-C}$= 50.3 Hz, BAr_F), 140.1 (quat. Ph), 136.1 (quat. Ph), 134.7 (BAr_F), 134.3 (quat. Ph), 133.9 (quat. Ph), 129.3-128.6 (m, CF_3), 125.9 (Ph), 123.1 (CH of imidazole), 120.8 (CH of benzimidazole), 117.4 (BAr_F), 81.1 (CH of cod), 80.2 (quat. Cp), 80.0 (quat. Cp), 75.2 (CH of cod), 74.6 (subst. Cp), 72.1 (subst. Cp), 71.7 (Cp and CH of cod), 68.7 (subst. Cp), 50.2 (CH_2), 47.7 (CH of *i*-Pr), 35.5 (CH_2 of cod), 31.8 (CH_2 of cod), 30.5 (CH_2 of cod), 28.5 (CH_2 of cod), 24.7 (CH_3 of *i*-Pr), 21.4 (CH_3 of *i*-Pr), 20.8 (CH_3 of Mes), 18.7 (CH_3 of Mes), 17.1 (CH_3 of Mes). HRMS (ESI) : 759.2055 (759.2047 calculated for $C_{34}H_{42}FeIrN_2S$, M-BAr_F).

3.6.4.8. General procedure for the asymmetric hydrogenation

The alkene (0.5 mmol) and Ir complex (1 mol %) were dissolved in CH_2Cl_2 (2 mL) and placed in a high-pressure autoclave. The autoclave was purged 4 times with hydrogen. Then, it was pressurized at the desired pressure. After the desired reaction time, the autoclave was depressurized and the solvent evaporated off. The residue was dissolved in Et_2O (1.5 mL) and filtered through a short plug of celite. The enantiomeric excess was determined by chiral GC or chiral HPLC and conversions were determined by ^{1}H NMR.

3.6.4.9. Reactivity studies of [Ir(cod)(L)]BAr_F towards H_2

In a typical experiment hydrogen was bubbled through a CD_2Cl_2 solution of the desired [Ir(cod)(L)]BAr_F catalyst precursor (5 mmol) at 195 K for 15-30 min. The reaction mixture was analyzed by NMR spectroscopy at the desired temperature. All attempts to isolate the *cis*-dihydride iridium complexes **42**–**48** were unsuccessful even at -70 ºC under a hydrogen atmosphere.

3.6.4.10. Computational details

Geometries of isomers of [Ir(cod)(**L**)]$^+$ were optimized using the Gaussian 16 program,[19] employing the B3LYP-D3[20] density functional and the LANL2DZ[21] basis set for iridium and iron and the 6-31G* basis set for all other elements.[22] Solvation correction was applied in the course of the optimizations using the PCM model with the default parameters of dichloromethane.[23] The complexes were treated with the charge +1 and in singlet state. No symmetry constraints were applied. The energies were further refined by performing single-point calculations using the above-mentioned parameters, with the exception that the 6-311+G**[24] basis set was used for all elements except iridium and iron. All energies reported are Gibbs free energies at 203.15 K

3.6.5. References

[1] Reviews about chiral ferrocenyl ligands in asymmetric catalysis: (a) Drusan, M.; Šebesta, R. Enantioselective C–C and C–heteroatom bond forming reactions using chiral ferrocene catalysts. *Tetrahedron* **2014**, *70*, 759–785. (b) Arrayás, R. G.; Adrio, J.; Carretero, J. C. Recent Applications of Chiral Ferrocene Ligands in Asymmetric Catalysis. *Angew. Chem. Int. Ed.* **2006**, *45*, 7674–7715. (c) Atkinson, R. C. J.; Gibson, V. C.; Long, N. J. The syntheses and catalytic applications of unsymmetrical ferroceneligands. *Chem. Soc. Rev.* **2004**, 33, 313–328. d) Colacot, T. J. A Concise update on the applications of chiral ferrocenyl phosphines in homogeneous catalysis leading to organic synthesis. *Chem. Rev.* **2003**, *103*, 3101–3118. (e) Cunningham, L. Benson, A.; Guiry, P. J. Recent developments in the synthesis andapplications of chiral ferrocene ligands and organocatalysts in asymmetric catalysis. *Org. Biomol. Chem.* **2020**, *18*, 9329–9370.

[2] See recent reviews: a) Fliedel C.; Labande, A.; Manoury, E.; Poli, R. Chiral N–heterocyclic carbene ligands with additional chelating group(s) applied to homogeneous metal–mediated asymmetric catalysis. *Coord. Chem. Rev.* **2019**, *394*, 65–103. b) Yoshida, K.; Yasue, R. Planar–Chiral Ferrocene–Based N–Heterocyclic Carbene Ligands. *Chem. Eur. J.* **2018**, *24*, 18575–18586.

[3] (a) Smilović, I. G.; Casas-Arcé, E.; Roseblade, S. J.; Nettekoven, U.; Zanotti-Gerosa, A.; Kovačevič, M.; Časar, Z. Iridium–catalyzed chemoselective and enantioselective hydrogenation of (1–chloro–1–alkenyl) boronic esters. *Angew. Chem. Int. Ed.* **2012**, *51*, 1014–1018. (b) Co, T. T.; Kim, T.–J. Chiral (iminophosphoranyl)ferrocenes: highly efficient ligands for rhodium– and iridium–catalyzed enantioselective hydrogenation of unfunctionalized olefins. *Chem. Commun.* **2006**, 3537–3539. (c) Gschwend, B.; Pugin, B.; Bertogg, A.; Pfaltz, A. P–Chiral Ferrocenephospholanes: Synthesis, Reactivity, Metal Complex Chemistry and Application in the Asymmetric Hydrogenation of Olefins. *Chem. Eur. J.* **2009**, *15*, 12993. (d) Metallinos, C.; Van Belle, L. Asymmetric hydrogenation of alkenes with planar chiral 2–phosphino–1–aminoferrocene–iridium(I) complexes. *J. Organomet. Chem.* **2011**, *696*, 141–149. (e) Li, X.; Li, Q.; Wu, X.; Gao, Y.; Xu, D.; Kong, L. Enantioselective hydrogenation of olefins with planar chiral iridium ferrocenyloxazolinylphosphine complexes. *Tetrahedron: Asymmetry* **2007**, *18*, 629–634. f) Biosca, M.; Coll, M.; Lagarde, F.; Brémond, E.; Routaboul, L.; Manoury, E.; Pàmies, O.; Poli, R.; Diéguez, M. Chiral ferrocene–based P,S ligands for Ir–catalyzed hydrogenation of minimally functionalized olefins. Scope and limitations. *Tetrahedron* **2016**, *72*, 2623–2631.

[4] Seo, H.; Park, H.–J.; Kim, B.Y.; Lee, J.H.; Son, S.U.; Chung, Y.K. Synthesis of P– and S–Functionalized Chiral Imidazolium Salts and Their Rh and Ir Complexes. *Organometallics* **2003**, *22*, 618–620.

[5] De La Cruz–Sánchez, P.; Faiges, J.; Mazloomi, Z.; Borràs, C.; Biosca, M.; Pàmies, O.; Diéguez, M. Ir/Thioether−Carbene, −Phosphinite, and −Phosphite Complexes for Asymmetric Hydrogenation. A Case for Comparison. *Organometallics* **2019**, *38*, 4193–4205.

[6] Honeychuck, R.-V.; Okoroafor, M.-O.; Shen, L.-H.; Brubaker Jr., C.-H. New ferrocenyl thio- and selenoether ligands. Preparation, characterization, and their palladium(II) complexes as catalysts for selective hydrogenation and Grignard cross-coupling. *Organometallics*, **1986**, *5*, 482-490.

[7] Xiao, L. A Practicable Synthesis of Enantiopure 2-Aminomethyl-1-bromo- and 2-Aminomethyl-1-iodoferrocenes. *Synthesis* **1999**, *8*, 1354-1362.

[8] (a) Merabet-Khelassi, M.; Aribi-Zouioueche, L.; Riant, O. Green methodology for enzymatic hydrolysis of acetates in non-aqueous media via carbonate salts. *Tetrahedron: Asymmetry*, **2008**, *19*, 2378-2384. (b) Anderson, J.-C.; Osborne, J. The synthesis of new planar chiral heterobidentate chelate ligands for asymmetric catalysis. *Tetrahedron: Asymmetry*, **2005**, *16*, 931-934.

[9] Lambusta, D.; Nicolosi, G.; Patti, A.; Piatelli, M. Lipase-mediated resolution of racemic 2-hydroxymethyl-1-methylthioferrocene. *Tetrahedron Lett.* **1996**, *37*, 127-130.

[10] (a) Speybrouck, D.; Lipka, E. Preparative supercritical fluid chromatography: A powerful tool for chiral separations. *J. Chromatog. A*, **2016**, *1467*, 33–55. (b) Gumustas, M.; Ozkan, S. A.; Chankvetadze, B. Analytical and Preparative Scale Separation of Enantiomers of Chiral Drugs by Chromatography and Related Methods. *Curr. Med. Chem.* **2018**, *25*, 4152-4188.

[11] Labande, A.; Daran, J.-C.; Manoury E.; Poli, R. New (1-Phosphanylferrocen-1'- and -2-yl)methyl-Linked Diaminocarbene Ligands: Synthesis and Rhodium(I) Complexes. *Eur. J. Inorg. Chem*. **2007**, *9*, 1205–1209.

[12] (a) Cui, X.; Burgess, K. Catalytic Homogeneous Asymmetric Hydrogenations of Largely Unfunctionalized Alkenes. *Chem. Rev.* **2005**, *105*, 3272– 3296. (b) Roseblade, S. J.; Pfaltz, A. Iridium-Catalyzed Asymmetric Hydrogenation of Olefins. *Acc. Chem. Res.* **2007**, *40*, 1402–1411. (c) Woodmansee, D. H.; Pfaltz, A. Asymmetric Hydrogenation of Alkenes Lacking Coordinating Groups. *Chem. Commun.* **2011**, *47*, 7912–7916. (d) Zhu, Y.; Burgess, K. Filling gaps in asymmetric hydrogenation methods for acyclic stereocontrol: application to chirons for polyketide-derived natural products. *Acc. Chem. Res.* **2012**, *45*, 1623–1636. (e) Verendel, J. J.; Pàmies, O.; Diéguez, M.; Andersson, P. G. Asymmetric Hydrogenation of Olefins Using Chiral Crabtree-type Catalysts: Scope and Limitations. *Chem. Rev.* **2014**, *114*, 2130– 2169. (f) Margarita, C.; Andersson, P. G. Evolution and Prospects of the Asymmetric Hydrogenation of Unfunctionalized Olefins. *J. Am. Chem. Soc.* **2017**, *139*, 1346– 1356. (g) Pàmies, O.; Zheng, J.; Faiges, J.; Andersson, P. G. Asymmetric hydrogenation of unfunctionalized olefins or with poorly coordinative groups. *Adv. Catal.* **2021**, *68*, 135–203.

[13] (a) Powell, M. T.; Hou, D.–R.; Perry, M. C.; Cui, X.; Burgess, K. Chiral imidazolylidine ligands for asymmetric hydrogenation of aryl alkenes. *J. Am. Chem. Soc.* **2001**, *123*, 8878–8879. (b) Bolm, C.; Focken, T.; Raabe, G. Synthesis of iridium complexes with novel planar chiral chelating imidazolylidene ligands. *Tetrahedron: Asymmetry* **2003**, *14*, 1733–1746. (c) Källström, K.; Andersson, P. G. Asymmetric Hydrogenation of Tri–substituted Alkenes with Ir–NHC–thiazole Complexes. *Tetrahedron Lett.* **2006**, *47*, 7477–7480. (d) Nanchen, S.; Pfaltz, A. Synthesis and application of chiral N-heterocyclic carbene–oxazoline ligands: iridium-catalyzed enantioselective hydrogenation. *Chem. Eur. J.* **2006**, *12*, 4550–4558. (e) Khumsubdee, S.; Fan, Y.; Burgess, K. A Comparison between oxazoline–imidazolinylidene, –imidazolylidine, –benzimidazolylidene

hydrogenation catalysts. *J. Org. Chem.* **2013**, *78*, 9969–9974. (f) Schumacher, A.; Bernasconi, M.; Pfaltz, A. Chiral N-ħHeterocyclic carbene/pyridine ligands for the iridium-catalyzed asymmetric hydrogenation of olefins. *Angew. Chem. Int. Ed.* **2013**, *52*, 7422–7425.

[14] The stereochemical description of the different dihydrido species is based on the location of the S–C ligands at the back of the octahedral.

[15] Warsink, S.; Venter, J.-A.; Roodt, A. NHC-amide donor ligands in rhodium complexes: Syntheses and characterisation. *J. Organomet. Chem.* **2015**, *775*, 195-201.

[16] Perry, M. C.; Cui, X.; Powell, M. T.; Hou, D.–R.; Reibenspies, J. H.; Burgess, K. Optically active iridium imidazol–2–ylidene–oxazoline complexes: preparation and use in asymmetric hydrogenation of arylalkenes. *J. Am. Chem. Soc.* **2003**, *125*, 113–123.

[17] Taipale, E.; Seipmann, M.; Truong, K.-N.; Rissanen, K. Iodine(I) and Silver(I) Complexes of Benzoimidazole and Pyridylcarbazole Derivatives. *Chem. Eur. J.* **2021**, *69*, 17412-17419

[18] Touj, N.; Özdemir, I.; Yasar, S.; Hamdi N. An efficient (NHC) Copper (I)-catalyst for azide–alkyne cycloaddition reactions for the synthesis of 1,2,3-trisubstituted triazoles: Click chemistry. *Inorganica Chim. Acta*, **2017**, *467*, 21-32.

[19] Gaussian 16, Revision C.01, Frisch, M. J.; Trucks, G. W.; Schlegel, H. B.; Scuseria, G. E.; Robb, M. A.; Cheeseman, J. R.; Scalmani, G.; Barone, V.; Petersson, G. A.; Nakatsuji, H.; Li, X.; Caricato, M.; Marenich, A. V.; Bloino, J.; Janesko, B. G.; Gomperts, R.; Mennucci, B.; Hratchian, H. P.; Ortiz, J. V.; Izmaylov, A. F.; Sonnenberg, J. L.; Williams-Young, D.; Ding, F.; Lipparini, F.; Egidi, F.; Goings, J.; Peng, B.; Petrone, A.; Henderson, T.; Ranasinghe, D.; Zakrzewski, V. G.; Gao, J.; Rega, N.; Zheng, G.; Liang, W.; Hada, M.; Ehara, M.; Toyota, K.; Fukuda, R.; Hasegawa, J.; Ishida, M.; Nakajima, T.; Honda, Y.; Kitao, O.; Nakai, H.; Vreven, T.; Throssell, K.; Montgomery, J. A., Jr.; Peralta, J. E.; Ogliaro, F.; Bearpark, M. J.; Heyd, J. J.; Brothers, E. N.; Kudin, K. N.; Staroverov, V. N.; Keith, T. A.; Kobayashi, R.; Normand, J.; Raghavachari, K.; Rendell, A. P.; Burant, J. C.; Iyengar, S. S.; Tomasi, J.; Cossi, M.; Millam, J. M.; Klene, M.; Adamo, C.; Cammi, R.; Ochterski, J. W.; Martin, R. L.; Morokuma, K.; Farkas, O.; Foresman, J. B.; Fox, D. J. Gaussian, Inc., Wallingford CT, 2016.

[20] (a) Grimme, S.; Ehrlich, S.; Goerigk, L. Effect of the damping function in dispersion corrected density functional theory. *J. Comput. Chem.* **2011**, *32*, 1456–1465. (b) Lee, C.; Yang, W.; Parr, R. G. Development of the Colle–Salvetti correlation–energy formula into a functional of the electron density. *Phys. Rev. B* **1988**, *37*, 785–789. (c) Becke, A. D. Density–functional thermochemistry. III. The role of exact Exchange. *J. Chem. Phys.* **1993**, *98*, 5648−5652. (d) Grimme, S.; Antony, J.; Ehrlich, S.; Krieg, H. A consistent and accurate ab initio parametrization of density functional dispersion correction (DFT-D) for the 94 elements H-Pu. *J. Chem. Phys.* **2010**, *132*, 154104.

[21]Hay, P. J.; Wadt, W. R. Ab initio effective core potentials for molecular calculations. Potentials for K to Au including the outermost core orbitals. *J. Chem. Phys.* **1985**, *82*, 299–310.

[22](a) Hehre, W. J.; Ditchfeld, R.; Pople, J. A. Self—consistent molecular orbital methods. xii. further extensions of gaussian—type basis sets for use in molecular orbital studies of organic molecules. *J. Chem. Phys.* **1972**, *56*, 2257–2261. (b) Hariharan, P. C.; Pople, J. A. The influence of polarization functions on molecular orbital hydrogenation energies. *Theor. Chim. Acta* **1973**, *28*, 213–222. (c) Francl, M. M.; Pietro, W. J.; Hehre W. J.; Binkley, J. S.; Gordon, M. S.; Defrees, D. J.; Pople, J. A. Self-consistent molecular orbital methods. XXIII. A polarization-type basis set for second-row elements. *J. Chem. Phys.* **1982**, *77*, 3654–3665.

[23] (a) Miertus, S.; Tomasi, J. Approximate evaluations of the electrostatic free energy and internal energy changes in solution processes. *Chem. Phys.* **1982**, *65*, 239−245. (b) Mennucci, B.; Tomasi, J. Continuum solvation models: A new approach to the problem of solute's charge distribution and

cavity boundaries. *J. Chem. Phys.* **1997**, *106*, 5151−5158. (c) Cossi, M.; Barone, V.; Mennucci, B.; Tomasi, J. Ab initio study of ionic solutions by a polarizable continuum dielectric model. *Chem. Phys. Lett.* **1998**, *286*, 253−260.

[24] (a) Krishnan, R.; Binkley, J. S.; Seeger, R.; Pople, J. A. Self−consistent molecular orbital methods. XX. A basis set for correlated wave functions. *J. Chem. Phys.* **1980**, *72*, 650−654. (b) McLean, A. D.; Chandler, G. S. Contracted Gaussian basis sets for molecular calculations. I. Second row atoms, *Z*=11−18. *J. Chem. Phys.* **1980**, *72*, 5639−5648.

UNIVERSITAT ROVIRA I VIRGILI
DEVELOPMENT OF CHIRAL METAL-CATALYSTS FOR THE SELECTIVE FORMATION OF C-H, C-C AND C-X BONDS. FROM DESIGN TO APPLICATION
Pol De La Cruz Sanchez Badia

CHAPTER 4

Pd-catalyzed asymmetric allylic substitution

UNIVERSITAT ROVIRA I VIRGILI
DEVELOPMENT OF CHIRAL METAL-CATALYSTS FOR THE SELECTIVE FORMATION OF C-H, C-C AND C-X BONDS. FROM DESIGN TO APPLICATION
Pol De La Cruz Sanchez Badia

4.1. Pd-catalyzed asymmetric allylic substitution using a methylene linked phosphite-oxazoline PHOX-based ligands

4.1.1. Introduction

Due to its mild reaction conditions, high functional group tolerance and the versatility of the alkene group for further functionalization, Pd-catalyzed asymmetric allylic substitution is an efficient tool for the formation of chiral C-C and C-heteroatom bonds with applications in the synthesis of enantiomerically pure relevant compounds.[1] To fully exploit their application in total synthesis there is a constant need to expand the range of substrate and nucleophiles. Over the last decades a great number of ligands have been successfully applied for this transformation.[1] However, catalysts are hardly suitable for a wide combination of substrates and nucleophiles. In addition, most catalysts still have a pronounced substrate specificity, with sterically hindered substrates requiring different ligands than unhindered substrates.[1] To reduce time-consuming ligand design synthesis, catalysts with wide substrate and nucleophile scope are desired. As comented in the introduction, the first breakthrough in ligand design was introduced by Trost with the development of diphosphine ligands, such as (*R*,*R*)-Ph-DACH, with a large bite angle which creates a more confined chiral cavity (Figure 4.1.1).[2] The stereoselectivity comes from an interplay between steric interactions imposed by the chiral cavity of the ligand and the H-bond and the electrostatic interactions of the amide groups with the nucleophile.[3] Trost ligands represent one of the most effective ligand families and are the ligands of choice for unhindered substrates, being the most widespread applied in total synthesis.[1,4] Another relevant breakthrough arrived with the application of the heterodonor phosphine-oxazoline PHOX ligands (Figure 4.1.1), whose application complemented the Trost ligands, providing high enantioselectivities with hindered substrates and low with narrow ones.[5] The stereoselectivity is based on the *trans* influence of the two donor groups that favors the nucleophilic attack predominantly trans to the donor group with the strongest trans influence. These facts, together with the excellent performance of PHOX ligands in other asymmetric unrelated catalytic reactions, have made them belong to the selected list of "privileged ligands".[6]

Inspired by the PHOX ligands, heterodonor bidentated P,N- and P,X-ligands (X= P' and S) have found a prominent position in the field of Pd-catalyzed asymmetric allylic substitution, with the development of many new families that have provided remarkable results.[1,7,8] In this respect, our group has taken advantage of the adaptability of biaryl phosphite-based ligands to overcome the substrate specificity and low nucleophile scope of the Pd-catalyzed asymmetric allylic substitution.[9] We found that the common substrate limitation of the phosphine-oxazoline PHOX-ligands **2** could be overcome by replacing the phosphine moiety by a biaryl phosphite group.[10] By introducing this group,

the catalyst can adapt to each substrate and the substrate scope has been significantly broadened. Therefore, and in contrast to the parent PHOX ligands , phosphite-oxazoline ligands **9** (Figure 4.1.1) show a wide substrate scope, providing high enantioselectivities for hindered and unhindered substrates, with a large variety of C, N and O-nucleophiles.[10] In addition, the acceptor capacity of the phosphite functionality had a positive effect on activity, inducing much higher TOF than the most common ligands. Since then, our group has developed other biaryl phosphite containing ligands, by modifying either the ligand backbone or by replacing the oxazoline by other N-donor groups[8i,k,l,m,n] (i.e. oxazole, pyridine, etc) and S-groups [8j, 8o,11] with remarkable results. Among them, they are to highlight the phosphite-oxazoline ligands **10**,[8p] where the *ortho*-phenylene tether of PHOX and of ligands **9** has been replaced by an alkyl backbone chain. Their Pd-catalysts provided enantioselectivities up to 99% in the allylic substitution of a wide range of substrate types and C, N and O-nucleophiles, even the challenging monosubstituted ones.

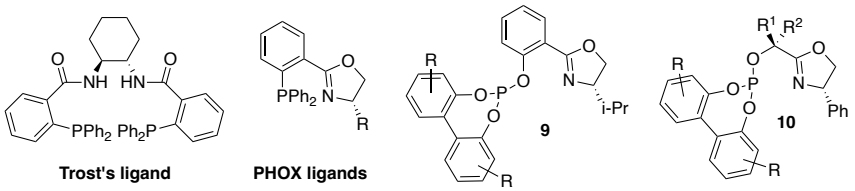

Figure 4.1.1. (*R*,*R*)-Ph-DACH Trost's ligand, phosphine-oxazoline PHOX ligands, phosphite-oxazoline based PHOX ligands **9** and phosphite-oxazoline ligands **10**.

Combining the advantages of the biaryl phosphite groups and the backbone's structure of PHOX ligands, we have recently designed a set of phosphite–oxazoline ligands **L1**–**L3a**–**c** with a methylene spacer between the oxazoline ring and the phenyl ring (Figure 4.1.2), that were applied in two different asymmetric transformation (hydrogenation and intermolecular Heck reactions) extending the range of substrates and triflate sources successfully used.[12] In this report, we studied these ligands in the Pd–catalyzed allylic substitution reaction to further investigate the possibilities of easily to synthetize phosphite-analogues of PHOX-type ligands in Pd-catalyzed asymmetric allylic substitution reactions. By tuning the ligand parameters, we have been able to achieve high enantioselectivities for a variety of substrates and nucleophiles (35 compounds in total). We have also performed DFT and NMR studies to gain further insight into the selectivity-determining step.

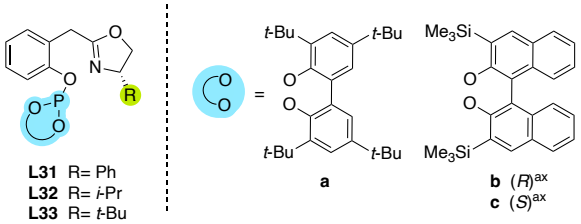

Figure 4.1.2. Phosphite-oxazoline ligands **L1**–**L3a**–**c** tested in this study.

4.1.2. Results and discussion

4.1.2.1. Initial screening. Allylic substitution of two disubstituted substrates with different steric requirement using dimethyl malonate

The usefulness of ligands **L31**–**L33a**–**c** in Pd-catalyzed asymmetric allylic substitution was first studied in the alkylation of two substrates with distinct steric properties, the benchmark lineal substrate *rac*-1,3-diphenyl-3-acetoxyprop-1-ene **S150** and the more challenging cyclic *rac*-3-acetoxycyclohexene **S151**. For comparison, we applied the same reaction conditions found in our previous studies with analogous Pd/**9** catalytic system, using dimethyl malonate as nucleophile (Table 4.1.1).[10b,13] Positively, high activities (TOF's up to >4000 mol substrate×(mol Pd×h)$^{-1}$) and enantioselectivities (ee's up to 96%) in both substrate types were obtained by selecting the right combination of oxazoline substituent and phosphite group. Concretely, the results showed that enantioselectivity depended on the biaryl phosphite group (**a**–**c**). For both substrates, ligands with an enantiopure (*S*)-biaryl phosphite functionality yielded the highest enantioselectivities (entries 3, 6 and 9 vs 1-2, 4-5 and 7-8, respectively). However, the effect of the oxazoline substituent is different for both substrates. While for substrate **S150** the oxazoline group has little effect on enantioselectivity, being somewhat best with Ph or *i*-Pr oxazoline substituents (entries 3 and 6, ee's up to 96%), for the small unhindered substrate **S151**, a bulkier *t*-Bu group was needed to maximize enantioselectivity (entry 9, ee's up to 86%). These results contrast with the parent phosphite-oxazoline ligands **9**, where for both type of substrates the oxazoline substituent has not effect on the achieved enantioselectivity. The consequence of introducing a methylene spacer between the oxazoline ring and the phenyl ring of ligands **9** is that the new catalytic system is not flexible enough to adjust the size of the chiral pocket to the steric demands of the substrate. There is a complex interplay between the biaryl phosphite moiety and the nature of the oxazoline substituent that determines the enantioselectivity for each substrate type. Thus, while the best enantioselectivity for hindered linear substrate **S150** is obtained with **L32c**, , for the cyclic substrate **S151** the use of **L33c** afforded the highest enantioselectivity.

In addition, the effect of the biaryl phosphite moiety on the catalytic performance is more pronounced in the cyclic substrate than in the linear one. Thus, while for **S150** the enantioselectivity varied from 82% (*S*) to 96% (*S*) by changing the configuration of the biaryl group due to a match/mismatch situation, for **S151** there was also an inversion in the configuration of the alkylation product (i.e. entries 8 vs 9).

Table 4.1.1. Pd-catalyzed asymmetric allylic alkylation of **S150**–**S151** with ligands **L31**–**L33a**–**c**.[a]

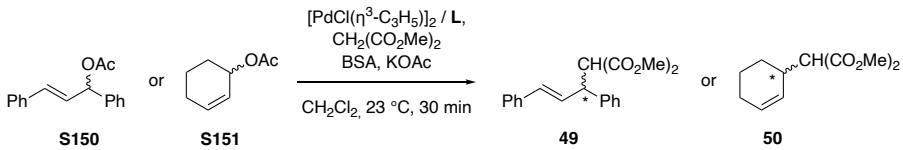

S150 **S151** **49** **50**

		49		**50**	
Entry	Ligand	%Conv[b]	% ee[c]	%Conv[b]	% ee[c]
1	**L31a**	100	92 (*S*)	100	60 (*R*)
2	**L31b**	100	86 (*S*)	100	51 (*R*)
3	**L31c**	100	95 (*S*)	100	66 (*S*)
4	**L32a**	100	89 (*S*)	100	40 (*R*)
5	**L32b**	100	82 (*S*)	100	30 (*R*)
6	**L32c**	100[d]	96 (*S*)[d]	100	48 (*S*)
7	**L33a**	100	73 (*S*)	100	30 (*R*)
8	**L33b**	100	72 (*S*)	100	80 (*R*)
9	**L33c**	100	92 (*S*)	100	86 (*S*)
10	**9**	100	>99 (*S*)[e]	100	99 (*S*)[e]
11	**10**	100	99 (*S*)[f]	100	99 (*S*)[f]

[a] 0.5 mol% $[PdCl(\eta^3\text{-}C_3H_5)]_2$, ligand (0.011 mmol), substrate (1 mmol), CH_2Cl_2 (2 mL), *N,O*-bis(trimethylsilyl)acetamide (BSA; 3 eq), dimethyl malonate (3 equiv), KOAc (3 mol%) at 23 °C. [b] Conversion percentage determined by ^{1}H-NMR spectroscopy after 30 min. [c] Enantiomeric excesses determined by HPLC or GC. Absolute configuration drawn in parentheses. [d] Reactions carried for 10 min using 0.1 mol% of catalyst precursor. TOF= 4048 mol **S150**×(mol Pd×h)$^{-1}$ measured after 5 min (68% conversion). [e] Data from ref. 10b. [f] Data from ref. 8p.

4.1.2.2. Scope and limitations. Allylic substitution of different disubstituted substrates with a range of C-, N- and O-nucleophiles

We next investigated the scope of Pd/**L31**–**L33a**–**c** catalytic systems with other C-nucleophiles and with N- and O-nucleophiles, as well as testing linear and cyclic substrates with different steric and electronic requirements. We initially considered the allylic substitution of the benchmark **S150** substrate with a range of C-, N- and O-nucleophiles, including the more challenging functionalized malonates and alkyl alcohols (Figure 4.1.3). Positively several malonates, even those substituted with propargyl-, pentenyl-, butenyl-, and allyl groups, reacted with **S150** to offer products **51**, **52**, **54**–**58** in high yields and enantioselectivities up to 99%, even higher in some cases than those achieved with dimethyl malonate. These are important results since products **54**–

57 are key building blocks for the synthesis of fine molecules.[8o,14] The reaction also performed well (ee's up to 96%) when the nucleophiles were acetylacetone (compound **53**) and malononitrile (compound **59**). As in previous publications the use of isopropyl cyanoacetate as nucleophile (compound **60**) give the formation of two diastereoisomers with low diastereoselectivity,[15] although both diastereoisomers were reached in high enantioselectivities (ee's up to 99%).

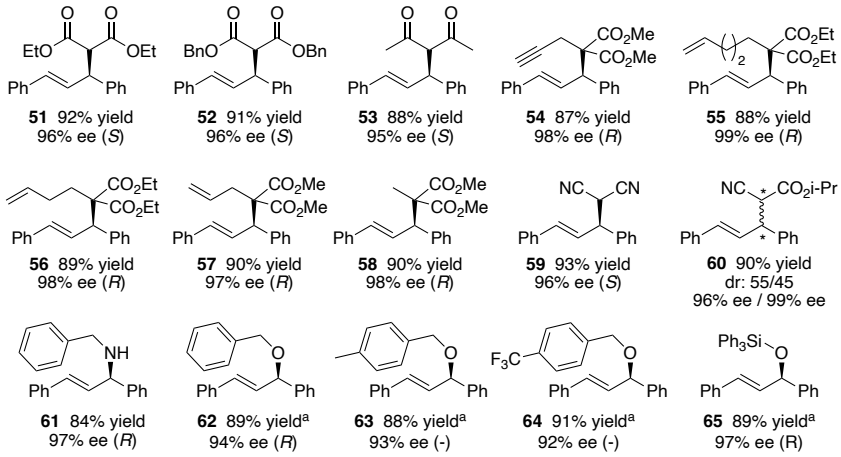

Figure 4.1.3. Pd-catalyzed allylic substitution of **S150** with Pd/**L32c** catalyst precursor using a range of C-, N- and O-nucleophiles. Reactions preformed in CH_2Cl_2 at 23 °C with $[PdCl(\eta^3\text{-}C_3H_5)]_2$ (0.5 mol %), ligand (1.1 mol %), BSA (3 equiv) and KOAc (3 mol%). Full conversions in 2 h. [a] Reactions carried out with 2 mol% $[PdCl(\eta^3\text{-}C_3H_5)]_2$, 4 mol% ligand and Cs_2CO_3 (3 equiv). Full conversions in 18 h.

Enantiocontrol was also high when benzylamine was used as an example of N-nucleophile (compound **61**, 97% ee). Interestingly, enantioselectivities as high as those with dimethyl malonate were also found in the addition of several aliphatic alcohols and silanols (compounds **62**–**65**, ee's up to 97%). Aliphatic alcohols are another relevant set of nucleophiles whose resulting chiral ethers are found in biologically active targets.[16] Despite the extensive research dedicate to the addition of aliphatic alcohols very few effective catalysts exist whose enantioselectivities largely depends on the type of alcohol and its electronic properties. [17] Thus, for example with Pd/**9** system the enantioselectivity dropped considerable when electron rich benzylic alcohols were used.[10] The reversed behavior was found with other Pd-catalysts.[17c,8p] Gratifyingly, the application of Pd/**L2c** in the etherification of **S150** with three aliphatic alcohols differing in their electronic properties, furnished the desired products in yields and enantioselectivities comparable to the best one reported so far. This represents an improvement regarding to the previously reported phosphite-based PHOX-ligands **9** and phosphite-oxazoline ligands **10**. High enantioselectivity were also reached with the triphenylsilanol as nucleophile (ee's up to 97%). As in previous publications a higher

amount of Pd/L was required to achieve full conversions, due to the lower nucleophilicity of the aliphatic alcohols.

The results collected in Scheme 4.1.1 showed that Pd/**L32c** can also be successfully used for the alkylation of other symmetrical linear substrates **S152**–**S156** with steric and electronic requirements different from those of **S150**. High yields and enantioselectivities were therefore attained with a range of malonates including those substituted with propargyl, pentenyl and allyl groups (compounds **66**–**73**, ee's from 96% to 99%). Among these results, to highlight that Pd/**L32c** is also able to adapt its chiral cavity to highly sterically demanding substrates such as **S155** and **S156** (compounds **72** and **73**, ee's up to 99%).

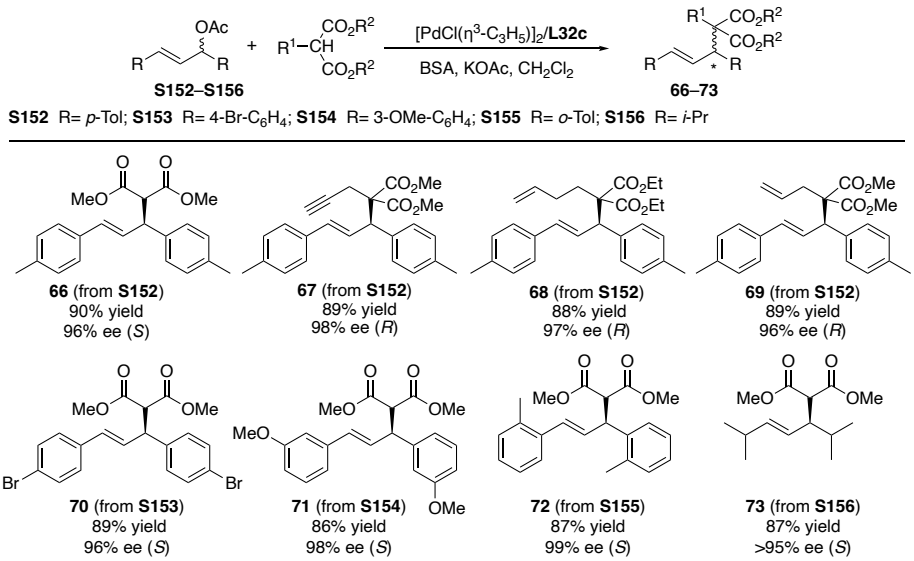

Scheme 4.1.1. Pd-catalyzed allylic substitution of **S152**–**S156** with C-nucleophiles using Pd/**L32c** catalytic system. Reactions were run at 23 °C with $[PdCl(\eta^3\text{-}C_3H_5)]_2$ (0.5 mol %), CH_2Cl_2 as solvent, ligand (1.1 mol %), BSA (3 equiv), and KOAc (3 equiv). Full conversions were achieved after 4 h.

We then studied the allylic substitution of cyclic substrate **S151** with more challenging nucleophiles than dimethyl malonate. We performed these studies with Pd/**L33c** catalytic system that provided the best results in the alkylation of **S151**. A wide range of C-nucleophiles, including acetylacetone and the less studied α-substituted malonates with propargyl, allyl and methyl groups, can react with **S151** to provide the desired corresponding compounds (**74**–**79**, Scheme 4.1.2) in high yields and enantioselectivities (ee's up to 92%), comparable to those achieved in the alkylation of **S151** with dimethyl malonate. Positively, Pd/**L33c** could also adjust its chiral pocket to cyclic substrates with higher (substrate **S157**) or lower (**S158**) ring sizes than **S151** (compounds **80**–**83**, ee's up to 94%), even using propargyl malonate as nucleophile.

As for the cyclic substrate **S2**, for **S8** and **S9** there is an inversion of the configuration of the final product by using ligand **L33b**, with opposite configuration of the biaryl phosphite moiety (see Suporting Inofrmation, S.I.4.1.3).

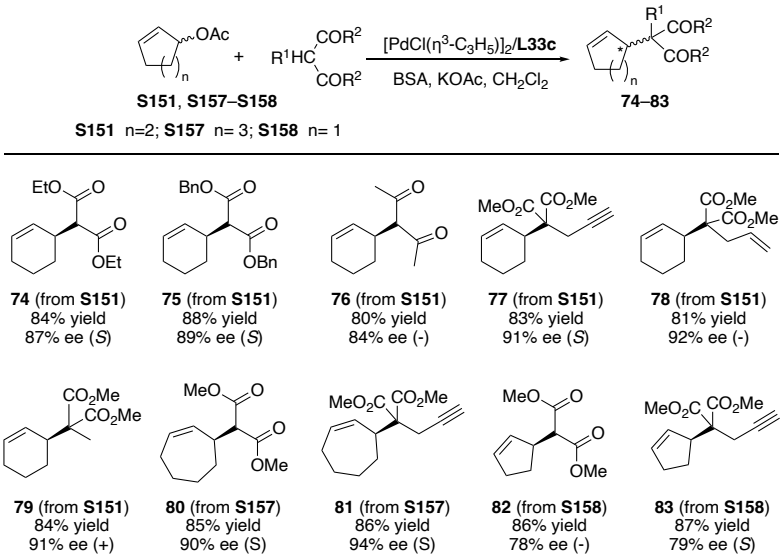

Scheme 4.1.2. Pd-catalyzed allylic alkylation of **S151**, **S157**–**S158** with the Pd/**L33c** catalyst precursor. Reactions were run at 23 °C with $[PdCl(\eta^3\text{-}C_3H_5)]_2$ (0.5 mol %), CH_2Cl_2 as solvent, ligand (1.1 mol %), BSA (3 equiv), and KOAc (3 equiv). Full conversions were achieved after 2 h.

4.1.2.3. Mechanistic studies. Origin of enantioselectivity

To better understand the effect of the ligand parameters on the enantioselectivities reached, we first performed a DFT study of the species involved in the nucleophilic attack, which is the enantiodetermining step. The transition state (TS) for this step, however, can be either early or late depending on the nucleophile, reaction conditions and ligands. In an early transition state, the enantioselectivity is controlled by both, the population of the Pd-η^3-allyl intermediates and the relative electrophilicity of the allylic carbon atoms, with an allyl terminus *trans* to a phosphorus atom being more reactive than one *trans* to a nitrogen in accordance with the stronger *trans* influence of the P atom.[18] For a late transition state the enantioselectivity is controlled by the Pd-olefin complex.[19]

The experimental catalytic results achieved with linear substrates show that the ligand parameter with the greatest effect on enantioselectivity is the chiral axis of the biaryl phosphite moiety. We therefore calculated the relative stability of the TSs and the Pd−olefin intermediates with the benchmark substrate **S150** with ligands **L32b** and **L32c** that differ only in the configuration of the biaryl phosphite moiety (Table 4.1.2).[20]

To accelerate the DFT calculations we used ammonia as nucleophile that also avoid the problems related to charge separation together with a continuum solvent model.[3,21] Note that the use of ammonia as nucleophile instead of dimethyl malonate results in the inversion of the CIP descriptor, due to the change in priority of the groups, although the sense of stereoselectivity is maintained. The results of most stable TSs ($TS_{exo\ (R)}$ and $TS_{endo\ (S)}$) and the most stable Pd−olefin complexes ($Pd–olefin_{exo(R)}$ and $Pd–olefin_{endo(S)}$) leading to the formation of both product enantiomers are shown in Table 4.1.2 (for the full set of calculated TSs and Pd−olefin complexes see Supporting Information). The difference of energy of the calculated TSs with ligand **L32c** was higher ($\Delta G^{\ddagger}$= 5.9 kJ/mol; ee_{calc}= 83% (*R*)) than with **L32b** (ΔG= 4.2 kJ/mol; ee_{calc}= 69% (*R*)), which match with the higher enantioselectivities found experimentally with **L32c**.

Table 4.1.2. Schematic representation and relative free energies in solution of the most stable *exo*- and *endo*-transition states (in kJ/mol) (left) and of the most stable Pd−olefin complexes (right) for substrate **S150** with ammonia and ligands **L32b** and **L32c**.

Pd-TS		Pd-olefin	
L32b	**L32c**	**L32b**	**L32c**
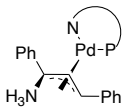 $TS_{exo(R)}$ 0 kJ/mol	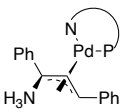 $TS_{exo(R)}$ 0 kJ/mol	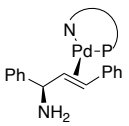 $Pd\text{-}olefin_{exo(R)}$ 0 kJ/mol	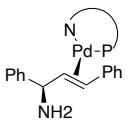 $Pd\text{-}olefin_{exo(R)}$ 0 kJ/mol
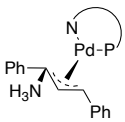 $TS_{endo(S)}$ 4.2 kJ/mol	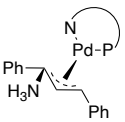 $TS_{endo(S)}$ 5.9 kJ/mol	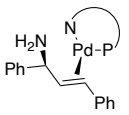 $Pd\text{-}olefin_{endo(S)}$ 19.3 kJ/mol	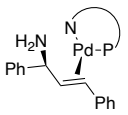 $Pd\text{-}olefin_{endo(S)}$ 3.1 kJ/mol

Moreover, the DFT correctly predicts the formation of the correct product enantiomer for both ligands. On the contrary, the predicted enantioselectivity of the Pd−olefin intermediates do not match with the experimental results. Although the calculations predict the formation of the correct product enantiomer for both ligands, a larger energy difference was found for the two Pd−olefin complexes with **L32b** (ΔG= 19.3 kJ/mol; ee_{calc}> 99% (*R*)) than for the two olefin complexes with **L32c** (ΔG= 3.1 kJ/mol; ee_{calc}= 55% (*R*)). According to these values, **L32b** should provide a higher enantioselectivity than **L32c**, which does not agree with the enantioselectivities achieved experimentally.

In order to further support the DFT calculations, we prepared Pd-allyl complex **40** by reaction of the 1,3-diphenyl ally Pd chloride dimer with two equivalents of ligand **L32c**, followed by counterion exchange with $AgBF_4$ (Scheme 4.1.3).

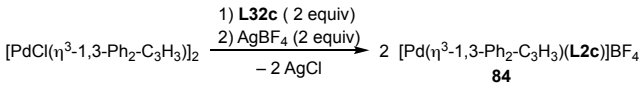

Scheme 4.1.3. Synthesis of [Pd(η^3-1,3-Ph$_2$-C$_3$H$_3$-C$_6$H$_9$)(L)]BF$_4$ complex **84**

The VT-NMR study showed a mixture of two isomers in equilibrium at a ca 4:1 ratio. As expected, NOE interactions indicated that these isomers corresponded to the *syn*/*syn* *exo* and *endo* intermediates, respectively (Scheme 4.1.4a). Thus, for both isomers there is a NOE interaction between the two terminal protons of the allyl group in agreement with a *syn/syn* disposition (Scheme 4.1.4b). In addition, for the major *exo* isomer there is an indicative NOE interaction between the terminal allylic proton *trans* to the P-moiety and the protons of one of the trimethylsilyl groups of the phosphite functionality that it is not present for the *endo* intermediate (Scheme 4.1.4b). The $^{13}C\{^1H\}$ NMR shifts of both isomers revealed that the most electrophilic allylic terminal carbons are found *trans* to the P-group. They also revealed that the terminal allylic carbon *trans* to P in the *exo* isomer is more electrophilic than the corresponding carbon for the *endo* isomer ($\Delta\delta(^{13}C)$ = 6.5 ppm). This indicates that the major *exo* isomer should react faster than the minor *endo* isomer, which is in line with the conclusions of the DFT calculations.[8k, 8n]

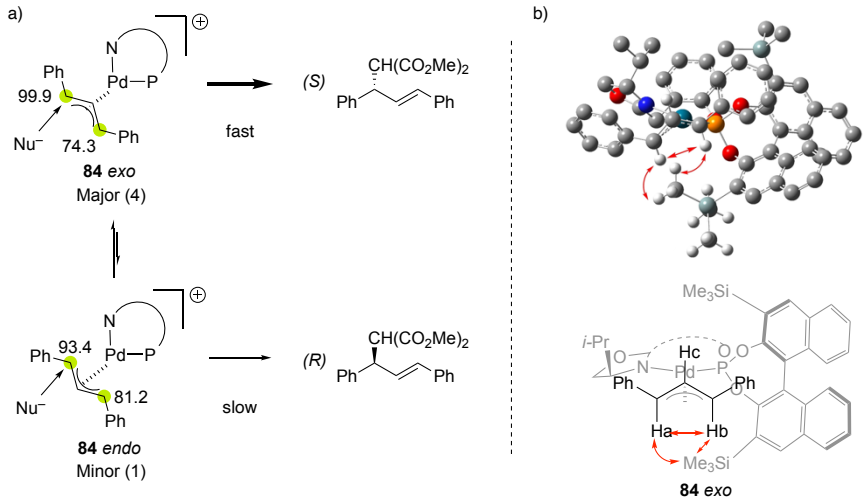

Scheme 4.1.4. a) Diastereoisomeric *exo* and *endo* Pd-η^3-allyl intermediates of complex **84**. The relative amounts of each isomer are shown in parentheses. The chemical shifts (in ppm) of the allylic terminal carbons are also shown. b) Calculated DFT structure for the major isomer of complex **84** (most of the hydrogen atoms have been omitted for clarity) and its schematic representation. Relevant NOE contacts that confirms its *exo* disposition are showed in red. H^a= terminal allyl proton *trans* to P; H^b= terminal allyl proton *trans* to N and H^c= central allyl proton.

To find out the impact of the configuration of the biaryl phosphite group in the enantioselectivity we then examined, for each ligand, the structures of the two most stable TSs, leading to both enantiomers of the substituted product (Figure 4.1.4).

For both ligands the major product enantiomer comes from a TS with an *exo* disposition of the substrate, while the *endo* disposition is responsible for the minor enantiomer. It is also interesting to see that the *exo* TSs of both ligands adopt a "boat-chair" conformation of the eight-membered chelate ring (Figure 4.1.4). In addition, for both ligands the *exo* TSs are stabilized due to an strong attractive interaction between the H of the methine group of the oxazoline and one of the phenyl rings of the substrate (see the noncovalent interaction (NCI) plots, in blue, Figure 4.1.5).

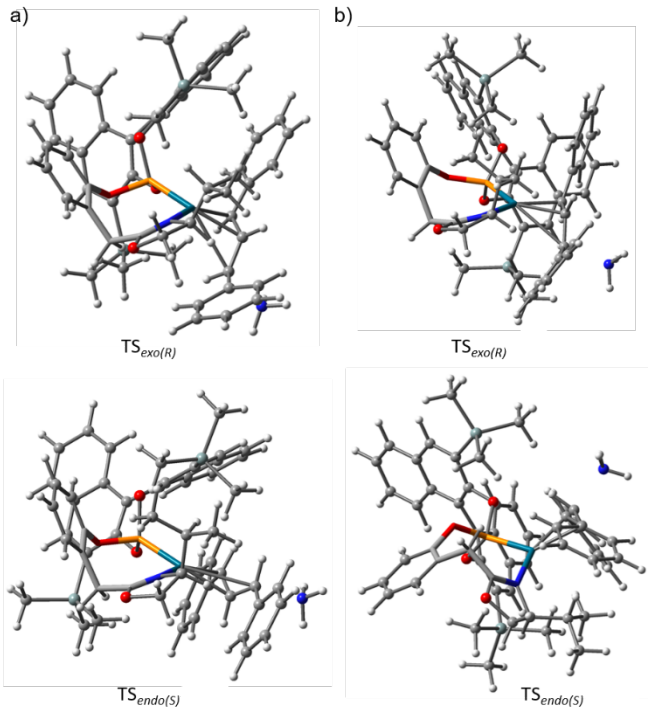

Figure 4.1.4. Most stable calculated TSs ($TS_{exo(R)}$ and $TS_{endo(S)}$) from **S150** using ligands (a) **L32b** and (b) **L32c**. The eight-membered chelate ring is highlighted using capped sticks, while the rest of the TS is shown using balls and sticks.

The difference between both ligands becomes evident when we analyzed the structures of the *endo* TSs. The *endo* TS of ligand **L32b** still maintains a boat-chair conformation which is destabilized with respect to the *exo* boat-chair conformation for two main reasons. Firstly, the above-mentioned attractive CH/π interaction is weaker than in the *exo* TS and secondly there is a steric repulsion between one of the Ph rings of the substrate and the binaphthyl phosphite moiety. In contrast to ligand **L32b**, the

endo TS of ligand **L32c** adopts a less stable "chair-chair" conformation (Figure 4.1.4). A TS with the same "boat-chair" disposition of the *endo* TS of ligand **L32b** is destabilized because the attractive CH/π interaction between the H from the oxazoline and the phenyl ring of the substrate does not exist because the H is pointing away from the coordination sphere (see Figure 4.1.6). Consequently, the ligand changes to a "chair-chair" conformation. This change of conformation increases the energy gap between the *endo* and the *exo* TSs and could explain the higher enantiomeric excess achieved with Pd/**L32c** over the Pd/**L32b**.

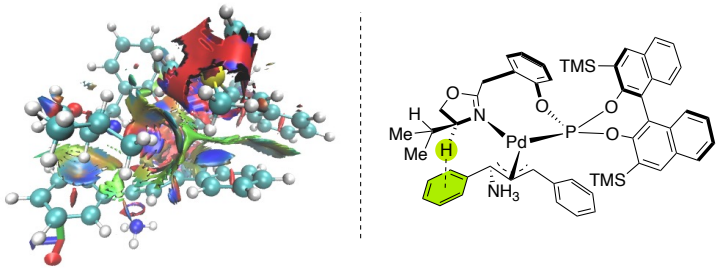

Figure 4.1.5. NCI plot of $TS_{exo(R)}$ with ligand **L32b** showing the CH/π interaction between the H of the methine group of the oxazoline and one of the phenyl rings of the substrate. NCIs were measured constructing the isosurface with the Multiwfn software, which were visualized with VMD.

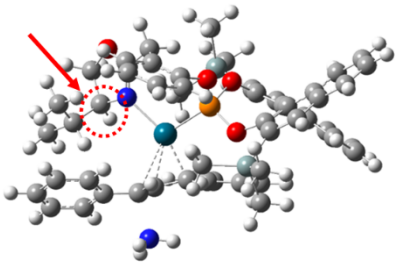

Figure 4.1.6. Calculated geometry for $TS_{endo(R)}$ using ligand **L32c**. The H of the methine group of the oxazoline is highlighted in red.

To shed some light on the different behavior of the allylic substitution of cyclic substrates, for which the enantioselectivity varied from 80% of the *R*-enantiomer (ligand **L33b**) to 86% of the *S*-enantiomer (ligand **L33c**) when the configuration of the biaryl phosphite group was changed, we studied the intermediate Pd-allyl complexes **85** and **86** (Scheme 4.1.5).

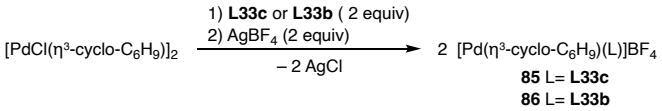

Scheme 4.1.5. Synthesis of [Pd(η^3-cyclo-C_6H_9)(L)]BF_4 complexes **85** and **84**.

For complex **85**, containing ligand **L33c** and a biaryl group with *S* configuration, two isomers were detected by NMR with ratio 1.2:1 (Scheme 4.1.6a). The NOESY spectrum indicated an *endo* disposition for the major isomer (responsible for the *S*-product) and an *exo* disposition for the minor (responsible for the *R*-product). For the minor isomer the *t*-butyl oxazoline group has NOE interactions with the terminal allyl proton *trans* to the phosphite group and also with the central allyl proton, whereas for the major *endo* isomer the central allyl proton showed a NOE interaction with one of the trimethyl silyl groups (TMS) of the phosphite group (see Supporting Information, Figure S5.1.80). The large difference on the chemical shifts of the allylic carbon *trans* to the phosphite group ($\Delta(^{13}C)$= 6.7 ppm) indicates that the major isomer reacts faster than the minor one, leading to observed preferential formation of the *S*-enantiomer.

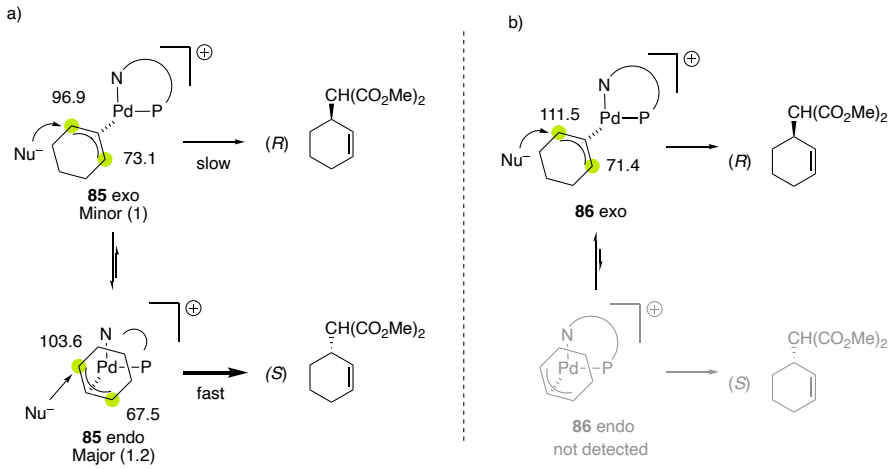

Scheme 4.1.6. Diastereoisomeric *exo* and *endo* Pd-η^3-allyl intermediates of: a) complex **85** and b) complex **86**. The relative amounts of each isomer are shown in parentheses. The chemical shifts (in ppm) of the allylic terminal carbons are also shown.

For complex **86** containing ligand **L33b** and a biaryl group with *R* configuration, only one isomer was found, whose NOE confirmed an *exo* disposition (Scheme 4.1.6b). As for the minor isomer of Pd/**L33c**, the NOE showed interactions of the *tert*-butyl oxazoline group with the terminal allyl proton *trans* to the phosphite group and also with the central allyl proton (see Supporting Information, Figure S5.1.85).

In summary, the configuration of the biaryl group affects which isomer is preferentially formed with ligands **L33b** and **L33c**. The *exo* isomer is favored with

ligands with an *R*-configuration of the biaryl moiety, while ligands with the opposite configuration favor the formation of the *endo* isomer.

The different effect of the configuration of the biaryl phosphite moiety on the outcome of the allylic substitution with linear and cyclic substrates can be explained by the different substrate geometry and the relative position of the trimethylsilyl groups of the biaryl phosphite group. Thus, in Figure 4.1.4 we can see that one of the TMS moiety are located above or below the Pd atom and in the space of the substrate coordination, depending on the configuration of the biaryl phosphite group. This feature is clearly illustrated in Figure 4.1.7a, where an apical view of the two *endo* TSs (TS_{endo}-**L32b** and TS_{endo}-**L32c**) is presented. In both cases one of the TMS groups is located almost at the same axis as the Pd atom, whereas the other TMS is located far from the substrate coordination sphere. However, whereas for the TS_{endo}-**L32b** the TMS group is located above the Pd atom, for the TS_{endo}-**L32c** the TMS group is located below the Pd atom. This disposition of the TMS groups has a small effect in favoring one of the two isomers (either *endo* or *exo*) for the linear substrate since the phenyl groups of the substrate are located far from the metal center and therefore far from the TMS group (Figure 4.1.7b). However, for the cyclic substrates the arrangement of the TMS group above or below to the Pd, has a direct effect in which of the two isomers is predominant (Figure 4.1.7c).

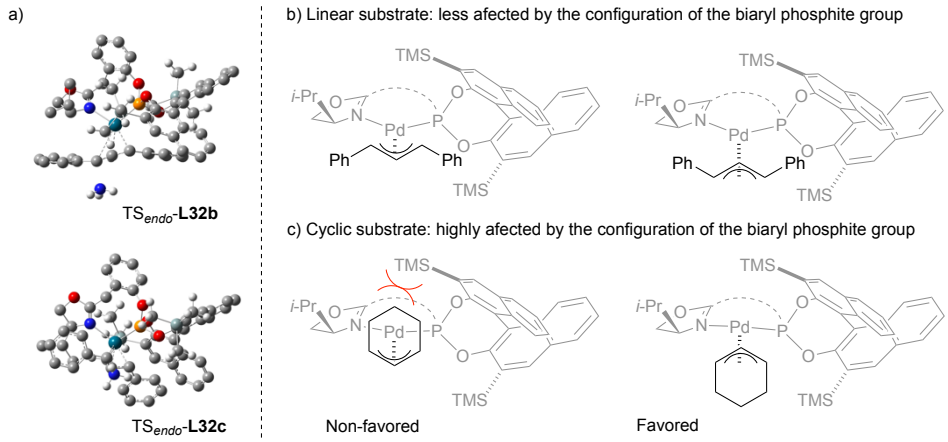

Figure 4.1.7. a) Apical view of the *endo* TSs with ligands **L32b** and **L32c**. Most of the hydrogen atoms except those of the TMS groups have been omitted for clarity. Steric environment found in *endo* and *exo* isomers in Pd/**L32b**-allyl complexes containing an *R*-biaryl phosphite moiety as example with: b) substrate **S150** and c) substrate **S151**.

4.1.3. Conclusions

A small library of air stable phosphite-oxazoline ligands has been tested in Pd-catalyzed allylic substitutions of a wide range of substrate types and nucleophiles (35 compounds in total), with high enantioselectivities (up to 99%) and activities (TOF's up to >4000 h^{-1}). These ligands, which are readily available in only two synthetic steps,

are derived from the PHOX ligand by replacing the phosphine moiety by biaryl phosphites and by introducing a methylene spacer between the oxazoline and the phenyl ring. These simple modifications allowed to increase the substrate and nucleophile scope of the PHOX ligands. We identified two ligands with good performance for a range of hindered (ligands **L32c**) and cyclic substrates (ligand **L33c**), with several nucleophiles. The two ligands have in common a chiral *S* biaryl phosphite moiety and differ at the oxazoline moiety. Mechanistic studies based on DFT calculations and NMR spectroscopy of the key Pd-intermediates allowed us to better understand the origin of the enantioselectivities. The wide substrate scope found is due to the ability of the ligand to adapt their ligand parameters to the reacting substrate. This contrasts to the parent phosphite-oxazoline ligands **9**. In this respect, while for hindered linear substrate the enantioselectivity is mainly affected by the biaryl phosphite functionality and therefore by the conformation adopted by the chelate ring, for the cyclic substrate the oxazoline group also has a crucial role. Accordingly a bulky oxazoline group is needed to adapt the size of the substrate binding pocket to the narrow substrate. In addition, the higher effect of the configuration of the biaryl phosphite moiety on the catalytic performance in cyclic substrates can be explained by the relative disposition of the trimethylsilyl groups of the biaryl phosphite moiety and their interactions with the substrates. These results open up the use of solid, air stable and readily available ligands to advance in the Pd-catalyzed asymmetric allylic substitution of several substrate types with diverse nucleophiles.

4.1.4. Experimental section

4.1.4.1. General considerations

All reactions were carried out using standard Schlenk techniques under an argon atmosphere. Commercial chemicals were used as received. Solvents were dried by means of standard procedures and stored under argon. ^{1}H, $^{13}C\{^{1}H\}$ and $^{31}P\{^{1}H\}$ NMR spectra were recorded using a Varian Mercury-400 MHz spectrometer. Chemical shifts are relative to that of NMR solvent for ^{1}H and $^{13}C\{^{1}H\}$ and of H_3PO_4 as internal standard for $^{31}P\{^{1}H\}$. The referenced $^{31}P\{^{1}H\}$ spectra in the Supporting Information are displayed without the internal standard. Racemic substrates **S150**-**S158**[22] and ligands **L31**–**L33a**–**c**[12a,b] were prepared as previously reported. For characterization and ee determination details, copies of the NMR spectra, copies of GC or HPLC traces as well as for DFT details see Supporting Information.

4.1.4.2. Typical procedure for the allylic alkylation reactions

A degassed solution of $[PdCl(\eta^3\text{-}C_3H_5)]_2$ (1.8 mg, 0.005 mmol) and the desired phosphite-oxazoline ligand (0.011 mmol) in dichloromethane (0.5 mL) was stirred for 30 min. After this time, a solution of substrate (1 mmol) in dichloromethane (1.5 mL), nucleophile (3 mmol), *N*,*O*-bis(trimethylsilyl)-acetamide (3 mmol) and KOAc (3 mg,

0.03 mmol) were added. The reaction mixture was stirred at room temperature. After the desired reaction time the reaction mixture was diluted with Et_2O (5 mL) and saturated NH_4Cl (aq) (25 mL) was added. The mixture was extracted with Et_2O (3 x 10 mL) and the extract dried over $MgSO_4$. For compounds **49**, **51**–**60**, **66**–**72**, **76**–**77** and **37**, the solvent was removed, conversions were measured by ^1H NMR and enantiomeric excesses were determined by HPLC. For compounds **50**, **74**–**75**, **78**–**80** and **83**, conversion and enantiomeric excesses were determined by GC. For compounds **73** and **82**, conversion was measured by ^1H NMR and ee's were determined by ^1H NMR using $[Eu(hfc)_3]$.

4.1.4.3. Typical procedure for the allylic amination of S150

A degassed solution of $[PdCl(\eta^3\text{-}C_3H_5)]_2$ (1.8 mg, 0.005 mmol) and the desired phosphite-oxazoline ligand (0.011 mmol) in dichloromethane (0.5 mL) was stirred for 30 min. After this time, a solution of substrate (1 mmol) in dichloromethane (1.5 mL) and benzylamine (262 µL, 3 mmol) were added. The reaction mixture was stirred at room temperature. After the desired reaction time the reaction mixture was diluted with Et_2O (5 mL) and saturated NH_4Cl (aq) (25 mL) was added. The mixture was extracted with Et_2O (3 x 10 mL) and the extract dried over $MgSO_4$. Conversion was measured by ^1H NMR and enantiomeric excesses of compound **61** were determined by HPLC.

4.1.4.4. Typical procedure for the allylic etherification and silylation of S150

A degassed solution of $[PdCl(\eta^3\text{-}C_3H_5)]_2$ (1.8 mg, 0.005 mmol) and the desired phosphite-oxazoline ligand (0.011 mmol) in dichloromethane (0.5 mL) was stirred for 30 min. Subsequently, a solution of **S150** (31.5 mg, 0.125 mmol) in dichloromethane (1.5 mL) was added. After 10 min, Cs_2CO_3 (122 mg, 0.375 mmol) and the corresponding alkyl alcohol or silanol (0.375 mmol) were added. The reaction mixture was stirred at room temperature. After the desired reaction time, the reaction mixture was diluted with Et_2O (5 mL) and saturated NH_4Cl (aq) (25 mL) was added. The mixture was extracted with Et_2O (3 x 10 mL) and the extract dried over $MgSO_4$. Conversions were measured by ^1H NMR and enantiomeric excesses for compounds **62**–**65** were determined by HPLC.

4.1.4.5. Computational details

The geometries of all intermediates were optimized using the Gaussian 09 program,[23] employing the B3LYP[24] density functional and the LANL2DZ[25] basis set for palladium and the 6-31G* basis set for all other elements.[26] Solvation correction was applied in the course of the optimizations using the PCM model with the default parameters for dichloromethane.[27] The complexes were treated with charge +1 and in the single state. No symmetry constraints were applied. The energies were further refined by performing

single point calculations using the above mentioned parameters, with the exception that the 6-311+G**[28] basis set was used for all elements except palladium, and by applying dispersion correction using DFT-D3[29] model. All energies reported are Gibbs free energies at 298.15 K and calculated as $G_{reported} = G_{6\text{-}31G^*} + (E_{6\text{-}311+G^{**}} - E_{6\text{-}31G^*}) + E_{DFT\text{-}D3}$.

We used the NCI method[30] to study the non-covalent interac-tions. The method is capable of mapping real-space regions where non-covalent interactions are important and is based exclusively on the electron density and its gradient. The information provided by NCI plots is essentially qualitative. To perform these calculations, we used promolecular approximation using xyz files.

4.1.4.6. Typical procedure for the preparation of [Pd(η³-allyl)(L)]BF_4 complexes 84–85

The corresponding ligand (0.05 mmol) and the complex $[Pd(\mu\text{-}Cl)(\eta^3\text{-}1,3\text{-}allyl)]_2$ (0.025 mmol) were dissolved in CD_2Cl_2 (1.5 mL) at room temperature under argon. $AgBF_4$ (9.8 mg, 0.05 mmol) was added after 30 minutes and the mixture was stirred for other 30 minutes more. The mixture was then filtered over celite under argon and the resulting solutions were analyzed by NMR.

[Pd(η³-1,3-Ph_2-C_3H_3)(L32c)]BF_4 84. Major isomer: $^{31}P\{^1H\}$ NMR (161.9 MHz, CD_2Cl_2): δ= 132.9 (s). ^1H NMR (400 MHz, CD_2Cl_2): δ= 0.44 (s, 9H, CH_3–Si), 0.62 (s, 9H, CH_3–Si), 0.70 (m, 6H, CH_3, *i*-Pr), 1.65 (m, 1H, CH, *i*-Pr), 2.48 (m, 1H, CH–N), 3.78 (d, 1H, CH_2, $^2J_{H\text{-}H}$= 14.8 Hz), 3.92–4.15 (m, 2H, CH_2–O), 4.35 (d, 1H, CH_2, $^2J_{H\text{-}H}$= 14.8 Hz), 4.77 (d, 1H, CH= trans to N, *J*= 11.2 Hz), 5.81 (m, 1H, CH= *trans* to P), 6.21 (m, 2H, CH=), 6.60 (m, 2H, CH=), 6.83 (m, 2H, CH= central and CH=), 6.92–8.32 (m, 19H, CH=). $^{13}C\{^1H\}$ (100.6 MHz, CD_2Cl_2): δ= 0.3 (CH_3, $SiMe_3$), 0.7 (CH_3, $SiMe_3$), 16.2 (CH_3, *i*-Pr), 18.9 (CH_3, *i*-Pr), 31.4 (CH, *i*-Pr), 35.1 (CH_2), 67.2 (CH–N), 70.6 (CH_2–O), 74.3 (d, CH= *trans* to N, $J_{C\text{-}P}$= 7.6 Hz), 99.9 (d, CH= *trans* to P, $J_{C\text{-}P}$= 33.0 Hz), 110.7 (d, CH= central, $J_{C\text{-}P}$= 10.4 Hz), 126.2-151.4 (aromatic carbons), 169.8 (C=N). Minor isomer: $^{31}P\{^1H\}$ NMR (161.9 MHz, CD_2Cl_2): δ= 134.4 (s). ^1H NMR (400 MHz, CD_2Cl_2): δ= 0.31 (s, 9H, CH_3–Si), 0.48 (s, 9H, CH_3–Si), 0.70 (m, 3H, CH_3, *i*-Pr), 0.86 (m, 3H, CH_3, *i*-Pr), 1.89 (m, 1H, CH, *i*-Pr), 2.27 (m, 1H, CH–N), 3.54 (d, 1H, CH_2, $^2J_{H\text{-}H}$= 13.6 Hz), 3.92–4.15 (m, 2H, CH_2–O), 4.09 (m, 1H, CH_2), 5.27 (d, 1H, CH= *trans* to N, *J*= 12 Hz), 5.44 (m, 1H, CH= trans to P), 6.38 (m, 2H, CH=), 6.65 (m, 1H, CH=), 6.83 (m, 2H, CH= central and 2xCH=), 6.92–8.32 (m, 19H, CH=). $^{13}C\{^1H\}$ (100.6 MHz, CD_2Cl_2): δ= -0.4 (CH_3, $SiMe_3$), -0.1 (CH_3, $SiMe_3$), 15.5 (CH_3, *i*-Pr), 18.0 (CH_3, *i*-Pr), 31.0 (CH, *i*-Pr), 34.7 (CH_2), 69.1 (CH–N), 69.7 (CH_2–O), 81.2 (d, CH= *trans* to N, $J_{C\text{-}P}$= 5.9 Hz), 93.4 (d, CH= *trans* to P, $J_{C\text{-}P}$= 40.5 Hz), 112.4 (d, CH= central, $J_{C\text{-}P}$= 12.6 Hz), 126.2-151.4 (aromatic carbons), 169.9 (C=N).

[Pd(η³-cyclo-C_6H_9)(L33c)]BF_4 85. Major isomer: $^{31}P\{^1H\}$ NMR (161.9 MHz, CD_2Cl_2): δ= 134.7 (s). ^1H NMR (400 MHz, CD_2Cl_2): δ= 0.32 (s, 9H, CH_3–Si), 0.57 (s,

9H, CH_3–Si), 0.99 (m, 9H, CH_3, *t*-Bu), 1.1-2.2 (b, 5H, CH_2), 2.49 (m, 1H, CH_2), 3.71 (d, 1H, CH_2, $^2J_{H-H}$= 14.4 Hz), 3.80 (d, 1H, CH_2, $^2J_{H-H}$= 14.4 Hz), 3.97 (b, 1H, CH= trans to N), 4.03 (dd, 1H, CH–N, *J*= 9.6 Hz, *J*= 3.2 Hz), 4.64 (m, 2H, CH_2–O), 5.50 (b, 1H, CH= central), 6.36 (b, 1H, CH= *trans* to P), 6.12-8.30 (m, 14H, CH=).$^{13}C\{^1H\}$ (100.6 MHz, CD_2Cl_2): δ= 0.0 (2xCH_3, $SiMe_3$), 20.3 (CH_2), 25.9 (CH_3, *t*-Bu), 26.6 (CH_2), 28.2 (d, CH_2, J_{C-P}= 8.3 Hz), 29.1 (C, *t*-Bu), 34.8 (d, CH_2, J_{C-P}= 10.2 Hz), 67.5 (b, CH= *trans* to N), 71.7 (CH_2–O), 78.2 (CH–N), 103.6 (d, CH= *trans* to P, J_{C-P}= 42.5 Hz), 112.7 (d, CH= central, J_{C-P}= 11.4 Hz), 120.8-151.4 (aromatic carbons), 169.8 (C=N). Minor isomer: $^{31}P\{^1H\}$ NMR (161.9 MHz, CD_2Cl_2): δ= 135.0 (s). ^1H NMR (400 MHz, CD_2Cl_2): δ= 0.43 (s, 9H, CH_3–Si), 0.52 (s, 9H, CH_3–Si), 0.90 (m, 9H, CH_3, *t*-Bu), 1.1-2.2 (b, 6H, CH_2), 4.15 (dd, 1H, CH–N, *J*= 9.6 Hz, *J*= 4.4 Hz), 4.47 (dd, 1H, CH_2, $^2J_{H-H}$= 14.4 Hz, *J*= 2.4 Hz), 4.52 (m, 2H, CH_2–O), 5.10 (b, 1H, CH= *trans* to N), 5.70 (b, 1H, CH= central), 6.29 (b, 1H, CH= trans to P), 6.12-8.30 (m, 14H, CH=).$^{13}C\{^1H\}$ (100.6 MHz, CD_2Cl_2): δ= 0.2 (CH_3, $SiMe_3$), 0.5 (CH_3, $SiMe_3$), 16.9 (CH_2), 25.6 (CH_3, *t*-Bu), 28.7 (CH_2), 29.1 (C, *t*-Bu), 29.8 (d, CH_2, J_{C-P}= 9.1 Hz), 35.9 (d, CH_2, J_{C-P}= 10.2 Hz), 71.4 (CH_2–O), 73.1 (b, CH= *trans* to N), 77.3 (CH–N), 96.9 (d, CH= *trans* to P, J_{C-P}= 31.2 Hz), 114.8 (d, CH= central, J_{C-P}= 9.9 Hz), 120.8-151.4 (aromatic carbons), 171.0 (C=N).

[Pd(η³-1,3-cyclo-C_6H_9)(L3b)]BF_4 86. $^{31}P\{^1H\}$ NMR (161.9 MHz, CD_2Cl_2): δ= 142.4 (s). ^1H NMR (400 MHz, CD_2Cl_2): δ= 0.06 (s, 9H, CH_3–Si), 0.32 (s, 9H, CH_3–Si), 0.48 (s, 9H, CH_3, *t*-Bu), 0.75 (m, 1H, CH_2), 0.89 (m, 1H, CH_2), 1.42 (m, 1H, CH_2), 1.56 (m, 1H, CH_2), 1.75 (b, 2H, CH_2), 3.17 (m, 1H, , CH= trans to N), 3.62 (d, 1H, CH_2, $^2J_{H-H}$= 14.4 Hz), 3.87 (m, 1H, CH–N), 4.22 (d, 1H, CH_2, $^2J_{H-H}$= 14.4 Hz), 4.38 (m, 2H, CH_2–O), 5.03 (m, 1H, CH= central), 6.07 (m, 1H, CH= trans to P), 6.81-7.38 (m, 10H, CH=), 7.82-7.84 (m, 2H, CH=), 8.01-8.03 (m, 2H, CH=). $^{13}C\{^1H\}$ (100.6 MHz, CD_2Cl_2): δ= 0.2 (CH_3, $SiMe_3$), 1.1 (CH_3, $SiMe_3$), 19.8 (CH_2), 25.6 (CH_3, *t*-Bu), 26.9 (CH_2 and C, *t*-Bu), 28.4 (d, CH_2, J_{C-P}= 7.6 Hz), 35.1 (CH_2), 70.6 (CH_2–O), 71.4 (b, CH= *trans* to N), 79.7 (CH–N), 111.1 (d, CH= central, J_{C-P}= 33.4 Hz), 111.5 (d, CH= *trans* to P, J_{C-P}= 9.1 Hz), 121.4-157.1 (aromatic carbons), 174.6 (C=N).

4.1.5. References

[1] See for example: (a) Pàmies, O.; Margalef, J.; Cañellas, S.; James, J.; Judge, e.; Guiry, P.J.; Moberg, C.; Bäckvall, J.-E.; Pfaltz, A.; Pericàs, M.A.; Diéguez, M. Recent advances in enantioselective pd-catalyzed allylic substitution: from design to applications. *Chem. Rev.* **2021,** *121*, 8, 4373–4505. (b) Huang, H.-M.; Bellotti, P.; Glorius F. Transition metal-catalysed allylic functionalization reactions involving radicals. *Chem. Soc. Rev.* **2020**, *49*, 6186–6197. (c) Lu, Z.; Ma, S. Metal-catalyzed enantioselective allylation in asymmetric synthesis**.** *Angew. Chem. Int. Ed*. **2008**, *47*, 258–297. (d) Yoshioka, E.; Kohtani, S. Miyabe, H. *Trends in Heterocyclic Chemistry* **2009**, *14*, 1–16. (e) Trost, B. M.; Zhang, T.; Sieber, J. D. Catalytic asymmetric allylic alkylation employing heteroatom nucleophiles: a powerful method for C–X bond formation. *Chem. Sci.* **2010**, *1*, 427-440. (f) Trost, B. M. Pd- and Mo-catalyzed asymmetric allylic alkylation. *Org. Process Res. Dev.* **2012**, *16*, 185-194. (g) Transition Metal Catalyzed Enantioselective Allylic substitution in organic synthesis.

(Ed.: U. Kazmaier), Springer, Cham, **2012**. (h) Kammerer. C.; Prestat, G.; Madec, D.; Poli, G. Synthesis of γ-lactams and γ-lactones via intramolecular Pd-catalyzed allylic alkylations. *Acc. Chem. Res*. **2014**, *47*, 3439–3447; (i) Butt, N. A.; Zhang, W. Transition metal-catalyzed allylic substitution reactions with unactivated allylic substrates. *Chem. Soc. Rev.* **2015**, *44*, 7929-7967. (j) Grange, R. L.; Clizbe, E. A.; Evans, P. A. Recent developments in asymmetric allylic amination reactions. *Synthesis* **2016**, *48*, 2911-296. (k) Butt, N.; Yang, G.; Zhang, W. Allylic alkylations with enamine nucleophiles. *Chem. Rec.* **2016**, *16*, 2687-2696.

[2] (a) (a) Trost, B. M.; van Vranken, D. L.; Bingel, C. A modular approach for ligand design for asymmetric allylic alkylations via enantioselective palladium-catalyzed ionizations. *J. Am. Chem. Soc.* **1992**, *114*, 9327-9343. (b) Trost, B. M. Designing a receptor for molecular recognition in a catalytic synthetic reaction: allylic alkylation. *Acc. Chem. Res.* **1996**, *29*, 355-364. (c) Trost, B. M.; Bunt, R. C. Asymmetric induction in allylic alkylations of 3-(acyloxy)cycloalkenes. *J. Am. Chem. Soc.* **1994**, *116*, 4089-4090. (d) Trost, B. M.; Krueger, A. C.; Bunt, R. C.; Zambrano, J. On the question of asymmetric induction with acyclic allylic substrates. an asymmetric synthesis of (+)-polyoxamic acid. *J. Am. Chem. Soc.* **1996**, *118*, 6520-6521.

[3] Butts, C. P.; Filali, E.; Lloyd-Jones, G. C.; Norrby, P.-O.; Sale, D. A.; Schramm, Y. FALTA TITOL *J. Am. Chem. Soc.* **2009**, *131*, 9945.

[4] Mata, G.; Kalnmals, C. A. Total synthesis in the Trost laboratories: selected milestones from the past twenty years**.** *Isr. J. Chem.* **2021**, *61*, 427–468 and references there in.

[5] (a) von Matt, P.; Pfaltz, A. Chiral Phosphinoaryldihydrooxazoles as ligands in asymmetric catalysis: Pd-catalyzed allylic substitution. *Angew. Chem. Int. Ed.* **1993**, *32*, 566-568. (b) Sprinz, J.; Helmchen, G. Phosphinoaryl- and phosphinoalkyloxazolines as new chiral ligands for enantioselective catalysis: Very high enantioselectivity in palladium catalyzed allylic substitutions. *Tetrahedron Lett.* **1993**, *34*, 1769-1772. (c) Dawson, G. J.; Frost, C. G.; Williams, J. M. J.; Coote, S. J. Asymmetric palladium catalysed allylic substitution using phosphorus containing oxazoline ligands. *Tetrahedron Lett.* **1993**, *34*, 3149-3150. (d) Helmchen, G.; Pfaltz, A. Phosphinooxazolines a new class of versatile, modular P,N-ligands for asymmetric catalysis, *Acc. Chem. Res.* **2000**, *33*, 336-345.

[6] (a) *Privileged Chiral Ligands and Catalysts*, (Ed.: Q.-L. Zhou), Wiley-VCH, Weinheim, 2011. (b) Sommer, W.; Weibel, D. *Sigma Aldrich's Chemfiles* **2008**, *2*, 1–91.

[7] (a) Chiral ligands. Evolution of ligand libraries for asymmetric catalysis, (Ed.: M. Diéguez), CRC Press, Boca Raton, **2021**. (b) Margalef, J.; Biosca, M.; De La Cruz-Sánchez, P.; Faiges, J.; Pàmies, O.; Diéguez, M. Evolution in heterodonor P-N, P-S and P-O chiral ligands for preparing efficient catalysts for asymmetric catalysis. From design to applications and references therein. *Coord. Chem. Rev*. **2021**, *446*, 214120-214205.

[8] For selected papers on Pd-catalyzed allylic substitution reaction see: (a) Wang, Q.-F.; He, W.; Liu, X.-Y.; Chen, H.; Qin, X.-Y.; Zhang, S.-Y. Facile one-pot synthesis of *cinchona alkaloid*-based P,N ligands and their application to Pd-catalyzed asymmetric allylic alkylation. *Tetrahedron: Asymmetry* **2008**, *19*, 2447−2450. (b) Cheung, H. Y.; Yu, W.-Y.; Au-Yeung, T. T. L.; Zhou, Z.; Chan, A. S. C. Effective chiral ferrocenyl phosphine-thioether ligands in enantioselective palladium-catalyzed allylic alkylations. *Adv. Synth. Catal*. **2009**, *351*, 1412−1422. (c) Cheng, H.-G.; Feng, B.; Chen, L.-Y. ;Guo W.; Yu, X.-Y.; Lu, L.-Q.; Chen, J.-R.; Xiao, W.-J. Rational design of sulfoxide–phosphine ligands for Pd-catalyzed enantioselective allylic alkylation reactions. *Chem. Comm*. **2014**, *50*, 2873−2875. (d) Qiu, Z.; Sun, R.; Teng, D. Synthesis of highly rigid phosphine–oxazoline ligands for palladium-catalyzed asymmetric allylic alkylation. *Org. Biomol. Chem*. **2018**,*16*, 7717-7724. (e) Noël, T.; Bert, K.; Van der Eycken, E.; Van der Eycken J. Imidate–phosphanes as highly versatile N,P ligands and their application in palladium-catalyzed asymmetric allylic alkylation reactions. *Eur. J. Org. Chem*.

2010, 4056–4061. (f) Liu, Q.-L.; Chen, W.; Jiang, Q.-Y.; Bai, X.-F.; Li, Z.; Xu, Z.; Xu, L.-W. A d-Camphor-based schiff base as a highly efficient N,P ligand for enantioselective palladium-catalyzed allylic substitutions. *ChemCatChem* **2016**, *8*, 1495–1499. (g) Nemoto, T.; Kanematsu, M.; Tamura, S.; Hamada, Y. Palladium-catalyzed asymmetric allylic alkylation of 2,3-allenyl acetates using a chiral diaminophosphine oxide. *Adv. Synth. Catal.* **2009**, *351*, 1773–1778; h) B. Lu, B. Feng, H. Ye, J.-R. Chen, W.-J. Xiao, *Org. Lett.* **2018**, *20*, 3473–3476. (i) Borràs, C.; Elías-Rodríguez, P.; Carmona, A. T.; Robina, I.; Pàmies, O.; Diéguez, M. Amino-P ligands from iminosugars: new readily available and modular ligands for enantioselective Pd-catalyzed allylic substitutions. *Organometallics*, **2018**, *37*, 1682–1694. (j) Margalef, J.; Coll, M.; Norrby, P.-O.; Pàmies, O.; Diéguez, M. Asymmetric catalyzed allylic substitution using a Pd/P–S catalyst library with exceptional high substrate and nucleophile versatility: DFT and Pd-π-allyl key intermediates studies. *Organometallics*, **2016**, *35*, 3323–3335. (k) Mata, Y.; Pàmies, O.; Diéguez, M. Pyranoside phosphite-oxazoline ligand library: highly efficient modular P,N ligands for palladium-catalyzed allylic substitution reactions. a study of the key palladium allyl intermediates. *Adv. Synth. Catal.* **2009**, *351*, 3217-3234. (l) Mazuela, J.; Paptchikhine, A.; Tolstoy, P.; Pàmies, O.; Diéguez, M.; Anderssom, P. G. A new class of modular P,N-ligand library for asymmetric Pd-catalyzed allylic substitution reactions: a study of the key Pd–π-allyl intermediates. *Chem. Eur. J.* **2010**, *16*, 620–638. (m) Mazuela, J.; Pàmies, O.; Diéguez, M. A new modular phosphite-pyridine ligand library for asymmetric Pd-catalyzed allylic substitution reactions: a study of the key Pd-π-allyl intermediates. *Chem. Eur. J.* **2013**, *19*, 2416–2432. (n) Magre, M.; Biosca, M.; Norrby, P.-O.; Pàmies, O.; Diéguez, M. Theoretical and experimental optimization of a new amino phosphite ligand library for asymmetric palladium-catalyzed allylic substitution. *ChemCatChem*. **2015**, *7*, 4091–4107. (o) Biosca, M.; Margalef, J.; Caldentey, X.; Besora, M.; Rodríguez-Escrich, C.; Saltó, J.; Cambeiro, X. C.; Maseras, F.; Pàmies, O.; Diéguez, M. Computationally guided design of a readily assembled phosphite–thioether ligand for a broad range of Pd-catalyzed asymmetric allylic substitutions. *ACS Catal*. **2018**, *8*, 3587−3601. (p) Biosca, M.; Saltó, J.; Magre, M.; Norrby, P.-O.; Pàmies, O.; Diéguez, M. An improved class of phosphite-oxazoline ligands for Pd-catalyzed allylic substitution reactions. *ACS Catal*. **2019**, *9*, 6033−6048.

[9] (a) Diéguez, M.; Pàmies, O. Biaryl Phosphites: New efficient adaptative ligands for Pd-catalyzed asymmetric allylic substitution reactions. *Acc. Chem. Res.* **2010**, *43*, 312.322. (b) van Leeuwen, P. W. N. M.; Kamer, P. C. J.; Claver, C.; Pàmies, O.; Diéguez, M. Phosphite-containing ligands for asymmetric catalysis. *Chem. Rev.* **2011**, *111*, 2077-2118. (c) Pàmies, O.; Diéguez, M. Adaptable P–X biaryl phosphite/phosphoroamidite-containing ligands for asymmetric hydrogenation and C–X bond-forming reactions: ligand libraries with exceptionally wide substrate scope. *Chem. Rec.* **2016**, *16*, 2460–2481. (d) Diéguez, M.; Pàmies, O.; Moberg, C. Self-adaptable tropos catalysts. *Acc. Chem. Res.* **2021**, *54*, 16, 3252–3263.

[10] (a) Pàmies, O.; Diéguez, M.; Claver, C. New phosphite−oxazoline ligands for efficient Pd-catalyzed substitution reactions. *J. Am. Chem. Soc.* **2005**, *127*, 3646-3647. (b) Bellini, R.; Magre, M.; Biosca, M.; Norrby, P.-O.; Pàmies, O.; Diéguez, M.; Moberg, C. Conformational preferences of a tropos biphenyl phosphinooxazoline–a ligand with wide substrate scope. *ACS Catal.* **2016**, *6*, 1701–1712.

[11] Margalef, J.; Pàmies, O.; Pericàs, M. A.; Diéguez, M. Evolution of phosphorus–thioether ligands for asymmetric catalysis. *Chem. Comm.* **2020**, *56*, 10795–10808.

[12] (a) Magre, M.; Pàmies, O.; Diéguez, M. PHOX–based phosphite–oxazoline ligands for the enantioselective Ir–catalyzed hydrogenation of cyclic β–enamides. *ACS Catal.* **2016**, *6*, 5186–5190. (b) Biosca, M.; Magre, M.; Coll, M.; Pàmies, O.; Diéguez, M. Alternatives to phosphinooxazoline (*t*-BuPHOX) ligands in the metal-catalyzed hydrogenation of minimally functionalized olefins and cyclic

β-enamides. *Adv. Synth. Catal.* 2017, *359*, 2801–2814. (c) Mazloomi, Z.; Magre, M.; Del Valle, E.; Pericàs, M. A.; Pàmies, O.; van Leeuwen, P. W.N.M.; Diéguez, M. Synthesis, Application and Kinetic studies of chiral phosphite-oxazoline palladium complexes as active and selective catalysts in intermolecular heck reactions**.** *Adv. Synth. Catal.* **2018**, *360*, 1650–1664

[13] We also studied the effect of Pd/L ratio. No effect on the catalytic performance was observed, see Supporting Information for details.

[14] See for example: a) Dugal-Tessier, J.; Dake, G. R.; Gates, D. P. Chiral phosphaalkene−oxazoline ligands for the palladium-catalyzed asymmetric allylic alkylation. *Org. Lett.* **2010**, *12*, 4667–4669. (b) Nakai. Y.; Uozumi. Cycloisomerization of 1,6-Enynes: Asymmetric multistep preparation of a hydrindane framework in water with polymeric catalysts. *Org. Lett.* **2005**, *7*, 291–293. c) Son, S. U.; Park, K. H.; Seo, H.; Chung, Y. K.; Lee, S.-G. Catalytic asymmetric synthesis of cyclopentenones from propargyl malonates and allylic acetate by successive action of homogeneous palladium(ii) and cobalt on charcoal catalysts in a one-pot reaction. *Chem. Commun.* **2001**, 2440–2441. (d) Farwick, A.; Engelhart, J. U.; Tverskoy, O.; Welter, C.; Umlauf, Q. E.; Rominger, F.; WillKerr, W. J.; Helmchen, G. Bicyclic cyclopentenones *via* the combination of an iridium- catalyzed allylic substitution with a diastereoselective intramolecular Pauson–Khand Reaction. *Adv. Synth. Catal.* **2011**, *353*, 349–370.

[15] (a) Kmentov I.; Gotov, B.; Solcniov, E.; Toma, S. Study of ligand and base effects on enantioselective allylation catalyzed by Pd(0) phosphine complexes in [bmim][PF_6] ionic liquid *Green Chem.* **2002**, 4, 103–106. (b) Liu, J.; Chen, G.; Xing, J.; Liao, J. *tert*-Butanesulfinylthioether ligands: synthesis and application in palladium-catalyzed asymmetric allylic alkylation*Tetrahedron:. Asymmetry* **2011**, *22*, 575–579. (c) Jin, Y.; Du, D. M. The synthesis of phosphine oxide-linked bis(oxazoline) ligands and their application in asymmetric allylic alkylation *Tetrahedron* **2012**, *68*, 3633–3640. (d) Martin, C. J.; Rawson, D. J.; Williams, J. M. J. The preparation of enantiomerically enriched γ-amino acids (GABAs) using palladium catalysed allylic substitution. *Tetrahedron: Asymmetry* **1998**, *9*, 3723–3730. (e) Deng, W. H.; Ye, F.; Bai, X. F.; Zheng, Z. J.; Cui, Y. M.; Xu, L. W. Multistereogenic Phosphine Ligand-promoted Palladium-Catalyzed Allylic Alkylation of Cyanoesters. *ChemCatChem* **2015**, *7*, 75–79.

[16] (a) *Dictionary of Natural Products*, (Ed.: J. Buckingham), Cambridge University Press., Cambridge, **1994**. (b) Lumbroso, A.; Cooke, M. L.; Breit, B. Catalytic asymmetric synthesis of allylic alcohols and derivatives and their applications in organic synthesis *Angew. Chem. Int., Ed.* **2013**, *52*, 1890–1932.

[17] The use of aliphatic alcohols has been much less studied than those using phenols. See: (a) Iourtchenko, A.; Sinou, D. Asymmetric palladium(0)-catalyzed synthesis of allylic ethers. *J. Mol. Catal. A* **1997**, *122*, 91–93. (b) Haight, A. R.; Stoner, E. J.; Peterson, M. J.; Grover, V. K. General Method for the Palladium-Catalyzed Allylation of Aliphatic Alcohols. *J. Org. Chem.* **2003**, *68*, 8092–8096. (c) Lam, F. L.; Au-Yeung, T. T. L.; Kwong, F. Y.; Zhou, Z.; Wong, K. Y.; Chan, A. S. C. Palladium–($S_{,p}R$)-FerroNPS-catalyzed asymmetric allylic etherification: electronic effect of nonconjugated substituents on benzylic alcohols on enantioselectivity. *Angew. Chem. Int. Ed.* **2008**, *47*, 1280–1283. (d) Ye, F.; Zheng, Z.-J.; Li, L.; Yang, K.-F.; Xia, C.-G.; Xu, L.-W. Development of a novel multifunctional n,p ligand for highly enantioselective palladium-catalyzed asymmetric allylic etherification of alcohols and silanols. *Chem. Eur. J.* **2013**, *19*, 15452–15457. (e) Caldentey, X.; Pericàs, M. A. Phosphinite thioethers derived from chiral epoxides. modular P,S-ligands for Pd-catalyzed asymmetric allylic substitutions. *J. Org. Chem.* **2010**, *75*, 2628–2644. (f) Liu, Z.; Du, H. Development of chiral terminal-alkene−phosphine hybrid ligands for palladium-catalyzed asymmetric allylic substitutions. *Org. Lett.* **2010**, *12*, 3054–3057. (g) Kato, M.; Nakamura, T.;

Ogata, K.; Fukuzawa, S.-I. Synthesis of novel ferrocenyl-based P,S ligands (ThioClickFerrophos) and their use in Pd-catalyzed asymmetric allylic substitutions. *Eur. J. Org. Chem.* **2009**, 5232–5238. (h) Feng, B.; Cheng, H.-G.; Chen, J.-R.; Deng, Q.-R.; Lu, L. Q.; Xiao, W.-J. Palladium/sulfoxide–phosphine-catalyzed highly enantioselective allylic etherification and amination. *Chem. Commun.* **2014**, *50*, 9550–9553.

[18] (a) Oslob, J. D.; Äkermark, B.; Helquist, P.; Norrby, P.-O. Steric influences on the selectivity in palladium-catalyzed allylation. *Organometallics* **1997**, 16, 3015–3021. (b) Hagelin, H.; Äkermark, B.; Norrby, P.-O. New molecular mechanics (MM3*) force field parameters for calculations on (η^3-allyl)palladium complexes with nitrogen and phosphorus ligands. *Organometallics* **1999**, *18*, 2884–2895.

[19] (a) Hagelin, H.; Svensson, M.; Äkermark, B.; Norrby, P.-O. Molecular mechanics (MM3*) force field parameters for calculations on palladium olefin complexes with phosphorus ligands. *Organometallics* **1999**, *18*, 4574–4583. (b) Moberg. C.; Bremberg, U.; Hallman, K.; Svensson, M.; Norrby, P.-O.; Hallberg, A.; Larhed, M.; Csöregh, I. Selectivity and reactivity in asymmetric allylic Alkylation. *Pure Appl. Chem*. **1999**, *71*, 1477–1483.

[20] In this study, only the two *syn-syn* allyl complexes were taken into account, neglecting the contribution of the *anti-anti* and *syn-anti* allylic species of higher energy.

[21] (a) Fristrup, P.; Ahlquist, M.; Tanner, D.; Norrby, P.-O. On the nature of the intermediates and the role of chloride ions in Pd-catalyzed allylic alkylations: added insight from density functional theory. *J. Phys. Chem.* **2008**, *112*, 12862–12867. (b) Wahlers. J.; Margalef, J.; Hansen, E.; Bayesteh, A.; Helquist, P.; Diéguez, M.; Pàmies, O.; Wiest, O.; Norrby, P.-O. Proofreading experimentally assigned stereochemistry through Q2MM predictions in Pd-catalyzed allylic aminations. *Nat. Commun.* **2021**, *12*, 6719-6725.

[22] (a) Auburn, P. R.; Mackenzie, P. B.; Bosnich, B. Asymmetric synthesis. Asymmetric catalytic allylation using palladium chiral phosphine complexes. *J. Am. Chem. Soc.***1985**, *107*, 2033–2046. (b) Jia, C.; Müller, P.; Mimoun, H. Palladium-catalyzed allylic acetoxylation of olefins using hydrogen peroxide as oxidant. *J. Mol. Cat. A: Chem.* **1995**, *101*, 127–136. (c) Lehman, J.; Lloyd-Jones, G. C. Regiocontrol and stereoselectivity in tungsten-bipyridine catalysed allylic alkylation. *Tetrahedron* **1995**, *51*, 8863–8874. d) Hayashi, T.; Yamamoto. A.; Ito, Y.; Nishioka, E.; Miura, H. Yanagi, K. Asymmetric synthesis catalyzed by chiral ferrocenylphosphine transition-metal complexes. 8. Palladium-catalyzed asymmetric allylic amination. *J. Am. Chem. Soc.* **1989**, *111*, 6301–6311.

[23] Frisch, M. J.; Trucks, G. W.; Schlegel, H. B.; Scuseria, G. E.; Robb, M. A.; Cheeseman, J. R.; Scalmani, G.; Barone, V.; Petersson, G. A.; Nakatsuji, H.; Li, X.; Caricato, M.; Marenich, A. V.; Bloino, J.; Janesko, B.G.; Gomperts, R.; Mennucci, B.; Hratchian, H.P.; Ortiz, J. V.; Izmaylov, A. F.; Sonnenberg, J. L.; Williams–Young, D.; Ding, F.; Lipparini, F.; Egidi, F.; Goings, J.; Peng, B.; Petrone, A.; Henderson, T.; Ranasinghe, D.; Zakrzewski, V. G.; Gao, J.; Rega, N.; Zheng, G.; Liang, W.; Hada, M.; Ehara, M.; Toyota, K.; Fukuda, R.; Hasegawa, J.; Ishida, M.; Nakajima, T.; Honda, Y.; Kitao, O.; Nakai, H.; Vreven, T.; Throssell, K.; Montgomery, J. A.; Peralta, J. E.; Ogliaro, F.; Bearpark, M. J.; Heyd, J. J.; Brothers, E. N.; Kudin, K. N.; Staroverov, V. N.; Keith, T. A.; Kobayashi, R.; Normand, J.; Raghavachari, K.; Rendell, A. P.; Burant, J. C.; Iyengar, S. S.; Tomasi, J.; Cossi, M.; Millam, J. M.; Klene, M.; Adamo, C.; Cammi, R.; Ochterski, J. W.; Martin, R. L.; Morokuma, K.; Farkas, O.; Foresman, J. B.; Fox, D. J. Gaussian 16, Revision A.03; Gaussian, Inc.: Wallingford CT, 2016.

[24] (a) Lee, C.; Yang, W.; Parr, R. G. Development of the Colle-Salvetti correlation-energy formula into a functional of the electron density. *Phys. Rev. B* **1988**, *37*, 785–789. (b) Becke, A. D. Density–functional thermochemistry. III. The role of exact Exchange. *J. Chem. Phys.* **1993**, *98*, 5648−5652.

[25] Hay, P. J.; Wadt, W. R. Ab initio effective core potentials for molecular calculations. Potentials for K to Au including the outermost core orbitals. *J. Chem. Phys.* **1985**, *82*, 299−310.

[26] (a) Hehre, W. J.; Ditchfield, R.; Pople, J. A. Self−consistent molecular orbital methods. XII. Further extensions of Gaussian−type basis sets for use in molecular orbital studies of organic molecules. *J. Chem. Phys*. **1972**, *56*, 2257−2261. (b) Hariharan, P. C.; Pople, J. A. The influence of polarization functions on molecular orbital hydrogenation energies. *Theor. Chim. Acta* **1973**, *28*, 213−222. (c) Francl, M. M.; Pietro, W. J.; Hehre, W. J.; Binkley, J. S.; Gordon, M. S.; Defrees, D. J.; Pople, J. A. Self−consistent molecular orbital methods. XXIII. A polarization−type basis set for second−row elements. *J. Chem. Phys*. **1982**, *77*, 3654−3665.

[27] (a) Miertus, S.; Tomasi, J. Approximate evaluations of the electrostatic free energy and internal energy changes in solution processes. *Chem. Phys.* **1982**, *65*, 239−245. (b) Mennucci, B.; Tomasi, J. Continuum solvation models: A new approach to the problem of solute's charge distribution and cavity boundaries. *J. Chem. Phys.* **1997**, *106*, 5151−5158. (c) Cossi, M.; Barone, V.; Mennucci, B.; Tomasi, J. Ab initio study of ionic solutions by a polarizable continuum dielectric model. *Chem. Phys. Lett.* **1998**, *286*, 253−260.

[28] (a) Krishnan, R.; Binkley, J. S.; Seeger, R. Pople, J. A. Self−consistent molecular orbital methods. XX. A basis set for correlated wave functions. *J. Chem. Phys.* **1980**, *72*, 650−654. (b) McLean, A. D.; Chandler, G. S. Contracted Gaussian basis sets for molecular calculations. I. Second row atoms, *Z*=11−18. *J. Chem. Phys.* **1980**, *72*, 5639−5648.

[29] (a) S. Grimme, S.; Antony, J.; Ehrlich, S.; Krieg, H. A consistent and accurate ab initio parametrization of density functional dispersion correction (DFT−D) for the 94 elements H−Pu. *J. Chem. Phys.* **2010**, *132*, 154104. (b) S. Grimme, S. Ehrlich, L. Goerigk, *J. Comput. Chem.* **2011**, *32*, 1456−1465.

[30] (a) Johnson, E.; Keinan, S.; Mori-Sánchez, P.; Contreras-García, J.; Cohen, A.; Yang, W. Revealing noncovalent interactions. *J. Am. Chem. Soc.* **2010**, *132*, 6498−6506. (b) Contreras-García, J.; Johnson, E.; Keinan, S.; Chaudret, R.; Piquemal, J.; Beratan, D.; Yang, W. NCIPLOT: A program for plotting noncovalent interaction regions. *J. Chem. Theory Comput.* **2011**, *7*, 625−632. (c) Contreras-García, J.; Yang, W.; Johnson, E. J. Analysis of hydrogen-bond interaction potentials from the electron density: integration of noncovalent interaction regions. *Phys. Chem. A* **2011**, *115*, 12983−12990.

CHAPTER 5

Pd-catalyzed [3+2] cycloaddition reaction

UNIVERSITAT ROVIRA I VIRGILI
DEVELOPMENT OF CHIRAL METAL-CATALYSTS FOR THE SELECTIVE FORMATION OF C-H, C-C AND C-X BONDS. FROM DESIGN TO APPLICATION
Pol De La Cruz Sanchez Badia

5.1. Synthesis of tetrahydrofuran-fused spirocyclic Meldrum's acid derivatives via asymmetric Pd-catalyzed [3+2] cycloaddition.

5.1.1. Introduction

Spirocyclic compounds are abundantly found in nature, and a significant number of them exhibit remarkable biological activity.[1] The optimal combination of conformational rigidity and flexibility in spirocyclic compounds plays a pivotal role in maximizing interactions with protein targets. As a result, spiro compounds have emerged as highly valuable scaffolds in the advancement of contemporary medicinal drugs.[1a,2] In this context, spirocyclic tetrahydrofurans exemplify a highly notable subclass of spiro compounds found in a diverse range of sources, including marine organisms,[3] plants,[4] insects [5] and can also have a fungal origin (Figure 5.1.1). [6] These attractive characteristics exhibited by spirocyclic tetrahydrofurans have served as a driving force behind the development of numerous synthetic pathways for their racemic or enantioselective synthesis.[7]

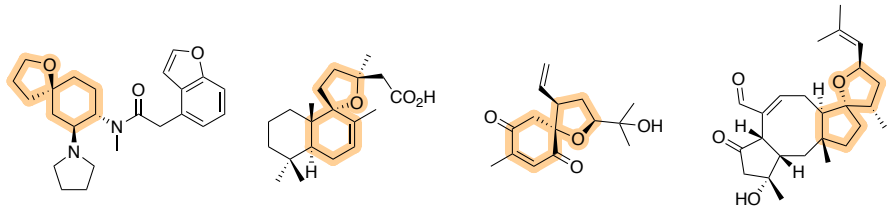

Figure 5.1.1. Representative examples of natural occurring compounds and drugs containing a chiral spirocyclic tetrahydrofuran scaffold.

Several cyclization strategies have been utilized to obtain spirocyclic tetrahydrofurans. These strategies encompass rearrangements/ring expansions, [8] epoxide opening, [9] hydroetherifications, [10] nucleophilic substitution by alcohols,[11] radical cyclizations,[12] and organocatalytic Csp^3–H functionalization.[13] In this context, cycloaddition reactions have emerged as versatile synthetic techniques, offering straightforward pathways to achieve diverse cyclic skeletons with high step economy. These methodologies are highly recognized for their ability to construct complex cyclic structures efficiently.[14] Transition-metal-catalyzed [3+2] cycloadditions represent a highly straightforward and appealing approach for the synthesis of these structures. These methods not only offer an efficient pathway to annulated complexes in a single step but also enable the simultaneous construction of multiple stereogenic centers, particularly multivicinal stereocenters, with controllable selectivity.[14]

Since Trost and Tsuji first reports, in 1979[15] and 1985[16] respectively, on the use of η-allylpalladium complexes as 1,3-dipoles with electron-deficient olefins in [3+2]

annulation, Pd-catalyzed cycloaddition reactions involving zwitterionic allylpalladium intermediates have gained considerable recognition. As discussed in the General Introduction, these transformations have become valuable methods for constructing cyclic scaffolds.[17] However, the Pd-catalyzed enantioselective synthesis of spirocyclic tetrahydrofurans with diverse structures remains underdeveloped with limited examples reported in the literature, with most of them involving the indane scaffold (Figure 5.1.2). Zhao and coworkers reported in 2016 the formal [3 + 2] cycloaddition of *para*-quinone methides with vinyl epoxides or cyclopropanes, which gave rise to a diverse array of spiro[4.5]decanes in high diastereo- and enantioselectivities (up to >20:1 dr and up to >99% ee's, Figure 5.1.2).[18] Later, in 2019, Yang and coworkers reported only one asymmetric example of the [3+2] cycloaddition of spirovinylcyclopropyl oxindole with 1-benzylindoline-2,3-dione (Figure 5.1.2), [19] albeit obtaining moderate enantioselectivities (ee's up to 71%). Later in 2020, Hu and coworkers developed the synthesis of spirooxindoles through a decarboxylative [3+2] cycloaddition of vinylethylene carbonates to methylene indolinenones (up to >20:1 dr and up to 99% ee, Figure 5.1.2).[20] In the same year, Guo's group described the decarboxylative cycloaddition of vinylethylene carbonate derivatives with several benzylidene 1,3-indandiones, resulting in spirocyclic tetrahydrofurans (up to 4:1 dr and up to 99% ee's, Figure 5.1.2).[21] More recently, Lee and coworkers, have developed a straightforward and stereodivergent [3+2] spiroannulation of vinyl ethylene carbonate with indole-based azadienes, affording all four stereoisomers in high diastereo- and enantioselectivities by simple selection of the adequate ligand (up to 13:1 dr and up to 99% ee, Figure 5.1.2).[22]

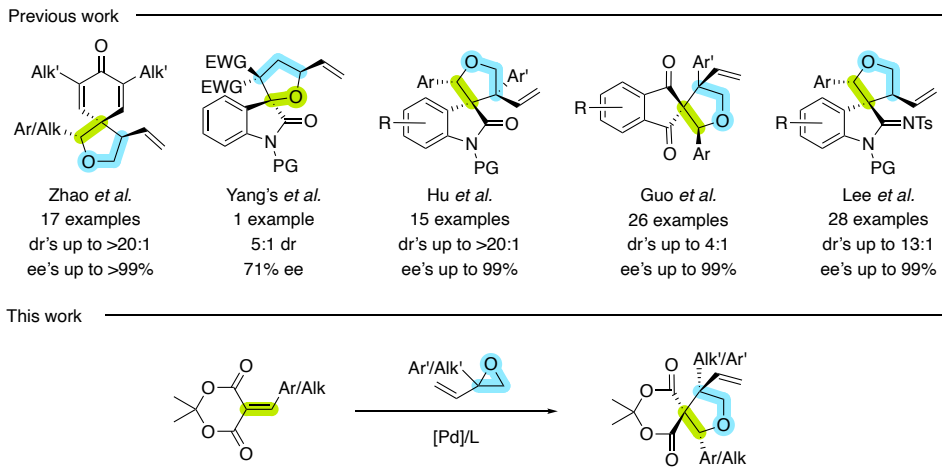

Figure 5.1.2. Precedents in the Pd-catalyzed [3+2] cycloaddition to construct structurally complex tetrahydrofuran-fused spirocyclic scaffolds.

In order to fill this gap, we envisioned a simple and straightforward methodology based on the enantioselective Pd-catalyzed [3+2] cycloaddition to construct structurally complex tetrahydrofuran-fused spirocyclic scaffolds. In the search for cross-partners for this reaction we were particularly interested in the use of 5-alkylidene Meldrum's acid derivatives as dipolarophiles, which have been scarcely studied.[23] Meldrum's acid derivatives are very easy to synthesize and their reactivity has been extensively studied, which would facilitate the access to more complex scaffolds in simple and straightforward ways (Scheme 5.1.1).[24] Therefore, in this chapter, we report a simple Pd-catalyzed [3+2] cycloaddition reaction of vinyl epoxides with 5-alkylidene Meldrum's acid derivatives for the synthesis of structurally complex tetrahydrofuran-fused spirocyclic scaffolds (Figure 5.1.2, bottom).

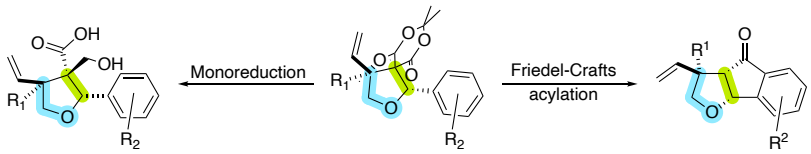

Scheme 5.1.1. Examples of more complex scaffolds that can be synthesized taking advantage of the Meldrum's acid derivatives reactivity.

5.1.2. Results and discussion

5.1.2.1. Initial screening and optimization of the reaction parameters

Initially, we studied the [3+2] cycloaddition reaction of 2-phenyl-2-vinyloxirane (**S159a**) with 5-(4-methoxybenzylidene)-2,2-dimethyl-1,3-dioxane-4,6-dione (**S160a**) under typical reaction conditions (e.g. $Pd_2dba_3{\cdot}CHCl_3$ as catalyst precursor, THF as solvent and at room temperature)[17]. The results are summarized in Table 5.1.1. It should be noted that the reaction does not proceed with the solely use of $Pd_2dba_3{\cdot}CHCl_3$ and that the formation of [5+2] cycloaddition products were not observed in any case.

We began testing some representatives of the commonly used ligand libraries for [3+2]-cycloadditions (ligands **L34**–**L36**; entries 1–3). To our surprise no reaction was observed when using PHOX ligand **L34** (entry 1). The use of diamidophosphite ligand **L35** led to formation of the spirocyclic compound **87aa** as the major diastereoisomer in almost full conversion and moderate selectivities (entry 2). The use of monophosphoramidite ligand **L36** afforded **87aa** in high yield and selectivities (entry 3). With this results in hand, we then focused on exploring a set of binol and spinol based phosphoramidite ligands (ligands **L37**–**L44**, entries 4–11). The results indicated that enantioselectivities were maximized by using phosphoramidite **L40** containing a small methyl substituent and a big $CHPh_2$ group attached to the N atom. Albeit, the diastereoselectivity decreased to 3:1. An interesting feature of the major diastereoisomer **87aa** is that it readily recrystallizes when adding isopropanol to a

concentrated dichloromethane solution of the diastereomeric mixture. Thus, by taking advantage of this feature we could attain **87aa** in good isolated yield (73%) and in excellent diastereo- and enantioselectivity (entry 12).

Table 5.1.1. Pd-catalyzed cycloaddition of **S159a** and **S160a** with ligands **L34**–**L44**.[a]

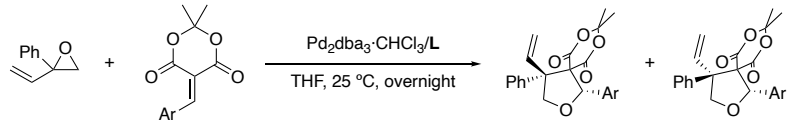

S159a **S160a** **87aa** **88aa**

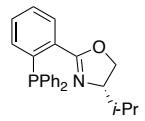

L34

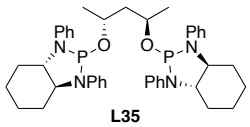

L35

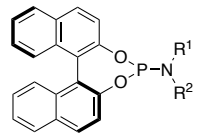

L36 R^1=R^2= *i*-Pr
L37 R^1=R^2= (*R*)-1-phenylethyl
L38 R^1=R^2= (*S*)-1-phenylethyl
L39 R^1= Me, R^2= Cy
L40 R^1= Me, R^2= $C(Ph)_2$
L41 R^1=R^2= dibenzoazepine

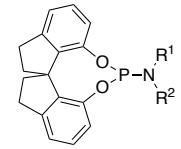

(*S*)-**L42** R^1=R^2= Me
(*R*)-**L43** R^1=R^2= (*R*)-1-phenylethyl
(*S*)-**L44** R^1=R^2= (*R*)-1-phenylethyl

Entry	Ligand	%Conv[b]	%Yield[c]	dr (**87aa**:**88aa**)[b]	%ee[d]
1	**L34**	—	—	—	—
2	**L35**	90	85	3:1	21 (*S*,*R*)
3	**L36**	100	98	8:1	93 (*S*,*R*)
4	**L37**	—	—	—	—
5	**L38**	27	19	1:1	22 (*S*,*R*)
6	**L39**	100	97	7:1	91 (*S*,*R*)
7	**L40**	100	>99	3:1	>99 (*S*,*R*)
8	**L41**	100	>99	3:1	90 (*S*,*R*)
9	**L42**	100	>99	6:1	33 (*S*,*R*)
10	**L43**	100	99	4:1	30 (*S*,*R*)
11	**L44**	50	49	2:1	63 (*S*,*R*)
12[e]	**L40**	100	73[f]	>20:1	>99 (*S*,*R*)

[a] Reaction conditions: $Pd_2(dba)_3$·$CHCl_3$ (2.5 mol%), ligand (10 mol% for **L34** and **L36**–**L44** and 5 mol% for **L35**), **S159a** (0.2 mmol), **S160a** (0.1 mmol), THF (1.0 mL), 25 ºC, overnight. [b] Measured by ^{1}H-NMR. [c] Isolated yields as a mixture of diastereomers. [d] Referred to the major diastereoisomer and determined by HPLC using a chiral stationary phase. The absolute configuration of **87aa** was confirmed by X-ray crystallography (see Figure 5.1.5). [e] Reaction carried out at 2 mmol scale. [f] Isolated yield after recrystallization.

The nature of both diastereoisomers **87aa** and **88aa** was determined by 1D-NOE (Nuclear Overhauser Effect) experiments. For example, when the methinic proton of the vinyl moiety of major product **87aa** was irradiated, a clear interaction with the methinic proton at the 2-position of the tetrahydrofuran scaffold was observed (Figure 5.1.3a). This spacial interaction indicates that both protons have a *cis* disposition. For isomer **88aa**, however, the only NOE interaction observed for the methinic proton is the one with the methyl protons of the methoxide group at the aryl group, which indicates that both groups are in *cis* disposition (Figure 5.1.3.b).

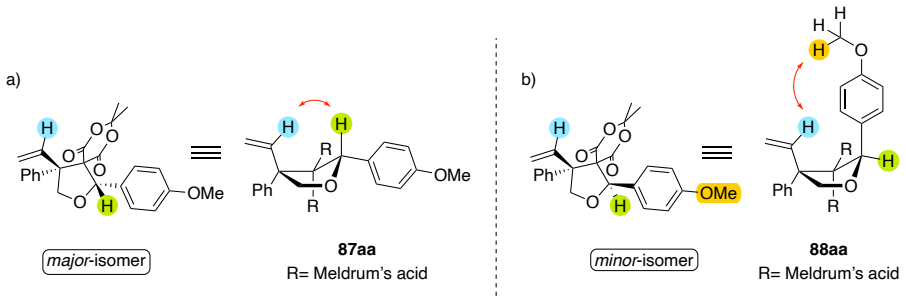

Figure 5.1.3. Representative NOE interactions with the methinic proton of: a) major product **87aa**; and b) minor product **88a**. The tetrahydrofuran scaffold is represented in a twisted conformation.

Furthermore, the absolute configuration of the major enantiomer **87aa** was determined by single X-ray diffraction after the separation of the diastereoisomers by recrystallization of an enantiopure sample (Figure 5.1.5).

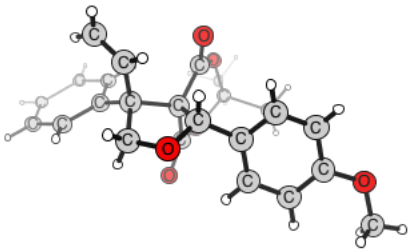

Figure 5.1.5. X-ray structure of enantiopure major (*S*,*R*)-**87aa**.

5.1.2.2. Reaction scope

With the optimal ligand in hand, we next studied the reaction scope. Firstly, a range of vinyl oxiranes **S159a–l** was examined in combination with 5-(4-methoxybenzylidene)-2,2-dimethyl-1,3-dioxane-4,6-dione **S160a** and also 2,2-dimethyl-5-(4-(trifluoromethyl)benzylidene)-1,3-dioxane-4,6-dione **S160b**. The latter was also considered because during the reaction scope we found that the use of **S160b** facilitates the determination of the enantiomeric excess of the corresponding

tetrahydrofurans (Scheme 5.1.2). A range of 2-aryl-2-vinyl oxiranes **S159a**–**h** containing both electron-donating and -withdrawing substituents at the *para* or *meta* position of the phenyl ring (R^1) were well-tolerated to produce the corresponding tetrahydrofurans in high yields and excellent enantioselectivity (ee's ≥94%). It should be noted that the different decoration of the aryl group also has little effect on the diastereoselectivity of the process. Notably, the cycloaddition of 2-alkyl-2-vinyl oxiranes proceeded well to form the corresponding tetrahydrofurans **87ja** and **87kb** in high yields and enantioselectivities (96% ee), albeit with poor-to-moderate diastereoselectivity (up to 2:1 dr). Furthermore, non-substituted 2-vinyl epoxide also reacted smoothly with **S160a** to provide product **87al** bearing two chiral tertiary carbon centers with high yield and ee.

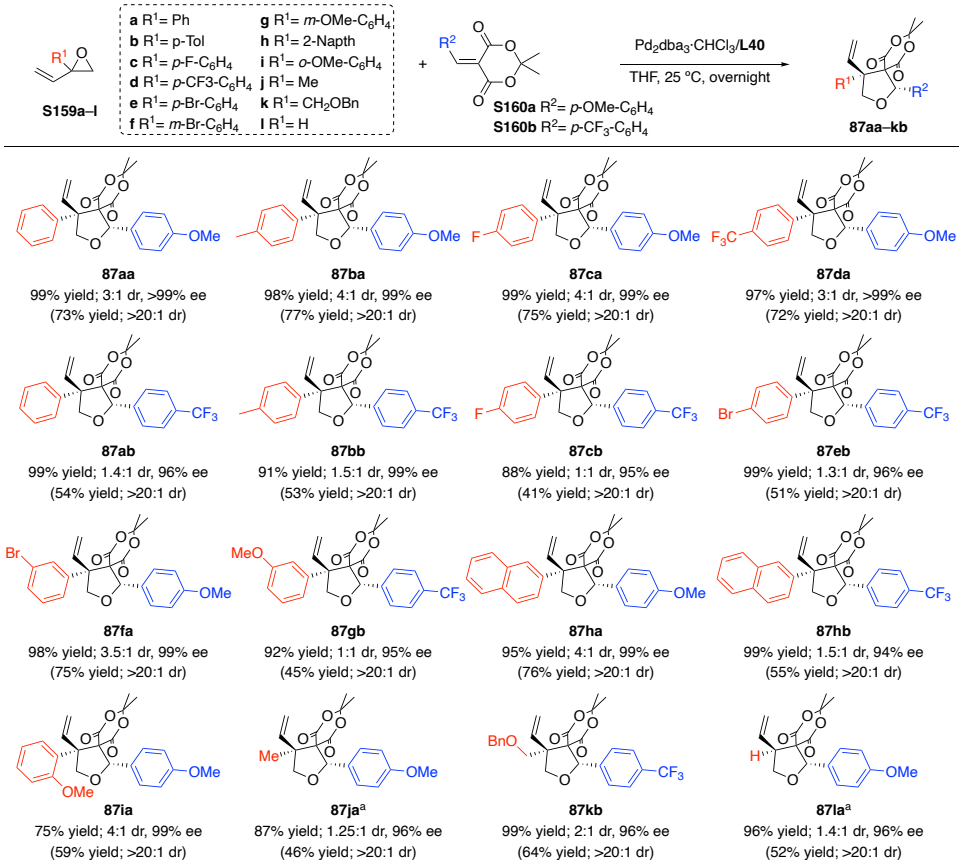

Scheme 5.1.2. Cycloaddition reactions using several vinyl oxiranes. Reactions carried out at 0.25 mmol scale. In parenthesis are shown the yields and diastereoselectivities after recrystallization. [a] Reaction carried out using 5 mol% of **L34**.

Next, a range of 5-substituted-2,2-dimethyl-1,3-dioxane-4,6-diones **S160a**–**l** was examined in combination with 2-phenyl-2-vinyloxirane **S159a** (Scheme 5.1.3). The use

of several 5-aryl alkylidene Meldrum's acid derivatives **S160a**–**h** led to the formation of the corresponding tetrahydrofurans **87aa**–**ah** in high yields and excellent enantioselectivities (ee's ≥ 98%) regardless of the aryl substitution pattern and electronic properties of the aryl substituents. Nevertheless, diastereoselectivities were affected by the electronic and steric properties of the substituents at the aryl group. Thus, whereas moderate diastereoselectivities (up to 3:1 dr) were attained for alkylidene Meldrum's acid derivatives containing *para*- and *meta*-substituents at the aryl ring, the use of *ortho* substituted ones led to better diastereoselectivities (up to 15:1 dr). The reaction also tolerated well the use of heteroaromatic alkylidene Meldrum's acid derivatives to produce tetrahydrofurans **87ai** and **87aj** in high yields with good diastereoselectivity and excellent enantiocontrol (dr's 7:1 and ee's up to 99%). Interestingly, the [3+2] cycloaddition reaction also performed well for non-aromatic alkylidenes. Thus, the use of 5-*tert*-butyl-2,2-dimethyl-1,3-dioxane-4,6-dione **S160k** afforded product **87ak** in 99% yield with an 8:1 dr and 97% ee. Notably, the cycloaddition of conjugated alkylidene Meldrum's derivative **S160l** proceeded well to form tetrahydrofuran **87al** with two distinct unsaturated substituents with a 4:1 dr and a 93% ee.

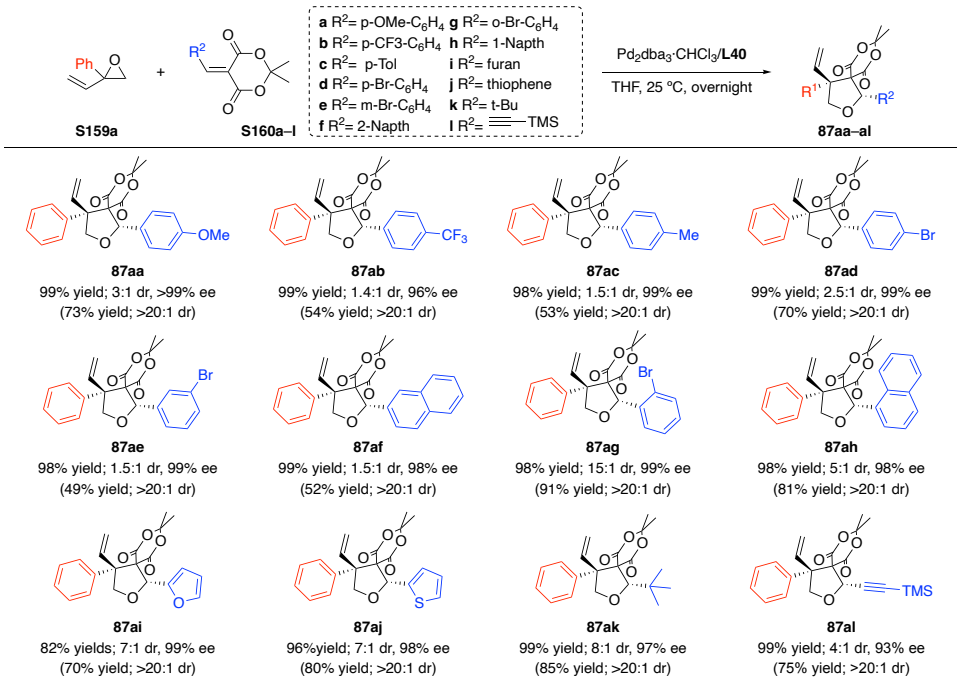

Scheme 5.1.3. Cycloaddition reactions using several 5-substituted-2,2-dimethyl-1,3-dioxane-4,6-diones. Reactions carried out at 0.25 mmol scale. In parenthesis are shown the yields and diastereoselectivities after recrystallization.

5.1.3. Conclusions

In summary, we have developed an efficient method for the synthesis of spirocyclic tetrahydrofurans via the Pd-catalyzed [3+2] cycloaddition reaction of vinyl epoxides with 5-alkylidene Meldrum's acid derivatives. By using a palladium complex generated *in situ* from $Pd_2(dba)_3{\cdot}CHCl_3$ and a phosphoramidite ligand, the cycloaddition reaction provided spiro-fused tetrahydrofurans bearing a quaternary stereocenter in high yields and enantioselectivities and good diastereoselectivities. Note that the both diastereomeric compounds are easily accessible by simple recrystallization. We were able to introduce successfully, in different positions of the tetrahydrofuran, several aryl, alkyl and heterocyclic groups with different electronic and steric abilities without compromising the high enantioselectivities obtained in the benchmark substrates. Furthermore, the stereochemistry of the major product was assigned by 1D-NOE NMR experiments and X-ray crystallography providing the absolute stereochemistry of the newly synthetized cycloadducts.

5.1.4. Experimental section

5.1.4.1. General considerations

All reactions were carried out using standard Schlenk techniques under an argon atmosphere unless otherwise noted. Commercial chemicals were used as received. Solvents were dried by means of standard procedures and stored under argon. ^{1}H, $^{13}C\{^{1}H\}$ and $^{19}F\{^{1}H\}$ NMR spectra were recorded using a Varian Mercury-400 MHz spectrometer. Chemical shifts are relative to that of NMR solvent for ^{1}H and $^{13}C\{^{1}H\}$ NMR spectra were recorded using a Varian Mercury-400 MHz spectrometer. Chemical shifts are relative to that of $SiMe_4$ (^{1}H and $^{13}C\{^{1}H\}$) as an internal standard. ^{1}H and ^{13}C assignments were made on the basis of ^{1}H-^{1}H gCOSY, ^{1}H-^{13}C gHSQC and NOESY experiments. $Pd_2(dba)_3{\cdot}CHCl_3$,[25] vinyl epoxides **S159a**,[26] **S159b**,[27] **S159c**–**e**,[26] **S159g**–**h**,[26] **S159j**,[28] and alkylidene Meldrum's acid derivatives **S160a**,[29] **S160b,**[30] **S160c**,[31] **S160d**–**e**,[30] **S160f**,[32] **S160g**–**h**,[33] **S160i**,[34] **S160j**,[30] and **S160k**[35] were prepared as previously reported in the literature. **S159l** was commercially available. Ligands tested for this transformation were all commercially available, except ligands **L39**[36] and **L40**[37] which were prepared following reported procedures. For copies of the NMR spectra, NOE experiments, X-ray data and HPLC traces see Supporting Information.

5.1.4.2. Typical procedure for the preparation of vinyl epoxides S159f and S159i

Following a reported methodology,[26] into solution of the corresponding α-bromoacetophenone (10 mmol, 1.0 equiv) in tetrahydrofuran (50 mL, 0.2 M) was added slowly vinylmagnesium bromide (15 mL, 15 mmol, 1.0 M in THF, 1.5 equiv) at 0 ºC.

The reaction mixture was kept under an ice bath for 1 hour. Then, a 1M NaOH aqueous solution (20 mL) was added. The mixture was gradually warmed to room temperature and stirred for 2 hours. Subsequently, the mixture was extracted with diethyl ether. The organic layers were combined and washed with brine, then dried using Mg_2SO_4. The organic phase was filtered, and the solvent was removed under reduced pressure using rotary evaporation. The resulting crude product was purified using Kugelrohr distillation under vacuum.

2-(3-Bromophenyl)-2-vinyloxirane (S159f). Colorless oil (1.8 g, 80% using 10 mmol of the corresponding α-bromoacetophenone). ^{1}H NMR (400 MHz, $CDCl_3$), δ= 2.96 (d, J_{H-H}= 5.5 Hz, 1H), 3.08 (d, J_{H-H}= 5.5 Hz, 1H), 5.26 (d, J_{H-H}= 17.2 Hz, 1H), 5.35 (d, J_{H-H}= 10.3 Hz, 1H), 6.01 (dd, J_{H-H}= 17.2, 10.3 Hz, 1H), 7.22-7.56 (m, 4H). ^{13}C{^{1}H} NMR (100.6 MHz, $CDCl_3$), δ= 56.8, 59.6, 119.6, 122.4, 125.6, 129.8, 130.0, 131.0, 136.4, 140.3.

2-(2-Methoxyphenyl)-2-vinyloxirane (S159i). Colorless oil (1.37 g, 77% using 10 mmol of the corresponding α-bromoacetophenone). ^{1}H NMR (400 MHz, $CDCl_3$), δ= 2.89 (d, J_{H-H}= 5.5 Hz, 1H), 2.96 (d, J_{H-H}= 5.5 Hz, 1H), 3.73 (s, 3H), 5.03 (dd, J_{H-H}= 17.1, 1.3 Hz, 1H), 5.10 (dd, J_{H-H}= 10.6, 1.3 Hz, 1H), 5.79 (dd, J_{H-H}= 17.1, 10.6 Hz, 1H), 6.78-6.86 (m, 2H), 7.25-7.28 (m, 2H) . ^{13}C{^{1}H} NMR (100.6 MHz, $CDCl_3$), δ= 55.4, 56.0, 58.6, 110.5, 117.7, 120.5, 126.4, 128.9, 129.3, 138.1, 157.4.

5.1.4.3. Preparation of 2-((benzyloxy)methyl)-2-vinyloxirane (S159k)

Following a modified procedure from the literature, [38] a solution of 2-((benzyloxy)methyl)oxirane (10.0 mmol) [39] in $CHCl_3$ (100 ml) was treated with concentrated HCl (30 mL) then stirred at room temperature until no starting material was observed (TLC). The organic phase was then washed with saturated aqueous $NaHCO_3$ and water and subsequently evaporated. The resulting crude of 1-(benzyloxy)-3-chloropropan-2-ol was used in the next step without further purification.

Then, to a stirred solution of 1-(benzyloxy)-3-chloropropan-2-ol (5.3 mmol) in acetone (11.6 mL) at 5 °C, a solution of H_2CrO_3 (prepared from H_2SO_4 (0.6 mL), CrO_3 (771 mg) and water (1.4 mL)) was added dropwise over 2 h. Next, the mixture was stirred until no starting product was observed (TLC) and subsequently quenched by the dropwise addition of 2-propanol (1.6 mL). The inorganic precipitate was then filtered off and washed with acetone (2x6 mL). The solvent was evaporated and to the resulting crude product water (70 mL) was added. The mixture was extracted with $CHCl_3$ (3x6 mL) and the organic layer washed with water (3x5 mL), dried over anhydrous Mg_2SO_4 and evaporated. The resulting crude 1-(benzyloxy)-3-chloropropan-2-ol was used in the next step without further purification. Then, the corresponding vinyl epoxide was prepared by the same means as in Section 5.1.4.2. Colorless oil (480 mg, 25% over 3 steps). ^{1}H NMR (400 MHz, $CDCl_3$), δ= 2.71 (d, J_{H-H}= 6.3 Hz, 1H), 2.94 (d, J_{H-H}= 6.3 Hz,

1H), 3.63 (d, J_{H-H}= 10.9 Hz, 1H), 3.77 (d, J_{H-H}= 10.9 Hz, 1H), 4.57 (dd, J_{H-H}= 20.8, 11.9 Hz, 1H), 5.28 (d, J_{H-H}= 11.0 Hz, 1H), 5.46 (d, J_{H-H}= 17.3 Hz, 1H), 5.86 (dd, J_{H-H}= 17.3, 11.0 Hz, 1H), 7.25-7.37 (m, 5H) . $^{13}C\{^1H\}$ NMR (100.6 MHz, $CDCl_3$), δ= 52.9, 57.6, 71.2, 73.2, 117.5, 127.7, 127.8 (2C), 128.4, 134.9, 137.8

5.1.4.4 Preparation of 2,2-dimethyl-5-(3-(trimethylsilyl)prop-2-yn-1-ylidene)-1,3-dioxane-4,6-dione (160l)

Following the method developed by Bigi *et al*.[29] a mixture of Meldrum's acid (5.5 mmol) and 3-(trimethylsilyl)propiolaldehyde (5 mmol) in water (10 mL) was stirred at 75 °C for 2 h. After cooling to room temperature the solid product was filtered and dried under vacuum. Recrystallisation in ethanol yielded the corresponding 5-alkylidene Meldrum's acid derivative in pure form. Off-white solid (570 mg, 45%). ^1H NMR (400 MHz, $CDCl_3$), δ= 0.15 (s, 9H), 1.61 (s, 6H), 7.35 (s, 1H). $^{13}C\{^1H\}$ NMR (100.6 MHz, $CDCl_3$), δ= 0.0 (3C), 28.6 (2C), 101.5, 105.9, 125.1, 128.2, 137.5, 158.8, 162.1.,

5.1.4.5. Typical procedure for the optimization of the asymmetric cycloaddition of S159a with S160a

A flame dried Schlenk was charged with $Pd_2(dba)_3{\cdot}CHCl_3$ (6.5 mg, 0.006 mmol), ligand (0.012 or 0.025 mmol, 5 or 10 mol%), 2-phenyl-2-vinyloxirane **S150a** (73 mg, 0.5 mmol) and 5-alkylidene Meldrum's acid derivative **S160a** (64.5 mg, 0.25 mmol). The reaction tube was sealed with rubber-septum, then purged with vacuum-argon cycles five times. Then, anhydrous solvent (1 mL) was added sequentially via syringe. The resulting mixture was stirred at room temperature overnight. After that, the solvent was evaporated *in vacuo*. Diastereomeric ratios were determined by NMR analysis of the crude product. Flash column chromatography on silica gel afforded the corresponding products as a mixture of diastereoisomers. The enantiomeric excess was determined by chiral HPLC, conversions were determined by ^1H NMR and isolated yields were determined after column chromatography.

1-(4-Methoxyphenyl)-8,8-dimethyl-4-phenyl-4-vinyl-2,7,9-trioxaspiro[4.5] decane-6,10-dione (87aa). The title compound was isolated through column chromatography (SiO_2, petroleum ether/ethyl acetate 4:1) as a white solid (91.9 mg, 90%). Enantiomeric excess determined by HPLC using Chiralcel AD column (90% hexane/2-propanol, flow 0.5 mL/min). t_R 31.7 min (*S,R*); t_R 35.7 min (*R*,*S*). ^1H NMR (400 MHz, $CDCl_3$), δ: 0.79 (s, 3H), 1.37 (s, 3H), 3.70 (s, 3H), 4.58 (d, J_{H-H}= 7.8 Hz, 1H), 4.81 (d, J_{H-H}= 17.0 Hz, 1H), 5.21 (d, J_{H-H}= 10.9 Hz, 1H), 5.43 (d, J_{H-H}= 7.8 Hz, 1H), 5.93 (s, 1H), 6.50 (dd, J_{H-H}= 17.0, 10.9 Hz, 1H), 6.77 (d, J_{H-H}= 8.3 Hz, 2H), 7.06 (d, J_{H-H}= 6.91 Hz, 2H), 7.19-7.30 (m, 5H). $^{13}C\{^1H\}$ NMR (100.6 MHz, $CDCl_3$), δ: 27.9, 30.1, 55.2, 64.9, 68.2, 76.4, 87.0, 105.5, 113.9 (2C), 115.4, 127.2 (2C), 127.5, 127.8, 128.5 (2C), 129.1 (2C), 138.3, 141.0, 160.2, 162.7, 165.5.

5.1.4.6. Typical procedure for the scope of the asymmetric cycloaddition of vinyl epoxides with 5-alkyledene Meldrum's acid derivatives

A flame dried Schlenk was charged with $Pd_2(dba)_3{\cdot}CHCl_3$ (6.5 mg, 0.06 mmol,), **L39** (12.8 mg, 0.025 mmol), vinyl epoxide (0.5 mmol) and 5-alkylidene Meldrum's acid derivative (0.25 mmol). The reaction tube was sealed with rubber-septum, then purged with vacuum-argon cycles five times. Then, anhydrous THF (1 mL) was added sequentially via syringe. The resulting mixture was stirred at room temperature overnight. After that, the solvent was evaporated *in vacuo*. Diastereomeric ratios were determined by NMR analysis of the crude product. Flash column chromatography on silica gel and recrystallization in *i*-PrOH/CH_2Cl_2 were performed to afford the major diastereoisomer in pure form. The enantiomeric excess was determined by chiral HPLC, conversions were determined by ^{1}H NMR and isolated yields were determined after column chromatography.

1-(4-Methoxyphenyl)-8,8-dimethyl-4-(*p*-tolyl)-4-vinyl-2,7,9-trioxaspiro[4.5] decane-6,10-dione (87ba). The title compound was isolated through column chromatography (SiO_2, petroleum ether/ethyl acetate 4:1) as a white solid (103.5 mg, 98%). Enantiomeric excess determined by HPLC using Chiralcel AD column (98% hexane/2-propanol, flow 1 mL/min). t_R 36.0 min (*R,S*); t_R 46.1 min (*S,R*). ^{1}H NMR (400 MHz, $CDCl_3$), δ: 0.79 (s, 3H), 1.43 (s, 3H), 2.25 (s, 3H), 3.70 (s, 3H), 4.55 (d, $J_{H\text{-}H}$= 7.7 Hz, 1H), 4.82 (d, $J_{H\text{-}H}$= 16.9 Hz, 1H), 5.19 (d, $J_{H\text{-}H}$= 10.0 Hz, 1H), 5.39 (d, $J_{H\text{-}H}$= 7.7 Hz, 1H), 5.92 (s, 1H), 6.48 (dd, $J_{H\text{-}H}$= 16.9, 10.0 Hz, 1H), 6.77 (d, $J_{H\text{-}H}$= 8.7 Hz, 2H), 6.94 (d, $J_{H\text{-}H}$= 8.3 Hz, 2H), 7.05 (d, $J_{H\text{-}H}$= 8.3 Hz, 2H), 7.28 (d, $J_{H\text{-}H}$= 8.7 Hz, 2H). ^{13}C{^{1}H} NMR (100.6 MHz, $CDCl_3$), δ: 21.0, 27.9, 30.2, 55.2, 64.7, 68.3, 76.4, 86.9, 105.4, 113.9 (2C), 115.2, 127.0 (2C), 127.6, 129.0 (2C), 129.2 (2C), 135.2, 137.5, 141.1, 160.2, 162.8, 165.5.

4-(4-Fluorophenyl)-1-(4-methoxyphenyl)-8,8-dimethyl-4-vinyl-2,7,9-trioxa spiro[4.5]decane-6,10-dione. (87ca). The title compound was isolated through column chromatography (SiO_2, petroleum ether/ethyl acetate 4:1) as a white solid (105.5 mg, 99%). Enantiomeric excess determined by HPLC using Chiralcel OD-H column (98% hexane/2-propanol, flow 0.5 to 1 mL/min, 60 min then 1ml/min). t_R 33.4 min (*S,R*); t_R 37.1 min (*R,S*). ^{1}H NMR (400 MHz, $CDCl_3$), δ: 0.88 (s, 3H), 1.51 (s, 3H), 3.91 (s, 3H), 4.63 (d, $J_{H\text{-}H}$= 8.2 Hz, 1H), 4.86 (d, $J_{H\text{-}H}$= 17.0 Hz, 1H), 5.31 (d, $J_{H\text{-}H}$= 10.6 Hz, 1H), 5.48 (d, $J_{H\text{-}H}$= 8.2 Hz, 1H), 6.03 (s, 1H), 6.59 (dd, $J_{H\text{-}H}$= 17.0, 10.6 Hz, 1H), 6.86 (d, $J_{H\text{-}H}$= 9.0 Hz, 2H), 7.02-7.15 (m, 4H), 7.37 (d, $J_{H\text{-}H}$= 9.0 Hz, 2H). ^{13}C{^{1}H} NMR (100.6 MHz, $CDCl_3$), δ: 27.9, 30.1, 55.2, 65.5, 68.4, 76.6, 87.0, 105.5, 113.9 (2C), 115.4, 115.6, 115.7, 127.3, 129.0 (3C), 129.1, 133.9, 140.8, 160.3, 162.8, 163.2, 165.4.

1-(4-Methoxyphenyl)-8,8-dimethyl-4-(4-(trifluoro-methyll)phenyl)-4-vinyl-2,7,9-trioxaspiro[4.5]decane-6,10-dione (87da). The title compound was isolated through column chromatography (SiO_2, petroleum ether/ethyl acetate 4:1) as a white solid (117.9 mg, 99%). Enantiomeric excess determined by HPLC using Chiralcel IA column (98% hexane/2-propanol, flow 1 mL/min). t_R 31.5 min (*S,R*); t_R 41.1 min (*R,S*). ^{1}H NMR (400 MHz, $CDCl_3$), δ: 0.77 (s, 3H), 1.45 (s, 3H), 3.71 (s, 3H), 4.60 (d, J_{H-H}= 8.2 Hz, 1H), 4.74 (d, J_{H-H}= 17.0 Hz, 1H), 5.23 (d, J_{H-H}= 11.1 Hz, 1H), 5.41 (d, J_{H-H}= 8.2 Hz, 1H), 5.93 (s, 1H), 6.48 (dd, J_{H-H}= 17.0, 11.1 Hz, 1H), 6.78 (d, J_{H-H}= 8.7 Hz, 2H), 7.19 (d, J_{H-H}= 7.4 Hz, 2H), 7.28 (d, J_{H-H}= 8.7 Hz, 2H), 7.52 (d, J_{H-H}= 7.4 Hz, 2H). ^{13}C{^{1}H} NMR (100.6 MHz, $CDCl_3$), δ: 28.1, 30.0, 55.3, 64.8, 67.9, 76.4, 87.2, 105.7, 114.0 (3C), 116.0, 125.6, 126.9, 127.6 (3C), 129.1 (3C), 140.4, 142.6, 160.4, 162.7, 165.2.

8,8-Dimethyl-4-phenyl-1-(4-(trifluoromethyl)phenyl)-4-vinyl-2,7,9-trioxa spiro[4.5]decane-6,10-dione (87ab). The title compound was isolated through column chromatography (SiO_2, petroleum ether/ethyl acetate 10:1) as a white solid (110.4 mg, 99%). Enantiomeric excess determined by HPLC using Chiralcel IA column (95% hexane/2-propanol, flow 1 mL/min). t_R 8.4 min (*R,S*); t_R 10.2 min (*S,R*). ^{1}H NMR (400 MHz, $CDCl_3$), δ: 0.83 (s, 3H), 1.38 (s, 3H), 4.60 (d, J_{H-H}= 8.6 Hz, 1H), 4.93 (d, J_{H-H}= 16.9 Hz, 1H), 5.28 (d, J_{H-H}= 11.1 Hz, 1H), 5.46 (d, J_{H-H}= 8.6 Hz, 1H), 6.05 (s, 1H), 6.50 (dd, J_{H-H}= 16.9, 11.1 Hz, 1H), 7.09-7.11 (m, 2H), 7.24-7.28 (m, 4H), 7.51 (s, 3H). ^{13}C{^{1}H} NMR (100.6 MHz, $CDCl_3$), δ: 27.7, 30.5, 64.8, 68.9, 76.2, 86.0, 105.7, 115.8, 116.2 (2C), 125.4, 125.5, 127.4 (2C), 128.0 (2C), 128.2, 128.6 (2C), 137.3, 140.1, 140.6, 162.4, 165.2

8,8-Dimethyl-4-(*p*-tolyl)-1-(4-(trifluoromethyl)phenyl)-4-vinyl-2,7,9-trioxaspiro[4.5]decane-6,10-dione (87bb). The title compound was isolated through column chromatography (SiO_2, petroleum ether/ethyl acetate 10:1) as a white solid (104.7 mg, 91%). Enantiomeric excess determined by HPLC using Chiralcel AD column (98% hexane/2-propanol, flow 1 mL/min). t_R 8.3 min (*S,R*); t_R 12.5 min (*R,S*). ^{1}H NMR (400 MHz, $CDCl_3$), δ: 0.84 (s, 3H), 1.39 (s, 3H), 2.25 (s, 3H), 4.58 (d, J_{H-H}= 8.1 Hz, 1H), 4.94 (d, J_{H-H}= 17.9 Hz, 1H), 5.26 (d, J_{H-H}= 11.3 Hz, 1H), 5.43 (d, J_{H-H}= 8.1 Hz, 1H), 6.05 (s, 1H), 6.57 (dd, J_{H-H}= 17.9, 11.3 Hz, 1H), 6.97 (d, J_{H-H}= 8.3 Hz, 2H), 7.07 (d, J_{H-H}= 8.3 Hz, 2H), 7.51 (s, 4H). ^{13}C{^{1}H} NMR (100.6 MHz, $CDCl_3$), δ: 21.0, 27.7, 30.6, 64.4, 68.3, 76.2, 85.9, 105.9, 115.9, 122.5, 125.4, 127.2 (2C), 128.0 (2C), 129.2 (2C), 131.0, 131.1, 134.1, 138.0, 140.2, 140.3, 162.4, 165.2.

4-(4-Fluorophenyl)-8,8-dimethyl-1-(4-(trifluoro-methyl)phenyl)-4-vinyl-2,7,9-trioxaspiro[4.5]decane-6,10-dione (87cb). The title compound was isolated through column chromatography (SiO_2, petroleum ether/ethyl acetate 10:1) as a white solid (102.1 mg, 88%). Enantiomeric excess determined by HPLC using Chiralcel AD column (98% hexane/2-propanol, flow 1 mL/min). t_R 12.6 min (*R,S*); t_R 15.1 min (*S,R*).

^{1}H NMR (400 MHz, $CDCl_3$), δ: 0.84 (s, 3H), 1.38 (s, 3H), 4.56 (d, J_{H-H}= 8.5 Hz, 1H), 4.90 (d, J_{H-H}= 17.3 Hz, 1H), 5.28 (d, J_{H-H}= 10.6 Hz, 1H), 5.42 (d, J_{H-H}= 8.5 Hz, 1H), 6.06 (s, 1H), 6.50 (dd, J_{H-H}= 17.3, 10.6 Hz, 1H), 6.95-7.19 (m, 4H), 7.49-7.54 (s, 4H). ^{13}C{^{1}H} NMR (100.6 MHz, $CDCl_3$), δ: 27.7, 30.5, 64.4, 76.4, 85.9, 105.8, 115.5, 115.7, 116.5, 125.4, 128.0 (2C), 129.2 (2C), 129.3 (2C), 131.1, 131.6, 132.9, 133.0, 139.8, 140.0, 162.4, 165.1.

4-(4-Bromophenyl)-8,8-dimethyl-1-(4-(trifluoro- methyl)phenyl)-4-vinyl-2,7,9-trioxaspiro[4.5]decane-6,10-dione (87eb). The title compound was isolated through column chromatography (SiO_2, petroleum ether/ethyl acetate 10:1) as a white solid (130.0 mg, 99%). Enantiomeric excess determined by HPLC using Chiralcel OAD column (95% hexane/2-propanol, flow 1 mL/min). t_R 8.3 min (*R,S*); t_R 11.5 min (*S,R*). ^{1}H NMR (400 MHz, $CDCl_3$), δ: 0.83 (s, 3H), 1.40 (s, 3H), 4.56 (d, J_{H-H}= 8.5 Hz, 1H), 4.89 (d, J_{H-H}= 16.9 Hz, 1H), 5.28 (d, J_{H-H}= 10.8 Hz, 1H), 5.40 (d, J_{H-H}= 8.5 Hz, 1H), 6.05 (s, 1H), 6.46 (dd, J_{H-H}= 16.9, 10.8 Hz, 1H), 6.97 (d, J_{H-H}= 8.6 Hz, 2H), 7.40 (d, J_{H-H}= 8.36 Hz, 2H), 7.48-7.54 (m, 4H). ^{13}C{^{1}H} NMR (100.6 MHz, $CDCl_3$), δ: 27.8, 30.5, 64.5, 68.1, 76.3, 86.1, 105.6, 116.6, 122.43, 125.5, 128.0 (2C), 129.1 (2C), 131.2, 131.5, 131.8 (2C), 136.3, 139.6, 139.8, 139.9, 162.4, 165.0.

4-(3-Bromophenyl)-1-(4-methoxyphenyl)-8,8-dimethyl-4-vinyl-2,7,9-tri oxaspiro[4.5]decane-6,10-dione (87fa). The title compound was isolated through column chromatography (SiO_2, petroleum ether/ethyl acetate 4:1) as a white solid (119.3 mg, 98%). Enantiomeric excess determined by HPLC using Chiralcel OX-H column (95% hexane/2-propanol, flow 1 mL/min). t_R 20.6 min (*S,R*); t_R 30.9 min (*R,S*). ^{1}H NMR (400 MHz, $CDCl_3$), δ: 0.87 (s, 3H), 1.61 (s, 3H), 3.80 (s, 3H), 4.66 (d, J_{H-H}= 8.0 Hz, 1H), 4.86 (d, J_{H-H}= 17.6 Hz, 1H), 5.32 (d, J_{H-H}= 10.5 Hz, 1H), 5.44 (d, J_{H-H}= 8.0 Hz, 1H), 6.00 (s, 1H), 6.54 (dd, J_{H-H}= 17.6, 10.5 Hz, 1H), 6.87 (d, J_{H-H}= 9.2 Hz, 2H), 7.04-7.07 (m, 1H), 7.24-7.44 (m, 6H). ^{13}C{^{1}H} NMR (100.6 MHz, $CDCl_3$), δ: 28.1, 30.1, 55.3, 64.7, 76.4, 87.1, 105.8, 114.0 (2C), 115.8, 122.7, 125.8 (2C), 127.1, 129.1 (2C), 130.2, 130.3, 131.0, 140.5, 140.8, 160.4, 162.7, 165.3.

4-(3-Methoxyphenyl)-8,8-dimethyl-1-(4-(trifluoro-methyl)phenyl)-4-vinyl-2,7,9-trioxaspiro[4.5]decane-6,10-dione (87gb). The title compound was isolated through column chromatography (SiO_2, petroleum ether/ethyl acetate 10:1) as a white solid (109.5 mg, 92%). Enantiomeric excess determined by HPLC using Chiralcel AD column (95% hexane/2-propanol, flow 1 mL/min). t_R 11.1 min (*R,S*); t_R 13.8 min (*S,R*). ^{1}H NMR (400 MHz, $CDCl_3$), δ: 0.83 (s, 3H), 1.42 (s, 3H), 3.72 (s, 3H), 4.60 (d, J_{H-H}= 7.9 Hz, 1H), 4.97 (d, J_{H-H}= 16.8 Hz, 1H), 5.27 (d, J_{H-H}= 10.9 Hz, 1H), 5.41 (d, J_{H-H}= 7.9 Hz, 1H), 6.03 (s, 1H), 6.45 (dd, J_{H-H}= 16.8, 10.9 Hz, 1H), 6.64-7.77 (m, 3H), 7.17-7.21 (m, 1H), 7.49-7.54 (m, 4H). ^{13}C{^{1}H} NMR (100.6 MHz, $CDCl_3$), δ: 27.6, 30.5, 55.2, 64.7, 68.1, 76.9, 86.1, 105.8, 112.2, 114.6, 116.1, 119.5, 125.4, 128.0 (3C), 129.7, 131.1, 131.4, 138.9, 139.9, 140.1, 159.5, 162.3, 165.1.

1-(4-Methoxyphenyl)-8,8-dimethyl-4-(naphthalen-2-yl)-4-vinyl-2,7,9-trioxaspiro[4.5]decane-6,10-dione (ha). The title compound was isolated through column chromatography (SiO_2, petroleum ether/ethyl acetate 4:1) as a white solid (108.8 mg, 95%). Enantiomeric excess determined by HPLC using Chiralcel OJ-H column (95% hexane/2-propanol, flow 1 mL/min). t_R 29.6 min (*R,S*); t_R 37.6 min (*S,R*). ^{1}H NMR (400 MHz, $CDCl_3$), δ: 0.88 (s, 3H), 1.54 (s, 3H), 3.80 (s, 3H), 4.77 (d, J_{H-H}= 8.1 Hz, 1H), 4.89 (d, J_{H-H}= 16.7 Hz, 1H), 5.32 (d, J_{H-H}= 10.4 Hz, 1H), 5.67 (d, J_{H-H}= 8.1 Hz, 1H), 6.09 (s, 1H), 6.69 (dd, J_{H-H}= 16.7, 10.4 Hz, 1H), 6.87 (d, J_{H-H}= 9.1 Hz, 2H), 7.25-7.27 (m, 1H), 7.40 (d, J_{H-H}= 8.3 Hz, 2H), 7.05 (d, J_{H-H}= 8.3 Hz, 2H), 7.28 (d, J_{H-H}= 8.3 Hz, 2H), 7.50-7.53 (m, 2H), 7.63 (s, 1H), 7.79-7.85 (m, 3H). $^{13}C\{^1H\}$ NMR (100.6 MHz, $CDCl_3$), δ: 28.0, 30.2, 55.3, 65.1, 68.2, 77.2, 87.1, 105.6, 114.0 (2C), 115.6, 125.1, 126.2, 126.5, 126.6, 127.5, 127.9, 128.3, 129.1 (2C), 132.5, 133.0, 135.6, 140.9 (2C), 160.3, 162.7, 165.6.

8,8-Dimethyl-4-(naphthalen-2-yl)-1-(4-(trifluoromethyl)phenyl)-4-vinyl-2,7,9-trioxaspiro[4.5]decane-6,10-dione (87hb). The title compound was isolated through column chromatography (SiO_2, petroleum ether/ethyl acetate 10:1) as a white solid (122.8 mg, 99%). Enantiomeric excess determined by HPLC using Chiralcel AD column (95% hexane/2-propanol, flow 1 mL/min). t_R 10.8 min (*R,S*); t_R 14.7 min (*S,R*). ^{1}H NMR (400 MHz, $CDCl_3$), δ: 0.84 (s, 3H), 1.39 (s, 3H), 4.70 (d, J_{H-H}= 8.1 Hz, 1H), 4.93 (d, J_{H-H}= 16.8 Hz, 1H), 5.29 (d, J_{H-H}= 10.7 Hz, 1H), 5.61 (d, J_{H-H}= 8.1 Hz, 1H), 6.12 (s, 1H), 6.60 (dd, J_{H-H}= 16.8, 10.7 Hz, 1H), 7.19-7.22 (m, 1H), 7.43-7.45 (m, 2H), 7.53-7.56 (m, 5H), 7.71-7.76 (m, 3H). $^{13}C\{^1H\}$ NMR (100.6 MHz, $CDCl_3$), δ: 27.7, 30.5, 65.1, 68.2, 76.6, 86.2, 105.8 (2C), 116.4 (2C), 125.1, 125.5, 126.5 (2C), 126.7 (3C), 127.6, 128.0 (2C), 128.3, 132.6, 132.9, 134.6, 140.1 (2C), 162.4, 165.7.

4-(2-Methoxyphenyl)-1-(4-methoxyphenyl)-8,8-dimethyl-4-vinyl-2,7,9-trioxaspiro[4.5]decane-6,10-dione (87ia). The title compound was isolated through column chromatography (SiO_2, petroleum ether/ethyl acetate 4:1) as a white solid (82.2 mg, 75%). Enantiomeric excess determined by HPLC using Chiralcel OX-H column (80% hexane/2-propanol, flow 1 mL/min). t_R 13.3 min (*R,S*); t_R 15.9 min (*S,R*). ^{1}H NMR (400 MHz, $CDCl_3$), δ: 0.61 (s, 3H), 1.37 (s, 3H), 3.66 (s, 3H), 3.70 (s, 3H), 4.62 (d, J_{H-H}= 8.0 Hz, 1H), 4.83 (d, J_{H-H}= 17.1 Hz, 1H), 5.09 (d, J_{H-H}= 9.9 Hz, 1H), 5.51 (d, J_{H-H}= 8.0 Hz, 1H), 5.80 (s, 1H), 6.62 (dd, J_{H-H}= 17.1, 9.9 Hz, 1H), 6.79 (m, 3H), 6.91 (m, 2H), 7.20 (m, 1H), 7.27 (d, J_{H-H}= 9.2 Hz, 2H). $^{13}C\{^1H\}$ NMR (100.6 MHz, $CDCl_3$), δ: 28.3, 29.5, 54.3, 55.3, 66.7, 88.8, 105.0, 111.8, 112.7, 114.0 (3C), 121.5, 127.5, 127.9, 128.3, 129.0 (3C), 129.2, 140.0, 156.0, 160.4, 163.3, 164.4.

1-(4-Methoxyphenyl)-4,8,8-trimethyl-4-vinyl-2,7,9-trioxaspiro[4.5]decane 6,10-dione (87ja). The title compound was isolated through column chromatography (SiO_2, petroleum ether/ethyl acetate 4:1) as a white solid (75.3 mg, 87%). Enantiomeric excess determined by HPLC using Chiralcel IB column (98% hexane/2-propanol, flow 1

mL/min). t_R 9.2 min (*S,S*); 15.2 min (*R,R*). ^{1}H NMR (400 MHz, $CDCl_3$), δ: 1.14 (s, 3H), 1.23 (s, 3H), 1.56 (s, 3H), 3.70 (s, 3H), 4.15 (d, J_{H-H}= 9.8 Hz, 1H), 4.27 (d, J_{H-H}= 9.8 Hz, 1H), 5.23 (d, J_{H-H}= 17.4 Hz, 1H), 5.25 (d, J_{H-H}= 10.5 Hz, 1H), 5.87 (s, 1H), 6.58 (dd, J_{H-H}= 17.4, 10.5 Hz, 1H), 6.75 (d, J_{H-H}= 8.7 Hz, 2H), 7.26 (d, J_{H-H}= 8.7 Hz, 1H). ^{13}C{^{1}H} NMR (100.6 MHz, $CDCl_3$), δ: 19.0, 28.2, 30.4, 55.2, 56.3, 68.8, 77.8, 85.2, 105.1, 113.5 (2C), 115.3, 128.2 (2C), 128.3, 139.6, 159.6, 163.5, 165.9.

4-((Benzyloxy)methyl)-8,8-dimethyl-1-(4-(trifluoromethyl)phenyl)-4-vinyl-2,7,9-trioxaspiro[4.5]decane-6,10-dione (87kb). The title compound was isolated through column chromatography (SiO_2, petroleum ether/ethyl acetate 4:1) as a white solid (120.1 mg, 98%). Enantiomeric excess determined by HPLC using Chiralcel IA column (98% hexane/2-propanol, flow 0.5 mL/min). t_R 27.9 min (*S,S*); t_R 31.7 min (*R,R*). ^{1}H NMR (400 MHz, $CDCl_3$), δ: 1.21 (s, 3H), 1.27 (s, 3H), 3.56 (d, J_{H-H}= 8.7 Hz, 1H), 3.82 (d, J_{H-H}= 9.7 Hz, 1H), 4.04 (dd, J_{H-H}= 13.2, 8.7 Hz, 2H), 4.24 (d, J_{H-H}= 11.2 Hz, 1H), 4.33 (d, J_{H-H}= 11.2 Hz, 1H), 45.34 (dd, J_{H-H}= 17.5, 10.5 Hz, 2H), 5.74 (s, 1H), 6.11 (dd, J_{H-H}= 17.5, 10.5 Hz, 1H), 7.21-7.22 (m, 5H), 7.36 (d, J_{H-H}= 7.8 Hz, 2H), 7.50 (d, J_{H-H}= 7.8 Hz, 2H). ^{13}C{^{1}H} NMR (100.6 MHz, $CDCl_3$), δ: 28.3, 29.6, 60.9, 64.9, 72.3, 73.4, 74.9, 89.5, 106.0, 117.6, 122.5, 125.1, 125.2, 126.5, 128.0, 128.3, 128.5, 130.1, 130.4, 130.7, 131.1, 136.7, 136.8, 139.9, 163.4, 166.4.

1-(4-Methoxyphenyl)-8,8-dimethyl-4-vinyl-2,7,9-trioxaspiro[4.5]decane-6,10 -dione (87ia). The title compound was isolated through column chromatography (SiO_2, petroleum ether/ethyl acetate 4:1) as a white solid (79.7 mg, 96%). Enantiomeric excess determined by HPLC using Chiralcel OD-H column (90% hexane/2-propanol, flow 1 mL/min). t_R 8.0 min (*S,S*), t_R 12.6 min (*R,R*). ^{1}H NMR (400 MHz, $CDCl_3$), δ: 1.05 (s, 3H), 1.48 (s, 3H), 3.72 (s, 3H), 4.03-4.07 (m, 1H), 4.25-4.38 (m, 2H), 5.16 (d, J_{H-H}= 10.5 Hz, 1H), 5.26 (d, J_{H-H}= 17.2 Hz, 1H), 5.43 (s, 1H), 5.68-5.75 (m, 1H), 6.78 (d, J_{H-H}= 6.7 Hz, 2H), 7.19 (d, J_{H-H}= 6.7 Hz, 1H). ^{13}C{^{1}H} NMR (100.6 MHz, $CDCl_3$), δ: 27.1, 29.5, 54.0, 54.2, 64.8, 71.3, 89.7, 104.6, 112.8 (2C), 120.5, 125.5, 126.8 (2C), 131.0, 159.3, 162.3, 166.7.

8,8-Dimethyl-4-phenyl-1-(*p*-tolyl)-4-vinyl-2,7,9-trioxaspiro[4.5]decane-6,10-dione (8ac). The title compound was isolated through column chromatography (SiO_2, petroleum ether/ethyl acetate 10:1) as a white solid (97.1 mg, 99%). Enantiomeric excess determined by HPLC using Chiralcel OX-H column (95% hexane/2-propanol, flow 1 mL/min). t_R 12.4 min (*S,R*); t_R 18.2 min (*R,S*). ^{1}H NMR (400 MHz, $CDCl_3$), δ: 0.77 (s, 3H), 1.41 (s, 3H), 2.23 (s, 3H), 4.58 (d, J_{H-H}= 7.9 Hz, 1H), 4.82 (d, J_{H-H}= 16.2 Hz, 1H), 5.21 (d, J_{H-H}= 10.3 Hz, 1H), 5.44 (d, J_{H-H}= 7.9 Hz, 1H), 5.95 (s, 1H), 6.51 (dd, J_{H-H}= 16.2, 10.3 Hz, 1H), 7.04-7.08 (m, 4H), 7.19-7.26 (m, 5H). ^{13}C{^{1}H} NMR (100.6 MHz, $CDCl_3$), δ: 21.2, 28.0, 30.1, 64.9, 68.2, 76.4, 87.1, 105.5, 115.4, 127.2 (2C), 127.5 (2C), 127.8, 128.5 (2C), 129.2 (2C), 132.5, 138.2, 139.0, 140.0, 162.6, 165.4.

1-(4-Bromophenyl)-8,8-dimethyl-4-phenyl-4-vinyl-2,7,9-trioxaspiro[4.5] decane-6,10-dione (87ad). The title compound was isolated through column chromatography (SiO_2, petroleum ether/ethyl acetate 10:1) as a white solid (112.0 mg, 98%). Enantiomeric excess determined by HPLC using Chiralcel AD column (98% hexane/2-propanol, flow 1 mL/min). t_R 22.2 min (*R,S*); t_R 28.2 min (*S,R*). ^{1}H NMR (400 MHz, $CDCl_3$), δ: 0.93 (s, 3H), 1.47 (s, 3H), 4.65 (d, J_{H-H}= 7.9 Hz, 1H), 4.96 (d, J_{H-H}= 16.8 Hz, 1H), 5.32 (d, J_{H-H}= 10.3 Hz, 1H), 5.50 (d, J_{H-H}= 7.9 Hz, 1H), 6.02 (s, 1H), 6.56 (dd, J_{H-H}= 16.8, 10.3 Hz, 1H), 7.14 (d, J_{H-H}= 7.2 Hz, 2H), 7.29-7.35 (m, 5H), 7.45 (d, J_{H-H}= 7.2 Hz, 2H). ^{13}C{^{1}H} NMR (100.6 MHz, $CDCl_3$), δ: 27.7, 30.5, 64.8, 68.1, 76.2, 86.2, 105.6, 115.9, 123.1, 127.2 (2C), 128.1, 128.6 (2C), 129.3 (2C), 131.6 (2C), 134.9, 137.5, 150.3, 162.5, 165.2.

1-(3-Bromophenyl)-8,8-dimethyl-4-phenyl-4-vinyl-2,7,9-trioxaspiro[4.5] decane-6,10-dione (87ae). The title compound was isolated through column chromatography (SiO_2, petroleum ether/ethyl acetate 10:1) as a white solid (112.1 mg, 98%). Enantiomeric excess determined by HPLC using Chiralcel AD column (98% hexane/2-propanol, flow 1 mL/min). t_R 15.3 min (*R,S*); t_R 25.6 min (*S,R*). ^{1}H NMR (400 MHz, $CDCl_3$), δ: 0.99 (s, 3H), 1.49 (s, 3H), 4.67 (d, J_{H-H}= 8.1 Hz, 1H), 4.98 (d, J_{H-H}= 17.3 Hz, 1H), 5.35 (d, J_{H-H}= 11.0 Hz, 1H), 5.53 (d, J_{H-H}= 8.1 Hz, 1H), 6.06 (s, 1H), 6.58 (dd, J_{H-H}= 17.3, 11.0 Hz, 1H), 7.17-7.46 (m, 8H), 7.45 (s, 1H). ^{13}C{^{1}H} NMR (100.6 MHz, $CDCl_3$), δ: 27.8, 30.5, 64.84, 68.2, 75.3, 86.0, 105.7, 116.0, 122.6, 126.1, 127.3 (2C), 128.1, 128.6 (2C), 130.1, 130.5, 132.2, 137.4, 138.3, 140.3, 162.4, 165.2.

8,8-Dimethyl-1-(naphthalen-2-yl)-4-phenyl-4-vinyl-2,7,9-trioxaspiro[4.5] decane-6,10-dione (87af). The title compound was isolated through column chromatography (SiO_2, petroleum ether/ethyl acetate 10:1) as a white solid (105.3 mg, 99%). Enantiomeric excess determined by HPLC using Chiralcel AD column (80% hexane/2-propanol, flow 1 mL/min). t_R 15.5 min (*R,S*); t_R 25.0 min (*S,R*). ^{1}H NMR (400 MHz, $CDCl_3$), δ: 0.72 (s, 3H), 1.43 (s, 3H), 4.72 (d, J_{H-H}= 8.4 Hz, 1H), 4.97 (d, J_{H-H}= 16.5 Hz, 1H), 5.34 (d, J_{H-H}= 10.3 Hz, 1H), 5.60 (d, J_{H-H}= 8.4 Hz, 1H), 6.26 (s, 1H), 6.64 (dd, J_{H-H}= 16.5, 10.3 Hz, 1H), 7.17-7-19 (m, 2H), 7.26-7.34 (m, 3H), 7.46-7.56 (m, 3H), 7.79-7.81 (m, 3H), 7.93 (s, 1H). ^{13}C{^{1}H} NMR (100.6 MHz, $CDCl_3$), δ: 27.8, 30.2, 64.9, 68.3, 76.4. 87.1, 87.2, 105.6, 115.7, 124.8, 126.4, 126.5, 127.0, 127.3, 127.6, 127.9, 128.2, 128.3, 128.5, 132.9, 133.2, 133.5, 137.8, 140.7, 140.8, 162.6, 165.5.

1-(2-Bromophenyl)-8,8-dimethyl-4-phenyl-4-vinyl-2,7,9-trioxaspiro[4.5] decane-6,10-dione (87ag). The title compound was isolated through column chromatography (SiO_2, petroleum ether/ethyl acetate 10:1) as a white solid (112.0 mg, 98%). Enantiomeric excess determined by HPLC using Chiralcel OX-H column (98% hexane/2-propanol, flow 1 mL/min). t_R 16.1 min (*S,R*); t_R 20.2 min (*R,S*). ^{1}H NMR (400 MHz, $CDCl_3$), δ: 1.13 (s, 3H), 1.54 (s, 3H), 4.58 (d, J_{H-H}= 8.4 Hz, 1H), 4.73 (d, J_{H-H}= 17.8 Hz, 1H), 5.25 (d, J_{H-H}= 11.4 Hz, 1H), 5.59 (d, J_{H-H}= 8.4 Hz, 1H), 6.45 (s, 1H), 6.73

(dd, J_{H-H}= 17.8, 11.4 Hz, 1H), 7.12-7.14 (m, 3H), 7.26-7.36 (m, 4H), 7.47(d, J_{H-H}= 7.9 Hz, 1H), 7.39 (d, J_{H-H}= 7.9 Hz, 1H).$^{13}C\{^1H\}$ NMR (100.6 MHz, $CDCl_3$), δ: 28.4, 29.9, 66.5, 66.9, 77.5. 85.4, 105.3, 122.5, 127.4 (3C), 127.7, 128.5 (3C), 130.4, 132.0, 132.4, 136.1, 137.6, 141.2 (2C), 162.8, 164.3.

8,8-Dimethyl-1-(naphthalen-1-yl)-4-phenyl-4-vinyl-2,7,9-trioxaspiro[4.5] decane-6,10-dione (87ah). The title compound was isolated through column chromatography (SiO_2, petroleum ether/ethyl acetate 10:1) as a white solid (104.5 mg, 98%). Enantiomeric excess determined by HPLC using Chiralcel AD column (95% hexane/2-propanol, flow 1 mL/min). t_R 17.8 min (*R,S*); t_R 35.7 min (*S,R*). ^1H NMR (400 MHz, $CDCl_3$), δ: 0.16 (s, 3H), 1.27 (s, 3H), 4.61 (d, J_{H-H}= 7.9 Hz, 1H), 4.76 (d, J_{H-H}= 16.7 Hz, 1H), 5.21 (d, J_{H-H}= 10.4 Hz, 1H), 5.59 (d, J_{H-H}= 7.9 Hz, 1H), 6.68 (dd, J_{H-H}= 16.7, 10.4 Hz, 1H), 6.84 (s, 1H), 7.02-7.05 (m, 2H), 7.21-7.23 (m, 2H), 7.34-7.43 (m, 3H), 7.67-7.70 (m, 2H), 7.86-7.94 (m, 2H). $^{13}C\{^1H\}$ NMR (100.6 MHz, $CDCl_3$), δ: 28.2, 29.0, 66.1, 67.6, 77.1, 82.8, 105.1, 115.1, 123.0, 125.6, 125.7, 126.9, 127.2 (2C), 127.8, 128.5 (2C), 128.9, 129.4, 130.6, 131.5, 133.3, 138.2, 141.6 (2C), 162.6, 165.5.

1-(Furan-2-yl)-8,8-dimethyl-4-phenyl-4-vinyl-2,7,9-trioxaspiro[4.5]-decane-6,10-dione (87ai). The title compound was isolated through column chromatography (SiO_2, petroleum ether/ethyl acetate 4:1) as a white solid (81.0 mg, 88%). Enantiomeric excess determined by HPLC using Chiralcel AD column (95% hexane/2-propanol, flow 1 mL/min). t_R 14.3 min (*R,S*); t_R 31.6 min (*S,R*). ^1H NMR (400 MHz, $CDCl_3$), δ: 1.12 (s, 3H), 1.56 (s, 3H), 4.53 (d, J_{H-H}= 9.2 Hz, 1H), 4.87 (d, J_{H-H}= 16.7 Hz, 1H), 5.27 (d, J_{H-H}= 10.3 Hz, 1H), 5.44 (d, J_{H-H}= 9.2 Hz, 1H), 6.02 (s, 1H), 6.35-6.36 (m, 1H), 6.46-6.53 (m, 2H), 7.12-7-14 (m, 2H), 7.26-7.35 (m, 5H). $^{13}C\{^1H\}$ NMR (100.6 MHz, $CDCl_3$), δ: 27.7, 29.5, 64.9, 66.3, 76.2, 81.1, 105.5, 110.7, 111.2, 115.8, 127.2 (2C), 128.0, 128.6 (2C), 137.5, 140.3, 142.5. 149.0, 162.9, 165.0.

8,8-Dimethyl-4-phenyl-1-(thiophen-2-yl)-4-vinyl-2,7,9-trioxaspiro[4.5] decane-6,10-dione (87aj). The title compound was isolated through column chromatography (SiO_2, petroleum ether/ethyl acetate 4:1) as a white solid (89.3 mg, 93%). Enantiomeric excess determined by HPLC using Chiralcel IA column (80% hexane/2-propanol, flow 1 mL/min). t_R 7.5 min (*R,S*); t_R 11.1 min (*S,R*). ^1H NMR (400 MHz, $CDCl_3$), δ: 0.95 (s, 3H), 1.52 (s, 3H), 4.63 (d, J_{H-H}= 8.2 Hz, 1H), 4.93 (d, J_{H-H}= 17.3 Hz, 1H), 5.30 (d, J_{H-H}= 11.4 Hz, 1H), 5.48 (d, J_{H-H}= 8.2 Hz, 1H), 6.27 (s, 1H), 6.50 (dd, J_{H-H}= 17.3, 11.4 Hz, 1H), 6.94-6.96 (m, 2H), 7.26-7.32 (m, 4H). $^{13}C\{^1H\}$ NMR (100.6 MHz, $CDCl_3$), δ: 27.8, 30.2, 76.0, 83.5, 105.7, 115.7, 126.6 (2C), 127.1 (2C), 127.2, 127.3, 128.0, 128.6 (2C), 137.9, 137.9, 140.5 (2C), 163.1, 165.1.

1-(*tert*-Butyl)-8,8-dimethyl-4-phenyl-4-vinyl-2,7,9-trioxaspiro[4.5]decane -6,10-dione (87ak). The title compound was isolated through column chromatography (SiO_2, petroleum ether/ethyl acetate 10:1) as a white solid (88.7 mg, 99%).

Enantiomeric excess determined by HPLC using Chiralcel AD column (98% hexane/2-propanol, flow 0.5 mL/min). (*R,S*); t_R 23.2 min (*S,R*). ^{1}H NMR (400 MHz, $CDCl_3$), δ: 0.93 (s, 9H), 1.21 (s, 3H), 1.63 (s, 3H), 4.33 (d, J_{H-H}= 7.4 Hz, 1H), 6.27 (s, 1H), 4.93 (s, 1H), 4.93 (d, J_{H-H}= 16.8 Hz, 1H), 5.23 (d, J_{H-H}= 11.4 Hz, 1H), 5.34 (d, J_{H-H}= 7.4 Hz, 1H), 6.59 (dd, J_{H-H}= 16.8, 11.4 Hz, 1H), 6.16-7.26 (m, 5H). $^{13}C\{^1H\}$ NMR (100.6 MHz, $CDCl_3$), δ: 27.1 (3C), 29.4, 29.5, 34.6, 62.9, 63.0, 73.2, 94.5, 105.8, 115.6, 128.0, 128.1, 128.5, 128.8, 137.4, 141.2, 143.4, 163.1, 164.5.

8,8-Dimethyl-4-phenyl-1-((trimethylsilyl)ethynyl)-4-vinyl-2,7,9-trioxaspiro [4.5]decane-6,10-dione (87al). The title compound was isolated through column chromatography (SiO_2, petroleum ether/ethyl acetate 10:1) as a white solid (98.6 mg, 99%). Enantiomeric excess determined by HPLC using Chiralcel OX-H column (90% hexane/2-propanol, flow 1 mL/min). t_R 5.2 min (*S,R*); t_R 6.5 min (*R,S*). ^{1}H NMR (400 MHz, $CDCl_3$), δ: 0.12 (s, 9H), 1.62 (s, 3H), 1.76 (s, 3H), 4.43 (d, J_{H-H}= 8.2 Hz, 1H), 4.81 (d, J_{H-H}= 17.9 Hz, 1H), 5.23 (d, J_{H-H}= 10.8 Hz, 1H), 5.36 (d, J_{H-H}= 8.2 Hz, 1H), 5.58 (s, 1H), 6.39 (dd, J_{H-H}= 17.9, 10.8 Hz, 1H), 7.10-7-12 (m, 2H), 7.30-7.33 (m, 3H). $^{13}C\{^1H\}$ NMR (100.6 MHz, $CDCl_3$), δ: -0.5 (3C), 27.3, 31.4, 65.7, 67.3, 74.8, 76.6, 95.9, 99.5, 105.4, 116.4, 127.4 (2C), 128.2, 128.5 (2C), 136.3, 139.4, 163.3, 165.1.

5.1.5. References

[1] For some reviews and exampels, see: (a) Chupakhin, E.; Babich, O.; Prosekov, A.; Asyakina, L.; Krasavin, M. Spirocyclic Motifs in Natural Products. *Molecules* **2019**, *24*, 4165. (b) Yadav, P.; Pratap, R.; Ji Ram, V. Naturaland Synthetic Spirobutenolides and Spirobutyrolactones. *Asian J. Org.Chem*. **2020**, *9*, 1377−1409. (c) Xie, J.; Wang, J.; Dong, G. Synthetic Study of Phainanoids. Highly Diastereoselective Construction of the 4,5-Spirocycle via Palladium-Catalyzed Intra-molecular Alkenylation. *Org. Lett.* **2017**, *19*, 3017−3020. (d) Half-penny, P. R.; Horwell, D. C.; Hughes, J.; Hunter, J. C.; Rees, D. C. Highly selective kappa-opioid analgesics. 3. Synthesis and structure-activity relationships of novel N-[2-(1-pyrrolidinyl)-4- or −5-substituted cyclohexyl]arylacetamide derivatives. *J. Med. Chem*. **1990**, *33*, 286−291. (e) Katsoulis, I. A.; Kythreoti, G.;Papakyriakou, A.; Koltsida, K.; Anastasopoulou, P.; Stathakis, C. I.;Mavridis, I.; Cottin, T.; Saridakis, E.; Vourloumis, D. Synthesis of 5,6-Spiroethers and Evaluation of their Affinities for the Bacterial A Site. *ChemBioChem*. **2011**, *12*, 1188−1192. (f) Yang, L.; Morriello, G.;Prendergast, K.; Cheng, K.; Jacks, T.; Chan, W. W.-S.; Schleim, K. D.;Smith, R. G.; Patchett, A. A. Potent 3-spiropiperidine growthhormone secretagogues. *Bioorg. Med. Chem. Lett*. **1998**, *8*, 107−112.

[2] Zheng, Y.; Tice, C. M.; Singh, S. B. The use of spirocyclic scaffolds in drug discovery. *Bioorg. Med. Chem. Lett*. **2014**, *24*, 3673−3682.

[3] Schmitz, F. J.; McDonald, F. J.; Vanderah, D. J. Marine natural products: sesquiterpene alcohols and ethers from the sea hare aplysia dactylomela. *J. Org. Chem*. **1978**, *43*, 4220−4225.

[4] (a) Panizzi, L.; Mangoni, L.; Belardini, M. The structure of grindelic acid, a new diterpene acid. *Tetrahedron Lett*. **1961**, *2*, 376−381. (b) Lee, E.; Lee, D. S.; Choi, Y. W.; Lee, K. H. Stereoselective reduction of α-iodospirolactones. Total synthesis of (±)-liguloxide. *Tetrahedron Lett.* **1992**, *33*, 6673−6676. (c) Hirasawa, Y.; Morita, H.; Shiro, M.; Kobayashi, J. i. Sieboldine A, a Novel Tetracyclic Alkaloid from Lycopodium sieboldii, Inhibiting Acetylcholinesterase. *Org. Lett*. **2003**, *5*, 3991−3993. (d) Miyawaki, A.; Kikuchi, D.; Niki, M.; Manabe, Y.; Kanematsu, M.; Yokoe, H.; Yoshida, M.;

Shishido, K. Total Synthesis of Natural Enantiomers of Heliespirones A and C via the Diastereoselective Intramolecular Hosomi-Sakurai Reaction. *J. Org. Chem*. **2012**, *77*, 8231−8243.

[5] For a review on insect's pheromones including spiroacetal moieties, see: Booth, Y. K.; Kitching, W.; De Voss, J. J. Biosynthesis of insect spiroacetals. *Nat. Prod. Rep*. **2009**, *26*, 490−525.

[6] (a) Bhatia, D. R.; Dhar, P.; Mutalik, V.; Deshmukh, S. K.; Verekar, S. A.; Desai, D. C.; Kshirsagar, R.; Thiagarajan, P.; Agarwal, V. Anticancer activity of Ophiobolin A, isolated from the endophytic fungus Bipolaris setariae. *Nat. Prod. Res*. **2016**, *30*, 1455−1458. (b) Thach, D. Q.; Brill, Z. G.; Grover, H. K.; Esguerra, K. V.; Thompson, J. K.; Maimone, T. J. Total Synthesis of (+)-6-epi-Ophiobolin A. *Angew. Chem. Int. Ed*. **2020**, *59*, 1532−1536.

[7] For representative reviews, see: (a) Rosenberg, S.; Leino, R. Synthesis of Spirocyclic Ethers. Synthesis **2009**, *2009*, 2651−2673. (b) Rios, R. Enantioselective methodologies for the synthesis of spiro compounds. *Chem. Soc. Rev*. **2012**, *41*, 1060−1074. (c) Xu, P.-W.; Yu, J.-S.; Chen, C.; Cao, Z.-Y.; Zhou, F.; Zhou, J. Catalytic Enantioselective Construction of Spiro Quaternary Carbon Stereo-centers. *ACS Catal*. **2019**, *9*, 1820−1882.

[8] (a) Lord, M. D.; Negri, J. T.; Paquette, L. A. Oxonium ion-initiated pinacolic ring expansion reactions. Application to the enantioselective synthesis of the spirocyclic sesquiterpene ethers dactyloxene-B and -C. *J. Org. Chem*. **1995**, *60*, 191−195. (b) Zhang, Q.-W.; Fan, C.-A.; Zhang, H.-J.; Tu, Y.-Q.; Zhao, Y.-M.; Gu, P.; Chen, Z.-M. Brønsted Acid Catalyzed Enantioselective Semipinacol Rearrangement for the Synthesis of Chiral Spiroethers. *Angew. Chem., Int. Ed*. **2009**, *48*, 8572−8574. (c) Branan, B. M.; Paquette, L. A. Heteroatomic Effects on the Acid-Catalyzed Rearrangements of Dispiro[4.0.4.4]tetradeca-11,13-dienes. *J. Am. Chem. Soc*. **1994**, *116*, 7658−7667. (d) Aggarwal, V. K.; Coldham, I.; McIntyre, S.; Warren, S. Transformation of cyclic α-phenylthio aldehydes by stereoselective aldol reactions and phenylthio migration into spirocyclic lactones and ethers, and E-allylic alcohols with 1,4-related chiral centres. *J. Chem. Soc., Perkin Trans. 1* **1991**, 451−460. (e) Chibale, K.; Warren, S. Asymmetric synthesis of spirocyclic pyrrolidines and tetrahydrofurans by chiral aldol reactions and phenylthio migration. *Tetrahedron Lett.* **1991**, *32*, 6645−6648. (f) Coldham, I.; Warren, S. Stereospecific Phenylthio Migrations in the Synthesis of Spirocyclic Lactones and Ethers from N-Methyl-4-Piperidone and Quinuclidin-3-one. *J. Chem. Soc., Perkin Trans. 1* **1992**, 2303−2307. (g) Palmer, L. I.; Read de Alaniz, J. Rapid and Stereoselective Synthesis of Spirocyclic Ethers via the Intramolecular Piancatelli Rearrangement. *Org. Lett.* **2013**, *15*, 476−479.

[9] (a) Ireland, R. E.; Maienfisch, P. The convergent synthesis of polyether ionophore antibiotics: the synthesis of the A ring carbamonensin spiro ether. *J. Org. Chem*. **1988**, *53*, 640−651. (b) Kumar, S.; Thornton, P. D.; Painter, T. O.; Jain, P.; Downard, J.; Douglas, J. T.; Santini, C. Synthesis of a family of spirocyclic scaffolds: building blocks for the exploration of chemical space. *J. Org. Chem.* **2013**, *78*, 6529−6539.

[10] (a) Hormuth, S.; Schade, W.; Reißig, H.-U. First Synthesis of Enantiomerically Pure Primary Helical Spirocycles Based on the Repetitive Addition of Lithiated Methoxyallene to Chiral 3(2H)-Dihydrofuranone Derivatives. *Liebigs Ann.* **1996**, *1996*, 2001−2006. (b) Kraft, P.; Popaj, K. Unexpected Tethering in the Synthesis of Methyl-Substituted Acetyl-1-oxaspiro[4.5]decanes: Novel Woody−Ambery Odorants with Improved Bioavailability. *Eur. J. Org. Chem*. **2008**, *2008*, 261−268.

[11] (a) Negri, J. T.; Paquette, L. A. Electrostatic Modulation of Hydroxyl Group Ionization in Acidic Media. Evidence for the Competitive Operation of Intramolecular SN2 Reactions. *J. Am. Chem. Soc.* 1992, 114, 8835−8841. (b) Bachki, A.; Falvello, L. R.; Foubelo, F.; Yus, M. Enantiomerically pure γ-oxidofunctionalised organolithium compounds from chiral oxetanes. Tetrahedron:Asymmetry **1997**, *8*, 2633−2643. (c) Young, J.-j.; Jung, L.-j.; Cheng, K.-m. Amberlyst-15-catalyzed

intramolecular SN2' oxaspirocyclization of tertiary allylic alcohols. *Tetrahedron Lett*. **2000**, *41*, 3411−3413.

[12] (a) Noto, N.; Koike, T.; Akita, M. Diastereoselective Synthesis of CF_3- and CF_2H-Substituted Spiroethers from Aryl-Fused Cyclo-alkenylalkanols by Photoredox Catalysis. *J. Org. Chem*. **2016**, *81*, 7064−7071. (b) Middleton, D. S; Simpkins, N. S; Begley, M. J.; Terrett, N. K. Synthesis of spiroethers using radical cyclisations*. Tetrahedron* **1990**, *46*, 545−564.

[13] Jiao, Z.-W.; Zhang, S.-Y.; He, C.; Tu, Y.-Q.; Wang, S.-H.; Zhang, F.-M.; Zhang, Y.-Q.; Li, H. Organocatalytic Asymmetric Direct Csp_3-H Functionalization of Ethers: A Highly Efficient Approach to Chiral Spiroethers. *Angew. Chem., Int. Ed*. **2012**, *51*, 8811−8815.

[14] (a) Lautens, M.; Klute, W.; Tam, W. Transition Metal-Mediated Cycloaddition Reactions. *Chem. Rev*. **1996**, *96*, 49-92. (b) Yet, L. Metal-Mediated Synthesis of Medium-Sized Rings. *Chem. Rev.* **2000**, *100*, 2963-3008; c) Xu. X.; Doyle, M. P. The [3 + 3]-Cycloaddition Alternative for Heterocycle Syntheses: Catalytically Generated Metalloenolcarbenes as Dipolar Adducts. *Acc. Chem. Res.* **2014**, *47*, 1396-1405. (d) Hashimoto, T.; Maruoka, K. Recent Advances of Catalytic Asymmetric 1,3-Dipolar Cycloadditions. *Chem. Rev*. **2015**, *115*, 5366-5412. (e) Trost, B. M.; Zuo, Z.; Schultz, J. E. *Chem. Eur. J*. **2020**, *26*, 15354-15377. (f) (a) Frühauf, H. Metal-Assisted Cycloaddition Reactions in Organotransition Metal Chemistry. *Chem. Rev.* **1997**, *97*, 523−596.

[15] Trost, B. M.; Chan, D. M. T. New Conjunctive Reagents. 2- Acetoxymethyl-3-Allyltrimethylsilane for Methylenecyclopentane Annulations Catalyzed by Palladium (0). *J. Am. Chem. Soc*. **1979**, *101*, 6429−6432.

[16] Shimizu, I.; Ohashi, Y.; Tsuji, J. Palladium-catalyzed [3 + 2] cycloaddition reaction of vinylcyclopropanes with α,β-unsaturated esters or ketones. *Tetrahedron Lett.* **1985**, *26*, 3825-3828.

[17] For reviews, see: (a) He, J.; Ling, J.; Chiu, P. Vinyl Epoxides in Organic Synthesis. *Chem. Rev*. **2014**, *114*, 8037-8128. (b) Allen, D.W.B.; Lakeland, C.P.; Harrity, J.P.A. Utilizing Palladium-Stabilized Zwitterions for the Construction of *N*-Heterocycles. *Chem. Eur. J*. **2017**, *23*, 13830-13857. (c) De, N.; Yoo, E.J. Recent Advances in the Catalytic Cycloaddition of 1,*n*-Dipoles. *ACS Catal*. **2018**, *8*, 48-58. (d) Liu, Y.; Oble, J.; Pradal, A.; Poli, G. Catalyic Domino Annulations through η^3-Allylpalladium Chemistry: A Never-Ending Story. *Eur. J. Inorg. Chem*. **2020**, 942-961. (e) Trost, B.M.; Mata. G. Forging Odd-Membered Rings: Palladium-Catalyzed Asymmetric Cycloadditions of Trimethylenemethane. *Acc. Chem. Res*. **2020**, *53*, 1293-1305. (f) Wang, J. Blaszczyk, S.A.; Li, X.; Tang, W. Transition Metal-Catalyzed Selective Carbon−Carbon Bond Cleavage of Vinylcyclopropanes in Cycloaddition Reactions. *Chem. Rev*. **2021**, *121*, 110-139. (g) Yang, C.; Yang, Z.-X.; Ding, C.-H.; Xu, B.; Hou, X.-L. Development of Dipolarophiles for Catalytic Asymmetric Cycloadditions through Pd-π-allyl zwitterions. *Chem. Rec.* **2021**, *21*, 1-14. (h) Pàmies, O.; Margalef, J.; Cañellas, S.; James, J.; Judge, E.; Guiry, P. J.; Moberg, C.; Bäckvall, J.-E.; Pfaltz, A.; Pericàs, M. A.; Diéguez, M. Recent Advances in Enantioselective Pd-Catalyzed Allylic 2 Substitution: From Design to Applications. *Chem. Rev.* **2021**, *121*, 4373–4505. (i) De la Cruz-Sánchez, P.; Pàmies, O. Metal-π-allyl mediated asymmetric cycloaddition reactions. In Advances in Catalysis; Elsevier:Amsterdam, The Netherlands, **2021**; Volume 69, pp. 103–180.

[18] Ma, C.; Huang, Y.; Xhao, Y. Stereoselective 1,6-Conjugate Addition/Annulation of *para*-Quinone Methides with Vinyl Epoxides/Cyclopropanes. *ACS. Catal.* **2016**, *6*, 6408−6412.

[19] Xiao, J.-A.; Li, Y.-C.; Luo, Z.-J.; Cheng, X.-L.; Deng, Z.-X.; Chen, W.-Q.; Su, W.; Yang, H. Construction of Bispirooxindole Heterocycles via Palladium-Catalyzed Ring-Opening Formal [3 + 2]-Cycloaddition of Spirovinylcyclopropyl Oxindole and 3-Oxindole Derivatives. *J. Org. Chem*. **2019**, *84*, 2297−2306.

[20] Wang, J.; Zhao, L.; Rong, Q.; Lv, R.; Lu, Y.; Pan, X.; Zhao, L.; Hu, L. Asymmetric Synthesis of 3,3′-Tetrahydrofuryl Spirooxindoles via Palladium-Catalyzed [3+2] Cycloadditions of Methyleneindolinones with Vinylethylene Carbonates. *Org. Lett*. **2020**, *22*, 5833−5838.

[21] Zhang, H.; Gao, X.; Jiang, F.; Shi, W.; Wang, W.; Wu, Y.; Zhang, C.; Shi, X.; Guo, H. Palladium-Catalyzed Asymmetric [3+2] Cycloaddition of Vinylethylene Carbonates with 2-Arylidene-1,3-Indandiones: Synthesis of Tetrahydrofuran-Fused Spirocyclic 1,3-Indandione *Eur. J. Org. Chem*. **2020**, *30*, 4801–4804.

[22] Jeon, H.J.; Park, S.M.; Lee, Y.M.; Lee, S.-G. Divergent Asymmetric Synthesis of Chiral Spiroheterocycles through Pd-Catalyzed Enantio-and Diastereoselective [3+2] Spiroannulation. *Org. Lett*. **2022**, *24*, 9189−9193.

[23] To the best of our knowledge there is only one report involving 5-alkylidene Meldrum's acid derivatives as dipolarophile species: Trost, B.M.; Morris, P.J.; Sprague, S.J. Palladium-Catalyzed Diastereo- and Enantioselective Formal [3+2]-Cycloadditions of Substituted Vinylcyclopropanes. *J. Am. Chem. Soc.* **2012**, *134*, 17823−17831.

[24] Some reviews on Meldrum's acid derivatives post-functionalization: (a) Ivanov, A.I. Meldrum's acid and related compounds in the synthesis of natural products and analogs. *Chem. Soc. Rev.* **2008**, *37*, 789–811. (b) Dumas, A.M.; Fillion, E. Meldrum's Acids and 5-Alkylidene Meldrum's Acids in Catalytic Carbon-Carbon Bond-Forming Processes. *Acc. Chem. Res*. **2010**, *43*, 440-454. (c) Brosge, F.; Singh, P.; Almqvist, F.; Bolm, C. Selected applications of Meldrum's acid – a tutorial. *Org. Biomol. Chem.* **2021**, *19*, 5014–5027.

[25] Zalesskiy, S., Ananikov, V.P. $Pd_2(dba)_3$ as a Precursor of Soluble Metal Complexes and Nanoparticles: Determination of Palladium Active Species for Catalysis and Synthesis. *Organometallics* **2012**, *6*, 2302–2309.

[26] Hu, W.; Lin, Z.; Wang, C. Synthesis of Multisubstituted Allylic Alcohols via a Nickel-Catalyzed Cross-Electrophile Ring-Opening Reaction. *Org. Lett.* **2022**, *31*, 5751–5755

[27] Zhang, J.; Yang, W.-L.; Zheng, H.; Wang, Y.; Deng, W.-P. Regio- and Enantioselective γ-Allylic Alkylation of In Situ-Generated Free Dienolates via Scandium/Iridium Dual Catalysis. Angew. Chem. Int. Ed. **2022**, *61*, e202117079.

[28] Hong, A.Y.; Stoltz, B.M. Enantioselective Total Synthesis of the Reported Structures of (−)-9-*epi*-Presilphiperfolan-1-ol and (−)-Presilphiperfolan-1-ol: Structural Confirmation and Reassignment and Biosynthetic Insights. *Angew. Chem. Int. Ed.* **2012**, *51*, 9674–9678

[29] Bigi, F.; Carloni, S.; Ferrari, L.; Maggi, R.; Mazzacani, A.; Sartori, G. Clean synthesis in water. Part 2: Uncatalysed condensation reaction of Meldrum's acid and aldehydes. *Tetrahedron Lett*. **2001**,*42*, 5203-5205.

[30] Jardim, M.; Baldassari, L.L.; Contreira, M.E.; Moro, A.V.; Lüdtke, D.S. Boron/zinc exchange for the conjugate arylation of unsaturated Meldrum's acid derivatives. Tetrahedron 76 (2020) 130967

[31] Deb, M.L.; Bhuyan, P.J. Uncatalysed Knoevenagel condensation in aqueous medium at room temperature. *Tetrahedron Letters* **2005**, *46*, 6453–6456.

[32] Das, T.K.; Rodriguez Treviño, A.M.; Pandiri, S.; Irvankoski, S.; Siitonen, J.; Rodriguez, S.M.; Yousufuddin, M.; Kürti, L. Catalyst-free transfer hydrogenation of activated alkenes exploiting isopropanol as the sole and traceless reductant. *Green Chem.* **2023**, *25*, 746-754

[33] Mohite, A.R.; Bhat, R.G. A Practical and Convenient Protocol for the Synthesis of (*E*)-α,β-Unsaturated Acids. *Org. Lett.* **2013**, *17*, 4564–4567.

[34] Helmy, S.; Leibfarth, F.A.; Oh, S.; Poelma, J.E.; Hawker, C.J.; Read de Alaniz, J. Photoswitching Using Visible Light: A New Class of Organic Photochromic Molecules. *J. Am. Chem. Soc.* 2014, *23*, 8169–8172.

[35] Dumas, A.M.; Fillion, E. $Sc(OTf)_3$-Catalyzed Conjugate Allylation of Alkylidene Meldrum's Acids. *Org. Lett.* **2009**, *9*, 1919–1922.

[36] Duursma, A.; Boiteau, J.-G.; Lefort, L.; Boogers, J.A.F.; de Vries, A.H.M.; De Vries, J.G.; Minnaard, A.J.; Feringa, B.L. Highly Enantioselective Conjugate Additions of Potassium Organotrifluoroborates to Enones by Use of Monodentate Phosphoramidite Ligands. *J. Org. Chem.* **2004**, *23*, 8045–8052.

[37] Kingsbury, A.; Brough, S.; McCarthy, A.P.; Lewis, W.; Woodward, S. Conjugate Addition Routes to 2-Alkyl-2,3-dihydroquinolin-4(1*H*)-ones and 2-Alkyl-4-hydroxy-1,2-dihydroquinoline-3-carboxylates. *Eur. J. Inorg. Chem*. **2019**, *2020*, 1011-1017.

[38] Lukowska, E.; Plenkiewicz, J. Asymmetric reduction of a-thiocyanatoketones by Saccharomyces cerevisiae and Mortierella isabellina—a new route to optically active thiiranes. *Tetrahedron: Asymmetry* **2007**, *18*, 1202-1209.

[39] Shimizu, K.; Sakamoto, M., Hamada, M.; Higashi, T.; Sugai, T.; Shoji, M. The scope and limitation of the regio- and enantioselective hydrolysis of aliphatic epoxides using *Bacillus subtilis* epoxide hydrolase, and exploration toward chirally differentiated tris(hydroxymethyl)methanol. *Tetrahedron: Asymmetry* **2010**, *21*, 2043-2049.

CHAPTER 6

General conclusions

UNIVERSITAT ROVIRA I VIRGILI
DEVELOPMENT OF CHIRAL METAL-CATALYSTS FOR THE SELECTIVE FORMATION OF C-H, C-C AND C-X BONDS. FROM DESIGN TO APPLICATION
Pol De La Cruz Sanchez Badia

6. General Conclusions

With the aim of finding catalysts able to reach unsolved substrates and novel combinations of substrate/nucleophile/dipolarophile for three asymmetric catalytic transformations of industrial interest, we have developed tailor-made ligand libraries, specially designed with the needs of the reaction under study and considering their industrial applicability (synthetized in few steps and from inexpensive starting materials, and simple manipulation). The specific conclusions for each transformation are collected below.

For the *asymmetric hydrogenation* of *chelating olefins* using easy-to-synthesize and air stable *Rh-catalysts*, we have successful prepared a family of P-stereogenic *N*-phosphine-phosphite ligands. The novelty in their design is that we used a chiral auxiliary for both, preparing the P-stereogenic moiety and as the ligand backbone. The latter allowed to reduce the number of synthetic steps. The usefulness of the corresponding Rh-catalytic systems was demonstrated with the synthesis of several valuable precursors of pharmacologically active compounds, with ee's at least as high (up to >99%) as the best ones reported, with the added advantages that the catalysts are easier to synthetize.

For the *asymmetric hydrogenation* of *olefins* with easy-to-synthesize and air stable *Ir-catalysts*, we have prepared five ligand libraries which take into account the needs of the substrate under study, with the aim to solve the problem of substrate specificity and reach the reduction of challenging substrates, whose hydrogenation is still unsolved.

In this respect, we have synthesized a family of phosphine-triazole ligands, specially designed to solve the asymmetric hydrogenation of exocyclic benzofused based non-chelating alkenes. Improving previous results reported, their air stable Ir-catalysts were able to successfully hydrogenate exocyclic olefins containing a benzofused six-membered ring motif (with ee's typically of 99%). Significantly, the results also extended to olefins bearing a five-membered benzofused ring (ee's typically ca 95%) and for the first time a promising enantioselectivity of 81% was reached for a seven-membered benzofused analogue. The absence of a competing isomerization process together with the perfect fit of the *E*-olefins in the catalyst chiral pocket are the keys for the success of this catalyst. In this fit the presence of non-covalent attractive interactions between the substrate and the ligand components has been crucial as well as the presence in the ligand of a triazole instead of the commonly oxazoline group.

We also take advantage of the thioether moiety with the application of an Ir-phosphite/phosphinite-thioether catalyst library, synthetized in four steps from inexpensive indene, that in contrast to most catalysts reported was able to reduce a

broad scope of olefins with a variety of coordination abilities, ranging from non-chelating olefins, through olefins with poorly coordinative groups to olefins with a coordinative functional group.

Two carbene-thioether ligand families, designed with the aim to combine the advantages of thioether and *N*-heterocyclic carbene functionalities were also prepared showing promising results.

Finally, we report the first family of ligands, P-stereogenic aminophosphine-oxazolines, that is able to successfully reduce a up to 106 di, tri- and tetrasubstituted olefins, including purely alkyl-trisubstituted olefins. DFT calculations and deuterium labeling experiments allowed the rationalization of the stereochemical outcomes of the reactions and helped in the selection of suitable substrates for these Ir-type catalysts.

For *Pd-catalyzed asymmetric allylic substitution* we show the application of a solid and air stable family of phosphite-oxazoline ligands, synthetized in few steps from readily available staring materials. Its design was based on the PHOX ligands, in which a methylene spacer has been added between the oxazoline and the phenyl ring and the phosphine moiety was replaced by biaryl phosphite groups. These simple modifications allowed to increase the substrate and nucleophile scope of the PHOX ligands. Excellent performance for a range of hindered and cyclic substrates, with several nucleophiles was observed. Mechanistic studies (DFT calculations and NMR spectroscopy of the key Pd-intermediates) showed that the wide substrate scope is due to the ability of the ligand to adapt their ligand parameters to the reacting substrate.

For the *Pd-catalyzed [3+2] cycloaddition reaction* we developed an efficient method for the synthesis of chiral spirocyclic tetrahydrofurans via the Pd-catalyzed [3+2] cycloaddition reaction of vinyl epoxides with 5-alkylidene Meldrum's acid derivatives. The novel cycloaddition products were attained in high yields, enantioselectivities and good diastereoselectivities independently of the nature of the substituents (dr's up to 15:1 and ee's up to >99%). We envision as future work in this field the post-functionalization of these cycloadducts taking advantage of the vinylic and Meldrum's acid moieties' reactivity to further demonstrate the synthetic potential of this newly developed protocol. In this manner we hope to achieve complex target molecules for medicinal chemistry or valuable intermediates in synthesis, in a simple way.

UNIVERSITAT ROVIRA I VIRGILI
DEVELOPMENT OF CHIRAL METAL-CATALYSTS FOR THE SELECTIVE FORMATION OF C-H, C-C AND C-X BONDS. FROM DESIGN TO APPLICATION
Pol De La Cruz Sanchez Badia

UNIVERSITAT ROVIRA I VIRGILI
DEVELOPMENT OF CHIRAL METAL-CATALYSTS FOR THE SELECTIVE FORMATION OF C-H, C-C AND C-X BONDS. FROM DESIGN TO APPLICATION
Pol De La Cruz Sanchez Badia

UNIVERSITAT ROVIRA I VIRGILI
DEVELOPMENT OF CHIRAL METAL-CATALYSTS FOR THE SELECTIVE FORMATION OF C-H, C-C AND C-X BONDS. FROM DESIGN TO APPLICATION
Pol De La Cruz Sanchez Badia

UNIVERSITAT ROVIRA I VIRGILI
DEVELOPMENT OF CHIRAL METAL-CATALYSTS FOR THE SELECTIVE FORMATION OF C-H, C-C AND C-X BONDS. FROM DESIGN TO APPLICATION
Pol De La Cruz Sanchez Badia

UNIVERSITAT
ROVIRA i VIRGILI